AD-A076 091 WOODWARD-CLYDE CONSULTANTS CHICAGO IL F/G 13/2
RESULTS AND INTERPRETATION OF CHEMICAL GROUTING TEST PROGRAM. V--ETC(U)
JUL 79 J PEREZ , Y LACROIX DACW43-78-C-0005
UNCLASSIFIED NL

1 OF 4
AD
A076091

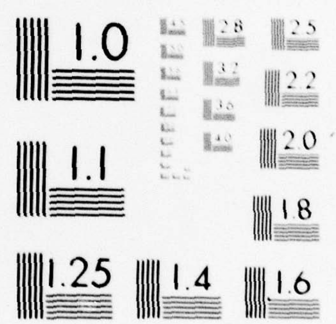

MICROCOPY RESOLUTION TEST CHART

NATIONAL BUREAU OF STANDARDS-1963-A

LEVEL III

PHASE IV REPORT

VOLUME II

RESULTS AND INTERPRETATION OF CHEMICAL GROUTING TEST PROGRAM

EXISTING LOCKS AND DAM NO. 26
MISSISSIPPI RIVER, ALTON, ILLINOIS

Prepared for

United States Army
Corps of Engineers
...Serving the Army
...Serving the Nation

St. Louis District

By

Woodward-Clyde Consultants
Chicago, Illinois

15 July 1979

Contract No. DACW43-78-C-0005

Y7C825

PHASE IV REPORT

VOLUME II

(6)

RESULTS AND INTERPRETATION OF CHEMICAL GROUTING TEST PROGRAM.

Volume II.

EXISTING LOCKS AND DAM ~~NO.~~ 26.
MISSISSIPPI RIVER, ALTON, ILLINOIS.

number

Phase IV Report.

Prepared for

United States Army
Corps of Engineers
...Serving the Army
...Serving the Nation

St. Louis District

(9) Final rept.,

By

(10) Jean-Yves Perez
Yves /Lacroix

Yves Lacroix

Woodward-Clyde Consultants
Chicago, Illinois

(12) 299

(11) 15 July 1979

Contract No. DACW43-78-C-0005
(15)

Y7C825

APPROVED FOR PUBLIC RELEASE - DISTRIBUTION UNLIMITED

411445

mt

Unclassified

SECURITY CLASSIFICATION OF THIS PAGE (When Data Entered)

REPORT DOCUMENTATION PAGE		READ INSTRUCTIONS BEFORE COMPLETING FORM
1. REPORT NUMBER	2. GOVT ACCESSION NO.	3. RECIPIENT'S CATALOG NUMBER
4. TITLE (and Subtitle) FOUNDATION INVESTIGATION AND TEST PROGRAM, LOCKS AND DAM 26, MISSISSIPPI RIVER, ALTON, ILLINOIS Volume II A076090		5. TYPE OF REPORT & PERIOD COVERED Final report 6. PERFORMING ORG. REPORT NUMBER
7. AUTHOR(s) Jean-Yves Perez Yves Lacroix		8. CONTRACT OR GRANT NUMBER(s) DACW43-78-C-0005
9. PERFORMING ORGANIZATION NAME AND ADDRESS Woodward-Clyde Consultants 11 East Adams Street Chicago, IL 60603		10. PROGRAM ELEMENT, PROJECT, TASK AREA & WORK UNIT NUMBERS
11. CONTROLLING OFFICE NAME AND ADDRESS U. S. Army Engineer District, St. Louis 210 North 12th Street St. Louis, MO 63101		12. REPORT DATE June 1979 13. NUMBER OF PAGES 257
14. MONITORING AGENCY NAME & ADDRESS(if different from Controlling Office)		15. SECURITY CLASS. (of this report) Unclassified 15a. DECLASSIFICATION/DOWNGRADING SCHEDULE

16. DISTRIBUTION STATEMENT (of this Report)

Approved for public release; distribution unlimited.

17. DISTRIBUTION STATEMENT (of the abstract entered in Block 20, if different from Report)

18. SUPPLEMENTARY NOTES

Vol I	Overview of Foundation Investigation and Test Program
Vol II	Results and Interpretation of Chemical Grouting Test Program
Vol IIA	Appendices A through G, Results and Interpretation of Chemical Grouting Test Program
Vol III	Results and Interpretation of Pile Driving Effects Test Program
Vol IIIA	Appendices H through T, Results and Interpretation of Pile Driving Effects Test Program
Vol IV	Results and Interpretation of Drilled-In Pile Test Program
Vol IVA	Appendices A through E, Results and Interpretation of Drilled-In Pile Test Program
Vol V	Results and Interpretation of Rock Anchor Test Program
Vol VA	Appendices A through E, Results and Interpretation of Rock Anchor Test Program

19. KEY WORDS (Continue on reverse side if necessary and identify by block number)

- Lock and Dam No. 26, Mississippi River
- Chemical grout test
- Rock anchor test
- Drilled-in pile test
- Pile driving effects test
- Timber piles
- Alluvial sands
- Benoto method
- Instrumentation of tests
- Vibrational effects on structures

20. ABSTRACT (Continue on reverse side if necessary and identify by block number)

A series of tests examining various foundation systems and construction techniques were conducted on Ellis Island near Locks and Dam No. 26 in alluvial sand deposits underlain by glacial deposits and limestone. The chemical grout test consisted of grouting the upper 20 feet of the alluvial sand by injecting a number of different silicate and cement-bentonite grout types, while varying the grouting method, hole spacing, and injecting rates. Heave, lateral displacement, and pore pressure were monitored during grout injection. The in situ properties of the sand were measured before and after grouting by standard

Cont

DD FORM 1 JAN 73 1473 EDITION OF 1 NOV 65 IS OBSOLETE

Unclassified

SECURITY CLASSIFICATION OF THIS PAGE (When Data Entered)

Cont'

20. penetration tests, static cone penetration tests, pressuremeter tests, bore hole permeability tests, and shear wave velocity tests. Concurrently laboratory tests were conducted to investigate the strength and creep behavior of the grouted sand. After completion of grouting, the site was excavated to examine and evaluate the grouted sand. In the rock anchor test, inclined rock anchors were installed in limestone through 130 feet of alluvial and glacial deposits using a pneumatic down-the-hole hammer with an offset reamer. Load tests were conducted on three instrumentated rock anchors and the feasibility of installation of the rock anchors was determined by evaluating loss of ground during installation, performance of the installation equipment, and rate of installation. The drilled-in pile test consisted of installation of large diameter high capacity pipe piles by the Benoto method. The feasibility of installing these piles was determined by evaluating loss of ground during installation, performance of the Benoto equipment, and rate of installation. In the pile driving effects test, pile founded monoliths were constructed, supported on either one, eight or twelve timber piles jetted and driven in alluvial sand to a depth of 35 feet. After applying lateral and vertical load to the monoliths, steel piles were driven at varying distances from the monoliths while monitoring movement of the monolith and supporting piles; shear, moment, and axial load in the timber piles; and pore pressure, movement, and particle velocity, in the soil. Parameters examined were pile type being driven (sheet, pipe, or H-pile), pile driving hammer (diesel, air-steam, or vibratory), distance of driven piles from monolith, driving of multiple piles at the same distance from the monolith, load level applied to the monolith, and soil properties (grouted and ungrouted). Vertical and lateral load tests were conducted on each pile founded monolith. Tests were also conducted to assess what effect grouted soil has on piles. Piles were driven in both grouted and ungrouted sand to examine driving characteristics and lateral load tests were conducted on H and pipe piles in both grouted and ungrouted sand.

TABLE OF CONTENTS

		Page
Title Page		i
Table of Contents		ii

0 SUMMARY OF CONCLUSIONS

Title Page		0-i
0.1	CHEMICAL GROUTING TEST PROGRAM	0-1
0.2	TEST AREA SUBSURFACE CONDITIONS	0-1
0.3	GROUTING ACTIVITIES	0-1
0.4	INSTRUMENTATION MONITORING	0-2
0.5	EVALUATION OF GROUTING RESULTS	0-2
0.6	COST	0-3

1 PURPOSE AND OBJECTIVES

Title Page		1-i
1.1	PURPOSE	1-1
1.2	OBJECTIVES	1-1
1.3	CONTRIBUTORS	1-2

TABLE OF CONTENTS

(Continued)

Page

2 CONCEPT AND DESCRIPTION OF TESTS

Title Page		2-i
2.1	TEST VARIABLES	2-1
2.1.1	Concept of Test Program	2-1
2.1.2	Grouting Methods	2-1
2.1.3	Grout Hole Spacing and Pattern	2-3
2.1.4	Grout Types	2-3
2.2	CONDUCT OF THE TESTS	2-4
2.2.1	Sequence of Activities	2-4
2.2.2	Test Area Configuration	2-5
2.3	MEASURED ASPECTS OF PERFORMANCE	2-6

List of Tables

Table 2.1	COMBINATION OF TEST VARIABLES	2-7

List of Figures

Figure 2.1	LAYOUT OF GROUT HOLES AND TEST SUBAREAS	2-8
Figure 2.2	DETAILS OF SLEEVE-PIPE AND PACKER	2-9
Figure 2.3	SEQUENCE OF ACTIVITIES	2-10
Figure 2.4	TEST AREA CONFIGURATION	2-11

TABLE OF CONTENTS

(Continued)

Page

3 TEST AREA SUBSURFACE CONDITIONS

Title Page		3-i
3.1	TEST AREA SELECTION	3-1
3.2	SUBSURFACE INVESTIGATIONS	3-1
3.2.1	Purpose and Scope	3-1
3.2.2	Dynamic Penetration Testing	3-1
3.2.3	Static Cone Penetration Testing	3-2
3.2.4	Pressuremeter Testing	3-3
3.2.5	Borehole Permeability Testing	3-3
3.2.6	Crosshole Shear Wave Velocity Measurements	3-3
3.2.7	Laboratory Testing	3-4
3.3	STRATIGRAPHY	3-5
3.3.1	General Geology	3-5
3.3.2	Description of Stratigraphic Units	3-5
3.4	INITIAL SOIL PROPERTIES	3-7
3.4.1	General	3-7
3.4.2	Index Properties	3-8
3.4.3	Stresses	3-8
3.4.4	Density	3-8
3.4.5	Strength-Deformation Properties	3-9
3.4.6	Permeability	3-11

List of Tables

Table 3.1	AVERAGE SOIL PROPERTIES BEFORE GROUTING	3-12

List of Figures

Figure 3.1	LOCATION OF SUBSURFACE INVESTIGATIONS BEFORE GROUTING	3-13
Figure 3.2	RESULT OF IN SITU TESTING BEFORE GROUTING	3-14
Figure 3.3	COMPARISON BETWEEN PENETRATION RESISTANCE N AND N_3 BEFORE GROUTING	3-15

TABLE OF CONTENTS

(Continued)

		Page
Figure 3.4	CORRELATION BETWEEN STANDARD AND STATIC CONE PENETRATION RESISTANCE BEFORE GROUTING	3-16
Figure 3.5	IDEALIZED PRESSUREMETER TEST RESULTS BEFORE GROUTING	3-17
Figure 3.6	SUBSURFACE PROFILE A-A OF TEST AREA	3-18
Figure 3.7	SUBSURFACE PROFILE B-B OF TEST AREA	3-19
Figure 3.8	SUBSURFACE PROFILE C-C OF TEST AREA	3-20
Figure 3.9	GRAIN-SIZE DISTRIBUTION OF STRATIGRAPHIC UNITS UNDERLYING TEST AREA	3-21
Figure 3.10	IN SITU STRESS PROFILES BEFORE GROUTING	3-22
Figure 3.11	SOIL UNIT WEIGHT PROFILE BEFORE GROUTING	3-23
Figure 3.12	RELATIVE DENSITY PROFILE BEFORE GROUTING	3-24
Figure 3.13	ELASTIC DEFORMATION MODULI BEFORE GROUTING	3-25
Figure 3.14	ANGLE OF INTERNAL FRICTION PROFILE BEFORE GROUTING	3-26
Figure 3.15	PRESSUREMETER LIMIT PRESSURE PROFILE BEFORE GROUTING	3-27
Figure 3.16	COEFFICIENT OF PERMEABILITY PROFILE BEFORE GROUTING	3-28

TABLE OF CONTENTS

(Continued)

		Page
	4 GROUTING PLANT	
Title Page		4-i
4.1	DESCRIPTION	4-1
4.1.1	General	4-1
4.1.2	Module 1	4-1
4.1.3	Module 2	4-1
4.1.4	Module 3	4-2
4.1.5	Module 4	4-2
4.2	OPERATION	4-3
4.2.1	Grouting Plant Operation Through Module 2	4-3
4.2.2	Grouting Plant Operation Through Module 4	4-3

List of Figures

Figure 4.1	VIEWS OF MODULAR GROUTING PLANT	4-4
Figure 4.2	VIEWS OF MODULAR GROUTING PLANT	4-5

TABLE OF CONTENTS

(Continued)

		Page
	5 GROUTS	
Title Page		5-i
5.1	LABORATORY TESTS	5-1
5.1.1	General	5-1
5.1.2	Preliminary Tests on Grouts	5-1
5.1.3	Tests on Reconstituted Sand Samples Grouted in the Laboratory	5-2
5.1.4	Investigation of Grout Neutralization Ratio	5-5
5.2	ON SITE LABORATORY TESTS	5-7
5.2.1	Purpose and Objectives	5-7
5.2.2	Grout Components and Fresh Grouts	5-7
5.2.3	Set Grouts	5-8
5.2.4	Results	5-8
5.3	GROUT COMPOSITIONS	5-9
5.3.1	Low-Strength Grouts	5-9
5.3.2	High-Strength Grouts	5-10
5.3.3	Cement-Bentonite Grouts	5-11

List of Tables

Table 5.1	COMPOSITION OF GROUTS PRELIMINARY LABORATORY TESTS	5-12
Table 5.2	RESULTS OF CHEMICAL ANALYSES OF TEST AREA GROUNDWATER AND MISSISSIPPI RIVER WATER	5-13
Table 5.3	GROUT PROPERTIES PRELIMINARY LABORATORY TESTS	5-14
Table 5.4	RESULTS OF UNCONFINED COMPRESSION TESTS, RECONSTITUTED SAND SAMPLES GROUTED IN THE LABORATORY	5-15
Table 5.5	RESULTS OF $\overline{\text{CID}}$ TRIAXIAL COMPRESSION AND PERMEABILITY TESTS, RECONSTITUTED SAND SAMPLES GROUTED IN THE LABORATORY	5-16
Table 5.6	RESULTS OF NEUTRALIZATION RATIO INVESTIGATIONS	5-17
Table 5.7	AVERAGE PROPERTIES OF GROUTS MEASURED ON SITE DURING GROUTING	5-18

TABLE OF CONTENTS

(Continued)

List of Figures

		Page
Figure 5.1	AVERAGE PROPERTIES OF SAND USED FOR LABORATORY GROUTING TESTS	5-19
Figure 5.2	LABORATORY GROUTING APPARATUS	5-20
Figure 5.3	RESULTS OF LONG-TERM UNCONFINED COMPRESSION TESTS, RECONSTITUTED SAND SAMPLES GROUTED IN THE LABORATORY	5-21
Figure 5.4	RESULTS OF LONG-TERM $\overline{\text{CID}}$ TRIAXIAL COMPRESSION TESTS, RECONSTITUTED SAND SAMPLES GROUTED IN THE LABORATORY	5-22

TABLE OF CONTENTS

(Continued)

Page

6 GROUTING PROCEDURES

Title Page		6-i
6.1	GENERAL	6-1
6.2	OPEN-BOTTOM PIPES	6-1
6.3	SLEEVE-PIPES	6-1
6.4	MULTI-STAGE GROUTING	6-2
6.5	HYDRAULIC FRACTURING TESTS	6-2

List of Tables

Table 6.1	HYDRAULIC FRACTURING TEST RESULTS	6-4

List of Figures

Figure 6.1	CALCULATION OF VOLUME OF GROUT TO BE INJECTED	6-5
Figure 6.2	EXAMPLE OF HYDRAULIC FRACTURING TEST RESULTS AND INTERPRETATION	6-6

TABLE OF CONTENTS

(Continued)

		Page
	7 MONITORING OF GROUTING ACTIVITIES	
Title Page		7-i
7.1	MONITORING SYSTEM	7-1
7.2	GROUT PUMPING PRESSURE	7-1
7.3	GROUT FLOW RATE	7-1
7.4	GROUT VOLUME	7-1

List of Tables

Table 7.1	GROUT VOLUME INJECTED IN EACH SUBAREA	7-2

TABLE OF CONTENTS

(Continued)

		Page
	8 EFFECTS OF GROUTING	
Title Page		8-i
8.1	OVERVIEW OF INSTRUMENTATION SYSTEM	8-1
8.2	HEAVE MEASUREMENTS	8-1
8.2.1	Instruments	8-1
8.2.2	Presentation of Results	8-2
8.2.3	Conclusions	8-4
8.3	LATERAL DISPLACEMENT MEASUREMENTS	8-5
8.3.1	Instrumentation	8-5
8.3.2	Presentation of Results	8-5
8.3.3	Conclusions	8-6
8.4	PORE PRESSURE MEASUREMENTS	8-7
8.4.1	Instruments	8-7
8.4.2	Presentation of Results	8-7
8.4.3	Conclusions	8-7

List of Tables

Table 8.1	GENERAL INSTRUMENTATION RESULTS	8-9
Table 8.2	HEAVE MEASURED IN EACH SUBAREA	8-10

List of Figures

Figure 8.1	INSTRUMENTATION LOCATION	8-11
Figure 8.2	VERTICAL CONTROL BENCHMARK BM-1	8-12
Figure 8.3	TYPICAL SURFACE REFERENCE POINT UNDER ASPHALT PAD	8-13
Figure 8.4	DETAILS OF BORROS HEAVE POINT	8-14
Figure 8.5	TYPICAL 3-D DEFORMATION GAGE	8-15
Figure 8.6	MAXIMUM VERTICAL MOVEMENT OF SURFACE REFERENCE POINTS AT EL 423	8-16
Figure 8.7	MAXIMUM VERTICAL MOVEMENT OF BORROS POINTS AT EL 402	8-17

TABLE OF CONTENTS

(Continued)

		Page
Figure 8.8	MAXIMUM VERTICAL MOVEMENT OF BORROS POINTS AT EL 384 TO EL 387	8-18
Figure 8.9	RESULTS OF HEAVE MEASUREMENTS BETWEEN SUBAREAS 8 AND 10	8-19
Figure 8.10	ANALYSIS OF VERTICAL MOVEMENT MEASURED BETWEEN SUBAREAS 8 AND 10	8-20
Figure 8.11	ADEQUATE INSTALLATION METHOD OF SONDEX RINGS ON INCLINOMETER CASING	8-21
Figure 8.12	COMPARISON BETWEEN TWO SUCCESSIVE MEASUREMENTS AND ACCURACY OF INCLINOMETER BEFORE GROUTING	8-22
Figure 8.13	COMPARISON BETWEEN TWO SUCCESSIVE MEASUREMENTS AND ACCURACY OF INCLINOMETER AFTER GROUTING	8-23
Figure 8.14	MAXIMUM TOTAL HORIZONTAL DISPLACEMENT FROM INCLINOMETER MEASUREMENTS	8-24
Figure 8.15	MAXIMUM HORIZONTAL DISPLACEMENT BETWEEN TWO SUCCESSIVE INCLINOMETER MEASUREMENTS	8-25
Figure 8.16	LATERAL MOVEMENT OF INCLINOMETER I-6 AT EL 407	8-26
Figure 8.17	LATERAL MOVEMENT OF INCLINOMETER I-6 AT EL 399	8-27
Figure 8.18	LATERAL MOVEMENT OF INCLINOMETER I-6 AT EL 385	8-28
Figure 8.19	DETAILS OF PNEUMATIC PIEZOMETER INSTALLATION	8-29
Figure 8.20	TYPICAL PORE WATER PRESSURE MEASUREMENTS IN TEST AREA	8-30
Figure 8.21	COMPARISON BETWEEN EXCESS PIEZOMETRIC PRESSURE IN P-3 AND GROUT PRESSURE IN GROUT HOLE 12-4	8-31

TABLE OF CONTENTS

(Continued)

		Page
	9 EVALUATION OF GROUTING RESULTS	
Title Page		9-i
9.1	METHODS OF EVALUATION	9-1
9.2	BOREHOLE SAMPLING AND IN SITU TESTING	9-1
9.2.1	Purpose and Scope	9-1
9.2.2	Boring and Sampling	9-1
9.2.3	Standard Penetration Tests	9-2
9.2.4	Static Cone Penetration Tests	9-3
9.2.5	Pressuremeter Tests	9-4
9.2.6	Borehole Permeability Tests	9-5
9.2.7	Crosshole Shear Wave Velocity Measurements	9-5
9.3	EXCAVATION INTO GROUTED SOIL	9-6
9.3.1	Purpose and Scope	9-6
9.3.2	Dewatering and Excavation Sequence	9-6
9.3.3	Mapping and Visual Observation	9-7
9.3.4	Plate Load Tests	9-12
9.3.5	In-Place Density Tests	9-13
9.3.6	Block and Core Samples	9-13
9.4	LABORATORY TESTING	9-14
9.4.1	Purpose and Scope	9-14
9.4.2	Borehole Samples	9-14
9.4.3	Excavation Block and Core Samples	9-15
9.4.4	Post-Grouting Groundwater Analyses	9-18
9.5	COMPARISON OF RESULTS	9-18
9.5.1	Grouting Effectiveness	9-18
9.5.2	Grouted Soil Properties	9-20

List of Tables

Table 9.1	RESULTS OF SHEAR WAVE VELOCITY MEASUREMENTS	9-30
Table 9.2	LOCATION AND RESULTS OF PLATE LOAD TESTS	9-31
Table 9.3	LOCATION AND RESULTS OF IN-PLACE DENSITY TESTS	9-32
Table 9.4	LOCATION OF GROUTED SOIL BLOCK AND CORE SAMPLES	9-33

TABLE OF CONTENTS

(Continued)

		Page
Table 9.5	CURING HISTORY OF UNDISTURBED BOREHOLE SAMPLES	9-34
Table 9.6	RESULTS OF UNCONFINED COMPRESSION AND PERMEABILITY TESTS ON UNDISTURBED BOREHOLE SAMPLES	9-35
Table 9.7	RESULTS OF UU TRIAXIAL COMPRESSION AND PERMEABILITY TESTS ON UNDISTURBED BOREHOLE SAMPLES	9-36
Table 9.8	RESULTS OF CID TRIAXIAL COMPRESSION AND MAX-MIN DENSITY TESTS ON RECONSTITUTED UNGROUTED SAND	9-37
Table 9.9	RESULTS OF UNCONFINED COMPRESSION AND SONIC VELOCITY ON EXCAVATION BLOCK AND CORE SAMPLES	9-38
Table 9.10	RESULTS OF TRIAXIAL AND OTHER TESTS ON BLOCK AND CORE SAMPLES	9-39
Table 9.11	RESULTS OF POST GROUTING GROUNDWATER ANALYSES	9-40
Table 9.12	CONDITIONS PREVAILING UNDER VARIOUS TESTS	9-41

List of Figures

Figure 9.1	LOCATION OF BORINGS DRILLED AFTER GROUTING	9-42
Figure 9.2	RESULTS OF IN SITU TESTING AFTER GROUTING IN SUBAREA 1	9-43
Figure 9.3	RESULTS OF IN SITU TESTING AFTER GROUTING IN SUBAREA 2	9-44
Figure 9.4	RESULTS OF IN SITU TESTING AFTER GROUTING IN SUBAREA 3	9-45
Figure 9.5	RESULTS OF IN SITU TESTING AFTER GROUTING IN SUBAREA 4	9-46

TABLE OF CONTENTS

(Continued)

		Page
Figure 9.6	RESULTS OF IN SITU TESTING AFTER GROUTING IN SUBAREA 5	9-47
Figure 9.7	RESULTS OF IN SITU TESTING AFTER GROUTING IN SUBAREA 5a	9-48
Figure 9.8	RESULTS OF IN SITU TESTING AFTER GROUTING IN SUBAREA 6	9-49
Figure 9.9	RESULTS OF IN SITU TESTING AFTER GROUTING IN SUBAREA 7	9-50
Figure 9.10	RESULTS OF IN SITU TESTING AFTER GROUTING IN SUBAREA 8	9-51
Figure 9.11	RESULTS OF IN SITU TESTING AFTER GROUTING IN SUBAREA 9	9-52
Figure 9.12	RESULTS OF IN SITU TESTING AFTER GROUTING IN SUBAREA 10	9-53
Figure 9.13	RESULTS OF *IN SITU* TESTING AFTER GROUTING IN SUBAREA 11	9-54
Figure 9.14	RESULTS OF IN SITU TESTING AFTER GROUTING IN SUBAREA 12	9-55
Figure 9.15	RESULTS OF IN SITU TESTING AFTER GROUTING IN SUBAREA 13	9-56
Figure 9.16	HORIZONTAL SECTION THROUGH TEST AREA AT EL 398	9-57
Figure 9.17	HORIZONTAL SECTION THROUGH TEST AREA AT EL 394	9-58
Figure 9.18	HORIZONTAL SECTION THROUGH TEST AREA AT EL 390	9-59
Figure 9.19	HORIZONTAL SECTION THROUGH TEST AREA AT EL 385	9-60
Figure 9.20	VERTICAL SECTION AA THROUGH TEST AREA	9-61
Figure 9.21	VERTICAL SECTION BB THROUGH TEST AREA	9-62
Figure 9.22	VERTICAL SECTION CC THROUGH TEST AREA	9-63
Figure 9.23	VERTICAL SECTION DD THROUGH TEST AREA	9-64
Figure 9.24	VERTICAL SECTION EE THROUGH TEST AREA	9-65
Figure 9.25	VERTICAL SECTION FF THROUGH TEST AREA	9-66
Figure 9.26	VERTICAL SECTION GG THROUGH TEST AREA	9-67
Figure 9.27	IDEALIZED GROUT PUMPING PRESSURE AND RATE RECORDS FOR ALLUVIAL GROUTING	9-68

TABLE OF CONTENTS

(Continued)

		Page
Figure 9.28	EXAMPLES AND INTERPRETATIONS OF ACTUAL GROUT PUMPING PRESSURE RECORDS	9-69
Figure 9.29	COMPARISON BETWEEN STATIC CONE PENETRATION RESISTANCE BEFORE AND AFTER GROUTING	9-70
Figure 9.30	SHEAR WAVE VELOCITY RESULTS FROM IN SITU CROSSHOLE MEASUREMENTS AND LABORATORY SONIC VELOCITIES ON EXCAVATION BLOCK SAMPLES	9-71
Figure 9.31	RELATIVE LOCATION OF GEOPHYSICAL ARRAYS AND GROUTED SOIL AT EL 398	9-72
Figure 9.32	RELATIVE LOCATION OF GEOPHYSICAL ARRAYS AND GROUTED SOIL AT EL 394	9-73
Figure 9.33	RELATIVE LOCATION OF GEOPHYSICAL ARRAYS AND GROUTED SOIL AT EL 390	9-74
Figure 9.34	RELATIVE LOCATION OF GEOPHYSICAL ARRAYS AND GROUTED SOIL AT EL 385	9-75
Figure 9.35	COMPARISON BETWEEN IN SITU HORIZONTAL P_o BEFORE AND AFTER GROUTING	9-76
Figure 9.36	COMPARISON OF GROUTING PRESSURE AND AFTER-GROUTING IN SITU HORIZONTAL STRESS	9-77
Figure 9.37	COMPARISON BETWEEN SOIL UNIT WEIGHT AND WATER CONTENT BEFORE AND AFTER GROUTING	9-78
Figure 9.38	COMPARISON BETWEEN ELASTIC DEFORMATION MODULUS FROM PRESSUREMETER TESTS BEFORE AND AFTER GROUTING	9-79
Figure 9.39	COMPARISON BETWEEN DEFORMATION MODULUS FROM PLATE LOAD TESTS	9-80
Figure 9.40	COMPARISON BETWEEN ELASTIC DEFORMATION MODULUS FROM SHEAR WAVE VELOCITY MEASUREMENTS	9-81
Figure 9.41	INFLUENCE OF VARIOUS FACTORS ON LABORATORY ELASTIC DEFORMATION MODULUS	9-82
Figure 9.42	INTERPRETATION OF $\overline{\text{CID}}$ TRIAXIAL TESTS ON UNGROUTED AND GROUTED SAND SAMPLES	9-83

TABLE OF CONTENTS

(Continued)

		Page
Figure 9.43	STRESS-STRAIN CURVES FROM UNCONFINED COMPRESSION TESTS FIELD AND LABORATORY SAMPLES GROUTED WITH 35 ± SIROC 142	9-84
Figure 9.44	INFLUENCE OF GROUT SILICATE CONTENT ON UNCONFINED STRESS-STRAIN CHARACTERISTICS	9-85
Figure 9.45	INFLUENCE OF STRAIN RATE ON UNCONFINED COMPRESSIVE STRENGTH OF GROUTED SAND	9-86
Figure 9.46	INFLUENCE OF CURING TIME ON STRESS-STRAIN CHARACTERISTICS OF GROUTED SAND	9-87
Figure 9.47	COMPARISON BETWEEN PRESSUREMETER LIMIT PRESSURES MEASURED BEFORE AND AFTER GROUTING	9-88
Figure 9.48	COMPARISON BETWEEN LONG-TERM UNCONFINED BEHAVIOR OF LAB GROUTED SAND USING 35, 50, and 70 ± SILICATE GROUTS	9-89
Figure 9.49	RESULTS OF LONG-TERM UNCONFINED COMPRESSION TESTS ON EXCAVATION BLOCK AND CORE SMAPLES	9-90
Figure 9.50	COMPARISON BETWEEN LONG-TERM TRIAXIAL BEHAVIOR OF LAB GROUTED SAND USING 35 ± and 70 ± SILICATE GROUTS	9-91
Figure 9.51	RESULTS OF LONG-TERM TRIAXIAL TESTS ON EXCAVATION BLOCK AND CORE SAMPLES	9-92
Figure 9.52	CREEP RATE VS GROUT SILICATE CONTENT INFERRED FROM PLATE LOAD TEST RESULTS	9-93
Figure 9.53	RESULTS OF LONG TERM PRESSUREMETER TESTS	9-94
Figure 9.54	FIELD AND LABORATORY FALLING HEAD PERMEABILITY TEST RESULTS	9-95

TABLE OF CONTENTS

(Continued)

		Page
	10 COST ANALYSES	
Title Page		10-i
10.1	GENERAL	10-1
10.2	GROUT PIPE INSTALLATION COST	10-1
10.2.1	Drill Rig Cost	10-1
10.2.2	Pipe Cost	10-1
10.2.3	Labor Cost	10-2
10.2.4	Sleeve Grouting Cost	10-2
10.2.5	Summary of Grout Pipe Installation Cost	10-2
10.3	GROUT COST	10-2
10.3.1	Grout Components	10-2
10.3.2	35% Siroc 142	10-3
10.3.3	25% Silicate/Aluminate	10-3
10.3.4	28% Silicate/R600	10-3
10.3.5	55% Siroc 142	10-4
10.3.6	55% Siroc 132	10-4
10.3.7	46% Silicate/R600	10-4
10.3.8	45% Siroc 132	10-5
10.3.9	Cement-Bentonite (c/w = 0.25)	10-5
10.3.10	Cement-Bentonite (c/w = 0.4)	10-5
10.3.11	Summary of Grout Cost	10-5
10.4	GROUT MIXING AND INJECTION COST	10-6
10.5	OTHER COSTS	10-6
10.6	TOTAL GROUTING COST	10-6

TABLE OF CONTENTS

(Continued)

Page

List of Tables

Table 10.1	SUMMARY OF GROUT PIPE INSTALLATION COST PER SUBAREA	10-7
Table 10.2	SUMMARY OF GROUT COST PER SUBAREA	10-8
Table 10.3	GROUT MIXING AND INJECTION COST PER TYPE OF GROUT	10-9
Table 10.4	SUMMARY OF GROUT MIXING AND INJECTION COST PER SUBAREA	10-10
Table 10.5	SUMMARY OF OTHER COSTS PER SUBAREA	10-11
Table 10.6	SUMMARY OF TOTAL GROUTING COST PER SUBAREA	10-12
Table 10.7	SUMMARY OF TOTAL GROUT COST PER GROUTING METHOD	10-13

REFERENCES

Title Page R-i

REFERENCES R-1

PHASE IV REPORT

VOLUME II

RESULTS AND INTERPRETATION OF CHEMICAL GROUTING TEST PROGRAM

SECTION 0

SUMMARY OF CONCLUSIONS

0 SUMMARY OF CONCLUSIONS

0.1 CHEMICAL GROUTING TEST PROGRAM

The feasibility and effectiveness of injecting silicate grouts into Mississippi River alluvial sand were tested near Locks and Dam No. 26 from April 1978 through August 1978. The field test program was supplemented by a laboratory test program undertaken in several steps from April 1978 through January 1979. The test program involved testing four different grouting methods, eight grout types, and two grout hole spacings. A total of 123,500 gal of grout was injected through 74 grout holes to grout approximately 1440 yd^3 of alluvial sand. The test area was explored by borings and instrumented before grouting, grouted, reexplored by borings after grouting, dewatered, and excavated to observe results of grouting.

0.2 TEST AREA SUBSURFACE CONDITIONS

The sand strata grouted during the test program comprised the upper 20 ft of the recent alluvium deposits of the Mississippi River valley. Initial subsurface conditions at the test area were assessed before grouting by borings, sampling, and in situ testing (standard penetration tests, static cone penetration tests, pressuremeter tests, borehole permeability tests, and shear wave velocity measurements). The alluvial sand is generally fine- to medium-grained and contained on the average no more than 5 percent fines (that is, 5 percent by weight of soil particles passed through a No. 200 US sieve). The coefficient of permeability in the zone that was grouted ranged from 5×10^{-3} cm/s to 3×10^{-2} cm/s.

During excavation of the test area, abundant concentrations of carbonaceous material (wood, charcoal, and lignite) ranging in size from silt to large tree trunks, were observed. The alluvial sand was always cross-bedded. Cross-beds were usually gently dipping and were from several inches to a few feet thick.

0.3 GROUTING ACTIVITIES

Grout injection was done by a joint venture of Raymond International Builders, Inc. and Soletanche and Rodio, Inc., subcontractors to Woodward-Clyde Consultants. A modular grouting plant was used to mix and pump silicate and cement-bentonite grouts and monitor grouting parameters (grout pumping pressure and pumping rate, and grout volume). Grout was pumped through open-bottom pipes and through sleeve-pipes. The pumping pressure was kept at less than 1 lb/in^2 per foot of soil above the bottom of open-bottom pipes. Grout was pumped at an average rate of 800 l/hr (3.5 gal/min) through each open-bottom pipe. The average grout take for open-bottom pipe was intended to be 25 percent of the volume of soil to be grouted. Actually, it averaged 25.6 percent.

Three grouting procedures were tested using sleeve-pipes. In one procedure, grout was pumped using a grouting pressure limiting criterion of 1 lb/in^2 per foot of overburden. Grout take was very small for this procedure. In a second procedure, the intended volume of grout was injected in one stage using a pumping rate less than 85 percent of the rate that would induce hydraulic fracturing of the soil. This pumping rate was usually between 300 l/hr and 450 l/hr (1.3 gal/min and 2 gal/min). The average grout take for the second sleeve-pipe procedure was intended to be 45 percent of the volume of soil to be grouted. Actually, it averaged 43.9 percent. In a third procedure, the intended volume of grout was injected in several separate stages, also using a rate of pumping of 300 l/hr to 450 l/hr. The actual grout take for the third procedure was 52.6 percent of the volume of soil to be injected.

0.4 INSTRUMENTATION MONITORING

Ground instruments were installed prior to grouting to monitor the effects of grouting (vertical and horizontal displacements of the soil mass, and pore water pressure). The maximum observed heave was 0.02 ft, except for one zone that heaved 0.048 ft. This localized, larger movement was attributed to injection of cement-bentonite grout. The predicted maximum heave was 0.02 ft. The maximum observed horizontal displacement was 0.018 ft as compared to a predicted value of 0.1 ft. Generally, the horizontal displacements were only slightly greater than the instrumentation accuracy. The maximum observed excess porewater pressure was about 12 lb/in^2 as compared to a predicted maximum change of 30 lb/in^2.

0.5 EVALUATION OF GROUTING RESULTS

Grouting results were evaluated by exploration and testing in boreholes drilled from ground surface, and by excavation, mapping, and in situ testing of the grouted soil. Standard and static cone penetration tests were used to assess the extent of grout penetration. Pressuremeter and borehole permeability tests, and shear wave velocity measurements were used to measure in situ properties of grouted soil. The in situ tests and measurements were found to be effective in assessing grouting results from ground surface.

The test area was dewatered and excavated. The extent of grout penetration was mapped and photographed. Observations indicated that open-bottom pipe grouting method was generally unsuccessful in achieving complete grout penetration. Low-pressure sleeve-pipe grouting was totally ineffective. Single-stage sleeve-pipe grouting yielded better, but not complete grout penetration. Multiple-stage sleeve-pipe grouting was generally very effective in achieving almost complete grout penetration. Six-ft grout hole spacing was sometimes not adequate, and 4.2-ft spacing was found to achieve the desired grout penetration and uniformity. Cement-bentonite grout did not permeate the alluvial sand. The small quantity of cement-bentonite injected resulted only in creating bulbs along geologic discontinuities. Hydraulic fractures were found in almost all grouted soil masses observed. The majority of the fractures were vertical or coincident to geologic discontinuities. Consistency of grouted soil varied from sandstone-like material for high-silicate-content grouts (55 to 45% silicate) to low-strength, cohesive material for low-silicate-content grouts (28 to 25% silicate).

Index and engineering properties of grouted soil were assessed by in situ and laboratory tests and measurements. Among the in situ testing methods, shear wave velocity measurements appeared to be a most appropriate method to detect both changes in soil properties and extent of grouting. In situ horizontal stresses increased by two to three times due to grouting. In-place dry unit weight of grouted soil averaged 1 to 3 lb/ft^3 more than before grouting. Strength and deformation modulus values were generally increased manyfold by grouting; the actual increases depended on the strength of the grout injected. The strength increase was due only to an increase in cohesion, the angle of internal friction remaining practically unchanged or decreasing slightly. Time dependent properties of grouted soil were tested. Significant creep was observed in some grouted zones, although tendency to creep failure was not generally pronounced. Siroc-type grouts exhibited less creep than grouts containing aluminate reactant. Grouts containing R600 reactant were the most creep-prone. Grouted soil was found to be much less permeable than ungrouted soil. Coefficient of permeability of grouted soil generally ranged from 10^{-4} cm/s to 10^{-6} cm/s. The reduction in permeability did not appear to be a function of grout type, but rather it was found to be a function of grouting method (that is, of grout penetration). Zones showing no decrease in permeability were zones left ungrouted.

A summary of grouted soil properties is given in Table 0.1. The data in the table give representative of average values of the results of the various tests performed on grouted soil during this program.

0.6 COST

The total cost of grouting (excluding earthwork, dewatering, and engineering) was $565,560. Grouting costs varied widely (from $210 to $618 per cubic yard of soil to be grouted) depending on grout type, grouting method, and grout hole spacing. When related to grout take, the range of cost variation was almost as wide ($7 to $20 per cubic yard of soil to be grouted and per percent grout take). Cost of open-bottom pipe grouting averaged $294 per cubic yard of soil to be grouted and $10 per cubic yard of soil to be grouted and per percent grout take. Cost of single-stage sleeve-pipe grouting averaged $425 per cubic yard of soil to be grouted and slightly less than $10 per cubic yard of soil to be grouted and per percent grout take. Cost of multiple-stage sleeve-pipe grouting averaged $437 per cubic yard of soil to be grouted and slightly more than $8 per cubic yard of soil to be grouted and per percent grout take.

These costs are not representative of production chemical grouting projects, especially for open-bottom pipe applications, because of the relatively large effect of mobilization and contractor's supervision costs inherent to the test program. It is likely that these costs could be decreased by a factor of two to four and be more representative of production grouting.

							Index Properties			Stress		Stiffness					
												Unconfined Compression		CID Triaxial Compression			
Subarea Number	GROUT TYPE	Grouting Method[8]	Grout-Hole Spacing, ft	Standard Penetration Resistance, bl/ft N	Static Cone Penetration Resistance t/ft² q_c	Shear Wave Velocity (Intact Mass), ft/s V_s	In-Situ Dry Density, lb/ft³ γ_d	Water Content, % ε_n	Specific Gravity G	In-Situ Horizontal Stress, t/ft² σ_h	Coefficient of Earth Pressure at Rest K_o	Initial Tangent Modulus, t/ft² E_t	Secant Modulus at Failure, t/ft² E_s	Initial Tangent Modulus, t/ft² E_t	Secant Modulus at Failure, t/ft² E_s	Plate Load Test Modulus, t/ft² E_{plt}	Pressuremeter E_p
U	Ungrouted	-	-	20	125	600	105	22	2.65	1.5	.45	-	-	500	150	144	1
6	25% Silicate/Aluminate	S_3	6	-	275	-	106.3	20	-	-	-	-	-	-	-	534	-
7	25% Silicate/Aluminate	S_3	6	-	280	-	110	17	-	-	-	-	-	-	-	311	-
8	25% Silicate/Aluminate	S_3	4.2	22	280	1,100	112.4	17	2.68	3.5	2.3	58	39	801	145	246	11
5a	25% Silicate/Aluminate	S_1	6	20	-	-	-	-	-	-	-	-	-	-	-	-	-
3	28% Silicate/R600	S_2	6	60	300	-	103.9	17	-	-	-	90[1]	55[1]	-	-	1,613	-
1	35% SIROC 142	0_1	4.2	45	320	1,190	110.3	19	2.68	2.2	1.3	1,231	757	902	155	338	1
2	35% SIROC 142	0_1	6	42	250	-	110.2	19	2.68	-	-	625	471	-	-	1,815	-
4	35% SIROC 142	S_2	6	100+	450	-	111.7	17	2.66	2.6	1.6	12,000	8,000	-	-	1,218	4
5	45% SIROC 132	S_2	6	100+	500+	-	-	-	-	4.4	3	-	-	-	-	8,233	1,57
12	46% Silicate/R600	S_3	6	100+	500+	-	-	-	-	-	-	-	-	-	-	911	-
13	46% Silicate/R600	S_3	4.2	100+	500+	2,110	105[3]	1.8	2.68	4.7	3.3	3,006	2,106	2,146	880	962	8
10	55% SIROC 142/132	S_2	6	100	425	-	-	0	-	-	-	-	-	-	-	9,290	-
11	55% SIROC 142/132	S_2	4.2	100+	500+	3,547	104[3]	20	2.72	3.8	2.5	5,192	4,910	6,667	3,673	12,098	1,32
9	55% SIROC	0_1	4.2	90	375	-	-	-	-	-	-	-	-	-	-	5,464	-

General Note

Unless otherwise noted, laboratory tests were made on excavation block and core samples.

Notes:

(1) *From undisturbed borehole samples*

(2) *Reconstituted sample grouted in the laboratory*

(3) *From excavation block sample*

(4) *Laboratory permeability test*

(5) *Borehole permeability test*

(6) *CSR = 30%, time range = 10 to 100 minutes*

(7) *CSR = 50%*

CSR = Constant stress ratio (see Fig. 9.48 and 9.50)

(8) *See Section 2.1.2 for definition of grouting method*

ss	Stiffness							Shear Strength							Creep		
	Unconfined Compression		CID Triaxial Compression					CID Triaxial Compression								
Coefficient of Earth Pressure at Rest K_o	Initial Tangent Modulus, t/ft² E_t	Secant Modulus at Failure, t/ft² E_s	Initial Tangent Modulus, t/ft² E_t	Secant Modulus at Failure, t/ft² E_s	Plate Load Test Modulus, t/ft² E_{plt}	Pressuremeter Modulus, t/ft² E_{pmt}	Cross Hole Shear Wave Velocity Modulus, t/ft² E_{csv}	Cohesion, t/ft² C	Friction Angle° ϕ	Unconfined Compressive Strength, t/ft² q_u	Ultimate Stress Plate Load Test, t/ft² q_{u_p}	Pressuremeter Limit Pressure, t/ft² P_L	Coefficient of Permeability, cm/s K	CID Triaxial Creep Strain Rate %/min E[6]	Pressuremeter Creep Radial Strain Rate %/min E[6]	Plate Load Test Creep Strain Rate %/min E[7]
.45	-	-	500	150	144	130	1,800	0	39.5	-	5	25	2×10^{-3}	7.8×10^{-5}	-	3×10^{-3}
-	-	-	-	-	534	-	-	-	-	-	8	-	-	-	-	-
-	-	-	-	-	311	-	-	-	-	-	6.4	-	-	-	-	-
2.3	58	39	801	145	246	119	4,000	.34	35	.32	8	59	1.5×10^{-4}	2.6×10^{-4}	1.9×10^{-2}	1.5×10^{-2}
-	-	-	-	-	-	-	-	-	-	-	-	-	-	-	-	-
-	90[1]	55[1]	-	-	1,613	-	-	-	-	.29[1]	11	-	1.2×10^{-5} [4] 1×10^{-4} [5]	-	-	5.4×10^{-3}
1.3	1,231	757	902	155	338	151	3,500	.36 .70[2]	35.5 39.5[2]	4.0	10	27	2×10^{-5} [4] 2×10^{-4} [5]	2.2×10^{-4}	-	2.6×10^{-2}
-	625	471	-	-	1,815	-	-	-	-	1.91	12	-	-	-	-	6.8×10^{-3}
1.6	12,000	8,000	-	-	1,218	459	-	-	-	18.38	>14	69	1.2×10^{-4}	-	-	3×10^{-3}
3	-	-	-	-	8,233	1,576	-	-	-	-	>17	100+	8×10^{-5}	-	2.7×10^{-2}	-
-	-	-	-	-	911	-	-	-	-	-	>18	-	-	-	-	2.6×10^{-2}
3.3	3,006	2,106	2,146	880	962	860	27,000	3.5	39.5	11.88	>14.5	100	1×10^{-4}	5.2×10^{-4}	1.4×10^{-1}	3.2×10^{-2}
-	-	-	-	-	9,290	-	-	-	-	-	>15.8	-	-	-	-	-
2.5	5,192	4,910	6,667	3,673	12,098	1,327	16,000	5.82	39	15.60	>14	100+	2×10^{-4}	1.4×10^{-4}	2.6×10^{-2} [7]	-
-	-	-	-	-	5,464	-	-	-	-	-	>16	-	-	-	-	1.5×10^{-2}

laboratory tests were made on excavation

borehole samples
ple grouted in the laboratory
lock sample
ability test
lity test
ange = 10 to 100 minutes

ess ratio
.50)
or definition of grouting method

2

CHEMICAL GROUTING TEST PROGRAM

SUMMARY OF GROUTED SOIL PROPERTIES

FOUNDATION INVESTIGATION AND TEST PROGRAM
EXISTING LOCKS AND DAM No. 26
ST LOUIS DISTRICT, CORPS OF ENGINEERS
DACW43-75-C-0055

Woodward-Clyde Consultants | **Table 0.1**

YTC828 Phase II

PHASE IV REPORT

VOLUME II

RESULTS AND INTERPRETATION OF
CHEMICAL GROUTING TEST PROGRAM

SECTION 1

PURPOSE AND OBJECTIVES

1 PURPOSE AND OBJECTIVES

1.1 PURPOSE

The chemical grouting tests described in Volume II of Phase IV Report were part of an investigation and test program designed to provide comprehensive technical bases for the evaluation of various overwater construction schemes and techniques that could be used adjacent to existing loaded structures. Chemical grouting may be used to improve the characteristics of the foundation soil. The investigation and test program also included assessment of pile driving effects (Volume III), and evaluation of construction feasibility of drilled-in piles (Volume IV) and rock anchors (Volume V). Summaries of conclusions for each of these tests are presented in Volume I.

The purpose of the chemical grouting test program was to assess the feasibility, applicability, and effectiveness of injecting silicate-based grouts into Mississippi River alluvial sand. Both low-strength and high-strength grouts were used for the tests. The primary intent of low-strength grouts was to decrease potential displacement and rearrangement of sand grains, and thus increase the stability of the sand, when subjected to vibrations induced by construction activities. The secondary intent was to moderately increase the strength of the sands, which would significantly augment the lateral resistance of piles. The tertiary intent was to increase resistance to erosion and to reduce the permeability of the sand.

The primary intent of high-strength grouts was to increase substantially the bearing capacity and the stability of the sand. The increased bearing capacity must be permanent. The secondary intent was to increase the resistance to erosion and reduce the permeability of the sand.

1.2 OBJECTIVES

The objectives of the chemical grouting test program were:

(1) to investigate the technical feasibility of satisfactorily grouting the sand without inducing objectionable heave, lateral movement, and excess pore pressure;

(2) to compare various grouts and provide a basis for selection of chemical grouts that will produce the desired grouted soil properties;

(3) to compare two common grouting methods, the open-bottom pipe and the sleeve-pipe methods;

(4) to establish an optimum grout-hole spacing by comparing the effects of two spacings, 4.2 ft and 6 ft, in achieving the desired grout penetration and uniformity;

(5) to provide bases for establishing criteria for acceptable and optimum grout quantities, grouting pressures, and optimum and maximum grout flow rates; and

(6) to provide cost elements for future estimating purposes.

1.3 ORGANIZATION OF VOLUME II

The chemical grouting test program is described in Section 2. The subsurface conditions of the test area were thoroughly investigated and are discussed in Section 3. Grouting was done using a modern grouting plant which is described in Section 4. Several studies of grout and grout properties were incorporated into the program and are presented in Section 5. The test grouting procedures and the monitoring of the grouting activities during the tests are discussed in Sections 6 and 7, respectively. The instrumentation installed to monitor the effects of grouting on the soil mass and the results of these measurements are presented in Section 8. The grouting results were thoroughly evaluated by various methods. The evaluation is discussed in Section 9.

PHASE IV REPORT

VOLUME II

RESULTS AND INTERPRETATION OF CHEMICAL GROUTING TEST PROGRAM

SECTION 2

CONCEPT AND DESCRIPTION OF TESTS

2 CONCEPT AND DESCRIPTION OF TESTS

2.1 TEST VARIABLES

2.1.1 Concept of Test Program

The intent of the test program was to inject high-strength and low-strength silicate grouts into the upper 20 ft of the recent alluvium deposit underlying the test area between el 400 and el 380. Attempts to inject cement-bentonite grout were also planned. Initially, the chemical grouting test program had been designed to allow a comparative evaluation of three grouting methods, two grout-hole spacings, and six grout types. During the course of the field implementation, the program was slightly expanded to include testing of one additional grouting method and two additional grout types. The actual combination of the test variables is presented in Table 2.1.

2.1.2 Grouting Methods

The four grouting methods tested were:

(1) the open-bottom pipe method with low-pressure criterion and single-stage injection (Method O_1);

(2) the sleeve-pipe method with low-pressure criterion and single-stage injection (Method S_1);

(3) the sleeve-pipe method with maximum rate of grout flow criterion and single-stage injection (Method S_2); and

(4) the sleeve-pipe method with maximum rate of grout flow criterion and multiple-stage injection (Method S_3).

Open-Bottom Pipe (Method O_1). One grouting method was tested with open-bottom pipes in Subareas 1, 2, and 9; see Fig. 2.1. In this method, an AW steel rod (1.75-in.-od, 1.22-in.-id), fitted with an expendable bottom plug, was driven into the ground to el 376 with a 140-lb or 360-lb drop-hammer. The expendable bottom plug was separated from the grout pipe when the initial grout pressure was applied and the pipe was slightly raised. Grout was injected through the bottom of the grout pipe. The grout pipe was raised 1 ft after each injection step. During each injection step, grout was injected until a predetermined volume of grout, equal to 25 percent of the volume of soil to be grouted, had been pumped or until the grouting pressure reached or exceeded 1 lb/in^2 per foot of soil above the bottom of the grout pipe. Grouting was also discontinued whenever grout leaks out of another pipe or along the grout pipe itself were noticed.

Sleeve-Pipe (Method S_1). Three grouting methods were tested with sleeve-pipes. The sleeve pipes consisted of 2.36-in.-od, 1.77-in.-id PVC pipes. The exterior wall of the pipes were ridged to minimize grout travel along the pipes; see Fig. 2.2. The sleeve-pipes were fabricated in 13-in. sections. A number of sections were screwed together to form the required grout pipe lengths. The pipes were provided with two diametrically opposed ports every 13 in. The ports were covered with tightly fitting 3-in.-long cylindrical rubber sleeves. The sleeve-pipes were installed in 3.6-in.-dia boreholes drilled by rotary method to approximately el 378. Some boreholes were drilled with bentonite drilling fluid; others were drilled with Revert. After the sleeve-pipes were inserted into the borehole, the annular spaces between the pipes and the borehole walls were filled with cement-bentonite grout (sleeve grout), having the following composition:

cement/water (by weight): 0.4

bentonite/water (by weight): 0.03 to 0.04

When boreholes were drilled with bentonite, the cement-bentonite sleeve grout was tremied to the bottom of the boreholes through a rubber hose lowered between the pipe and the borehole walls. After the grout had completely displaced the bentonite fluid, the rubber hose was removed. When boreholes were drilled with Revert, the degradation of the Revert did not allow this procedure to be used. In these cases, the sleeve grout was placed by injecting it through the inside of the sleeve-pipes, using packers to build up grout pressure and open the rubber sleeves. The purpose of the sleeve-grout was to prevent upward travel of grout along the sleeve-pipe during subsequent injections.

The procedure for injecting grout through a sleeve-pipe involved the use of a double packer; see Fig. 2.2. Rubber-cup packers were mainly used for injecting cement-bentonite grout. O-ring packers were mainly used for injecting chemical grouts. The double packer was connected to a grout pipe extending to the ground surface. The grout pipe was in turn connected to a grouting pump through a rubber hose. Grout injection proceeded from bottom of the sleeve-pipes upward through one or two sleeves at one time.

In grouting Method S_1, tested in Subarea 5a, chemical grout was injected once at every sleeve level. The grouting pressure was kept below 1 lb/in^2 per foot of soil above the sleeve being injected. This pressure criterion is unusually low for sleeve-pipe grouting. Method S_1 was tested in only two holes, mainly for the purpose of demonstrating that the low-pressure criterion is incompatible with sleeve-pipe grouting.

Sleeve-Pipe (Method S_2). This grouting method, tested in Subareas 3, 4, 5, 10, and 11, involved injection of a predetermined volume of chemical grout once at each sleeve level, at a rate of grout flow not exceeding a predetermined maximum allowable value. The volume of grout was determined as 45 percent of the volume of soil to be grouted. The maximum allowable rate of grout flow was established on the basis of the contractor's experience in alluvial grouting and attempts were made to confirm this maximum allowable rate by hydraulic fracturing tests; see Section 6.2. The intent was to estimate the rate of grout flow inducing hydraulic fracturing during these tests and to establish a maximum allowable rate of grout flow for subsequent injection equal to 85 percent of the fracturing rate. In fact, interpretation of the fracturing tests results was difficult and ambiguous, and the selection of the maximum allowable rate of grout flow generally relied on engineering judgment. The reasons for setting the limiting criterion in terms of rate of grout flow rather than in terms of grout pressure are discussed in Section 6.2. Injection was discontinued and restarted at a later time whenever evidence of grout leaking along the sleeve-pipe or through adjacent grout-holes was noted.

Sleeve-Pipe (Method S_3). This grouting method was tested in Subareas 6, 7, 8, 12, and 13. It involved injection of predetermined volumes of chemical grouts at two or more separate times at each sleeve level, at a rate of grout flow not exceeding a predetermined maximum allowable value. The total volume of grout to be injected was determined as 45 percent of the volume of soil to be grouted. Two-thirds of the intended grout volume was injected in a first injection stage. One-third of the intended grout volume was injected in a second injection stage. Generally, the two injection stages were carried out a few days apart. In some grout-holes, where low grouting pressure was recorded during the second stage grouting, a third injection stage was implemented at selected sleeve levels. The volume of grout injected in this third injection stage ranged from 1.2 percent to 13 percent of the volume of soil to be grouted. During any of the grouting stages, injection was discontinued and restarted at a later time whenever evidence of grout leaking along the sleeve-pipe or through adjacent grout-holes was noted. This grouting procedure resulted in actual volume of grout injected greater than 45 percent of the volume of soil (see Section 7).

Injection of cement-bentonite grout was attempted as a first-stage injection in every grout hole in Subareas 7 and 8, and in one grout hole each in Subareas 12 and 13. Cement-bentonite grout take was small. These tests are discussed in more detail in subsequent sections.

2.1.3 Grout Hole Spacing and Pattern

Two grout hole spacings, 6 ft and 4.2 ft, were used for the grouting tests. The test subareas were designed such that the basic grout hole pattern was 6 ft by 6 ft. Intermediate grout holes, located at the mid points of the 6-ft by 6-ft grid, were used to form the 4.2-ft by 4.2-ft pattern. The 6-ft grout hole spacing was selected because it is consistent with the 3-ft spacing of the piles under the existing locks and dam structures; however, it was felt that this spacing might be too large to achieve uniform grout penetration and complete grouting of the soil between grout holes. The 4.2-ft spacing was selected because it is within the range of grout hole spacings found to be successful in past alluvial grouting projects.

2.1.4 Grout Types

Eight grout types were tested; seven were sodium silicate grouts, one was cement-bentonite grout. Three sodium silicate grouts, having sodium silicate concentrations of 25, 28 and 35 percent by volume, were intended to be low-strength grouts. Four sodium silicate grouts, having sodium silicate concentrations of 45, 46, and 55 percent* by volume, were intended to be high-strength grouts.

---

* *Both 55% Siroc 132 (calcium chloride reactant) and 55% Siroc 142 (sodium aluminate reactant) were used (Section 5.3.2)*

The cement-bentonite grout was intended to fill the larger voids in coarse-grained zones. Other chemical components used included sodium aluminate, formamide, calcium chloride and di-methyl-succinate (R600). Mixing water was pumped out of a small diameter well located near the test area. The average compositions of the eight grouts tested are given in Section 5.3.2.

2.2 CONDUCT OF THE TESTS

2.2.1 Sequence of Activities

The field implementation of the chemical grouting test program involved four phases that are illustrated in Fig. 2.3 and described below.

Phase 1. Phase 1, implemented in March and April 1978, consisted of preparatory work. It included drilling of borings for confirming test area selection, grading of test area and construction of an asphalt working surface or grouting pad at el 423, measurement of initial ungrouted soil properties by borehole in situ testing and sampling, installation of surface and subsurface instrumentation, and installation of grout pipes.

Phase 2. Phase 2 was the grout injection phase. During Phase 2, implemented in May and June 1978, the grouting plant was installed, grout was injected, grouting operations were monitored and documented, and the effects of grouting were assessed by monitoring the surface and subsurface instrumentation. The extent of the grouted zone and the properties of the grouted soil were investigated after grouting by borings, sampling, and subsurface in situ testing from el 423. During the grout injection phase, the groundwater surface in the test area varied between approximately el 420 and el 407. The dewatering system was constructed during the latter part of Phase 2.

Phase 3. Phase 3 was an intermediate phase of the test program, during which the test area was dewatered to el 383 to 382, and excavated to el 402. This phase was implemented in July 1978. Additional borehole in situ tests were made from el 402.

Phase 4. Phase 4 was the test excavation phase. During Phase 4, implemented in August 1978, the test area was excavated from el 402 to between el 385 and el 382. This controlled excavation was carefully made in 3-ft to 5-ft lifts to expose and document by mapping and photography the results of the grouting tests. Block and core samples were taken, and plate load tests and in-place density tests were made in grouted and ungrouted soil during this phase. The dewatering system was shut down at the end of Phase 4, on the evening of 22 August, and was dismantled soon thereafter.

Preceeding, concurrent with, and subsequent to the field implementation of the test program, several laboratory test activities were carried out. These activities included grout mix property tests (April 1978); strength and permeability tests on reconstituted sand samples grouted in the laboratory (April to August); on-site grout mix tests (May and June); chemical neutralization tests

(July); strength and permeability tests on grouted sand samples recovered in post-grouting boreholes (July); grain-size analyses on samples recovered in the test excavation (September); chemical analyses of groundwater sampled in the test area after grouting (September and October); and strength and permeability tests on block and core samples taken during test excavation (October 1978 to February 1979).

2.2.2 Test Area Configuration

The chemical grouting tests were conducted in an area immediately adjacent to US Route 67, downstream of the left abutment of the dam, on the Missouri side of the Mississippi River; see Fig. 2.4. At that location, the natural ground surface was at approximately el 420. The test area was filled and graded at el 423. An 8-in.-thick asphalt grouting pad, 70 ft by 67 ft, was constructed at el 423 at the center of the test area to serve as a working surface. The grout holes, installed from the asphalt pad, were arranged to form fourteen test subareas as shown in Fig. 2.1. The test variables corresponding to each subarea are given in Table 2.1.

Test Subareas 1 and 2. The test variables for Subareas 1 and 2 were identical, except for grout hole spacing. Grout hole spacings were 4.2 ft for Subarea 1 and 6 ft for Subarea 2. Both subareas were grouted by grouting method O_1 with 35% Siroc 142 grout (low strength). Subareas 1 and 2 consisted of seven and four grout holes, respectively.

Test Subarea 3. Subarea 3 consisted of four grout holes spaced 6 ft apart. Low-strength 28% silicate/R600 grout was injected by grouting method S_2 in this subarea. Grout was injected only between el 380 and el 393 in this subarea, because of limited supply of R600 reactant.

Test Subareas 4 and 6. The test variables for Subareas 4 and 6 were identical, except for grout type and grouting method. Subarea 4 was injected with 35% Siroc 142 grout (low strength) using grouting method S_2. Subarea 6 was injected with 25% silicate/aluminate grout (low strength) using grouting method S_3. Grout hole spacing was 6 ft. Both subareas consisted of five grout holes each.

Test Subarea 5. Subarea 5 consisted of four grout holes spaced 6 ft apart. High-strength grout 45% Siroc 132 was injected by method S_2 in this subarea.

Test Subarea 5a. Subarea 5a consisted of only two grout holes spaced 6 ft apart. This was the only subarea where grouting method S_1 was attempted. The grout used was low-strength 25% silicate/aluminate.

Test Subareas 7 and 8. The test variables for Subareas 7 and 8 were identical, except for grout hole spacing. Grout hole spacings were 6 ft for Subarea 7 and 4.2 ft for Subarea 8. Both subareas were grouted by grouting method S_3 with 25% silicate/aluminate grout (low strength). A very small volume of cement-bentonite was injected in every hole of each subarea as a first-stage grouting.

Test Subarea 9. Subarea 9 consisted of six grout holes spaced 4.2 ft apart. High-strength 55% Siroc 142 grout was injected by grouting method O_1 in this subarea.

Test Subareas 10 and 11. The test variables for Subareas 10 and 11 were identical, except for grout hole spacing. Grout holes were spaced 6 ft apart in Subarea 10 and 4.2 ft apart in Subarea 11. Both subareas were grouted with high-strength 55% Siroc 132/142 grout by method S_2. Subareas 10 and 11 consisted of six and eight grout holes, respectively.

Test Subareas 12 and 13. The test variables for Subareas 12 and 13 were identical, except for grout hole spacing. Grout holes were spaced 6 ft apart in Subarea 12 and 4.2 ft apart in Subarea 13. Both subareas were grouted with high-strength 46% silicate/R600 grout by method S_3. A very small quantity of cement-bentonite was injected in one grout hole of each subarea as a first-stage grouting. Subareas 12 and 13 consisted of four and five holes, respectively.

2.3 MEASURED ASPECTS OF PERFORMANCE

The significant aspects of performance of the chemical grouting test program identified during design were displacement of the soil mass, extent and properties of grouted soil, and cost of grouting. During implementation of the program, the displacements produced by grouting were measured by means of instrumentation installed in the soil prior to grouting (Section 8). Grouted soil extent and properties were evaluated by means of borings, in situ measurements, direct visual and photographic observations, and laboratory tests (Section 9). Costs of grouting related to the quantity of grout injected, grouting method, grout type, injection time, and amount of labor and equipment required were documented (Section 10).

In addition to monitoring the significant aspects of performance, other technical activities were performed during the field implementation of the program. These activities consisted of documenting the set-up and operation of the grouting plant (Section 4), supplementing the understanding of grouts and grout chemistry (Section 5), testing various grouting procedures (Section 6), and monitoring the injection process (Section 7).

<table>
<tr><th></th><th>GROUT TYPE</th><th>GROUTING METHOD</th><th>GROUT-HOLE SPACING ft</th><th>MAXIMUM GROUT PRESSURE OR RATE OF PUMPING</th><th>TEST SUBAREA NO.</th></tr>
<tr><td rowspan="8">LOW-STRENGTH</td><td rowspan="3">35% SIROC 142</td><td rowspan="2">O_1</td><td>4.2</td><td rowspan="2">1 lb/in^2/ft</td><td>1</td></tr>
<tr><td rowspan="5">6</td><td>2</td></tr>
<tr><td>S_2</td><td>85% of hydraulic fracturing rate of pumping</td><td>4</td></tr>
<tr><td rowspan="2">25% Silicate/ Aluminate</td><td>S_1</td><td>1 lb/in^2/ft</td><td>5a</td></tr>
<tr><td rowspan="3">S_3</td><td rowspan="4">85% of hydraulic fracturing rate of pumping</td><td>6</td></tr>
<tr><td rowspan="2">Some Cement-Bentonite and 25% Silicate/ Aluminate</td><td>7</td></tr>
<tr><td>4.2</td><td>8</td></tr>
<tr><td>28% Silicate/R600</td><td>S_2</td><td>6</td><td>3</td></tr>
<tr><td rowspan="6">HIGH-STRENGTH</td><td>45% SIROC 132</td><td>S_2</td><td>6</td><td>85% of hydraulic fracturing rate of pumping</td><td>5</td></tr>
<tr><td rowspan="3">55% SIROC 142/132</td><td>O_1</td><td>4.2</td><td>1 lb/in^2/ft</td><td>9</td></tr>
<tr><td rowspan="2">S_2</td><td>6</td><td rowspan="5">85% of hydraulic fracturing rate of pumping</td><td>10</td></tr>
<tr><td>4.2</td><td>11</td></tr>
<tr><td rowspan="2">46% Silicate/R600</td><td rowspan="2">S_3</td><td>6</td><td>12</td></tr>
<tr><td>4.2</td><td>13</td></tr>
</table>

CHEMICAL GROUTING TEST PROGRAM

COMBINATION OF TEST VARIABLES

FOUNDATION INVESTIGATION AND TEST PROGRAM
EXISTING LOCKS AND DAM No. 26
ST LOUIS DISTRICT, CORPS OF ENGINEERS.
DACW43-78-C-0005

Woodward-Clyde Consultants
Y7C825 Phase IX

Table 2.1

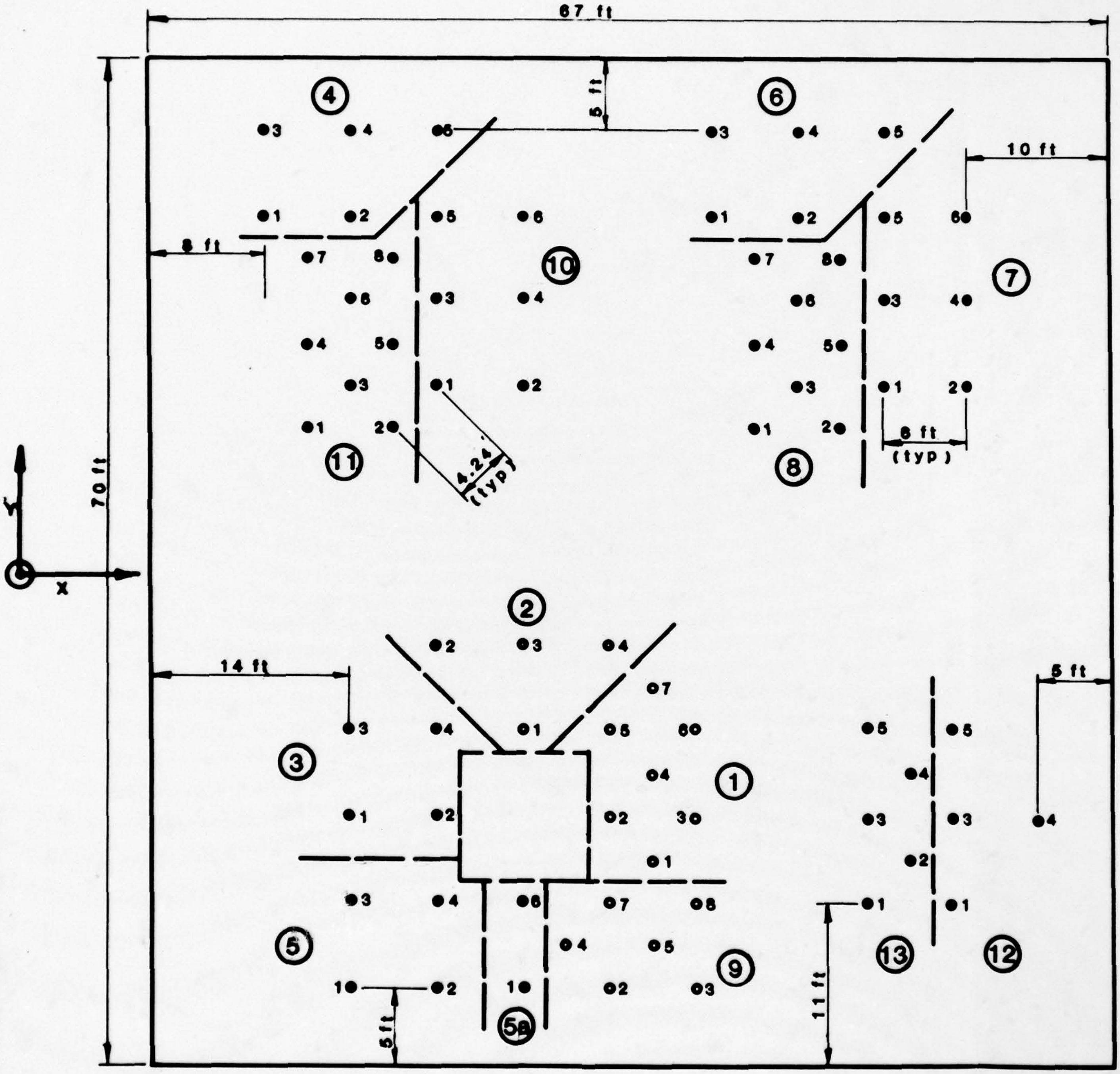

67 ft
70 ft
5 ft
10 ft
8 ft
4.24 (typ)
8 ft (typ)
14 ft
5 ft
5 ft
11 ft
y
x
1
2
3
4
5
5a
6
7
8
9
10
11
12
13

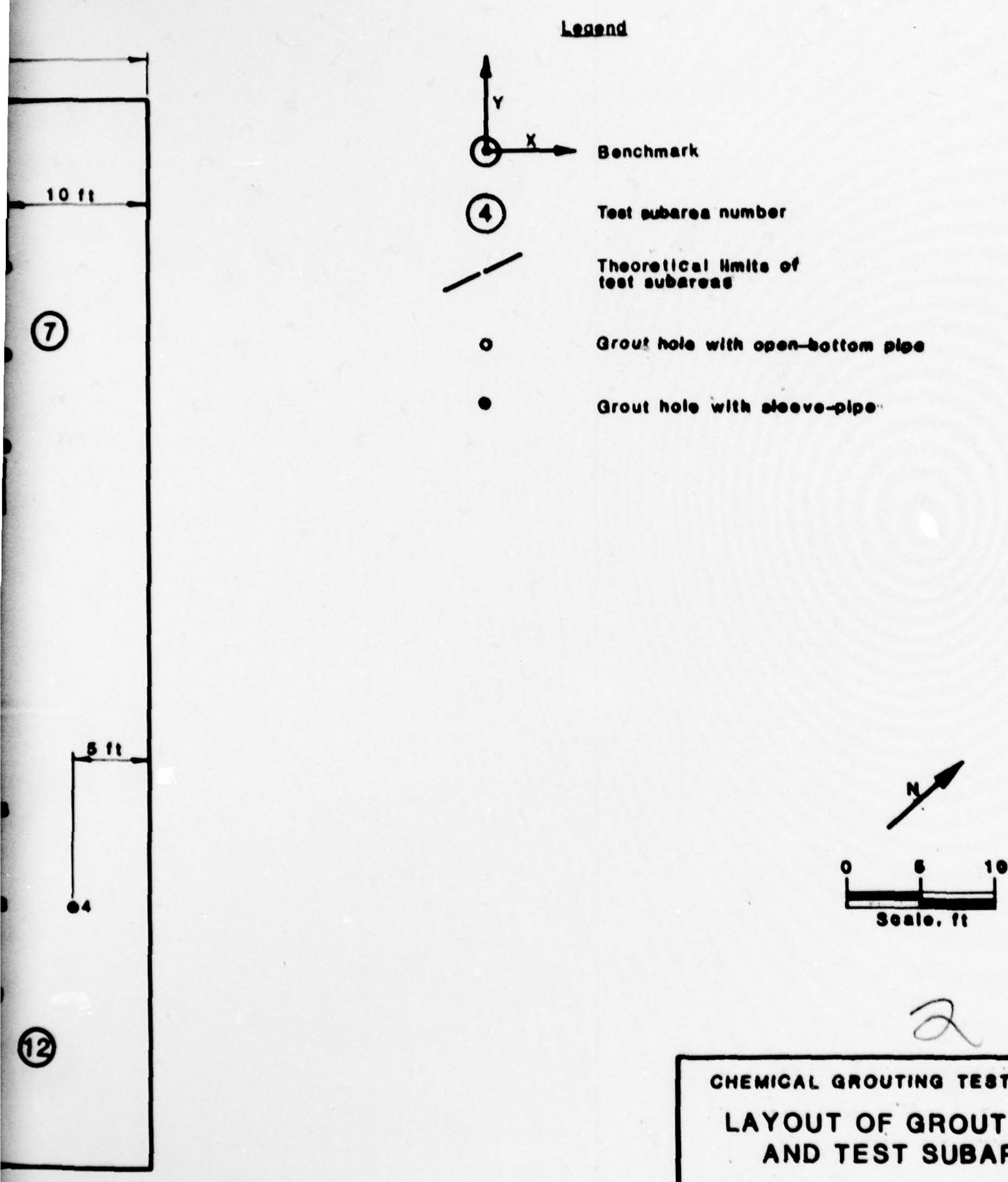

CHEMICAL GROUTING TEST PROGRAM

LAYOUT OF GROUT HOLES AND TEST SUBAREAS

FOUNDATION INVESTIGATION AND TEST PROGRAM
EXISTING LOCKS AND DAM No. 26
ST LOUIS DISTRICT, CORPS OF ENGINEERS.
DACW43-76-C-0005

Woodward-Clyde Consultants

Y7C826 Phase IX

Fig. 2.1

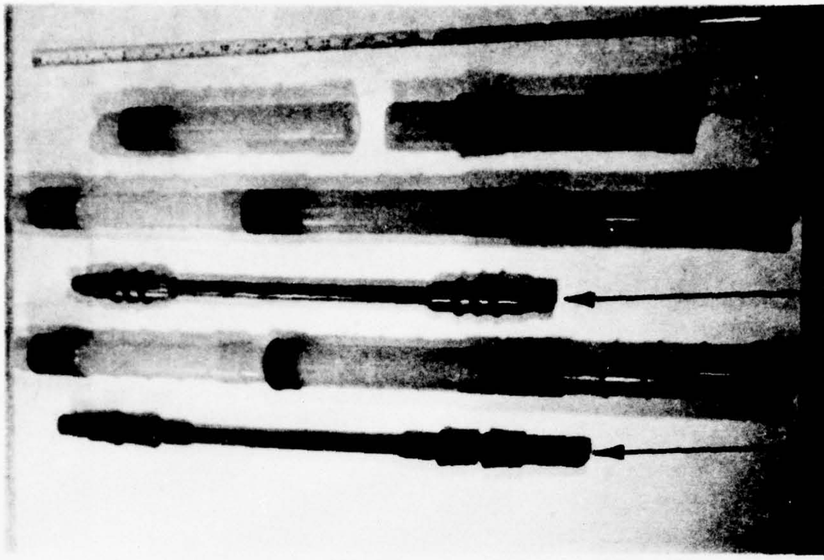

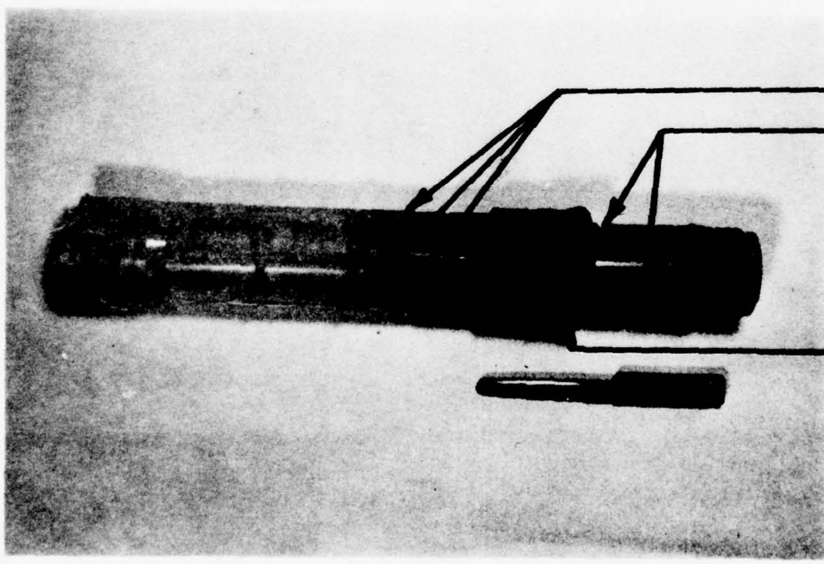

CHEMICAL GROUTING TEST PROGRAM

DETAILS OF SLEEVE-PIPE AND PACKER

FOUNDATION INVESTIGATION AND TEST PROGRAM
EXISTING LOCKS AND DAM No. 26
ST LOUIS DISTRICT, CORPS OF ENGINEERS.
DACW43-78-C-0005

Woodward-Clyde Consultants
Y7C825 Phase IX

Fig. 2.2

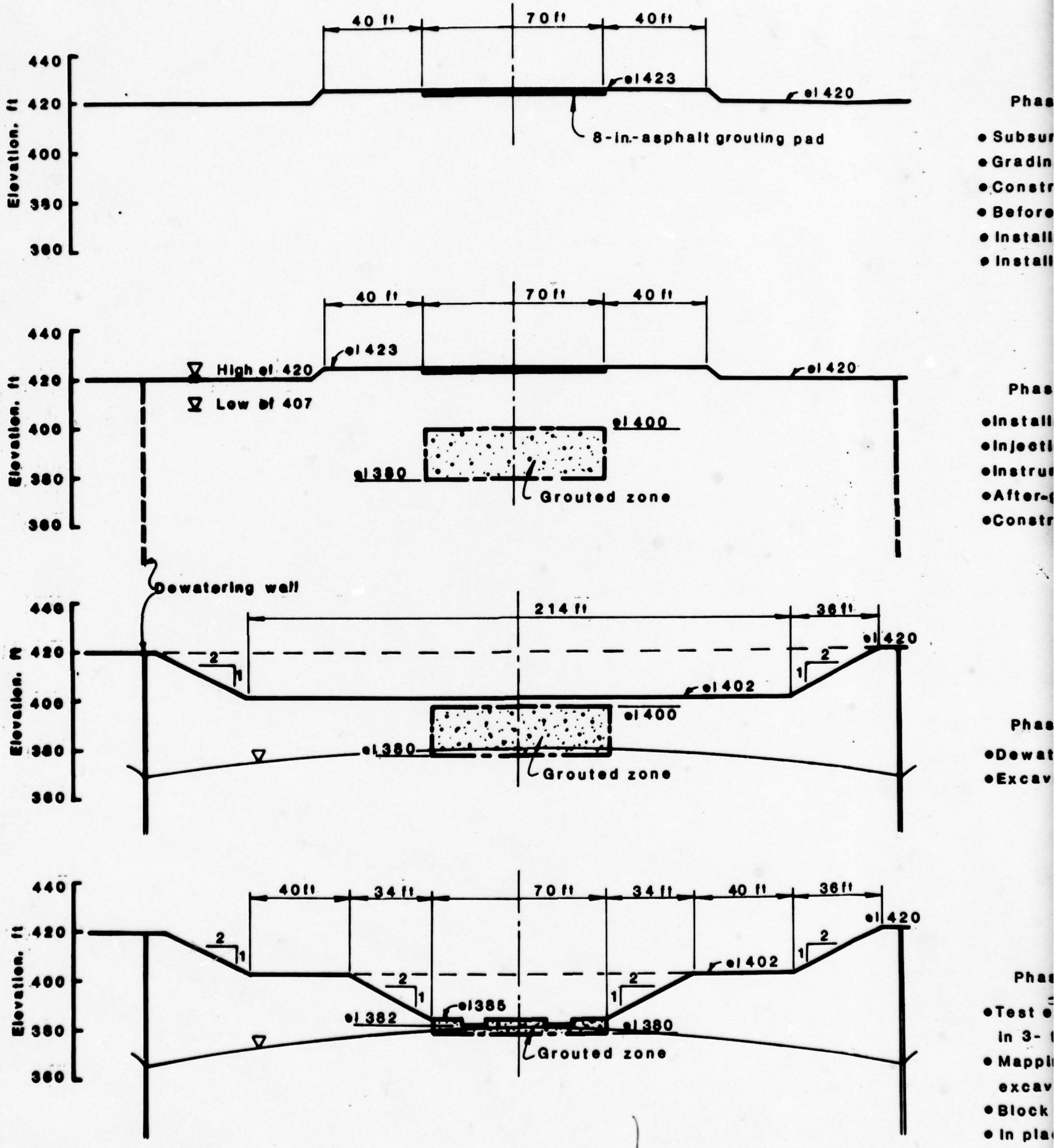
40 ft
70 ft
40 ft
el 423
el 420
8-in.-asphalt grouting pad
Elevation, ft
440
420
400
380
360
High el 420
Low el 407
el 400
el 380
Grouted zone
Dewatering well
214 ft
36 ft
el 402
34 ft
el 385
el 382
2
1
Phas
Subsur
Gradin
Constr
Before
Install
Install
Installi
Injecti
Instrur
After-
Constr
Dewat
Excav
Test e
in 3-
Mappi
excav
Block
In plac
Plate
Shutd
dewat

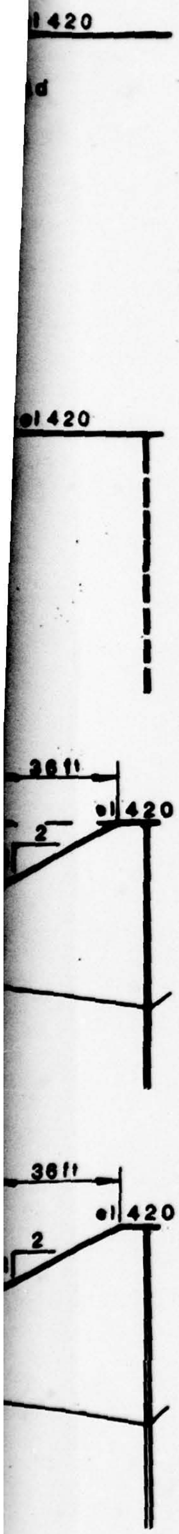

Activities

Phase 1 (Mar-Apr 1978)

- Subsurface investigations
- Grading of test area at el 423
- Construction of asphalt grouting pad
- Before-grouting borehole in situ testing and sampling
- Installation of instrumentation
- Installation of grout holes

Phase 2 (May-Jun 1978)

- Installation of grouting plant
- Injection of grout
- Instrumentation monitoring
- After-grouting borehole in situ testing and sampling
- Construction of dewatering system

Phase 3 (Jul 1978)

- Dewatering of test area to el 383/382
- Excavation to el 402

2

0 25 50
Scale, ft

Phase 4 (Aug 1978)

- Test excavation to el 385/382 in 3- to 5-ft increments
- Mapping and documentation of excavation faces
- Block and core samples
- In place density tests
- Plate load tests
- Shutdown and dismantlement of dewatering system

CHEMICAL GROUTING TEST PROGRAM

SEQUENCE OF ACTIVITIES

FOUNDATION INVESTIGATION AND TEST PROGRAM
EXISTING LOCKS AND DAM No. 26
ST LOUIS DISTRICT, CORPS OF ENGINEERS.
DACW43-78-C-0005

Woodward-Clyde Consultants
Y7C826 Phase IX

Fig.2.3

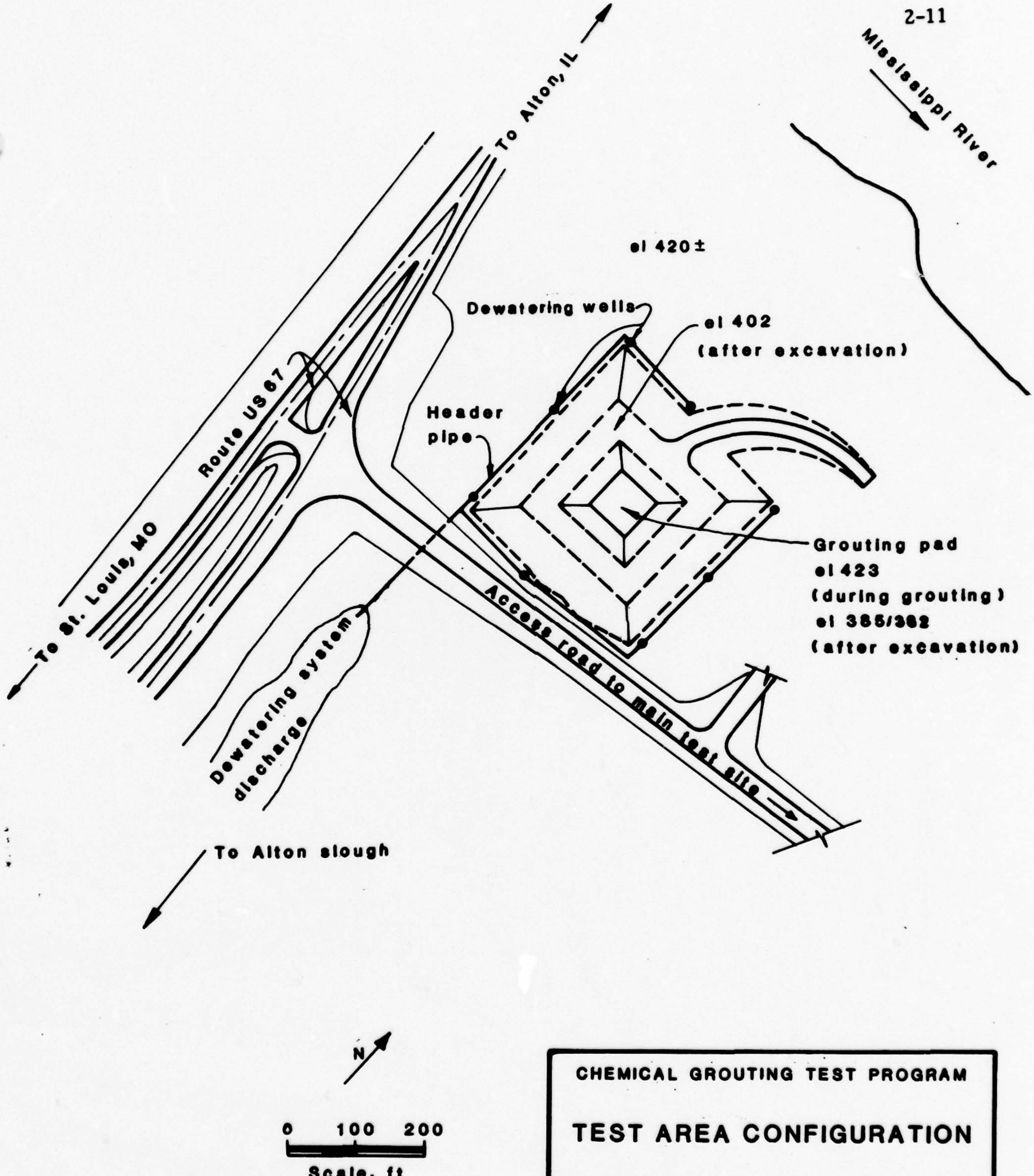

CHEMICAL GROUTING TEST PROGRAM

TEST AREA CONFIGURATION

FOUNDATION INVESTIGATION AND TEST PROGRAM
EXISTING LOCKS AND DAM No. 26
ST LOUIS DISTRICT. CORPS OF ENGINEERS.
DACW43-78-C-0005

Woodward-Clyde Consultants

Y7C825 Phase IX

Fig.2.4

PHASE IV REPORT

VOLUME II

RESULTS AND INTERPRETATION OF
CHEMICAL GROUTING TEST PROGRAM

SECTION 3
TEST AREA SUBSURFACE CONDITIONS

3 TEST AREA SUBSURFACE CONDITIONS

3.1 TEST AREA SELECTION

It was originally planned to conduct the chemical grouting test program at the main test site*, which is located near the downstream end of Ellis Island. Several borings were drilled there for confirming the test area selection. Although the subsurface conditions were found to be adequate for the chemical grouting test purpose, it became apparent that access to that remote location would remain very difficult, and danger of flooding would be high until completion of the site preparation work scheduled for June or July 1978. On the basis of these considerations, it was decided to conduct the chemical grouting test program at the upstream end of Ellis Island, at a location adjacent to US Route 67 (Fig. 2.4). At this location, the natural ground surface was at approximately el 420, high enough to minimize the risk of flooding, and access was easy.

Subsurface investigations were undertaken to confirm the suitability of the new test area. On the basis of field visual classification and laboratory tests performed on split-spoon samples recovered in one test boring (D-21), it was concluded that the subsurface conditions at the selected location were representative of the alluvial and glacial sand deposits found under Locks and Dam No. 26, and that the area was adequate for the test program purposes.

3.2 SUBSURFACE INVESTIGATIONS

3.2.1 Purpose and Scope

A program of borings, sampling, and in situ and laboratory tests was undertaken in March 1978 to measure properties of natural, ungrouted soil underlying the test area. Some of the boreholes were also used to install subsurface instrumentation. These initial properties were intended to serve as a base for future comparison with grouted soil properties.

Boreholes were drilled at locations shown in Fig. 3.1. In situ testing performed in these boreholes included dynamic and static penetration tests, pressuremeter tests, and falling head permeability tests. Grain-size analyses were made on samples recovered in conjunction with dynamic penetration testing. Shear wave velocity of the alluvial sand deposit within the zone to be grouted was measured in four arrays of geophysical boreholes (Fig. 3.1).

3.2.2 Dynamic Penetration Testing

These tests consisted of driving a split-spoon into the soil. Two split-spoons were used: a 2-in.-od spoon driven with a 140-lb hammer falling 30 in. (standard penetration test, ASTM D 1586-67), and a 3-in.-od spoon driven with a

---

* *The other tests of the Foundation Investigation and Test program were conducted at the main test site beginning in September 1978 (Volume I)*

350-lb hammer falling 18 in. (a procedure commonly used by the St Louis District in alluvial deposits). The dynamic penetration resistance was recorded as the number of hammer blows N or N_3 required to drive the 2-in. or 3-in. spoon, respectively, 12 in. into the soil. In addition to yielding penetration resistance values, these tests also provided a means for recovering disturbed soil samples used for visual classification and laboratory index property tests.

Standard penetration tests were made in Boring D-21 for confirmation of the test area selection, in Boring D-22 to correlate with pressuremeter test results, in Borings D-23 and D-26 to correlate with static cone penetration test results, and in Boring D-28 to correlate with falling head permeability test results. Dynamic penetration tests using the 3-in. spoon were made continuously in Boring D-25 and in the borehole drilled for installation of benchmark BM-1. Samples from Borings D-21, D-22, and D-23 were used for the preparation of reconstituted samples for laboratory grouting tests (Section 5.1.3).

The results of standard penetration tests are compared with other in situ test results in Fig. 3.2. The N-values measured in Boring D-28 are outside the range of values obtained in the other borings. In Boring D-28, a steel casing was driven and washed out with water for permeability testing. Water washing was probably not successful in removing the coarser sand and gravel particles. These particles probably accumulated at the bottom of the borehole and became lodged in the sampling spoon, resulting in increased N-values above approximately el 390. Below el 390, the hydraulic head became great enough to cause the sand to flow into the casing, resulting in loosening and decreased N-values. These phenomena were not experienced in the other borings, probably because they were drilled with bentonite slurry.

A comparison between N-values and N_3-values is presented in Fig. 3.3. The N_3-values fall within, but at the low end, of the N-value range. This is consistent with previous results obtained at or near this site, and with the St Louis District experience.

3.2.3 Static Cone Penetration Testing

Static cone penetration tests were made in two borings (D-23 and D-26). The cone system used was developed by WCC. The cone has a 10-cm^2 cross sectional area, and an angle of 60°. The load applied on the cone to push it into the soil at a constant rate of penetration of 4 ft/min was measured by a load cell and was recorded on a strip chart. Continuous cone penetration profiles were otained by alternately pushing the cone 5 ft to 10 ft into the soil at the bottom of the borehole, and reaming the borehole after each cone run by rotary drilling.

The results of the two static cone penetration soundings made before grouting are shown in Fig. 3.2, together with other in situ test results. The correlation between cone penetration resistance q_c and standard penetration resistance N measured in the test area is presented in Fig. 3.4. This correlation is approximated by:

$$q_c \ (t/ft^2) = 5 \text{ to } 6N \ (bl/ft)$$

3.2.4 Pressuremeter Testing

Pressuremeter tests were made in two borings (D-22 and D-27). The Menard type GAm pressuremeter used for the measurements consisted of a BX-size probe that were expanded at the bottom of a borehole. The volume change of the probe was measured as a function of the applied pressure. The data were used to obtain elastic and plastic characteristics of the soil. The boreholes were carefully prepared by slow drilling with a drag bit and thick Revert or bentonite drilling fluid.

An idealized pressuremeter volume change vs applied pressure curve is shown in Fig. 3.5. At the beginning of the test, the probe begins to expand through the drilling fluid with little lateral restraint, until it makes contact with the borehole walls. This corresponds to the steep initial portion of the volume change curve. As the probe continues to expand, the soil resistance is mobilized and the volume change curve is linear (pseudo-elastic response). At higher pressure, plastic deformation occurs. The soil then sustains large deformations for small pressure increases. The asymptote of the volume change vs pressure curve corresponds to the ultimate strength of the soil (or limit pressure).

The results of the actual pressuremeter tests performed in Borings D-22 and D-27 are presented in Fig. A.1 through Fig. A.8, Appendix A, Volume IIA. A lesser degree of disturbance was experienced in Boring D-27 than in D-22, resulting in higher measured soil modulus and strength. Boring D-22 was drilled with bentonite slurry which, if not cleared of suspended sand particles, tended to scour the borehole walls during drilling. Revert, on the other hand, was used in Boring D-27 and appeared to provide more lubrication during drilling, yielding a more uniformly sized hole.

3.2.5 Borehole Permeability Testing

Falling head permeability tests were performed in Boring D-28. The tests were conducted by driving an NX-size, flush-joint casing into the soil to the desired testing depths, cleaning out the soil with a rotary drill bit and circulating water, and flushing the casing with clean water to remove bottom sediment. The casing was filled with water and the elevation of the water surface in the casing was measured as a function of time. The coefficients of permeability obtained from these tests are given in Fig. 3.2, together with other in situ test results.

3.2.6 Crosshole Shear Wave Velocity Measurements

Crosshole seismic shear wave velocity measurements were made in the test area shortly before grouting started (23 April 1978). Seismic wave velocity depends on the elastic and density characteristics of the soil medium through which the waves propagate. These characteristics are modified by grouting. Shear wave velocity measurements were selected because in loose sand below the water table, compressional wave velocities of the soil deposits would be masked by the much higher velocity of the groundwater. On the other hand, shear wave velocity is only affected by the characteristics of the soil. The equipment used was developed by WCC and is manufactured by Bison Instruments (Mirafuente et al 1975, Auld 1977, and Statton et al 1978). The energy signal source consisted of a downhole hammer jacked against the wall of a 5-in.-dia steel casing grouted with cement in a 7-in.-dia borehole (Borehole S-0, Fig. 3.1). The borehole hammer is designed such that an uniaxial impact is imparted along the axis of the borehole. The direction of impact, however, can be in either direction (upward or downward), providing for symmetrical reversal of impact motion. The polarity of the first arrival shear wave can be reversed by reversal of impact direction, because the shear waves being measured are in a common plane with the impact motion. The shear wave motions detected along the vertical axis of the source are uniquely reversed with source reversal, while other seismic waves generated have constant polarity independent of source impact direction. The signal generated by the hammer was detected in four sets of geophysical boreholes (S-1 through S-8) drilled along lines radiating from S-0, using pairs of vertical geophones placed at the same depth as the hammer in two adjacent boreholes. The geophones were housed in PVC capsules containing both a geophone and a pneumatic bladder that was inflated to couple the capsule firmly to a 3-in.-dia PVC casing. Seismic wave data detected by the geophones were fed to a storage oscilloscope and/or a multichannel signal en hancement seismograph, where trace and arrival time were displayed. Polaroid photographs of the screen displays were taken for each recording. Shear wave velocity was calculated from arrival times and distances between boreholes. Borehole inclinometer measurements were made in each of the nine geophysical boreholes to determine the precise distances between source and receiver at any depth.

Results of shear wave velocity measurements before grouting are given in Table 9.1, Section 9. Signals at the four near geophone boreholes were strong and sharp. However, poor to marginal data were obtained at the distant geophone boreholes. No arrival data could be obtained at borehole S-6 due to the very weak signals detected in that borehole. Shear wave velocity of the soil in the test area calculated from the near geophone data ranged from 505 ft/s to 670 ft/s and averaged 586 ft/s. The data indicated no significant variation with depth within the vertical extent of the zone to be grouted.

3.2.7 Laboratory Testing

Grain-size analyses were made on split-spoon samples recovered in D-series borings, in geophysical boreholes, and in several instrumentation installation boreholes (Section 8). Several samples from Boring D-28 indicate unusual concentrations of fine to coarse gravel. This may be because that boring was washed with water only and the washing action may not have been successful in removing some of the coarser particles that accumulated at the bottom of the borehole.

Samples were also obtained during excavation of the grouted area (Section 9.3). Grain-size distribution curves for these samples are presented in Fig. A.9 and Fig. A.10, Appendix A, Volume IIA.

3.3 STRATIGRAPHY

The understanding of the stratigraphy and geology of the test area is based on the information obtained from borings made before grouting (Section 3.2), and after grouting (Section 9.2), and by mapping of the excavation made after grouting (Section 9.3).

3.3.1 General Geology

The sand strata grouted during the chemical grouting test program are located entirely within the recent alluvium deposits of the Mississippi River valley. The recent alluvium is overlain by 5 to 8 ft of fill and clayey floodplain deposit, and it is underlain by a sequence of glacial outwash, ice contact flood-plain deposits, and limestone bedrock, similar to that found under Locks and Dam No. 26.

The recent alluvium is a relatively uniform deposit because of a common depositional environment and history, and because of the scale of the Mississippi-Missouri fluvial system. It is uniform in such characteristics as composition, grain size, roundness, sorting, distribution and orientation of primary depositional structures, and abundance and distribution of carbonaceous material. The grouted strata range in grain-size from coarse silt to fine gravel but are predominantly fine to medium sand. These sediments are characteristically clean, well-sorted (poorly graded) sand composed of at least 70 percent and frequently more than 80 percent quartz grains. They also contain abundant concentrations of carbonaceous material including wood, charcoal, and lignite which range in size from coarse silt to large tree trunks. Fresh water shells are also abundant. All the grouted sediments are pervasively and consistently cross-bedded; the majority of the cross-beds dip generally N to NE at an angle of 5 to 35 degrees. These cross-beds are broad and continuous, and they occur in sets from several inches to a few feet thick. Associations of contiguous beds with similar grain size and sorting characteristics comprise the sheet and shoestring sand that make up the recent alluvium of the valley. Laterally extensive sand sheets were deposited as a result of continuous lateral migration of fluvial channels. Narrow elongate sand shoestrings were deposited as a result of occasional, discontinuous channel shifts or jumps, and subsequent in-filling of the resulting abandoned channel. These associations of cross-bed sets extend laterally as distinct geologic units. Contacts between these geologic units are somewhat irregular, but are generally horizontal to gently dipping. These contacts are either abrupt or gradational, but they are usually fairly well defined by subtle discontinuities in grain size across the contact.

3.3.2 Description of Stratigraphic Units

Ten distinct stratigraphic units have been identified in the chemical grouting test area. These units extend from the surface into the underlying alluvial outwash deposit. Subsurface profiles have been developed for the cross sections shown on Fig. 3.1. On these profiles, Fig. 3.6 through 3.8, the contacts between the various units have been inferred. Results and locations of in situ testing performed prior to grouting are also shown in these figures. These units are described in order of stratigraphic position from highest to lowest.

Unit A. Unit A is a 5-to 6-ft-thick layer of fill that was borrowed from Unit C and compacted in the asphalt pad area to replace the miscellaneous fill that was removed. The miscellaneous fill contained bricks, concrete, car wrecks, tires, and other debris that would have interfered with installation of grout pipes and drilling. The replacement fill is brown, medium, dense fine sand with some silt to silty fine sand (SM). It was compacted with CAT 955 and 977 front-end loaders.

Unit B. Unit B is the surficial natural flood-plain deposit. Miscellaneous debris is mixed into this deposit. This unit is brown, firm to stiff silty clay to clayey silt (CH-CL, ML) which is desiccated. The desiccation is caused by drying out and oxidation which occurs because the groundwater level only reaches this elevation during river flood stage conditions. The varying degrees of desiccation cause this unit to have a wide range of plasticity and consistency.

Unit C. Unit C is the highest layer of recent alluvial sand. It is brown, medium dense, silty fine sand to fine sand with some silt (SM). It is subrounded to angular, poorly graded sand. This unit is subject to fluctuating groundwater levels and is dry for most of the year. It exhibits the characteristic cross-bedding structures and general uniformity of recent alluvium.

Unit D. Unit D is brown, firm to stiff, fine sandy silt to clayey silt with a trace of sand (ML). It resembles Unit B to some extent, except that it has a coarser grain size and some of the cross-bedded structure of Unit C. It is suspected that Unit D has thin seams and pockets of clayey silt which were deposited in a quiescent environment similar to that which existed during deposition of Unit B. A thickening of this unit, trending approximately SW-NE, was observed in the southeast corner of the test area. This geometry suggests that this unit resulted from channel filling deposition.

Unit E. Unit E is brown to grey, medium dense, fine to medium sand and has a trace of silt (SP-SM,SP). The sand is rounded to subrounded and poorly graded. This unit is cross-bedded with occasional concentrations of predominantly fine sand. Coloration grades from brown to grey because of the fluctuating level of the groundwater table. The groundwater table generally does not fall below el 400, and this elevation corresponds to the contact between the brown and grey sand. The sand above el 400 is periodically subjected to drying and desiccation that exposes the soil minerals to air. This exposure results in oxidation of the iron, thus the brownish coloration. The sand below the water table is oxygen-poor and retains a more greyish hue. During excavation of the test area, the dewatered sand below el 400 turned from grey to brown.

Within the limits of Unit E are several stratigraphic discontinuities. In the northwest corner of the test area, a large tree trunk was discovered. Around this wood, material similar to that found in Unit C was deposited as a result of the obstruction to flow caused by the fallen tree. Along the eastern portion of the test area, a lens-shaped deposit of Unit C material was observed. This finer grained deposit trended approximately SW-NE and had a variably shaped contact with Unit E (see Fig. 3.6 for an inferred profile of these discontinuities).

Unit F. Unit F is grey, medium dense to dense, fine to coarse sand with trace of fine gravel and silt (SP). Generally, the sand is rounded to subangular and poorly graded. This unit is very similar to Unit E, except that it is more well graded, coarser grained, and contains locally significant concentrations of fine gravel. It does, however, contain many intercalated beds and cross-beds of fine to medium sand having characteristics identical to those of Unit E. The contact between Units E and F is usually abrupt; the contact between Units F and G is gradational and irregular.

Unit G. Unit G is grey, medium dense to dense, fine to medium sand with trace of silt and fine gravel (SP). It is rounded to subangular, generally poorly graded sand, but it has occasional well-graded cross-beds of coarser material. This unit is very similar to Unit E, except for the local concentrations of coarser material. Carbonaceous material is more abundant in Unit G than in the other recent alluvial units.

Unit H. Unit H is grey, dense to very dense, fine sand with trace of silt (SP, SP-SM). It is generally poorly graded and has at least 80 percent subrounded quartz grains. There are local traces of medium sand and coarse silt. This unit is cross-bedded and exhibits the greatest uniformity of characteristics of the recent alluvial sand.

Unit I. Unit I is grey, dense to very dense, fine to medium sand with trace of silt (SP). It is poorly graded and very similar to Unit H; however, it contains a larger percentage of medium sand and has a slightly lower density. It was encountered only in Borings BM-1 and D-26 (Fig. 3.7).

Unit J. Unit J is the lowest unit investigated in the chemical grouting test area, and it is the contact deposit between the recent alluvium and the alluvial outwash. It is an intergrading of the alluvial sand with the glacial outwash sand and gravel. This unit is grey, medium dense to dense, fine to coarse sand with trace of silt and fine gravel, occasionally grading with rock fragments (SP). The sand is typically subrounded and poorly graded.

3.4 INITIAL SOIL PROPERTIES

3.4.1 General

The in situ and laboratory testing results were interpreted in light of the stratigraphic information to provide initial soil property characterization for the chemical grouting test area. Index properties such as natural water content, specific gravity, and grain-size distribution; in situ state of stress; unit weight, and relative density; strength-deformation properties such as modulus, drained angle of internal friction, and pressuremeter limit pressure; and permeability were evaluated for each stratigraphic unit. Table 3.1 presents a summary of average soil properties for each soil layer before grouting. Soil properties are discussed in the following sections.

3.4.2 Index Properties

Natural water content was measured in samples obtained during previous investigations in the general testing area. Similar stratigraphic units were identified in these borings enabling moisture contents in the chemical grouting test area to be estimated. Previous investigations also provided data on specific gravity from which chemical grouting test area parameters could be estimated.

Laboratory grain-size analyses performed on samples obtained from borehole sampling and excavation mapping were significant in differentiating stratigraphic units. The ranges of grain-size distribution for units C through H are given in Fig. 3.9.

3.4.3 Stresses

The in situ state of stress was evaluated from pressuremeter and density tests results, and field observations. The vertical effective stress profile calculated from estimated unit weights is shown in Fig. 3.10. The horizontal total stress was measured during pressuremeter testing as the cell pressure at which the undisturbed elastic resistance of the soil was mobilized, that is, the stress at which the pressure-volume change curve becomes linear. The horizontal effective stress was obtained by subtracting the static pore pressure because the tests are assumed to be fully drained. The inferred horizontal effective stress profile before grouting is shown in Fig. 3.10. The coefficient of lateral earth pressure at rest K_o is the ratio of horizontal to vertical effective stress. For the test area, before grouting, K_o ranged from 0.4 to 0.6 and averaged 0.48, indicative of normally consolidated sand.

3.4.4 Density

Total and dry unit weights were determined from Phase II laboratory testing of undisturbed samples and from in-place density tests of ungrouted soil made during excavation of the test area (Section 9.3). Maximum and minimum dry unit weights were determined in the laboratory from undisturbed samples taken during Phase II investigations. These results were supported by Proctor and Providence testing of borehole samples reconstituted in the laboratory in preparation for the laboratory grouting program (Section 5.1). In-place unit weights are plotted vs maximum and minimum unit weights from Phase II studies in Fig. 3.11.

Relative density profiles were determined from the results of static cone and standard penetration tests. Relative density was calculated from static cone penetration point resistance using an empirical correlation (Schmertmann 1976) established with an electrical cone in normally consolidated, fine sand (SP). The correlation takes into account the effect of vertical effective overburden stress. The relative density profiles for borings D-23 and D-26 are shown in Fig. 3.12. The lower relative densities in Boring D-23 may be due to the presence of Unit C material down to el 398, whereas the top portion of Boring D-26 was completely in Unit E. The two cone profiles are in close agreement below el 390.

Relative density can be calculated from the results of in-place density tests made during excavation and of laboratory maximum and minimum unit weight determinations made during Phase II. Using the results in Fig. 3.11, relative densities at various depths were calculated and plotted on Fig. 3.12. In general, they confirm the relative density profile determined from the cone. The scatter of data observed was anticipated because of nonhomogeneities across the site and the lack of maximum and minimum unit weight data specific to the chemical grouting test area.

Standard penetration resistances were related to relative density using Gibbs and Holtz (1953) correlation. This correlation was chosen because the sands tested in that study were similar to Ellis Island recent alluvial sand. Using the upper and lower bounds of standard penetration resistances shown on Fig. 3.2, a relative density profile was calculated and plotted in Fig. 3.12. Between el 400 and el 392, relative densities calculated from standard penetration tests appear to be slightly lower than those predicted from static cone. However, below el 392, the static cone and standard penetration resistances yield equivalent relative density values. Below el 380, very high cone and standard penetration resistances were encountered, reflecting the high relative density of Unit H.

3.4.5 Strength-Deformation Properties

Deformation Modulus. The elastic deformation modulus (Young's Modulus) was inferred from results of static cone penetration tests, pressuremeter tests, plate load tests and crosshole shear wave velocity measurements. Each of these moduli represent a drained modulus, however, the strain amplitude and plane of deformation were different for each test (see Section 9.5.2).

Static Cone Modulus. Modulus was determined from the static cone penetration test using a strictly empirical correlation first suggested by Vesic (1970):

$$E_s = 2(1 + D_r^2)\, q_c$$

where: D_r = relative density; and
q_c = cone penetration resistance.

There are many other correlations, primarily derived from plate load tests in various types of sand, that give similar results. This modulus is therefore representative of three dimensional (deviatoric) compression. Modulus values calculated from static cone penetration tests in Borings D-23 and D-26 are presented in Fig. 3.13.

Pressuremeter Modulus. Elastic deformation modulus values were calculated from pressuremeter tests using the slope of the linear pseudo-elastic portion of the pressure-volume change curve. An equation for cylindrical cavity expansion of a linearly elastic material under conditions of axial symmetry and plane strain was used:

$$E_s = 2V_o (1 + \nu) \Delta P / \Delta V$$

where: V_o = initial volume of measuring cell;

ν = Poisson's ratio;

ΔP = pressure increment; and

ΔV = volume increment resulting from ΔP.

Modulus values calculated from pressuremeter tests in Boring D-27 are presented in Fig. 3.13.

Plate Load Test Modulus. The initial modulus from plate load tests was calculated from the initial slope of the pressure-settlement curve using:

$$E_s = I(1 - \nu^2) B K$$

where: I = shape factor;

ν = Poisson's ratio;

B = width or diameter of plate;

K = modulus of subgrade reaction, which is the slope of the pressure-deflection curve.

This value is an initial recompression modulus representing the three dimensional compression caused by a model footing. Moduli computed from plate load tests performed on ungrouted soil during excavation are plotted on Fig. 3.13.

Shear Wave Modulus. Elastic deformation modulus can be determined from crosshole shear wave velocity measurements using:

$$G = \rho V_s^2 \qquad \text{and} \qquad E = 2(1+\nu)G$$

where: G = shear modulus;

ρ = mass density of soil;

V_s = shear wave velocity; and

ν = Poisson's ratio.

Moduli calculated from shear wave velocity measurements averaged over the four arrays for each depth are presented in Fig. 3.13. Reviewing Fig. 3.13, differences between moduli are apparent (see Section 9.5.2). Pressuremeter moduli are the lowest; they correspond to the highest strain amplitude (up to 25 percent strain), and properties are measured along a horizontal plane, whereas the cone and plate load test measure vertical properties. The plate load test values generally fall between the cone and pressuremeter results, except for one test that may have been made on partially grouted soil. The cone modulus results vary from 200 to 500 t/ft^2 which is similar to the range of initial tangent modulus values of 280 to 525 t/ft^2 obtained in $\overline{CID}$ triaxial tests of main testing area samples during Phase II. The crosshole shear wave velocity moduli are substan tially greater than those inferred from the other tests because of the very small strain amplitude caused during transmission of a shear wave (10^{-8} percent strain).

Angle of Internal Friction. The drained angle of internal friction was determined from the results of static cone penetration and pressuremeter tests. Static cone penetration resistance was correlated to friction angle $\bar{\phi}$ using an empirical chart developed by Meyerhof (1974). This correlation is independent of the in situ stress conditions. Friction angles calculated from the cone point resistance are plotted with depth in Fig. 3.14. The drained angle of internal friction was also determined from pressuremeter tests using a new method developed by Hughes et al (1977). Friction angles calculated using this method are plotted on Fig. 3.14.

The average values for friction angle calculated from the cone vary within a range of 35 to 39 degrees, remaining relatively constant with depth. The pressuremeter, however, predicted values ranging from 29 degrees in the upper, fine-grained material to 40 degrees in the denser, deeper deposits. Correlation between friction angles determined from cone and pressuremeter results is difficult due to differences in stratigraphy at actual test elevations. For comparable soil types, however, the results match reasonably well. The lower friction angles determined from pressuremeter tests in the upper deposits may also be an indication of a residual instead of a peak friction angle which was determined in the deeper tests. The shallow tests were carried further into the range of plastic deformation and closer to ultimate failure.

Pressuremeter Limit Pressure. The pressuremeter limit pressure (asymptote to which the pressure-volume curve tends at large strains) has been used in design of shallow and deep foundations as representative of ultimate soil strength. The limit pressure has been related theoretically to ultimate bearing capacity, shear strength in cohesive soils, and friction angle in sand. For this program, however, it provided an index to ultimate strength. Pressuremeter limit pressures from Boring D-27 are plotted in Fig. 3.15.

3.4.6 Permeability

Borehole permeability testing in Boring D-28 provided a profile of the permeability coefficient with depth (Fig. 3.2 and Fig. 3.16). Also shown in Fig. 3.16 is the stratigraphic profile for this boring. In the upper, finer-grained portion of Unit C, low permeabilities were encountered. As the sand became coarser in Unit E and fine gravel was encountered in the upper portion of Unit F, permeabilities increased. With less coarse-grained sand and fine gravel in Units F and G, the permeability decreased.

UNIT	INDEX PROPERTIES						STRESS	DENSITY					STRENGTH-DEFORMATION						PERMEABIL
													E_s						
	w_n %	G	Fine Content %	Gravel Content %	D_{10} mm	D_{60} mm	K_o	γ_t lb/ft³	γ_d lb/ft³	γ_{dmax} lb/ft³	γ_{dmin} lb/ft³	D_r %	PMT t/ft²	PLT t/ft²	CPT t/ft²	CSV t/ft²	$\bar{\phi}$ °	P_L t/ft²	k cm/s
A	18	2.65	29	0	-	0.1	-	128	-	-	-	60	-	-	-	-	-	-	-
B	29.7	2.67	-	-	-	-	-	113	-	-	-	-	-	-	-	-	-	-	$6\times10^{-\text{[illegible]}}$
C	18	2.65	29.2	0	-	0.18	0.31	128	-	-	-	60	-	-	160	-	32	7	-
D	20	2.65	76	0	-	0.05	1.97	120	-	-	-	50	41.0	-	-	-	-	-	-
E	22	2.65	4	0.4	0.17	0.47	0.64	125	102	108	86.4	65	33.1	-	320	1800	35	8.7	$1.7\times10^{-\text{[illegible]}}$
F	22	2.65	2.1	5.9	0.28	0.75	0.79	129	106.5	112.5	94.3	70	53.1	197	320	1730	37	20.3	$3\times10^{-\text{[illegible]}}$
G	22	2.66	2	0.9	0.25	0.53	0.68	128	105.6	114.4	95.5	68	137.8	91	350	1830	39	26.8	$5\times10^{-\text{[illegible]}}$
H	26	2.66	4.8	0.3	0.14	0.28	0.65	132	104.6	107.4	84.9	90	176.9	-	600	-	40	49	$6\times10^{-\text{[illegible]}}$
I	-	-	-	-	-	-	-		-	-	-	70	-	-	-	-	-	-	$2\times10^{-\text{[illegible]}}$
J	-	-	1.9	5.8	0.3	1.0	-		-	-	-	70	-	-	-	-	-	-	$3\times10^{-\text{[illegible]}}$

…T t/ft²	STRENGTH-DEFORMATION E_s PLT t/ft²	CPT t/ft²	CSV t/ft²	$\bar{\phi}$ °	P_L t/ft²	PERMEABILITY k cm/s
-	-	-	-	-	-	-
-	-	-	-	-	-	$6x10^{-5}$
-	-	160	-	32	7	-
1.0	-	-	-	-	-	-
3.1	-	320	1800	35	8.7	$1.7x10^{-3}$
3.1	197	320	1730	37	20.3	$3x10^{-2}$
7.8	91	350	1830	39	26.8	$5x10^{-3}$
6.9	-	600	-	40	49	$6x10^{-4}$
-	-	-	-	-	-	$2x10^{-3}$
-	-	-	-	-	-	$3x10^{-2}$

Notes

UNIT	Stratigraphic unit described in Section 3.3.2
W_n	Natural Water Content
G	Specific Gravity
FINE CONTENT	Percent by weight of soil particles passing through a No. 200 US standard sieve (0.074 mm)
GRAVEL CONTENT	Percent by weight of soil particles retained by a No. 4 US standard sieve (4.76 mm)
D_{10}	Effective grain-size or grain-size for which 10 percent by weight of the soil particles are finer
D_{60}	Grain-size for which 60 percent by weight of the soil particles are finer
K_o	Ratio of in situ *effective* horizontal stress to effective vertical stress
γ_t	Total unit weight
γ_d	Dry unit weight
$\gamma_{d\ max}$	Maximum dry unit weight
$\gamma_{d\ min}$	Minimum dry unit weight
D_r	Relative density
E_s	Elastic deformation modulus
PMT	Pressuremeter test
PLT	Plate load test
CPT	Static cone penetration test
CSV	Shear wave velocity measurements
$\bar{\phi}$	Drained angle of internal friction
P_L	Pressuremeter limit pressure
k	Coefficient of permeability (measured by falling-head borehole permeability test)

2

CHEMICAL GROUTING TEST PROGRAM

AVERAGE SOIL PROPERTIES BEFORE GROUTING

FOUNDATION INVESTIGATION AND TEST PROGRAM
EXISTING LOCKS AND DAM No. 26
ST LOUIS DISTRICT, CORPS OF ENGINEERS.
DACW43-76-C-0006

Woodward-Clyde Consultants
Y7C825 Phase IX

Table 3.1

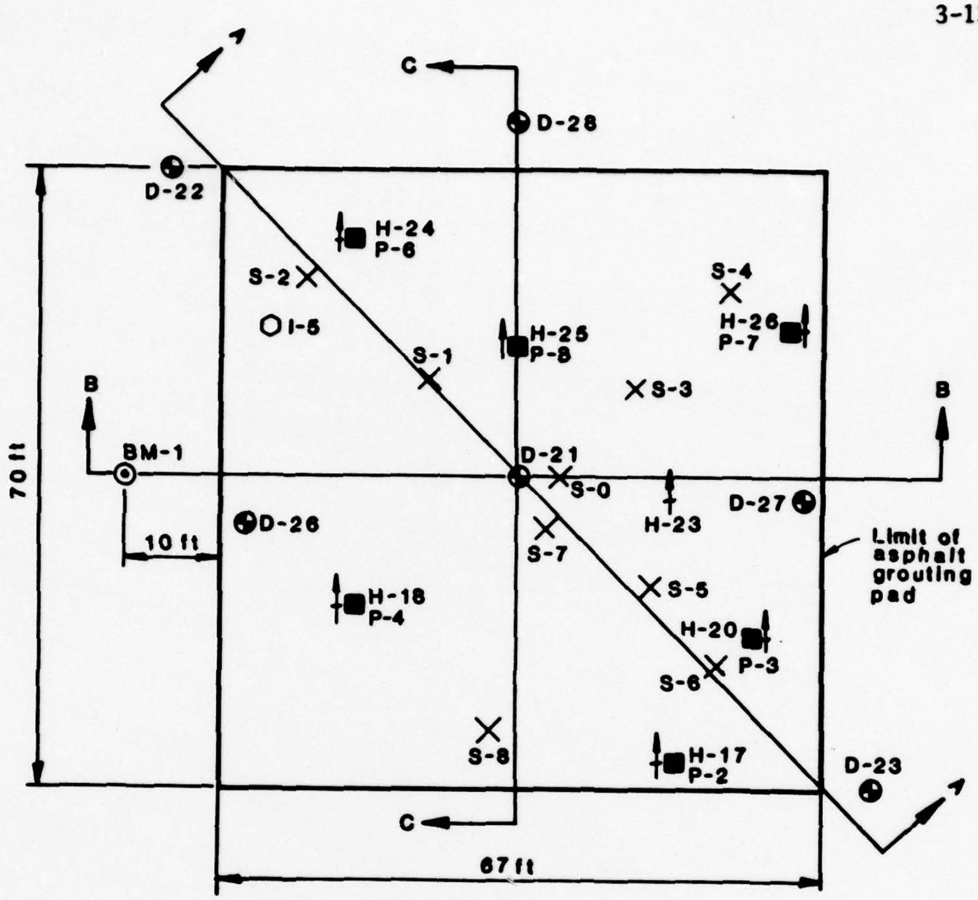

Legend

Boreholes used for subsurface investigation

- BM Benchmark
- H Subsurface heave/settlement point
- P Pore pressure transducer
- I 3-D gage inclinometer
- S Geophysical borehole
- D Insitu testing boring

N

0 10 20

Scale, ft

Note: D-25 is located 250 ft to the north of D-22

CHEMICAL GROUTING TEST PROGRAM

LOCATION OF SUBSURFACE INVESTIGATIONS BEFORE GROUTING

FOUNDATION INVESTIGATION AND TEST PROGRAM
EXISTING LOCKS AND DAM No. 26
ST LOUIS DISTRICT, CORPS OF ENGINEERS.
DACW43-78-C-0006

Woodward-Clyde Consultants

Y7C828 Phase IX

Fig.3.1

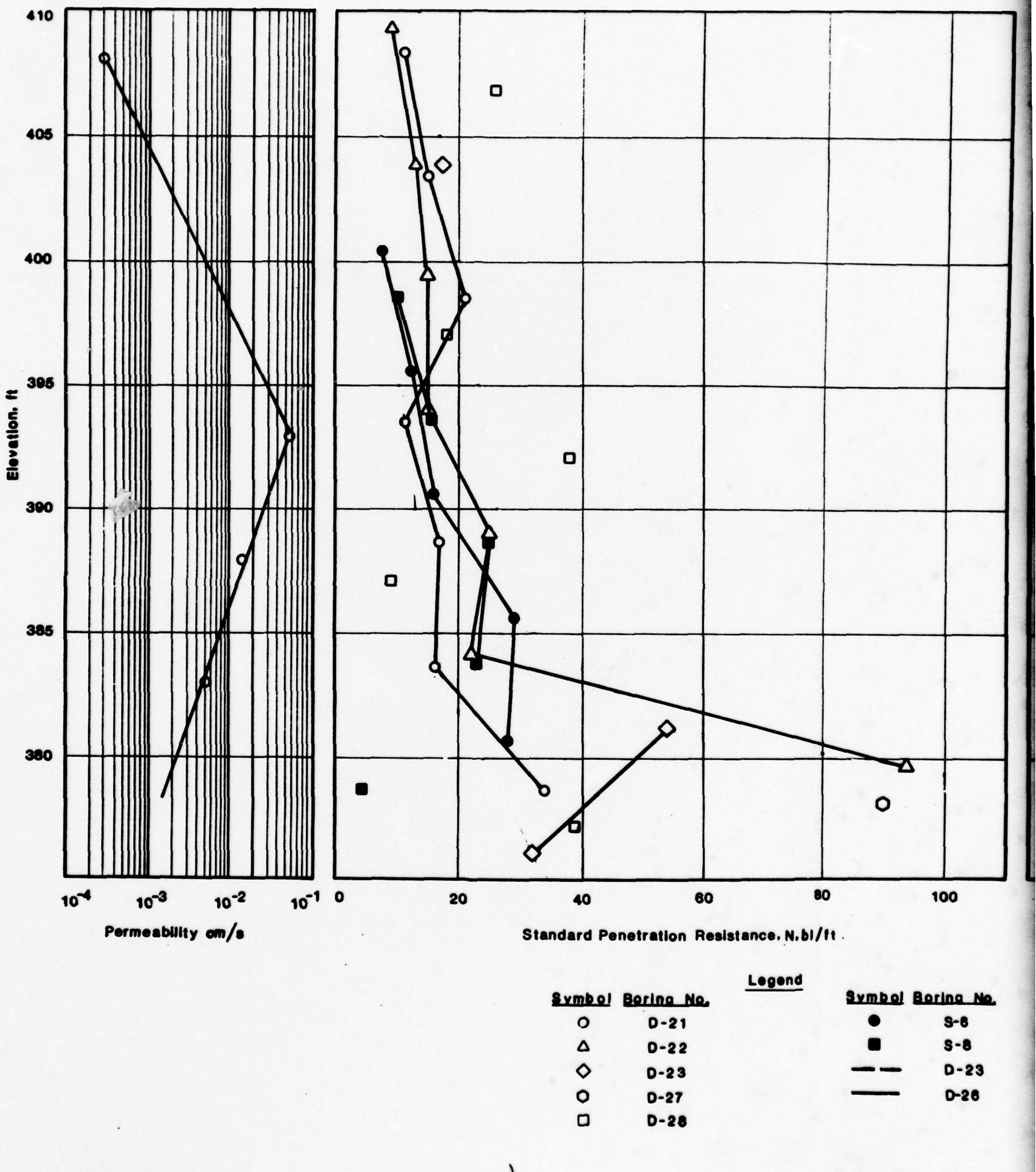

410
405
400
395
390
385
380
Elevation, ft
10^{-4}
10^{-3}
10^{-2}
10^{-1}
Permeability cm/s
0
20
40
60
80
100
Standard Penetration Resistance, N, bl/ft
Legend
Symbol Boring No.
○ D-21
△ D-22
◇ D-23
⬡ D-27
□ D-28
Symbol Boring No.
● S-6
■ S-8
— — D-23
—— D-26

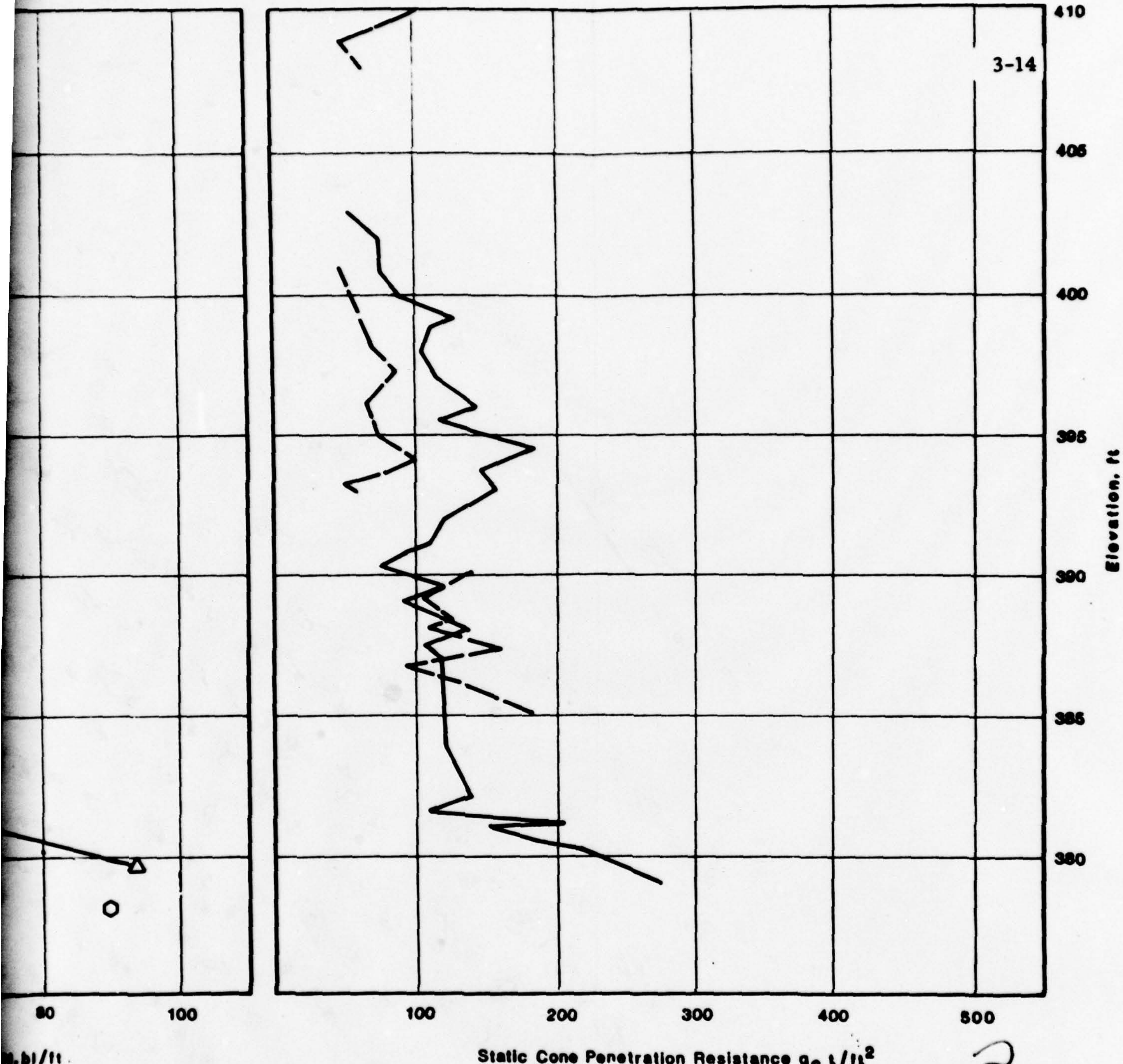

2

nd

Symbol	Boring No.
●	S-6
■	S-8
— —	D-23
——	D-26

CHEMICAL GROUTING TEST PROGRAM

RESULTS OF IN SITU TESTING BEFORE GROUTING

FOUNDATION INVESTIGATION AND TEST PROGRAM
EXISTING LOCKS AND DAM No. 26
ST LOUIS DISTRICT, CORPS OF ENGINEERS.
DACW43-78-C-0065

Woodward-Clyde Consultants

Fig. 3.2

77C825 Phase IX

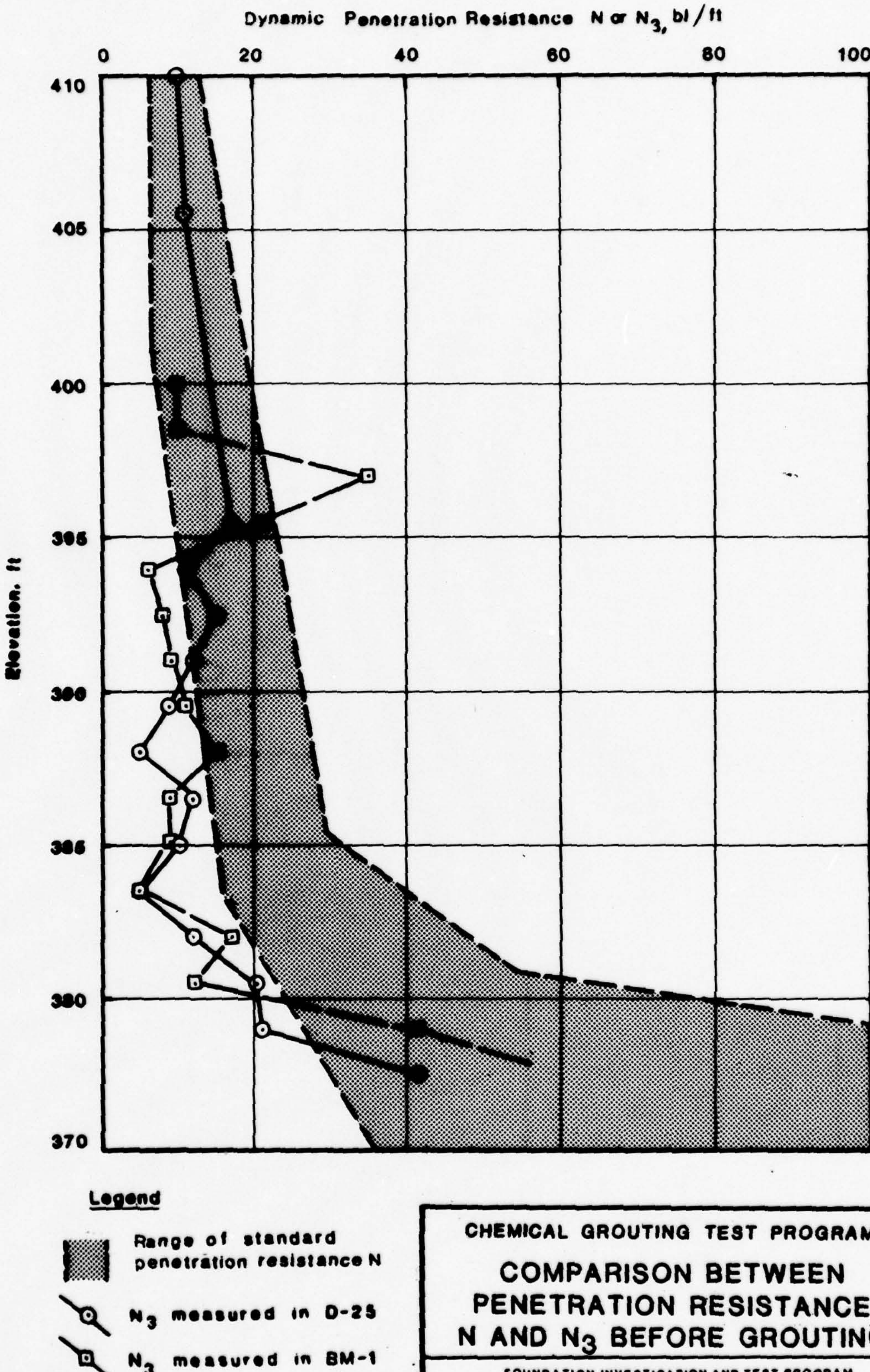

CHEMICAL GROUTING TEST PROGRAM

COMPARISON BETWEEN PENETRATION RESISTANCE N AND N_3 BEFORE GROUTING

FOUNDATION INVESTIGATION AND TEST PROGRAM
EXISTING LOCKS AND DAM No. 26
ST LOUIS DISTRICT, CORPS OF ENGINEERS.
DACW43-78-C-0005

Woodward-Clyde Consultants

Y7C825 Phase IX

Fig. 3.3

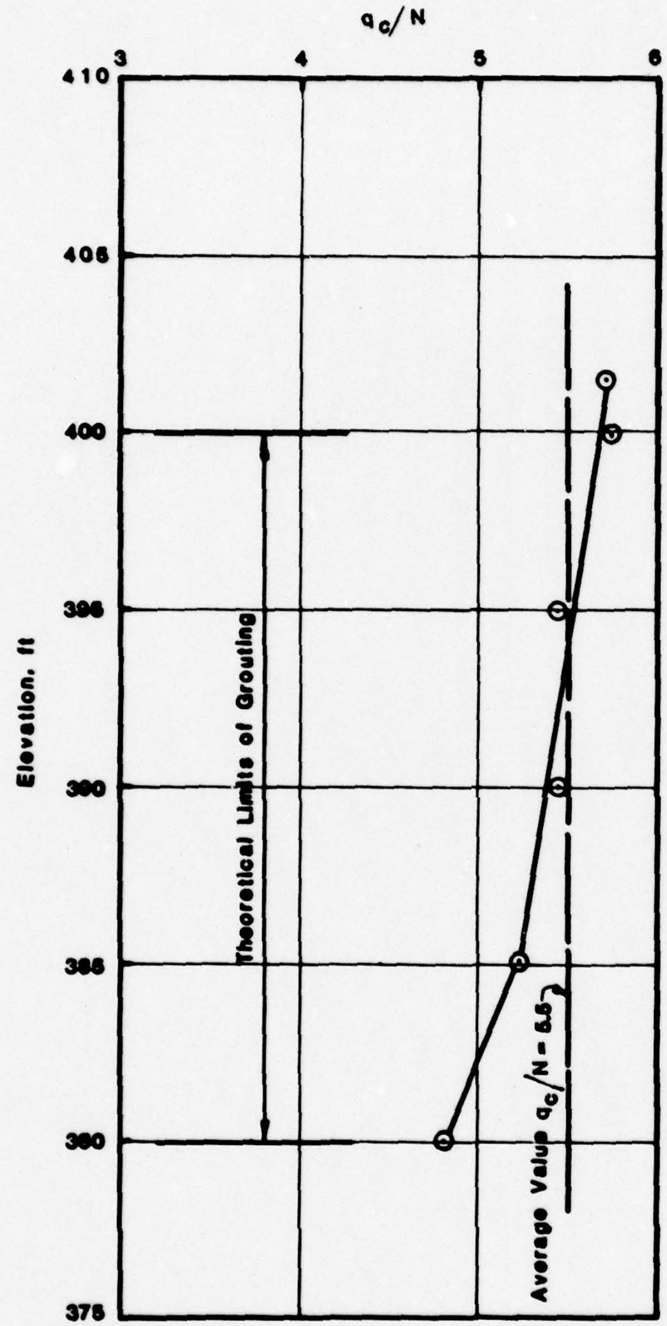

CHEMICAL GROUTING TEST PROGRAM

CORRELATION BETWEEN STANDARD AND STATIC CONE PENETRATION RESISTANCE BEFORE GROUTING

FOUNDATION INVESTIGATION AND TEST PROGRAM
EXISTING LOCKS AND DAM No. 26
ST LOUIS DISTRICT, CORPS OF ENGINEERS.
DACW43-78-C-0008

Woodward-Clyde Consultants
Y7C028 Phase III

Fig. 3.4

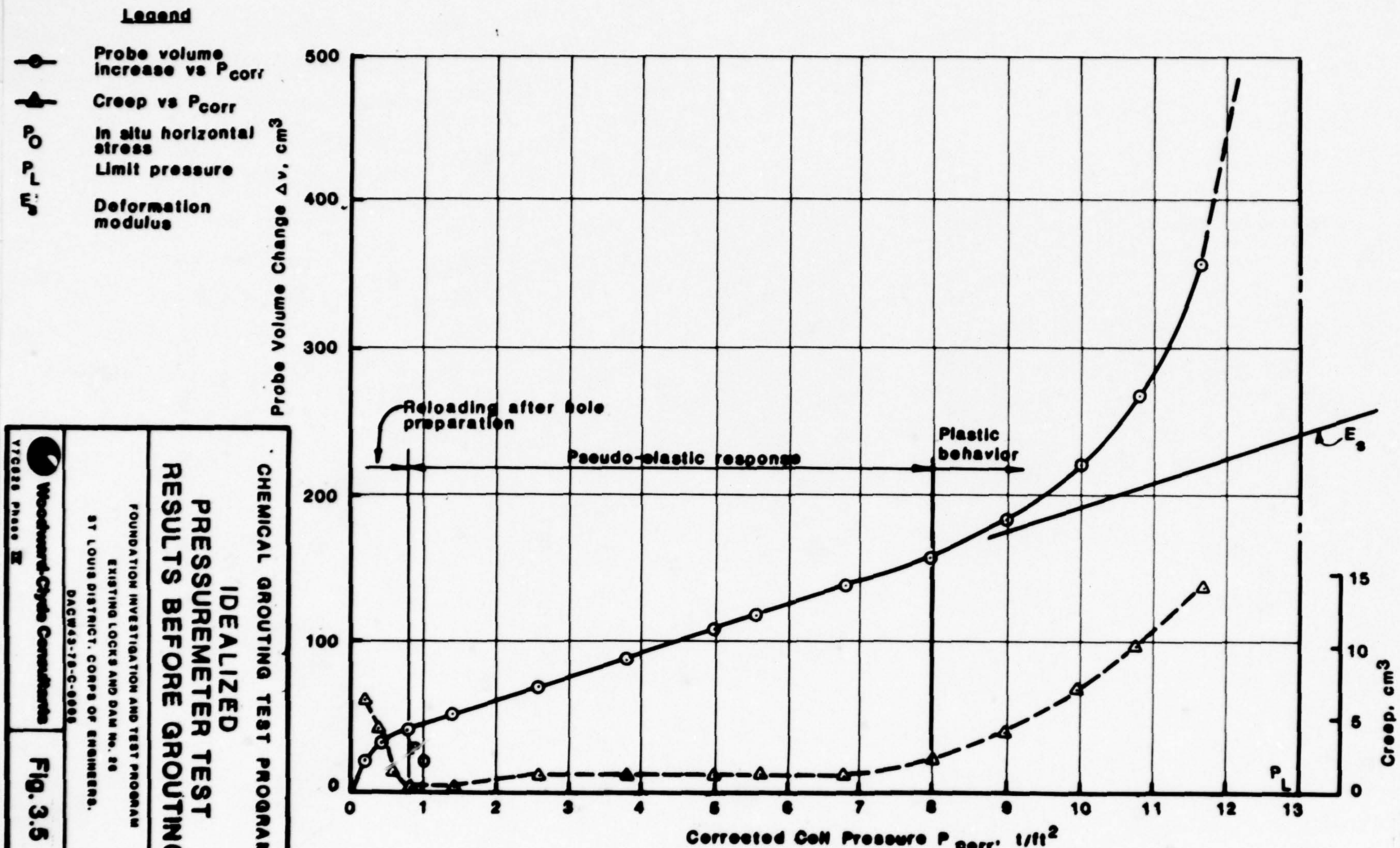

CHEMICAL GROUTING TEST PROGRAM

IDEALIZED PRESSUREMETER TEST RESULTS BEFORE GROUTING

FOUNDATION INVESTIGATION AND TEST PROGRAM
EXISTING LOCKS AND DAM No. 26
ST LOUIS DISTRICT, CORPS OF ENGINEERS.
DACW43-78-C-0066

Woodward-Clyde Consultants

Fig. 3.5

Y7C626 Phase II

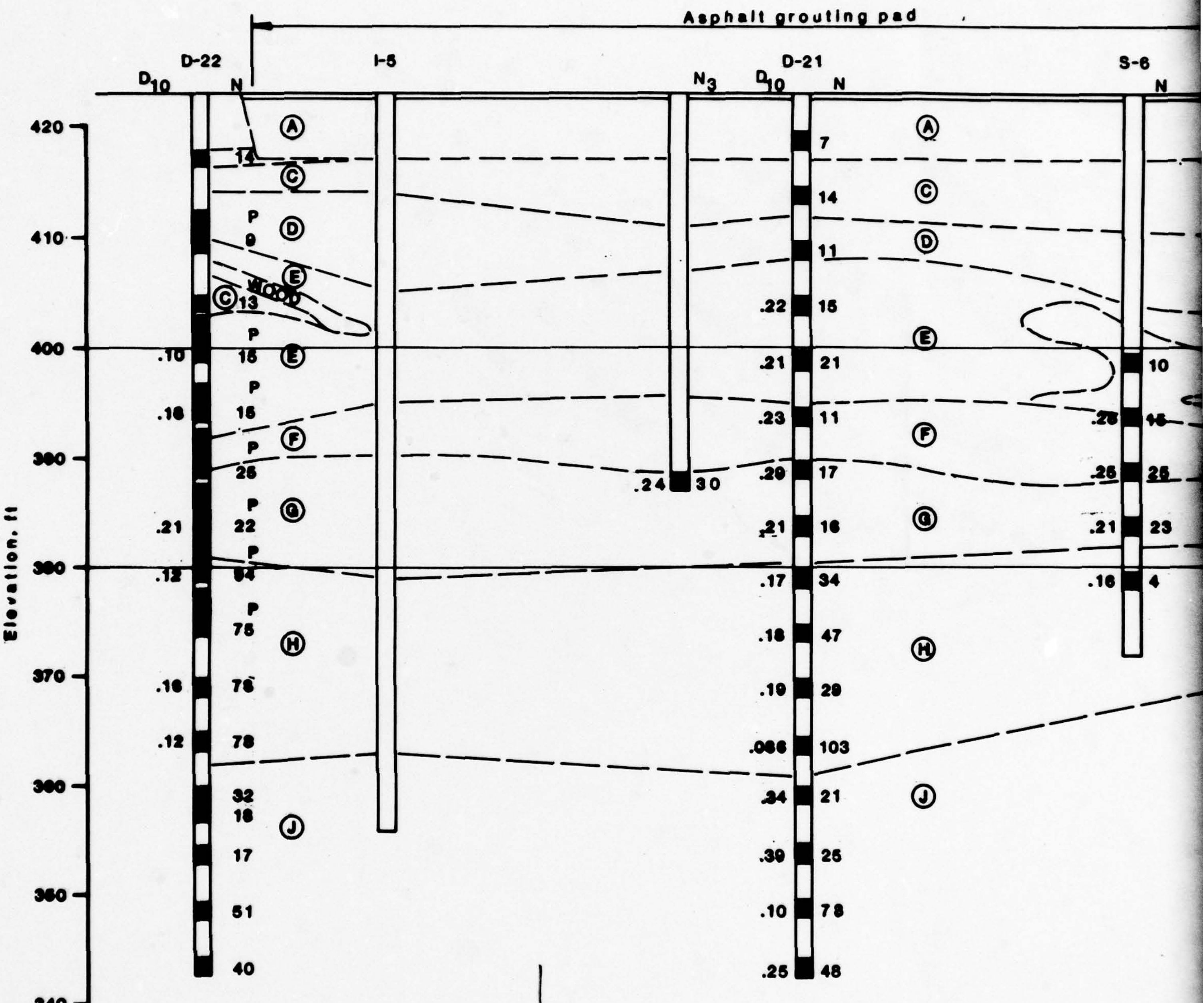

Ⓐ Medium dense brown fine SAND with some silt to silty fine SAND (SM) FILL

Ⓑ Soft to stiff brown silty CLAY to clayey SILT (CH-CL-ML) FLOOD PLAIN DEPOSIT

Ⓒ Medium dense brown silty fine SAND to fine SAND with some SILT (SM) RECENT ALLUVIUM

Ⓓ Firm to stiff brown fine sandy SILT to clayey SILT with trace sand (ML) RECENT ALLUVIUM

Ⓔ Medium dense brown to grey fine to medium SAND with a trace of silt (SP-SM/SP) RECENT ALLUVIUM

Ⓕ Medium dense to dense grey fine to coarse SAND with a trace of fine gravel and silt (SP) RECENT ALLUVIUM

Ⓖ Medium dense to dense grey fine t[o …] trace of silt and fine gravel (SP) [...]

Ⓗ Dense to very dense grey fine SA[ND …] (SP/SP-SM) RECENT ALLUVIUM

Ⓘ Medium dense to dense grey fine t[o …] trace of silt (SP) RECENT ALLU[VIUM]

Ⓙ Medium dense grey fine to coarse [...] silt and fine gravel, occasionally [...] ments (SP) ALLUVIAL OUTWASH

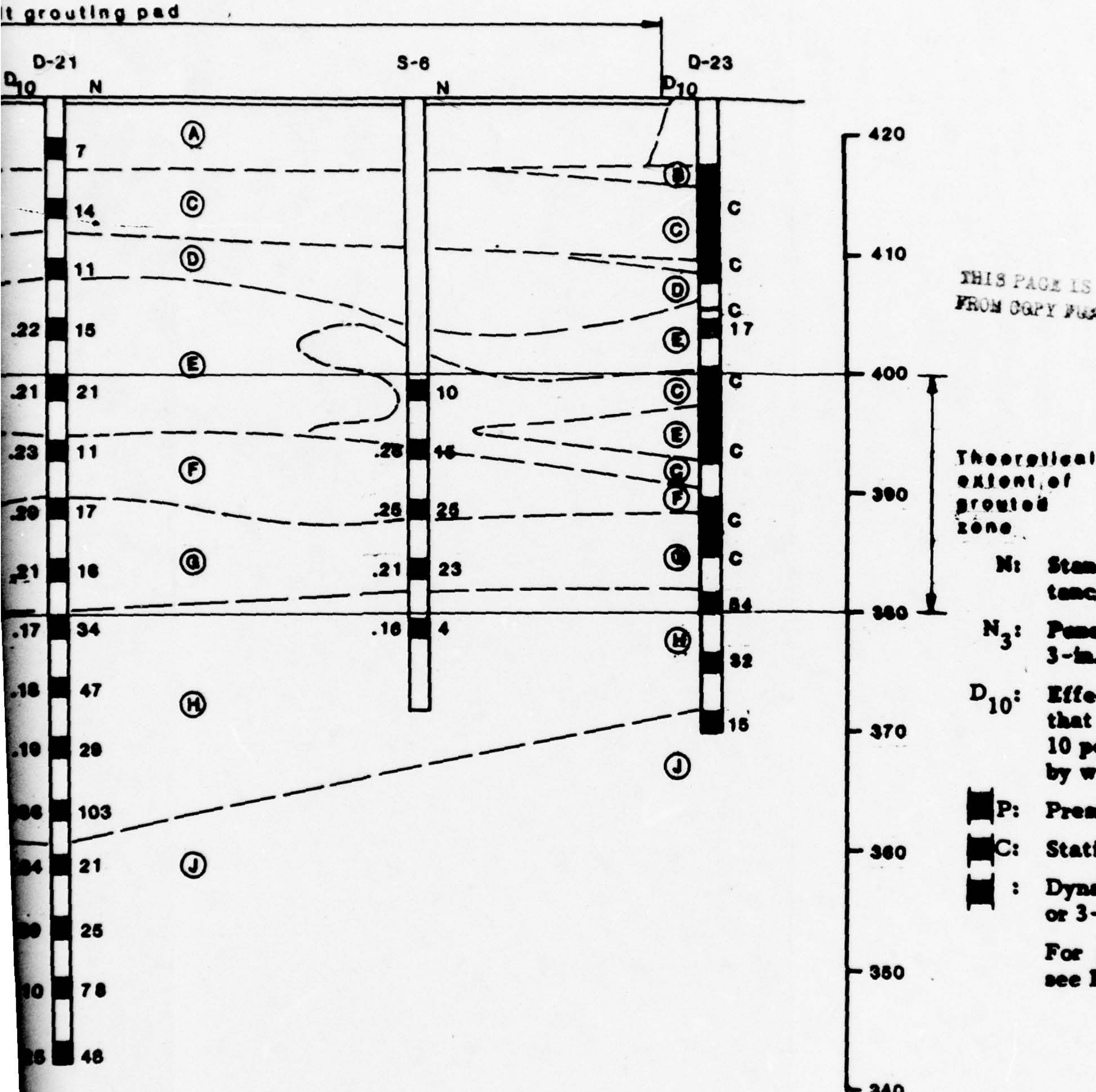

Legend

N: Standard Penetration Resistance, bl/ft

N_3: Penetration Resistance for 3-in.-dia split spoon, bl/ft

D_{10}: Effective grain size (mm), that is grain size for which 10 percent of the soil is finer by weight

P: Pressuremeter test

C: Static cone penetration test

: Dynamic penetration test (2- or 3-in. split spoon)

For plan location of profile, see Fig. 3.1

2

Ⓖ Medium dense to dense grey fine to medium SAND with a trace of silt and fine gravel (SP) RECENT ALLUVIUM

Ⓗ Dense to very dense grey fine SAND with a trace of silt (SP/SP-SM) RECENT ALLUVIUM

Ⓘ Medium dense to dense grey fine to medium SAND with a trace of silt (SP) RECENT ALLUVIUM

Ⓙ Medium dense grey fine to coarse SAND with a trace of silt and fine gravel, occasionally grading with rock fragments (SP) ALLUVIAL OUTWASH

CHEMICAL GROUTING TEST PROGRAM

SUBSURFACE PROFILE A-A OF TEST AREA

FOUNDATION INVESTIGATION AND TEST PROGRAM
EXISTING LOCKS AND DAM No. 26
ST LOUIS DISTRICT, CORPS OF ENGINEERS.
DACW43-78-C-0008

Woodward-Clyde Consultants

Y7C823 Phase III

Fig. 3.8

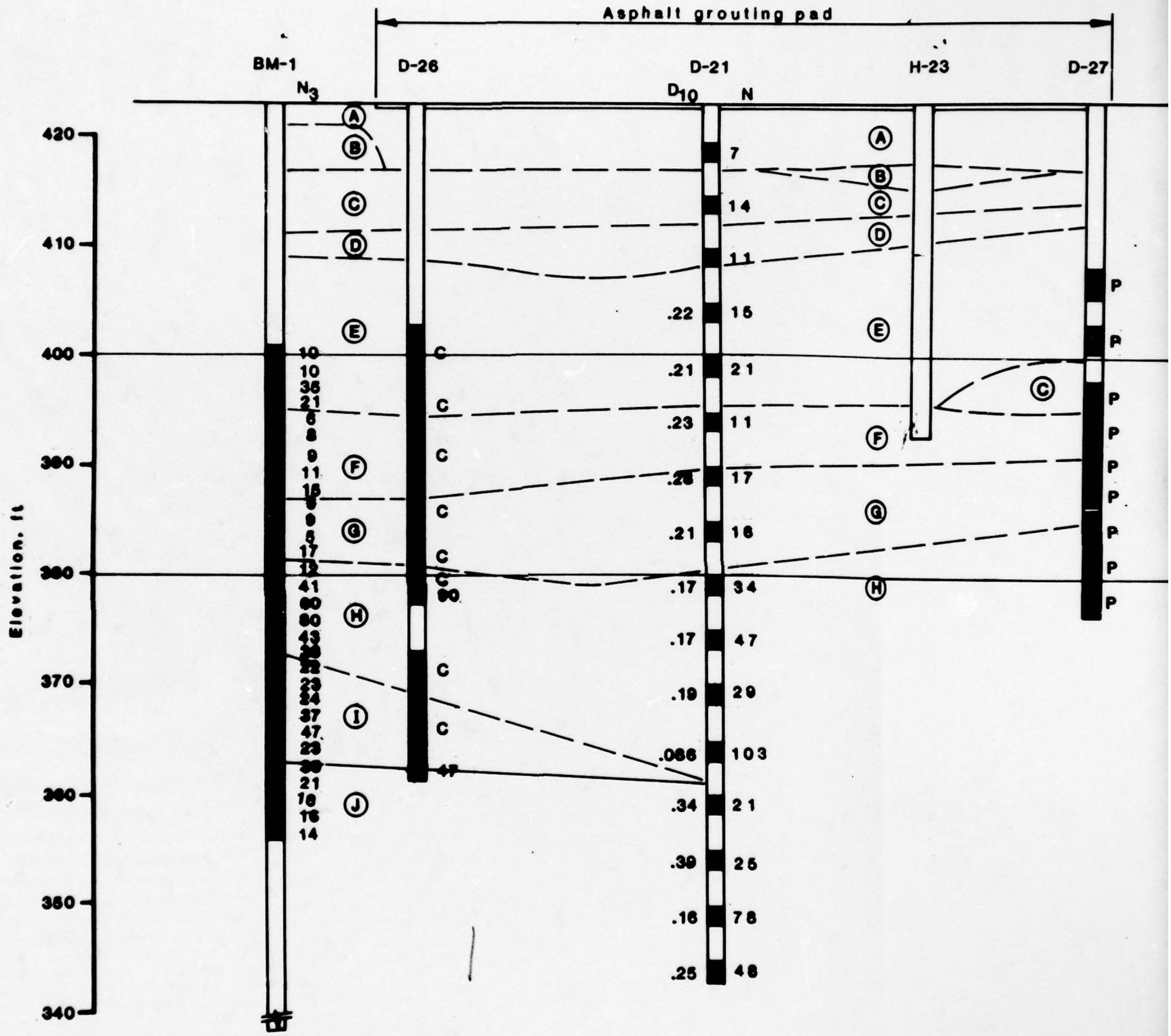

Ⓐ Medium dense brown fine SAND with some silt to silty fine SAND (SM) FILL

Ⓑ Soft to stiff brown silty CLAY to clayey SILT (CH-CL-ML) FLOOD PLAIN DEPOSIT

Ⓒ Medium dense brown silty fine SAND to fine SAND with some SILT (SM) RECENT ALLUVIUM

Ⓓ Firm to stiff brown fine sandy SILT to clayey SILT with trace sand (ML) RECENT ALLUVIUM

Ⓔ Medium dense brown to grey fine to medium SAND with a trace of silt (SP-SM/SP) RECENT ALLUVIUM

Ⓕ Medium dense to dense grey fine to coarse SAND with a trace of fine gravel and silt (SP) RECENT ALLUVIUM

Ⓖ Medium dense to dense grey fi[ne ...] trace of silt and fine gravel ([...]

Ⓗ Dense to very dense grey fine [...] (SP/SP-SM) RECENT ALLUV[IUM]

Ⓘ Medium dense to dense grey fi[ne ...] trace of silt (SP) RECENT A[LLUVIUM]

Ⓙ Medium dense grey fine to co[arse ...] silt and fine gravel, occasion[al ...] ments (SP) ALLUVIAL OUTWA[SH]

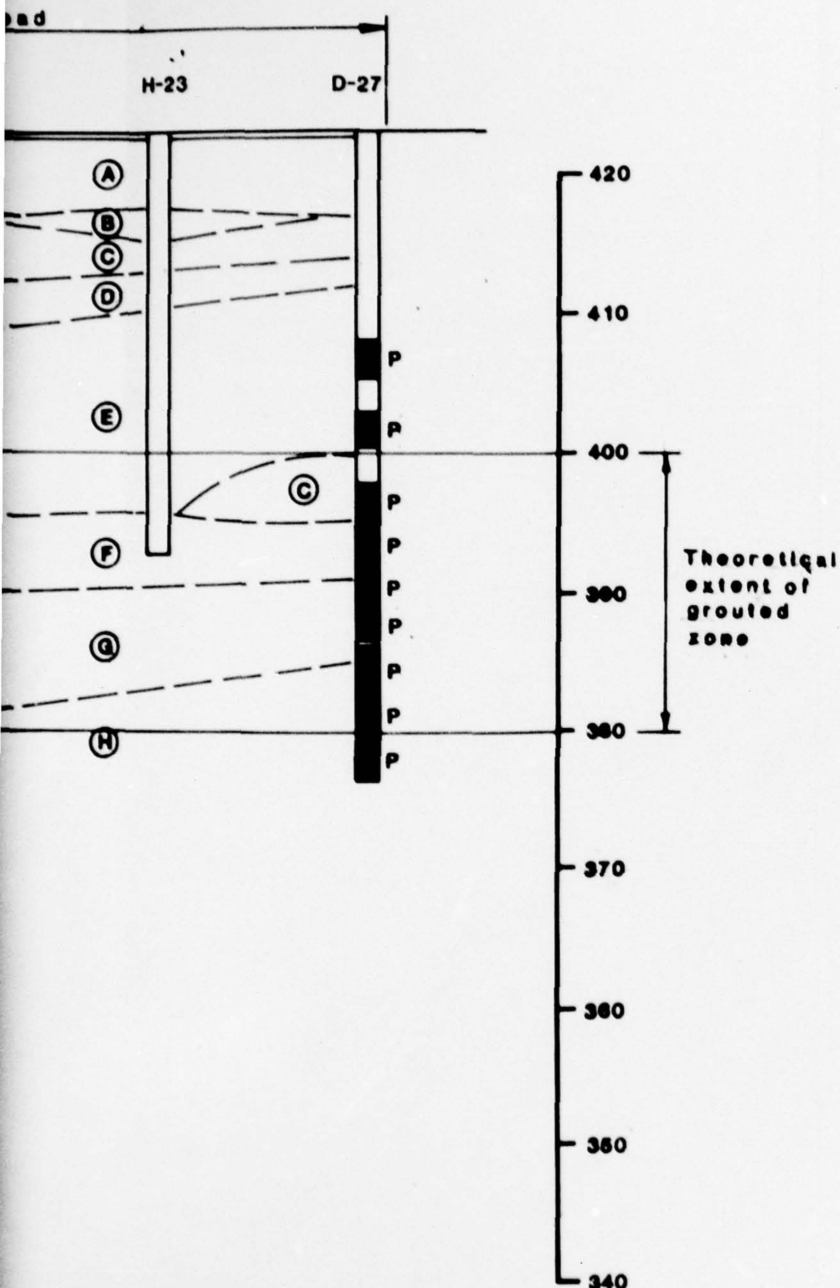

Legend

N: Standard Penetration Resistance, bl/ft

N_3: Penetration Resistance for 3-in.-dia split spoon, bl/ft

D_{10}: Effective grain size (mm), that is grain size for which 10 percent of the soil is finer by weight

P: Pressuremeter test

C: Static cone penetration test

: Dynamic penetration test (2- or 3-in. split spoon)

For plan location of profile, see Fig. 3.1

2

Ⓖ Medium dense to dense grey fine to medium SAND with a trace of silt and fine gravel (SP) RECENT ALLUVIUM

Ⓗ Dense to very dense grey fine SAND with a trace of silt (SP/SP-SM) RECENT ALLUVIUM

Ⓘ Medium dense to dense grey fine to medium SAND with a trace of silt (SP) RECENT ALLUVIUM

Ⓙ Medium dense grey fine to coarse SAND with a trace of silt and fine gravel, occasionally grading with rock fragments (SP) ALLUVIAL OUTWASH

CHEMICAL GROUTING TEST PROGRAM

SUBSURFACE PROFILE
B-B' OF TEST AREA

FOUNDATION INVESTIGATION AND TEST PROGRAM
EXISTING LOCKS AND DAM No. 26
ST. LOUIS DISTRICT, CORPS OF ENGINEERS.
DACW43-76-C-[illegible]

Woodward-Clyde Consultants
[illegible] Phase IX

Fig. 3.7

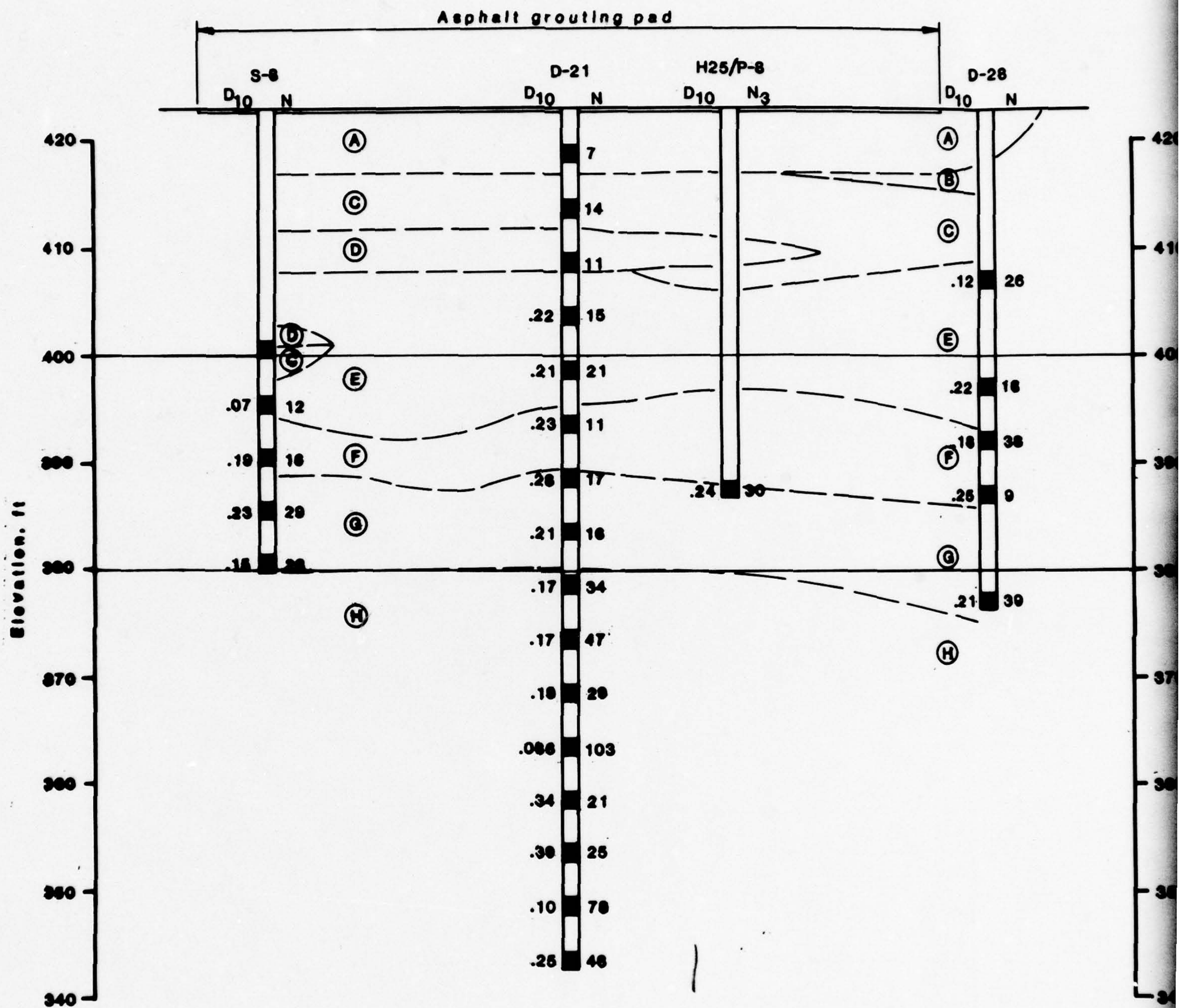

Ⓐ Medium dense brown fine SAND with some silt to silty fine SAND (SM) FILL

Ⓑ Soft to stiff brown silty CLAY to clayey SILT (CH-CL-ML) FLOOD PLAIN DEPOSIT

Ⓒ Medium dense brown silty fine SAND to fine SAND with some SILT (SM) RECENT ALLUVIUM

Ⓓ Firm to stiff brown fine sandy SILT to clayey SILT with trace sand (ML) RECENT ALLUVIUM

Ⓔ Medium dense brown to grey fine to medium SAND with a trace of silt (SP-SM/SP) RECENT ALLUVIUM

Ⓕ Medium dense to dense grey fine to coarse SAND with a trace of fine gravel and silt (SP) RECENT ALLUVIUM

Ⓖ Medium dense to dense grey fine trace of silt and fine gravel (SP

Ⓗ Dense to very dense grey fine S (SP/SP-SM) RECENT ALLUVIU

Ⓘ Medium dense to dense grey fine trace of silt (SP) RECENT ALL

Ⓙ Medium dense grey fine to coar silt and fine gravel, occasional ments (SP) ALLUVIAL OUTWASH

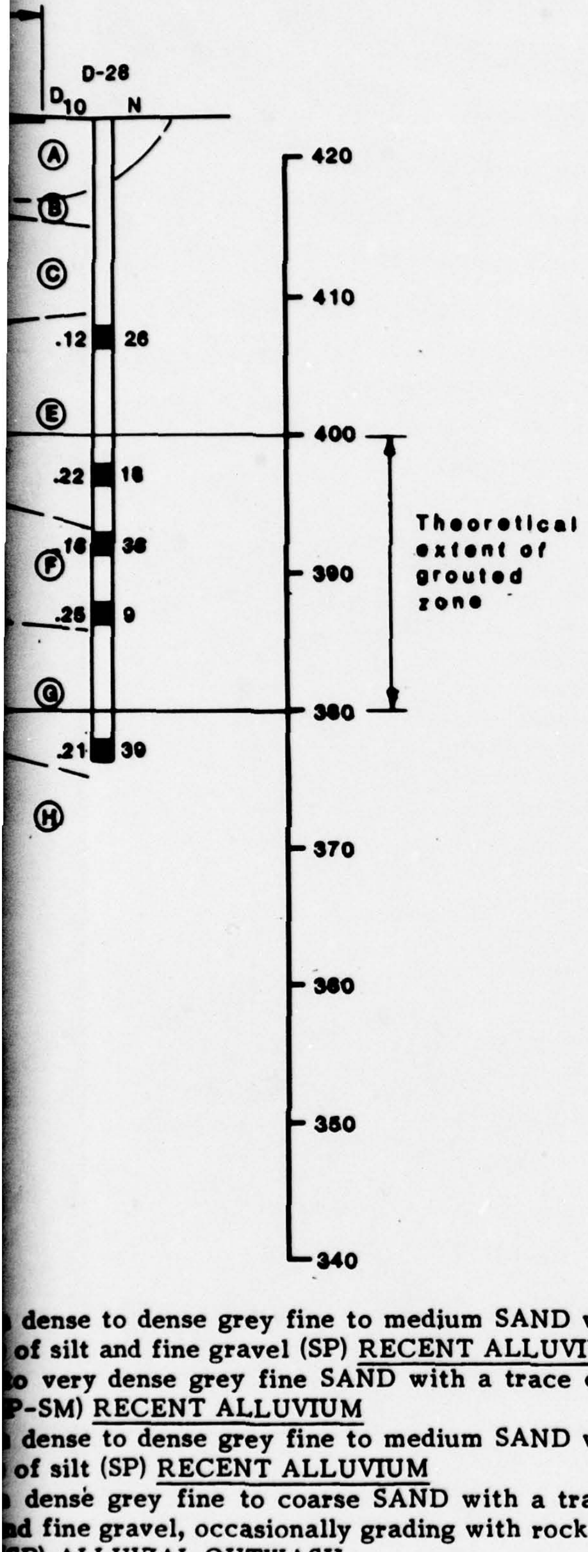

dense to dense grey fine to medium SAND with a
of silt and fine gravel (SP) RECENT ALLUVIUM
o very dense grey fine SAND with a trace of silt
P-SM) RECENT ALLUVIUM
dense to dense grey fine to medium SAND with a
of silt (SP) RECENT ALLUVIUM
dense grey fine to coarse SAND with a trace of
d fine gravel, occasionally grading with rock frag-
SP) ALLUVIAL OUTWASH

Legend

N: Standard Penetration Resistance, bl/ft

N_3: Penetration Resistance for 3-in.-dia split spoon, bl/ft

D_{10}: Effective grain size (mm), that is grain size for which 10 percent of the soil is finer by weight

P: Pressuremeter test

C: Static cone penetration test

: Dynamic penetration test (2- or 3-in. split spoon)

For plan location of profile, see Fig. 3.1

2

CHEMICAL GROUTING TEST PROGRAM

SUBSURFACE PROFILE
C-C OF TEST AREA

FOUNDATION INVESTIGATION AND TEST PROGRAM
EXISTING LOCKS AND DAM No. 26
ST LOUIS DISTRICT, CORPS OF ENGINEERS.
DACW43-78-C-0005

Woodward-Clyde Consultants

Y7C825 Phase IX

Fig. 3.8

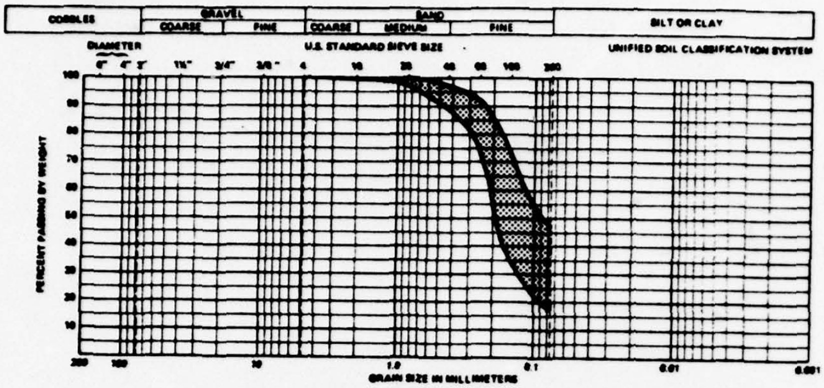

Stratigraphic Unit C

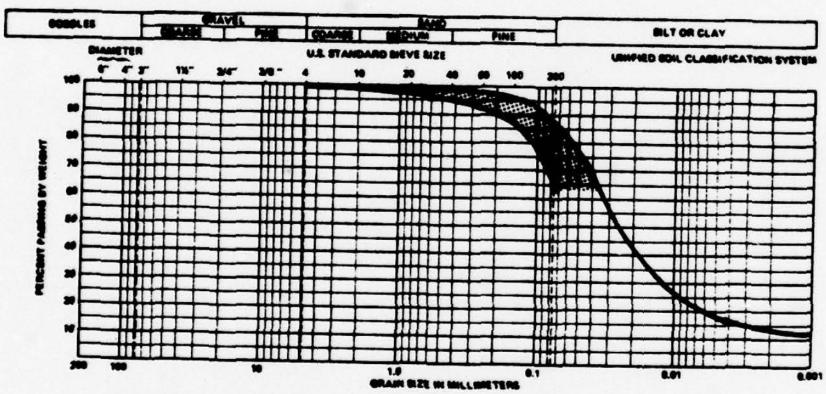

Stratigraphic Unit D

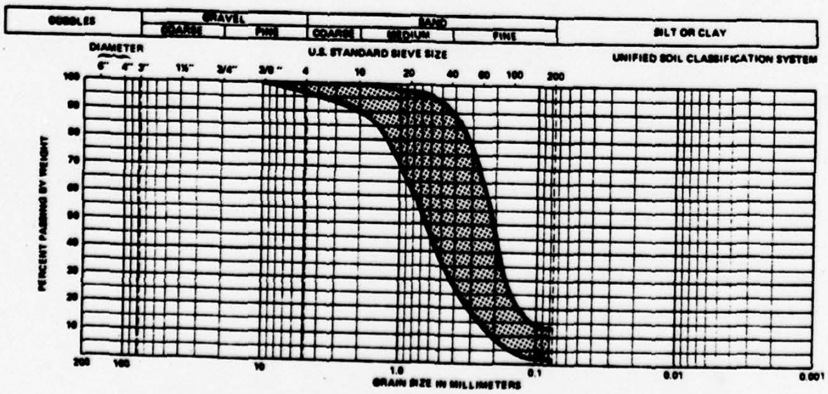

Stratigraphic Unit E

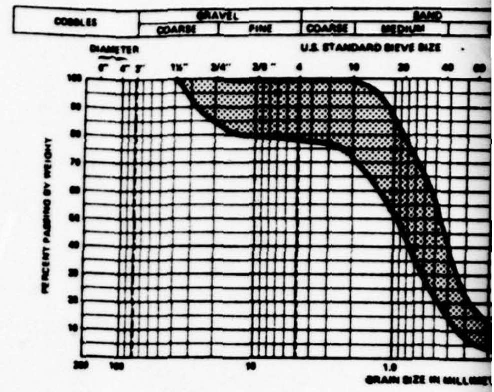

Stratigraphic

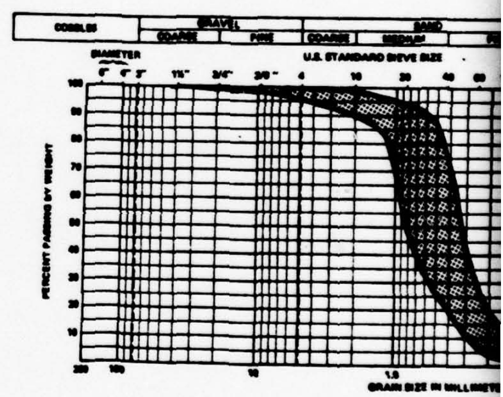

Stratigraphic U

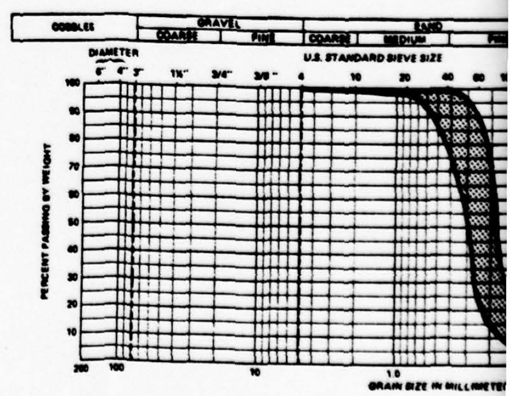

Stratigraphic U

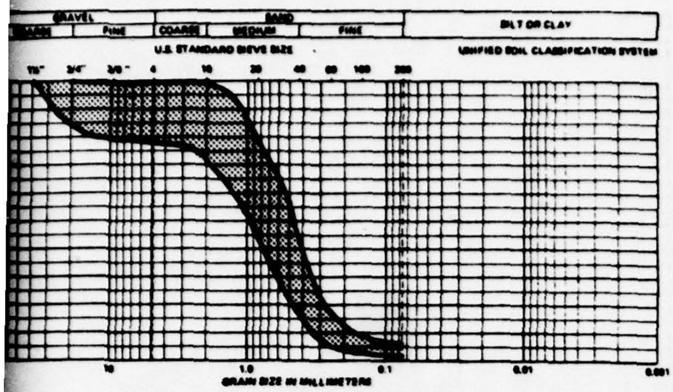

Stratigraphic Unit F

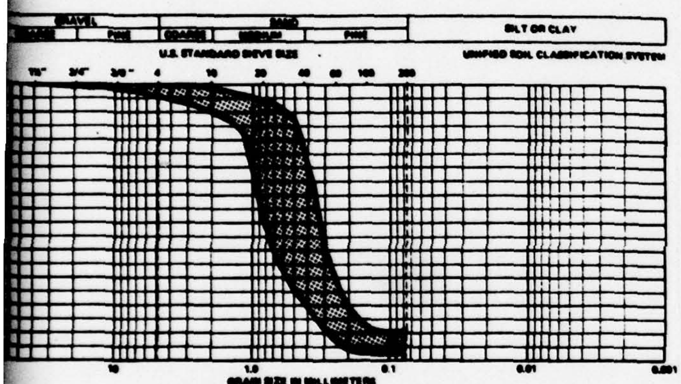

Stratigraphic Unit G

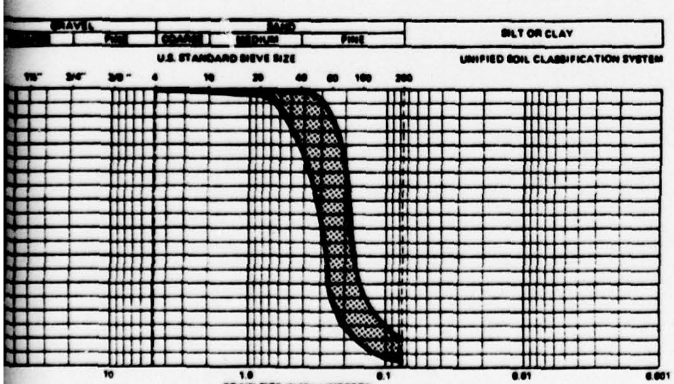

Stratigraphic Unit H

2

CHEMICAL GROUTING TEST PROGRAM

GRAIN-SIZE DISTRIBUTION OF STRATIGRAPHIC UNITS UNDERLYING TEST AREA

FOUNDATION INVESTIGATION AND TEST PROGRAM
EXISTING LOCKS AND DAM No. 26
ST LOUIS DISTRICT, CORPS OF ENGINEERS.
DACW43-78-C-0008

Woodward-Clyde Consultants

Y7C825 Phase IX

Fig. 3.9

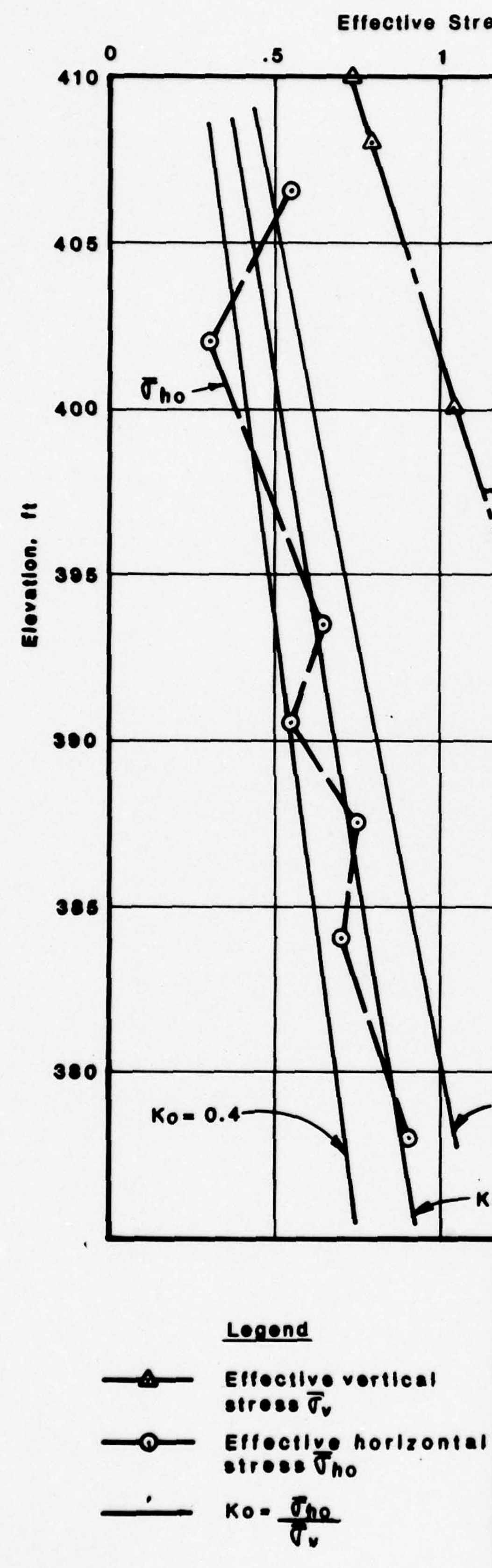

CHEMICAL GROUTING TEST PROGRAM

IN SITU STRESS PROFILE BEFORE GROUTING

FOUNDATION INVESTIGATION AND TEST PROGRAM
EXISTING LOCKS AND DAM No. 26
ST LOUIS DISTRICT, CORPS OF ENGINEERS.
DACW43-78-C-0005

Woodward-Clyde Consultants

Y7C825 Phase IX

Fig. 3.10

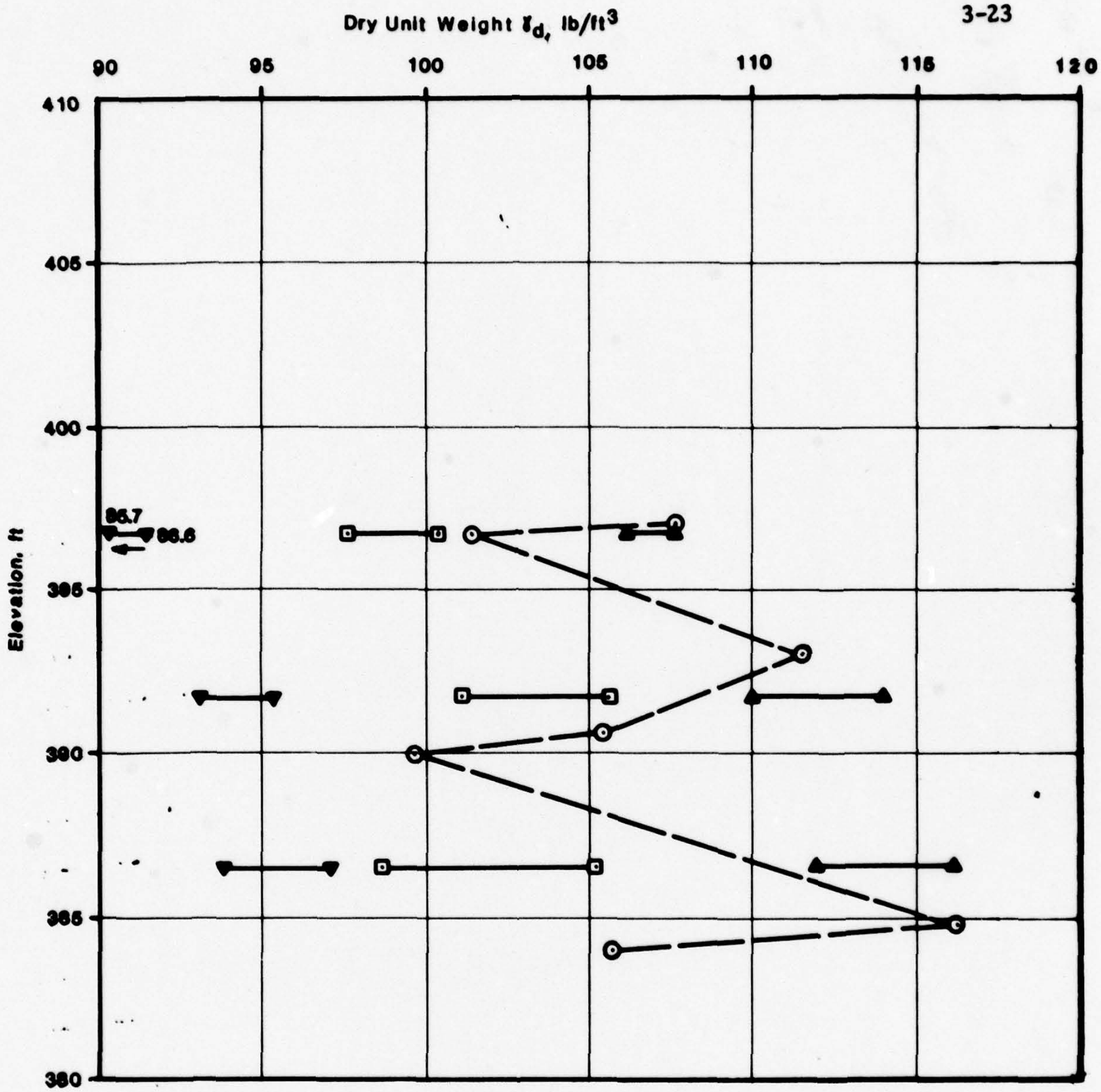

Legend

- In-place dry unit weight from excavation
- Lab dry unit weight
- Minimum dry unit weight
- Maximum dry unit weight

CHEMICAL GROUTING TEST PROGRAM

SOIL UNIT WEIGHT PROFILE BEFORE GROUTING

FOUNDATION INVESTIGATION AND TEST PROGRAM
EXISTING LOCKS AND DAM No. 26
ST LOUIS DISTRICT, CORPS OF ENGINEERS.
DACW43-78-C-0068

Woodward-Clyde Consultants | **Fig. 3.11**

Y7C828 Phase III

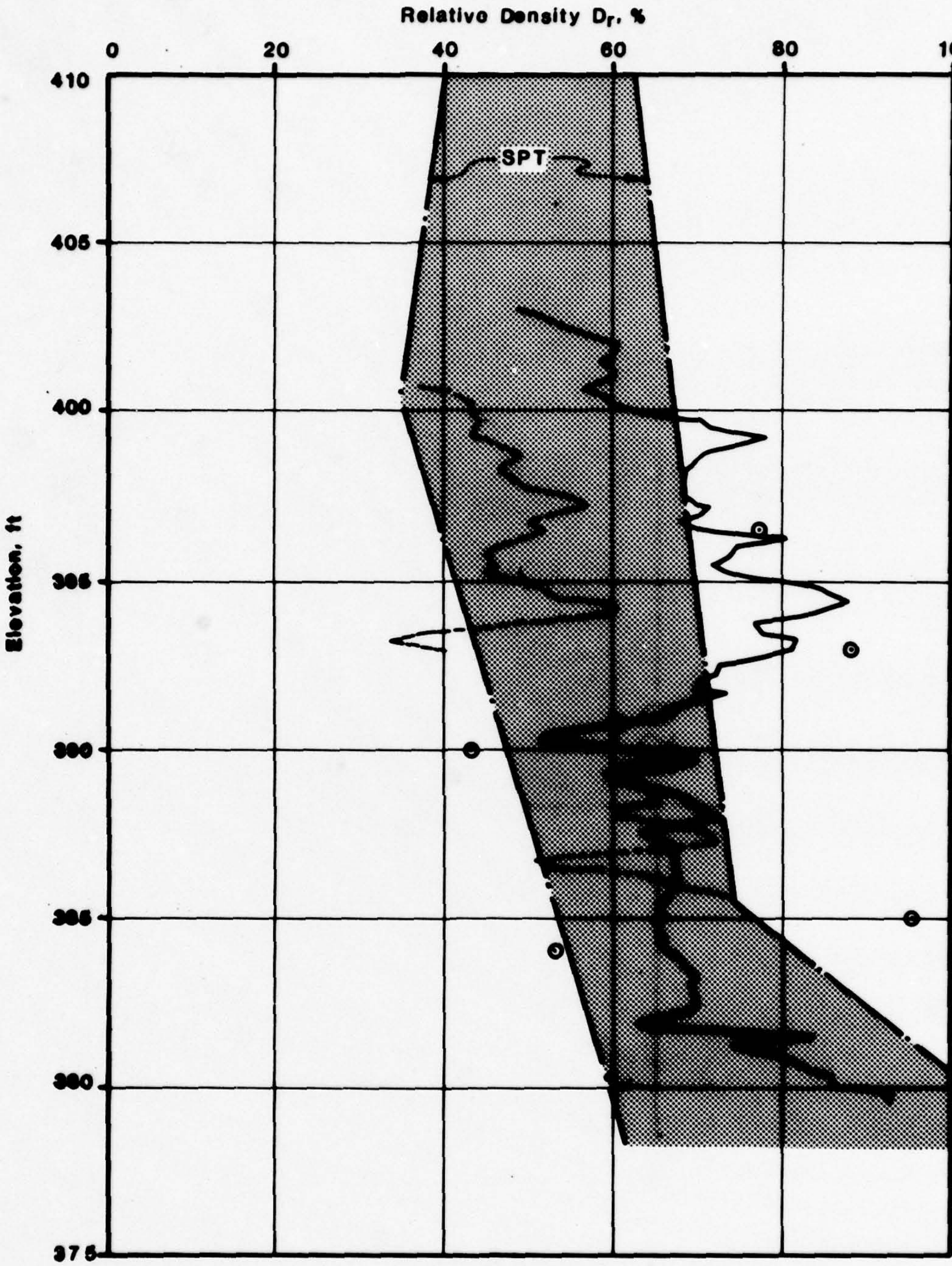

Legend

---- Boring D-23
—— Boring D-26
Determined from cone penetration resistance using Schmertmann's (1976) correlation

Determined from SPT using Gibbs and Holtz (1953) relationship. Borings D-21, D-22, D-23, D-26, D-28, S-5, S-6

From in-place density tests and lab max-min density tests

CHEMICAL GROUTING TEST PROGRAM	
RELATIVE DENSITY PROFILE BEFORE GROUTING	
FOUNDATION INVESTIGATION AND TEST PROGRAM EXISTING LOCKS AND DAM No. 26 ST LOUIS DISTRICT, CORPS OF ENGINEERS. DACW43-78-C-0005	
Woodward-Clyde Consultants Y7C825 Phase II	Fig. 3.12

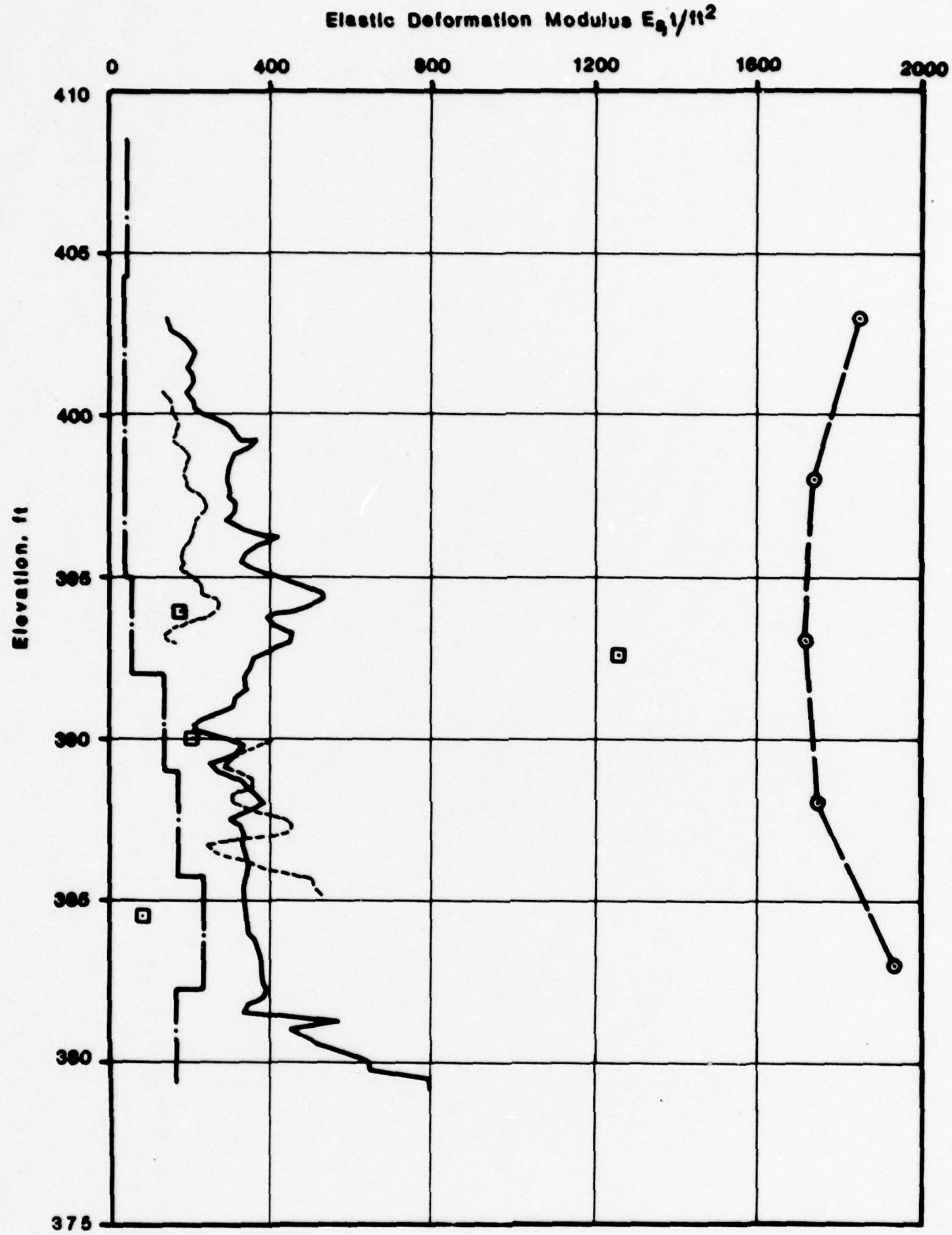

Legend

- - - - Boring D-23 } From cone penetration
——— Boring D-26 } tests

—·— From pressuremeter tests Boring D-27

□ From plate load tests

○ From cross-hole shear wave velocity measurements

CHEMICAL GROUTING TEST PROGRAM

ELASTIC DEFORMATION MODULI PROFILE BEFORE GROUTING

FOUNDATION INVESTIGATION AND TEST PROGRAM
EXISTING LOCKS AND DAM No. 26
ST LOUIS DISTRICT, CORPS OF ENGINEERS.
DACW43-78-C-0008

Woodward-Clyde Consultants

Y7C825 Phase IX

Fig. 3.13

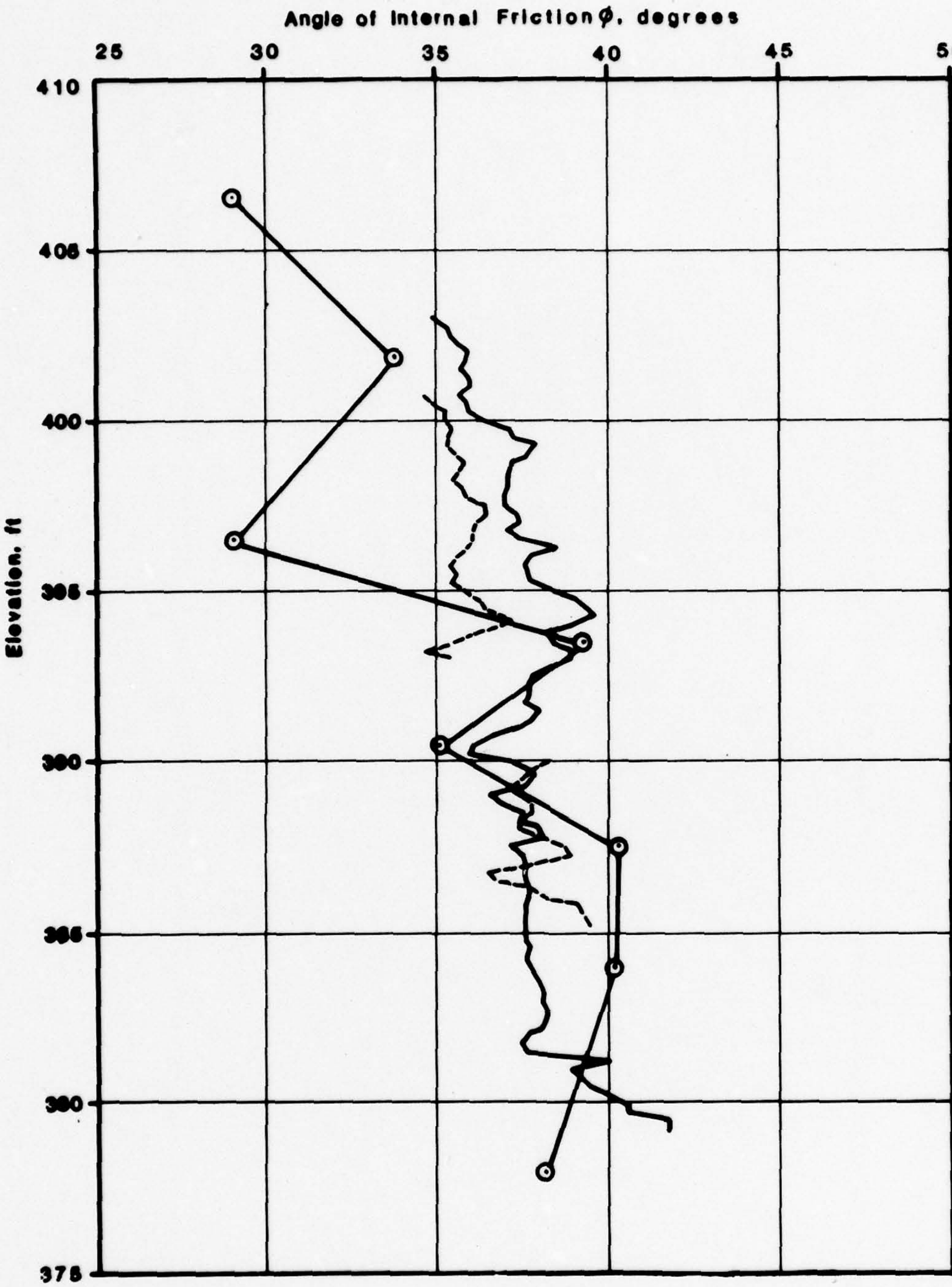

Legend

- - - - - Boring D-23 } From static cone penetration point resistance using Meyerhof (1974) correlation

——— Boring D-26 }

—o—·— Boring D-27 From pressuremeter tests using Hughes, Wroth & Windle (1977) approach

CHEMICAL GROUTING TEST PROGRAM

ANGLE OF INTERNAL FRICTION PROFILE BEFORE GROUTING

FOUNDATION INVESTIGATION AND TEST PROGRAM
EXISTING LOCKS AND DAM No. 26
ST LOUIS DISTRICT, CORPS OF ENGINEERS.
DACW43-78-C-0005

Woodward-Clyde Consultants

Y7C825 Phase IX

Fig. 3.14

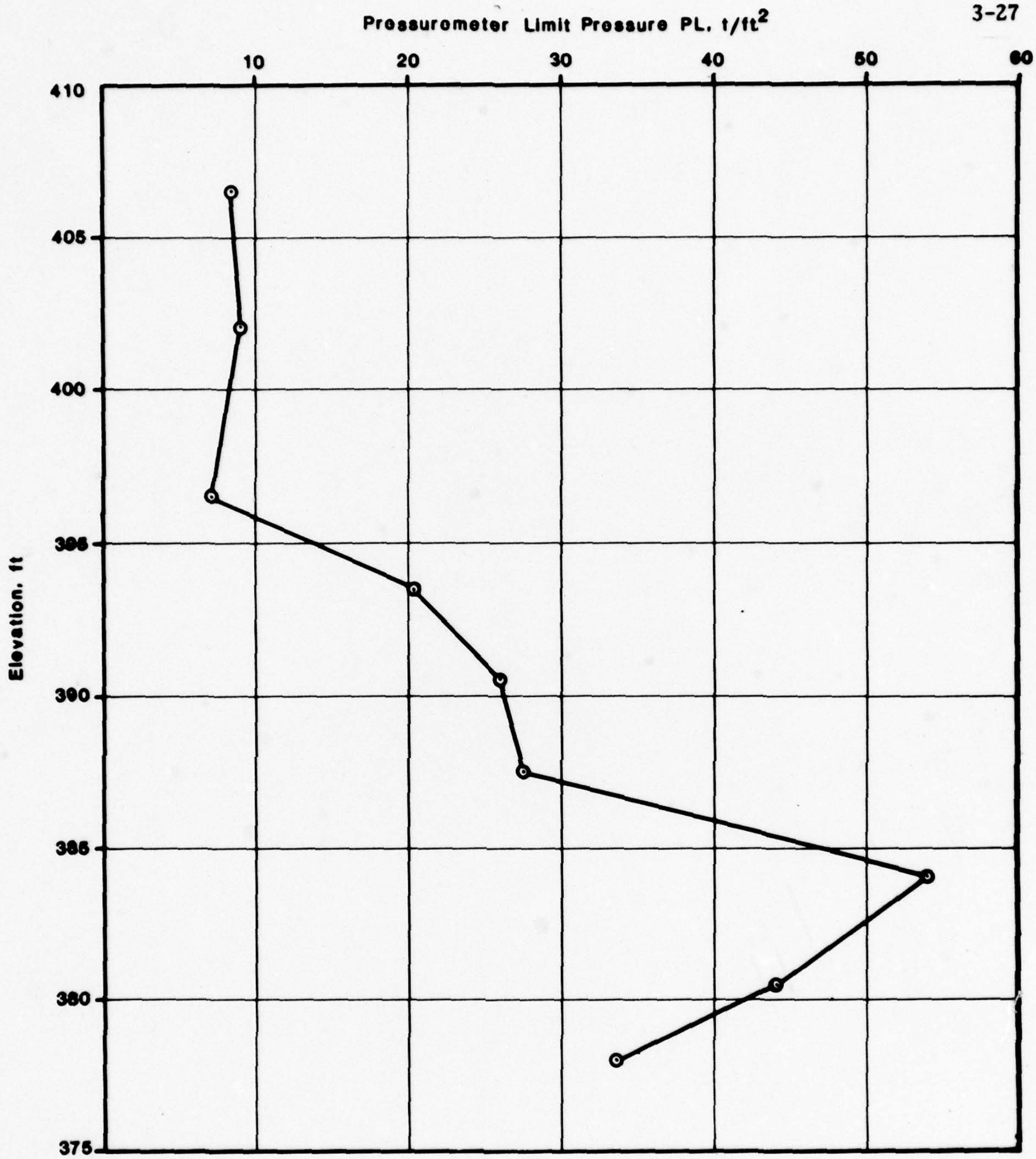

CHEMICAL GROUTING TEST PROGRAM

PRESSUREMETER
LIMIT PRESSURE PROFILE
BEFORE GROUTING

FOUNDATION INVESTIGATION AND TEST PROGRAM
EXISTING LOCKS AND DAM No. 26
ST LOUIS DISTRICT, CORPS OF ENGINEERS.
DACW43-78-C-0005

Woodward-Clyde Consultants
Y7C825 Phase IX

Fig. 3.15

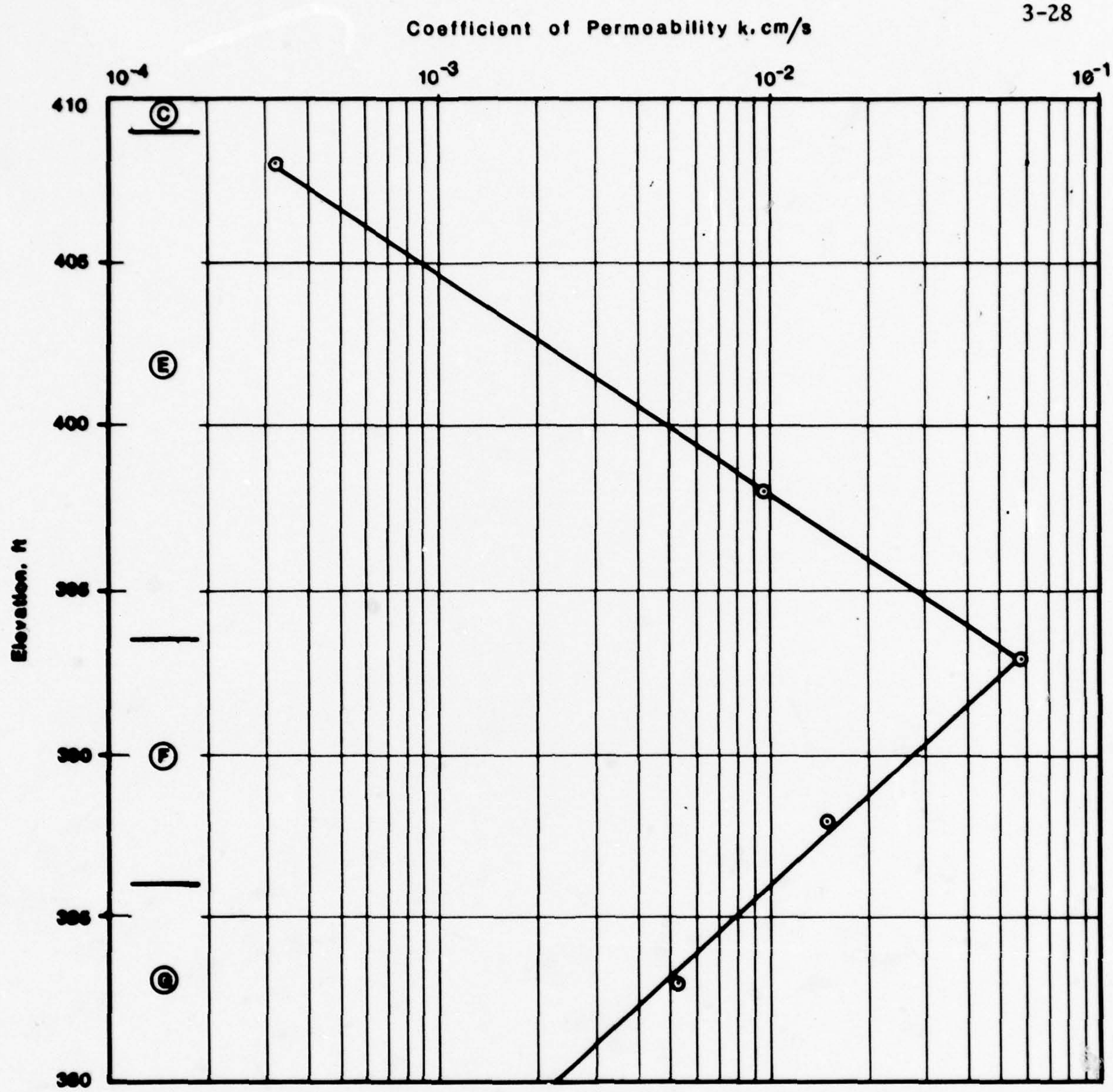

Note

k measured by falling head borehole permeability tests

Legend

(E) Stratigraphic unit E

CHEMICAL GROUTING TEST PROGRAM

COEFFICIENT OF PERMEABILITY PROFILE BEFORE GROUTING

FOUNDATION INVESTIGATION AND TEST PROGRAM
EXISTING LOCKS AND DAM No. 26
ST LOUIS DISTRICT, CORPS OF ENGINEERS.
DACW43-78-C-0005

Woodward-Clyde Consultants

Y7C825 Phase IX

Fig. 3.16

PHASE IV REPORT

VOLUME II

RESULTS AND INTERPRETATION OF
CHEMICAL GROUTING TEST PROGRAM

SECTION 4

GROUTING PLANT

4 GROUTING PLANT

4.1 DESCRIPTION

4.1.1 General

All electrical, mechanical and pneumatic equipment required for storing and diluting grout components; proportioning, mixing, metering, and pumping grout; and monitoring grout pumping pressure and flow rate were assembled in a modular grouting plant. The plant consisted of four modules, compact enough to be transportable by truck. Each module could perform independent grouting tasks, or could be combined with one or more other modules to form units of larger capacity. Photographs of the grouting plant are shown in Fig. 4.1 and 4.2.

4.1.2 Module 1

Module 1 was designed to proportion, dilute, and store the various silicate-based grout components. It included:

(1) one high-speed mixer (16*) for diluting concentrated sodium silicate;

(2) one tank (14) for storing diluted sodium silicate;

(3) one pump (15) for supplying diluted sodium silicate out of tank 14 to other modules;

(4) one mixer (17) for dissolving solid grout components (sodium aluminate and calcium chloride);

(5) two tanks (12 and 13) for storing solutions of sodium aluminate and calcium chloride; and

(6) one tank (11) for storing formamide or R600 reactants.

4.1.3 Module 2

Module 2 was the main pumping unit for the chemical grouts. Module 2 was a highly automated equipment capable of proportioning and mixing the various grout components, pumping grout into four grout holes simultaneously, and monitoring the grouting parameters for each hole being injected. It included:

(1) one tank (24) for proportioning and mixing up to four grout components. This tank was called "mother unit", because of its important role in the grout fabrication;

(2) one piston pump (22) receiving the grout from the mother unit and discharging it under pressure into secondary pumps;

---

* *Equipment code number is illustrated in Fig. B.1 through Fig. B.3, Appendix B, Volume IIA*

(3) four secondary reciprocating pumps (25 through 28). These pumps were actually metering devices, each stroke of their reciprocating pistons displacing exactly one liter (0.26 gal) of grout, thus their name "grout counters". The grout counters were connected directly to the grout pipes; and

(4) a control panel (23) where all control, monitoring and recording equipments were gathered, including controls for rate of pumping, four grout counters (stroke recorders), five pressure gages and five pressure recorders; and

(5) an electrical distribution panel.

4.1.4 Module 3

Module 3 was designed for injection of solid suspensions, such as cement-bentonite grout. The cement-bentonite grout was directly injected using the main grouting pump, without going through grout counters, because of the high pressure required to inject the more viscous grout and to avoid the abrasive effects of cement grains on the grout counters pistons and cylinders. Module 3 was also used to inject chemical grout when Module 2 was being used for another grout. Module 3 consisted of:

(1) two metering tanks (31 and 32);

(2) two piston pumps (33 and 34) similar to pump 22 of Module 2, receiving the grout from the metering tanks and directly connected to one grout pipe each; and

(3) an electrical panel comprising all 60-Hz switches for the grouting plant, and a generator providing 50-Hz* AC current to Module 2 and Module 3.

4.1.5 Module 4

Module 4 was an independent unit primarily used to proportion and mix grout to be injected through Module 3, while the mother unit was being used with another type of grout. Module 4 was used for cement-bentonite grout, 25% silicate/aluminate grout, and, at times, for 45% Siroc 142 grout. It consisted of:

(1) two proportioning tanks (42 and 42a); one for proportioning sodium aluminate, or calcium chloride and formamide; the other for proportioning diluted sodium silicate;

(2) one mixer (43) connected to the water line and tanks 42 or 42a, and discharging into buffer tank 44;

(3) one buffer tank (44); and

---

* *Most of the plant was from Europe, thus the 50-Hz electrical power requirements*

(5) one pump (41) intaking from buffer tank 44 and discharging into metering tanks 31 and 32 of Module 3.

4.2 OPERATION

4.2.1 Grouting Plant Operation Through Module 2

Module 2 was used for injection of the following grouts;

(1) 35% Siroc 142;

(2) 45% Siroc 132

(3) 55% Siroc 132 and 142;

(4) 25% silicate/aluminate

(5) 46% silicate/R600; and

(6) 28% silicate/R600.

The operation of the grouting plant through Module 2 for preparation and injection of Siroc and silicate/R600 grouts is illustrated in Fig. B.1 and Fig. B.2, Appendix B, Volume IIA, respectively.

4.2.2 Grouting Plant Operation Through Module 4

Module 4 was used for injection of the following grouts;

(1) cement-bentonite grout, in connection with Module 3;

(2) 25% silicate/aluminate grout, when another chemical grout was being prepared using the mother unit of Module 2; and

(3) 45% Siroc 132, after it became apparent that premixing formamide and sodium aluminate in proportioning tank 42 before adding the sodium silicate, reduced the formation of lumps in the grout. Until that time, Siroc grouts had been prepared in the mother unit of Module 2 by mixing sodium aluminate and silicate first, then adding the formamide.

The operation of the grouting plant through Module 4 for preparation and injection of silicate grouts is illustrated in Fig. B.3, Appendix B, Volume IIA.

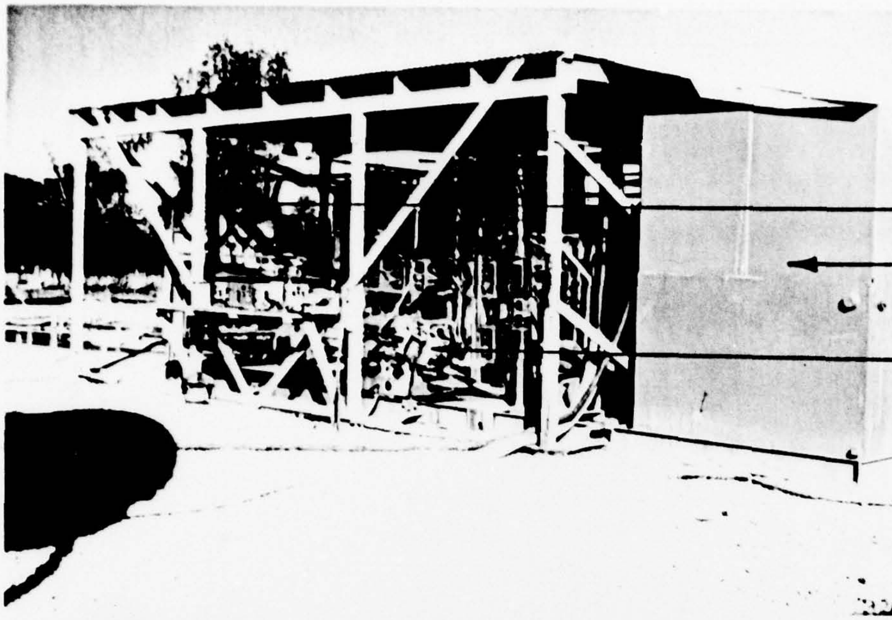

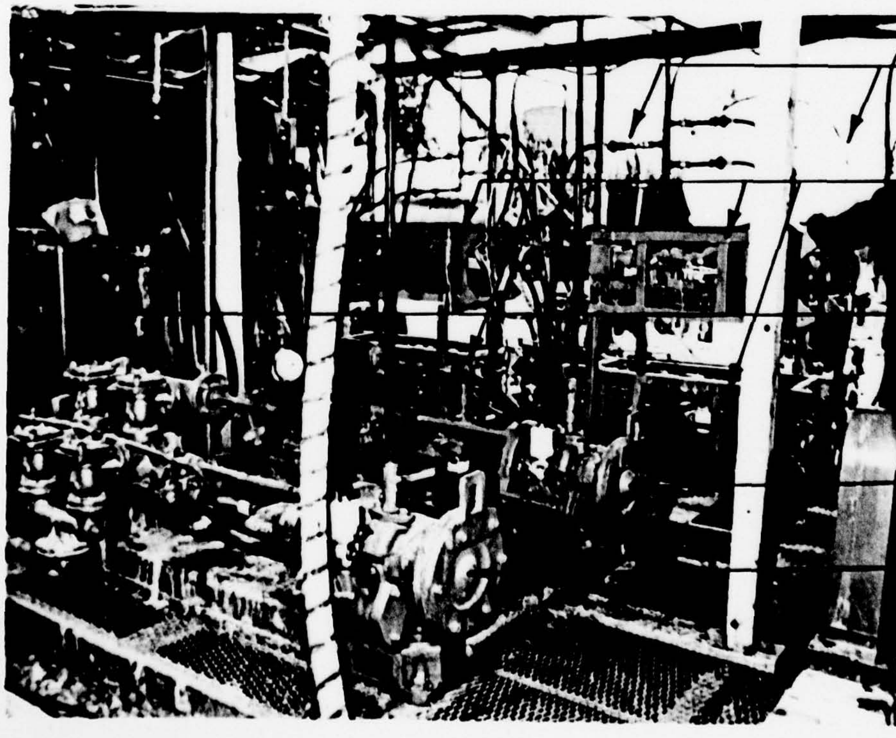

Grouting Contractor:

Raymond/Soletanche, Joint Venture

CHEMICAL GROUTING TEST PROGRAM

VIEWS OF MODULAR
GROUTING PLANT

FOUNDATION INVESTIGATION AND TEST PROGRAM
EXISTING LOCKS AND DAM No. 26
ST. LOUIS DISTRICT, CORPS OF ENGINEERS
DACW43-78-C-0005

Woodward-Clyde Consultants

Fig. 4.1

Y7C825 Phase IV

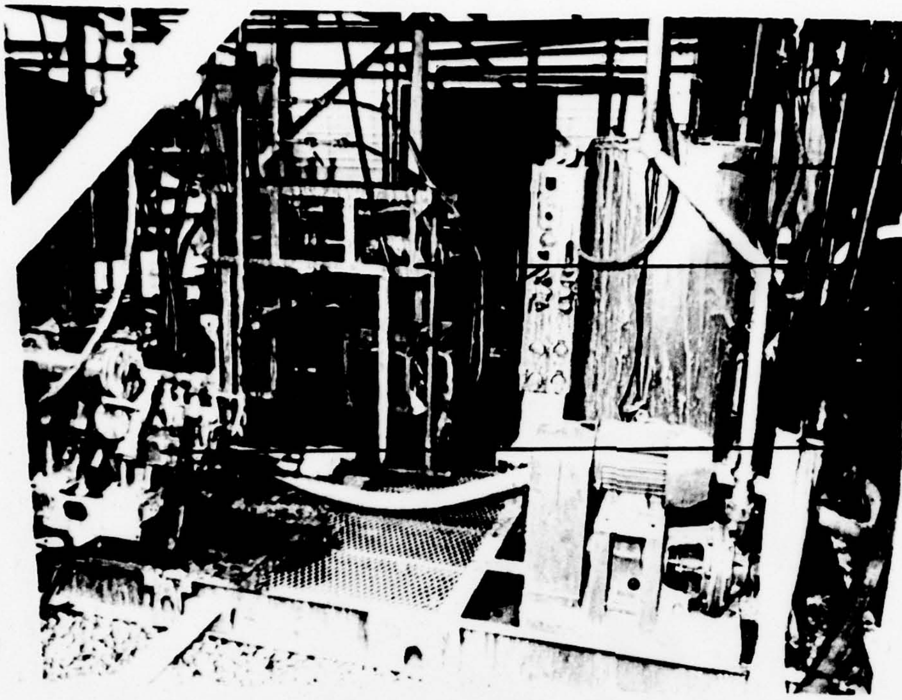

Mother Unit 24

"Grout Counters" 25,27

Grout pump 22

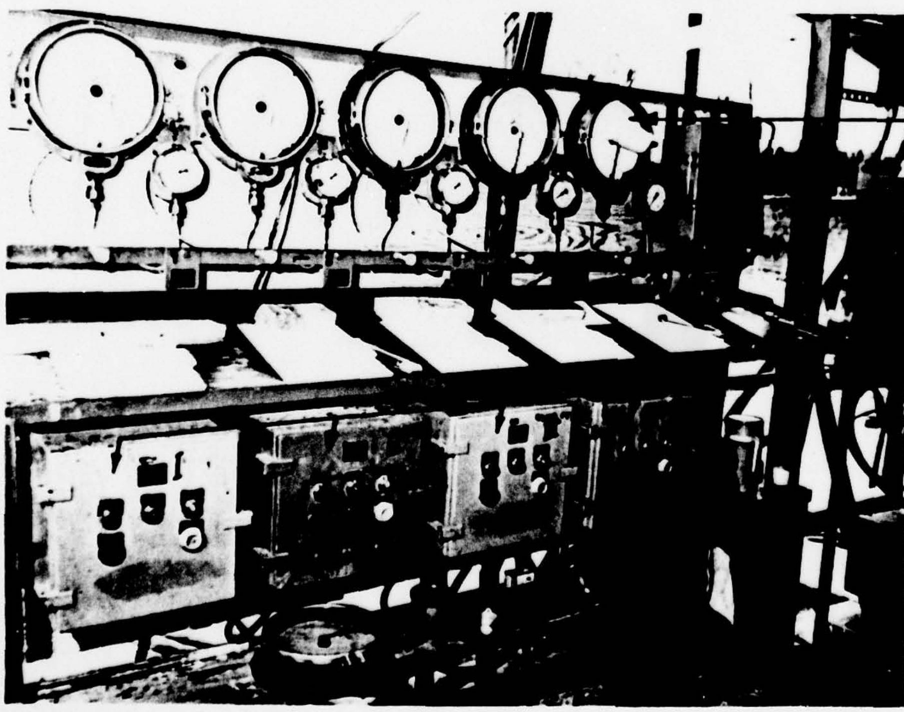

Pressure recorders

Pressure gages

"Grout Counter" stroke recorders and rate of pumping controls

Grouting Contractor:

Raymond Solentanche, Joint Venture

CHEMICAL GROUTING TEST PROGRAM

VIEWS OF MODULAR GROUTING PLANT

FOUNDATION INVESTIGATION AND TEST PROGRAM

EXISTING LOCKS AND DAM No. 26

ST. LOUIS DISTRICT, CORPS OF ENGINEERS.

DACW43-78-C-0005

Woodward-Clyde Consultants

Fig. 4.2

Y7C825 Phase IX

PHASE IV REPORT

VOLUME II

RESULTS AND INTERPRETATION OF
CHEMICAL GROUTING TEST PROGRAM

SECTION 5

GROUTS

5 GROUTS

5.1 LABORATORY TESTS

5.1.1 General

During the course of the chemical grouting test program, laboratory tests were made to study grout and grouted sand properties. This section describes the tests made on grouts, grout components, and reconstituted sand samples grouted in the laboratory.

5.1.2 Preliminary Tests on Grouts

Purpose. A preliminary grout testing program was implemented in April in WCC Plymouth Meeting, Pennsylvania laboratory. The purpose of those tests was to confirm the compositions of the grouts proposed for field testing, to measure and document the properties of grout components and grout mixes, and to establish criteria, procedures and testing equipment requirements for field quality control.

Grout Compositions. Grout compositions were established on the basis of Phase II work and information provided by the grouting contractor. For all grouts, mixing water was groundwater obtained from boreholes drilled in the test area. The chemical grouts were prepared with sodium silicate (Grade 40) manufactured by Diamond Shamrock. The proportions of sodium silicate and reactants selected for this testing were established with the assistance of the grouting contractor to attempt to achieve a setting time of approximately 1 hour at 68°F (20°C) for both low-strength and high-strength silicate grouts.

The cement-bentonite grouts were proportioned to achieve a relatively high-strength grout for use as sleeve grout, and a relatively low-strength grout for use in first stage grouting before injection of chemical grout. The composition of the grouts tested in the laboratory are given in Table 5.1.

The grouts were prepared in 1-gal batches. The reactants were dissolved and mixed in a separate container, then poured into the sodium silicate while the mixture was mechanically agitated. This mixing procedure was generally successful in producing a homogeneous grout, except for 55% Siroc 142. For this grout, lumps could not be avoided. Lumps also occurred during preparation of this grout in the grouting plant at the test site.

Water Quality. Samples of test area groundwater and Mississippi River water were analyzed to assess the suitability of these waters for chemical grout fabrication. The results of these tests are presented in Table 5.2. This table also shows the results of groundwater analyses reported by McClelland Engineers (1975).

Properties of Pure Grouts. The following properties of pure grouts were measured:

(1) unit weight before setting;

(2) viscosity immediately after mixing and as a function of time elapsed after mixing, using a Brookfield Synchro-Lectric Viscometer, Model LV;

(3) setting time as recommended by Tallard and Caron (1977);

(4) shear strength after setting and as a function of time elapsed after mixing, using a shear vane (Wickerham-Farrance miniature vane, Model IV), pocket penetrometer (Soiltest Model CL-700), Proctor Penetrometer (Soiltest, Model CN-419), or unconfined compression tests (ASTM D 2166-66); and

(5) shrinkage, that is, the ratio of the volume of synergic liquid over the initial volume of grout.

The results of these tests are presented in Table 5.3.

5.1.3 Tests on Reconstituted Sand Samples Grouted in the Laboratory

Purpose. Consistent with laboratory tests conducted at the Waterways Experiment Station, Corps of Engineers (WES), a low-strength grout (35% Siroc 142) was selected to study the effectiveness of chemically grouting granular soil similar to that underlying Locks and Dam No. 26. The laboratory tests were conducted in WCC's Plymouth Meeting laboratory.

Sand Sample Preparation Procedure. All sand samples to be grouted in the laboratory were prepared from a mixture of natural sand recovered between el 380 and el 400 in borings D-21, D-22, and D-23 drilled in the chemical grouting test area (Fig. 3.1). Average index and physical properties of the sand to be grouted were determined (grain-size distribution, water content, maximum-minimum unit weight). The sand was grey, medium to fine with trace of gravel and trace of silt. The results of these measurements are presented in Fig. 5.1. On the basis of Phase II investigations, the average in situ relative density of the recent alluvial deposit was estimated to be approximately 70 percent. Samples of sand to be grouted were reconstituted at a relative density of 70 percent. The reconstituted sand samples had the following average characteristics:

Diameter:	2.822 in.
Height:	6.60 in.
Dry Unit Weight:	107.9 lb/ft^3
Water Content:	16.2 percent
Total Unit Weight:	125.4 lb/ft^3

To provide a basis for comparison with grouted sand samples, three isotropically consolidated drained ($\overline{CID}$) triaxial compression tests were performed on ungrouted, reconstituted sand samples. The results of these tests are shown in Fig. C.1, Appendix C. From the test results, the following strength parameters were determined for the ungrouted sand:

cohesion intercept, $c = 0.1\ t/ft^2$

Friction angle, $\phi = 39.5°$

Sand Sample Grouting Procedure. The reconstituted sand samples were saturated and grouted under a back pressure equivalent to the average in situ water pressure anticipated in the field at midpoint of the grouted zone. The apparatus used for grouting the samples was designed and constructed for this purpose. It consists of three parts (Fig. 5.2):

(1) four sample reconsitution tubes;

(2) four saturating tanks; and

(3) a grouting tank assembly.

The sample reconstitution tubes were lined with a 2.82-in.-dia, 6-to 8-in.-long, lucite, split tube. The saturation tanks could allow the sand samples to be saturated under a backpressure as high as 140 lb/in^2. Actually, the samples were saturated under a backpressure of 6.5 lb/in^2 during grouting. The grouting tank assembly included an agitation system and a four-way T manifold that allowed four samples to be grouted simultaneously while the grout was kept under agitation.

The grout used for these tests had the following composition (35% Siroc 142):

Sodium Silicate:	35 percent
Formamide:	6 percent
Sodium Aluminate:	0.0179 g/cm^3 (15 lb/100 gal of grout)
Water:	58 percent

The grout was injected at the bottom of the sand samples. The grouting pressure was first set at 6.5 lb/in^2 (that is, equal to the backpressure), then increased to 33 lb/in^2 in three increments. The grouting pressure of 33 lb/in^2 was selected because it represents a pressure of 1 lb/in^2 per foot of soil above the mid-point of the zone to be grouted in the test area. Grouting was continued until grout filled up the upper space above the sand samples.

Curing of Grouted Sand Samples. The grouted sand samples were cured in the lucite split-liner for 24 hours in 100 percent humidity. The samples were then submerged in groundwater in a curing tank pressurized to 6.5 lb/in^2. This pressure corresponds to the average hydrostatic groundwater pressure at mid-point of the grouted zone (see Section 9.5.2).

This curing method was selected to simulate expected field conditions and after the following observations were made on early samples:

(1) air curing results in large syneresis and slight reduction in strength;

(2) unpressurized water curing results in very little syneresis and large reduction in strength; and

(3) humid-room curing results in little syneresis and no reduction in strength.

Scope of Testing. The following tests were made on grouted sand samples:

Unconfined compression (Strain rate = 0.5%/min)	*3 tests at 2-day curing time*
	2 tests at 7-day curing time
	3 tests at 28-day curing time
	1 test at 84-day curing time
Unconfined compression at other strain rates: (ESR)	*3 tests at 28-day curing time*
Long-term unconfined compression (creep tests):	*4 tests at 28-day curing time*
Triaxial compression ($\overline{CID}$):	*2 series of 3 tests at 7-day curing time*
	2 series of 3 tests at 28-day curing time
	1 series of 3 tests and 2 tests at 84-day curing time
Long-term triaxial compression (creep tests):	*3 tests at 84-day curing time*
Permeability:	*6 tests at 7-day curing time*
	6 tests at 28-day curing time
	2 tests at 84-day curing time

Test results are presented in the following paragraphs and are discussed further in Section 9.5.

Unconfined Compression Tests. All samples were tested at a strain rate of 0.5 percent per minute. The tests were continued to failure or to 20 percent axial strain, whichever occurred first. The results of the tests are presented in Table 5.4 and in Fig. C.2, Appendix C, Volume IIA.

Triaxial Compression Tests. Consolidated drained ($\overline{CID}$) triaxial compression tests (Bishop and Henkel 1962) were conducted on grouted samples. The samples were isotropically consolidated with a backpressure of approximately 20 lb/in^2 to obtain a high degree of saturation. After consolidation, the samples were tested for permeability and then sheared under drained conditions at an axial strain rate of approximately 0.15 percent per minute. The results of the tests are presented in Table 5.5 and in Fig. C.3 through Fig. C.8, Appendix C, Volume IIA.

Permeability Tests. Constant-head permeability tests were conducted on all $\overline{CID}$ specimens at a backpressure of 20 lb/in^2 (Lambe 1951). Immediately following consolidation but prior to shearing, a series of permeability measurements were made on triaxial samples. The permeant was de-aired water. The results are tabulated in Table 5.5.

Creep Tests. Four long-term unconfined compression tests were made on sand samples grouted in the laboratory following a procedure used by Clough et al (1979). The samples were cured for 28 days. A constant axial stress of 15, 25, 37, or 50 percent of the average unconfined compressive strength obtained from tests made at a strain rate of 0.5 percent per minute was applied for approximately 8 days. The results of unconfined compression creep tests are presented in Fig. 5.3.

Three long-term triaxial compression tests ($\overline{CID}$) were also made on grouted sand samples cured for 84 days. The samples were consolidated at 2 t/ft^2 and loaded in steps up to a constant deviator stress equivalent to 40, 59, and 79 percent of the maximum deviator stress $(\sigma_1-\sigma_3)_{max}$ obtained from a reference $\overline{CID}$ test made at a strain rate of 0.15 percent per minute. The results of the triaxial compression creep tests are presented in Fig. 5.4.

Effects of Strain Rate. Three reconstituted grouted sand samples were tested in unconfined compression at strain rates of 0.34 and 0.15 percent per minute. The tests were to assess the effects of low strain rates on the ultimate strength of the grouted sand. The results are presented in Table 5.4 and Fig. C.2, Appendix C, Volume IIA.

5.1.4 Investigation of Grout Neutralization Ratio

Purpose. Sodium silicate in aqueous solution transforms into a gel under the action of appropriate reactants. The properties of that gel are determined by the silicate content of the sodium silicate solution (volume of silicate/volume of silicate plus water), the reactant ratio of the grout mixture (weight or volume of reactant(s)/volume of silicate), and the neutralization ratio R_N of the solidified gel (weight of sodium neutralized by reactant/initial weight of sodium in the sodium silicate solution). A laboratory investigation was undertaken in July 1978 to measure the neutralization ratios of sodium silicate gels produced by grouts similar to those used in the field tests. This investigation was conducted by Dr Gerardine Meerman in New Jersey.

Mechanism of Gelation of Sodium Silicate Grouts. Sodium silicate is stable only in some basic solutions. Upon acidifying, an unstable silicic acid is formed. The unstable silicic acid rapidly loses water to form a series of partially hydrated polymerized silicas. Theoretically, any acid will cause gelation. However, in grouting applications, the neutralization of the basic sodium silicate solution is controlled by the slow release of hydrogen ions produced by hydrolisis of a reactant, usually an organic compound such as formamide or an aliphatic ester (R600, dimethyl succinate). Inorganic reactants such as calcium chloride and sodium aluminate are also used.

The polymerization of the silicic acid, described above, normally continues until all monosilicic and polysilicic ions are bound together to form a solid gel. Water, sodium salts, unused reactants, and non-neutralized sodium silicate remaining within the gel structure are slowly released in a liquid form. This phenomenon is called syneresis, and the liquid expelled from the gel structure is called synergic liquid.

Principle of Neutralization Ratio Determination. The neutralization ratio was determined by titration of the hydroxyl ions in the synergic liquid. The following assumptions were made:

(1) all non-neutralized sodium silicate was expelled from the gel structure during syneresis;

(2) the silica/sodium ratio* (SiO_2/Na_2O) of the non-neutralized sodium silicate in the synergic liquid remained the same as that of the initial sodium silicate solution;

(3) the sodium salts and unused reactants contained in the synergic liquid did not interfer with the titration of the hydroxyl ion; and

(4) the number of excess hydroxyl ions in the synergic liquid was equal to the number of excess sodium ions.

The neutralization ratio was calculated as:

$$R_N = \frac{\text{Initial Volume of NaOH - Volume of NaOH in Synergic Liquid}}{\text{Initial Volume of NaOH}}$$

Results and Interpretation. The unit weight of the sodium silicate grade 40 used for grout preparation was found to be 1.38 g/cm^3. The ratio weight of sodium oxide/weight of sodium silicate was found to be 0.0733. The neutralization ratios determined for all samples tested are presented in Table 5.6. The data indicate that the measured neutralization ratios were generally about one. This would imply that, under the conditions of this investigation, all hydroxyl ions initially present in the sodium silicate solution had been neutralized and that none were found in the synergic liquid. Tests made by Soletanche (1978), however, indicated that for a 50% silicate/R600 grout having a R600 concentration of 8.7 percent by volume, the neutralization ratio was 0.54. For a similar type of grout with a R600 concentration of 6.9 percent, the neutralization ratio determined by Dr Meerman was almost 1.

Observations. During the course of this investigation, several observations were made that are of significance to grout chemistry. These observations are:

(1) no synergic liquid was observed after two days of curing in 25% silicate/aluminate grout samples. Some liquid was found in some samples after 5 days;

---

* *Grade 40 sodium silicate used in test program had a SiO_2/Na_2O ratio of 3.22*

(2) the synergic liquid of the silicate/R600 grouts consisted of two phases: a yellow aqueous liquid on top of a dark brown oily liquid. Infrared spectral examination disclosed that the oily liquid was pure R600. The presence of acidic R600 in the synergic liquid probably neutralized the hydroxyl ions, rendering the results of the titration unreliable; and

(3) the quantity of synergic liquid for Siroc grouts appeared to be a function of the size of the grout sample. The larger the grout sample, that is the larger the surface area, the larger the percentage of synergic liquid observed.

5.2 ON SITE LABORATORY TESTS

5.2.1 Purpose and Objectives

The purpose of the laboratory tests performed on site during the field implementation of the chemical grouting test program was to document the properties of the grouts actually used, and to serve as quality control. The objectives were:

(1) measure the physical properties of the various grouts and compare them to data previously obtained in the laboratory (Section 5.1.2) and data provided by the grouting contractor;

(2) control the uniformity of grout quality and use the test results to modify grout composition, if required; and

(3) obtain additional data regarding grout strength to correlate with properties of sand grouted in situ.

5.2.2 Grout Components and Fresh Grouts

Sodium Silicate. The following properties and characteristics of both undiluted and diluted sodium silicate were measured regularly at the site:

(1) temperature;

(2) viscosity;

(3) unit weight; and

(4) degree Baume.

Water. Water temperature was monitored at the well and at the storage tank before use in grout fabrication.

Fresh Grouts. The following properties and characteristics of fresh grouts were measured regularly at the site:

(1) temperature;

(2) unit weight;

(3) viscosity;

(4) degree Baume; and

(5) setting time.

Frequency of Testing. For each 8-hour shift, the following number of tests were made, on the average, on grout components and fresh grouts.

Material	Temp	Unit Weight	Degree Baume	Viscosity	Setting Time
Well Water	2	-	-	-	-
Tank Water	2	-	-	-	-
Diluted Sod Silicate	1	1	1	1	-
Concentrated Sod Silicate	1	1	1	1	-
Each Type of Grout	4	4	4	4	4

5.2.3 Set Grouts

During the field implementation of the chemical grouting test program, samples of pure grout were preserved and cured. The shear strength of the samples was measured with a Wickerham-Farrance miniature vane and an unconfined compression test machine, depending on the strength of the set grout.

5.2.4 Results

The average values of the various properties measured in the site laboratory on sodium silicate and grout samples are presented in Table 5.7 and are briefly discussed below.

Sodium Silicate. The average degree Baume measured at the site was 40.7°, slightly less than the value of 41.5° expected for sodium silicate Grade 40. At 68°F, the average measured viscosity was 114.6 cp, compared to the expected value of 206 cp.

35% Siroc 142. The unit weight of 35% Siroc 142 measured in the on-site laboratory is in good agreement with the theoretical unit weight. No trend could be seen in the relationships of viscosity vs time or setting time vs temperature, probably because the grout composition was constantly adjusted during grouting. Very little or no syneresis was observed in samples of this grout. However, many lucite sample tubes were found cracked after a few days of curing. This could be attributed to the ammonia released during curing. This phenomenon was observed with all Siroc grouts.

45% Siroc 132. Only a relatively small quantity of this grout was used in the program. The few samples of 45% Siroc 142 tested in the on-site laboratory yielded results similar to those of 35% Siroc 142, except for higher viscosity and strength.

55% Siroc 132/142. The viscosity and setting time of 55% Siroc 132 and to a lesser degree of 55% Siroc 142 grouts were found to be erratic. The samples of 55% Siroc 132/142 were generally characterized by the presence of lumps in the liquid grout, and by the large volume of synergic liquid produced during curing. The hardened grout was always too hard to be tested with the miniature vane. The shape of the hardened grout samples was so distorted because of large syneresis, that trimming acceptable cylinders for unconfined compression tests was almost always impossible. For most samples, lower bound values of shear strength were obtained with a pocket penetrometer.

46% Silicate/R600. The viscosity and setting time of 46% Silicate/R600 grout were found to be constant. Results of strength tests were erratic, mostly due to testing difficulties. The large syneresis distorted the hardened grout samples, making it difficult to trim acceptable cylinders for unconfined compression tests. The samples of this grout exhibited a much more plastic behavior than the Siroc grouts. During curing, it was not uncommon to observe that the samples would creep under their own weight.

28% Silicate/R600. A relatively small quantity of this grout was used in the program, and only a few samples were tested. The amount of syneresis in these samples was significantly less than for the high-strength 45% silicate/R600, probably due to the lesser sodium silicate content in the mix. However, samples of 28% silicate/R600 exhibited a greater tendency to creep than samples of the higher strength grout.

25% Silicate/Aluminate. No syneresis was observed on samples of this low-strength grout. The strength of the pure grout was generally too low to be adequately measured with the testing equipment available in the on-site laboratory.

Cement-Bentonite. Results of tests on cement-bentonite grout samples were consistent with expected properties (Caron 1972).

5.3 GROUT COMPOSITIONS

The average composition of the grouts actually used during field implementation of the chemical grouting test program are given in the following sections.

5.3.1 Low-Strength Grouts

35% Siroc 142. Average composition for 100 gal of grout:

Sodium Silicate (Grade 40):	35 gal
Sodium Aluminate (dry):	8 to 12 lb

AD-A076 091 WOODWARD-CLYDE CONSULTANTS CHICAGO IL F/G 13/2

RESULTS AND INTERPRETATION OF CHEMICAL GROUTING TEST PROGRAM. V--ETC(U)

JUL 79 J PEREZ , Y LACROIX DACW43-78-C-0005

UNCLASSIFIED NL

2 OF 4

AD A076091

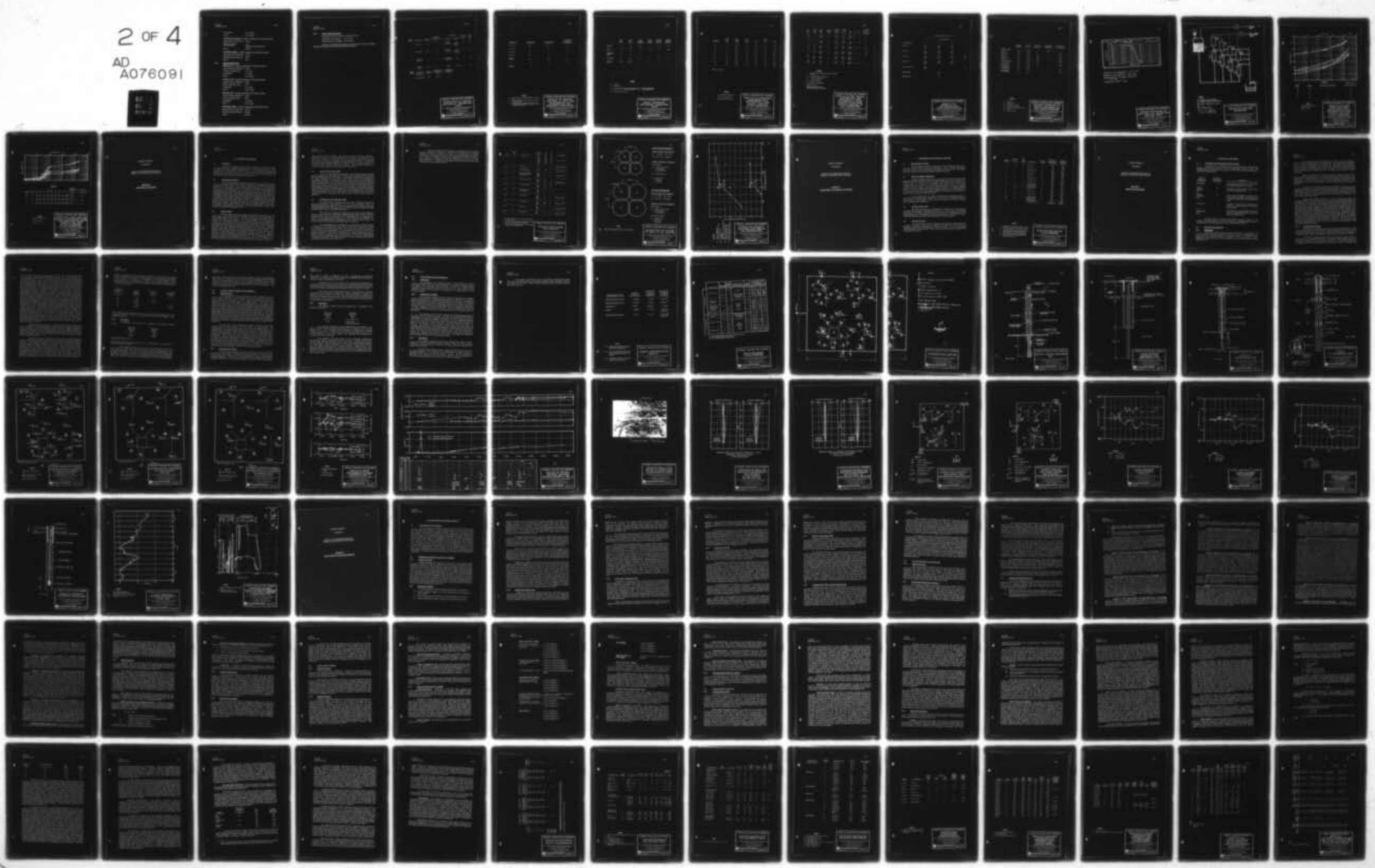

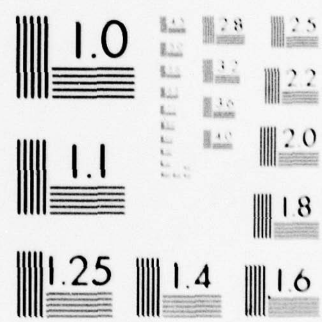

MICROCOPY RESOLUTION TEST CHART
NATIONAL BUREAU OF STANDARDS-1963-A

Formamide:	6 to 10 gal
Water:	55 to 59 gal

25% Silicate/Aluminate. Average composition for 100 gal of grout:

Sodium Silicate (Grade 40):	25 gal
Sodium Aluminate (10% Solution):	13 lb (approx 15 gal of solution)
Water:	60 gal

28% Silicate/R600. Average composition for 100 gal of grout:

Sodium Silicate (Grade 40):	28 gal
R600 (dimethyl succinate):	6 gal
Water:	66 gal

5.3.2 **High-Strength Grouts**

45% Siroc 132. Average composition for 100 gal of grout:

Sodium Silicate (Grade 40):	45 gal
Calcium chloride (dry):	5 to 11 lb
Formamide:	7 to 8 gal
Water:	47 to 48 gal

55% Siroc 142. Average composition for 100 gal of grout:

Sodium Silicate (Grade 40):	55 gal
Sodium Aluminate (dry):	10 lb
Formamide:	8 to 10 gal
Water:	35 to 37 gal

55% Siroc 132. Average composition for 100 gal of grout:

Sodium Silicate (Grade 40):	55 gal
Calcium Chloride (dry):	5.6 lb
Formamide:	8 to 10 gal
Water:	35 to 37 gal

46% Silicate/R600. Average composition for 100 gal of grout:

Sodium Silicate (Grade 40):	46.3 gal
R600 (dimethyl succinate):	7.4 gal
Water:	46.3 gal

5.3.3 Cement-Bentonite Grouts

The range of cement-bentonite composition was:

Cement/water by weight:	0.2 to 0.42
Bentonite/water by weight:	0.03 to 0.035

Cement was Portland Type III from Universal Atlas Cement Company. Bentonite was Quick Gel from Baroid Petroleum Services.

GROUT MIX NO.	GROUT TYPE	STRENGTH	QUANTITY OF SODIUM SILICATE gal	REACTANTS TYPE	REACTANTS QUANTITY	QUANTITY OF WATER gal	TOTAL VOLUME gal
1	35% Siroc 142	low	35	Formamide Sod Aluminate	7 gal 10, 15 or 20 lb/100 gal	58	100
2	55% Siroc 142	high	55	Formamide Calc Chloride	7 gal 10, 15 or 20 lb/100 gal	38	100
3	25% Silicate/ Aluminate	low	25	Sod Aluminate (10% Solution)	23 gal	52	100
4	45% Silicate R600	high	45	R600C	7.35 gal	55	100

GROUT MIX NO.	GROUT TYPE	STRENGTH	BENTONITE/WATER BY WEIGHT	CEMENT/WATER BY WEIGHT
5	Cement-Bentonite	low	0.03-0.04	0.3
6	Cement-Bentonite	high	0.03-0.04	0.4

CHEMICAL GROUTING TEST PROGRAM

COMPOSITION OF GROUTS PRELIMINARY LABORATORY TESTS

FOUNDATION INVESTIGATION AND TEST PROGRAM
EXISTING LOCKS AND DAM No. 26
ST LOUIS DISTRICT, CORPS OF ENGINEERS.
DACW43-78-C-0005

Woodward-Clyde Consultants

V7C525 Phase III

Table 5.1

TYPE OF TEST[3]	RIVER WATER[1]	GROUNDWATER[1]	REPLACEMENT SITE GROUNDWATER[2]
Hardness, ppm	284	330	347
Sulfate, ppm	30	20	2.7
Chloride, ppm	20	7	4
Sodium, ppm	57.5	8.5	5
Alkalinity at pH 4.5, ppm	169	268	343
pH	7.25	7.3	7.1
Acidity as $CaCO_3$, ppm	8	9	-

Notes

(1) *Tests made by Betz Environmental Engineers, Inc (BEE) for WCC*

(2) *Results reported by McClelland (1975) for Locks and Dam No. 26 replacement site*

(3) *BEE tests performed in accordance with "Standard Methods for the Examination of Water and Wastewater", American Public Health Association, 1971*

CHEMICAL GROUTING TEST PROGRAM

RESULTS OF CHEMICAL ANALYSES OF TEST AREA GROUNDWATER AND MISSISSIPPI RIVER WATER

FOUNDATION INVESTIGATION AND TEST PROGRAM
EXISTING LOCKS AND DAM No. 26
ST LOUIS DISTRICT, CORPS OF ENGINEERS.
DACW43-78-C-0006

Woodward-Clyde Consultants

Y7C026 Phase IX

Table 5.2

	35% SIROC 142	55% SIROC 142	25% SILICATE/ ALUMINATE	45% SILICATE/ R600	CEMENT/ BENTONITE c/w = 0.3	CEMENT/ BENTONITE c/w = 0.4
Unit weight lb/ft^3	71.7	76.4	68.4	-	72.7	79.5
Viscosity	6.5 (1)	15 (1)	7 (1)	8 (1)	35 (2)	35 (2)
Shear Strength at 28 days t/ft^2	1.2	1.2	~0	-	6	9
Shrinkage, % (3)	5.3	6.5	2.7	-	46	25
Setting time min	8.5 to 7.0	Erratic (4)	6	172	-	-

Notes

(1) *Centipoises*

(2) *Marsh Seconds*

(3) *Shrinkage* $= \dfrac{\text{Initial Volume of Grout - Volume of Solid Grout}}{\text{Initial Volume of Grout}} = \dfrac{\text{Volume of Synergic Liquid}}{\text{Initial Volume of Grout}}$

(4) *Too variable to be meaningful*

CHEMICAL GROUTING TEST PROGRAM

GROUT PROPERTIES PRELIMINARY LABORATORY TESTS

FOUNDATION INVESTIGATION AND TEST PROGRAM
EXISTING LOCKS AND DAM No. 26
ST LOUIS DISTRICT, CORPS OF ENGINEERS.
DACW43-78-C-0086

Woodward-Clyde Consultants

Y7C626 Phase IX

Table 5.3

SAMPLE NO.	CURING TIME days	UNIT WEIGHT lb/ft^3	STRAIN RATE %/min	q_u t/ft^2	STRAIN AT FAILURE %	E_{50} t/ft^2
13	2	124.0	0.5	2.05	3.04	68.8
14	2	125.1	0.5	1.49	3.21	41.1
33	2	122.2	0.5	2.16	1.69	140.2
2	7	125.6	0.5	2.16	2.17	192.4
12	28	123.0	0.5	2.08	1.69	188.4
15	28	124.7	0.5	1.56	2.05	127.4
20	28	125.0	0.5	2.43	1.38	280.5
22	28	125.3	0.15	1.57	1.87	116.6
23	28	125.0	0.34	2.10	1.70	159.9
25	28	122.6	0.15	1.77	1.90	156.6
16	84	124.2	0.5	1.72	2.50	100.0

(See Fig. C.2, Appendix C)

Notes

q_u = Unconfined compressive strength

E_{50} = Secant modulus at 50% q_u

Samples grouted with 35% Siroc 142

CHEMICAL GROUTING TEST PROGRAM

RESULTS OF UNCONFINED COMPRESSION TESTS RECONSTITUTED SAND SAMPLES GROUTED IN THE LABORATORY

FOUNDATION INVESTIGATION AND TEST PROGRAM
EXISTING LOCKS AND DAM No. 26
ST LOUIS DISTRICT, CORPS OF ENGINEERS.
DACW43-78-C-0005

Woodward-Clyde Consultants

Y7C825 Phase IX

Table 5.4

SAMPLE NO.	CURING TIME days	UNIT WEIGHT lb/ft³	CONFINING STRESS t/ft²	PEAK DEVIATOR STRESS t/ft²	STRAIN AT FAILURE %	E_{50} (2) t/ft²	ϕ (3) °	C (4) t/ft²	COEFFICIENT OF PERMEABILITY 10^{-7} x cm/s
34	7	126.1	1	6.85	2.62	840.7			3
36	7	125.5	2	11.16	2.34	1190.0	39	0.9	3
35	7	124.8	4	16.69	4.40	1336.1			4
1 (5)	7	123.7	1	5.73	3.56	-			6
3	7	123.4	2	9.21	3.61	499.4	39	0.45	10
4	7	123.4	4	14.98	4.73	1358.5			5
17	28	124.0	1	5.54	3.18	316.6			2.6
18	28	124.7	2	9.31	3.33	572.1	40	0.45	5.5
19	28	125.0	4	17.01	4.22	954.9			3.2
6	28	122.4	1	5.52	4.78	336.2			5.4
7	28	125.1	2	10.04	3.09	782.3	39	0.5	5.5
8	28	124.9	4	15.80	4.64	3184.6			4.1
26	82	124.3	1	6.57	2.87	293.9			-
24	80	125.3	2	10.67	3.21	479.4	40	0.8	-
21	80	125.5	4	18.31	2.68	1181.3			-
27 (1)	84	127.9	2	10.87	1.23	2352.0	40	0.8	-
31 (1)	98	122.5	2	10.39	2.53	2008.0			-

Notes

(1) Samples 27 and 31 were tested to failure at end of $\overline{CID}$ creep tests

(2) E_{50} = Secant Modulus at 50% of failure

(3) ϕ = Angle of internal friction

(4) C = Cohesion intercept

(5) Sample No. 1 was unsaturated

Strain rate 0.15%/min

Samples grouted with 35% Siroc 142
(See Fig. C.3 through Fig. C.8, Appendix C)

CHEMICAL GROUTING TEST PROGRAM

RESULTS OF $\overline{CID}$ TRIAXIAL COMPRESSION AND PERMEABILITY TESTS RECONSTITUTED SAND SAMPLES GROUTED IN THE LABORATORY

FOUNDATION INVESTIGATION AND TEST PROGRAM
EXISTING LOCKS AND DAM No. 26
ST LOUIS DISTRICT, CORPS OF ENGINEERS.
DACW43-78-C-0008

Woodward-Clyde Consultants

Table 5.5

Y7C825 Phase IX

GROUT TYPE	MEASURED NEUTRALIZATION RATIO R_n — TEST BATCH NUMBER I	Ia	II	III
55% Siroc 132	0.87	0.87	0.90	-
	0.88	0.88	0.90	-
	0.87	0.88	0.90	-
55% Siroc 142	0.93	0.90	0.93	-
	0.87	0.89	0.93	-
	0.88	0.90	0.94	-
35% Siroc 142	0.98	0.99	1.00	1.00
	0.98	0.99	1.00	1.00
	0.98	0.99	1.00	1.00
45% Siroc 142	0.87	0.89	0.89	-
	0.88	0.99	0.88	-
	0.87	0.99	0.88	-
25% silicate/aluminate	0.99	-	-	1.00
	0.99	-	-	-
	1.00	-	-	1.00
28% silicate/R600	-	1.00	-	-
	-	1.00	-	-
	-	-	-	-
46% silicate/R600	-	1.00	-	-

CHEMICAL GROUTING TEST PROGRAM

RESULTS OF NEUTRALIZATION RATIO INVESTIGATIONS

FOUNDATION INVESTIGATION AND TEST PROGRAM
EXISTING LOCKS AND DAM No. 26
ST LOUIS DISTRICT, CORPS OF ENGINEERS.
DACW43-78-C-0005

Woodward-Clyde Consultants

Y7C825 Phase III

Table 5.6

	UNIT WEIGHT lb/ft³	VISCOSITY	SETTING TIME min	DEGREE BAUME at 68°F	SHEAR STRENGTH t/ft²
Concentrated Sodium Silicate	86.5	114.6 (1)	-	40.66	-
35% Siroc 142	70.4	6.6 (1)	58	-	0.15
45% Siroc 132	74.4	11.1 (1)	67	-	1.27
55% Siroc 142	77.7	13.5 (1)	195 (3)	-	> 4.5 (5)
55% Siroc 132	77.8	11.3 (1)	576 (4)	-	> 4.5 (5)
25% Silicate/Aluminate	69.9	6.3 (1)	65	-	0.03 (7)
28% Silicate/R600	70.3	7.2 (1)	59	-	0.57
46% Silicate/R600	74.0	11.5 (1)	48	-	2.10 (6)
Cement-Bentonite c/w - 0.40 to 0.42	80.4	43.6 (2)	-	-	9.84
Cement-Bentonite c/w = 0.20 to 0.25	74.0	33.6 (2)	-	-	0.84

Notes

(1) *Centipoises*
(2) *Marsh Seconds*
(3) *Varied from 10 to 300 min*
(4) *Varied from 130 to 1500 min*
(5) *Lower bound from pocket penetrometer*
(6) *Erratic*
(7) *Difficult to measure*

CHEMICAL GROUTING TEST PROGRAM

AVERAGE PROPERTIES OF GROUTS MEASURED ON SITE DURING GROUTING

FOUNDATION INVESTIGATION AND TEST PROGRAM
EXISTING LOCKS AND DAM No. 26
ST LOUIS DISTRICT, CORPS OF ENGINEERS.
DACW43-78-C-0006

Woodward-Clyde Consultants

Table 5.7

Y7C826 Phase IX

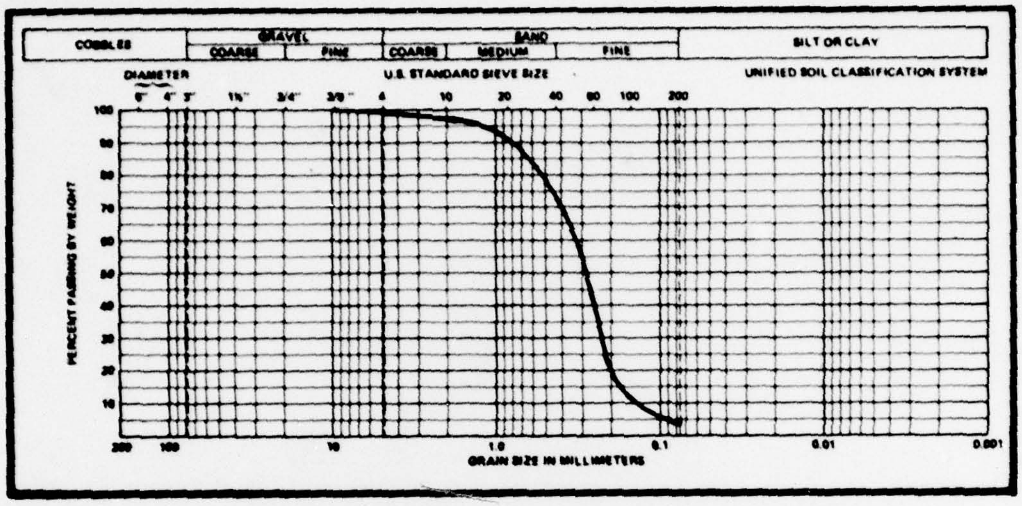

Maximum dry unit weight γ_{max}: 116.2 lb/ft^3

Minimum dry unit weight γ_{min}: 94.3 lb/ft^3

Reconstituted dry unit weight: 107.6 lb/ft^3
(Dr 70%)

Average water content: 16.2%

CHEMICAL GROUTING TEST PROGRAM

AVERAGE PROPERTIES OF SAND USED FOR LABORATORY GROUTING TESTS

FOUNDATION INVESTIGATION AND TEST PROGRAM
EXISTING LOCKS AND DAM No. 26
ST LOUIS DISTRICT, CORPS OF ENGINEERS.
DACW43-78-C-0006

Woodward-Clyde Consultants

77C625 Phase IX

Fig 5.1

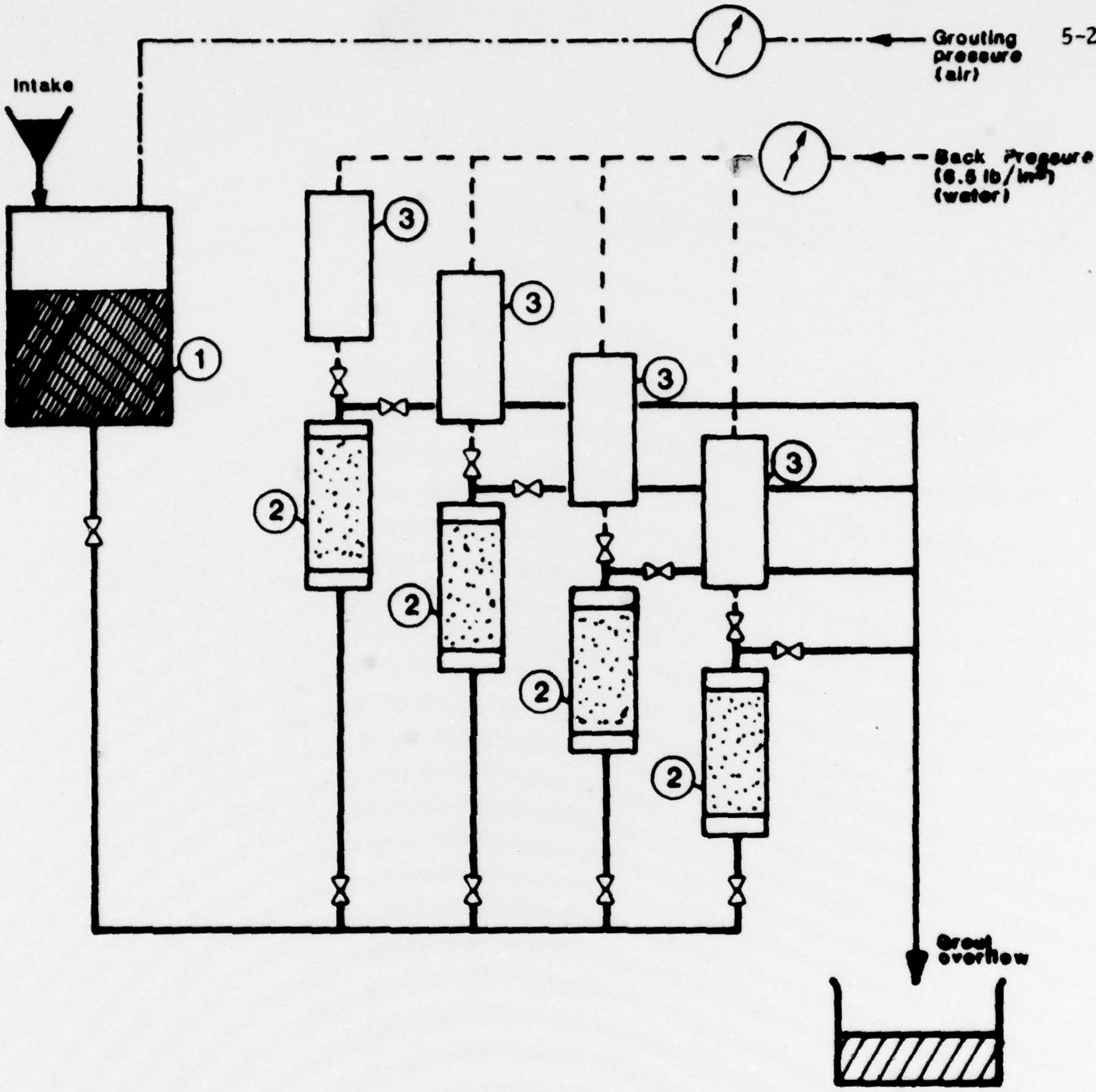

Legend

1. Grouting tank assembly (Mixing, agitating, pressurizing)
2. Sample reconstitution tubes
3. Saturating tanks

—·—·— Air line
- - - - - Water line
———— Grout line

CHEMICAL GROUTING TEST PROGRAM

LABORATORY GROUTING APPARATUS

FOUNDATION INVESTIGATION AND TEST PROGRAM
EXISTING LOCKS AND DAM No. 26
ST LOUIS DISTRICT, CORPS OF ENGINEERS.
DACW43-78-C-0005

Woodward-Clyde Consultants
Y7C025 Phase IX

Fig. 5.2

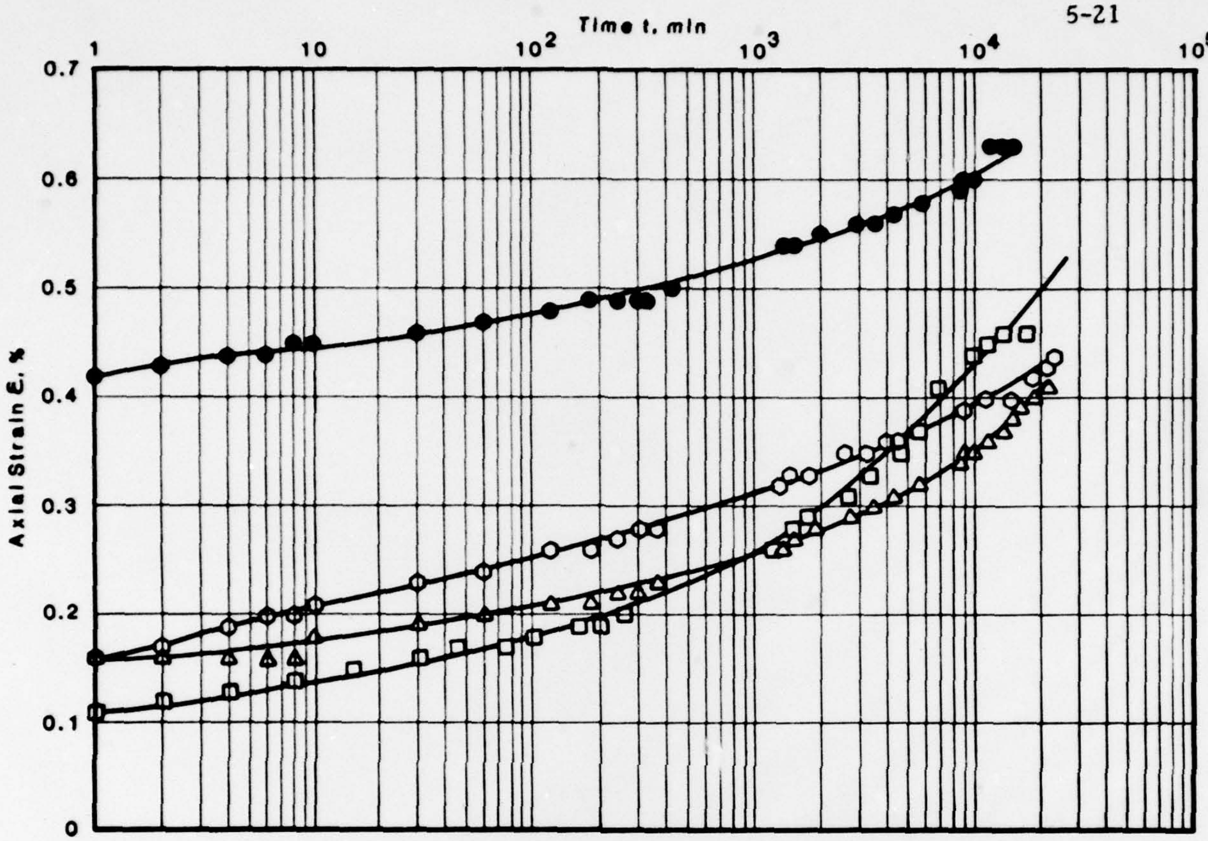

Legend

SYMBOL	TEST NO.	CONSTANT AXIAL STRESS σ_1, t/ft²	CONSTANT STRESS RATIO CSR = σ_1/σ_{max}
●	T-29	1	0.5
○	T-30	0.75	0.375
△	T-31	0.5	0.25
□	T-32	0.25	1.25

Notes

Samples grouted with 35% Siroc 142

Curing time = 28 days

$\sigma_{max} = q_u = 2$ t/ft²

CHEMICAL GROUTING TEST PROGRAM

RESULTS OF LONG-TERM UNCONFINED COMPRESSION TESTS RECONSTITUTED SAND SAMPLES GROUTED IN THE LABORATORY

FOUNDATION INVESTIGATION AND TEST PROGRAM
EXISTING LOCKS AND DAM No. 26
ST LOUIS DISTRICT. CORPS OF ENGINEERS.
DACW43-78-C-0005

Woodward-Clyde Consultants

Y7C825 Phase IX

Fig 5.3

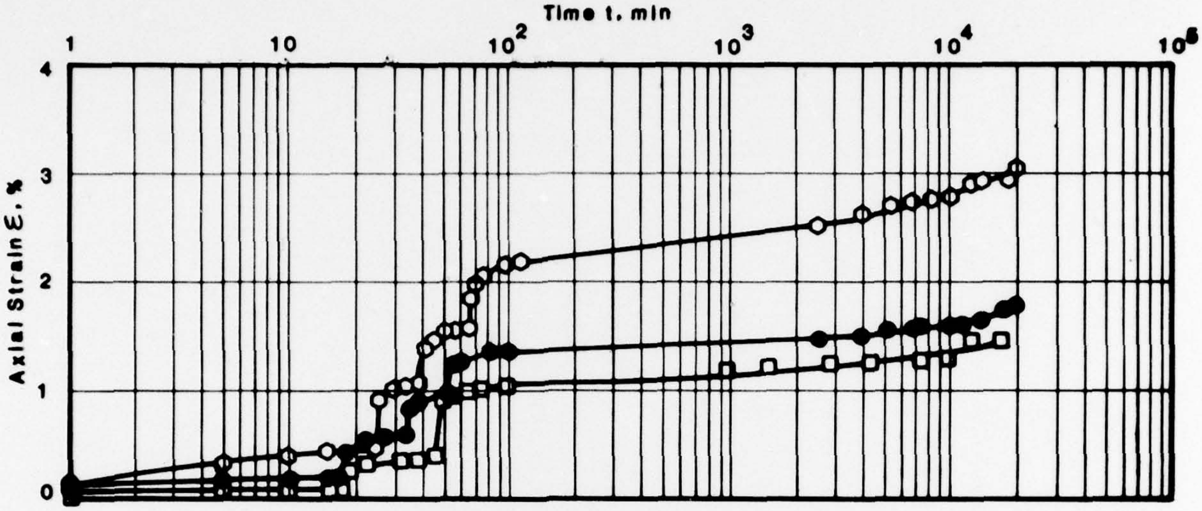

Legend

SYMBOL	TEST NO.	Time t, min: 0	17	24	33	34	40	48	52	65
●	T-27	1.58 (0.15)	3.12 (0.29)	3.12 (0.29)	3.12 (0.29)	4.75 (0.45)	4.75 (0.45)	4.75 (0.45)	6.34 (0.59)	6.34 (0.59)
○	T-28	2.12 (0.20)	2.12 (0.20)	4.20 (0.39)	4.20 (0.39)	4.20 (0.39)	6.30 (0.59)	6.30 (0.59)	6.30 (0.59)	8.40 (0.79)
□	T-31	1.05 (0.10)	2.15 (0.20)	2.15 (0.20)	3.15 (0.30)	3.15 (0.30)	3.15 (0.30)	4.25 (0.40)	4.25 (0.40)	4.25 (0.40)

CONSTANT DEVIATOR STRESS APPLIED $(\sigma_1-\sigma_3)$ t/ft^2

CONSTANT STRESS RATIO $(\sigma_1-\sigma_3)/(\sigma_1-\sigma_3)_{max}$

Notes

Sample grouted with 35% Siroc 142

Curing time = 98 [illegible]

$(\sigma_1-\sigma_3)_{max}$ = 10.67 t/ft^2

Confining Pressure σ_3 = 2 t/ft^2

CHEMICAL GROUTING TEST PROGRAM

RESULTS OF LONG-TERM CID TRIAXIAL COMPRESSION TESTS RECONSTITUTED SAND SAMPLES GROUTED IN THE LABORATORY

FOUNDATION INVESTIGATION AND TEST PROGRAM
EXISTING LOCKS AND DAM No. 26
ST LOUIS DISTRICT, CORPS OF ENGINEERS.
DACW43-78-C-0006

Woodward-Clyde Consultants

Y7C826 Phase IX

Fig 5.4

PHASE IV REPORT

VOLUME II

RESULTS AND INTERPRETATION OF
CHEMICAL GROUTING TEST PROGRAM

SECTION 6
GROUTING PROCEDURES

6 GROUTING PROCEDURES

6.1 GENERAL

The chemical grouting test program essentially compared two grout placement techniques: through open-bottom pipes, as it has been done in the USA for many years; and through sleeve-pipes, as it is commonly done in Europe and recently has been done in the USA. A joint venture of Raymond International Builders, Inc and Soletanche and Rodio, Inc was selected to combine US and European chemical grouting techniques and experience.

6.2 OPEN-BOTTOM PIPES

The open-bottom pipe grouting procedure has been extensively used in the USA. Grout pipe installation is relatively inexpensive, requiring simple driving equipment and steel pipes. The grouting method (Method O_1) is described in Section 2.1.2. The volume of grout to be injected was selected as being equivalent to 25 percent of the volume of soil to be grouted, on the basis of the contractor's (Raymond International Builders, Inc) usual practice in this type of alluvial sand. By making this selection, it was implicitly acknowledged that the soil would not be completely saturated with grout because its porosity is approximately 35 percent. Calculations of the volume of grout to be injected are presented in Fig. 6.1. The actual volume of grout injected is given in Table 7.1. Although the grout pumping pressure was kept at less than 1 lb/in^2 per foot of soil above the bottom of the grout pipe, the grout was pumped at 800 l/hr (3.5 gal/min) through each open-bottom pipe, which is approximately twice the rate of grout flow rate used with sleeve-pipes. As discussed in Section 9.3.3, this relatively high rate of grout flow resulted in hydraulic fracturing of the soil.

6.3 SLEEVE-PIPES

The sleeve-pipe grouting procedure was developed in Europe several decades ago. There it became the most widely used method of alluvial grouting. It allows regrouting several times in the same grout pipe and permits special treatment in specific soil horizons. The method (Method S_2) is described in Section 2.1.2. The volume of grout to be injected was selected as being equivalent to 45 percent of the volume of soil to be grouted, on the basis of the Contractor's (Soletanche and Rodio, Inc) usual practice in this type of alluvial sand. By making this selection, it was implicitly acknowledged that the soil would be completely saturated with grout, allowing for some dispersion, losses, and leakages. Calculations of the volume of grout to be injected through each sleeve are presented in Fig. 6.1. The actual volume of grout injected is given in Table 7.1. Injection through sleeve-pipes required an initial grout pumping pressure high enough to crack the sleeve grout surrounding the sleeves. This cracking pressure was sometimes as high as several hundred lb/in^2, but was of very short duration. Once the sleeve grout was cracked, the grout pumping pressure decreased, usually to a value between 20 and 120 lb/in^2. The grout was usually pumped at 300 l/hr to 450 l/hr (1.3 gal/min to 2 gal/min) through each sleeve pipe. The optimum rate of grout flow was selected on the basis of the contractor's experience and attempts were made to confirm it by hydraulic fracturing tests (Section 6.5). As expected, limiting the grout pumping pressure to 1 lb/in^2 per foot of soil above the sleeves was inconsistent with the sleeve-pipe method. This procedure (Method S_1, Section 2.1.2) was attempted without success in Subarea 5a.

6.4 MULTI-STAGE GROUTING

One of the advantages of sleeve-pipes is to allow regrouting or multiple grouting stages in the same grout pipe. This procedure (Method S_3, Section 2.1.2) was used in Subareas 6, 7, 8, 12, and 13. The volume of grout to be injected (that is, a volume equivalent to 45 percent of the volume of soil to be treated) was divided into two parts. The first part, equal to two-thirds of the total volume of grout, was injected first at every sleeve level. The second part, equal to one-third of the total volume of grout, was injected several hours to several days after the first injection at every sleeve level. In several grout holes, a third-stage injection, and sometimes a fourth- and fifth-stage, were done through selected sleeves when leaks or low pressure were noticed during the second-stage grouting. The volume of grout injected in these later stages varied from 1.2 percent to 13.1 percent of the volume of soil to be grouted. The actual volume of grout injected is given in Table 7.1.

6.5 HYDRAULIC FRACTURING TESTS

Several hydraulic fracturing tests were made during the course of the grout injection phase. The purpose of the tests was to establish criteria for grouting through sleeve-pipes in terms of grout pumping pressure and rate. Theoretically, hydraulic fracturing of the soil by grout occurs when grout pumping pressure and rate reach certain threshold values.

The tests were conducted by pumping a given type of grout through a sleeve at a given elevation. Both grout pumping pressure and rate were increased gradually until a drop or a stabilization of the pumping pressure accompanied by a faster increase in pumping rate were noticed. This phenomenon corresponded to a break in the pumping pressure vs pumping rate curve plotted during testing. This break was taken as the point representing hydraulic fracturing.

Grout pumping pressure was difficult to control and to measure because of variations. Grout pumping rate was easily controlled and measured on the grout line immediately after the grout pump. The actual grout pressure beyond the sleeve and into the soil was unknown. Grout pumping rate, however, could not vary along the grout path and therefore appeared to be a better parameter to use for grouting criterion. On this basis, it was decided to inject grout through sleeve-pipes at a grout pumping rate not exceeding 85 percent of the rate corresponding to hydraulic fracturing. This limiting criterion was used for all grout injection by Grouting Methods S_2 and S_3 (Section 2.1.2).

Results of hydraulic fracturing tests are pesented in Fig. D.1 through Fig. D.11, Appendix D, Volume IIA. Actually, it was difficult and sometimes impossible to readily interpret the test data. The interpretation was strongly influenced by the contractor's previous successful alluvial grouting experience. Two examples of hydraulic fracturing test interpretation are shown in Fig. 6.2; these examples are untypical in that they illustrate two of the few easily interpretable tests. A complete list of hydraulic fracturing tests and test results field interpretation are given in Table 6.1

DATE	GROUT HOLE NO.	GROUT USED	TEST ELEVATION ft	Q_f (1) l/hr	P_f (2) bar	REMARKS
5 May 78	10-2	55% Siroc 142	380 383.3 386.6 389.9 393.2 396.4 399.7	450 515 610 720 756 600 670	6 4.9 3.8 4.2 4.3 3.6 4.4	Use Q_{allow} = 400 l/hr (3)
10 May	10-3	55% Siroc 132	387.7			Data not interpretable
11 May	7-1	Cement-Bentonite (c/w = 0.25; b/w = 0.03)	380 383.3	370	8.5	Use Q_{allow} = 370 l/hr (3)
16 May	7-2	25% Silicate/Aluminate (after 1st stage grouting with C-B)	380 383.3 386.6 389.9	590	6.8	Use Q_{allow} = 450 l/hr (3)
17 May	6-1	25% Silicate/Aluminate	389.9 393.3 396.4	460 430	3 3.4	Results questionable
18 May	6-3	25% Silicate/Aluminate	380 383.3 386.6	410 630	2.8 3.4	
22 May	12-2	Cement-Bentonite (c/w = 0.25; b/w = 0.03)	380 383.3 386.6	390	3.2	
22 May	12-4	46% Silicate/R600	380 383.3 386.6 389.9	580	1.4	Use Q_{allow} = 400 l/hr (3)
25 May	13-2	46% Silicate/R600	380 383.3 386.6	500 to 570	3.6	Use Q_{allow} = 400 l/hr (3)
2 June	4-2	35% Siroc 142	380 383.3 386.6	575	4.4	Use Q_{allow} = 450 l/hr (3)
8 June	3-3	28% Silicate/R600	380 383.3	675	2.5	Use Q_{allow} = 500 l/hr (3)

(1) Q_f = Grout pumping rate at which hydraulic fracturing appeared to occur

(2) P_f = Grout pumping pressure at which hydraulic fracturing appeared to occur (hydraulic fracturing pressure)

(3) $Q_{allow} < 0.85\ Q_f$: Grout pumping rate not to be exceeded when grouting in corresponding subarea

CHEMICAL GROUTING TEST PROGRAM

HYDRAULIC FRACTURING TEST RESULTS

FOUNDATION INVESTIGATION AND TEST PROGRAM
EXISTING LOCKS AND DAM No. 26
ST LOUIS DISTRICT, CORPS OF ENGINEERS.
DACW43-78-C-0005

Woodward-Clyde Consultants
Y7C825 Phase IX

Table 6.1

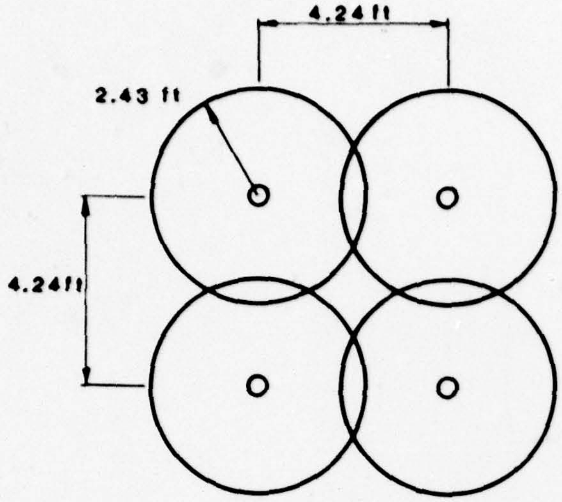

4.24-ft Grout Hole Spacing

Volume of Soil to be Grouted:

$V_s = \pi \times \overline{2.43}^2 = 18.5\ ft^3/ft$

$V_s = 525\ l/ft = 139\ gal/ft$

Volume of Grout to be Injected:

Sleeve-pipe:

$V_G = 525 \times 1.08 \times 0.45$
$= 255\ l/sleeve$
$= 67\ gal/sleeve$

Open-bottom pipe:

$V_G = 525 \times 0.25$
$= 132\ l/ft$
$= 35\ gal/ft$

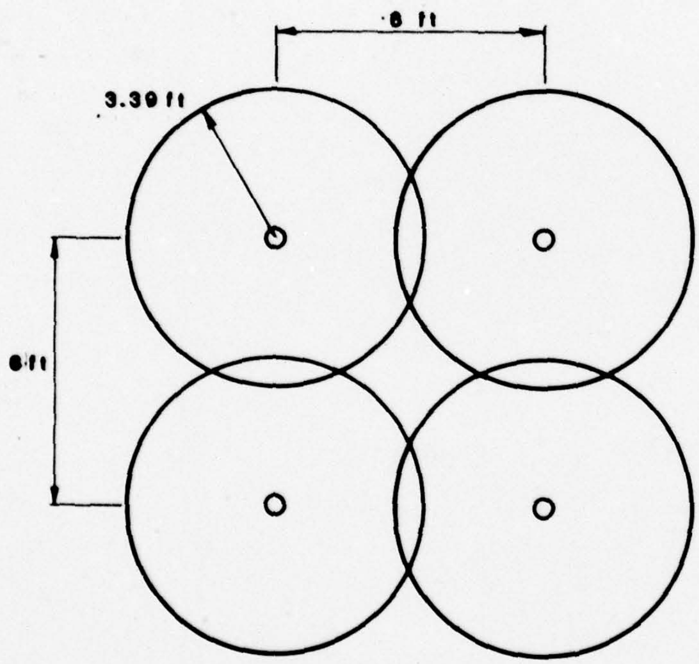

6-ft Grout Hole Spacing

Volume of Soil to be Grouted:

$V_s = \pi \times \overline{3.39}^2 = 36.1\ ft^3/ft$

$V_s = 1022\ l/ft = 270\ gal/ft$

Volume of Grout to be Injected:

Sleeve-pipe:

$V_G = 1022 \times 1.08 \times 0.45$
$= 497\ l/sleeve$
$= 131\ gal/sleeve$

Open-bottom pipe:

$V_G = 1022 \times 0.25$
$= 256\ l/ft$
$= 68\ gal/ft$

Note

Sleeves are spaced 33 cm = 1.08 ft apart

CHEMICAL GROUTING TEST PROGRAM

CALCULATION OF VOLUME OF GROUT TO BE INJECTED

FOUNDATION INVESTIGATION AND TEST PROGRAM
EXISTING LOCKS AND DAM No. 26
ST LOUIS DISTRICT, CORPS OF ENGINEERS.
DACW43-78-C-0008

Woodward-Clyde Consultants

Y7C825 Phase IX

Fig 6.1

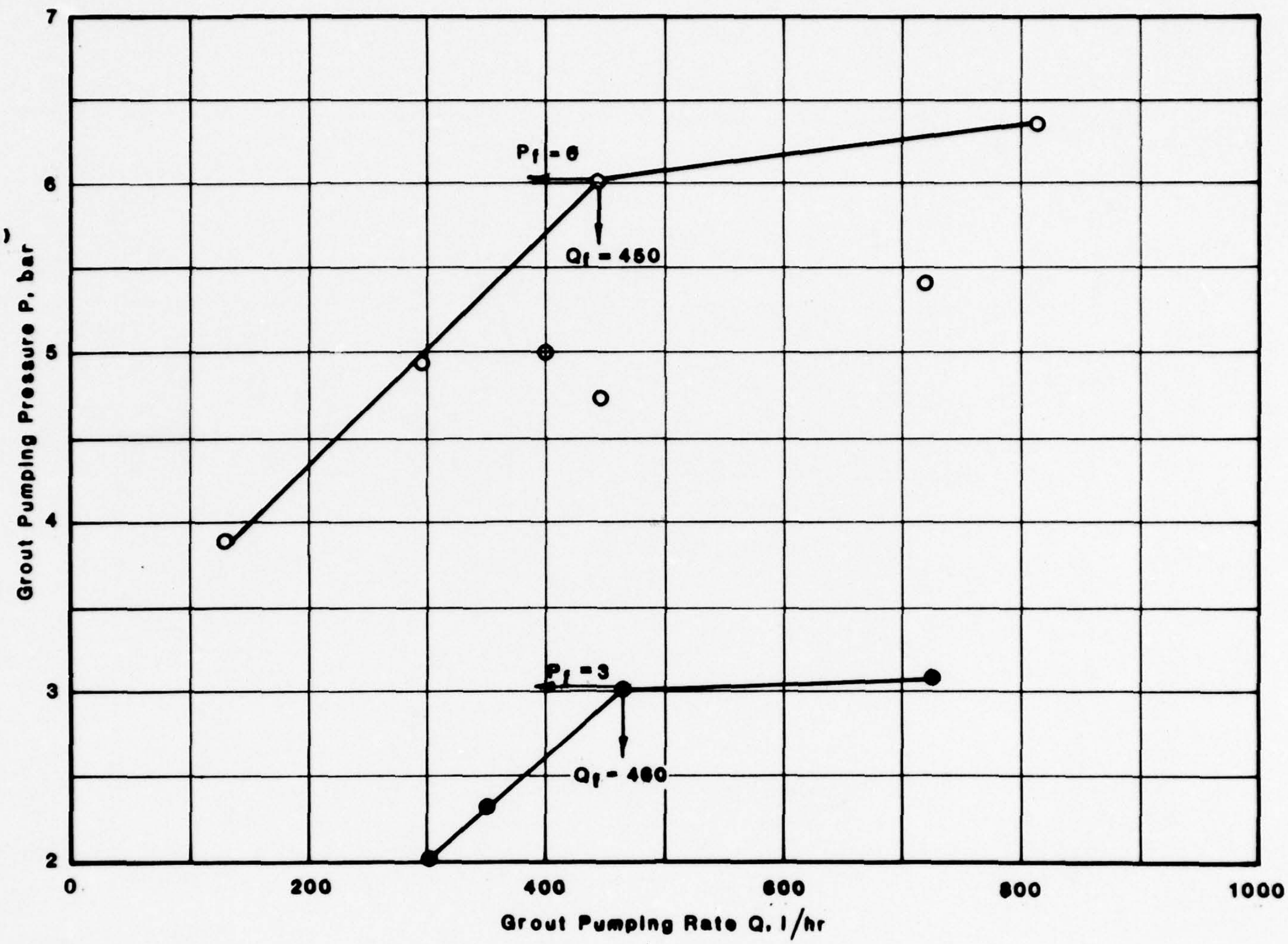

Legend

- ○ Grout hole 10-2, el 380 (55% Siroc 142)
- ● Grout hole 6-1, el 389.9 (25% Silicate/Aluminate)

Q_f = Hydraulic fracturing grout pumping rate

P_f = Hydraulic fracturing grout pumping pressure

CHEMICAL GROUTING TEST PROGRAM

EXAMPLE OF HYDRAULIC FRACTURING TEST RESULTS AND INTERPRETATION

FOUNDATION INVESTIGATION AND TEST PROGRAM
EXISTING LOCKS AND DAM No. 26
ST LOUIS DISTRICT, CORPS OF ENGINEERS.
DACW43-78-C-0005

Woodward-Clyde Consultants

Y7C625 Phase IX

Fig. 6.2

PHASE IV REPORT

VOLUME II

RESULTS AND INTERPRETATION OF CHEMICAL GROUTING TEST PROGRAM

SECTION 7

MONITORING OF GROUTING ACTIVITIES

7 MONITORING OF GROUTING ACTIVITIES

7.1 MONITORING SYSTEM

During grouting, injection parameters (grout pumping pressure, flow rate, and volume) were continuously monitored. Most of these monitoring activities were done from the grouting plant (Module 2, Section 4.1.3). The control panel from which the monitoring was done is shown in Fig. 4.2.

7.2 GROUT PUMPING PRESSURE

The grout pumping pressure was continuously recorded with five disk pressure recorders. Initially, pressure recorders having ranges of 0 to 50 bar (0 to 725 lb/in^2) and 0 to 100 bar (0 to 1450 lb/in^2) were used. New recorders with smaller range of 0 to 20 bar (0 to 390 lb/in^2) were installed after a few days, consistent with the range of actual grout pumping pressures. The grout pumping pressure was also measured with pressure gages. Initially, three gages graduated from 0 to 60 bar (0 to 870 lb/in^2) and two gages graduated from 0 to 1450 lb/in^2 (0 to 14 bar) were used. Five gages graduated from 0 to 14 bar (0 to 200 lb/in^2) were added to the control panel after a few days.

For each grout hole, the average maximum grout pumping pressure was documented at each injection level (that is, for every foot of open-bottom pipe or every sleeve of sleeve-pipe). These data are presented in Fig. E.1 through Fig. E.74, Appendix E, Volume IIA.

7.3 GROUT FLOW RATE

The grout flow rate was determined on the basis of the contractor's experience and hydraulic fracturing tests (Section 6). The speed of the grouting pumps and of the "grout counters" (Section 4.1.3) was set to supply grout at the predetermined rate. During grouting, the rate of grout flow was usually constant. Deviations from this rate were documented whenever they occurred.

7.4 GROUT VOLUME

At each injection level, the volume of grout injected (or grout take) was recorded. The data is presented in Appendix E, Volume IIA. For multi-stage grouting, the grout take was cumulated. Table 7.1 presents a summary of the grout volume injected in each subarea. The actual volumes injected are compared with the predicted volumes.

TEST SUBAREA	GROUT HOLE SPACING ft	NO. OF GROUT HOLES	GROUT TYPE	GROUTING METHOD	THEORETICAL[1] VOL OF GROUT TO BE INJECTED	ACTUAL[1] VOL OF GROUT INJECTED
1	4.24	7	35% Siroc 142	O_1	4640 (25)	5584 (30.1)
2	6	4	35% Siroc 142	O_1	5330 (25)	5348 (25.1)
3	6	4	28% Silicate/R600	S_2	6710 (45)	6231 (41.8)
4	6	5	35% Siroc 142	S_2	11860 (45)	11836 (44.9)
5	6	4	45% Siroc 132	S_2	9550 (45)	9548 (45)
5a[2]	6	2	25% Silicate/Alum	S_1	2045 (25)	303 (3.7)
6	6	5	25% Silicate/Alum	S_3	11930 (45)	12246 (46.2)
7[3]	6	6	25% Silicate/Alum Cement-Bentonite[5]	S_3	13743 (45)	16049 (52.5)
8[3]	4.24	8	25% Silicate/Alum Cement-Bentonite[5]	S_3	8900 (45)	11100 (56.1)
9	4.24	6	55% Siroc 142	O_1	4000 (25)	3357 (21)
10	6	6	55% Siroc 132/142	S_2	14360 (45)	13750 (43.1)
11	4.24	8	55% Siroc 132/142	S_2	9550 (45)	9353 (44.1)
12[4]	6	4	46% Silicate/R600 Cement-Bentonite[5]	S_3	9350 (45)	11243 (54.1)
13[4]	4.24	5	46% Silicate/R600 Cement-Bentonite[5]	S_3	5870 (45)	7574 (58.1)
			Total Volume of Grout, gal		118000 (approx)	123522

Notes

(1) *First figure is volume in gal; second figure ( ) is volume expressed as a percent of volume of soil to be treated*

(2) *Grout take was practically zero; test was discontinued*

(3) *A very small volume of cement-bentonite grout was injected in every grout hole as a first-stage grouting*

(4) *A very small volume of cement-bentonite grout was injected in one grout hole as a first-stage grouting*

(5) *Cement/water by weight = 0.25*

CHEMICAL GROUTING TEST PROGRAM

GROUT VOLUME INJECTED IN EACH SUBAREA

FOUNDATION INVESTIGATION AND TEST PROGRAM
EXISTING LOCKS AND DAM No. 26
ST LOUIS DISTRICT, CORPS OF ENGINEERS.
DACW43-78-C-0008

Woodward-Clyde Consultants

Y7C825 Phase IX

Table 7.1

PHASE IV REPORT

VOLUME II

RESULTS AND INTERPRETATION OF
CHEMICAL GROUTING TEST PROGRAM

SECTION 8

EFFECTS OF GROUTING

8 EFFECTS OF GROUTING

8.1 OVERVIEW OF INSTRUMENTATION SYSTEM

Measurements of vertical and horizontal displacements, and porewater pressure were made to monitor the effects of grouting on the soil mass. The following ground instruments were used in the chemical grouting test program to make these measurements:

Type of Instrument	Number of Instruments	Comments
Benchmark	1	First-order benchmark for vertical control installed adjacent to test area
Surface reference point	35	Installed 2 ft below asphalt pad to monitor vertical displacement
Heave/ settlement point	26	Borros gages installed at various elevations above and within the grouted zone to monitor differential vertical displacement
Piezometer	9	Pneumatic pore-pressure transducer installed at various elevations to measure pore pressure
3-D deformation gage	7	Inclinometer casing installed with Sondex rings to monitor differential vertical and horizontal displacement

The plan location of ground instruments is shown in Fig. 8.1. The accuracy of the instruments, and the expected and measured maximum values of the parameters monitored during the test are presented in Table 8.1.

8.2 HEAVE MEASUREMENTS

8.2.1 Instruments

Vertical movements were measured with reference to a benchmark. An as-built sketch of the benchmark (BM-1) is shown in Fig. 8.2. Horizontal control points were also installed outside the asphalt pad for initial layout of the instruments and grout holes, and for surveying the top of the inclinometer casings during the test.

The instrumentation for measurement of surface heave consisted of reference points located just below the asphalt pad. The reference point consisted of a No. 6 re-bar with diagonal saw cut at the top. An as-built sketch is shown in Fig. 8.3. Survey measurements were made with a Wild NAK1 self-leveling level with a vernier rod. The rod was read to the nearest 0.001 ft. The accuracy of the surface reference point measurements may be slightly better than the 0.005 ft anticipated.

Borros heave/settlement points were used to measure vertical movements just above the grouted zone at el 402 and within the lower portion of the grouted soil at el 385 and el 387. The Borros gage consisted of an anchored point attached to a 0.25-in.-dia steel riser that was isolated from friction of the surrounding soil by a 1-in.-dia steel pipe. A sketch of the Borros gage is shown in Fig. 8.4.

The elevation of the Borros gages was determined with the same survey equipment described above for the surface reference points. A steel extension rod machined to a length of exactly 1.00 ft was used to position the survey rod on the riser because the top end of the 0.25-in-dia riser was recessed inside the 1-in. pipe. The accuracy of the measurements on the Borros points was similar to that of the surface reference points.

Sondex rings firmly attached to a PVC inclinometer casing (3-D deformation gage) were used to measure vertical movements at depth intervals of 5 ft, generally. The elevations of the Sondex rings were usually 418, 405, 400, 395, 390, 385, 378, 368, and 360. The Sondex rings consisted of stainless steel wire loops attached to short segments of thin, corrugated polyethylene casing. The segments of polyethylene casing were attached to the PVC casing with duct tape. The rings had only limited ability for movement relative to the PVC casing. An as-built sketch of the 3-D deformation gage is given in Fig. 8.5. The distance to the rings was determined by lowering a torpedo-shaped sensor through the inclinometer. A signal was generated by induction when the sensing device was opposite the wire ring. The distance from the top of the inclinometer casing to the ring was determined with a surveyor's chain attached to the sensor. The accuracy of the instrument was probably no better than 0.005 ft. Absolute elevations of the rings were not determined because the top of the casing was only surveyed at the beginning of the grouting test.

8.2.2 Presentation of Results

The gross vertical movements of each surface reference point at el 423 and each Borros point at either el 402 or el 385/387 are shown in Fig. 8.6, Fig. 8.7 and Fig. 8.8, respectively. The range of heave measured at these elevations are compared with the chemical grouting test variables for each subarea in Table 8.2.

The heave measurements are plotted as a function of time in Fig. F.1 throug Fig. F.23, Appendix F, Volume IIA. The largest heave (0.048 ft) appears to have been measured at el 402 with Borros gage H-11. The data from H-11 are compared with the data obtained from surface reference point R-22, Borros gage

H-25 at el 384, and 3-D deformation gage I-6, in Fig. 8.9. All these instruments were located in a cluster between Subareas 8 and 10. The vertical movement of 3-D deformation gage I-6 does not follow the pattern observed with Borros gages and surface reference points. Analyses of these and other 3-D gage data indicated that the predominant Sondex movement was downward. The results obtained with the 3-D gages are also more erratic. Two possible reasons for these discrepancies have been identified. The implicit assumption that the top of the casing was fixed in space was not valid. If the ground surface heaved, it is probable that the top of the casing heaved also. Attempts were made to correct for this condition by subtracting the distances measured to each ring from the distance to the lowest ring (that is, by assuming the base was fixed). This eliminated the predominant downward displacement (settlement), but the corrected data remained very erratic. Since this cluster of instruments (H-11, H-25, and R-22) were the only gages that indicated significant heave, these data were analyzed in detail. The results are plotted on an expanded time scale in Fig. 8.10. Certain grouting activities in the area are also summarized on this plot along with the tailwater elevation at Locks and Dam No. 26 and the pore pressure monitored in piezometer P-8 at el 387. The displacement of H-11 (el 402) seems to have occurred primarily between approximately 9 and 13 May. The grouting activities during this period included injection in Grout Holes 10-6, 10-3, 10-4, 10-5, and all the grout holes in Subarea 8. A hydraulic fracturing test was made in Grout Hole 10-3 on 10 May. In Subarea 8, grouting method S_3 was used. Cement-bentonite was injected in the first stage and 25% silicate/aluminate grout was injected in the subsequent stages. During excavation of the chemical grout test area, a relatively large mass of cement-bentonite grouted sand, observed as a nearly horizontal lens, was identified at approximately el 393 (Section 9.3.3). This was the only area where such a large mass of cement-bentonite grouted sand was observed and could be the source of the observed heave at el 402.

Although the measured heave was generally small, and not much larger than the accuracy of the instrumentation, certain trends are apparent. There was no measured heave at el 423 in Subareas 3 and 5, and only a slight movement in Subarea 2. The surface heave in the remaining areas was generally in the range of 0.006 to 0.019 ft (0.07 to 0.23 in.). With the exception of H-11, the heave at el 402 ranged from 0.002 to 0.015 ft (0.024 to 0.18 in.). The heave at el 385/387 ranged from 0 to 0.020 ft (0.24 in.).

Analysis of the vertical displacement vs time plots generally indicated heave occurred between about 4 May and 13 to 15 May, after which settlement occurred. The magnitude of heave was typically between 0.005 ft and 0.015 ft (0.06 in. and 0.18 in.) and the subsequent settlement was somewhat larger, approximately 0.010 ft to 0.025 ft (0.12 in. to 0.30 in.). The reason for the cyclic movement may be the change in groundwater level. Between 7 May and 16 May, the tailwater elevation at the dam rose about 10 ft. Between 16 May and 14 June, the tailwater elevation decreased approximately 16 ft; see Fig. 8.10. A rise in groundwater level resulted in a decrease in effective stress, which could have caused an elastic heave of the ground surface that was proportional to the thickness of overburden soil and the deformation modulus of the soil. Similarly, a decrease in groundwater level could have resulted in a settlement of the ground surface. Bedrock in the area of the chemical grout test was encountered at about el 283, therefore the thickness of overburden soil was approximately 140 ft. Assuming that the soil deformation modulus ranges between 5,000 lb/in^2 and 25,000 lb/in^2, the heave/settlement corresponding to groundwater level changes of 10 to 16 ft are as follows:

Change of Groundwater Elevation ft	Assumed Modulus lb/in^2	Calculated Heave ft	Calculated Settlement ft
+10	5,000	0.12	-
+10	25,000	0.023	-
-16	5,000	-	0.18
-16	25,000	-	0.037

This simplified analysis indicates that it is probable that the gradual heave and subsequent settlement observed in most gages were the result of changes in the groundwater level.

8.2.3 Conclusions

The maximum observed heave is compared to the predicted value below:

Predicted Maximum Value ft	Maximum Observed Value ft
0.020	0.020*

*Excluding 0.048 ft at H-11

The relatively large heave observed at H-11 is attributed to the injection of cement-bentonite in Subarea 8.

The reliability and effectiveness of the surface reference points and Borros gages was satisfactory. This was not the case for the Sondex rings on the 3-D deformation gage. A special test installation was made subsequent to the grouting test to evaluate the source of the erratic results. This test installation was used to compare three methods of attaching Sondex rings to the inclinometer casing. The top of the casing was surveyed using a level each time Sondex readings were made. The results of this test indicated that the method of attaching the rings to the PVC casing that was used in the chemical grouting test did not allow them to move freely with the soil. The test results also indicated that the rings are free to move vertically with the soil if attached as shown in Fig. 8.11. This method was used for the remaining installations in the pile driving effects, rock anchor, and drilled-in pile tests.

8.3 LATERAL DISPLACEMENT MEASUREMENTS

8.3.1 Instrumentation

The instrumentation for measurement of lateral displacements consisted of seven inclinometer casings installed at the locations indicated in Fig. 8.1. These casings were also used to measure vertical heave/settlement and were referred to as 3-D deformation gages. The casings were 2.75-in.-od PVC flush-joint casing provided by Slope Indicator Company (Sinco). The casings were installed to depths of 64 ft (el 359) in boreholes drilled using a stabilizing fluid. After the casing was installed and the grooves aligned in the desired direction, pea gravel was used to backfill the annulus between the casing and the borehole. Details of the installation are given in the as-built sketches; Fig. 8.5. Horizontal displacements were measured with Sinco Model 50325 Digitilt probe and a Sinco Model 50309 LCD digital readout. The data were processed using a local computer vendor and batch processing. The horizontal location of the top of the casing was surveyed before and after grouting. It was necessary to add a short segment of casing to extend it above the ground surface when measurements were being made because the inclinometer casing was recessed below the top of the asphalt pad for protection.

The accuracy of the inclinometer system is reported by the manufacturer to be one part in 1000 or 0.1 ft in 100 ft of casing length. The repeatability of the measurements made in the chemical grouting test area are compared with the accuracy limits in Fig. 8.12 and Fig. 8.13. Measurements were made on 1 May and again on 8 May before grouting commenced. The difference in casing position between these two dates for each of the seven instruments is shown in Fig. 8.12. The casings were also monitored on 12 June and 14 June after grouting was completed. The difference in casing position between these two dates for each of the seven instruments is shown in Fig. 8.13. Comparison of these results indicate that the repeatability of the instruments was well within the the 0.1 ft in 100 ft limit claimed by the manufacturer. The measurements were more repeatable after grouting than before grouting and the results were more repeatable in the north-south direction than in the east-west direction.

8.3.2 Presentation of Results

Vectors of the maximum horizontal displacement within the grouted soil mass for the duration of the grouting tests are plotted in Fig. 8.14. The vectors range from 0.008 to 0.018 ft in magnitude and have a predominantly southerly orientation. Vectors of the maximum horizontal displacement between successive readings on each casing are plotted in Fig. 8.15. These vectors range from 0.006 to 0.014 ft in magnitude and have a predominant southwesterly orientaton. In considering these data, it should be remembered that the results are within the range of repeatability cited above.

Inclinometers I-1, I-3, I-5, and I-7 were located around the periphery of the grouted area and should not have undergone as much lateral movement as the other inclinometers. This assumption tends to be supported by the data in Fig. 8.14 and Fig. 8.15 where the largest lateral movements were measured in I-6 and I-4.

The results of all measurements made in I-6 are presented in Fig. F.24 through Fig. F.27, Appendix F, Volume IIA. Lateral movements are plotted as functions of time at el 407, el 399, and el 385 in Fig. 8.16, Fig. 8.17, and Fig. 8.18, respectively. Measurements made in the other inclinometers were usually less than the accuracy of the system and, in some cases, the direction of movement was towards the area being grouted.

8.3.3 Conclusions

The maximum observed horizontal displacement is compared to the predicted value below:

Predicted Maximum Value ft	Maximum Observed Value ft
0.10	0.018 total 0.014 incremental

The maximum observed horizontal displacement was measured in I-6 which correlates with the maximum recorded heave of 0.048 ft at H-11 located adjacent to I-6. These relatively large movements are attributed to grouting activities in Subarea 8. It should be noted that the maximum heave at H-11 occurred between 9 and 11 May, whereas the maximum lateral displacement occurred between 22 and 23 May.

The reliability and effectiveness of the horizontal displacement measurements using the inclinometers were satisfactory. All seven of the inclinometer casings functioned reliably. The accuracy of the instrumentation appears to be about 0.01 ft. With the exception of I-6, the observed horizontal movements were only slightly greater than the system accuracy. Despite the fact that fractures produced by grouting were primarily oriented vertically (Section 9.3.3), significant horizontal movements were not observed. This is a qualified conclusion since most of the inclinometer casings were located at least several feet away from the grout holes.

8.4 PORE PRESSURE MEASUREMENTS

8.4.1 Instruments

Pore pressures were monitored prior to and during the chemical grouting tests with Sinco Model 51481 pneumatic pore pressure transducers and a Sinco Model 51411 precision digital indicator. A sketch of a typical as-built installation of the piezometer is shown in Fig. 8.19. In a few cases, the pore pressure transducers were installed in conjunction with a Borros point or a 3-D deformation gage.

8.4.2 Presentation of Results

Pore pressure measurements were made in each piezometer beginning shortly after installation. During grouting, piezometers adjacent to or within a subarea being grouted were monitored approximately once per hour. Although the units of measurement were force per unit area (lb/in^2), the results were converted into pressure head (elevation) for comparison with river level. This comparison is shown as a function of time in Fig. F.28 through Fig. F.36, Appendix F, Volume IIA. A typical comparison is shown in Fig. 8.20. These data demonstrate that the piezometers were functioning and the groundwater level was following closely the river level.

Pore pressures have also been compared to the grout pumping pressure measured at the top of the grout pipe. The best such correlation was made by comparing the pore pressure change in piezometer P-3 with the grout pressure in Grout Hole 12-4 during a hydraulic fracturing test and subsequent grouting activity; see Fig. 8.21. Pressures measured at the grout pipe were typically in a range of 20 to 30 lb/in^2, whereas the excess pore water pressure was about 5 to 12 lb/in^2. The difference was attributed to head losses in the sleeve pipe and surrounding sleeve grout, as well as radial dissipation of grout pressure between the point of injection and the pore pressure transducer. The transducer was located at el 387 and about 3 ft horizontally from the grout hole. For most other piezometers, the observed pore pressure changes during hydraulic fracturing and grouting were negligible (that is, less than 1 lb/in^2) even though the transducers were sometimes as close as 3 ft from the grout holes.

8.4.3 Conclusions

The maximum observed excess pore pressure was about 12 lb/in^2, compared to a predicted maximum change of 30 lb/in^2. This latter value was quite conservative because pressures at the top of the grout pipe were usually in the range of 30 to 60 lb/in^2.

The pneumatic piezometers were reliable and sufficiently accurate for the intended purpose. The accuracy of the instrumenation was about an order of magnitude better than the expected value of 1 lb/in^2. All nine transducers functioned for the duration of the test; however, they did cease to respond once they were encapsulated in grout and the grout set. This was expected.

One possible improvement in the pore pressure instrumentation would have been to install electronic pore pressure transducers with a continuous readout. This might have allowed a closer correlation between grout pressures and pore pressures in the soil.

INSTRUMENTATION	SYSTEM ACCURACY	PREDICTED MAXIMUM CHANGE	MEASURED MAXIMUM CHANGE
Surface Reference Point	0.005 ft	0.02 ft	0.025 ft(1)
Heave/Settlement Point	0.005 ft	0.02 ft	0.025 ft(1)
Piezometers	1 lb/in^2	30 lb/in^2	11 lb/in^2
Sondex	0.005 ft	0.02 ft	0.07 ft (0.04 ft)(2)
Horizontal Inclinometer	0.01 ft	0.1 ft	0.014 ft(1) 0.018 ft(3)

Notes

(1) Maximum changes measured from incremental data

(2) 0.04 ft was the nearest maximum change observed after 0.07 ft

(3) Maximum changes measured from total deflections

CHEMICAL GROUTING TEST PROGRAM

GENERAL INSTRUMENTATION RESULTS

FOUNDATION INVESTIGATION AND TEST PROGRAM
EXISTING LOCKS AND DAM No. 26
ST LOUIS DISTRICT, CORPS OF ENGINEERS
DACW43-78-C-0005

Woodward-Clyde Consultants
Y7C825 Phase IX

Table 8.1

	GROUT TYPE	GROUTING METHOD	GROUT-HOLE SPACING ft	MAXIMUM GROUT PRESSURE OR RATE OF PUMPING	TEST SUBAREA NO.	MEASURED HEAVE[1] ELEVATION 423	402	385 ±
LOW-STRENGTH	35% SIROC 142	O_1	4.2	1 lb/in²/ft	1	.013 to .017	—	—
			6		2	.000 to .007	.000 to .005	.000 to .004
		S_2		85% of hydraulic fracturing rate of pumping	4	.013 to .017	.008 to .015[2]	.008 to .009
	25% Silicate/ Aluminate	S_1		1 lb/in²/ft	5a	—	—	—
		S_3		85% of hydraulic fracturing rate of pumping	6	.001 to .013	.002	.001
	Some Cement-Bentonite and 25% Silicate/ Aluminate				7	.008 to .012	.008	.002
			4.2		8	.007 to .008	.048[3]	.005
	28% Silicate/R600	S_2	6		3	.000	.002	.000
HIGH-STRENGTH	45% SIROC 132	S_2	6	85% of hydraulic fracturing rate of pumping	5	.000	—	—
	55% SIROC 142/132	O_1	4.2	1 lb/in²/ft	9	.012 to .019	—	—
		S_2	6	85% of hydraulic fracturing rate of pumping	10	.011 to .016	.048[3]	—
			4.2		11	.010	—	—
	46% Silicate/R600	S_3	6		12	.006 to .009	.012	.013
			4.2		13	.008 to .014	.002 to .012	.003 to .020

(1) Heave measured with surface reference and Borros points
(2) H-8 located between areas 2 and 10
(3) H-11 located between areas 8 and 10

CHEMICAL GROUTING TEST PROGRAM

HEAVE MEASURED IN EACH SUBAREA

FOUNDATION INVESTIGATION AND TEST PROGRAM
EXISTING LOCKS AND DAM No. 26
ST LOUIS DISTRICT, CORPS OF ENGINEERS.
DACW43-78-C-0005

Woodward-Clyde Consultants

Y7C825 Phase IX

Table 8.2

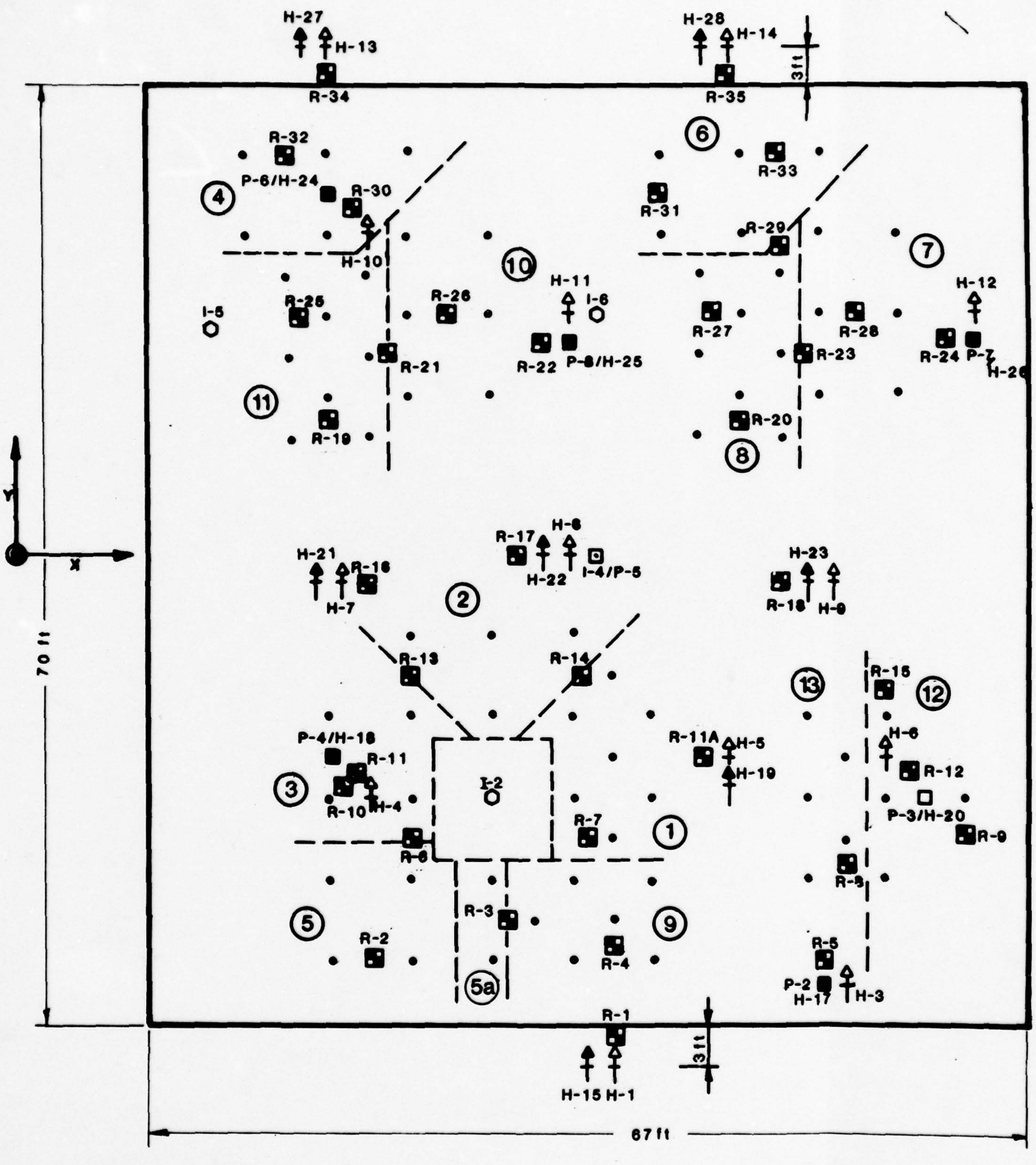

H-27
H-13
R-34
H-28
H-14
R-35
3 ft
R-32
P-6/H-24
R-30
H-10
R-31
R-33
R-29
R-25
R-26
H-11
I-6
I-5
R-21
R-22
P-8/H-25
R-27
R-28
R-23
H-12
R-24
P-7
H-26
R-19
R-20
Y
X
70 ft
R-17
H-8
H-22
I-4/P-5
H-21
R-16
H-7
H-23
R-18
H-9
R-13
R-14
R-15
P-4/H-18
R-11
R-10
H-4
I-2
R-11A
H-5
H-19
H-6
R-12
P-3/H-20
R-9
R-7
R-6
R-3
R-8
R-2
R-4
R-5
P-2
H-17
H-3
R-1
H-15
H-1
67 ft
1
2
3
4
5
5a
6
7
8
9
10
11
12
13

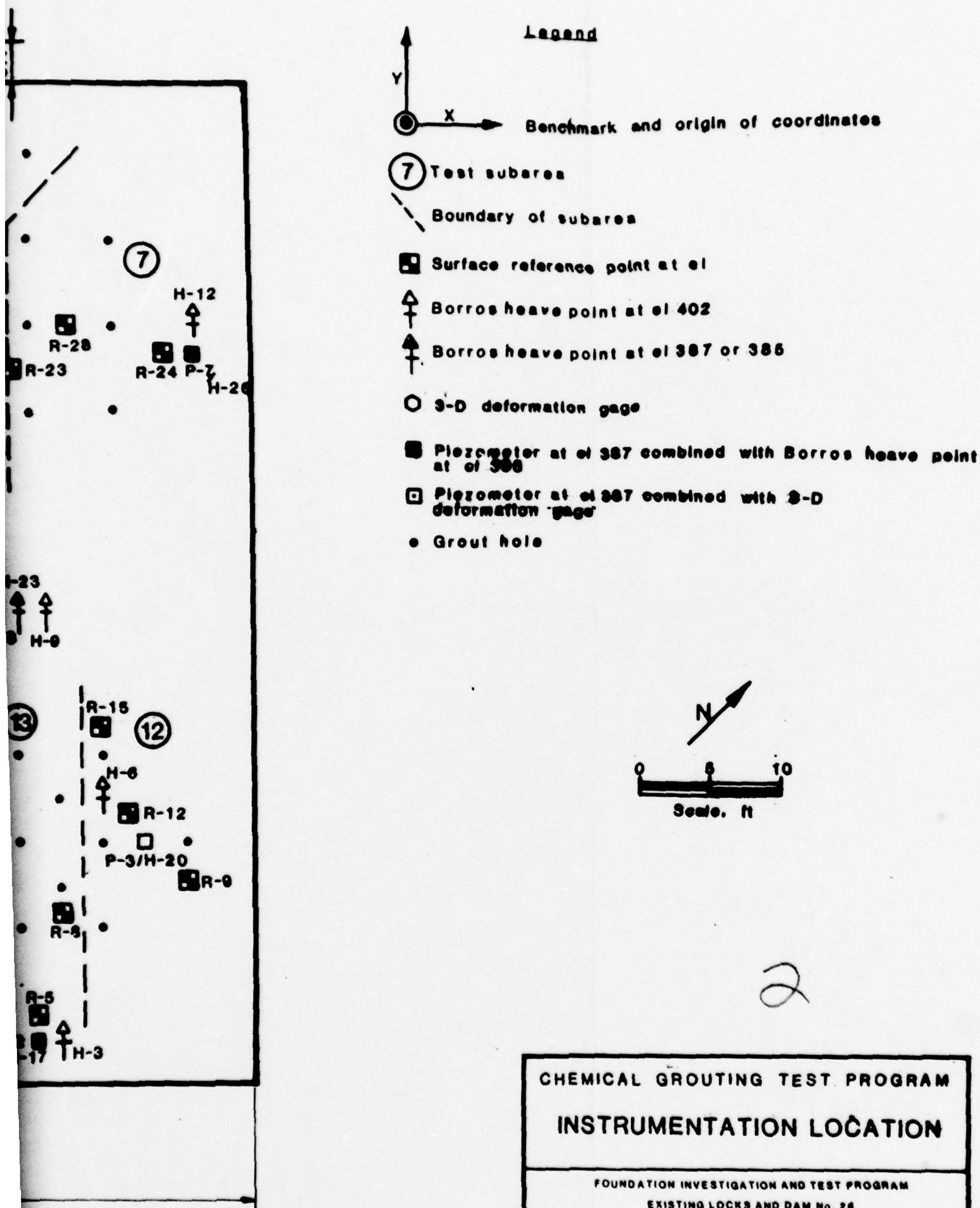

2

CHEMICAL GROUTING TEST PROGRAM

INSTRUMENTATION LOCATION

FOUNDATION INVESTIGATION AND TEST PROGRAM
EXISTING LOCKS AND DAM No. 26
ST LOUIS DISTRICT, CORPS OF ENGINEERS.
DACW43-78-C-0005

Woodward-Clyde Consultants

Y7C825 Phase IX

Fig. 8.1

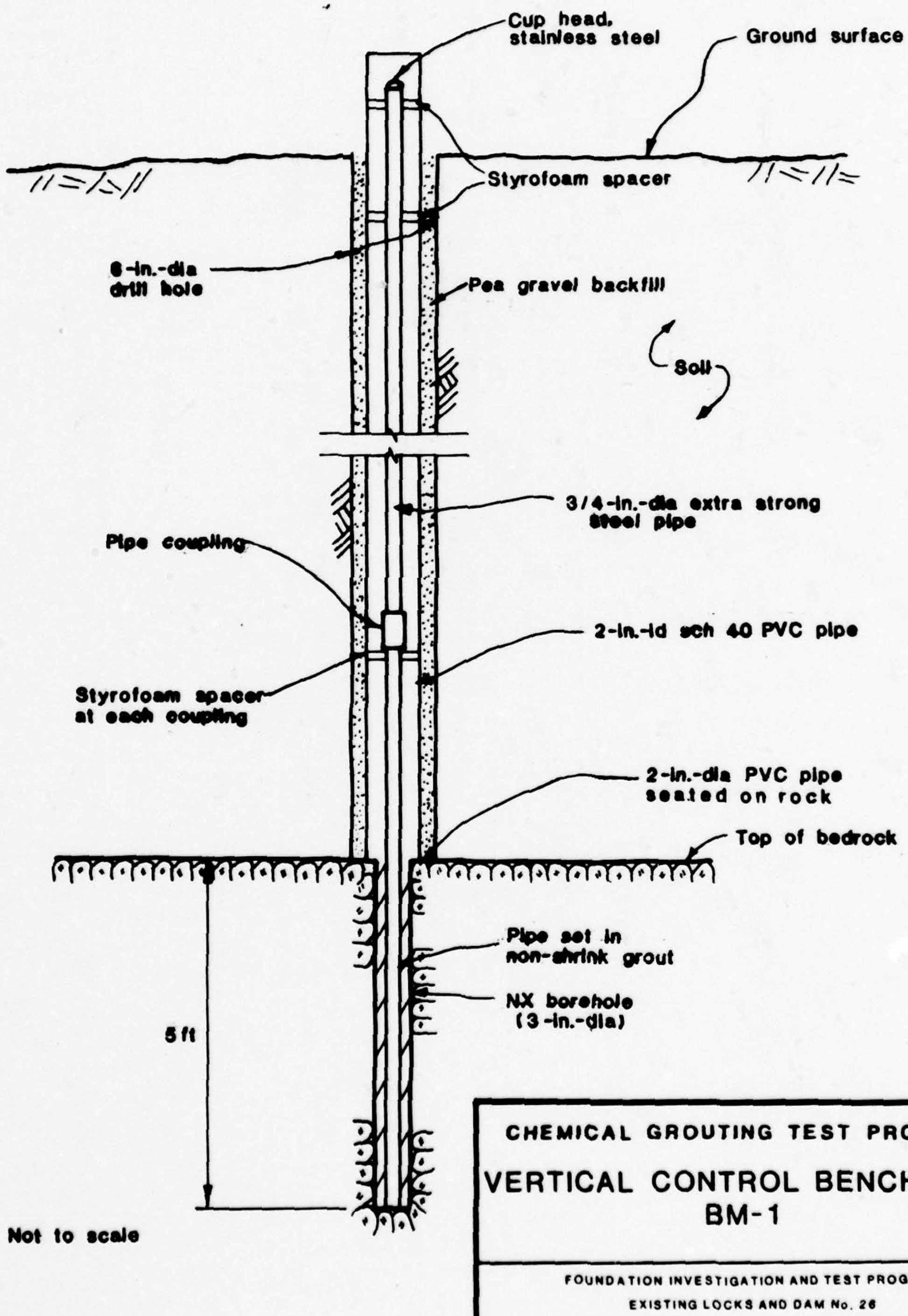

CHEMICAL GROUTING TEST PROGRAM

VERTICAL CONTROL BENCHMARK BM-1

FOUNDATION INVESTIGATION AND TEST PROGRAM
EXISTING LOCKS AND DAM No. 26
ST LOUIS DISTRICT, CORPS OF ENGINEERS.
DACW43-78-C-0005

Woodward-Clyde Consultants

Y7C825 Phase IX

Fig. 8.2

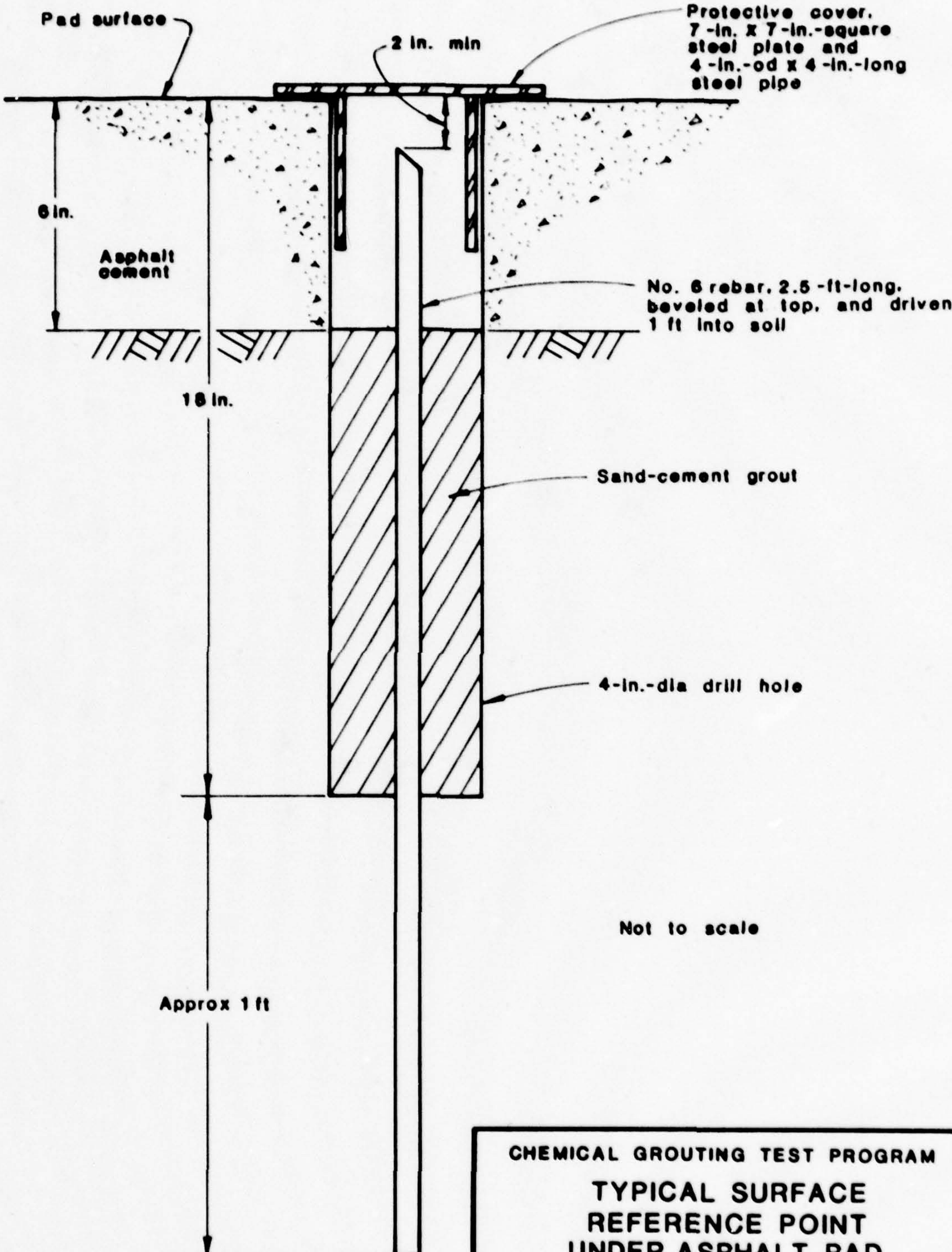

CHEMICAL GROUTING TEST PROGRAM

TYPICAL SURFACE REFERENCE POINT UNDER ASPHALT PAD

FOUNDATION INVESTIGATION AND TEST PROGRAM
EXISTING LOCKS AND DAM No. 26
ST LOUIS DISTRICT, CORPS OF ENGINEERS.
DACW43-78-C-0005

Woodward-Clyde Consultants

Y7C828 Phase IX

Fig. 8.3

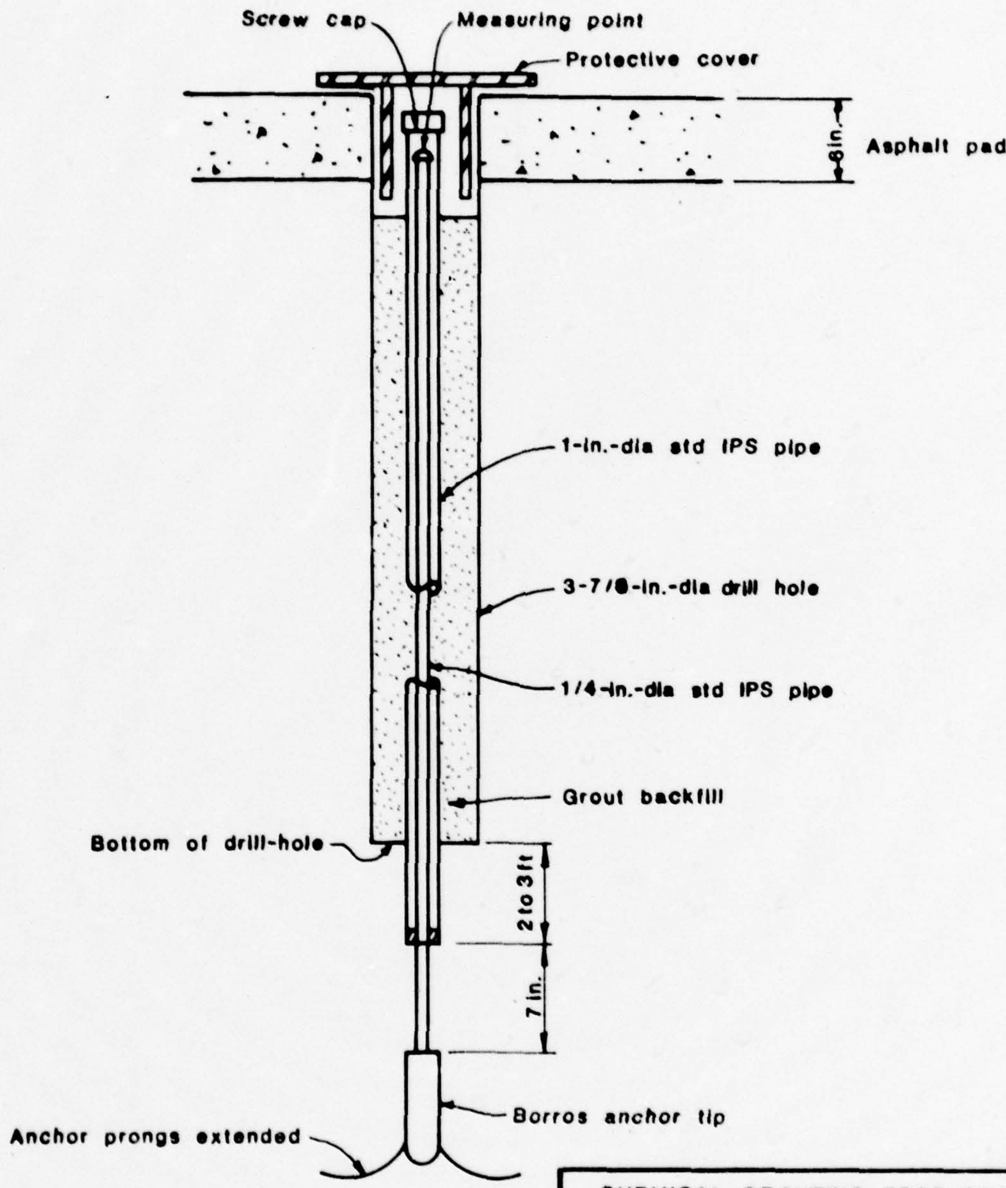

Not to scale

CHEMICAL GROUTING TEST PROGRAM

DETAILS OF
BORROS HEAVE POINT

FOUNDATION INVESTIGATION AND TEST PROGRAM
EXISTING LOCKS AND DAM No. 26
ST LOUIS DISTRICT, CORPS OF ENGINEERS.
DACW43-78-C-0005

Woodward-Clyde Consultants
Y7C825 Phase IX

Fig. 8.4

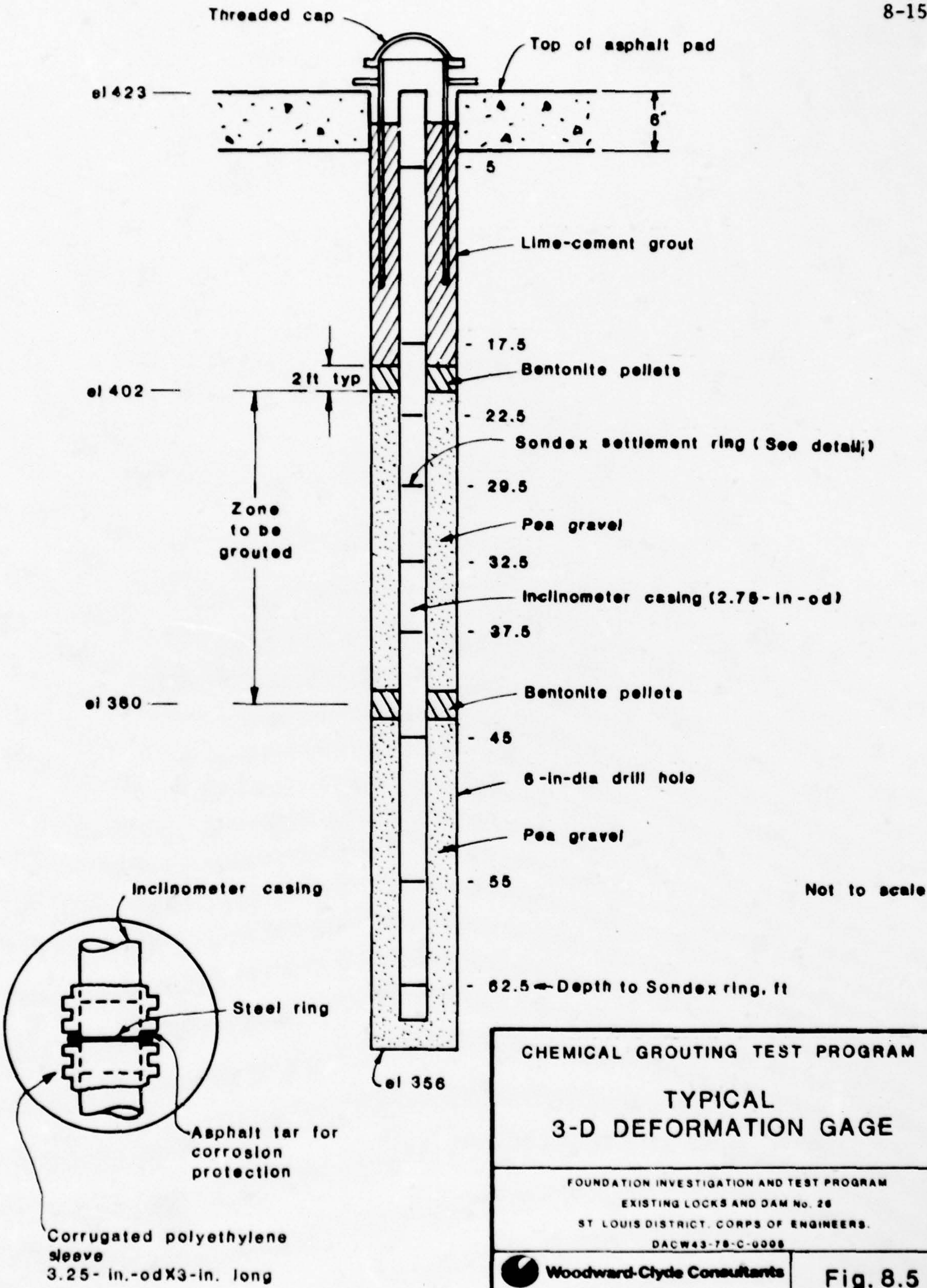

CHEMICAL GROUTING TEST PROGRAM

TYPICAL
3-D DEFORMATION GAGE

FOUNDATION INVESTIGATION AND TEST PROGRAM
EXISTING LOCKS AND DAM No. 26
ST LOUIS DISTRICT, CORPS OF ENGINEERS.
DACW43-78-C-0008

Woodward-Clyde Consultants

Y7C825 Phase IX

Fig. 8.5

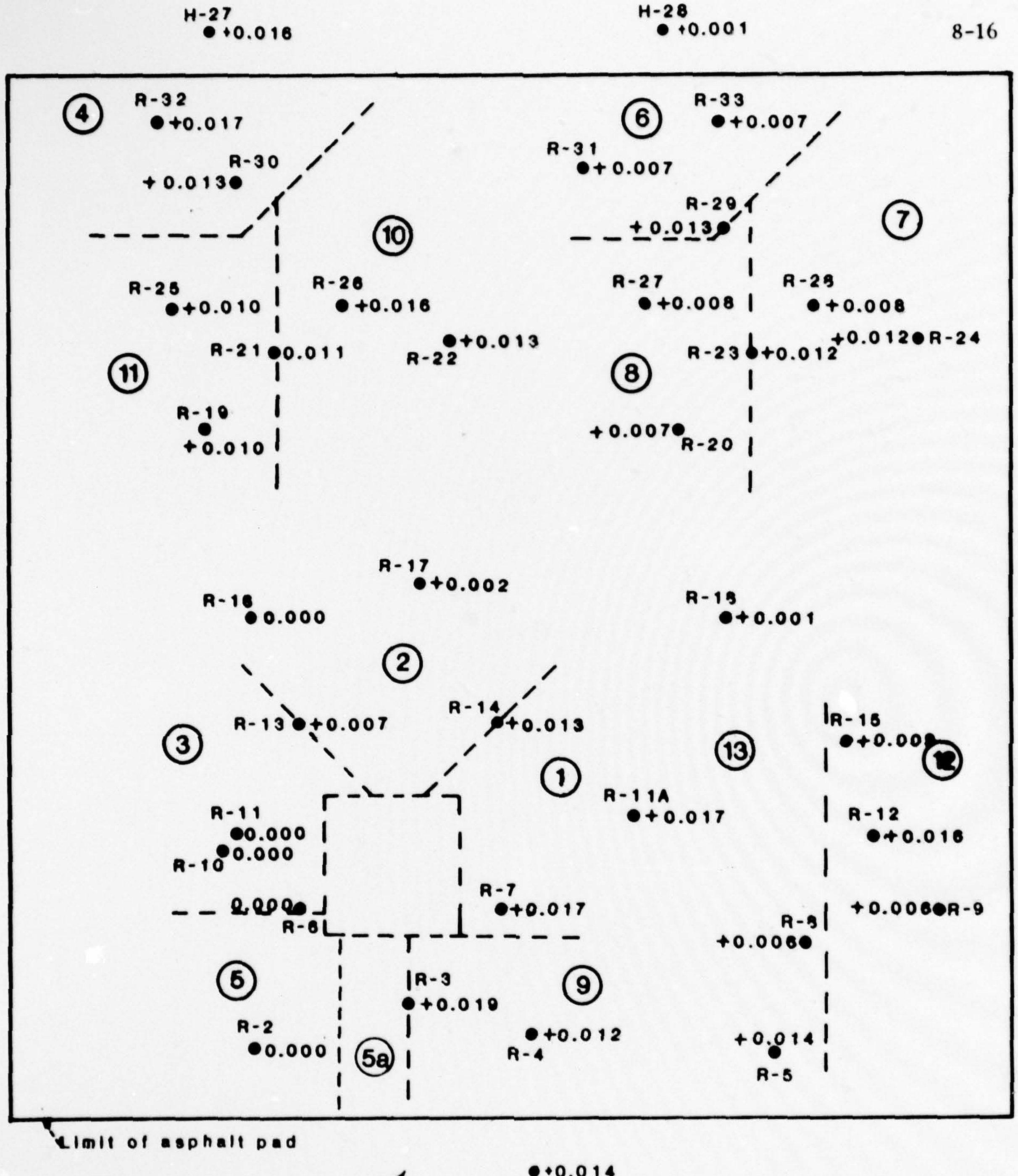

Legend

(5) Test Subarea No.

● R-26 Instrument location and number

+0.004 Heave in feet

CHEMICAL GROUTING TEST PROGRAM

MAXIMUM VERTICAL MOVEMENT OF SURFACE REFERENCE POINTS AT EL 423

FOUNDATION INVESTIGATION AND TEST PROGRAM
EXISTING LOCKS AND DAM No. 26
ST LOUIS DISTRICT, CORPS OF ENGINEERS.
DACW43-78-C-0005

Woodward-Clyde Consultants

Fig. 8.6

Y7C825 Phase IV

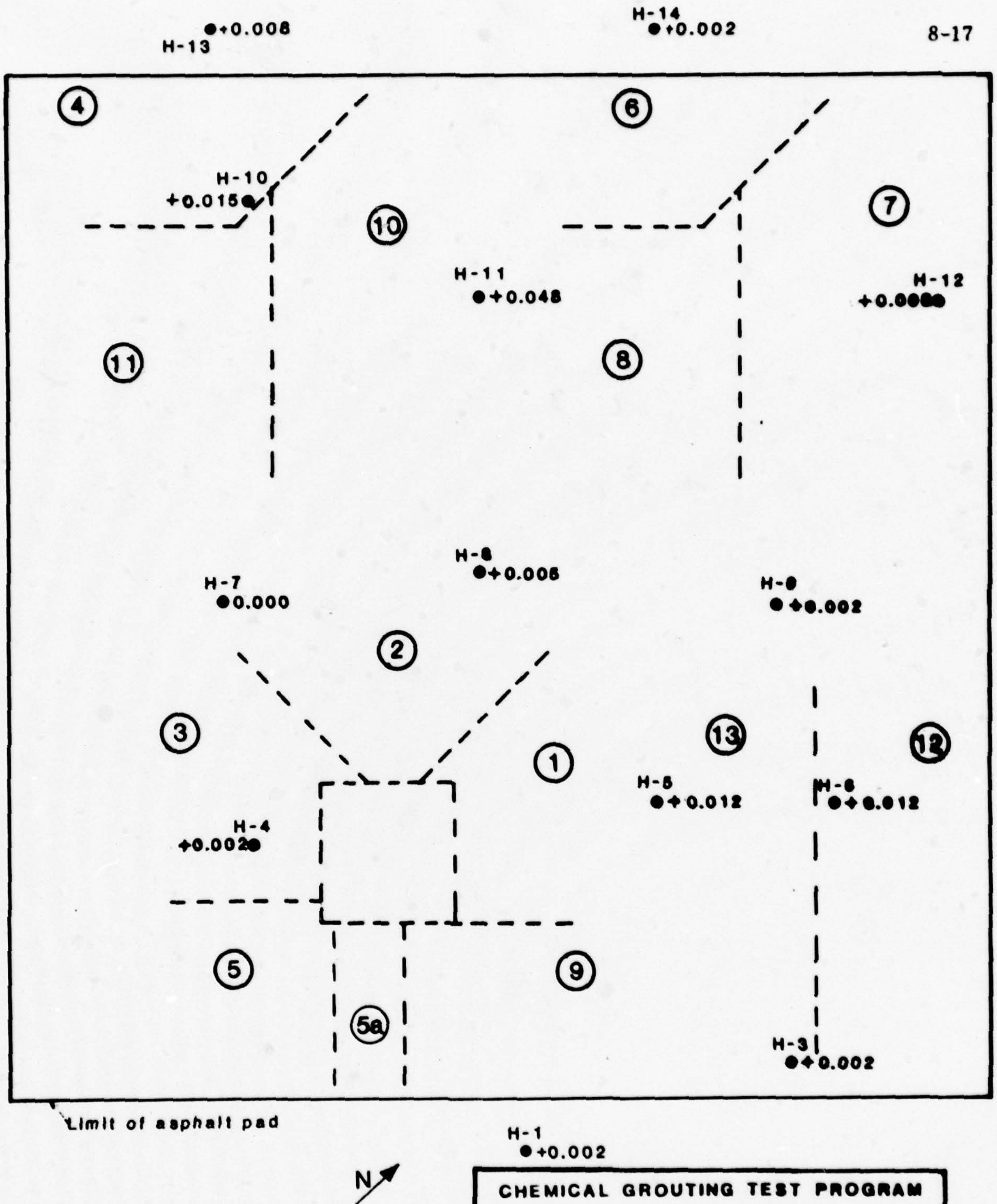

Legend

5 Test Subarea No.

● H-12 Instrument location and numbers

+0.004 Heave in ft

CHEMICAL GROUTING TEST PROGRAM

MAXIMUM VERTICAL MOVEMENT OF BORROS POINTS AT EL 402

FOUNDATION INVESTIGATION AND TEST PROGRAM
EXISTING LOCKS AND DAM No. 26
ST LOUIS DISTRICT, CORPS OF ENGINEERS.
DACW43-78-C-0005

Woodward-Clyde Consultants

Y7C825 Phase IX

Fig. 8.7

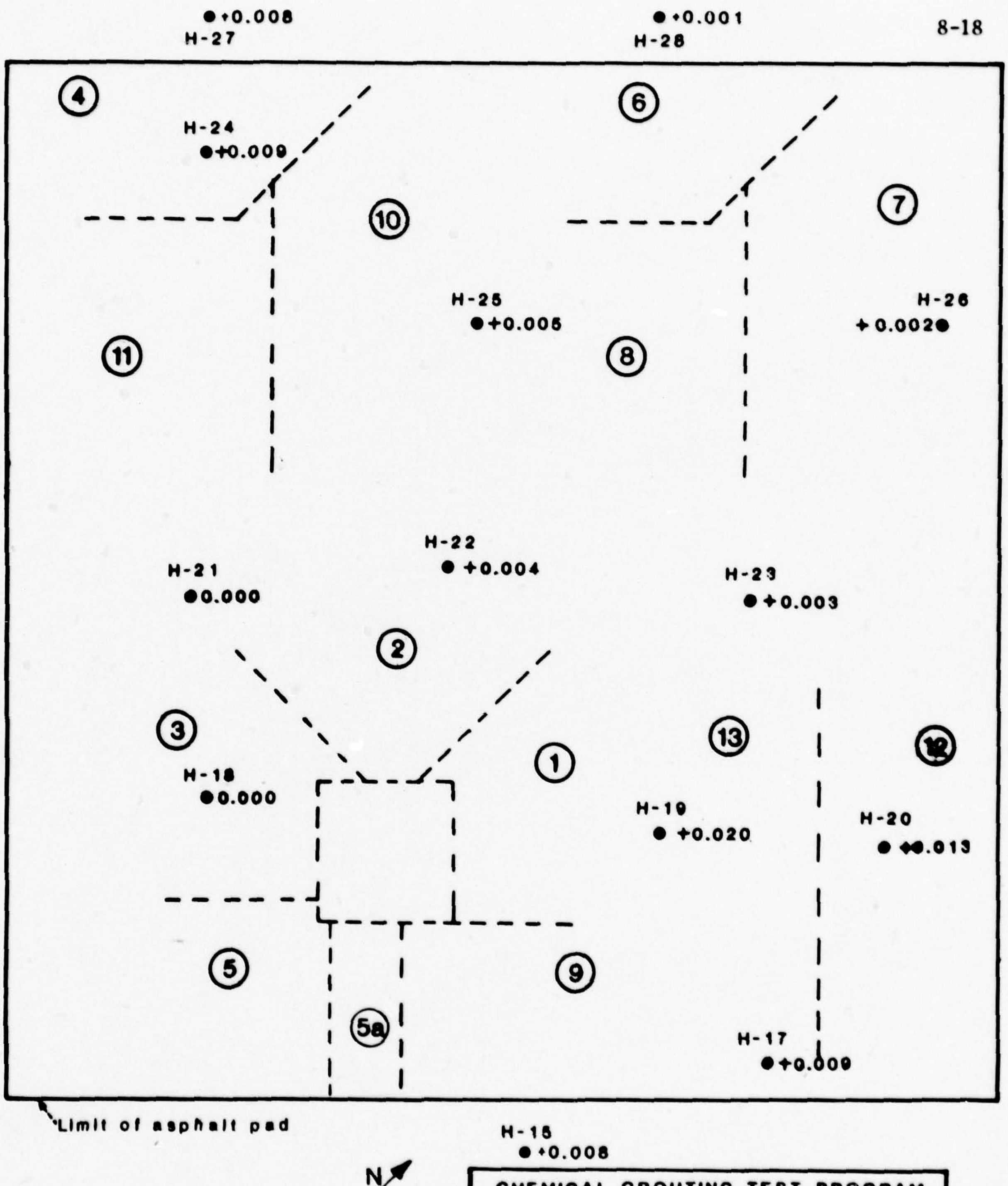

Legend

5 Test Subarea No.

● H-19 Instrument location and numbers

+0.004 Heave in ft

CHEMICAL GROUTING TEST PROGRAM

MAXIMUM VERTICAL MOVEMENT OF BORROS POINTS AT EL 385 TO 387

FOUNDATION INVESTIGATION AND TEST PROGRAM
EXISTING LOCKS AND DAM No. 26
ST LOUIS DISTRICT, CORPS OF ENGINEERS.
DACW43-78-C-0005

Woodward-Clyde Consultants

Fig. 8.8

Y7C825 Phase IX

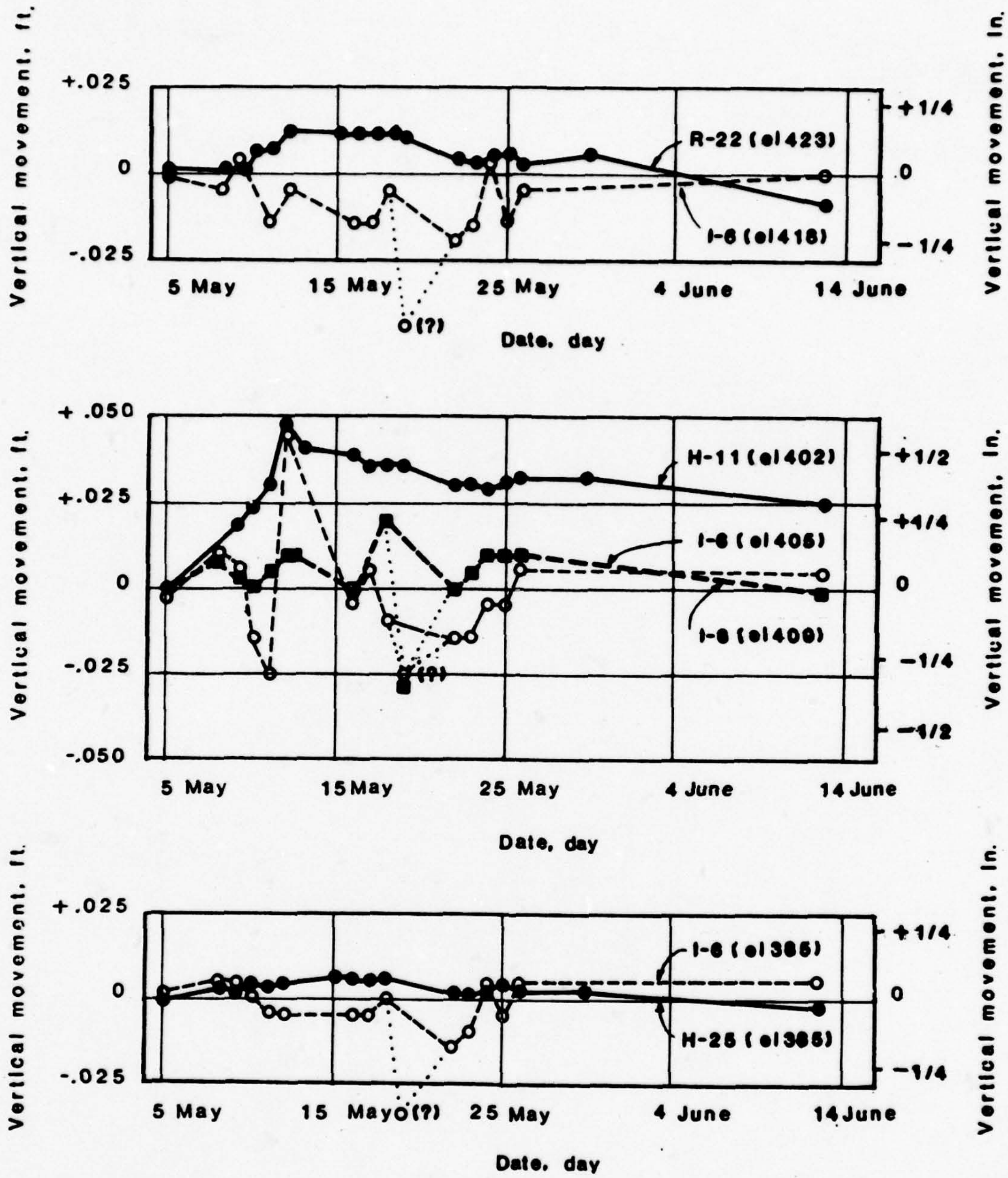

Legend

R = Surface reference point

I = Sondex ring

H = Borros Gage

CHEMICAL GROUTING TEST PROGRAM

RESULTS OF HEAVE MEASUREMENTS BETWEEN SUBAREAS 8 AND 10

FOUNDATION INVESTIGATION AND TEST PROGRAM
EXISTING LOCKS AND DAM No. 26
ST LOUIS DISTRICT, CORPS OF ENGINEERS.
DACW43-78-C-0005

Woodward-Clyde Consultants

Y7C825 Phase IV

Fig. 8.9

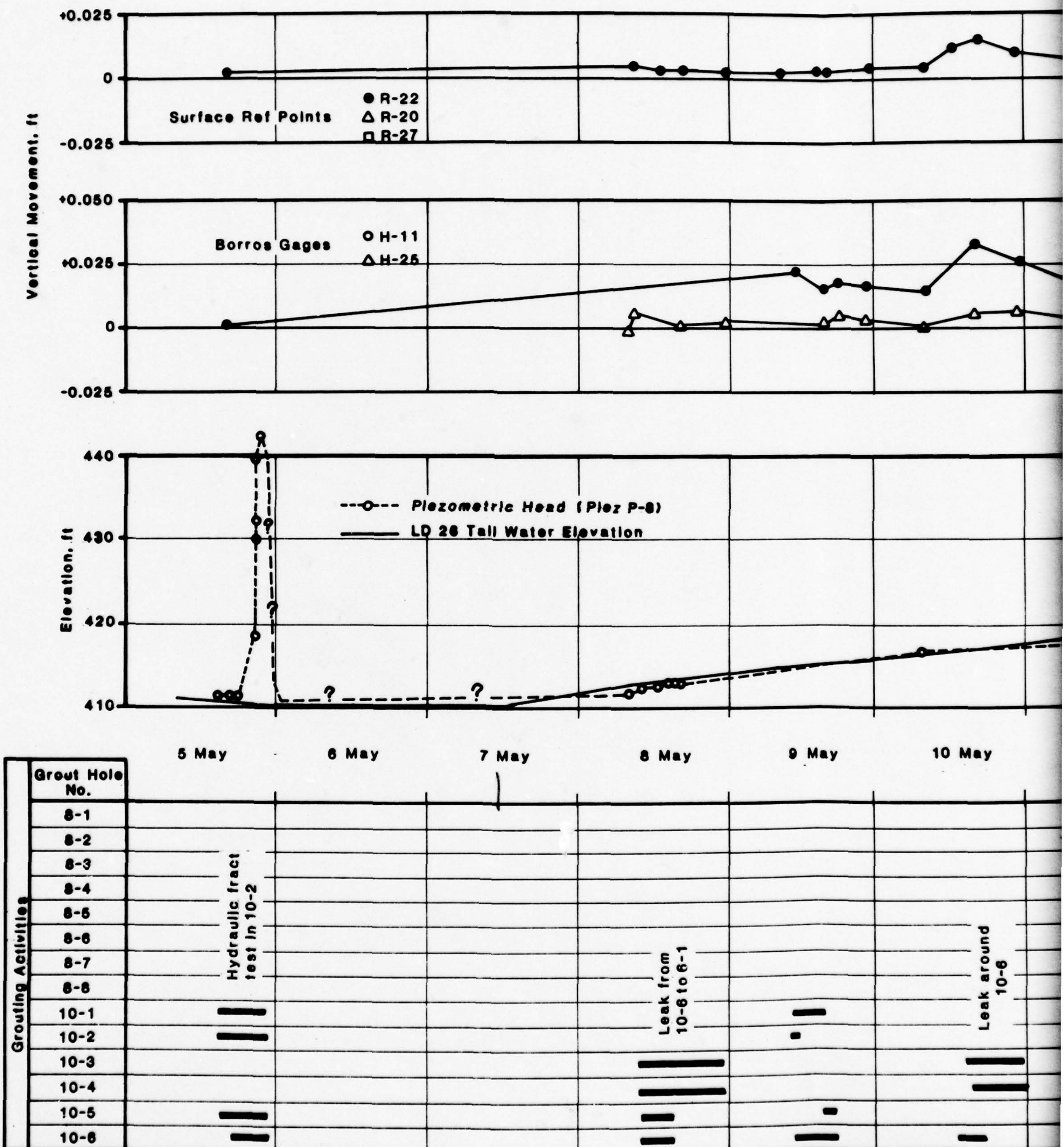

Vertical Movement, ft
+0.025
0
-0.025
Surface Ref Points
R-22
R-20
R-27
+0.050
+0.025
0
-0.025
Borros Gages
H-11
H-25
Elevation, ft
440
430
420
410
Piezometric Head (Piez P-8)
LD 26 Tail Water Elevation
5 May
6 May
7 May
8 May
9 May
10 May
Grouting Activities
Grout Hole No.
8-1
8-2
8-3
8-4
8-5
8-6
8-7
8-8
10-1
10-2
10-3
10-4
10-5
10-6
Hydraulic fract test in 10-2
Leak from 10-6 to 6-1
Leak around 10-6

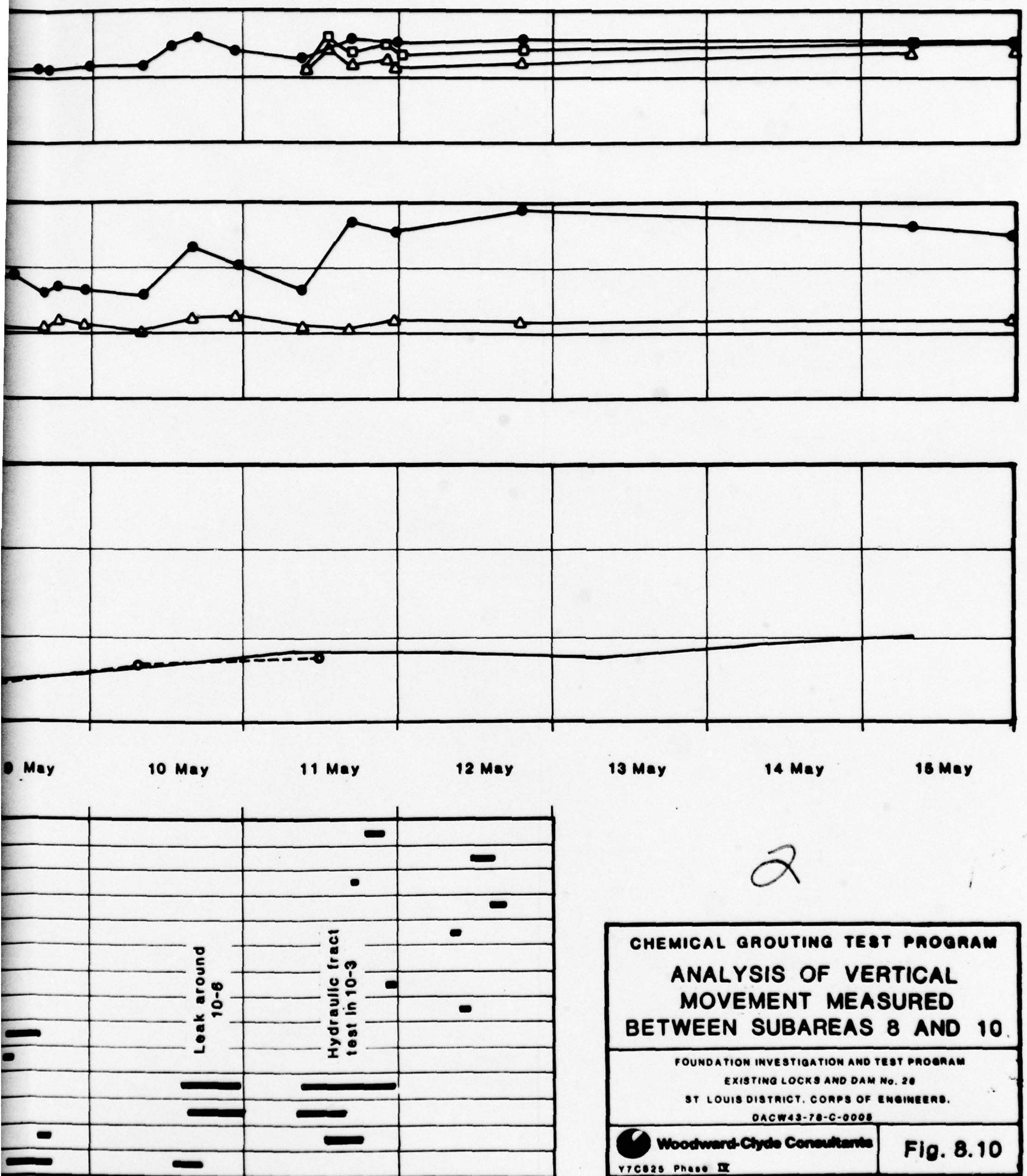

CHEMICAL GROUTING TEST PROGRAM

ANALYSIS OF VERTICAL MOVEMENT MEASURED BETWEEN SUBAREAS 8 AND 10

FOUNDATION INVESTIGATION AND TEST PROGRAM
EXISTING LOCKS AND DAM No. 26
ST LOUIS DISTRICT, CORPS OF ENGINEERS.
DACW43-78-C-0008

Woodward-Clyde Consultants

Fig. 8.10

Y7C825 Phase IX

CHEMICAL GROUTING TEST PROGRAM

ADEQUATE INSTALLATION METHOD OF SONDEX RINGS ON INCLINOMETER CASING

FOUNDATION INVESTIGATION AND TEST PROGRAM
EXISTING LOCKS AND DAM No. 26
ST LOUIS DISTRICT, CORPS OF ENGINEERS.
DACW43-78-C-0005

Woodward-Clyde Consultants
Y7C825 Phase IX

Fig. 8.11

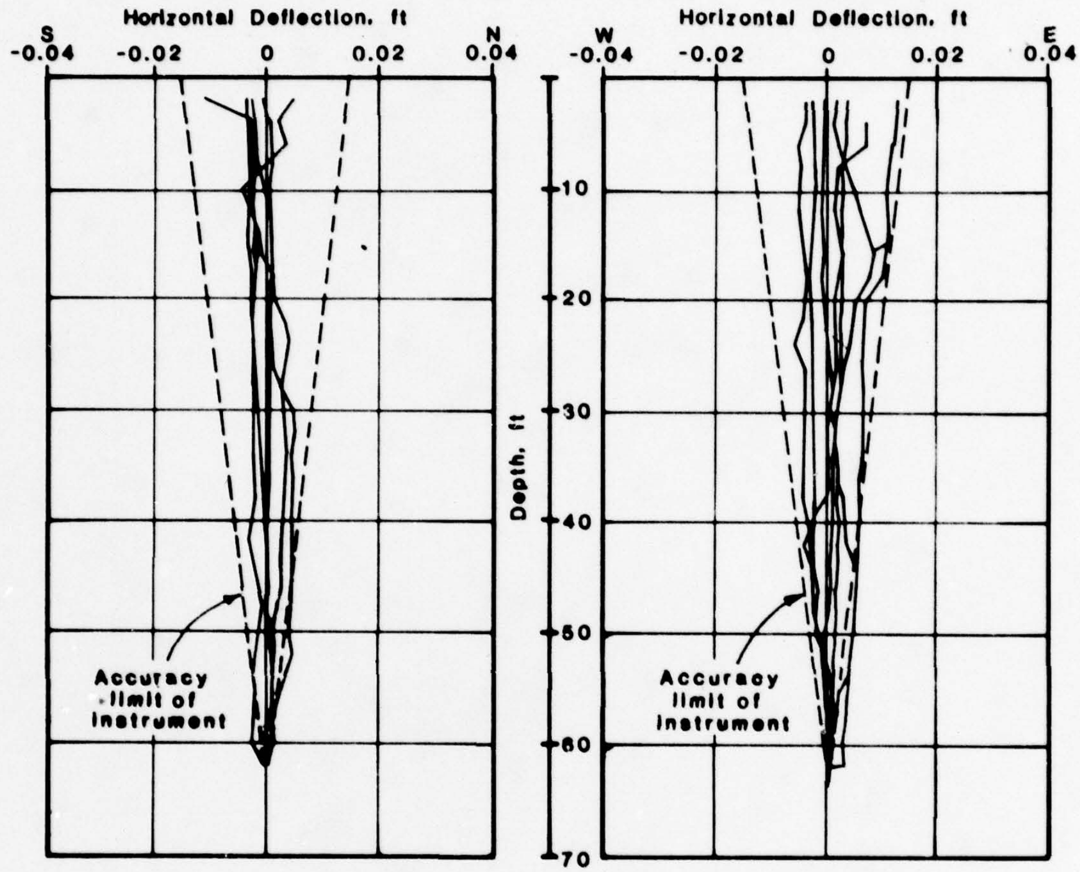

Difference between two successive measurements of seven inclinometers made before grouting (1 May and 8 May 1978)

CHEMICAL GROUTING TEST PROGRAM

COMPARISON BETWEEN TWO SUCCESSIVE MEASUREMENTS AND ACCURACY OF INCLINOMETER BEFORE GROUTING

FOUNDATION INVESTIGATION AND TEST PROGRAM
EXISTING LOCKS AND DAM No. 26
ST. LOUIS DISTRICT, CORPS OF ENGINEERS.
DACW43-78-C-0005

Woodward-Clyde Consultants

Fig. 8.12

Y7C825 Phase IX

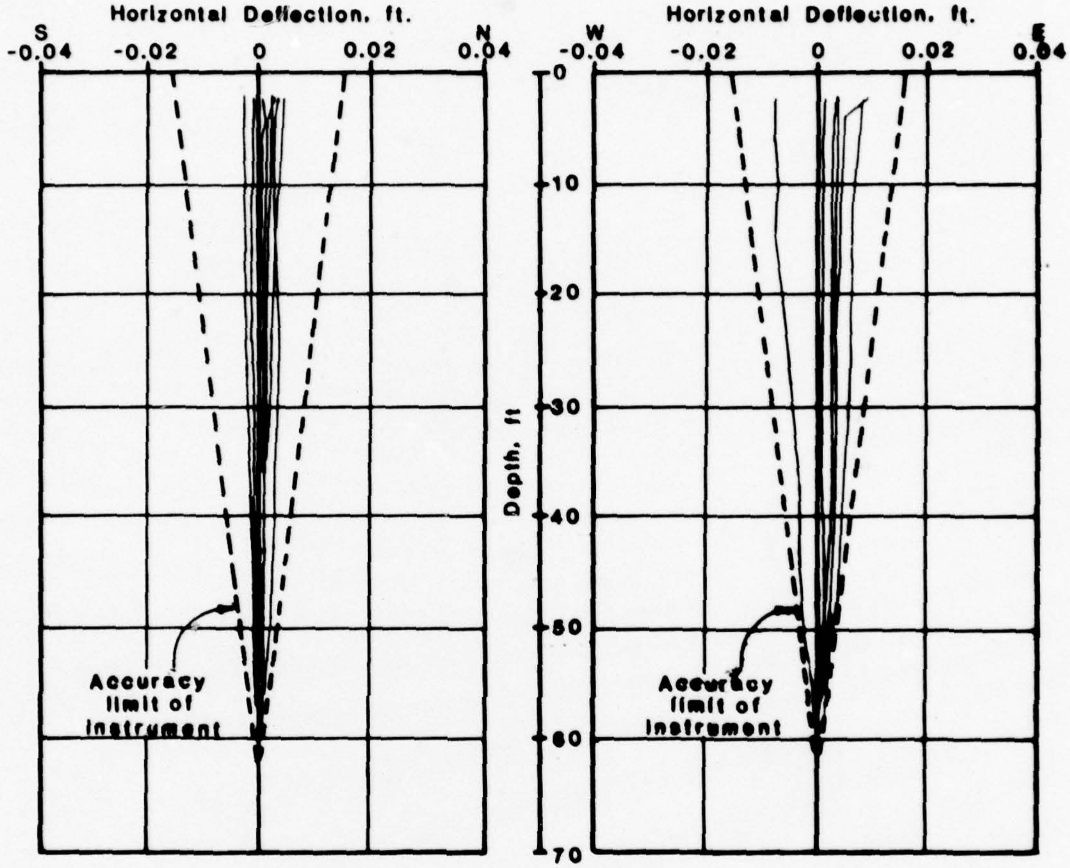

Difference between two successive measurements of seven inclinometers made after grouting
(12June and 14 June 1978)

CHEMICAL GROUTING TEST PROGRAM

COMPARISON BETWEEN TWO SUCCESSIVE MEASUREMENTS AND ACCURACY OF INCLINOMETER AFTER GROUTING

FOUNDATION INVESTIGATION AND TEST PROGRAM
EXISTING LOCKS AND DAM No. 26
ST LOUIS DISTRICT, CORPS OF ENGINEERS.
DACW43-78-C-0005

Woodward-Clyde Consultants

Y7C825 Phase IX

Fig. 8.13

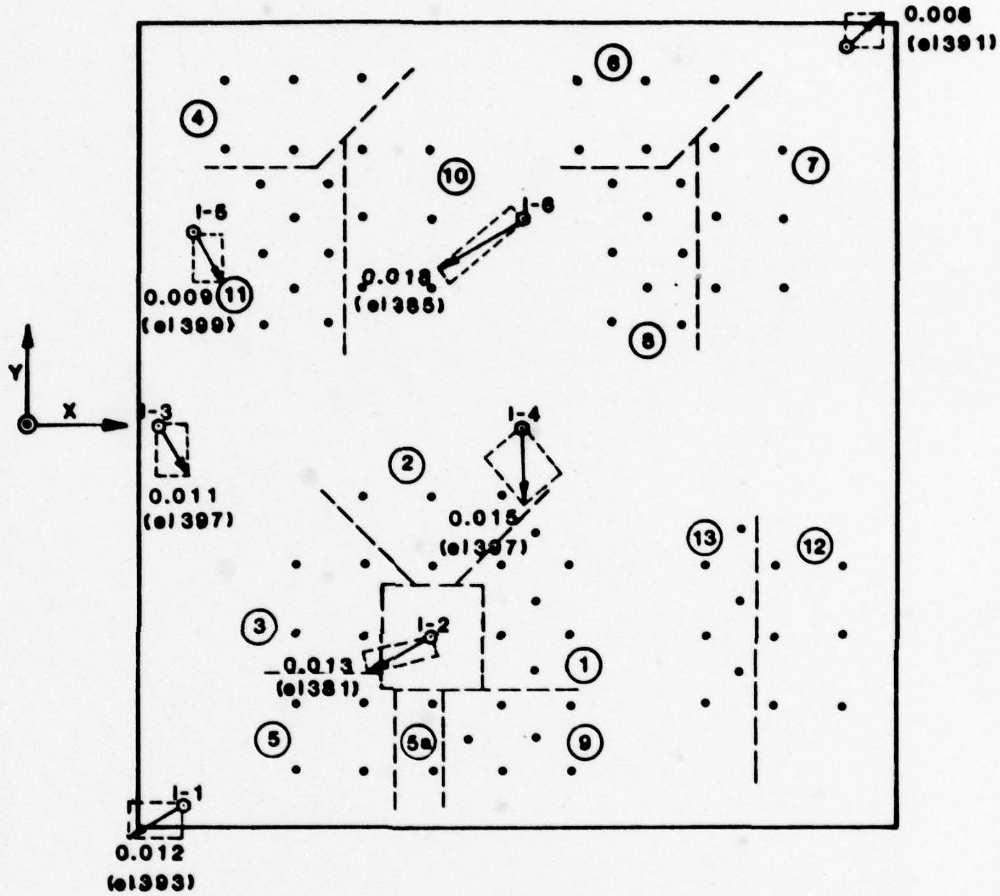

Legend

Benchmark

5 Grout Subarea No.

Grout hole

Boundary of subarea

Asphalt pad limits

Inclinometer movement, ft

(el 393) Elevation at which maximum displacement occurred

CHEMICAL GROUTING TEST PROGRAM

MAXIMUM TOTAL HORIZONTAL DISPLACEMENT FROM INCLINOMETER MEASUREMENTS

FOUNDATION INVESTIGATION AND TEST PROGRAM
EXISTING LOCKS AND DAM No. 26
ST LOUIS DISTRICT, CORPS OF ENGINEERS.
DACW43-78-C-0008

Woodward-Clyde Consultants
Y7C828 Phase IX

Fig. 8.14

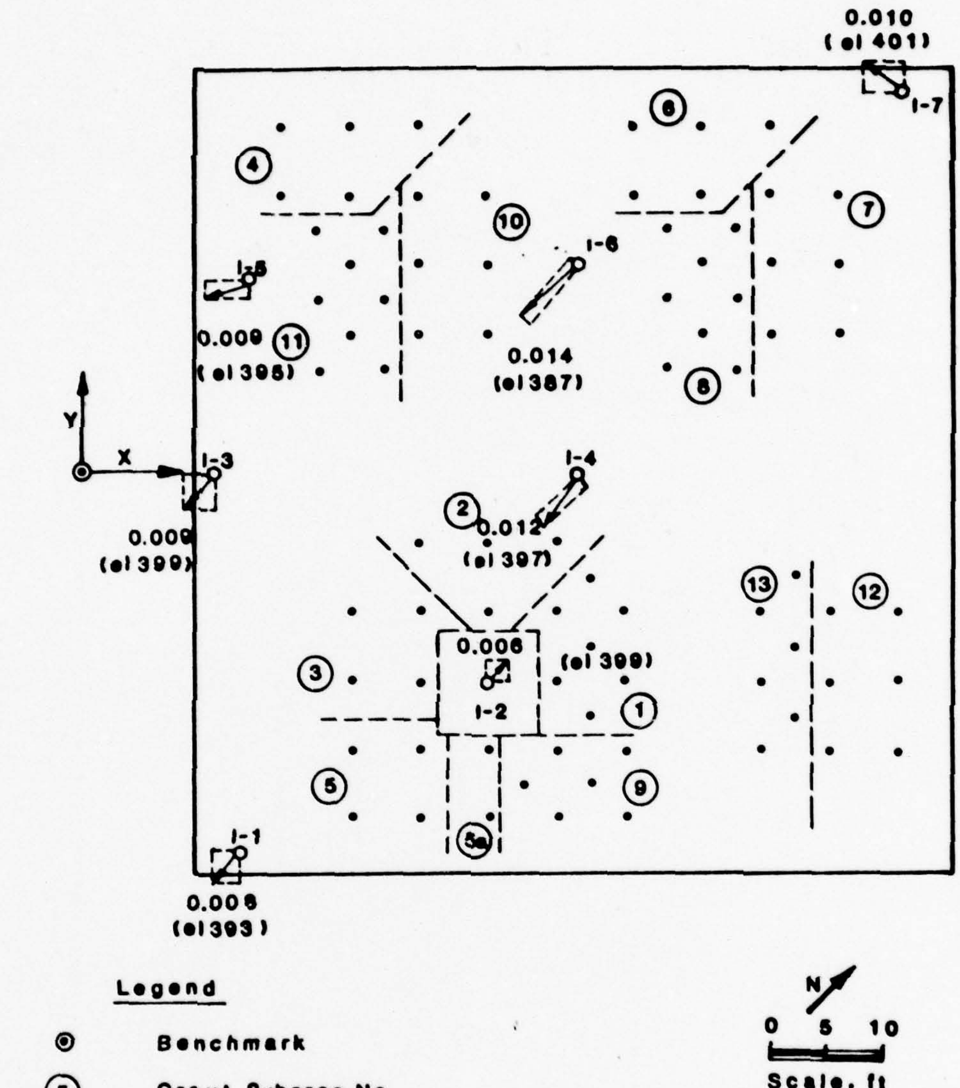

Legend

- Benchmark
- (5) Grout Subarea No.
- Grout hole
- Boundary of subarea
- Asphalt pad limits
- Inclinometer movement, ft
- (el 393) Elevation at which maximum displacement occurred

CHEMICAL GROUTING TEST PROGRAM

MAXIMUM HORIZONTAL DISPLACEMENT BETWEEN TWO SUCCESSIVE INCLINOMETER MEASUREMENTS

FOUNDATION INVESTIGATION AND TEST PROGRAM
EXISTING LOCKS AND DAM No. 26
ST LOUIS DISTRICT, CORPS OF ENGINEERS.
DACW43-78-C-0008

Woodward-Clyde Consultants

Y7C825 Phase IX

Fig. 8.15

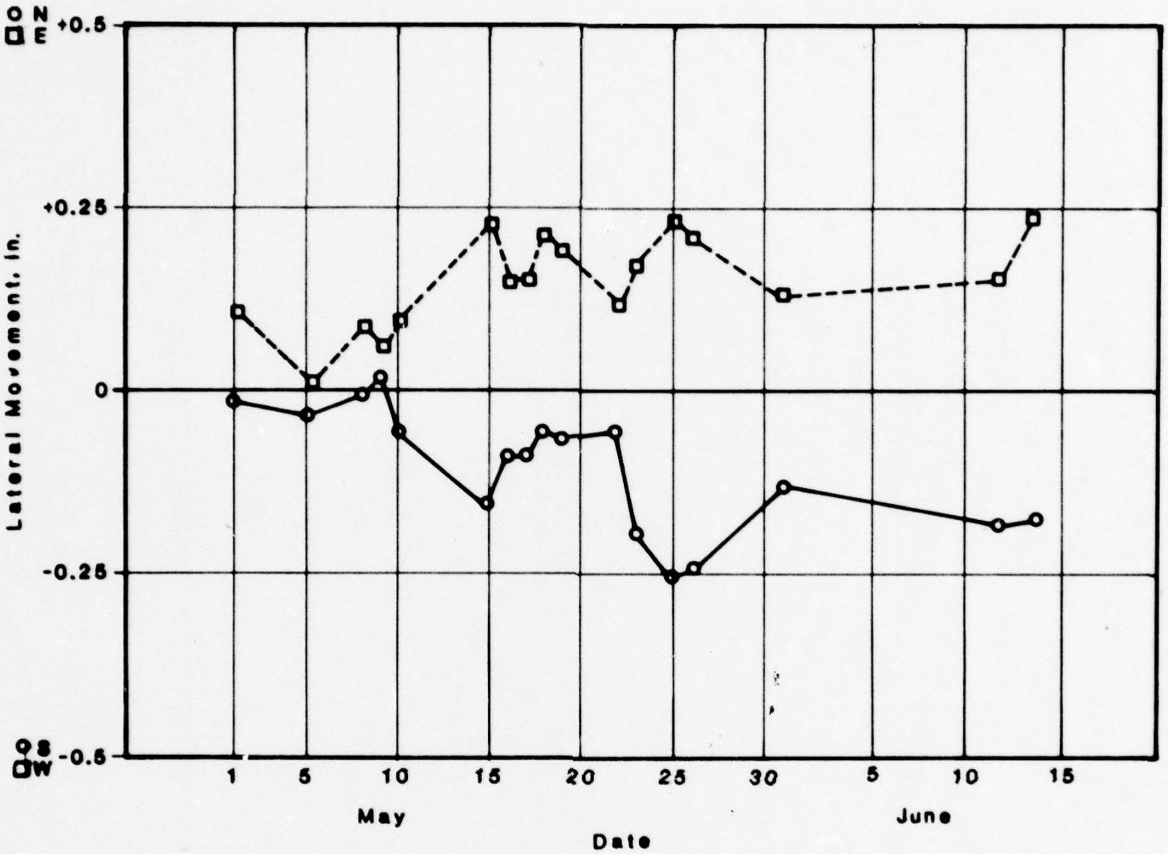

Legend

Symbol	Direction
O	North-South
□	East-West

CHEMICAL GROUTING TEST PROGRAM

LATERAL MOVEMENT
OF INCLINOMETER
I-6 AT EL 407

FOUNDATION INVESTIGATION AND TEST PROGRAM
EXISTING LOCKS AND DAM No. 26
ST LOUIS DISTRICT, CORPS OF ENGINEERS.
DACW43-78-C-0005

Woodward-Clyde Consultants
Y7C825 Phase IX

Fig. 8.16

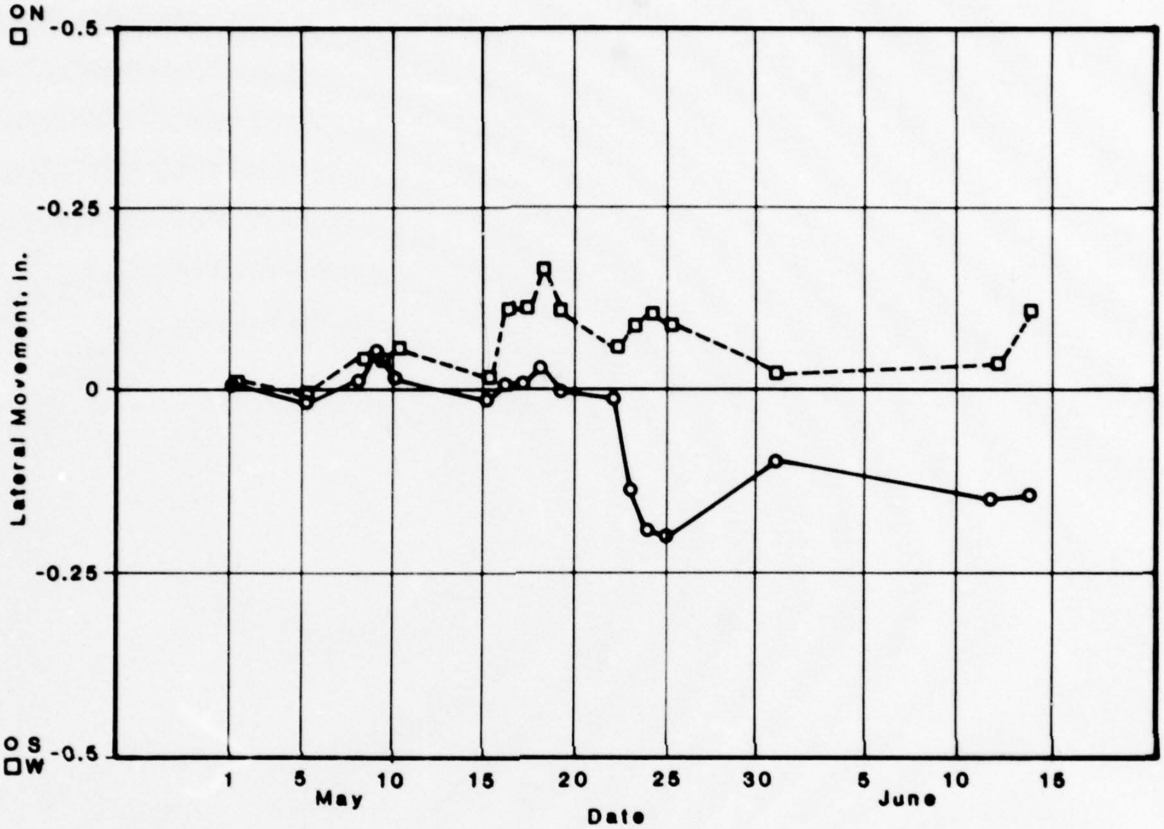

Legend

Symbol	Direction
O	North-South
□	East-West

CHEMICAL GROUTING TEST PROGRAM

LATERAL MOVEMENT OF INCLINOMETER I-6 AT EL 399

FOUNDATION INVESTIGATION AND TEST PROGRAM
EXISTING LOCKS AND DAM No. 26
ST LOUIS DISTRICT, CORPS OF ENGINEERS.
DACW43-78-C-0005

Woodward-Clyde Consultants

Y7C825 Phase IX

Fig 8.17

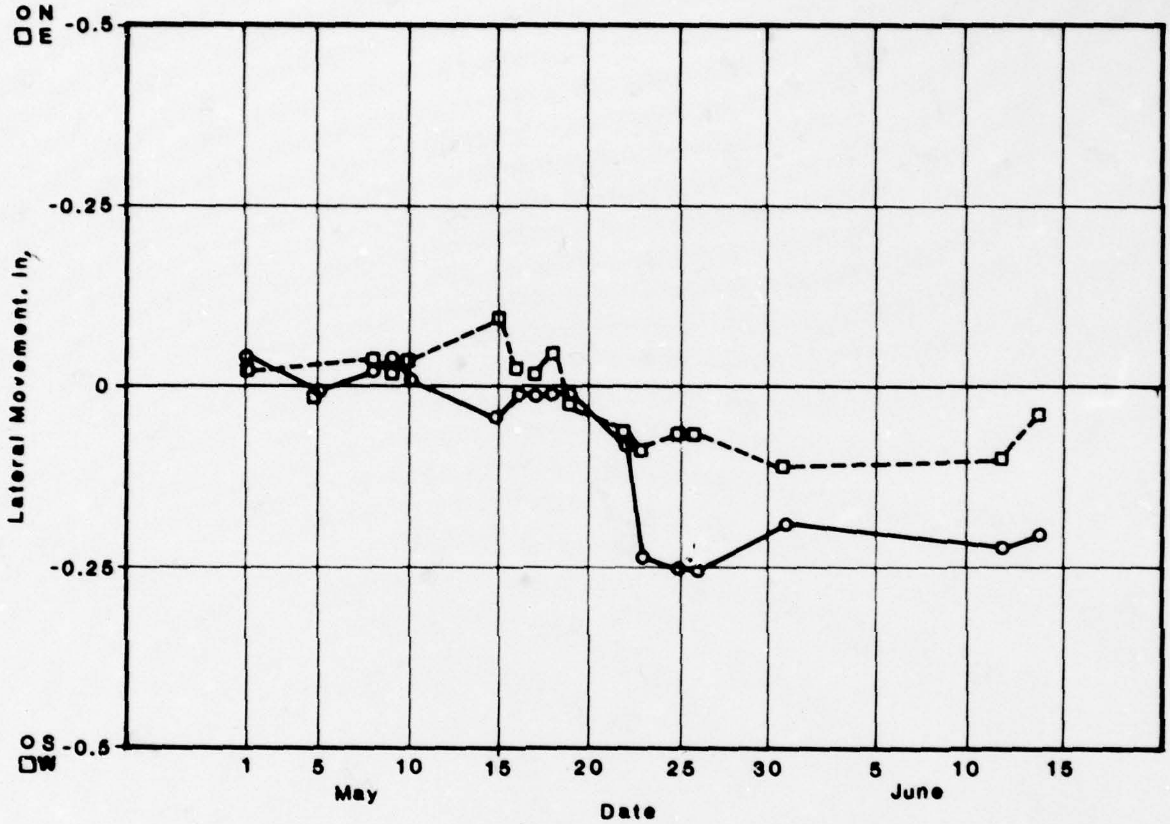

Legend

Symbol	Direction
O	North-South
□	East-West

CHEMICAL GROUTING TEST PROGRAM

LATERAL MOVEMENT OF INCLINOMETER I-6 AT EL 385

FOUNDATION INVESTIGATION AND TEST PROGRAM
EXISTING LOCKS AND DAM No. 26
ST LOUIS DISTRICT, CORPS OF ENGINEERS.
DACW43-78-C-0005

Woodward-Clyde Consultants

Y7C825 Phase IX

Fig. 8.18

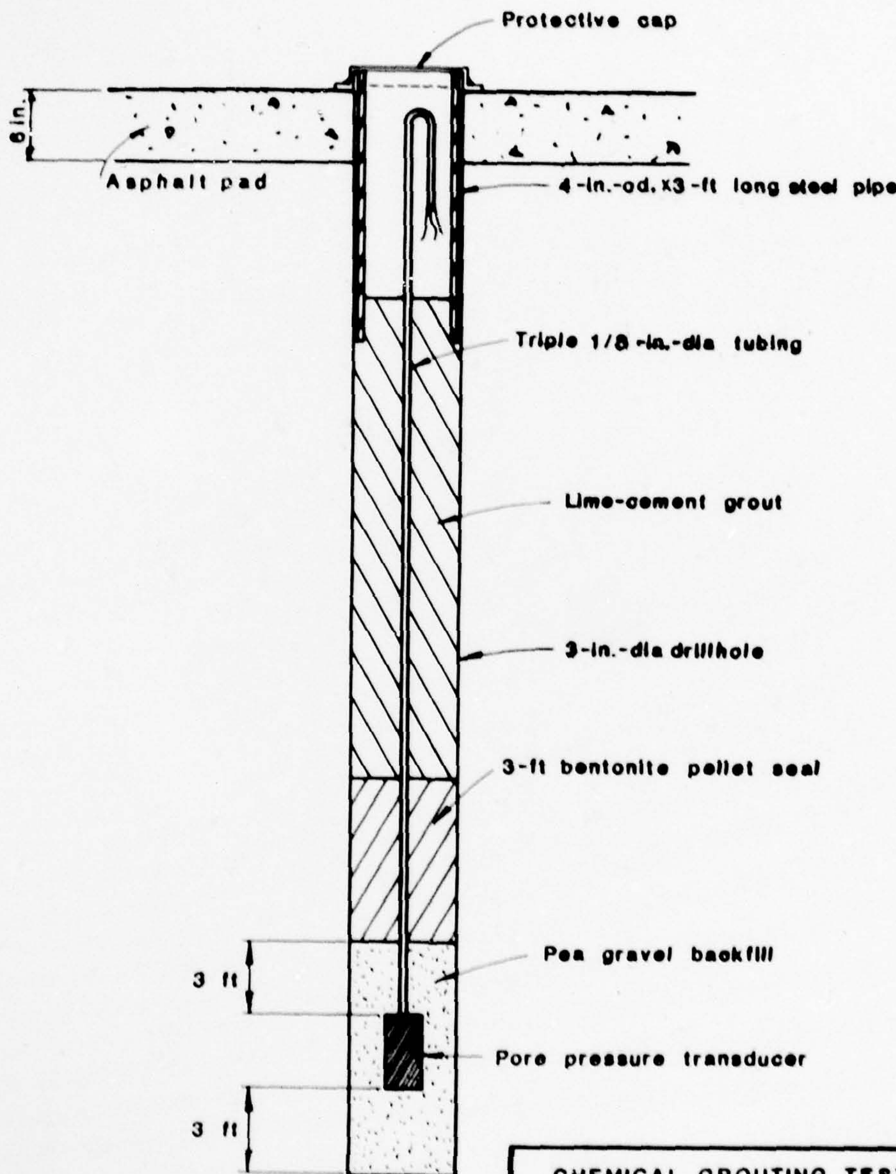

Not to scale

CHEMICAL GROUTING TEST PROGRAM

DETAILS OF PNEUMATIC PIEZOMETER INSTALLATION

FOUNDATION INVESTIGATION AND TEST PROGRAM
EXISTING LOCKS AND DAM No. 26
ST LOUIS DISTRICT, CORPS OF ENGINEERS.
DACW43-78-C-0006

Woodward-Clyde Consultants
Y7C825 Phase IX

Fig. 8.19

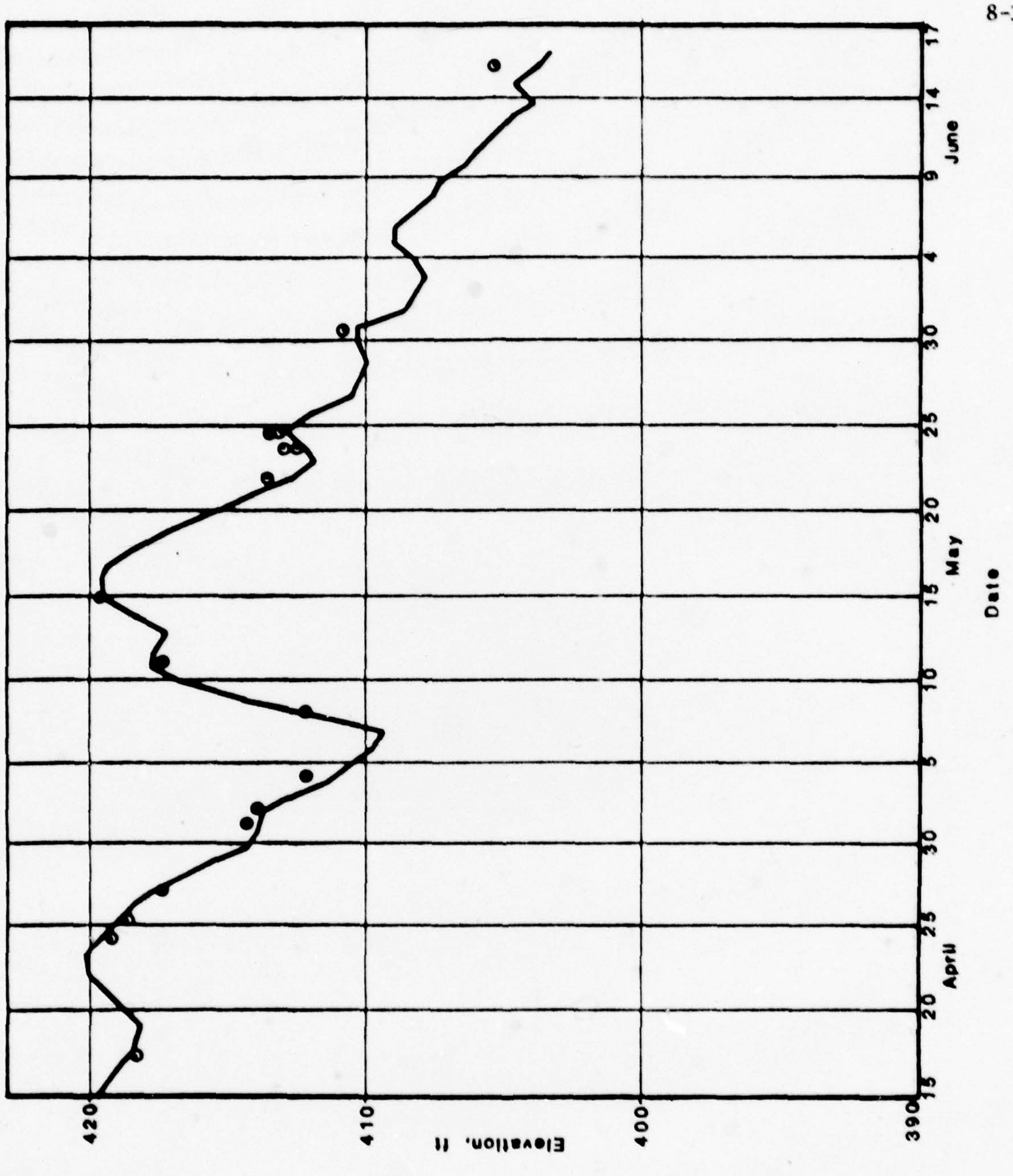

Legend

Tail water elevation at Locks and Dam No. 26 ________

Piezometric head in P-9 o

CHEMICAL GROUTING TEST PROGRAM

TYPICAL PORE WATER PRESSURE MEASUREMENTS IN TEST AREA

FOUNDATION INVESTIGATION AND TEST PROGRAM
EXISTING LOCKS AND DAM No. 26
ST LOUIS DISTRICT CORPS OF ENGINEERS
DACW43 76 C 0005

Woodward-Clyde Consultants

Fig. 8.20

Y7C825 Phase IV

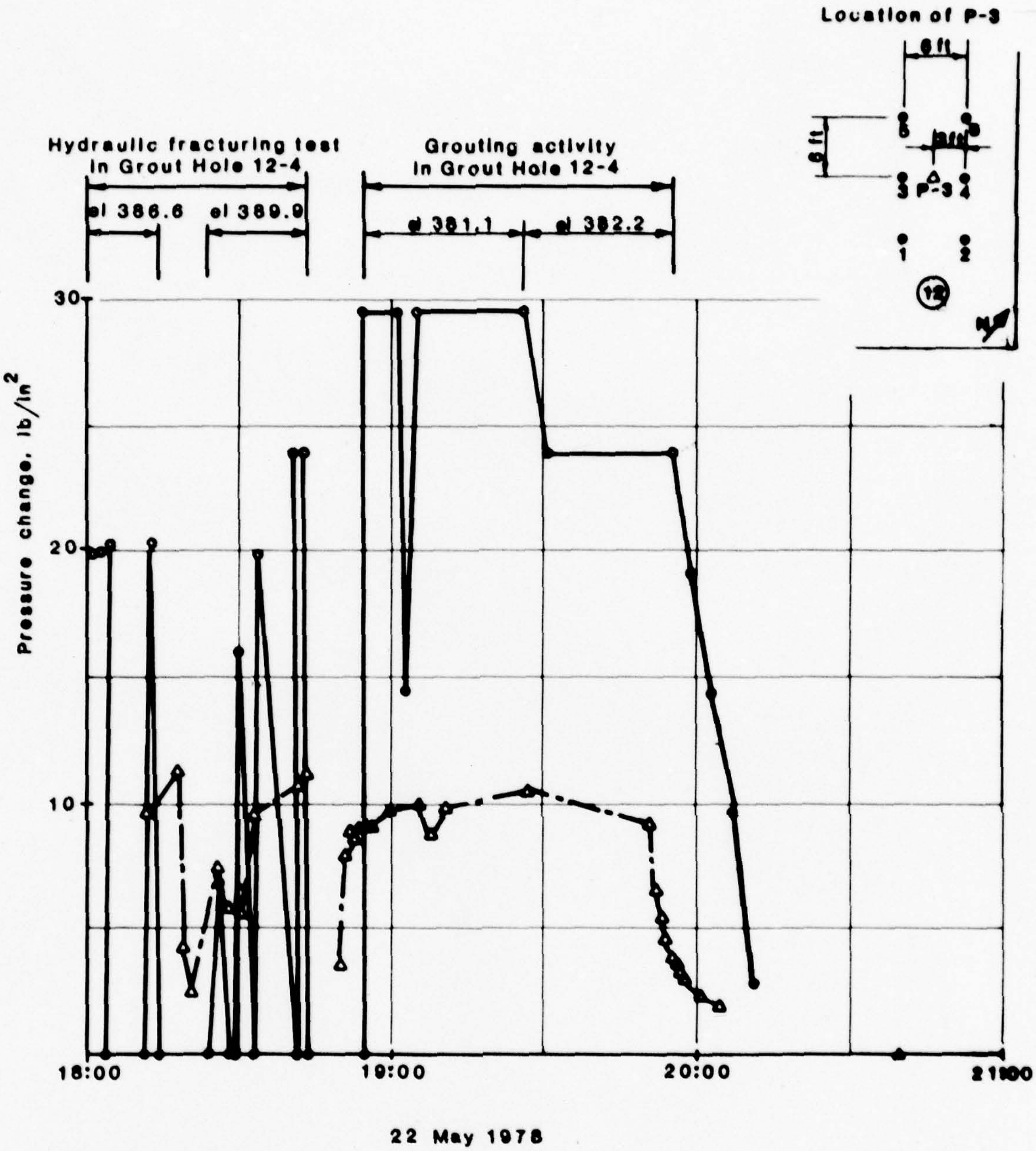

Legend

- o Grout pressure in Grout Hole 12-4
- Δ Excess pressure in Piezometer P-3 (el 387)

CHEMICAL GROUTING TEST PROGRAM

COMPARISON BETWEEN EXCESS PIEZOMETRIC PRESSURE IN P-3 AND GROUT PRESSURE IN GROUT HOLE 12-4

FOUNDATION INVESTIGATION AND TEST PROGRAM
EXISTING LOCKS AND DAM No. 26
ST LOUIS DISTRICT, CORPS OF ENGINEERS
DACW43-78-C-0006

Woodward-Clyde Consultants

Y7C825 Phase III

Fig. 8.21

PHASE IV REPORT

VOLUME II

RESULTS AND INTERPRETATION OF CHEMICAL GROUTING TEST PROGRAM

SECTION 9

EVALUATION OF GROUTING RESULTS

9 EVALUATION OF GROUTING RESULTS

9.1 METHODS OF EVALUATION

After grouting was completed, results of grout injection activities were evaluated using two approaches. The first approach was to evaluate the results from existing ground surface through boreholes drilled into the grouted zone (Section 9.2). The borehole evaluation was made immediately after grouting; in fact, it started in some completed subareas as grouting continued in others. The borehole evaluation consisted of sampling (Section 9.2.2), standard penetration tests (Section 9.2.3), static cone penetration tests (Section 9.2.4), pressuremeter tests (Section 9.2.5), borehole permeability tests (Section 9.2.6), and crosshole shear wave velocity tests (Section 9.2.7). The second approach was to excavate into the grouted zone for visual observation and documentation of the results (Section 9.3.3), and sampling (Section 9.3.6) and in situ testing (Sections 9.3.4 and 9.3.5) of the grouted soil. Both borehole and excavation evaluations were supplemented by laboratory tests (Section 9.4). The results of the various methods of evaluation of grouting effectiveness and grouted soil properties are discussed in Section 9.5.

9.2 BOREHOLE SAMPLING AND IN SITU TESTING

9.2.1 Purpose and Scope

Borehole samples were taken and in situ tests were performed after grouting to evaluate the effects of grouting on the soil and to measure strength-deformation properties of the grouted soil. Forty-five borings (series AG-A) were drilled from el 423 in June 1978, and five borings (series AG-B) were drilled from el 402 in July. In situ testing performed in these borings included standard penetration, static cone penetration, pressuremeter, and falling head permeability tests. Disturbed and undisturbed samples were also taken in some of these borings. The locations of the AG-series borings are shown in Fig. 9.1, in relation to the grout holes and the test subareas. Laboratory tests were made on samples recovered in the borings. These tests, consisting of unconfined and triaxial compression tests and permeability tests, are discussed in Section 9.4. Shear wave velocity measurements were made after grouting in the same four arrays of geophysical boreholes that were used before grouting (Section 3.2.6).

9.2.2 Boring and Sampling

The after-grouting boring and sampling program had three purposes:

(1) provide disturbed samples for visual classification and evaluation of grout content;

(2) provide supplemental information on the stratigraphic profile; and

(3) provide undisturbed samples of grouted soil for laboratory testing.

Disturbed samples were obtained from standard penetration test split-spoon samples. Eleven continuous standard penetration test borings were made in the chemical grouting test area and split-spoon samples were taken after every permeablity test in other borings. The standard penetration test borings were advanced with a tricone roller bit and bentonite drilling fluid, which provided good sample recovery. In the permeability test borings drilled with water, split-spoon sample recovery was generally poor in the ungrouted to lightly grouted soils, and satisfactory in more heavily grouted soils.

The spraying of phenolphtalein solution on disturbed split-spoon samples provided an effective method for identifying the extent and concentration of silicate grout in the samples. The high alkalinity of the sodium silicate grouts turned the clear solution to bright purple. During drilling, prior to reaching the desired testing depth, phenolphtalein was sprayed on the returning drilling fluid and the observed color changes were used to detect the presence of grouted strata.

Odor was also an effective identification tool. The Siroc grouts had a strong ammonia odor due to the formamide reactant. The silicate/aluminate grout did not have any formamide and therefore was odorless. The silicate/R600 grouts produced an odor similar to that of a fruit salad. Dyes had been mixed with the grouts for later identification, but much of the color was diluted during injection through the soil. Some color was observed in the grout fractures that were occasionally found in the samples.

Undisturbed sampling was attempted with thin-wall (Shelby) tubes, and Pitcher and Denison samplers. In each case, the hole was advanced with rotary drilling and bentonite drilling fluid. Shelby tubes were effective in low-strength grouts where the standard penetration resistance N was less than 30. The fixed-piston tube sampler (Denison) was found to be ineffective due to the hardness of the grouted soil. The Pitcher sampler was successful as the spring force on the sampling tube varied in response to the hardness of the soil being sampled. The cutting head was able to effectively advance the sampler as long as rotation, thrust, and drilling fluid flow were maintained at a constant, moderately slow rate. However, inspection of the tube samples in the laboratory revealed that the many soft seams in the grouted soil mass limited the number and length of samples that could be effectively tested. Sample shipment was a key consideration because of the varying sensitivities to vibration and impact within each sample. The samples were carefully transported by car to the laboratory. Seven undisturbed sampling borings were made in the various test subareas, yielding 41 samples.

9.2.3 Standard Penetration Tests

A program of continuous standard penetration test borings was performed to provide a universally used numerical index related to soil compactness and hardness. Standard penetration resistance or N-value has been empirically related to relative density, angle of internal friction and other soil properties, but no such correlations exist for grouted soil. However, the wealth of experience behind the use of this test in all types of soil can be used to provide a practical "feel" for the material. The numerical index was also a means by which comparisons of before and after grouting results could be used to assess relative magnitude of changes. Different grout types and grouting procedures could also be effectively compared. Standard penetration test results were also compared to other in situ testing results.

The continuous standard penetration resistance profiles from the eleven AG-series borings performed after grouting are presented in Fig. 9.2 through Fig. 9.15. The SPT profiles are plotted along with static cone penetration and permeability test results for each subarea. In situ testing data obtained before grouting (Fig. 3.2) are also shown in these figures for comparison purposes.

The influence of testing procedures on the quality of the results is well illustrated by three standard penetration resistance profiles shown in Fig. 9.2 and Fig. 9.3. In Boring AG-A1-1 in Subarea 1, the borehole was advanced by driving a steel casing and washing it out with water. Rotary drilling with bentonite drilling fluid was not used because the borehole was also used for falling head permeability tests at certain depths. In Borings AG-A1-2 in Subarea 1 and AG-A2-1 in Subarea 2, the boreholes were advanced by rotary drilling with bentonite drilling fluid. The N-values measured in Boring AG-A1-1 were significantly lower than those measured in the other two borings and, in fact, were at the lower limit of the range of N-values obtained before grouting. Although Borings AG-A1-1 and AG-A1-2 were only 9 ft apart in Subarea 1, the after-grouting subsurface conditions were sometimes different at these two locations. However, even when the conditions did not differ significantly, the N-values measured in AG-A1-1 were lower than those measured in AG-A1-2. The low N-values were attributed to loosening of the grouted sand below the casing in AG-A1-1 when the water level inside the casing dropped significantly several times during drilling. The low hydrostatic pressure inside the casing may have resulted in sand flow into the casing and loosening of the soil to be penetrated during the standard penetration test.

9.2.4 Static Cone Penetration Tests

A program of continuous static cone penetration test soundings was made to supplement the standard penetration tests and provide a numerical index that could facilitate comparison between grouted and ungrouted soil, and between various types of grouted soil. The empirical correlations between cone point resistance and various soil properties used in Section 3.2 are not valid for grouted soil. However, magnitudes of change were clearly indicated by the cone profiles, providing good comparative data. Like the standard penetration resistance profiles, the cone soundings were used for evaluating grouting effectiveness. The static cone differed from the standard penetration tests in that cone measurements were made under a sustained quasi-static loading while the standard split-spoon was driven dynamically.

Static cone penetration resistance profiles from the fourteen AG-series borings performed after grouting are presented in Fig. 9.2 through Fig. 9.15. In general, the cone profiles compared favorably with the standard penetration test profiles. Differences in the profiles generally result from testing different grouting products, as each test was performed between a different set of grout holes.

The procedure for static cone penetration testing was identical to the testing performed before grouting (Section 3.2). This procedure involved alternately drilling and pushing the cone. In most of the high-strength grouted soil, testing had to be discontinued before completing the nominal 5-ft run and the hole had to be drilled deeper because the load limit of the load cell (16,000 lb) was reached. In many cases, only 1 in. to 3 in. of penetration was achieved before exceeding the cone load limit. In any event, cone point resistances above 500 t/ft^2 have little meaning as they are indicative of rock-like material and penetration would be impossible without some damage to the cone.

9.2.5 *Pressuremeter Tests*

Pressuremeter tests were made to provide in situ stress and strength-deformation properties of the chemically grouted soil. These properties were used to compare grouted and ungrouted soil, and to compare various types of grouted soil. The results of pressuremeter tests performed in five AG-A-series borings and four AG-B-series borings are presented in Fig. G.1 through Fig. G.10, Appendix G. These results are in the form of pressure-volume change plots.

The pressuremeter borings were drilled following the same procedure used for Boring D-27 (Section 3.2). Thick Revert drilling fluid was used, and the borehole was advanced with a three-prong drag bit that was the same size as the pressuremeter probe. In some high-strength grout subareas, where the grout was injected under high pressure, some difficulty was encountered with insertion and removal of the probe in and out of the hole without damaging it. The high-pressure grouting appears to have locked in large horizontal stresses, which caused the borehole to squeeze after drilling or after probe expansion. A slightly larger drag bit was used with some success in some of the high-pressure subareas. This drilling procedure generally produced somewhat oversized test holes, requiring moderate to high initial consumption of probe fluid to expand the probe through the annular space, before mobilizing the strength of the surrounding soil.

In high-strength grout subareas, small probe deformations and high pressures were experienced. Corrections for dilation of the system became important and were made. In many instances, the limit pressure of the grouted soil was not reached, as it exceeded the capacity of the pressuremeter. Modulus values could be calculated in most cases, and limit pressures were extrapolated for the shape of the volume change-pressure curves.

The creep or time-dependent deformation response of the grouted soil under constant stress was studied in situ with the pressuremeter. The probe pressure was increased up to a certain percentage of the estimated limit pressure. This percentage was generally 30 to 50 percent. The pressure was maintained at this level for several hours, and volume change measurements were made at regular time intervals. After the creep test, the probe pressure was increased to soil failure or up to the limit of the system. The results of the creep tests in subareas 5, 11, and 13 are discussed further in Section 9.5.2. The pressuremeter was found to be a good tool for studying creep behavior because the soil was tested in its in situ condition under the stress that existed in the field. Difficulties with sample disturbance and reproduction of actual stresses, inherent to laboratory testing, were thus avoided or minimized.

9.2.6 Borehole Permeability Tests

Falling head borehole permeability tests were performed in eight AG-A-series borings and one AG-B-series boring to provide coefficient of permeability profiles in the grouted soil. These profiles were used to compare the effectiveness of various types of grouts and grouting methods in reducing the permeability of the natural soil. The results of falling head permeability tests performed in the various test subareas are presented in Fig. 9.2 through Fig. 9.15, along with the other in situ testing results.

The procedures followed in the falling head permeability testing in the grouted soil was identical to testing in ungrouted soil (Section 3.2) except that 6 in. of soil was left in the bottom of the casing. It was found that, in some of the grouted soil, cleaning out the soil to the bottom of the casing resulted in washing out of the grout in the 6 in. of soil directly below the casing. This made the soil directly below the casing more pervious resulting in overestimated permeabilities. Examination of split-spoon samples taken after permeability tests where the soil was cleaned out to the bottom of the casing clearly showed this zone of washed-out grout. During washing, a milky white fluid was often noticed. Leaving 6 in. of soil in the casing allowed the soil below the casing to be relatively undisturbed. In boring AG-A11-2, the soil was cleaned to the bottom of the casing whereas in Boring AG-A11-6, 6 in. of soil were left inside the casing. Comparing the results of these two borings in Fig. 9.13, at an equivalent elevation in identical grouted soil, the permeability in Boring AG-A11-6 is one order of magnitude less than in Boring AG-A11-2. Permeability tests in grouted soil were generally time consuming. Driving the casing through the grouted soil took much time and many tests were continued overnight to obtain sufficient data to interpret the basic time lag.

9.2.7 Crosshole Shear Wave Velocity Measurements

Crosshole shear wave velocity measurements were made shortly after grouting (10 and 24 June 1978) in the boreholes where the initial measurements were made (Section 3.2.6). Two sets of measurements were needed after grouting due to interference from high electrical background noise, and high signal attenuation rates requiring amplification of the most distant borehole geophone signals. The results of measurements made on 10 June were considered unsatisfactory and are not presented. Measurements were made at el 383, 388, 393, 398, and 403; grout was injected between el 380 and el 400. A new series of inclinometer measurements was made in the boreholes to determine changes in location that might have resulted from grout injection. Measured changes were small and within the expected accuracy of the measurement method.

Seismic shear wave velocities calculated from travel time data and distances between boreholes are summarized in Table 9.1. The initial velocities, before grouting, are also indicated in this table. The purpose of the measurements being to detect changes in velocity resulting from changes in density and rigidity of the soil, velocities were calculated between source and near geophone boreholes (S0-S1; S0-S31 S0-S5; and S0-S7) where no grouting was done, and between near and distant geophone boreholes (S1-S2; S3-S4; S5-S6; and S7-S8) where grouting was done. Velocities were not calculated for source to distant geophone boreholes, which would simply average lower and higher velocity zones.

The summary of velocity increases resulting from grouting (Table 9.1) demonstrates a significant increase in seismic shear wave velocities in all four arrays measured. Comparing velocities calculated for source to near geophone boreholes prior to grouting (the most accurate pre-grouting velocities) and for near to distant geophone boreholes after grouting, it is found that velocity increases due to grouting ranged from 1.5 to 3.3 times the original velocity. Average velocity increased by 2.5 times (603 ft/s to 1493 ft/s) in subareas 10 and 11 where 55% Siroc 132/142 was injected by grouting method S_2; by 1.5 times (623 ft/s to 920 ft/s) in Subareas 7 and 8 where 25% silicate/aluminate was injected by grouting method S_3; by 3.3 times (600 ft/s to 1953 ft/s) in Subareas 12 and 13 where 46% silicate/R600 was injected by grouting method S_3; and by 1.6 times (516 f/s to 853 ft/s) in Subareas 1 and 9 where 35% Siroc 142 and 55% Siroc 132/142 were injected by grouting method O_1.

9.3 EXCAVATION INTO GROUTED SOIL

9.3.1 Purpose and Scope

After grouting was completed and the AG-A series borehole in situ tests were made from el 423, the test area was dewatered and excavated to investigate and observe the results of grouting. At el 402, the AG-B series borehole in situ tests were made. Below el 402, the excavation was planned to expose the test area in sequential steps. At each step, the extent of grout penetration was mapped along vertical and horizontal sections, and in situ tests (plate load tests and density tests) were made. The excavation provided a means to carve or core samples of grouted soil for laboratory testing.

9.3.2 Dewatering and Excavation Sequence

As the injection of grout in the test area was being completed (Phase 2, Section 2.2.1), a dewatering system was installed around the area to lower the groundwater to el 382 during excavation. Eight deep wells were installed at an average spacing of 150 ft at the periphery of the proposed excavation. The wells were 32-in.-dia with gravel filter and 16-in.-dia screens extending from el 320 to el 368. Multi-stage turbine pumps of 3500 gal/min capacity were installed in the wells. The pumps were driven with surface diesel engines through right-angle drives. The dewatering system was installed and operated under Dewatering Contract No. DACW43-78-C-0094, by J. S. Alberici Construction Company, Inc of St Louis, Missouri.

The dewatering system was started on 3 July and the groundwater was drawn down to el 382 by 5 July 1978. After excavation and testing in the excavation were completed, the system was shut down on 22 August 1978. During the course of the system operation, the natural groundwater level (that is, the tailwater elevation of the Mississippi River) varied between el 402 and el 413. The pumping rate of the dewatering system averaged 850 gal/min per foot of drawdown. The aquifer being 100 ft thick and the line source being 600 ft away from the dewatered area, the measured rate of pumping corresponded to an average coefficient of permeability of 1.8×10^{-1} cm/s for the soil underlying the test area.

The first stage of the excavation from el 423 to el 402 (Phase 3, Section 2.2.1) was started on 5 July and completed by 14 July 1978. This first stage excavation was done under Site Preparation Contract DACW43-78-C-0093, by Luhr Bros, Inc of St Louis, Missouri. The mass excavation was made with scapers, and the excavated soil was used for constructing part of the embankment for the access road to the main test site. No particular excavation sequence was required for this first stage, except that the slopes were to be maintained at 2 (hor) to 1 (ver). After completion of the first stage of excavation and before commencing the second stage, the AG-B series boreholes were drilled and the borehole in situ testing program was completed from 15 to 25 July 1978.

The second stage of the excavation from el 402 to approximately el 382 (Phase 4, Section 2.2.1) was also done by Luhr Bros, Inc, under a modification to the Site Preparation Contract. Initially, the second stage excavation was to be done as part of the General Testing Contract. The Site Preparation Contract, however, was modified to include the second stage of excavation because the General Testing Contract had not been awarded at that time.

Generally, the excavation was made in four steps to el 398, el 394, el 390, and el 385. Portions of the test area were excavated to el 382. Each step was excavated by creating a series of vertical cuts approximately 4 ft deep.

9.3.3 Mapping and Visual Observation

A systematic mapping and visual observation program was implemented during excavation of the chemical grouting test area between el 402 and el 382. A team of two engineers familiar with the grout injection work (Phase 1, Section 2.2.1) and one Quarternary geologist were assigned to this task. The scope of this documentation task was to:

(1) identify and map the limits of grout penetration and observe the thickness and orientation of grout seams (hydraulic fractures);

(2) identify and map the primary geologic structures, mainly cross-bedding and depositional contacts;

(3) sample and visually inspect grouted and ungrouted soil to estimate general composition, grain size, sorting, and roundness characteristics; and

(4) inspect excavation faces for evidence of secondary geologic structures, such as jointing, faulting, and folding.

Documentation techniques relied heavily on conventional and Polaroid photography. Moveable grids consisting of 6-in. by 6-in. wire mesh panels were used to facilitate sketching observed features to scale. The results of the mapping program are presented in Fig. 9.16 through Fig. 9.19 (horizontal sections), and in Fig. 9.20 through Fig. 9.26 (vertical sections). Some of the results of the excavation documentation program are also discussed in Section 3.3, Stratigraphy. The most significant observations concerning grout penetration and influence of the geology on grout penetration are discussed below.

Subarea 1 (35% Siroc 142, Grouting Method O_1, 4-ft Spacing). Vertical cuts were made through Grout Holes 1-2, and 1-5 (Section AA, Fig. 9.20). Grout was found to be massive in coarse-grained strata (medium to coarse sand with minor amounts of fine gravel and fine sand). Grout penetration ranged from 2 ft to 3 ft from grout holes between el 394 to el 390. In finer strata (fine to medium sand), grouting was somewhat irregular and limits of grout penetration in some strata were as close as 1 ft to 0.5 ft from grout holes, between el 400 to el 394 and el 390 to el 385. Abundant vertical grout fractures were found in this area, even though the traditional, supposedly low-pressure, grouting method O_1 (Section 2.1.2) was used. Generally, vertical fractures predominated in the finer grained strata between el 390 to el 385, whereas diagonal fractures were more common in the coarser grained strata between el 394 to el 390. No significant horizontal fractures were observed.

Subarea 2 (35% Siroc 142, Grouting Method O_1, 6-ft Spacing). Vertical cuts were made through Grout Holes 2-1, 2-2 (Section BB, Fig. 9.21) and 2-4 (Section AA, Fig. 9.20). Grout penetration from the most isolated grout hole (Grout-Hole 2-2) was found to be approximately 2.5 ft in medium to coarse sand (el 393 to el 390), 2 ft in fine to medium sand (el 388 to el 386), and less than 1 ft in fine sand (el 401 to el 396). Similar but wider variations in grout penetration were observed around Grout Hole 2-1. An opposite trend was found at Grout Hole 2-4. There, a downward expanding cone was observed in coarser strata (el 393 to el 391) that capped a 2-ft- to 2.5-ft-radius grouted column in fine sand (el 391 to el 387). Vertical grout fractures were more abundant in the finer strata, and one thick diagonal fracture, coincident with cross-bedding, was observed in coarse grained sand near Grout Hole 2-1.

Subarea 3 (28% Silicate/R600, Grouting Method S_2, 6-ft Spacing). Vertical sections were excavated through Grout Holes 3-2 and 3-4 (Section BB, Fig. 9.21). Narrow grout columns were found above el 393 to el 395, as no grout was injected above el 393 due to shortage of R600 reactant. Grout penetration was broad and massive below el 390 in fine to medium sand. Radius of penetration was at least 3 ft. No significant grout fractures were observed in vertical sections in this area.

Subarea 4 (35% Siroc 142, Grouting Method S_2, 6-ft Spacing). Vertical sections were excavated through Grout Holes 4-2 and 4-4 (Section CC, Fig. 9.22) and Grout Holes 4-3 and 4-5. Grout distribution in this subarea was strongly influenced by sediment grain size. Grout penetration in medium to coarse sand was generally in excess of 3 ft, whereas grout penetration in fine sand varied from 0.5 ft to 2 ft (el 393 to el 391). Grout penetration in fine to medium sand was variable, but generally intermediate between these two extremes. Intrusions of 55% Siroc 132/142, from adjacent Subarea 11, were often observed in Subarea 4 near Grout Holes 4-1 and 4-2. Vertical grout fractures were very abundant throughout the exposed surfaces examined. The fracture network extended into Subarea 11. Only one 2-mm-thick diagonal fracture was observed between Grout Holes 4-1 and 4-3 at approximately el 386.5. This diagonal fracture was coincident with cross-bedding.

Subarea 5 (45% Siroc 132, Grouting Method S_2, 6-ft Spacing). Vertical cuts were excavated through Grout Holes 5-2 and 5-5 (Section BB, Fig. 9.21), and Grout Holes 5-1 and 5-4. Grout distribution in this subarea was strongly influenced by geologic conditions. Along medium to very coarse grained sand strata, grouted sand lenses 0.5 ft to 1.5 ft thick extended outward 6 ft to 8 ft from the grout holes, generally to the southwest. At el 393 to el 391, a massive grouted sand mass, several feet thick, was found throughout Subarea 5. Below el 390, in fine to medium sand, grout distribution was more limited and irregular. With the exception of Grout Hole 5-2, grouted sand columns in these finer sediments were generally less than 1 ft in radius, and frequently less than 0.5 ft in radius (horizontal section at el 385, Fig. 9.19). Relatively few grout fractures were observed in Subarea 5, most of them diagonal and coincident with cross-bedding.

Subarea 5a (25% Silicate/Aluminate, Grouting Method S_1, 6-ft Spacing). Virtually no grout penetration was observed from the two grout holes of Subarea 5a. Grout found in this subarea was due to intrusions from adjacent Subareas 5 and 9. As stated previously, Grouting Method S_1 (Section 2.1.2) was not expected to give satisfactory results.

Subareas 6, 7, and 8 (25% Silicate/Aluminate, Grouting Method S_3, 4-ft and 6-ft Spacings). Vertical cuts were excavated through Grout Holes 6-2, 6-4, 8-0, 8-3, 8-4, 8-6, and 8-7 (Section EE, Fig. 9.24). Chemical grout penetration was found to be uniformly high in all cuts examined, extending 3 ft to 5 ft from the grout holes. Grout fractures were not pronounced, generally less than 2 mm thick, and predominantly vertical. Cement-bentonite grout was injected at selected elevations in Subarea 8. Lenses of sand grouted with cement-bentonite were observed at el 393, el 390, and el 398 (Section EE, Fig. 9.24). These lenses dipped to the north and were as much as 1 ft thick and 4 ft wide. The orientation of these lenses was strongly controlled by the orientation of cross-bedding. Many cement-bentonite lenses were coated with pure silicate grout, indicating that they constituted a preferential path for the silicate grout.

Subarea 9 (55% Siroc 132/142, Grouting Method O_1, 4-ft Spacing). Vertical cuts were excavated through Grout Holes 9-1 and 9-5 (Section AA, Fig. 9.20). Below el 393, only narrow (less than 0.5 ft in radius) grout columns were observed around each grout hole, regardless of the grain size or structure of the surrounding alluvial sand. Above el 393, a relatively massive grouted sand mass was observed. This is undoubtedly due to the influence of a large, partially decomposed, tree trunk interred at this level, which acted as a conduit for the grout. Few grout seams were observed in Subarea 9.

Subareas 10 and 11 (55% Siroc 132/142, Grouting Method S_2, 4-ft and 6-ft Spacings). Vertical cuts were excavated through Grout Holes 10-2, 10-4 and 10-6 (Section DD, Fig. 9.23), Grout Holes 10-1, 10-3 and 10-5, and Grout Holes 11-1, 11-3, 11-4, 11-6 and 11-7 (Section CC, Fig. 9.22). Throughout these two subareas, significant grout penetration was generally limited to less than 2.5 ft from the grout holes in all but occasional strata of medium to coarse sand. Grout columns less than 1 ft in radius were characteritic of the fine sand strata (el 394 to el 391, Section DD). In the coarser grained strata, grout penetration was better but more irregular (el 389 to el 384, Section CC and DD). In these strata, the grout had a tendency to form irregularly shaped lenses as much as 1 ft thick and 4 ft wide. Around Grout Holes 10-4 and 10-6, an anomalous thinning of the grout columns was observed between el 391 and el 389 in medium to coarse sand. One explanation of this phenomenon may be that the grout injected at these elevations had an excessively long gel time and percolated downward through the soil, forming a cone-shaped bulb. Another explanation may be that there was communication between grout holes during injection, as can be inferred from grouting records and the connection between Grout Holes 10-4 and 10-2 at el 389 shown in Fig. 9.18. Numerous evidences of invasion of 55% Siroc 132/142 from Subarea 11 to Subarea 4 were observed. Pronounced vertical grout fractures were common in the more heavily grouted zones of Subarea 11, but were relatively thin and infrequent in the isolated grouted columns. Some of the vertical fractures were very thick. One of them, radiating easterly from Grout Hole 11-3, was 30 mm thick at el 390 (Fig. 9.18). Several diagonal fractures were observed in the most heavily grouted zones of Subarea 11. The orientation of most of these diagonal fractures was influenced by cross-bedding; however, some fractures were not coincident with these planes of weakness.

Subareas 12 and 13 (46% Silicate/R600, Grouting Method S_3, 4-ft and 6-ft Spacings). Vertical cuts were excavated through Grout Holes 12-1, 12-3, and 12-5 (Section GG, Fig. 9.26) and through Grout Holes 13-3 and 13-5. Grout penetration was found to be uniformly high in all cuts examined, extending 3 ft to 5 ft from the grout holes. Grout distribution was found to be largely independent of geologic control. Only a few minor grout fractures were observed. The ungrouted sand surrounding these two subareas was removed between el 389 and el 385 leaving the grouted mass relatively intact in the form of a massive rectangular block.

Influence of Grain Size on Grout Distribution. Throughout the test area, grout distribution was found to be directly related to the average grain size of the alluvial sediments. Grout penetration was greater in coarse sand than in fine sand. This general relationship appears to have been influenced by grout viscosity, and penetration of more viscous grouts was more dependent on the sediment grain size than was penetration of less viscous grouts. Exceptions to this general conclusion were found in Subareas 2, 3, and 10, but they may be explained by incomplete grouting, excessively long gel times, and low pressures resulting from communication between grout holes.

Influence of Depositional Structures and Secondary Geologic Structures on Grout Distribution. Except where they formed the boundaries between sediments of different grain size, depositional structures such as bedding contacts and cross-bedding were found to have only a minor influence on the general distribution of the silicate grouts. Cement-bentonite grout, however, characteristically formed well defined lenses that were usually bounded by cross-bedding or bedding contacts. Secondary geologic structures, such as joints, faults, and folds, were not observed in any of the subareas.

Influence of Depositional Structures on Grout Fracture Orientation. Hydraulic fracturing caused by grout injection occurred in most of the test subareas. Several of those fractures were intentionally produced by hydraulic fracturing tests (Section 6.5). Many were produced during the injection process. The large majority of the grout fractures observed were vertical or nearly vertical. The orientation of these vertical fractures did not appear to have been influenced by any natural structures in the sediments. No vertical or near-vertical primary or secondary structures were found in either the grouted or ungrouted portions of the test area excavation. Cross-bedding, however, was found to have a strong influence on the orientation of the more gently dipping grout fractures. Most of these more gently dipping fractures were either subparallel or coincident with cross-bedding. Only very few diagonal fractures were observed to intersect cross-bedding at high angles. Diagonal fractures coincident with cross-beddings were more abundant in coarser grained strata, whereas vertical fractures were more abundant in finer grained strata. Generally, grout fractures were observed to strike N-S or E-W, although exceptions were not unusual.

Influence of Carbonaceous Materials on Grout Distribution. Carbonaceous materials (wood, lignite, charcoal) were abundant and widely distributed throughout the grouted soil in the test area. Wood was only found between el 400 and el 393. Some of these materials significantly influenced grout penetration and consistency of grouted soil. Concentrations of wood fragments, charcoal and lignite pebbles were often found to be only partly grouted or less firmly grouted than surrounding soils free of carbonaceous inclusions. Large wood pieces, such as buried tree branches and tree trunks sometimes controlled grout distribution. These materials, being far more compressible than the surrounding sand in which they were buried, were probably compressed under the grout pressure. They acted as conduits for the grout, enabling the grout to flow far from the injection point. Examples of this phenomenon occurred in Subarea 9 between el 394 and el 398 (Fig. 9.16) and between Subareas 11 and 3 at approximately el 394 (Fig. 9.17).

Partially Grouted Transition Zones. Partially grouted transition zones were observed in many subareas. These zones varied in width from a few inches to

4 ft, and were very irregular in shape. They appeared to be the result of ungelled grout or grout components that migrated away from grouted masses. This migration seemed to have occurred through all strata, but preferentially along coarse grained cross-bedding and bedding contacts. The increase in cohesion and reduction in permeability of the soil in these partially grouted zones were slight as compared with firmly grouted zones. However, in the partially grouted zones, the phenolphtalein reaction was almost as strong as in the firmly grouted zones. This phenomenon was particularly pronounced in the subareas injected with the weaker or less viscous grouts (Subareas 6, 7, 8, 12, and 13) but also occurred in other subareas.

9.3.4 Plate Load Tests

Seventeen plate load tests were made at various elevations on grouted and ungrouted sand. The tests were made to measure strength, and short- and long-term deformation properties of grouted soil. The location and elevation of each test and the soil tested in each test are given in Table 9.2.

The tests were made by applying an incremental load to a 13.5-in.-dia (1 ft^2) steel plate. The plate was placed on top of a leveled soil surface. The load was applied using a hydraulic jack reacting against the rear hitch of a CAT D-8 dozer. The load was measured with a 10-t or 50-t load cell. Plate movement was measured with three dial gages (0.001-in. sensitivity) mounted on a stable reference beam. After a seating load was applied, the plate load was increased in increments of 20 percent of the anticipated failure load. Each incremental load was maintained for 10 minutes before loading to the next increment. Dial gages were read every 2 min. In three of the tests in Subareas 8, 11, and 13, a load equal to one-half the anticipated failure load was maintained up to 30 hours to study creep behavior of the grouted soil. These tests were then continued to failure in load increments.

Load-deflection curves are shown in Fig. G.11 through Fig. G-15, Appendix G. Plate deflection vs time are presented in Fig. G.16 through Fig. G.20, Appendix G. Properties of the tested soil inferred from plate load tests are presented in Table 9.2 and are discussed in the following paragraphs.

Moduli of Elasticity and of Subgrade Reaction. A modulus of subgrade reaction was calculated from load-deflection data for each test for loads ranging from zero to one-half the failure load. Calculated moduli of subgrade reaction are presented in Table 9.2. A modulus of elasticity was calculated from modulus of subgrade reaction (Terzaghi, 1951):

$$E_s = I(1 - \nu^2)B$$

where I = shape factor, 0.88 for circular plate;

ν = Poisson's ratio, assumed to be 0.33 for grouted sand;

B = diameter of plate, 13.5 in; and

K = modulus of subgrade reaction.

Calculated moduli of elasticity are presented in Table 9.2.

Ultimate Plate Bearing Capacity. The failure load indicative of ultimate plate bearing capacity was chosen on the basis of one of the following criteria:

(1) disproportionate increase in deflection versus load;

(2) increase in creep rate at any sustained incremental load; or

(3) signs of soil distress around the plate.

Tests in soil grouted with high-strength grout did not reach failure as described above because of the limitation of the maximum load attainable. The maximum test load that could be applied by test set up was 14 t to 18 t, depending on the positioning of the dozer. Measured or estimated ultimate plate bearing capacities q are presented in Table 9.2.

Creep Rate. A creep rate, expressed as plate deflection in inches per log cycle of time, was calculated for each test at one-half failure load and at failure load. Calculated creep rates are presented in Table 9.2.

9.3.5 In-Place Density Tests

As the excavation proceeded, 21 in-place density tests were made in grouted and ungrouted soil. Table 9.3 gives the location, elevation, and soil condition of each density test. The in-place unit weight was measured using a water-balloon method (Washington Densometer). Each test involved a volume of soil 6 in. in diameter by 6 in. deep. The results of the in-place density tests are also given in Table 9.3. The dry unit weight of the ungrouted soil varied from 99.7 lb/ft^3 for coarse to fine sand, with traces of silt and gravel, to 116.2 lb/ft^3 for medium to fine sand with some coarse sand. The soil most prevalent in the test area within the grouted zone gray medium to fine sand, averaged 104.2 lb/ft^3 dry unit weight. Assuming a specific gravity of 2.65 for the sand particles, the average void ratio of the ungrouted soil was estimated at 0.59 (that is a porosity of approximately 37 percent). The unit weight of grouted soil is also presented in Table 9.3 and discussed in Section 9.5.2.

9.3.6 Block and Core Samples

As the excavation proceeded, 50 undisturbed samples were taken from exposed grouted soil masses. The samples were taken for laboratory tests and for preservation in case future studies were to be considered at a later date. Table 9.4 gives the location, elevation, and soil condition of every sample. Twenty-two samples were carved block samples, approximately 10-in. cubes. All block samples, except BS-11, were carved from horizontal surfaces. Tools used for sampling included saws, knives, and trowels. The samples were waxed and wrapped in cheese cloth and parafin, placed individually in padded wood crates, and shipped to WCC Clifton, New Jersey laboratory by moving van to WES, Vicksburg, Mississippi, by air freight.

In soil grouted with high-strength grout, block sampling was difficult and time consuming. After some attempts at block sample carving, a small electric diamond core drill was successfully used. Twenty-eight 4.5-in.-dia core samples were taken in hard grouted soil. The samples were generally taken in groups of four 10-in.-long cores which were equivalent to one block sample. The quality of the core samples was generally good, but the walls of the samples were usually rough and uneven due to vibrations of the single-tube core barrel and erosion by the flushing water. The cores were wrapped with plastic film and aluminum foil before being waxed and wrapped in cheese cloth and parafin. The cores were placed in padded wood crates in groups of four for shipment to the laboratory.

9.4 LABORATORY TESTING

9.4.1 Purpose and Scope

After grouting was completed, a laboratory testing program was undertaken on samples of grouted sand taken in boreholes and in the excavation. The water that flooded the test area excavation after removal of the dewatering system was also sampled and tested.

The purpose of the laboratory tests was to measure properties of sand grouted in situ. The results of the tests were used to compare samples obtained in boreholes (which were typical of the type of samples that could be easily obtained on most grouting projects) with samples obtained by direct carving or coring in the test excavation (which would not be obtained normally on other projects). The results of the tests were also compared with results obtained on reconstituted sand samples grouted in the laboratory (Section 5.1.3). Grain-size analyses were made on disturbed samples taken during excavation mapping to confirm visual classification and stratigraphic contacts.

9.4.2 Borehole Samples

Borehole undisturbed samples (AG-A series borings) were obtained with a 3-in.-dia Pitcher sampler (Section 9.2). The samples were capped with expandable, draining end packers to allow free water to drain. The tubes were then sealed with parafin. The tubes were stored in a trailer at the test site, then transported by car to WCC laboratories in Kansas City, Missouri, or Plymouth Meeting, Pennsylvania. In the laboratories, the tubes were stored in a humid room until they were opened for testing. The parafin and end packers were removed and the samples were inspected for evidence of disturbance. The tubes were then cut into 6-in. lengths and the grouted sand was expelled using a hydraulic extractor. Some samples could not be expelled and the tubes had to be longitudinally sawed. Samples used for permeability testing were saturated in the testing cell; all other samples were saturated by soaking in water before extraction from the tubes. After testing, the samples were used for unit weight determination. The curing history of samples from each AG-series boring is presented in Table 9.5. The effects of curing time are discussed in Section 9.5

The number of useable samples was reduced by the presence of hydraulic fractures and ungrouted seams. Even though sample recovery was generally excellent, disturbance during sampling and shipment resulted in breakage along discontinuities. In Kansas City, an attempt was made to saturate some samples after splitting the tube. This resulted in disintegration of the samples.

Unconfined Compression Tests. Seventeen unconfined compression tests were made on undisturbed borehole samples from Subareas 1, 3, 4, 8, 11, and 13. All tests were made at a strain rate of 0.5 percent per minute. The results of these tests are presented in Fig. G.21 through G.25, Appendix G, and are summarized in Table 9.6.

Triaxial Compression Tests. Two unconsolidated undrained (UU) triaxial compression tests were made on undisturbed borehole samples from Subarea 13. The samples were tested for permeability and then sheared, in undrained condition, under a confining pressure of 2.5 t/ft^2 at an axial strain rate of 0.15 percent per minute. Test results are presented in Fig. G.26, Appendix G, and are summarized in Table 9.7. This table also shows other samples, which were found unsuitable for strength testing.

Permeability Tests. Eleven constant-head permeability tests were made on unconfined or triaxial test specimens prior to shearing. The permeant used was de-aired water under a backpressure of 20 lb/in^2. Test results are summaried in Tables 9.6 and 9.7.

9.4.3 Excavation Block and Core Samples

Sample Preparation. Twenty-two 10-in.-cube block samples and twenty-eight 4.5-in.-dia, 10- to 12-in.-long core samples were obtained during excavation of the test area (Section 9.3.6). These samples were shipped to WCC laboratory in Clifton, New Jersey via a moving van. In the laboratory, the samples were stored in a humid room.

Although the samples appeared to be homogeneous during field sampling, close observation in the laboratory revealed many ungrouted zones, lignite seams, grout fractures and other discontinuities. Some block and core samples were found to be homogeneous enough for testing. Samples of sand grouted with low-strength 25% silicate/aluminate grout could be trimmed using standard soil procedures. Samples of sand grouted with high-strength 55% Siroc 132/142 and 46% silicate/R600 grouts required coring. To do so, the block samples were placed into a box backfilled with sand. For unconfined compression test specimens, saturation was achieved by soaking in water; however, this could not be done for samples grouted with 25% silicate/aluminate. Triaxial compression specimens were saturated by back pressure in the testing cell.

Scope of Testing. The following tests were performed on excavation block and core samples:

Short-Term Static Loading

Unconfined Compression: (Strain rate = 0.15 percent per minute)	*4 test for Subarea 1*
	1 test for Subarea 2
	1 test for Subarea 4
	2 tests for Subarea 8
	2 tests for Subarea 11
	3 Tests for Subarea 13
Triaxial Compression ($\overline{CID}$): (Confining pressure = 1, 2, and 4 t/ft^2)	*1 series of 3 tests for Subarea 1*
	1 series of 3 tests for Subarea 8
	1 series of 3 tests for Subarea 11
	1 series of 3 tests for Subarea 13
(Confining pressure = 2 t/ft^2	*1 test on reconstituted ungrouted sand sample*

Long-Term Static Loading

Unconfined Compression: (sustained load ≃ 0.35 q_u)	*2 tests for Subarea 1*
	1 test for Subarea 2
	2 tests for Subarea 8
	1 test for Subarea 11
	1 test for Subarea 13
Triaxial Compression ($\overline{CID}$): (Sustained load ≃ 0.1, 0.35 and 0.7 peak deviator stress for series of tests)	*1 series of 3 tests for reconstituted ungrouted sand sample*
	1 series of 3 tests for Subarea 8
(Sustained load ≃ 0.35 peak deviator stress for single test)	*1 test for Subarea 1*
	1 test for Subarea 11
	1 test for Subarea 13

Sonic Velocity	*1 test for Subarea 1*
	1 test for Subarea 8
	2 tests for Subarea 11
	1 test for Subarea 13

Permeability:	*1 test for Subarea 1*
	1 test for Subarea 8
	1 test for Subarea 11
	1 test for Subarea 13
Maximum-Minimum Unit Weight:	*2 series of tests on ungrouted sand samples*

Short-Term Static Loading.

Unconfined compression Tests. The samples were tested at a strain rate of 0.15 percent per minute. The tests were continued to failure or to 20 percent axial strain, whichever occurred first. The results of these tests are presented in Fig. G.27, Appendix G, Volume IIA and are summarized in Table 9.8.

Triaxial Compression Tests. The samples were isotropically consolidated with a back pressure of 5 t/ft^2 to achieve a high degree of saturation. After consolidation, some samples were tested for permeability and then sheared under drained condition at an axial strain rate of 0.12 to 0.15 percent per minute. Each test series consisted of three tests at confining stresses of 1, 2, and 4 t/ft^2. The tests were continued to failure or to 20 percent axial strain, whichever occurred first. The results of these tests are presented in Fig. G.28 through G.33, Appendix G, Volume IIA, and are summarized in Tables 9.9 and 9.10.

Long-Term Static Loading (Creep Tests).

Unconfined Compression Tests. The samples were subjected to a sustained axial load of 35 percent of the ultimate unconfined compressive strength determined during the short-term unconfined compression tests. The sustained load was maintained for a maximum of 6000 minutes. If the soil did not creep-rupture prior to 6000 minutes, the load was increased and the samples were sheared at a strain rate of 0.15 percent per minute. Test results are presented in Fig. 9.49, and Fig. G.27, Appendix G, Volume IIA, and are summarized in Table 9.8.

Triaxial Compression Tests ($\overline{\text{CID}}$). The samples were isotropically consolidated under a confining pressure of 2 t/ft^2 with a back pressure of 5 t/ft^2 to achieve a high degree of saturation. After consolidation, the samples were loaded at a strain rate of 0.15 percent per minute up to a deviator stress of 10, 35, or 70 percent of the peak deviator determined during the short-term $\overline{\text{CID}}$ triaxial compression tests. This deviator stress was maintained for approximately 8000 minutes. After 8000 minutes, the load was increased and the samples were sheared at a strain rate of 0.15 percent per minute. Test results are presented in Fig. 9.51, Fig. G.28 and G.30 through G.32, Appendix G, Volume IIA, and are summarized in Tables 9.9 and 9.10.

Sonic Velocity Tests. The samples were isotropically confined at a stress of 0, 0.7, 1.4, 2.1 and 2.8 t/ft^2, during which shear wave travel time measurements were made. Shear wave velocities were calculated from precise measurements of the sample height between the seismic source and receiver.

Permeability Tests. Constant-head permeability tests were made on some $\overline{CID}$ triaxial specimens after consolidation but prior to shearing. The tests were made using a back pressure of 20 lb/in^2. De-aired water was used as the permeant. The results of these tests are presented in Fig. 9.52 and are summarized in Table 9.9.

Maximum-Minimum Unit Weight Tests. The maximum unit weight of ungrouted sand sampled during excavation was determined by the modified Providence method using an electromagnetic jack hammer. Minimum unit weights were determined using the tube method developed by Lucks (1970), funnel method in 0.1-ft^3 mold (ASTM) and small 432-cm^3 mold, and cylinder tilt method (Kolbuszewski 1948). Test results are summarized in Table 9.10.

9.4.4 Post-Grouting Groundwater Analyses

After shut-down of the dewatering system on 22 August, groundwater flooded the test area excavation. The water in the flooded excavation was dark brown. A sample of that water was taken on 26 September and analyzed by Raltech Scientific Services of St Louis, Missouri. Results of these analyses and of similar analyses of groundwater out of the dewatering system of the main test site are presented in Table 9.11.

9.5 COMPARISON OF RESULTS

9.5.1 Grouting Effectiveness

The effectiveness of grouting was measured by how well the grout was injected into the soil. Mapping of the extent of grouted soil provided a direct evaluation of grouting effectiveness. Excavation and mapping would not be possible on actual production grouting projects. Therefore, this test program provided a rare opportunity to compare direct observations (mapping) with indirect or remote measurements (borehole in situ testing and grouting records) of grouting effectiveness. These comparisons were used to check reliability and accuracy of indirect methods to assess grouting effectiveness.

Monitoring of Grouting Activities. During grouting, the injection parameters (grout pumping pressure, grout pumping rate, and grout take) were monitored (Section 7). From these measurements some understanding of the mechanisms of grouting can be inferred. The optimum grout pumping pressure and flow rate are controlled by the soil permeability to grout. The soil permeability to grout is function of soil void ratio, particle structure, grain-size distribution, grout viscosity, and presence of previously injected grout. Four typical, idealized pumping pressures and flow rate records for sleeve-pipe grouting are illustrated in Fig. 9.27. Case A corresponds to a high grout pumping pressure and moderate pumping rate, indicative of a soil of medium to low permeability to grout. The grout was probably injected into a fine or medium to fine sand, and the grout penetration was probably good. Case B corresponds to a lower pumping pressure and a higher pumping rate, indicative of a soil of higher permeability to grout than in Case A. This soil is probably coarser grained and, therefore requires less pressure for satisfactory grout flow and penetration. In Case C, the pumping pressure increases rapidly to a high average value with relatively large fluctuations from this average value, and the grout pumping rate remains small. Case C behavior is indicative of very low soil permeability to grout. The soil in Case C could be very fine grained or has been grouted previously. Case D is an illustration of a typical hydraulic fracturing grouting record. The grout pumping pressure and the pumping rate increase to a point where the pumping pressure drops significantly while the pumping rate increases suddenly. At that point, hydraulic fracturing has occurred. Grout can now flow through the open conduit of the fracture at low pressure and relatively high rate of flow, until the conduit becomes plugged with grout. At that time, the pumping pressure begins to increase again, and the pumping rate decreases.

Open-bottom pipe grouting records can be interpreted in a similar fashion. Lower pumping pressure and faster grout flow rate were used with open-bottom grout pipes. In the same soil, Case B would be representative of open-bottom pipe grouting while Case A would be representative of sleeve-pipe grouting.

Examples of actual grout pumping pressure vs time are shown in Fig. 9.28. The interpretation of each of these records was confirmed by the results of the excavation mapping. These examples illustrate how grouting records can be interpreted to follow progress and assess efficiency of the grouting process.

Borehole In Situ Testing. Results of continuous standard penetration and static cone penetration tests were compared with information obtained by mapping. Both in situ tests were effective in detecting the extent of grouting. Comparison between penetration resistances and mapping results are presented in Fig. 9.2 through Fig. 9.15. On these figures, the notation UG indicates that the soil was ungrouted, PG indicates that the soil was poorly grouted or partially grouted, and G indicates that the soil was well grouted with uniform grout penetration. The increase in static cone resistance due to grouting (q_c after grouting/q_c before grouting) is plotted vs elevation in Fig. 9.29 for Subareas 8, 3, 5, and 9. For zones that were found ungrouted (UG) during excavation the ratio (q_c after q_c before) remained approximately one. For zones that were found to be poorly grouted (PG), the ratio ranged from one to two. For zones that were found to be well grouted (G), the ratio was always greater than two. For low-strength grout (Subarea 8), although the increase in static cone resistance was marked, the increase in standard penetration resistance was small, even in well-grouted zones. This may indicate some reduction in strength induced by dynamic driving stresses. In addition to penetration resistances, standard penetration tests yielded disturbed samples for visual classification. The subsurface profiled inferred from these samples correlated well with the profiles of grouting effectiveness obtained by subsequent excavation mapping.

Crosshole shear wave velocity measurements were found to be an effective non-destructive means for evaluating grouting effectiveness. The results tabulated in Table 9.1 are plotted vs elevation in Fig. 9.30. The highest crosshole shear wave velocities were measured in Subareas 12 and 13, exceeding those measured in Subareas 10 and 11 by approximately 35 percent. Velocities in Subareas 1 and 9 were approximately 10 percent less than those measured in Subareas 7 and 8. Results of other tests have shown that strength and stiffness of grouted soil increased with silicate content of the grout (Section 9.5.2). This appears inconsistent with the crosshole shear wave velocity results: grout used in Subareas 10 and 11 had a higher silicate content (55 percent) than that used in Subareas 12 and 13 (46 percent); grouts used in Subareas 1 and 9 (55 and 35 percent) had a higher silicate content that that used in Subareas 7 and 8 (25 percent). An explanation of this apparent discrepancy can be developed on the basis of the excavation mapping (Section 9.3.3) as follows.

The elevation of the horizontal sections shown in Fig. 9.16 through 9.19 are indicated in Fig. 9.30. These sections are reproduced in Fig. 9.31 through 9.34 together with the location of the geophysical borehole arrays. From these figures, it can be seen in a simplified manner that the shear wave velocities were not only influenced by the type of grout, but also, and probably more significantly, by the extent of grout penetration. Subareas 7 and 8, and 12 and 13 were massively grouted. Subareas 10 and 11 were not entirely grouted. Subareas 1 and 9 were poorly grouted. Ungrouted zones significantly reduced shear wave velocities, because these measurements reflect the bulk properties of the mass through which the waves propagate.

The results of laboratory sonic velocity tests on specimens of grouted soil carved from excavation block and core samples are plotted as dark symbols in Fig. 9.30. The laboratory velocities from samples of Subareas 8 and 13 agree closely with the in situ crosshole velocities. The laboratory velocities from samples of Subareas 1 and 11 exceed the in situ crosshole velocities. The ratio laboratory to in situ velocities for these subareas is roughly equal to the ratio of the volume of grouted soil mass to ungrouted soil mass along the wave path. The laboratory sonic velocity measurements were made on small, intact grouted sand specimens which did not contain the discontinuities and ungrouted seams found in situ in the large grouted soil mass. From these results, it appears that comparison between in situ crosshole shear wave velocity and laboratory sonic velocity measurements can be useful to evaluate grouting effectiveness.

9.5.2 Grouted Soil Properties

Properties of grouted soil were measured through in situ and laboratory tests. The program of testing implemented after grouting coincided with the testing performed before grouting (Section 3).

Stresses. In situ horizontal stresses were inferred from pressuremeter test results. Comparisons between horizontal total stresses measured before and after-grouting in selected subareas are presented in Fig. 9.35. In all cases, the in situ horizontal stresses measured after grouting were higher than those measured before grouting, even in poorly grouted or ungrouted soil, regardless of the grouting method used.

The influence of the grouting pressure on the after-grouting horizontal stress is illustrated in Fig. 9.36. The ratio of the after-grouting in situ horizontal stress to the average peak grouting pressure in the two nearest grout holes ranged from 0.5 to 1.1 and averaged 0.77. Therefore, it appears that the pressure applied to the soil during injection had not completely dissipated at the time the pressuremeter tests were made. The tests in borings of the AG-B series were made more than one month after completion of grouting. This phenomenon should be considered when designing foundation elements which would be influenced by high K_o stress state.

Density. The unit weight of the grouted soil was determined by three different methods:

(1) laboratory measurements on Pitcher tube samples (Section 9.4.2);

(2) in-place measurements with Washington Densometer during excavation (Section 9.3.4); and

(3) laboratory measurements on block and core samples (Section 9.4.3).

The results of these determinations are summarized in Fig. 9.37. The Pitcher tube samples were obtained before dewatering. The in-place measurements were made and the block and core samples were obtained after dewatering. The water content of the grouted soil averaged 3 to 6 percent less than the water content before grouting (Fig. 9.37b and Table 3.1). The dry unit weight of the grouted soil measured in place averaged 1 to 3 lb/ft^3 more than the dry unit weight of the ungrouted soil (Fig. 9.37c). The dry unit weight of the grouted soil measured in Pitcher tube and excavation block and core samples ranged from 0 to 8 lb/ft^3 less, and were typically 2 to 4 lb/ft^3 less than the dry unit weight of the grouted soil measured in place. These results are in agreement with data for ungrouted soil presented by Horn (1978) which show a 3 to 4 lb/ft^3 discrepancy between block sample unit weights and unit weights measured by in situ methods.

Elastic Deformation Modulus. The elastic deformation modulus of grouted soil was calculated from the results of pressuremeter, plate load, crosshole shear velocity, and laboratory unconfined and $\overline{\text{CID}}$ triaxial compression tests. The conditions prevailing in these tests are outlined in Table 9.9. Modulus values are largely influenced by test conditions. The selection of an appropriate modulus value for a particular design application can be facilitated by using Table 9.9. For example, in estimating the settlement of a footing, the modulus value obtained from plate load test results would be most appropriate, because this test duplicates all the conditions existing under a loaded footing, except for the size of the soil sample tested. Therefore, the plate load test modulus would have to be modified for scale effects. As another example, to predict the lateral load capacity of piles in grouted soil, the most appropriate test method would be the pressuremeter because it duplicates most of the actual conditions, except for stress durations. To evaluate earthquake loading on a structure, crosshole shear wave velocity measurements would yield the most appropriate modulus because they model best the simple shear loading, stress duration, and strain amplitude produced by the seism. If an excavation were to be made in grouted soil, and a finite element analysis were to be used to predict the stresses and deformations of the excavation support system and soil mass, laboratory test results would be used. For soil elements near the excavation surface before installation of the support systems, unconfined compression test results would be applicable. For soil elements within the soil mass and wall elements after the support system is installed, results of triaxial compression tests at the proper confining stress would be used.

Pressuremeter Modulus. An elastic deformation modulus was calculated from the pseudo-elastic portion of the pressuremeter curves as it was done before grouting (Section 3.4.5). Results of these calculations are presented in Fig. 9.38 for Subarea 1, 5, 8, 4, 11, and 13, where they are compared to the pressuremeter modulus profile obtained before grouting from Boring D-27. Grouting was ineffective in increasing the deformation modulus in Subarea 1 (35% Siroc 142, Grouting Method O_1). In Subarea 4, however, the same grout injected by Grouting Method S_2 resulted in a noticeable increase in pressuremeter deformation modulus. Significant increases in modulus were measured in Subareas 5 and 11 (55% Siroc 142, Grouting Method S_2). The low modulus values at el 400, el 397, and el 386 in Subarea 11 corresponded to ungrouted soil. Only two pressuremeter tests were made in Subarea 8, but these measurements indicated a slight increase in modulus due to grouting, consistent with the low-strength of 25% silicate/aluminate grout. Modulus values increased in the high-strength grout in Subarea 13 (46% silicate/R600, Grouting Method S_3), but the magnitude of the increase is less than that observed in the high-strength Siroc subareas.

Plate Load Test Modulus. An elastic deformation modulus was calculated from the initial portion of plate load tests pressure-settlement curves (Section 9.39). Results of these calculations are presented in Fig. 9.34 for all test subareas, except Subarea 5a, and for ungrouted sand. Four range of modulus values can be inferred from this figure: ungrouted soil (less than 250 t/ft^2), low-modulus (Subareas 1, 6, 7, and 8) (250 t/ft^2), medium-modulus (Subareas 2, 3, 4, 12, and 13) (500 to 2000 t/ft^2), and high-modulus grouted soil (Subareas 5, 9, 10, and 11) (2000 to 12000 t/ft^2). Subarea 1 (35% Siroc 142, Grouting Method O_1) had a lower modulus than all other subareas injected with the same grout. Sand grouted with 25% silicate/aluminate had a low modulus. For the high-strength Siroc grouts, modulus values increased with increasing percentage of silicate and decreasing grout hole spacing. Subarea 9 (55% Siroc 132/142, Grouting Method O_1) had a significantly lower modulus than the other three high-strength Siroc subareas injected using grouting Method S_2. Of significance are the relatively low modulus values obtained in Subareas 12 and 13 (46% silicate/R600), although failure was not approached during the plate load tests in these subareas. These results may be explained by the creep-prone behavior of this material combined with the long stress duration of the tests. This is discussed later in this section.

Shear Wave Modulus. An elastic deformation modulus was calculated from crosshole shear wave velocity measurements as discussed in Section 3.4.5.

Results of these calculations are presented in Fig. 9.40. In Subareas 1 and 9, the shear wave modulus doubled due to grouting. In Subareas 7 and 8, the increase was slightly more than twofold. In Subareas 10 and 11, the modulus increased as much as 8 times. In Subareas 12 and 13, the modulus increased as much as 14 times. As discussed in Section 9.5.1, shear wave-derived moduli were not only influenced by the type of grout, but also, and probably more significantly, by the extent of grout penetration. These modulus values are representative of the bulk of the entire grouted and ungrouted soil mass.

Laboratory Modulus. Elastic modulus values were calculated from laboratory unconfined and triaxial ($\overline{CID}$) compression tests on undisturbed field and laboratory reconstituted grouted samples (Sections 5.1.3 and 9.5). Initial tangent modulus, secant modulus at 50 percent of peak stress, and secant modulus at peak stress (failure) were obtained from stress-strain curves. Initial tangent modulus values were affected by seating of the initial test load especially for unconfined compression tests. Secant modulus values at failure E_{sf}, were the most consistent and the least affected by discrepancies associated with the initial portion of the tests. The influence of silicate content on modulus is illustrated in Fig. 9.41a. Modulus values increased with silicate content as expected, which is in agreement with recent work by Clough et al (1979). The excavation block and core samples, however, were significantly stiffer than the laboratory reconstituted or borehole samples. For grouts having a silicate content greater than 25 percent, unconfined compression moduli were greater than $\overline{CID}$ triaxial moduli for tests made on block samples. This brittle response of block samples in unconfined compression is discussed later in this section. Generally, the moduli measured in situ with pressuremeter (Fig. 9.38) and plate load tests (Fig. 9.39) are lower than those measured in the laboratory on reconstituted samples grouted with similar grout. This may have been caused by field sampling disturbance.

The influence of strain rate on modulus is illustrated in Fig. 9.41b. From the limited range of strain rates studies, it appears that modulus values increased with faster strain rates, although considerable scatter was found at strain rate of 0.5 percent per minute. This is consistent with the trend observed by Clough et al (1979). Koenzen (1978) showed that the effect of strain rate on modulus diminishes with decreasing percentage of silicate.

The influence of confining pressure on modulus is illustrated in Fig. 9.41c. Modulus values increased with confining pressure. Clough et al (1979) showed similar trends, with the rate of increase of modulus with confining pressure being greater for higher silicate content. The influence of curing time on modulus is illustrated in Fig. 9.41d. Modulus values did not appear to increase with curing time, contrary to the findings of Clough et al (1979).

Shear Strength. The shear strength of grouted soil was found to be the result of a frictional component ϕ mobilized between sand grains and a cohesion component c induced by the grout. Shear strength of ungrouted and grouted sand was assessed from results of unconfined compression tests on undisturbed borehole samples of grouted sand (Section 9.4.2), excavation block and core samples

samples (Section 9.4.3), and on reconstituted sand samples grouted in the laboratory (Section 5.1.3); from results of triaxial compression tests on reconstituted sand samples ungrouted and grouted in the laboratory (Section 5.1.3), and on excavation block and core samples (Section 9.4.3); and from pressuremeter test results made before and after grouting (Sections 3.2.4 and 9.2.5).

Triaxial Test Results. The ϕ and c components of shear strength calculated using Mohr-Coulomb law (Mohr circles, Fig. C.1 and C.3 through C.8, Appendix C and Fig. G.28 through G.33, Appendix G, Volume IIA):

$$\tau_f = c + \sigma_f \tan \phi$$

where: τ_f = shear strength;

c = cohesion

σ_f = peak deviator stress; and

ϕ = angle of internal friction.

The ϕ and c components of shear strength were also calculated using p-q diagrams, where each Mohr circle is represented by one point. Such a p-q diagram is shown in Fig. 9.42. All CID triaxial test results analyzed are summarized in this figure. The curve drawn through points on this figure is the K_f-line. The slope α of the K_f-line and its origine intercept a are related to ϕ and c as follows:

$$\sin \phi = \tan \alpha \quad \text{and} \quad c = \frac{a}{\cos \phi}$$

The p-q method was found to be less susceptible to variability in interpretation than the Mohr circle method. Both methods, however, yielded similar averages for ϕ and c. For ungrouted sand, the following average results were found:

ϕ = 39.5°; and

c = 0 to 0.1 t/ft^2.

For reconstituted sand samples grouted in the laboratory with 35% Siroc 142 grout, the following results were found:

ϕ = 39.5°; and

c = 0.7 t/ft^2.

For excavation block and core samples, the following results were found:

Subarea No.	Silicate Content %	c t/ft^2	ϕ degrees
1	35	0.36	35.5
8	25	0.34	35
11	55	5.82	39
13	46	3.50	39.5

Results from tests on reconstituted sand samples grouted in the laboratory (35% Siroc 142), and on samples from Subarea 11 (55% Siroc 132/142) and Subarea 13 (46% Silicate/R600) are in agreement with results reported by other investigators (Clough et al, 1979): injection of silicate grouts did not change the angle of internal friction but increased the cohesion. The increase in cohesion increased with the silicate content of the grout. Results from Subareas 1 and 8, however, show a lesser increase in cohesion, and a decrease in friction. In the case of low-strength grouts (Subarea 8), it may be postulated that the grout tended to lubricate the sand grains, thus reducing the internal friction. In the case of medium-strength grouts (Subarea 1), the lower friction angle may have resulted from sampling disturbance. This sampling disturbance may not have been experienced for high-strength grouts because the grouts were strong enough to keep the sand particles bound together despite stress relief during sample carving or coring, and vibrations and shocks during shipping. Further testing is necessary to illuminate the strength disparity.

Unconfined Test Results. Unconfined compression tests are not appropriate to measure the shear strength of grouted sand because of the large frictional component of the material. The unconfined compressive strength, however, was useful as an index to shear strength. Undisturbed borehole samples, excavation block and core samples, and laboratory reconstituted samples were used in unconfined compression testing. The test results are shown in Fig. C.2, Appendix C and Fig. G.21 through G.25, and Fig. G.27, Appendix G, Volume IIA. Results from specimens prepared in the laboratory fall within a relatively narrow range, while results from field samples are much more scattered. This is explained by the variability of the natural soil structure and non-uniform in situ grout penetration. Average results for 35% Siroc 142 from tests on laboratory reconstituted samples, borehole samples, and excavation block and core samples are plotted in Fig. 9.43. The block samples had the highest unconfined compressive strength and showed a brittle response. The borehole samples had the lowest strength and were the lest stiff, indicative of the highest degree of disturbance. The brittle behavior of the excavation block samples may be related to the sampling process. The grouted soil in the block samples followed an unloading stress path (first, vertical unloading during excavation, then, horizontal unloading during carving) which may have resulted in yielding, depending on the shear strength of the grouted soil. Yielding could have resulted in micro-fractures developing in the grout matrix. The samples were stored without confinement in the shipping boxes, then subjected to vibration and shock during transportation to the laboratory. This may have aggravated the postulated micro-fracturing process. During unconfined compression testing, samples with micro-fractures would be expected to fail in a brittle manner once the strength along the fractures is mobilized. But, under confinement during triaxial testing, the micro-fractures might tend to heal, the samples would behave more as an intact mass, and the response would be less brittle with failure occurring at a higher strain.

The data suggests that the effect of micro-fracturing, if indeed this mechanism occurred, was only significant for medium strength grouts (for example, 35% Siroc 142). For these grouts yielding during sampling and shipping may have exceeded the shear strength of the grouted soil, whereas for stronger samples (such as those from Subareas 13 and 11), yielding was probably very small. The ductile response of samples grouted with very low-strength 25% silicate/aluminate grout (Subarea 8) may be due to the fact that this grout was plastic enough to yield without inducing micro-fractures. Although block sampling still appears to be the best method presently available for obtaining undisturbed samples of grouted soil, unconfined compression testing on specimens trimmed from block samples may underestimate the in situ strength.

Influence of Various Factors. The influence of silicate content on unconfined stress-strain characteristics is illustrated in Fig. 9.44. The unconfined compressive strength increased with silicate content, as expected. Data scatter for field samples is attributed to sampling disturbance, but the general trend is in agreement with findings reported by Clough et al (1979) for laboratory reconstituted samples. The axial strain at failure decreased as the silicate content increased (that is, the response became more brittle and the modulus larger as the silicate content increased).

The influence of strain rate on unconfined compressive stress is illustrated in Fig. 9.45. The strength increased as the strain rate increased. This is in agreement with results reported by Clough et al (1979). Koenzen (1978) found that for 70% silicate grouts, the strength decreased by 45 percent when strain rate was decreased by three orders of magnitude. From those results, it is concluded that conventional laboratory loading rates (that is, about 0.5 percent per minute) may yield strength results up to 50 percent greater than slower loading rates that are more likely to occur in actual field loading.

The influence of curing time on stress-strain characteristics is illustrated in Fig. 9.46. No significant strength and axial strain at failure change were noted as curing time increased from 2 days to 100 days, contrary to results reported by Clough et al (1979). The disparity can be explained by the different curing environments used in WCC and Clough laboratories. Clough allowed the grouted samples to stand in air for 24 hours before placing them in a humid room. Locks and Dam No. 26 samples were placed in a humid room immediately after grouting, then submerged in groundwater in a curing tank pressurized to the average hydrostatic pressure expected at midpoint of the grouted zone (Section 5.1.3). The later curing procedure was more representative of the expected field curing conditions.

Pressuremeter Test Results. Although no method has been developed to calculate shear strength from pressuremeter tests for soils exhibiting both frictional and cohesive strength, pressure limit pressure was a useful index to shear strength and to compare the various test subareas. Limit pressures measured before and after grouting are presented in Fig. 9.46. Ungrouted zones corresponded to zones where no increase in limit pressure was noted. After-grouting values lower than before-grouting values were noted in Subarea 1. This may have resulted from borehole disturbance or maybe related to open-bottom pipe injection process. In several cases (Subareas 5, 11, and 13) failure was not approached during pressuremeter testing and limit pressure values could not be estimated. These values are plotted as 100(+) t/ft^2.

Time-Dependent Properties. Laboratory, pressuremeter, and plate load tests indicated that grouted soil behavior under a sustained or slowly applied load was different than under a fast loading rate.

Unconfined Compression Tests. Results of long-term unconfined compression tests on reconstituted sand samples grouted in the laboratory are presented in Section 5.1.3 and Fig. 5.3. From these results, it appears that none of the tests approached failure or creep rupture. Creep rates, that is the ratio change in strain/change in time, were almost identical at CSR* of 50, 37 and 25 percent. At CSR of 15 percent, the creep rate is somewhat different, probably due to sample differences. Similar tests were performed by Clough et al (1979) and Koenzen (1978). Results of these tests are compared with Locks and Dam No. 26 test results in Fig. 9.48 and are summarized below.

TEST	SILICATE CONTENT %	CSR %	CREEP FAILURE
LD26 (1978)	35	37	No
		50	No
Clough et al (1979)	50	40	No
		60	Yes
Koenzen (1978)	70	36	No
		43	Yes
		57	Yes

The greater tendency towards creep rupture reported by Clough and Koenzen may be attributed to the greater silicate content of the grouts used by these investigators. However, the greater silicate content used by Koenzen does not result in faster creep rate, as would be expected.

---

* *CSR: Constant stress ratio or ratio of sustained axial stress to unconfined compressive strength measured at strain rate of 0.5 percent per minute*

Long-term unconfined compression tests were also performed on excavation block and core samples. The results of these tests are presented in Fig. 9.49. Samples from Subareas 8 and 11 did not undergo creep rupture. Samples from Subareas 1, 3, and 13, however, failed at CSR as low as 30 to 35 percent. This is inconsistent with the results obtained on reconstituted samples grouted in the laboratory. Again, block samples from Subareas 1 and 2 showed a brittle response in unconfined compression characterized by a small creep strain until the strain or stress duration reached a point where rapid, brittle failure developed. The block sample from Subarea 13 showed a steady increase in strain up to failure. The creep behavior of soil grouted with 46% silicate/R600 appears to be inherent to this type of grout and not related to sampling disturbance. The block sample from Subarea 8 (25% silicate/aluminate) showed a tendency for stabilization of creep strain at about 300 minutes, indicative of strain-hardening.

Triaxial Compression Tests. Results of long-term triaxial compression tests on reconstituted sand samples grouted in the laboratory are presented in Section 5.1.3 and Fig. 5.4. No creep rupture was observed under CSR of 40, 59 and 79 percent. Failure was induced by increasing the deviator stress at the end of the creep tests. Koenzen (1978) reported creep rupture for CSR greater than 65 percent for similar tests on samples injected with grout containing 70 percent silicate. From these results, presented in Fig. 9.50, it can be concluded that confinement significantly decreased creep tendency of grouted soil, and that creep tendency decreased when silicate content was reduced.

Results of long-term triaxial compression tests on excavation block and core samples from Subareas 1, 8, 11, and 13 are presented in Fig. 9.51. For reference, results of a similar test on an ungrouted sand sample obtained in the excavation and reconstituted in the laboratory are also plotted in that figure. No creep rupture was observed at CRS of as much as 38 percent for all grouted samples, and for one sample from Subarea 8 at a CSR of 68 percent. At CSR values of as much as 38 percent, creep rates for samples from Subareas 1, 8, and 11 did not differ significantly from the results obtained with the ungrouted sample. The sample from Subarea 13 (46% silicate/R600), however, showed a much larger creep rate than the other samples and a tendency towards creep rupture.

The stress path followed during triaxial compression more realistically models typical field loading conditions than unconfined compression. It is recommended that triaxial creep tests be performed instead of unconfined creep tests to assess long-term behavior of grouted soil. In triaxial compression, creep did not appear to be significant up to CSR values of about 60 percent for all grouts tested, except for 46% silicate/R600. On the basis of these results, lower allowable load levels should be used in design for R600 grouts than for Siroc grouts.

Plate Load Tests. Results of long-term plate load tests are presented in Section 9.3.4. Creep rates $d\varepsilon/dt$ deduced from these tests are plotted vs silicate content in Fig. 9.52. Creep rate increased with increasing silicate content. In Subareas 5, 10, and 11 (55% Siroc 132/142), the maximum applied stress never reached 50 percent of the ultimate plate bearing capacity, and the test data are not shown in Fig. 9.52. Creep rates for these subareas were less than 0.007 percent per minute. However, in Subareas 12 and 13 (46% silicate/R600), which exhibited short-term strength similar to that of 55% Siroc 132/142, the observed creep rate was at least two orders of magnitude faster. Low-strength 25% silicate/aluminate also had a noticeable creep deformation tendency.

Pressuremeter Tests. Results of pressuremeter creep tests are presented in Section 9.2.5. Radial strain vs time during which constant probe pressure was applied is plotted in Fig. 9.53. Results of pressuremeter creep tests showed trends similar to those found in triaxial creep tests. Small creep strain occurred up to a CSR level of 33 percent in subareas grouted with Siroc and 25% silicate/aluminate grouts. But again, sand grouted with 46% silicate/R600 had a much faster creep rate. Tendency for strain hardening at a CSR of 50 percent was also noted for sand grouted with low-strength 25% silicate/aluminate.

On the basis of the creep test results, it can be concluded that pressuremeter tests, plate load tests, and laboratory triaxial compression tests can be effectively used in evaluating time-dependent properties of grouted soil.

Permeability. The reduction of permeability due to grouting was assessed from results of borehole falling-head permeability tests (Section 9.2.6) and laboratory permeability tests on borehole undisturbed samples, excavation block and core samples, and reconstituted sand samples grouted in the laboratory (Sections 9.4.2, 9.4.3, and 5.1.3). A summary of the results is presented in Fig. 9.54, together with results obtained before grouting in Boring D-28. Generally, grouting reduced permeability by one to two orders of magnitude. The reduction did not appear to be a function of the grout type; rather, it was found to be a function of the grouting method. Comparison between mapping observations and field permeability test results clearly showed that zones in which permeability was not decreased were ungrouted. Ungrouted zones surrounded by well-grouted zones, however, showed a marked decrease in permeability.

Permeability measured on reconstituted sand samples grouted in the laboratory averaged 4.8×10^{-7} cm/s; that is, two to three orders of magnitude less than field and laboratory tests on sand grouted in situ. The difference is explained by natural soil discontinuities and borehole disturbance.

ELEVATION	SUBAREAS 10 AND 11		SUBAREAS 7 AND 8		SUBAREAS 12 AND 13		SUBAREAS 1 AND 9		MEASUREMENT SERIES*
	55% SIROC 132/142 GROUTING METHOD S_2		25% SILICATE/ALUMINATE GROUTING METHOD S_3		46% SILICATE/R600 GROUTING METHOD S_3		35% SIROC 142 55% SIROC 132/142 GROUTING METHOD O_1		
	SHEAR WAVE VELOCITY ft/s		SHEAR WAVE VELOCITY ft/s		SHEAR WAVE VELOCITY ft/s		SHEAR WAVE VELOCITY ft/s		
	S0-S1	S1-S2	S0-S3	S3-S4	S0-S5	S5-S6	S0-S7	S7-S8	
403	600	(465)**	565	(610)	560	-	670	(515)	B
	(725)	945	(640)	780	(720)	2190	(680)	890	A
398	570	(730)	650	(580)	600	-	505	(605)	B
	(825)	1055	(770)	850	(755)	2095	(650)	770	A
393	590	(675)	625	(620)	590	-	505	(525)	B
	(775)	1745	(745)	950	(705)	2430	(675)	820	A
388	615	(630)	555	(715)	585	-	550	(490)	B
	(810)	1750	(715)	920	(660)	2300	(710)	820	A
383	635	(610)	660	(990)	625	-	505	(545)	B
	(795)	1420	(750)	960	(630)	985	(575)	970	A
Array Average	603		623		600		516		B
Array Average		1493		920		1953		853	A
Velocity Increase (A/B)		2.5		1.5		3.3		1.6	

* B: Measurements before grouting, 22 and 23 April 1978; reading accuracy good (±1 ms) for near geophones.
A: Measurements after grouting, 24 and 25 June 1978; reading accuracy excellent (±0.2 ms) for all readings.

** Values in parentheses ( ) not used for computing array average.

CHEMICAL GROUTING TEST PROGRAM

RESULTS OF SHEAR WAVE VELOCITY MEASUREMENTS

FOUNDATION INVESTIGATION AND TEST PROGRAM
EXISTING LOCKS AND DAM No. 26
ST LOUIS DISTRICT, CORPS OF ENGINEERS.
DACW43-78-C-0005

Woodward-Clyde Consultants

Y7C825 Phase IX

Table 9.1

MATERIAL TESTED	TEST SUBAREA	LOCATION	ELEVATION ft	TEST NO.	$K^{(3)}$ t/ft^3	$E_s^{(4)}$ t/ft^2	$q^{(5)}$ t/ft^2	CREEP RATE in./cycle at q	at q/2
Ungrouted Soil									
grey m-f SAND	-	16.5 ft N 2.5 ft E of 4-5[6]	392.6	P-4	1429[1]	1261[1]	5.5	0.007	0.001
tan m-f SAND some coarse	-	8 ft W 5 ft N of BM-1	393.9	P-5	208	183	5.1	0.037	0.006
grey m-f SAND some coarse	-	17.5 ft N 6 ft W of 6-1	390.6	P-8	238	210	3.7	0.006	0.002
grey brown m-f SAND trace coarse	-	14.5 ft S of 9-1	384.3	P-17	103	91	3.6	0.019	0.009
Low-Strength Grout									
25% Silicate/Aluminate	6	3.5 ft NE of 6-1	398	P-1[2]	605	534	8.0	-	-
	8	2 ft NE of 8-3	398	P-2	278	246	8.0	0.085	0.035
	7	2 ft NW of 7-3	390.9	P-10	353	311	6.4	0.039	0.010
35% Siroc 142	4	3.5 ft W of 4-2	390	P-9	1385	1218	>14	-	0.010
	2	1.5 ft N of 2-2	389.4	P-12	2057	1815	12.0	0.028	0.004
	1	1.5 ft S of 1-5	389.6	P-13	384	338	10.0	0.134	0.035
28% Silicate/R600	3	2 ft W of 3.2	390	P-11	1833	1613	11.0	0.015	0.007
High-Strength Grout									
55% Siroc 132/142	10	2 ft S of 10-1	384.6	P-15	10533	9290	>15.8	-	0.001
	9	1.5 ft W of 9-5	397.6	P-3[2]	6194	5464	>16	-	0.02
	11	2.5 ft W of 11-6	384.2	P-16	13714	12098	>14	-	< 0.001
45% Siroc 142	5	3 ft W of 5-2	393.3	P-7	9333	8233	>17.0	-	< 0.001
46% Silicate/R600	13	3 ft S of 13-5	393.4	P-6[2]	1091	962	>14.5	-	0.044
	12	1.5 ft N of 12-3	390	P-14	1033	911	>18	-	0.035

Notes

(1) Difficulty in setting dozer may have resulted in preloading area

(2) Long-term tests

(3) K: Modulus of subgrade reaction

(4) E_s: Modulus of elasticity

(5) q: Ultimate plate bearing capacity

(6) Location given in relation to nearest grout hole or Benchmark BM-1

CHEMICAL GROUTING TEST PROGRAM

LOCATION AND RESULTS OF PLATE LOAD TESTS

FOUNDATION INVESTIGATION AND TEST PROGRAM
EXISTING LOCKS AND DAM No. 26
ST LOUIS DISTRICT, CORPS OF ENGINEERS.
DACW43-78-C-0005

Woodward-Clyde Consultants

Y7C825 Phase III

Table 9.2

MATERIAL TESTED	TEST SUBAREA	LOCATION[1]	ELEVATION ft	TEST NO.	TOTAL UNIT WEIGHT lb/ft³	WATER CONTENT %	DRY UNIT WEIGHT lb/ft³	AVERAGE DRY UNIT WEIGHT lb/ft³
Ungrouted Sand								
tan m-f SAND some coarse	-	9 ft N 10 ft E of 4-5	397	D-4	113	5	107.6	
gray-brown m-f SAND	-	7 ft NE of 1-3	396.7	D-5	106.5	5	101.4	
gray-brown m-f SAND some coarse	-	4 ft SE of 10-2	393	D-8	114.3	3	111.5	
gray c-f SAND trace silt and gravel	-	2.5 ft SE of 10-6	390	D-10	102.7	3	99.7	111.8
gray m-f SAND	-	2 ft E of P-8	390.6	D-14	108.6	3	105.4	
gray-brown m-f SAND	-	14.5 ft S of 9-1 (at P-17)	383.8	D-18	109.9	4	105.7	
gray m-f SAND trace coarse	-	11.1 ft N of 12-5	384.7	D-21	120.8	4	116.2	
25% Silicate/Aluminate								
brown m-f SAND	6	2 ft W of 6-4	397.5	D-2	126.6	21	104.7	106.3
gray m-f SAND	6	3 ft E of 6-4	391	D-13	129.5	20	107.9	
brown c-f SAND	7	1.5 ft W of 7-4	397.5	D-3	129.7	19	109	110
gray m-f SAND	7	1.2 ft SE of 7-3	390.7	D-12	128.4	16	110.9	
brown c-f SAND	8	2 ft S of 8-8	397.5	D-1	133.4	17	114	112.4
gray c-f SAND	8	6 ft S of 8-6	390.7	D-11	129.6	17	110.7	
35% Siroc 142								
gray m-f SAND	1	2 ft W of 1-2	392.9	D-6	132.9	18	113.6	
gray m-f SAND	1	1.5 ft W of 1-3	389.6	D-16	127.5	19.3	106.9	110.2
gray m-f SAND	2	1 ft E of 2-3	393.5	D-7	135.6	16	116.9	
gray m-f SAND	2	2 ft E of 2-2	390	D-15	125.2	21	103.5	
gray m-f SAND	4	2 ft S of 4-3	390.2	D-9	130.9	16	112.8	111.7
gray m-f SAND	4	2 ft N of 4-1	383.9	D-19	131.5	19	110.5	
28% Silicate/R600								
gray m-f SAND	3	2 ft NE of 3-1	389.6	D-17	123.3	17.5	104.9	103.9
gray m-f SAND	3	1.3 ft N of 3-2	384.6	D-20	119.3	16	102.9	

Note

(1) Locations are given in relation to nearest grout hole

CHEMICAL GROUTING TEST PROGRAM

LOCATION AND RESULTS OF IN-PLACE DENSITY TESTS

FOUNDATION INVESTIGATION AND TEST PROGRAM
EXISTING LOCKS AND DAM No. 26
ST LOUIS DISTRICT, CORPS OF ENGINEERS.
DACW43-78-C-0005

Woodward-Clyde Consultants
Y7C825 Phase II

Table 9.3

TYPE OF GROUT	TEST SUBAREA	SAMPLE LOCATION[1]	ELEVATION ft	SAMPLE NUMBER[2]
25% Silicate/Aluminate	6	1 ft NE of 6-1	394.4	BS-9[3]
	7	1 ft N of 7-4	393.5	BS-8
	8	1.5 ft W of 8-7	398	BS-3
	8	1 ft SW of 8-5	393.3	BS-15[3]
	8	2 ft SW of 8-7	384.3	BS-22
35% Siroc 142	1	1 ft N of 1-2	397	BS-6
	1	1 ft SW of 1-4	393	BS-14
	1	4 ft W of 1-2	390	C-11/12[4]
	1	3 ft SE of 1-4	389.7	C-13/14/15/16
	2	1 ft NE of 2-2	396.7	BS-7
	2	3.5 ft NE of 2-2	389.6	BS-21
	4	3 ft W of 4-5	398	BS-2
	4	1 ft NW of 4-4	390.2	BS-18
28% Silicate/R600	3	1 ft SW of 3-2	393	BS-16
	3	3 ft SW of 3-4	390.1	BS-20
	3	0.7 ft N 1.5 ft E of 3-4	384.8	C-17/18/19/20
45% Siroc 142	5	3.5 ft N of 5-1	396.6	BS-5
	5	Around 5-4	390.8	C-5/6/7/8
	5	2.5 ft SW of 5-2	390	C-9/10[4]
55% Siroc 132/142	9	1 ft NE of 9-5	397	BS-11[5]
	9	4 ft SW of 9-2	393.7	BS-17
	9	1 ft SW of 9-5	384.9	C-22/23/24
	9	0.7 ft N of 9-6	384.9	C-21
	10	2.5 ft NW of 10-2	390.8	BS-19[3]
	11	4.2 ft NE of 11-3	399	BS-1
	11	1.5 ft N of 11-5	393.8	BS-10
	11	Between 11-2 and 10-1	389.6	C-1/2/3/4[6]
46% Silicate/R600	12	1 ft NE of 12-4	393.4	BS-12[7]
	13	1.5 ft S of 13-3	397.2	BS-4
	13	1.5 ft N of 13-1	393.5	BS-13
	13	2 ft W of 13-2	385.2	C-25/26/27/28

Notes

(1) Location given in relation to nearest grouthole
(2) BS = Block Sample; C = Core
(3) Sample cracked during carving
(4) Cores shipped to WES
(5) Sample carved from vertical cut face; all others carved from horizontal exposures
(6) Cores C-3/4 shipped to WES
(7) Sample is only 8 in. high

CHEMICAL GROUTING TEST PROGRAM

LOCATION OF GROUTED SOIL BLOCK AND CORE SAMPLES

FOUNDATION INVESTIGATION AND TEST PROGRAM
EXISTING LOCKS AND DAM No. 26
ST LOUIS DISTRICT, CORPS OF ENGINEERS.
DACW43-78-C-0009

Woodward-Clyde Consultants
Y7C825 Phase IX

Table 9.4

BORING	GROUT TYPE	IN SITU CURING TIME days	TIME IN TUBE DRY(1) days	TIME IN TUBE MOIST(2) days	TIME OUT OF TUBE BEFORE TESTING days	TOTAL AGE AT TESTING days
AG-A1-4	35% Siroc 142	46	13	17	0	76
AG-A3-3	28% Silicate/R600	20	5	11 to 17	5 to 0	41 to 42
AG-A4-3	35% Siroc 142	19	12	18	0 to 3	49 to 52
AG-A5-4	45% Siroc 132	12	15	15	-	42
AG-A8-4	25% Silicate/Aluminate	16	27	14	0	57
AG-A11-4	55% Siroc 132/142	35	20	10	1 to 3	66 to 68
AG-A13-3	46% Silicate/R600	20	17	10	1 to 5	48 to 52

Notes

(1) *Samples stored in sealed tubes at test site*

(2) *Samples stored in sealed tubes in laboratory humid room*

CHEMICAL GROUTING TEST PROGRAM

CURING HISTORY OF UNDISTURBED BOREHOLE SAMPLES

FOUNDATION INVESTIGATION AND TEST PROGRAM
EXISTING LOCKS AND DAM No. 26
ST LOUIS DISTRICT, CORPS OF ENGINEERS.
DACW43-78-C-0005

Woodward-Clyde Consultants

Y7C825 Phase IX

Table 9.5

BORING	SUBAREA	ELEVATION ft	UNIT WEIGHT lb/ft^3	STRAIN RATE %/min	q_u t/ft^2	STRAIN AT FAILURE %	E_{50} (3) t/ft^2	COEFFICIENT OF PERMEABILITY K, cm/s
AG-A1-4	1	389	124.7	0.5	0.44	1.69	46.8	2.1×10^{-5}
AG-A1-4	1	390	124.1	0.5	0.27	2.44	36.8	-
AG-A1-4	1	385	126.0	0.5	0.58	1.2	65.9	-
AG-A3-3	3	389	125.5	0.5	0.17	1.47	222.5	1.1×10^{-5}
AG-A3-3	3	390	128.6	0.5	0.40	0.83	153.9	-
AG-A4-3 (1)	3	394	119.6	0.5	3.67	0.52	1360.0	-
AG-A4-3	4	393	126.3	0.5	1.29	1.42	140.0	-
AG-A4-3	4	388	127.1	0.5	1.50	1.17	150.0	1.1×10^{-4}
AG-A4-3	4	478	127.6	0.5	1.34	1.26	124.8	-
AG-A8-4	8	388	119.8	0.5	0.11	3.96	8.6	3.8×10^{-4}
AG-A8-4	8	387	120.6	0.5	0.09	0.85	91.7	-
AG-A11-4	11	390	122.3	0.5	14.99	1.71	894.8	2.9×10^{-4}
AG-A11-4	11	385	125.8	0.5	7.89	0.11	8393.6	7.3×10^{-4}
AG-A13-3	13	391	129.8	0.5	4.46	1.05	495.2	1.7×10^{-5}
AG-A13-3	13	390	124.8	0.5	5.24	1.54	375.4	-
AG-A13-3 (2)	13	386	123.5	0.5	1.06	3.64	32.9	3.9×10^{-4}
AG-A13-3	13	385	125.8	0.5	7.30	1.40	527.8	-

Notes

(1) Sample infiltrated with 55% Siroc 142

(2) Fracture in sample

(3) E_{50} = Secant modulus at 50 percent of q_u

CHEMICAL GROUTING TEST PROGRAM

RESULTS OF UNCONFINED COMPRESSION AND PERMEABILITY TESTS ON UNDISTURBED BOREHOLE SAMPLES

FOUNDATION INVESTIGATION AND TEST PROGRAM
EXISTING LOCKS AND DAM No. 26
ST LOUIS DISTRICT, CORPS OF ENGINEERS.
DACW43-78-C-0005

Woodward-Clyde Consultants

Y7C825 Phase IX

Table 9.6

BORING	SUBAREA	ELEVATION ft	UNIT WEIGHT lb/ft³	CONFINING STRESS t/ft²	PEAK DEVIATOR STRESS t/ft²	STRAIN AT FAILURE %	E_{50} t/ft²	COEFFICIENT OF PERMEABILITY cm/s
AG-A5-4(2)	5	396	130.9	-	-	-	-	-
AG-A5-4(2)	5	395	112.3	-	-	-	-	-
AG-A8-4(2)	8	386.5	116.9	-	-	-	-	-
AG-A8-4(2)	8	386	123.9		Unsuitable for Strength Testing			
AG-A8-4(2)	8	385	117.6	-	-	-	-	-
AG-A11-4	4	398	120.1	-	-	-	-	9.5×10^{-6}
AG-A11-4(2)	4	382	122.0	-	-	-	-	-
AG-A13-3(1)	13	397	125.8	2.5	9.49	18.60	148.3	3.4×10^{-7}
AG-A13-3(2)	13	388	126.7		Unsuitable for Strength Testing			
AG-A13-3(1)	13	387	124.9	2.5	3.42	4.60	333.3	1.4×10^{-4}

Notes

(1) *Strain rate = 15%/min*

(2) *Sample deteriorated and was unsuitable for strength testing*

CHEMICAL GROUTING TEST PROGRAM

RESULTS OF UU TRIAXIAL COMPRESSION AND PERMEABILITY TESTS ON UNDISTURBED BOREHOLE SAMPLES

FOUNDATION INVESTIGATION AND TEST PROGRAM
EXISTING LOCKS AND DAM No. 26
ST LOUIS DISTRICT, CORPS OF ENGINEERS.
DACW43-78-C-0005

Woodward-Clyde Consultants

Y7C825 Phase IX

Table 9.7

TEST SUBAREA	BLOCK SAMPLE OR CORE NUMBER	SPECIMEN NUMBER	ELEVATION ft	DRY UNIT WEIGHT γ_d lb/ft³	q_u (1) t/ft²	STRAIN AT FAILURE ϵ_f %	INITIAL TANGENT MODULUS E_i t/ft²	MODULUS AT FAILURE E_{sf} t/ft²	SONIC VELOCITY V_s ft/s
1	BS-6	2	397	105.1	3.94	0.56	1,290.3	704.3	-
1	BS-6	7	397	107.2	4.13	0.55	1,290.3	750.5	-
1	BS-6	5	397	106.1	3.92	0.48	1,111.1	816.3	-
1	BS-6	1 (2)	397	106.8	1.40	∞	-	-	-
1	BS-6	3 (2)	397	102.3	1.40	∞	-	-	-
1	BS-6	6	397	106.5	-	-	-	-	1,190
1	BS-14	5	393	102.3	0.71	0.50		143.0	-
2	BS-7	1	396.7	105.6	1.91	0.41	625.0	471.4	-
2	BS-7	4 (2)	396.7	105.1	0.67	∞	-	-	-
4	BS-2	1	398.0	101.5	18.38	0.34	12,000	8,000	-
8	BS-22	5	384.3	102.2	0.32	0.76	50.0	42.1	-
8	BS-22	6	384.3	104.0	0.29	0.81	66.7	35.2	-
8	BS-22	7 (2)	384.3	102.8	0.34	0.35	454.5	95.2	-
11	C-1	-	389.6	100.0	13.69	1.17	1,538.5	1,538.5	-
11	C-4	-	389.6	98.8	8.59	0.72	1,538.5	1,538.5	-
11	C-2 (2)	-	389.6	97.6	24.53	0.21	12,500	11,652	-
13	BS-13	1	393.5	107.4	16.32	0.78	3,000	3,000	-
13	BS-13	3 (2)	395.5	105.4	3.53	∞	-	-	-
13	BS-13	4	393.5	106.3	4.15	0.91	845.1	710.1	-
13	BS-4	1	397.4	96.5	15.18	0.58	5,172	2,609	-

Notes

(1) Strain Rate = 0.15%/min

(2) Creep Test

CHEMICAL GROUTING TEST PROGRAM

RESULTS OF CID TRIAXIAL COMPRESSION AND MAX-MIN DENSITY TESTS ON RECONSTITUTED UNGROUTED SAND

FOUNDATION INVESTIGATION AND TEST PROGRAM
EXISTING LOCKS AND DAM No. 26
ST LOUIS DISTRICT, CORPS OF ENGINEERS.
DACW43-78-C-0005

Woodward-Clyde Consultants

Y7C825 Phase IX

Table 9.8

TEST SUBAREA	BLOCK SAMPLE OR CORE NUMBER	SPECIMEN NUMBER	ELEVATION ft	DRY UNIT WEIGHT γ_d lb/ft³	CONFINING STRESS $\bar{\sigma}_{3c}$ t/ft²	PEAK DEVIATOR STRESS $(\sigma_1 - \sigma_3)_{max}$ t/ft²	STRAIN AT FAILURE ϵ_f %	INITIAL TANGENT MODULUS E_i t/ft²	MODULUS AT FAILURE E_{sf} t/ft²	SONIC VELOCITY V_s ft/s	COEFFICIENT OF PERMEABILITY K cm/s
1	BS-14	1	393	103.1	1.0	3.99	3.37	578	118.5	-	-
1	BS-14	2	393	102.7	2.0	6.95	4.59	852.1	151.2	-	-
1	BS-14	4	393	103.5	4.0	12.48	6.36	1,266	196.2	-	-
1	BS-14	3 (1)	393	103.7	2.0	7.13	5.93	-	120.2	-	-
1	BS-6	6	397	105.2	1.0	-	-	-	-	-	1.8×10^{-5}
8	BS-22	1	384.3	100.7	1.0	3.95	3.78	634.9	104	-	1.33×10^{-4}
8	BS-22	2	384.3	104.1	2.0	7.02	5.32	754.7	132	-	-
8	BS-22	3	384.3	103.0	4.0	12.14	6.08	1,012.7	199.7	-	-
8	BS-22	8 (1)	384.3	103.3	2.0	7.48	6.63	4,137.9	112.9	-	-
8	BS-22	9 (1)	384.3	101.5	2.0	6.74	5.07	4,137.9	133	-	-
8	BS-22	10 (1)	384.3	100.9	2.0	7.14	4.05	1,250	176.2	-	-
8	BS-22	11	384.3	102.7	0-3.9	-	-	-	-	1,100	-
11	BS-10	1	393.8	108.4	1.0	28.14	0.70	6,667	4,036	-	7.1×10^{-5}
11	BS-10	2	393.8	108.1	2.0	22.95	0.70	6,667	3,292	-	-
11	BS-10	4	393.8	108.4	4.0	37.56	1.02	6,667	3,690	-	-
11	BS-10	3 (1)	393.8	108.2	1.99	28.27	0.35	11,000	8,072	-	-
11	BS-10	5	393.8	108.2	0-2.8	-	-	-	-	3,611	-
11	BS-10	7	393.8	-	0-2.8	-	-	-	-	3,484	-
13	C-25	-	385.2	108.2	4.0	28.66	3.05	2,828	940.8	-	-
13	C-26 (1)	-	385.2	107.2	2.0	11.61	3.04	2,828	381.5	-	-
13	C-27	-	385.2	104.9	2.0	11.59	1.27	2,154	912.6	-	-
13	C-28	-	385.2	101.8	0, 1.0	6.71	0.85	1,455	786.1	2,110	-
13	BS-13	2	393.5	103.0	1.0	-	-	-	-	-	2.95×10^{-3}

Notes

(1) *Creep Test; Strain Rate = 0.15%/min*

CHEMICAL GROUTING TEST PROGRAM

RESULTS OF UNCONFINED COMPRESSION AND SONIC VELOCITY ON EXCAVATION BLOCK AND CORE SAMPLES

FOUNDATION INVESTIGATION AND TEST PROGRAM
EXISTING LOCKS AND DAM No. 26
ST LOUIS DISTRICT, CORPS OF ENGINEERS.
DACW43-78-C-0005

Woodward-Clyde Consultants

Y7C825 Phase IX

Table 9.9

AD-A076 091 WOODWARD-CLYDE CONSULTANTS CHICAGO IL F/G 13/2
RESULTS AND INTERPRETATION OF CHEMICAL GROUTING TEST PROGRAM. V--ETC(U)
JUL 79 J PEREZ , Y LACROIX DACW43-78-C-0005

UNCLASSIFIED NL

3 OF 4
AD
A076091

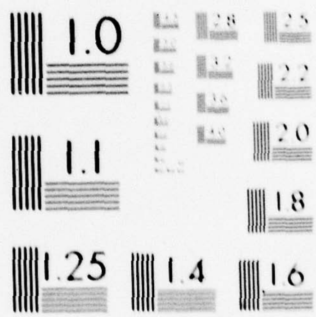

MICROCOPY RESOLUTION TEST CHART

NATIONAL BUREAU OF STANDARDS-1963-A

SAMPLE NUMBER	SPECIMENS NUMBER	DRY UNIT WEIGHT γ_d lb/ft³	MAX-MIN UNIT WEIGHT γ_{dmax} (2) lb/ft³	γ_{dmin} (3) lb/ft³	CONFINING STRESS $\bar{\sigma}_{3c}$	PEAK(1) DEVIATOR STRESS $(\sigma_1 - \sigma_3)_{max}$	STRAIN AT FAILURE ϵ_f	INITIAL TANGENT MODULUS E_i	MODULUS AT FAILURE E_{sf}
1	-	111.8	122.4	98.6	-	-	-	-	-
2	-	111.8	118.9	99.4	-	-	-	-	-
2	3	111.8	–	–	2.0	10.41	1.38	1,905	756.7
2	6 (4)	111.9	–	–	2.0	10.16	1.50	1,482	676.6
2	4 (4)	111.7	–	–	2.0	10.39	1.25	2,667	832.7
2	5 (4)	111.9	–	–	2.0	10.20	0.91	4,000	1,126.7

Notes

(1) *Strain Rate = 0.15%/min*

(2) *Maximum density obtained by horizontal vibration*

(3) *Minimum density average of density obtained by tube, funnel in small mold, ASTM 0.1 ft³ mold, and cylinder tilt*

(4) *Creep Test*

CHEMICAL GROUTING TEST PROGRAM

RESULTS OF TRIAXIAL AND OTHER TESTS ON BLOCK AND CORE SAMPLES

FOUNDATION INVESTIGATION AND TEST PROGRAM
EXISTING LOCKS AND DAM No. 26
ST LOUIS DISTRICT, CORPS OF ENGINEERS.
DACW43-78-C-0005

Woodward-Clyde Consultants
Y7C825 Phase IV

Table 9.10

ASSAY	WATER FROM TEST AREA EXCAVATION	WATER FROM MAIN TEST SITE DEWATERING	UNITS
Ammonia (as Nitrogen)	27.7	2.5	ppm
Calcium	103	144	ppm
Sodium	230	39.6	ppm
Silicon	29.9	15.3	percent
Total Organic Carbon	44	54.9	ppm
Aluminum	<1	<1	ppm

Tests made by Raltech Scientific Services for WCC

CHEMICAL GROUTING TEST PROGRAM

RESULTS OF POST-GROUTING GROUNDWATER ANALYSES

FOUNDATION INVESTIGATION AND TEST PROGRAM
EXISTING LOCKS AND DAM No. 26
ST LOUIS DISTRICT, CORPS OF ENGINEERS.
DACW43-78-C-0005

Woodward-Clyde Consultants

YTC825 Phase IX

Table 9.11

	TEST CONDITION \ TEST TYPE	PRESSUREMETER	PLATE LOAD TEST	CROSSHOLE SHEAR WAVE VELOCITY	UNCONFINED COMPRESSION	CID TRIAXIAL COMPRESSION
1	LOADING TYPE	Stress-controlled plane strain cyl cavity expansion	Stress-controlled 1-D confined compression	Stress-controlled simple shear	Strain-controlled uniaxial compression	Strain-controlled triaxial compression
2	VOLUME OF SOIL TESTED	2-ft-long, 1-ft-dia cylinder of in situ soil	In situ soil mass under 13.5-in.-dia plate	In situ bulk soil mass	7-in.-long, 3-in.-dia tube or block sample	7-in.-long, 3-in.-dia tube or block sample
3	TYPE OF DISTURBANCE	Borehole disturbance	Excavation disturbance	None	Sampling and trimming	Sampling and trimming
4	STATE OF CONFINING STRESS	In situ stresses	Removal of vertical stress	In Situ stresses	Unconfined	Confined under selected stresses
5	MAJOR PRINCIPAL STRESS	Horizontal	Vertical	Vertical	Vertical	Vertical
6	DRAINAGE CONDITIONS	Assume fully Drained	Drained	Undrained	Drained	Drained
7	STRESS PATH			-		
8	FAILURE PLANE	Multiple	Single	No failure	Single	Single
9	STRAIN RATE %/min	0.25	0.01	-	0.5	0.5
10	STRESS DURATION $^{min}/_{t/ft^2}$	1	5	10^{-5}	5.6	0.65
11	STRAIN AMPLITUDE %	15	1.2	10^{-6} to 10^{-8}	2	4

CHEMICAL GROUTING TEST PROGRAM

CONDITIONS PREVAILING UNDER VARIOUS TESTS

FOUNDATION INVESTIGATION AND TEST PROGRAM
EXISTING LOCKS AND DAM No. 26
ST LOUIS DISTRICT, CORPS OF ENGINEERS.
DACW43-78-C-0005

Woodward-Clyde Consultants

Table 9.12

V7C628 Phase III

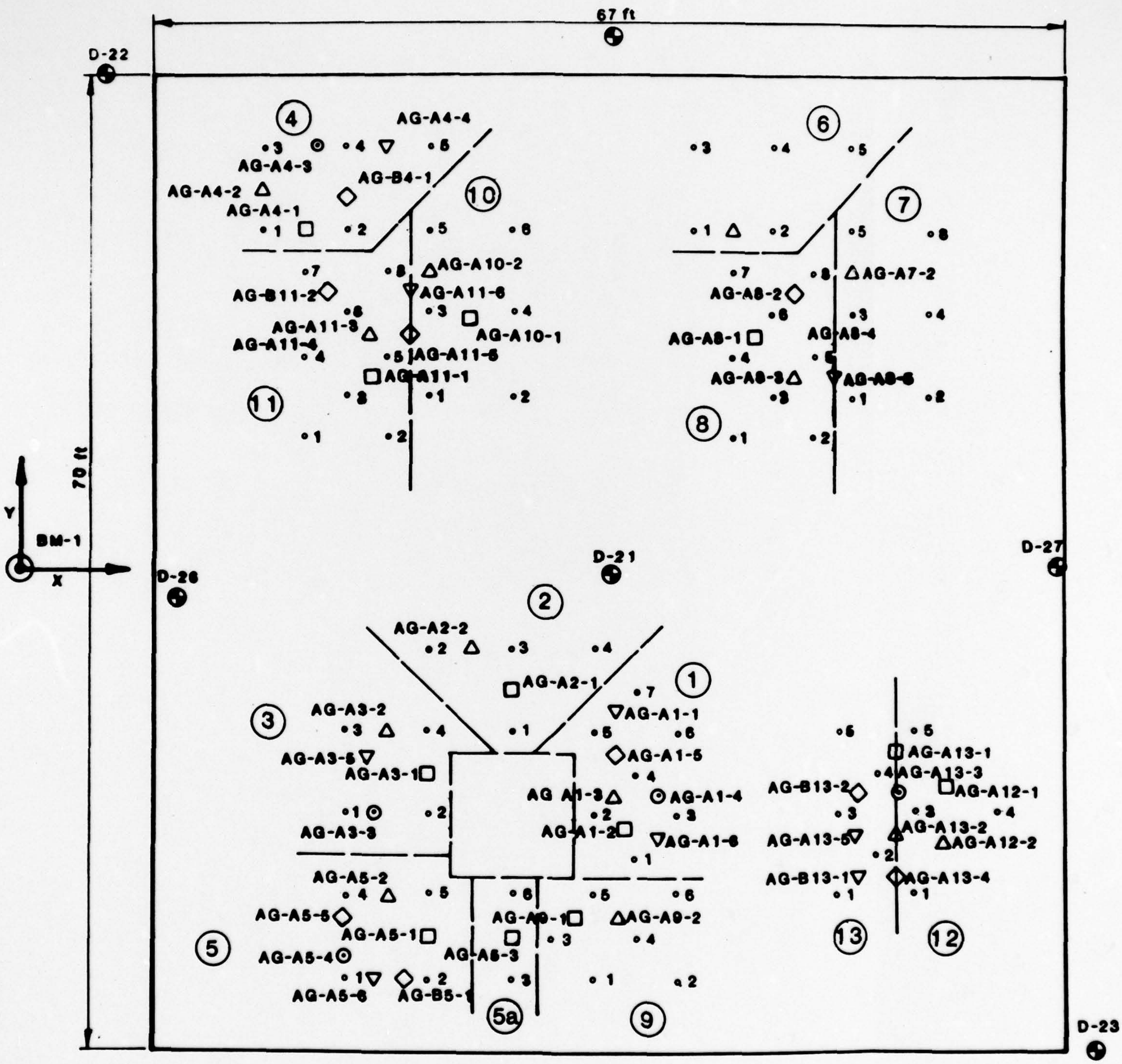

67 ft
70 ft
D-22
D-21
D-23
D-26
D-27
BM-1
Y
X
AG-A4-4
AG-A4-3
AG-A4-2
AG-A4-1
AG-B4-1
AG-A10-2
AG-A10-1
AG-A11-6
AG-B11-2
AG-A11-3
AG-A11-4
AG-A11-5
AG-A11-1
AG-A7-2
AG-A8-2
AG-A8-1
AG-A8-4
AG-A8-3
AG-A8-5
AG-A2-2
AG-A2-1
AG-A1-1
AG-A1-5
AG-A1-3
AG-A1-4
AG-A1-2
AG-A1-6
AG-A3-2
AG-A3-5
AG-A3-1
AG-A3-3
AG-A5-2
AG-A5-5
AG-A5-1
AG-A5-4
AG-A5-3
AG-A5-6
AG-B5-1
AG-A9-1
AG-A9-2
AG-A13-1
AG-A13-3
AG-B13-2
AG-A12-1
AG-A13-5
AG-A13-2
AG-A12-2
AG-B13-1
AG-A13-4
5a

1

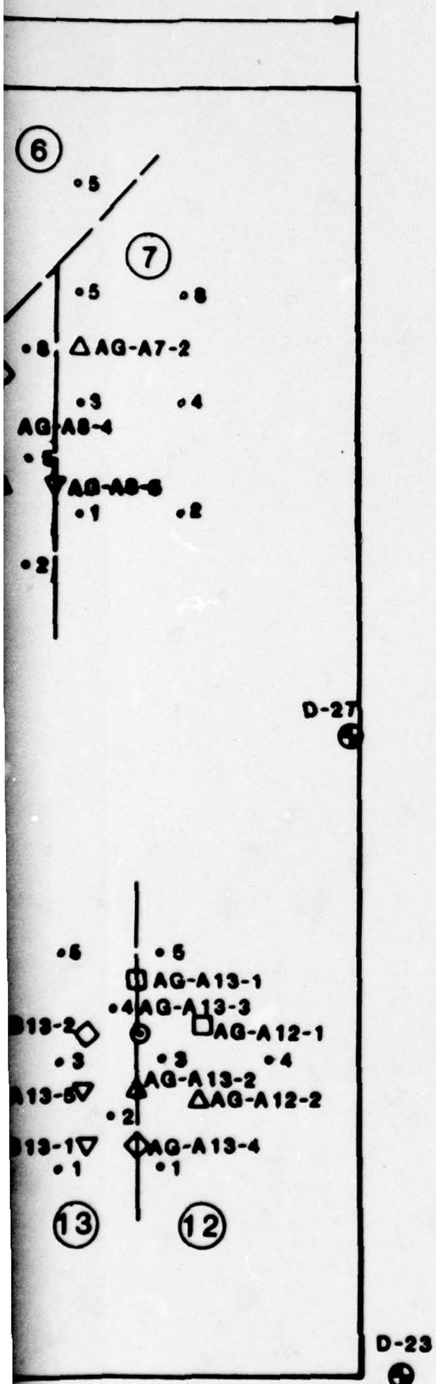

Legend

Y X Benchmark and origins of coordinates

□ SPT Standard penetration test

△ CPT Cone penetration test sounding

▽ K Permeability testing

◇ PMT Pressuremeter test

⊙ ST Undisturbed sampling

D Series boring locations

• Grout holes

N

0 10 20

Scale, ft

2

CHEMICAL GROUTING TEST PROGRAM

LOCATION OF BORINGS DRILLED AFTER GROUTING

FOUNDATION INVESTIGATION AND TEST PROGRAM
EXISTING LOCKS AND DAM No. 26
ST LOUIS DISTRICT, CORPS OF ENGINEERS,
DACW43-78-C-0006

Woodward-Clyde Consultants

Y7C026 Phase II

Fig. 9.1

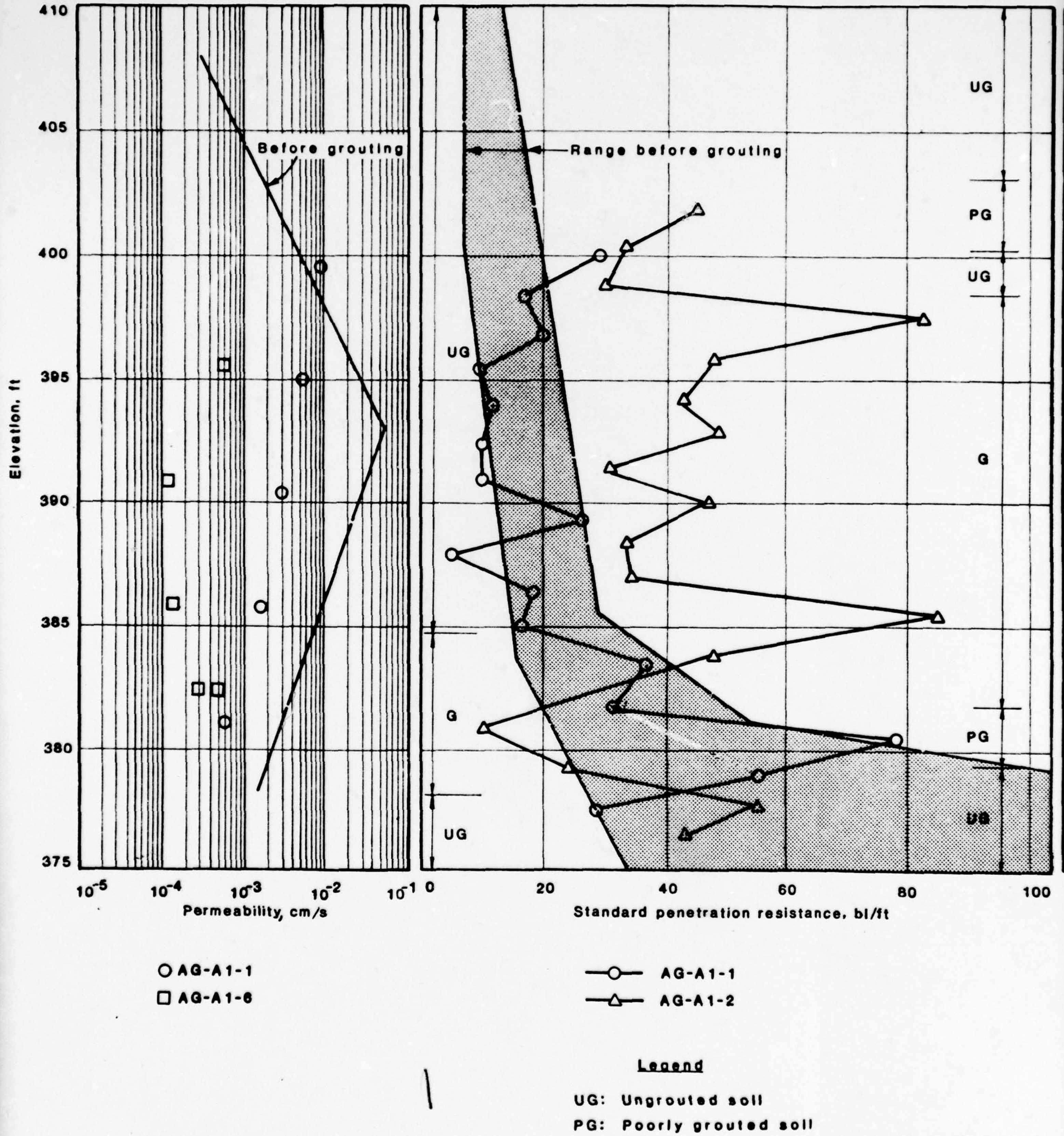

<u>Legend</u>

UG: Ungrouted soil

PG: Poorly grouted soil

G: Grouted soil

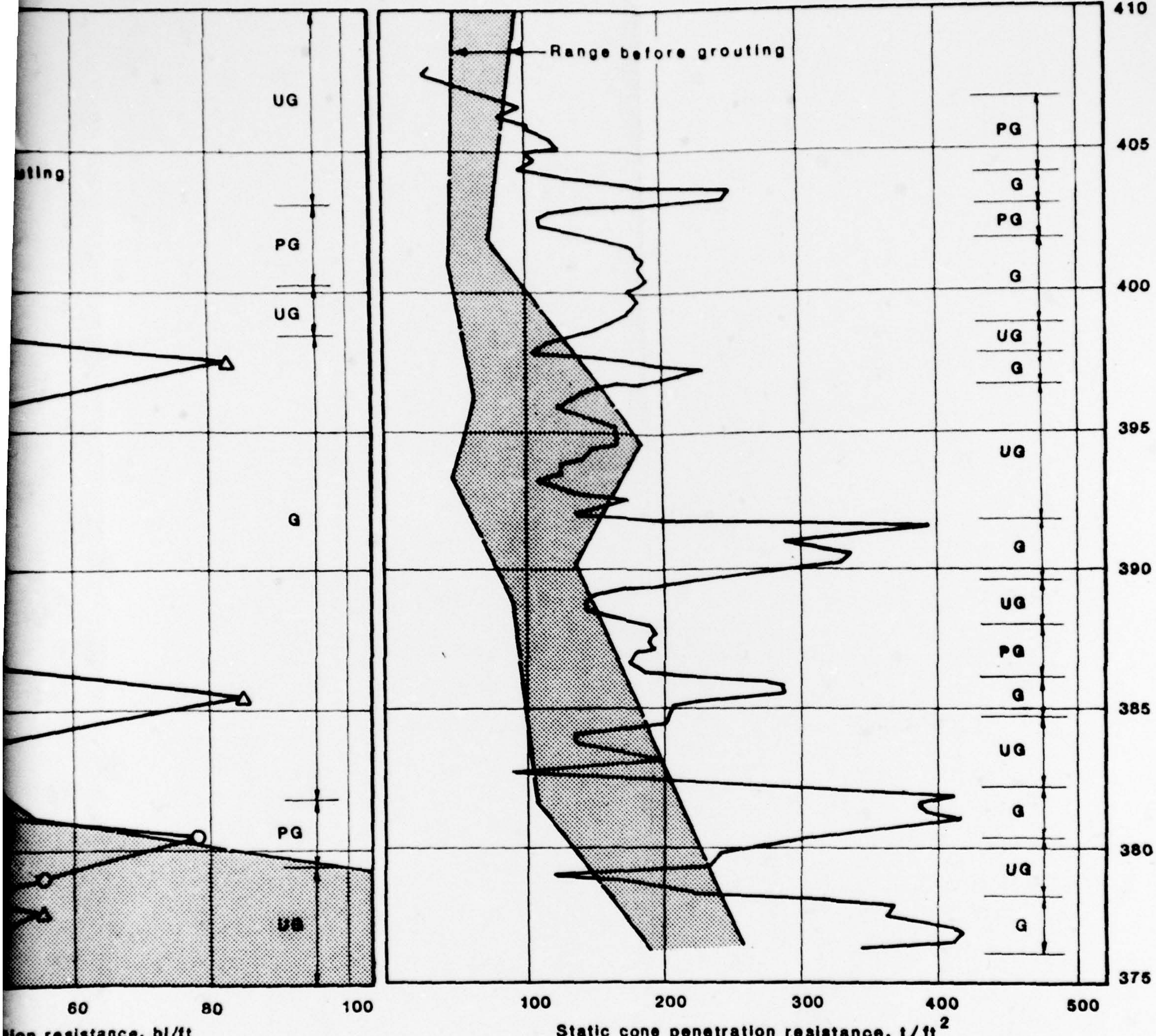

-1

-2

AG-A1-3

soil

outed soil

oil

CHEMICAL GROUTING TEST PROGRAM

RESULTS OF IN SITU TESTING AFTER GROUTING SUBAREA 1

FOUNDATION INVESTIGATION AND TEST PROGRAM
EXISTING LOCKS AND DAM No. 26
ST LOUIS DISTRICT, CORPS OF ENGINEERS.
DACW43-78-C-0008

Woodward-Clyde Consultants

Y7C825 Phase IX

Fig. 9.2

2

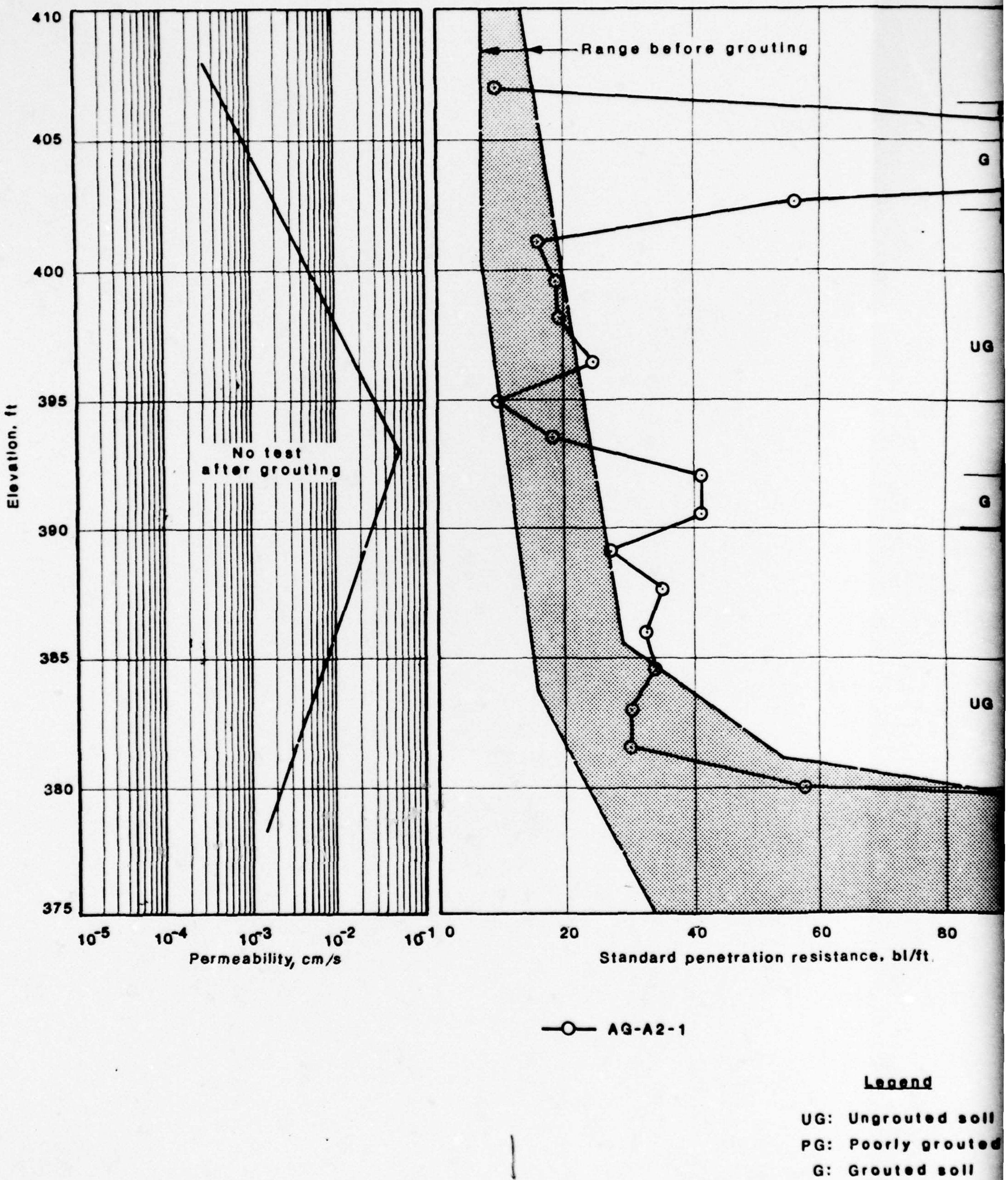

Range before grouting
No test
after grouting
Elevation, ft
410
405
400
395
390
385
380
375
10^-5
10^-4
10^-3
10^-2
10^-1
Permeability, cm/s
0
20
40
60
80
Standard penetration resistance, bl/ft
G
UG
G
UG
AG-A2-1
Legend
UG: Ungrouted soil
PG: Poorly grouted
G: Grouted soil

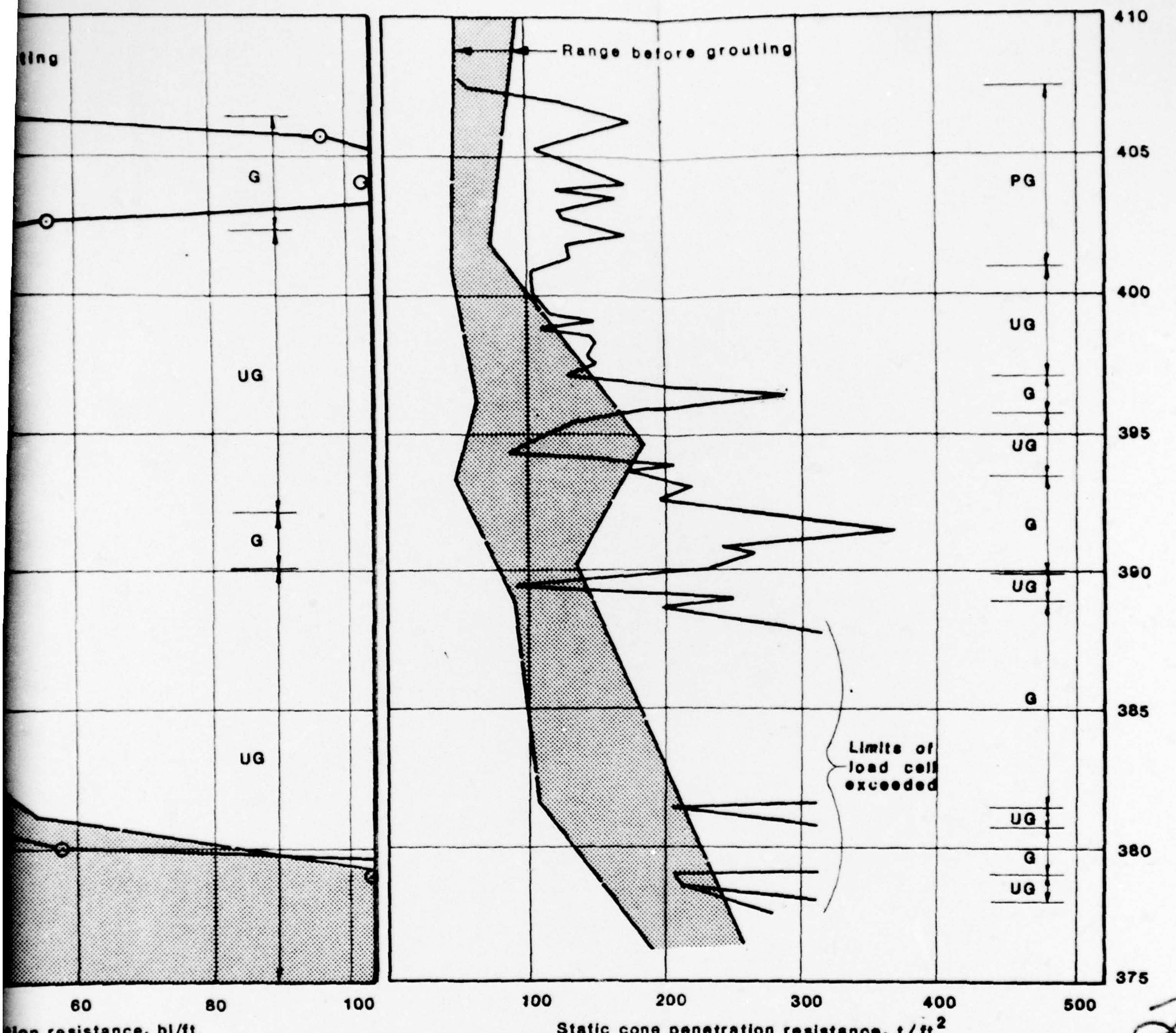

2

— AG-A2-2

Legend

UG: Ungrouted soil
PG: Poorly grouted soil
G: Grouted soil

CHEMICAL GROUTING TEST PROGRAM

RESULTS OF IN SITU TESTING AFTER GROUTING SUBAREA 2

FOUNDATION INVESTIGATION AND TEST PROGRAM
EXISTING LOCKS AND DAM No. 26
ST LOUIS DISTRICT, CORPS OF ENGINEERS.
DACW43-78-C-0088

Woodward-Clyde Consultants
Y7C825 Phase IX

Fig. 9.3

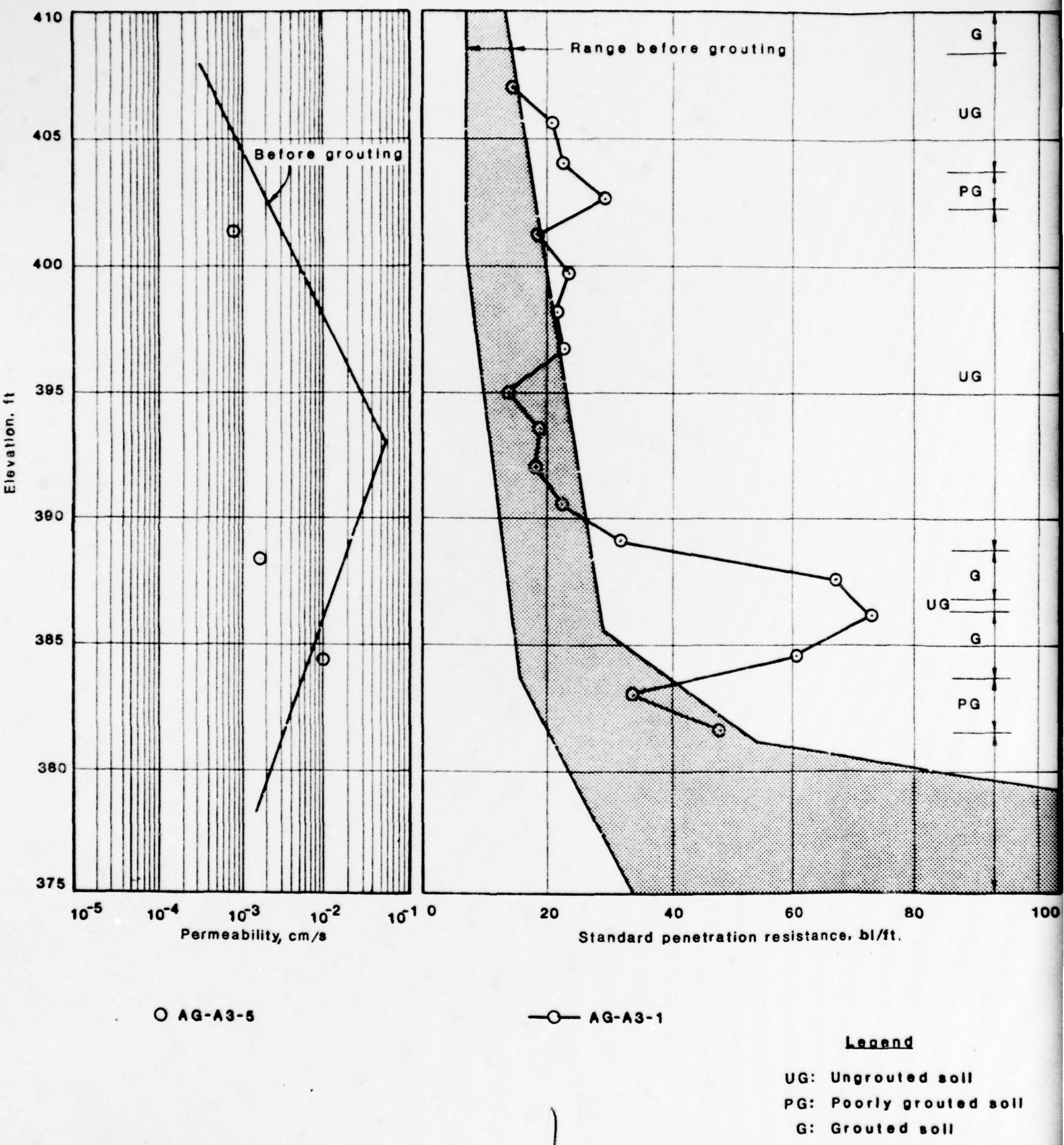

Elevation, ft
410
405
400
395
390
385
380
375
Before grouting
10^{-5}
10^{-4}
10^{-3}
10^{-2}
10^{-1}
Permeability, cm/s
Range before grouting
0
20
40
60
80
100
Standard penetration resistance, bl/ft.
G
UG
PG
UG
G
UG
G
PG
O AG-A3-5
AG-A3-1
Legend
UG: Ungrouted soil
PG: Poorly grouted soil
G: Grouted soil

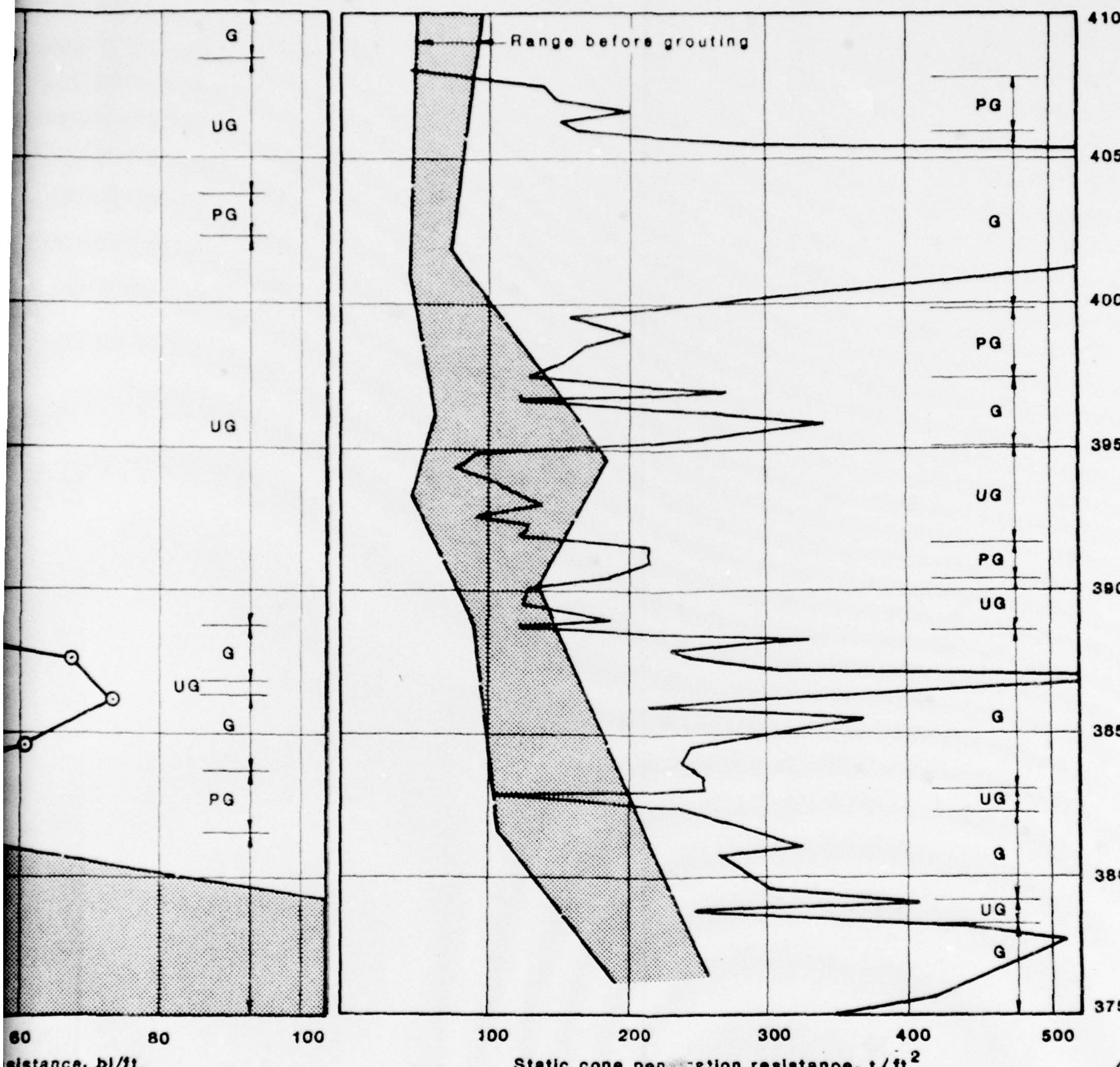

AG-A3-2

Legend

UG: Ungrouted soil

PG: Poorly grouted soil

G: Grouted soil

CHEMICAL GROUTING TEST PROGRAM

RESULTS OF IN SITU TESTING AFTER GROUTING SUBAREA 3

FOUNDATION INVESTIGATION AND TEST PROGRAM
EXISTING LOCKS AND DAM No. 26
ST LOUIS DISTRICT, CORPS OF ENGINEERS.
DACW43-78-C-0006

Woodward-Clyde Consultants
Y7C825 Phase IX

Fig. 9.4

2

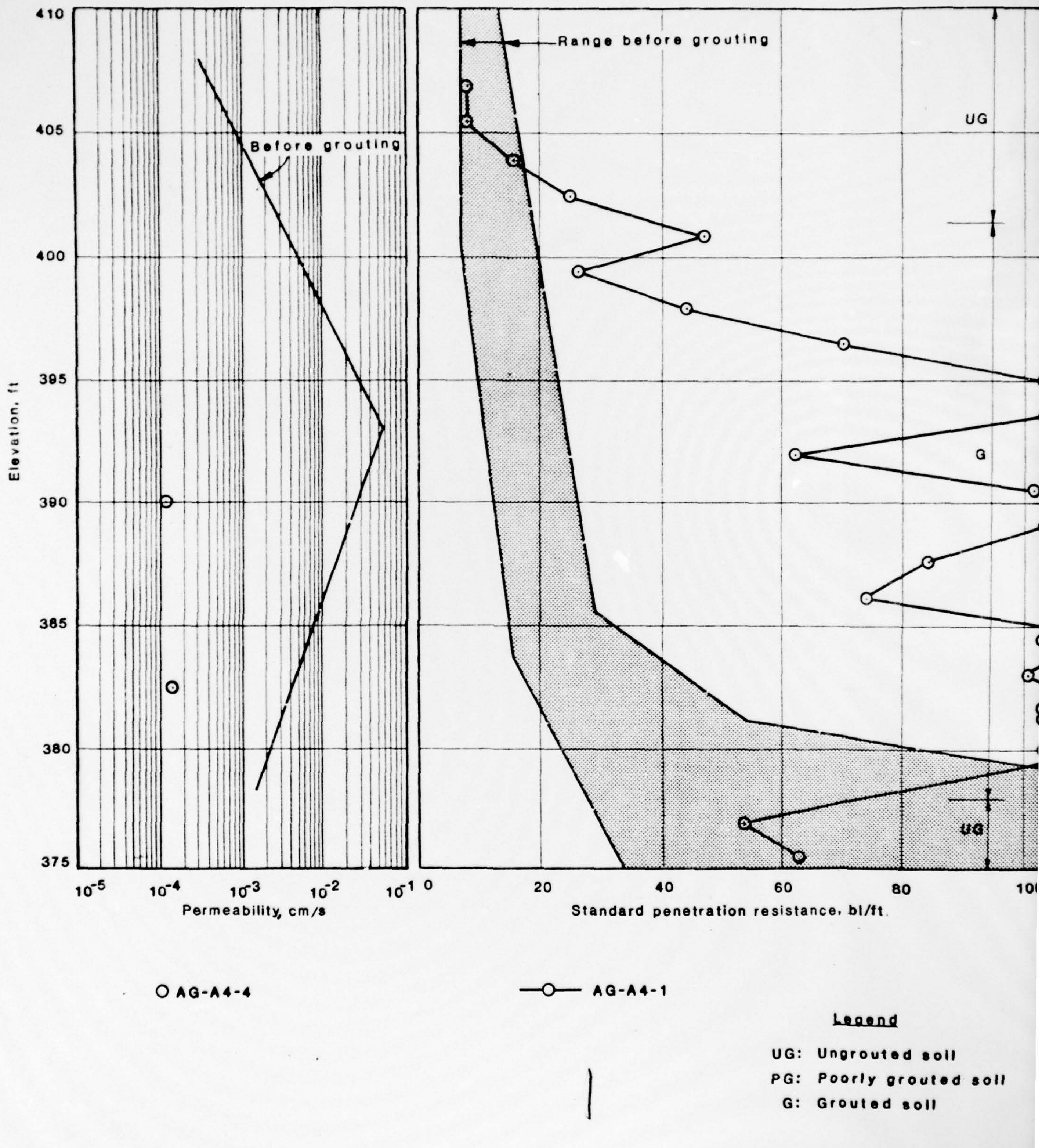

Range before grouting
Before grouting
UG
G
UG
Elevation, ft
410
405
400
395
390
385
380
375
10^{-5}
10^{-4}
10^{-3}
10^{-2}
10^{-1}
Permeability, cm/s
0
20
40
60
80
Standard penetration resistance, bl/ft
○ AG-A4-4
—○— AG-A4-1
Legend
UG: Ungrouted soil
PG: Poorly grouted soil
G: Grouted soil

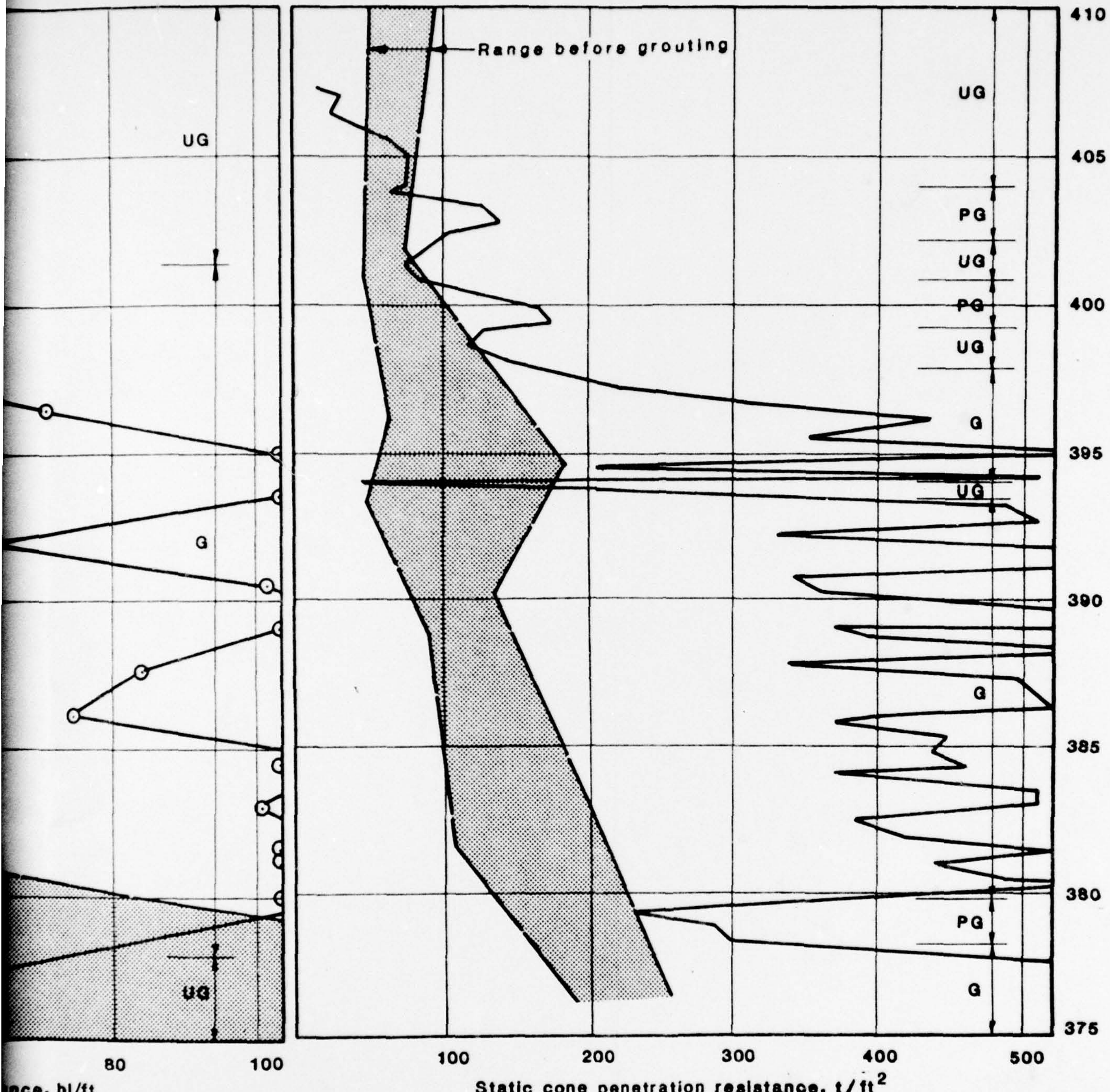

— AG-A4-2

Legend

Ungrouted soil

Poorly grouted soil

Grouted soil

2

CHEMICAL GROUTING TEST PROGRAM

RESULTS OF IN SITU TESTING AFTER GROUTING SUBAREA 4

FOUNDATION INVESTIGATION AND TEST PROGRAM
EXISTING LOCKS AND DAM No. 26
ST LOUIS DISTRICT, CORPS OF ENGINEERS,
DACW43-78-C-0005

Woodward-Clyde Consultants

Y7C825 Phase IX

Fig. 9.5

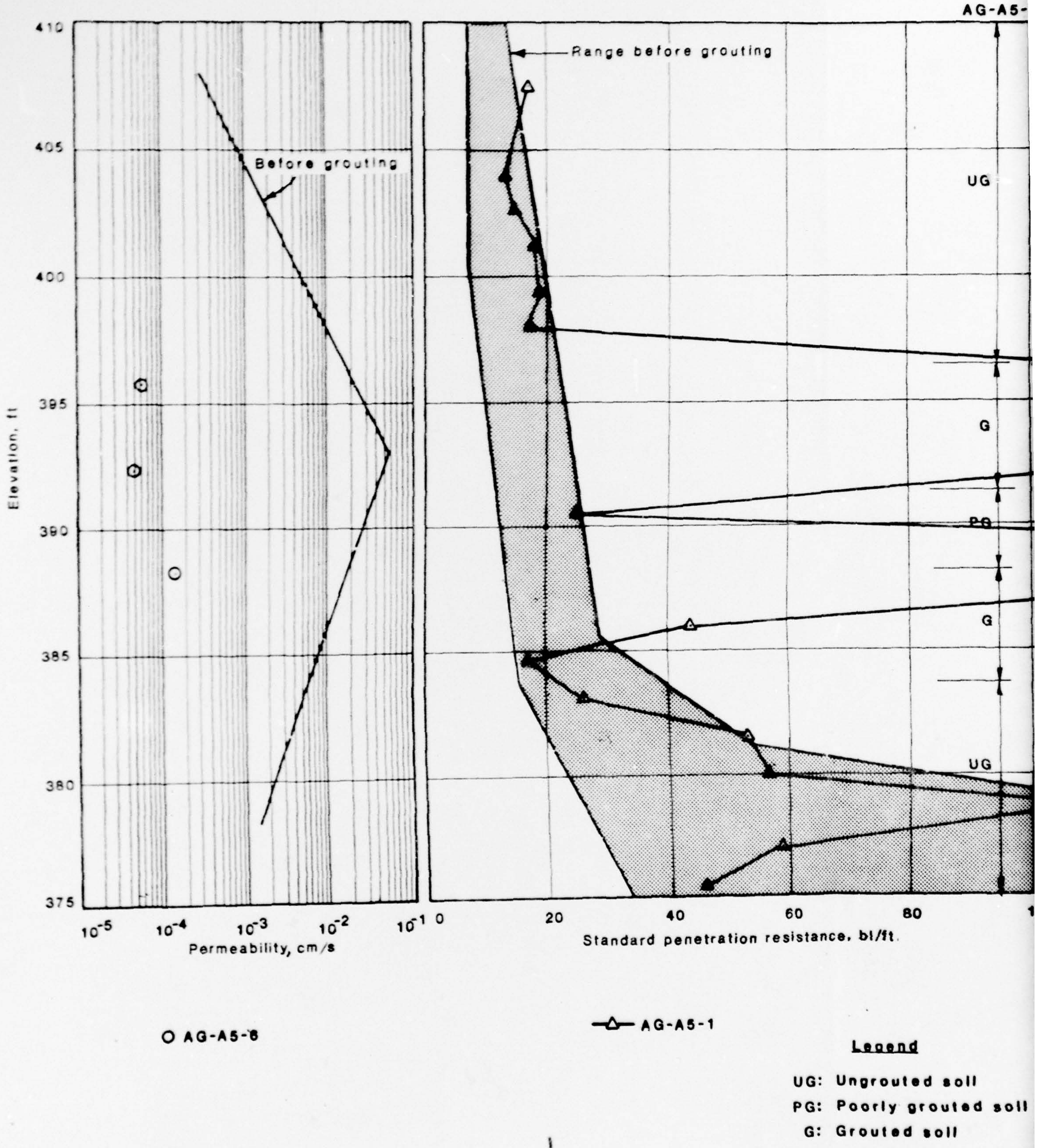

AG-A5-
Range before grouting
Before grouting
Elevation, ft
410
405
400
395
390
385
380
375
10^{-5}
10^{-4}
10^{-3}
10^{-2}
10^{-1}
Permeability, cm/s
0
20
40
60
80
Standard penetration resistance, bl/ft.
UG
G
PG
G
UG
O AG-A5-8
AG-A5-1
Legend
UG: Ungrouted soil
PG: Poorly grouted soil
G: Grouted soil

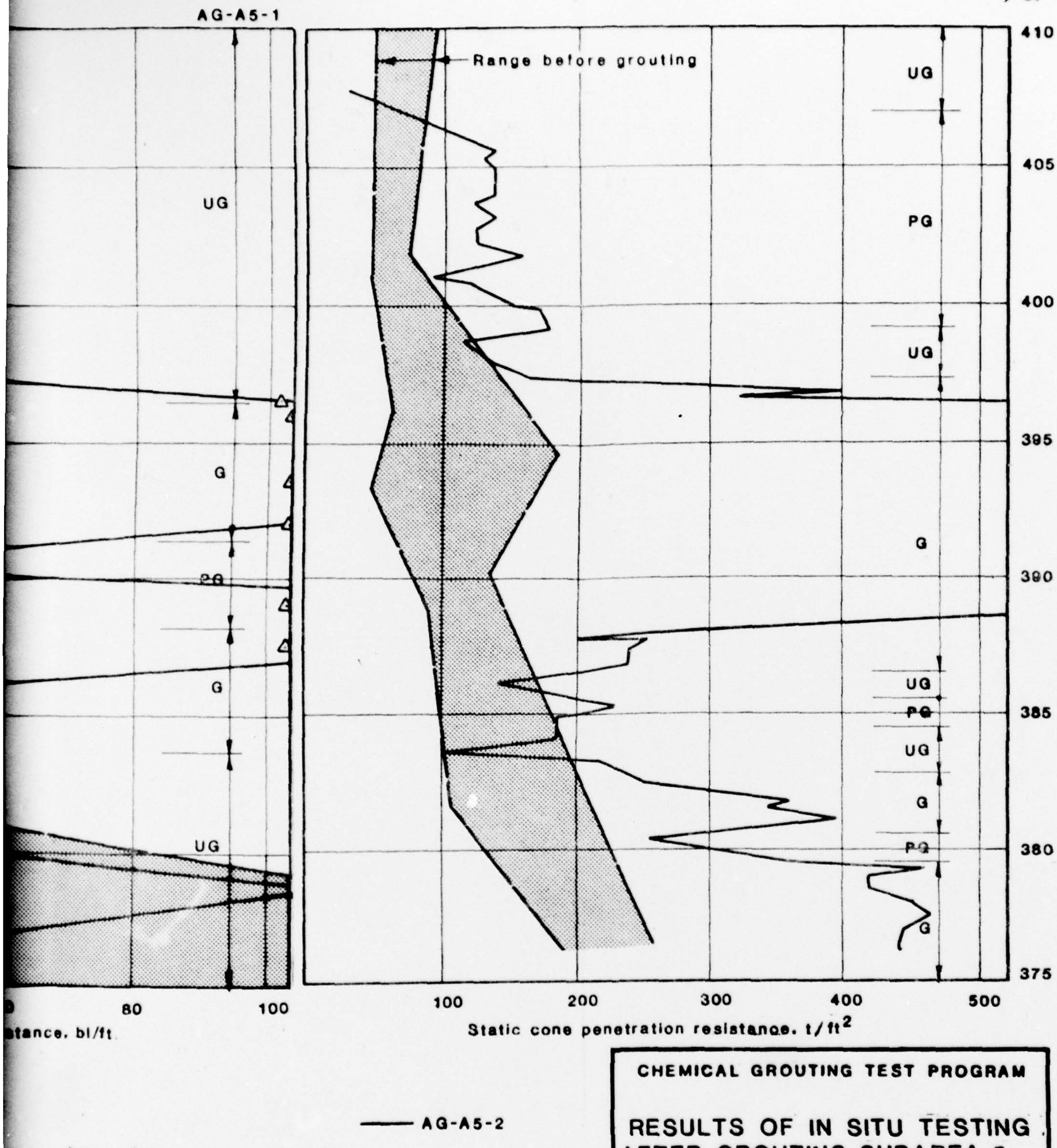

Legend

UG: Ungrouted soil

PG: Poorly grouted soil

G: Grouted soil

CHEMICAL GROUTING TEST PROGRAM

RESULTS OF IN SITU TESTING AFTER GROUTING SUBAREA 5

FOUNDATION INVESTIGATION AND TEST PROGRAM
EXISTING LOCKS AND DAM No. 26
ST. LOUIS DISTRICT, CORPS OF ENGINEERS.
DACW43-78-C-0006

Woodward-Clyde Consultants

Y7C825 Phase II

Fig. 9.6

2

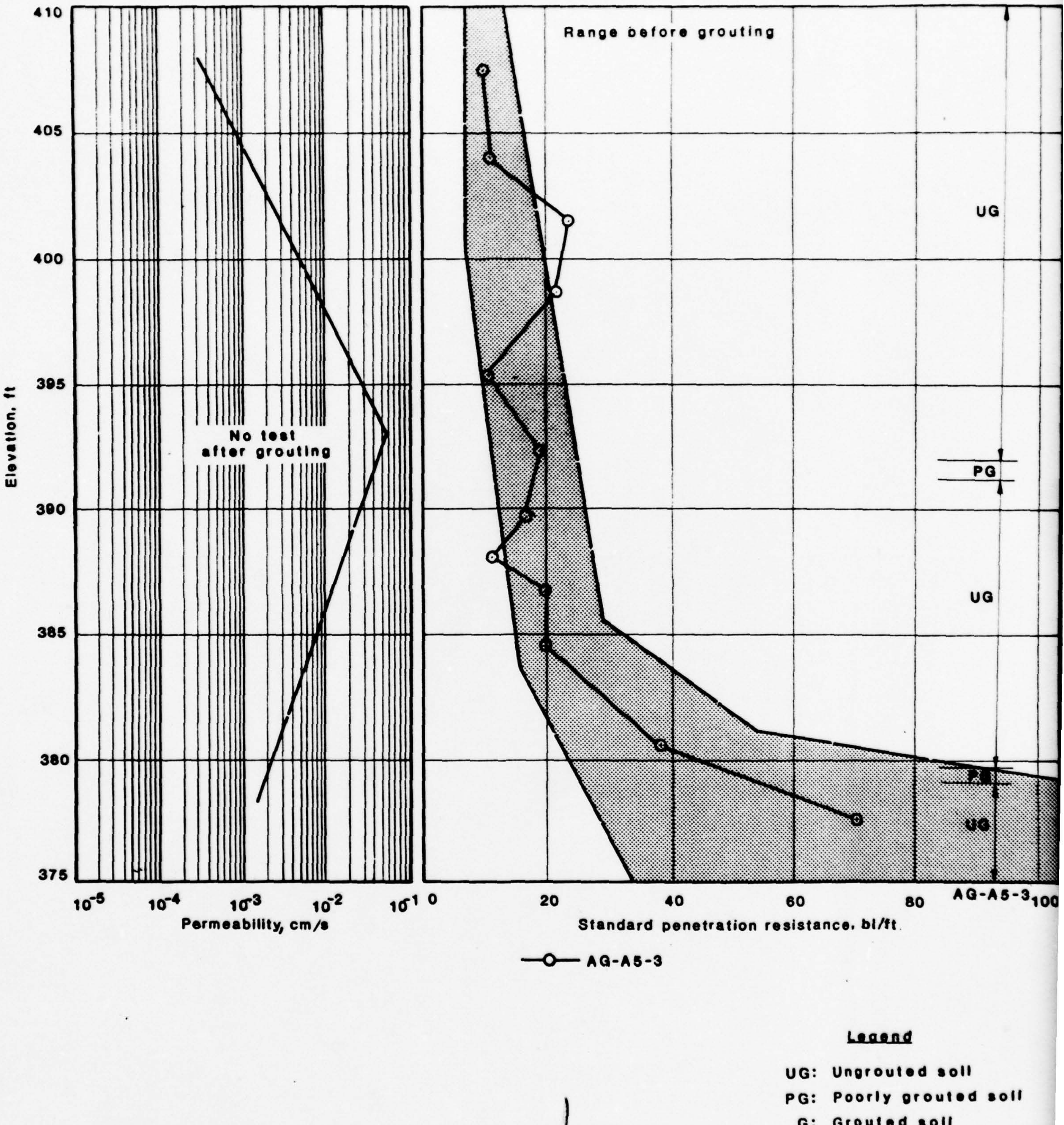

Range before grouting
No test
after grouting
Elevation, ft
410
405
400
395
390
385
380
375
10-5
10-4
10-3
10-2
10-1
Permeability, cm/s
0
20
40
60
80
100
Standard penetration resistance, bl/ft
UG
PG
UG
PG
UG
AG-A5-3
AG-A5-3
Legend
UG: Ungrouted soil
PG: Poorly grouted soil
G: Grouted soil

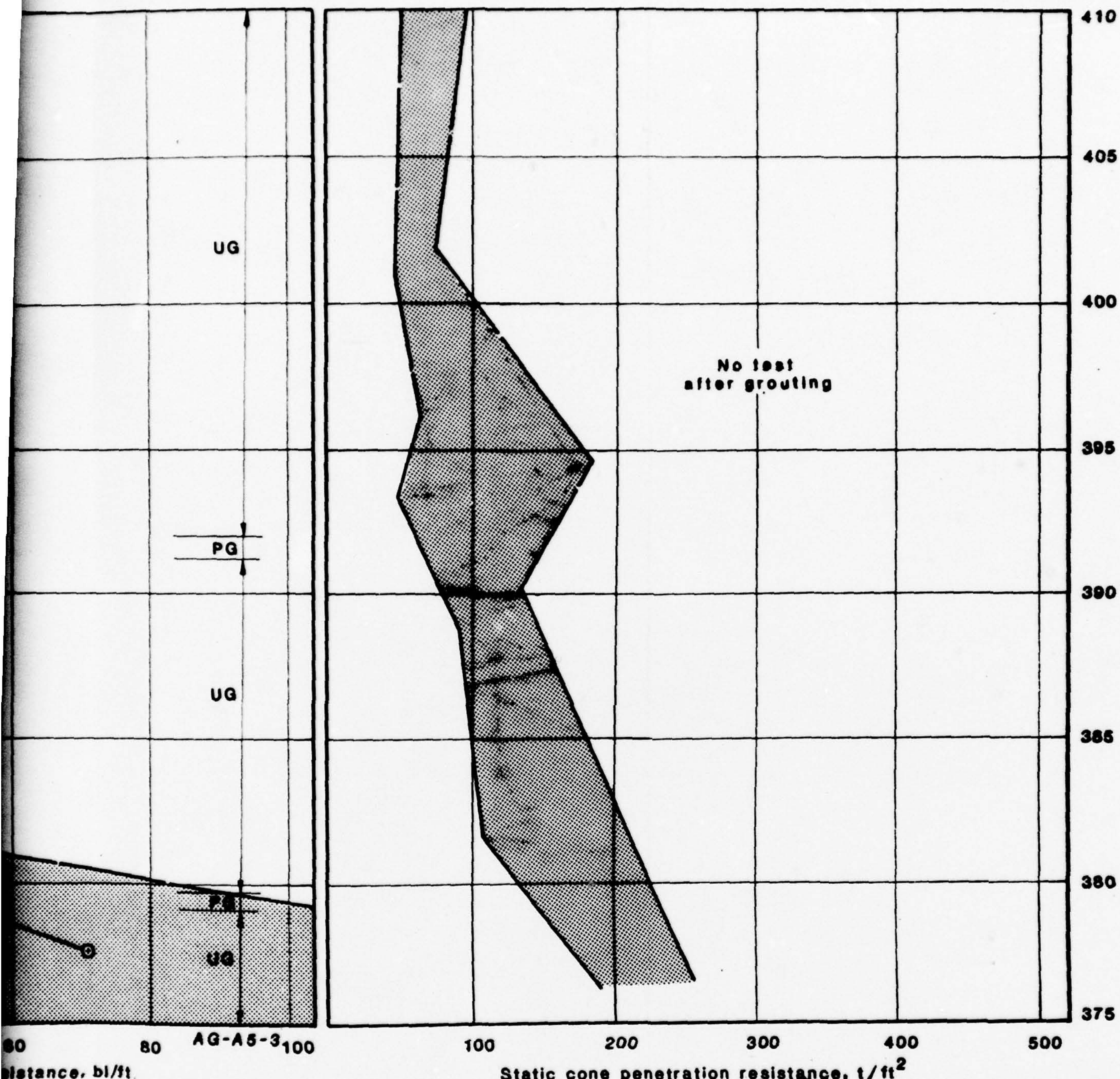

2

Legend

UG: Ungrouted soil
PG: Poorly grouted soil
G: Grouted soil

CHEMICAL GROUTING TEST PROGRAM

RESULTS OF IN SITU TESTING AFTER GROUTING SUBAREA 5a

FOUNDATION INVESTIGATION AND TEST PROGRAM
EXISTING LOCKS AND DAM No. 26
ST LOUIS DISTRICT, CORPS OF ENGINEERS.
DACW43-78-C-0005

Woodward-Clyde Consultants

Fig. 9.7

Y7C825 Phase IX

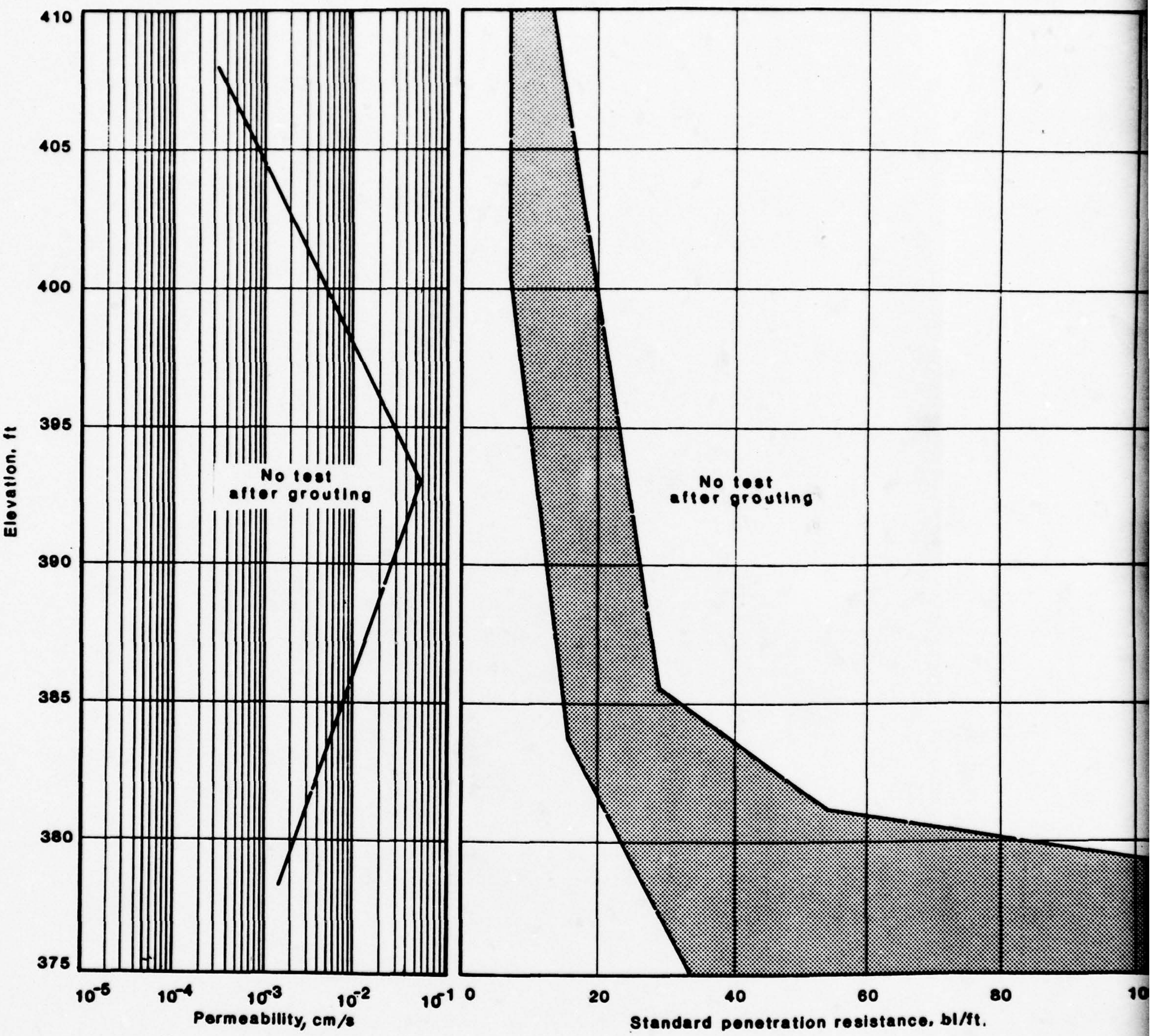

<u>Legend</u>

UG: Ungrouted soil

PG: Poorly grouted soil

G: Grouted soil

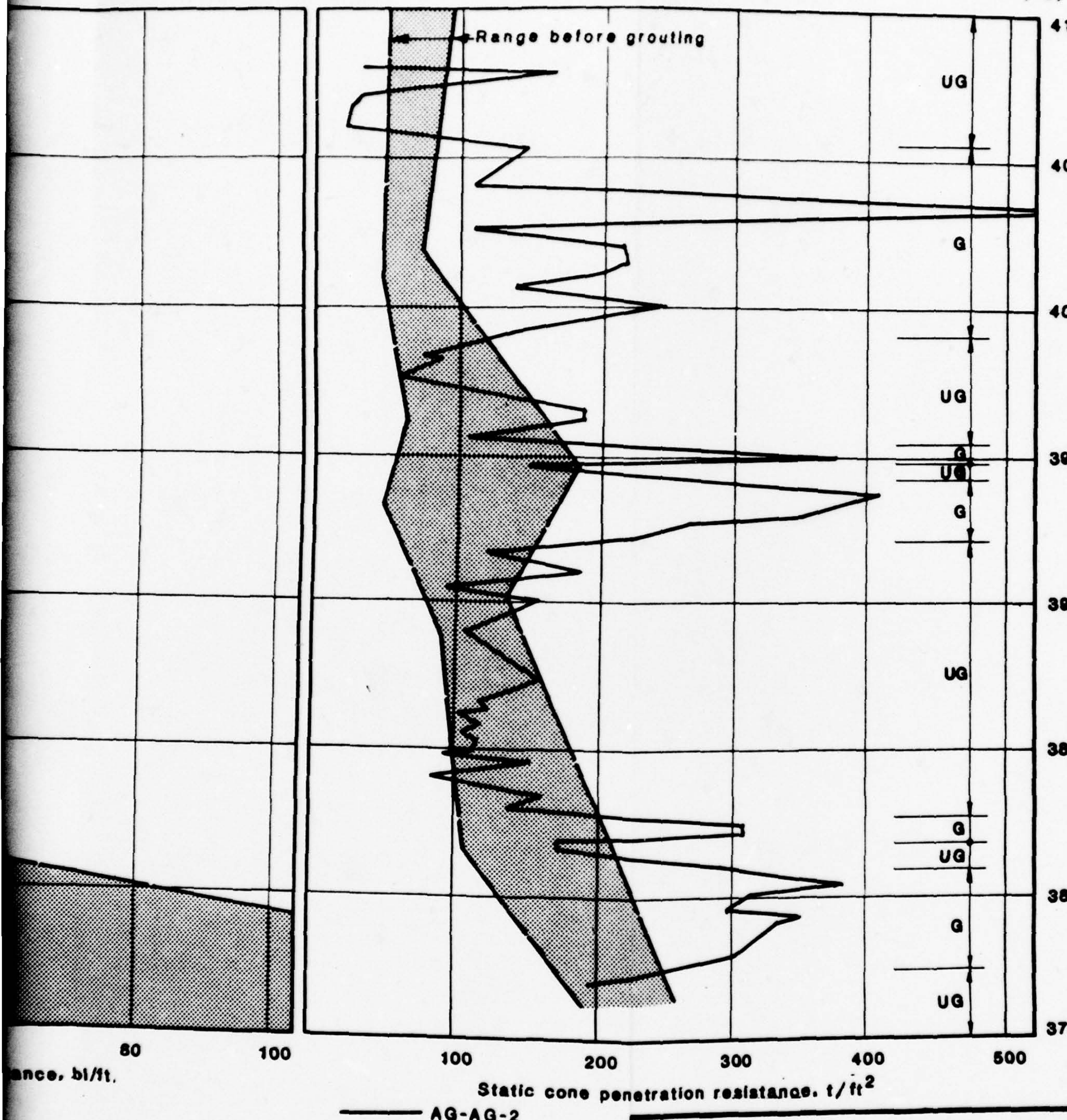

oil
ted soil
l

2

CHEMICAL GROUTING TEST PROGRAM

RESULTS OF IN SITU TESTING AFTER GROUTING SUBAREA 6

FOUNDATION INVESTIGATION AND TEST PROGRAM
EXISTING LOCKS AND DAM No. 26
ST LOUIS DISTRICT, CORPS OF ENGINEERS.
DACW43-78-C-0005

Woodward-Clyde Consultants

Fig. 9.8

Y7C825 Phase IX

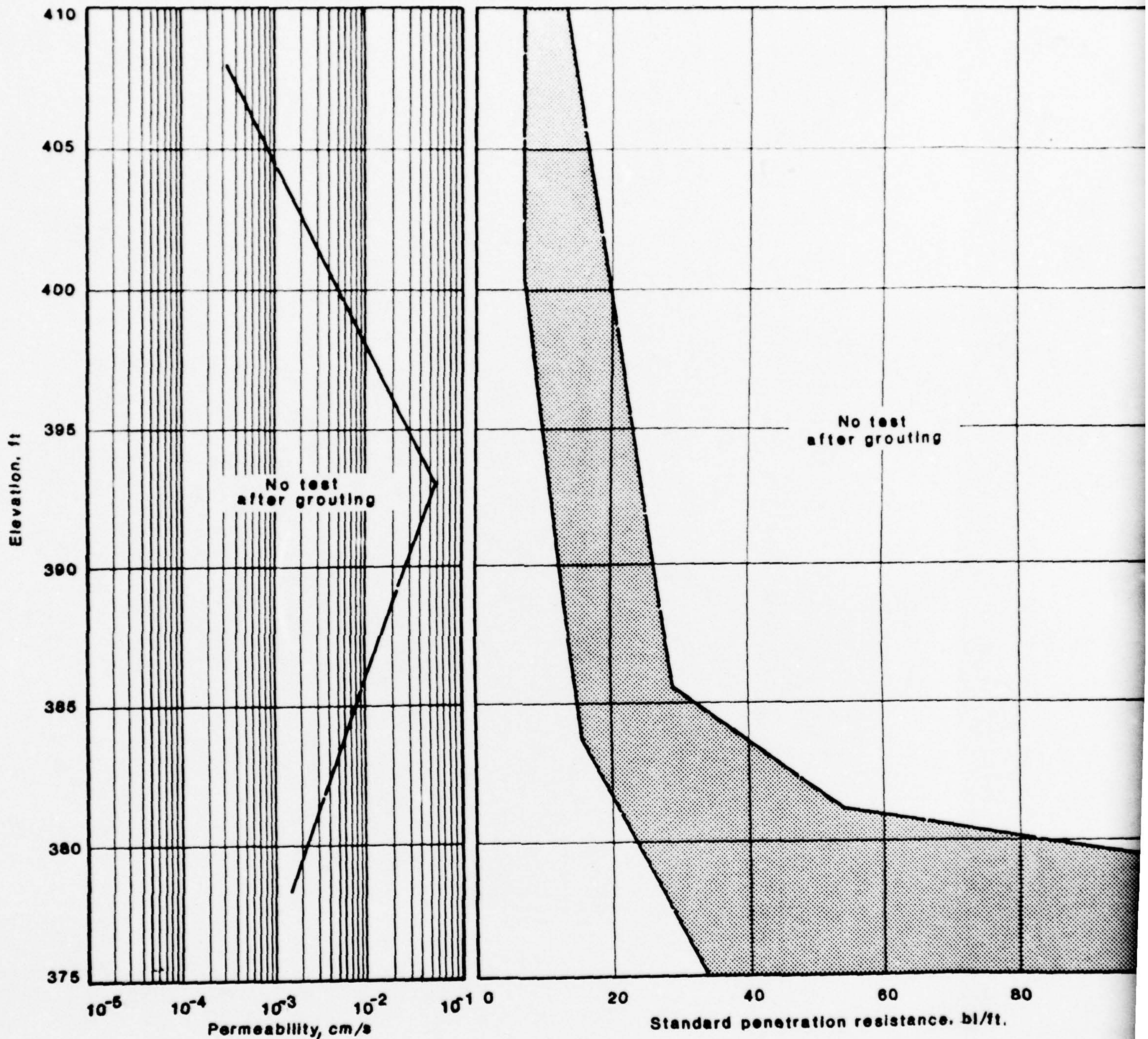

Legend

UG: Ungrouted soil
PG: Poorly grouted soil
G: Grouted soil

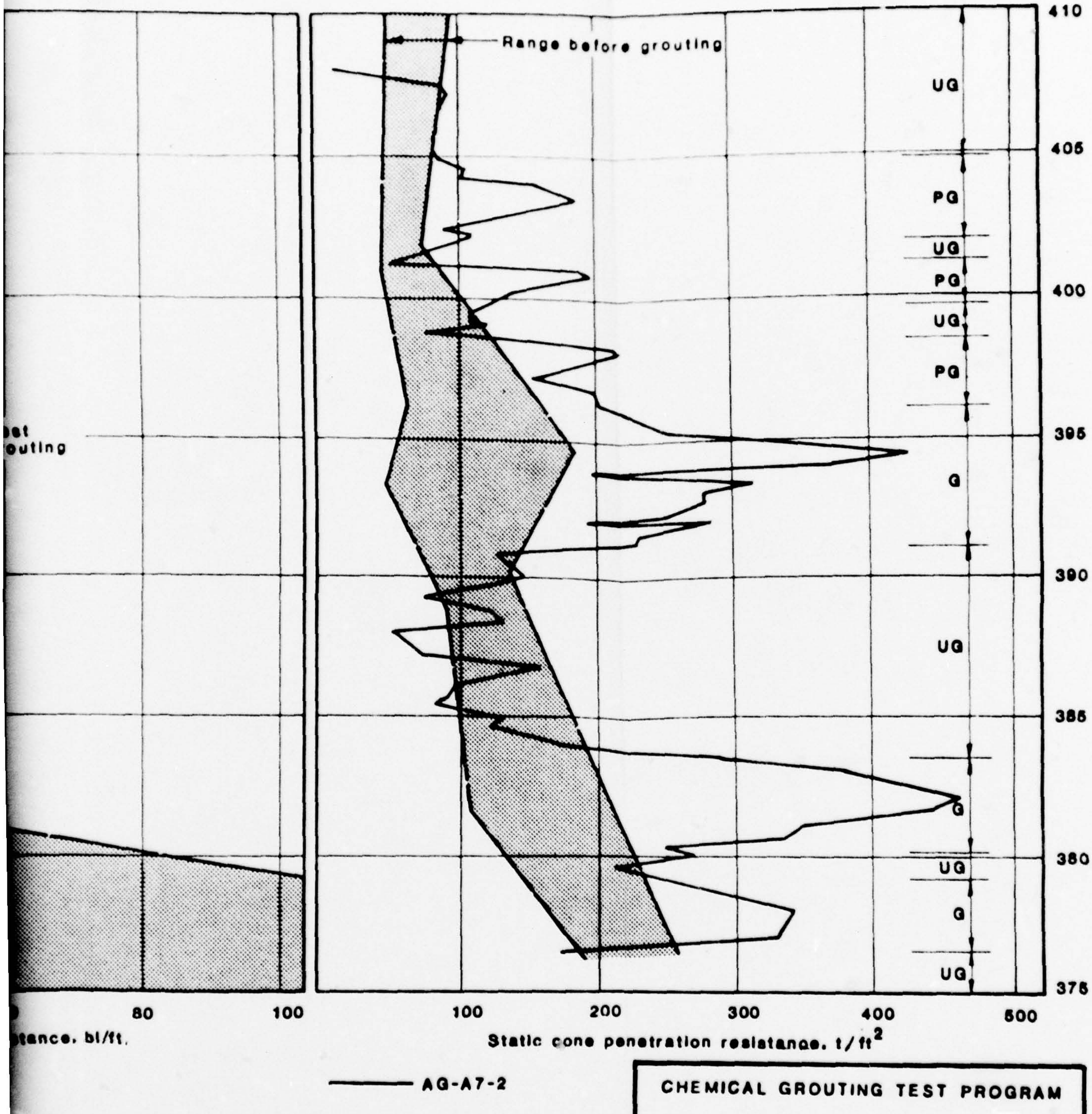

CHEMICAL GROUTING TEST PROGRAM

RESULTS OF IN SITU TESTING AFTER GROUTING SUBAREA 7

FOUNDATION INVESTIGATION AND TEST PROGRAM
EXISTING LOCKS AND DAM No. 26
ST LOUIS DISTRICT, CORPS OF ENGINEERS.
DACW43-78-C-0008

Woodward-Clyde Consultants

Y7C828 Phase IX

Fig. 9.9

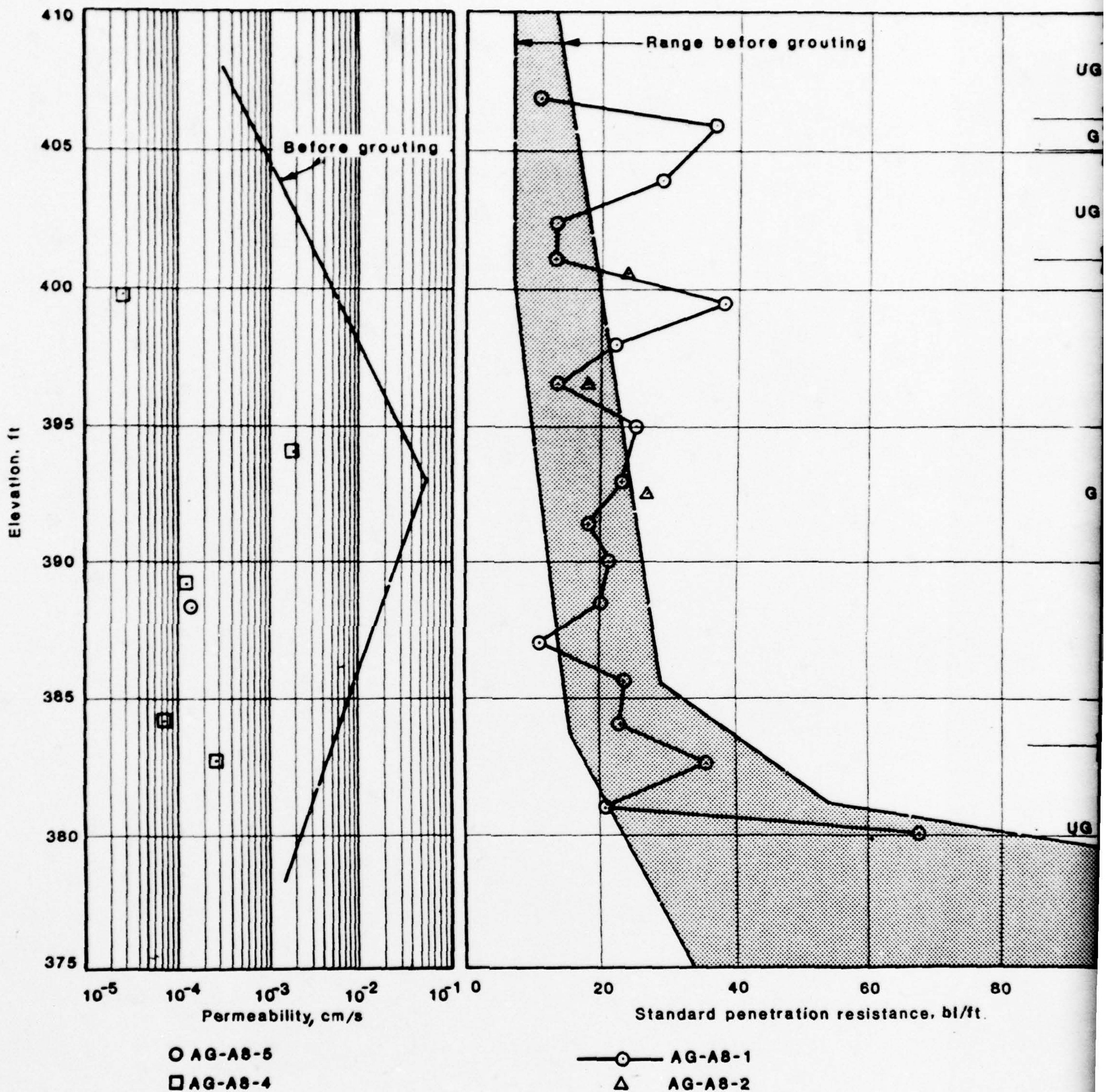

Legend

UG: Ungrouted soil
PG: Poorly grouted soil
G: Grouted soil

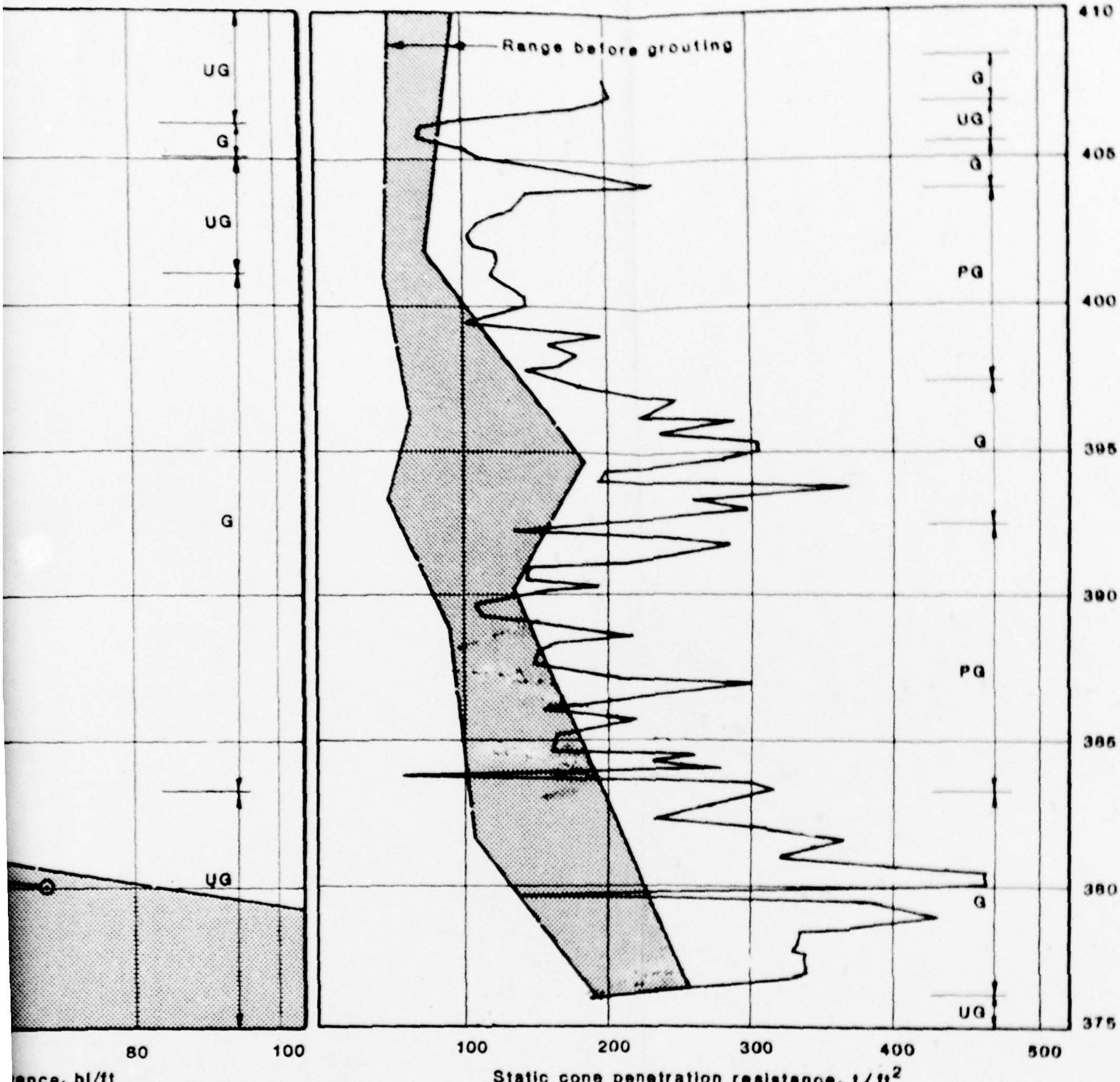

—— AG-A8-3

– – – – AG-A8-2

Legend

ngrouted soil

oorly grouted soil

routed soil

CHEMICAL GROUTING TEST PROGRAM

RESULTS OF IN SITU TESTING AFTER GROUTING SUBAREA 8

FOUNDATION INVESTIGATION AND TEST PROGRAM
EXISTING LOCKS AND DAM No. 26
ST. LOUIS DISTRICT, CORPS OF ENGINEERS
DACW43-78-C-0005

Woodward-Clyde Consultants

77C825 Phase IV

Fig. 9.10

2

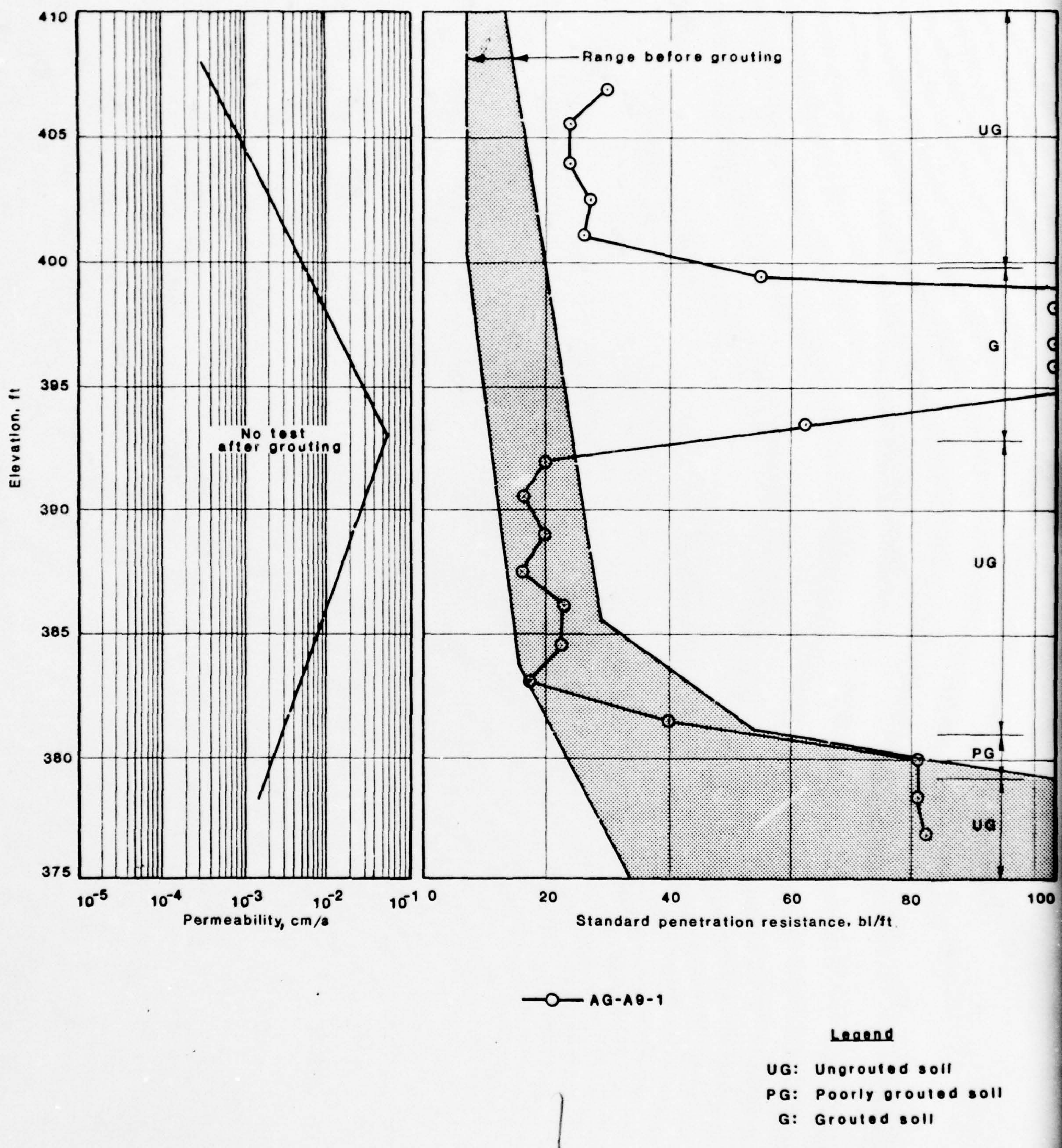

Range before grouting
No test after grouting
Elevation, ft
410
405
400
395
390
385
380
375
10^{-5}
10^{-4}
10^{-3}
10^{-2}
10^{-1}
Permeability, cm/s
0
20
40
60
80
100
Standard penetration resistance, bl/ft
UG
G
UG
PG
UG
AG-A9-1
Legend
UG: Ungrouted soil
PG: Poorly grouted soil
G: Grouted soil

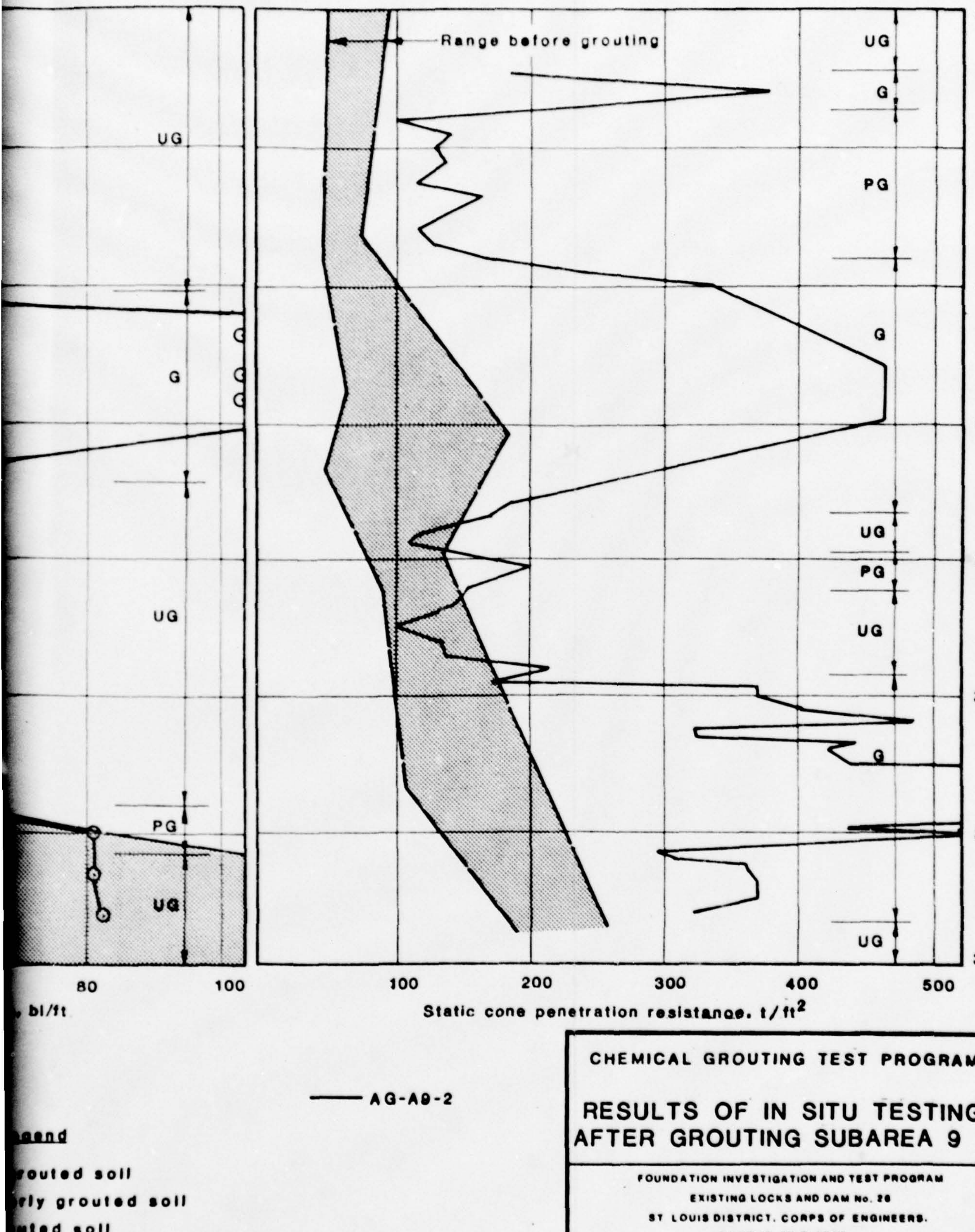

CHEMICAL GROUTING TEST PROGRAM

RESULTS OF IN SITU TESTING AFTER GROUTING SUBAREA 9

FOUNDATION INVESTIGATION AND TEST PROGRAM
EXISTING LOCKS AND DAM No. 26
ST LOUIS DISTRICT, CORPS OF ENGINEERS.
DACW43-78-C-0005

Woodward-Clyde Consultants

Y7C825 Phase IX

Fig. 9.11

G: Grouted soil

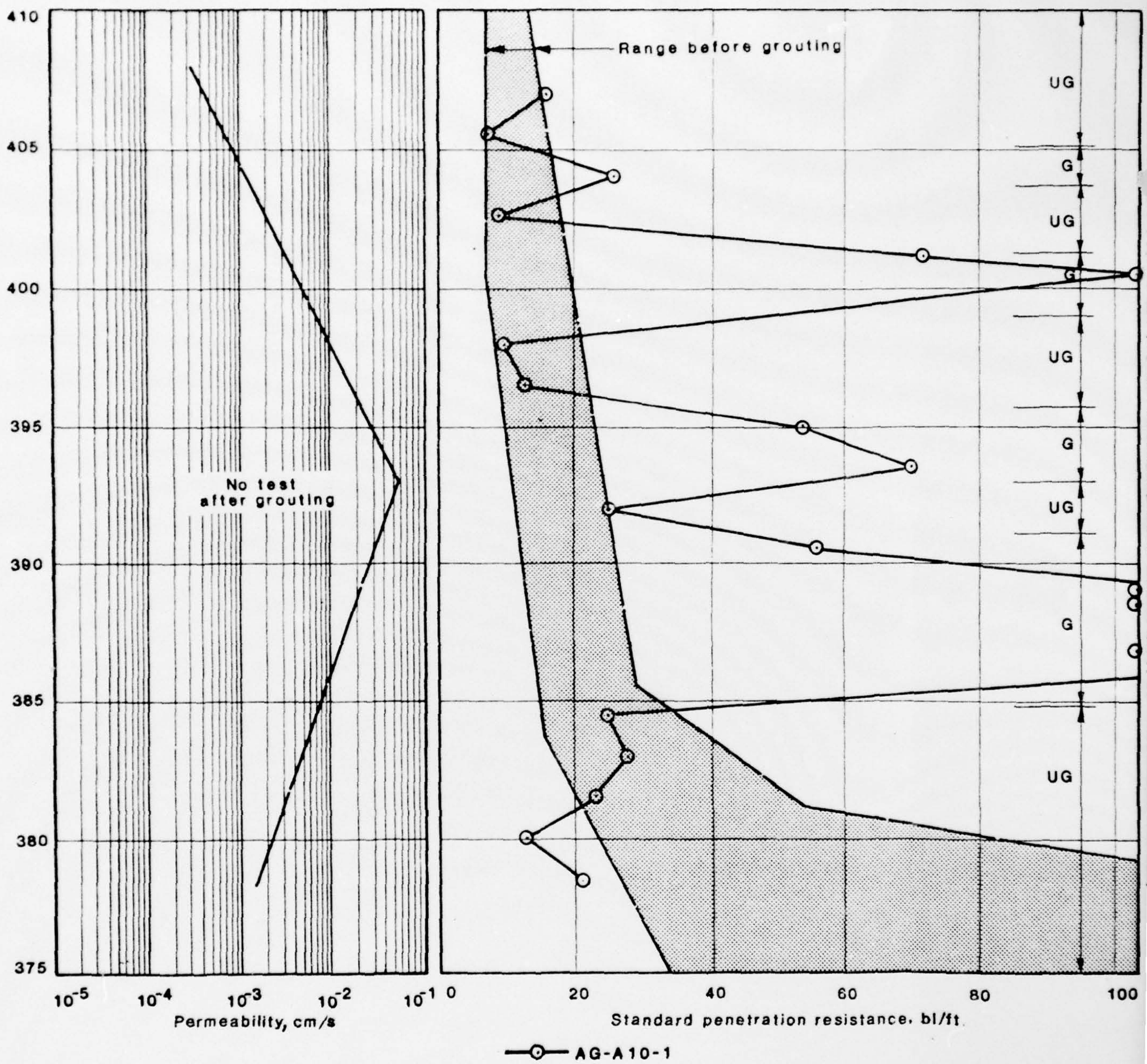

Legend

UG: Ungrouted soil

PG: Poorly grouted soil

G: Grouted soil

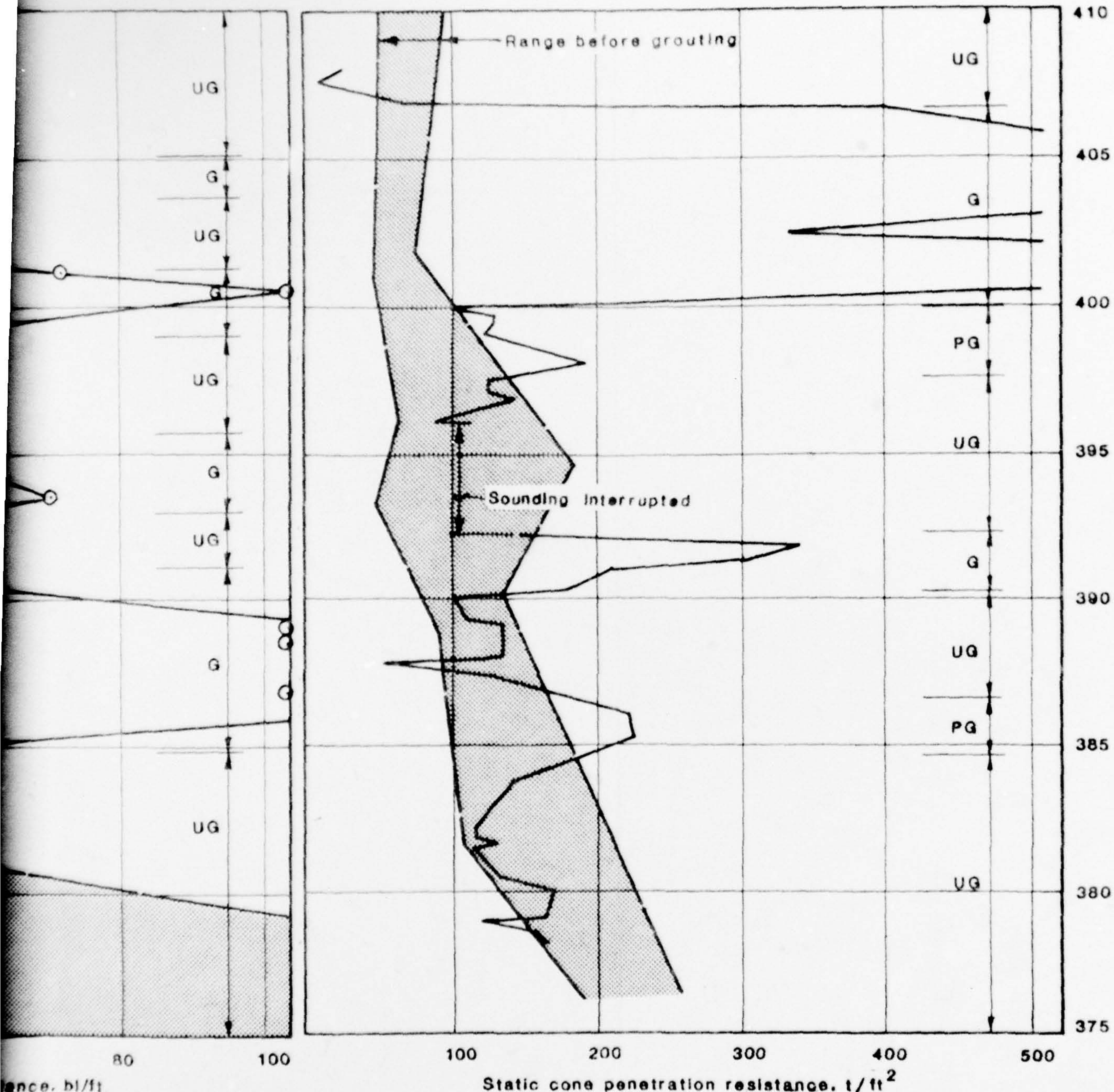

2

Legend

UG: Ungrouted soil
PG: Poorly grouted soil
G: Grouted soil

CHEMICAL GROUTING TEST PROGRAM

RESULTS OF IN SITU TESTING AFTER GROUTING SUBAREA 10

FOUNDATION INVESTIGATION AND TEST PROGRAM
EXISTING LOCKS AND DAM No. 26
ST LOUIS DISTRICT, CORPS OF ENGINEERS.
DACW43-78-C-0005

Woodward-Clyde Consultants

Y7C825 Phase III

Fig. 9.12

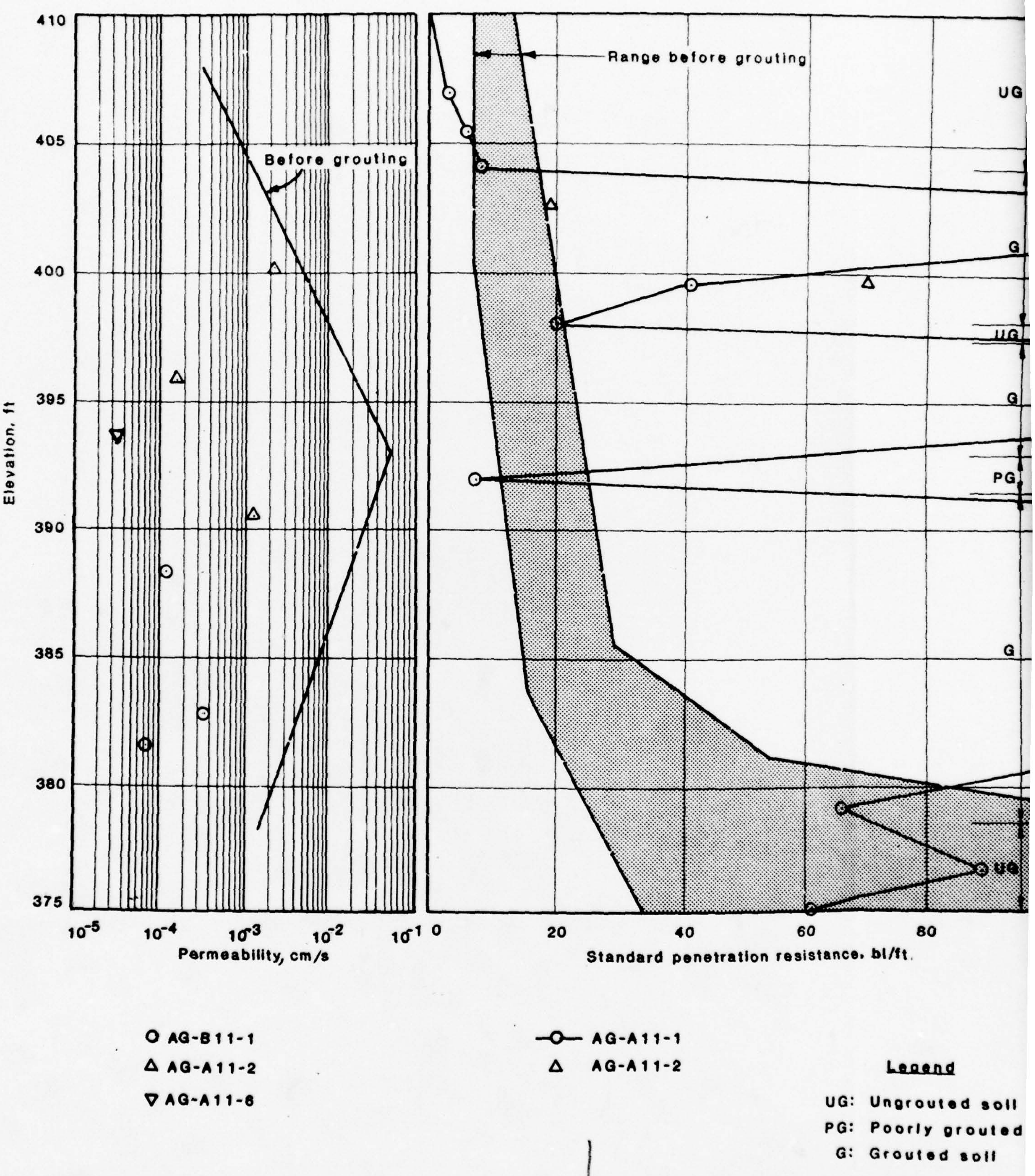

Elevation, ft
410
405
400
395
390
385
380
375
Before grouting
10^{-5}
10^{-4}
10^{-3}
10^{-2}
10^{-1}
Permeability, cm/s
Range before grouting
UG
G
UG
G
PG
G
UG
0
20
40
60
80
Standard penetration resistance, bl/ft.
O AG-B11-1
Δ AG-A11-2
∇ AG-A11-6
—O— AG-A11-1
Δ AG-A11-2
Legend
UG: Ungrouted soil
PG: Poorly grouted
G: Grouted soil

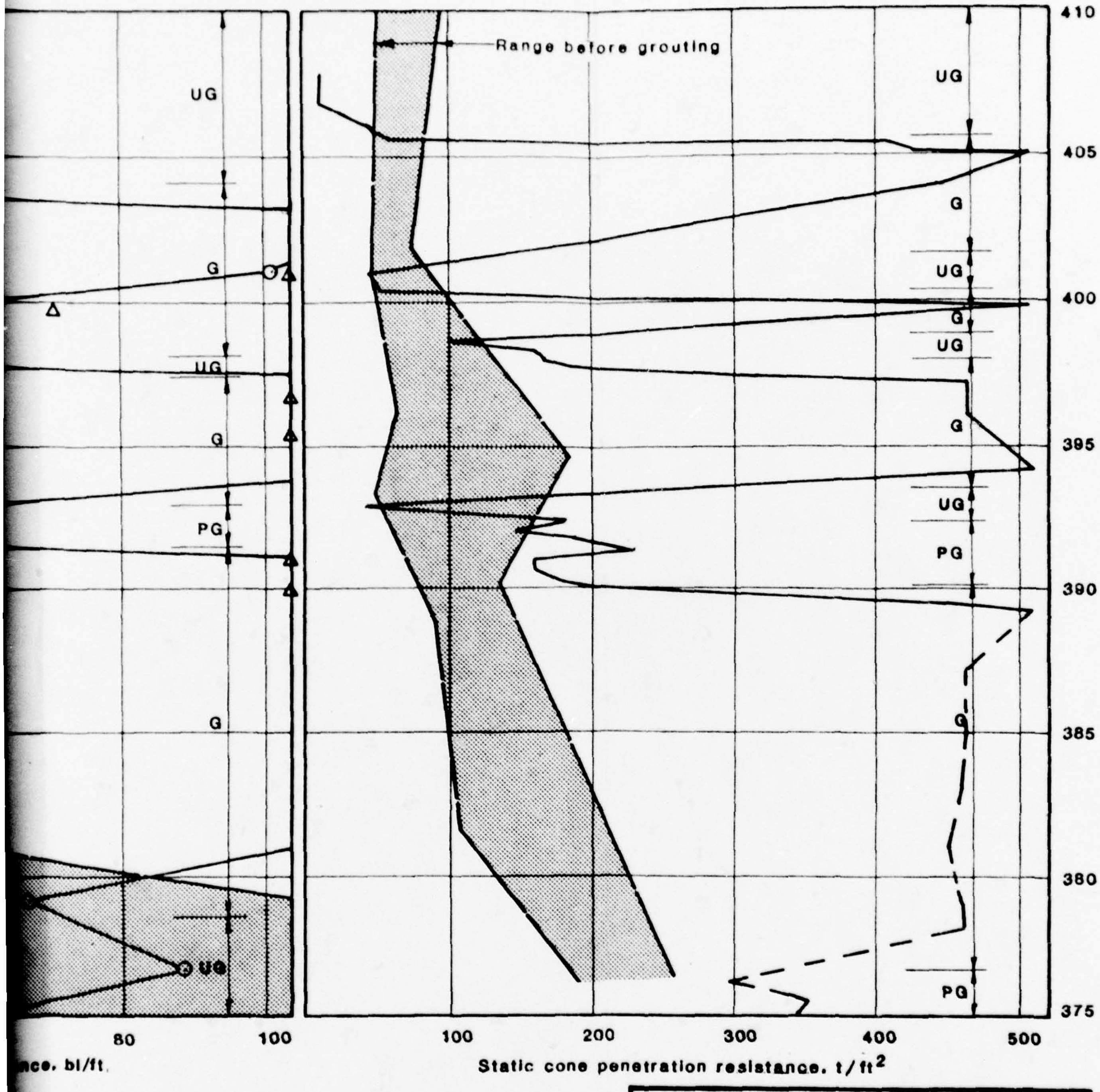

Legend

UG: Ungrouted soil
PG: Poorly grouted soil
G: Grouted soil

CHEMICAL GROUTING TEST PROGRAM

RESULTS OF IN SITU TESTING AFTER GROUTING SUBAREA 11

FOUNDATION INVESTIGATION AND TEST PROGRAM
EXISTING LOCKS AND DAM No. 26
ST LOUIS DISTRICT, CORPS OF ENGINEERS.
DACW43-78-C-0005

Woodward-Clyde Consultants

Y7C625 Phase IX

Fig. 9.13

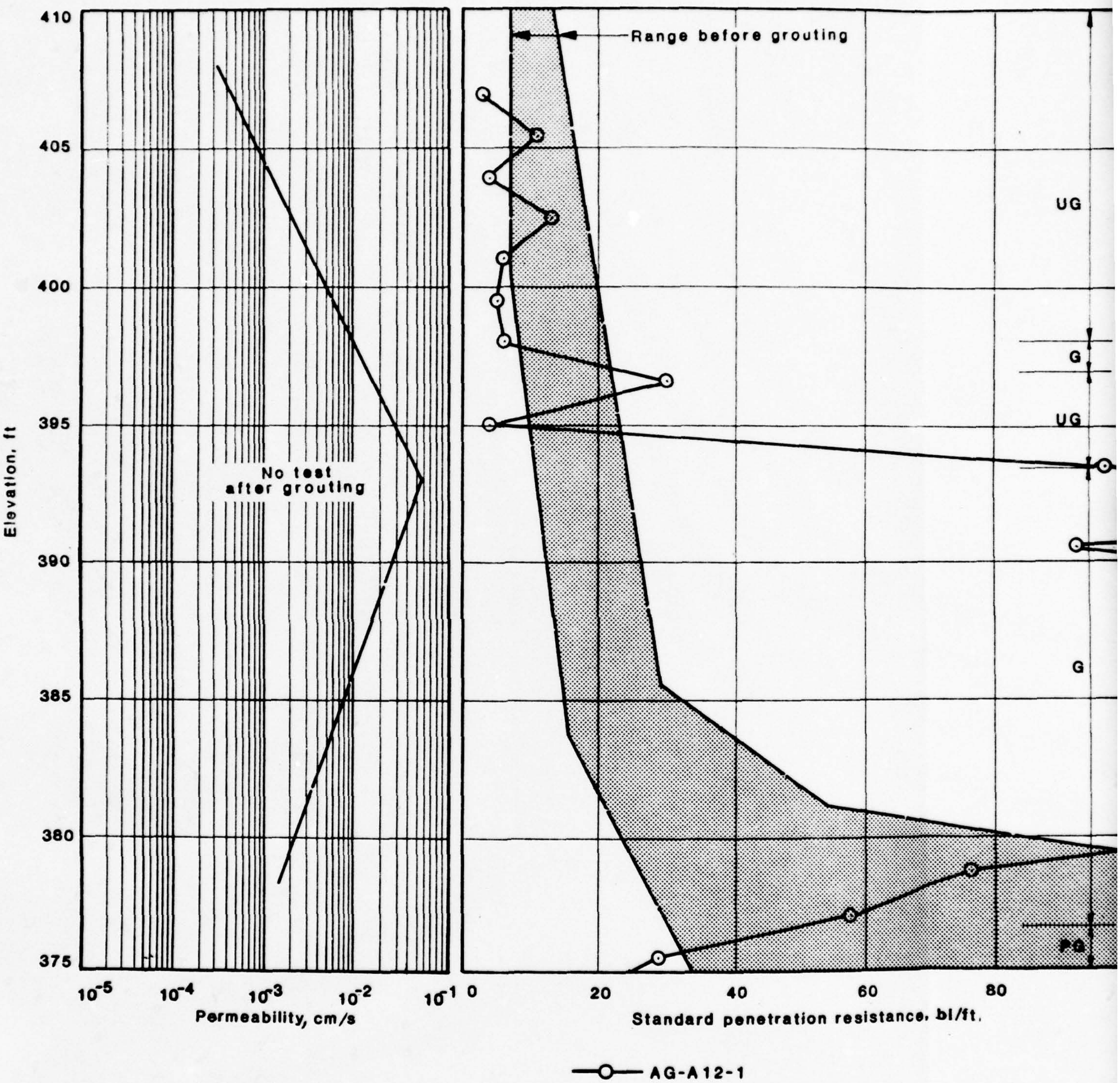

<u>Legend</u>

UG: Ungrouted soil

PG: Poorly grouted soil

G: Grouted soil

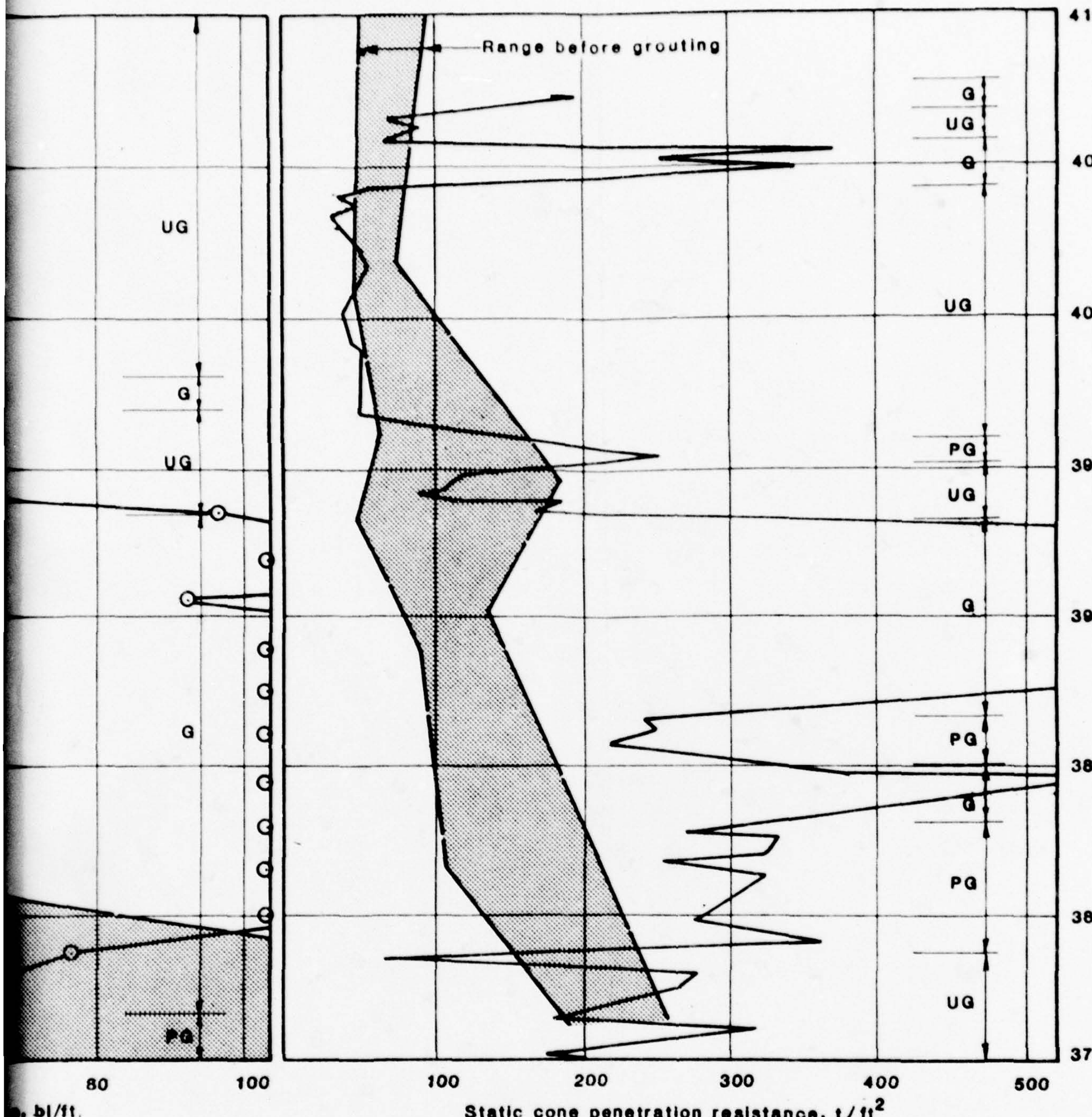

2

CHEMICAL GROUTING TEST PROGRAM

RESULTS OF IN SITU TESTING AFTER GROUTING SUBAREA 12

FOUNDATION INVESTIGATION AND TEST PROGRAM
EXISTING LOCKS AND DAM No. 26
ST LOUIS DISTRICT, CORPS OF ENGINEERS.
DACW43-78-C-0006

Woodward-Clyde Consultants

Y7C825 Phase IX

Fig. 9.14

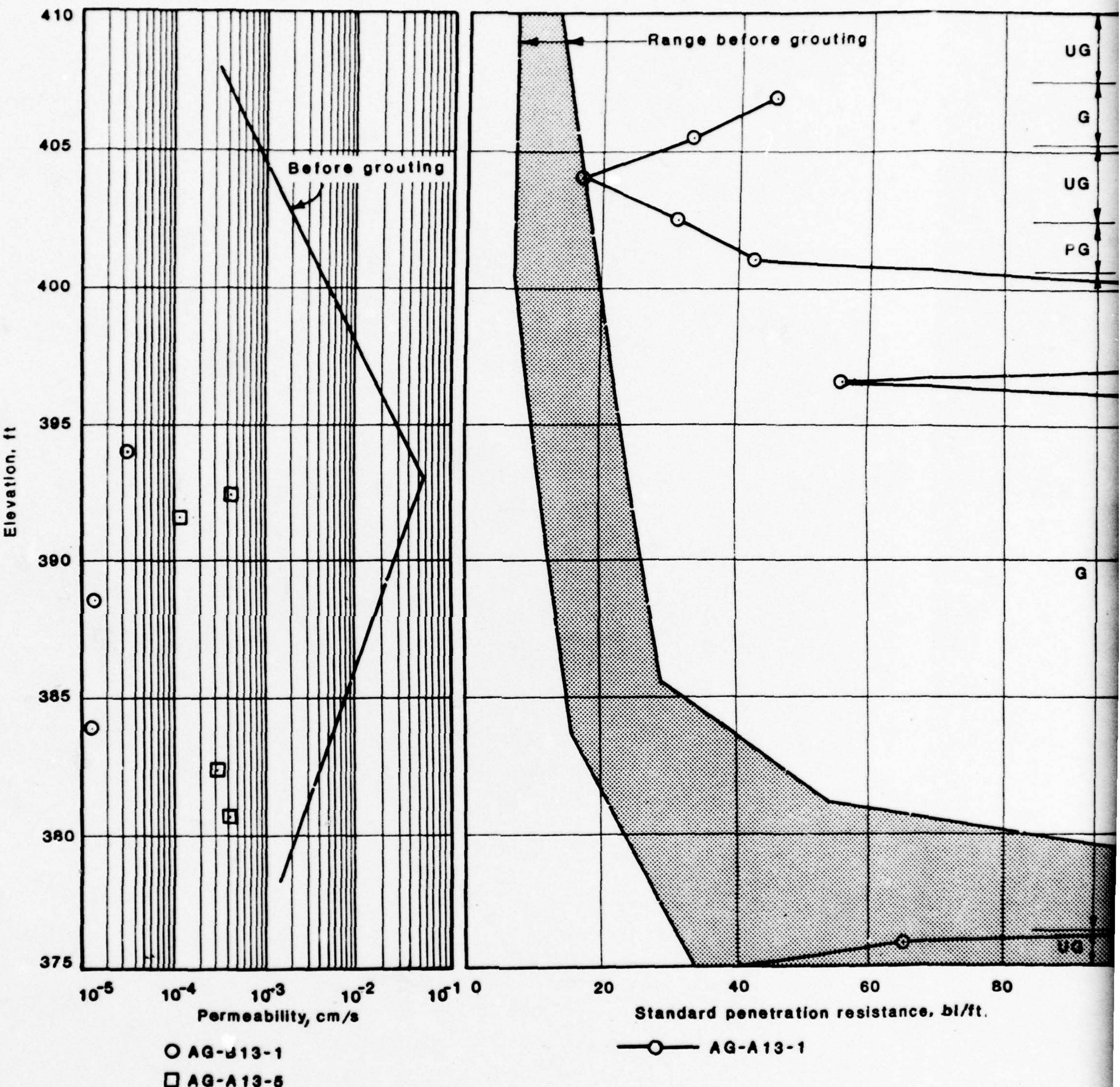

<u>Legend</u>

UG: Ungrouted soil

PG: Poorly grouted

G: Grouted soil

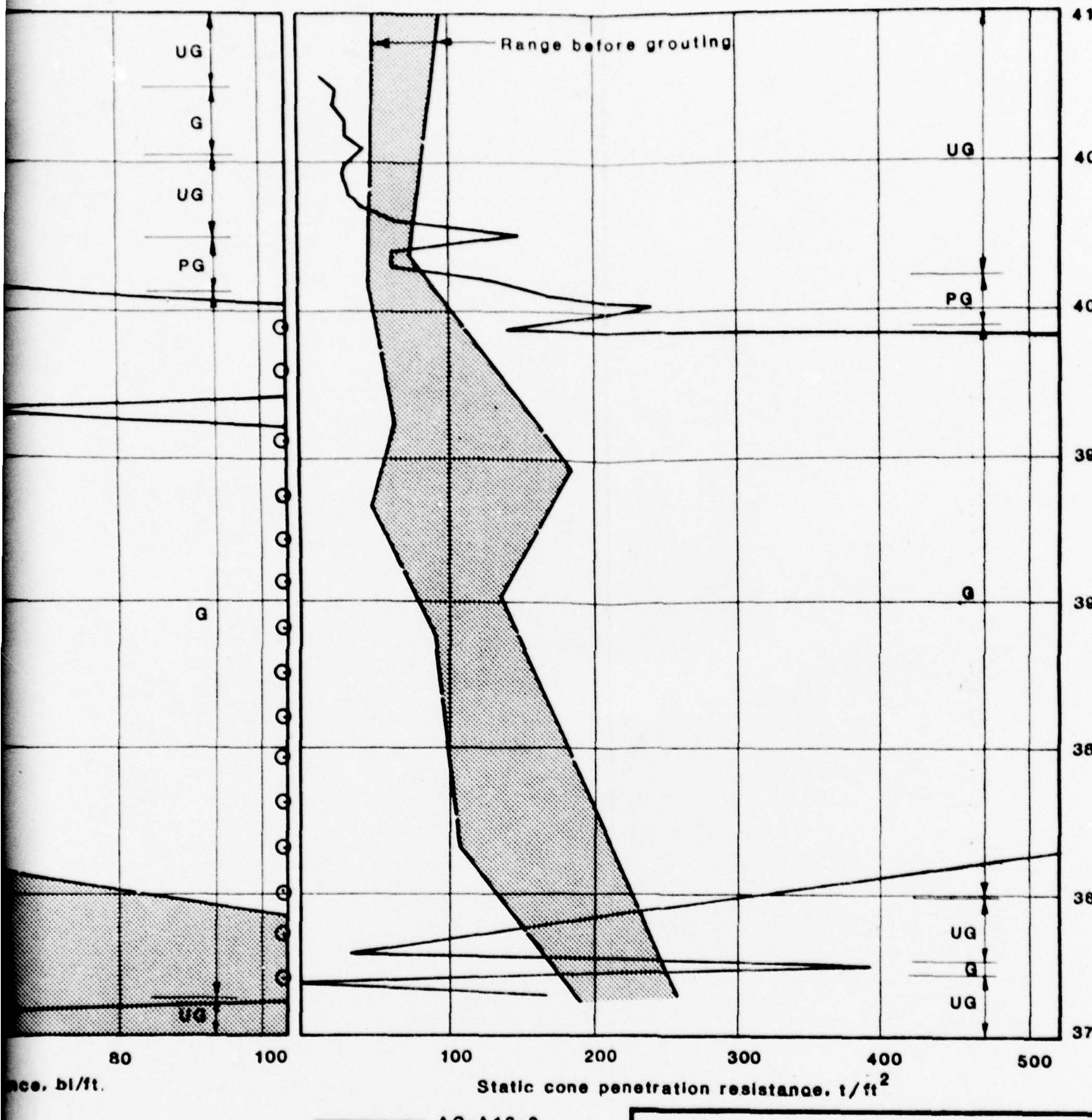

Legend

UG: Ungrouted soil

PG: Poorly grouted soil

G: Grouted soil

CHEMICAL GROUTING TEST PROGRAM

RESULTS OF IN SITU TESTING AFTER GROUTING SUBAREA 13

FOUNDATION INVESTIGATION AND TEST PROGRAM
EXISTING LOCKS AND DAM No. 26
ST LOUIS DISTRICT, CORPS OF ENGINEERS.
DACW43-78-C-0008

Woodward-Clyde Consultants

Y7C825 Phase IX

Fig. 9.15

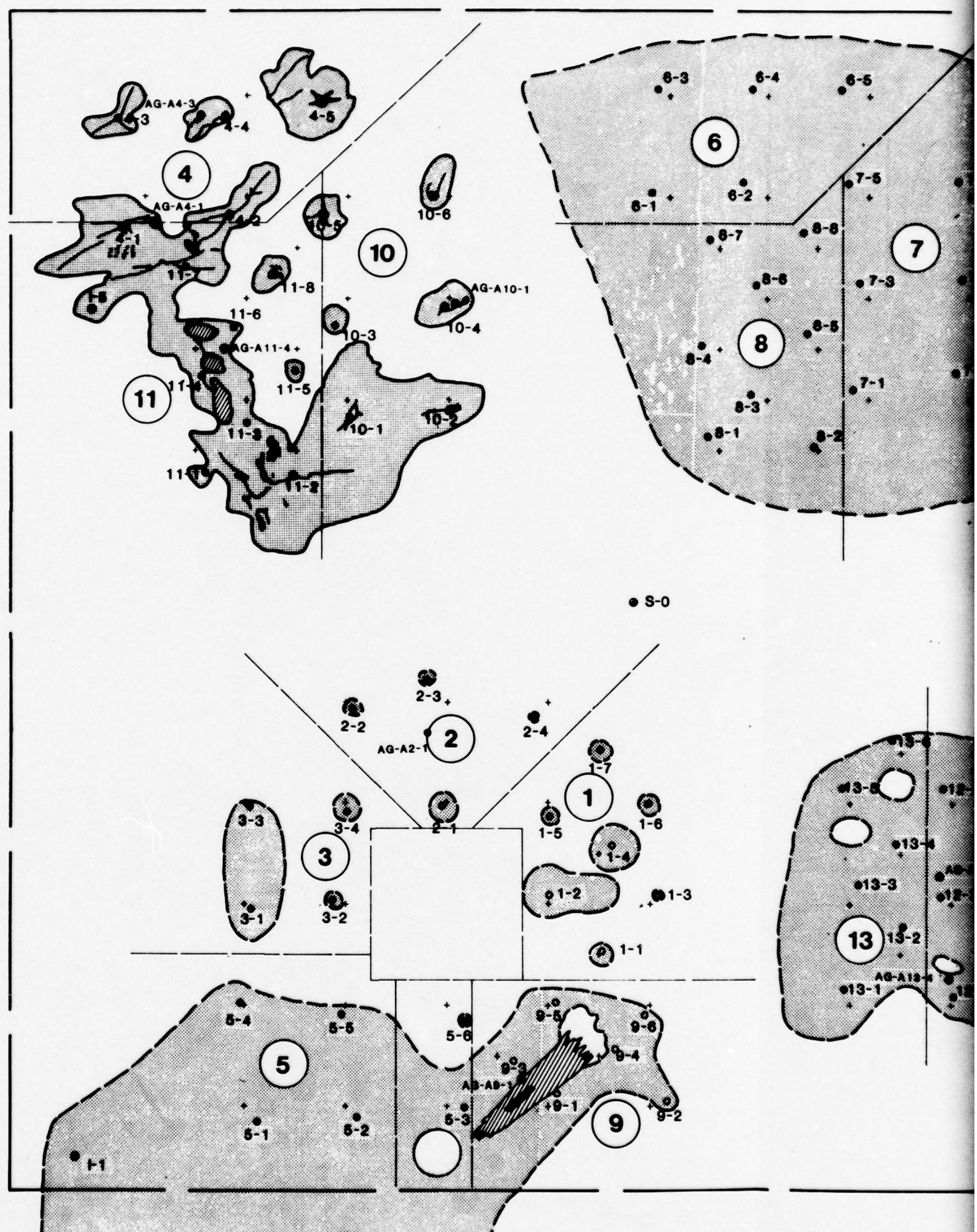

AG-A4-3
4-3
4-4
4-5
4
AG-A4-1
4-1
4-2
10-5
10-6
10
AG-A10-1
10-4
10-3
11-8
11-6
11-5
AG-A11-4
11
11-3
10-1
10-2
11-2
6-3
6-4
6-5
6
6-1
6-2
7-5
7
8-7
8-6
7-3
8
8-4
8-5
7-1
8-3
8-1
8-2
S-0
2-3
2-2
2-4
AG-A2-1
2
1-7
1
3-3
3-4
2-1
1-5
1-6
3
1-4
1-2
1-3
3-1
3-2
1-1
13-5
13-4
13-3
13
13-2
13-1
5-4
5-5
5-6
9-5
9-6
5
9-4
9-3
9-1
5-3
5-1
5-2
9
9-2

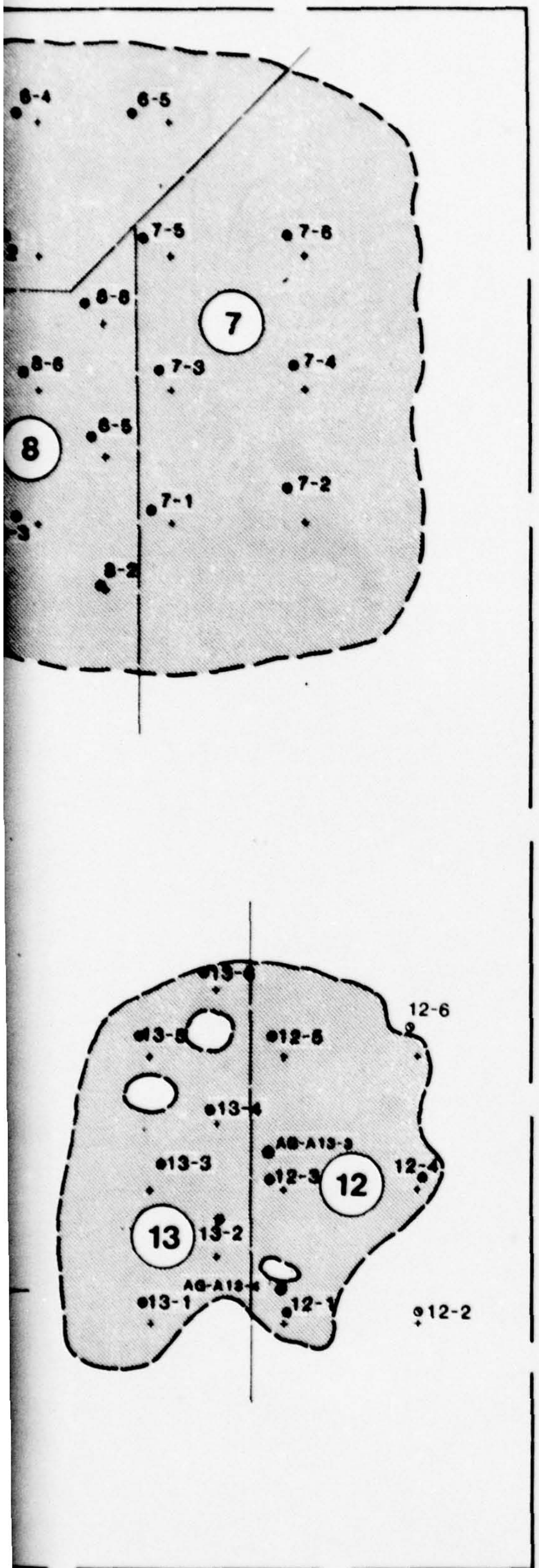

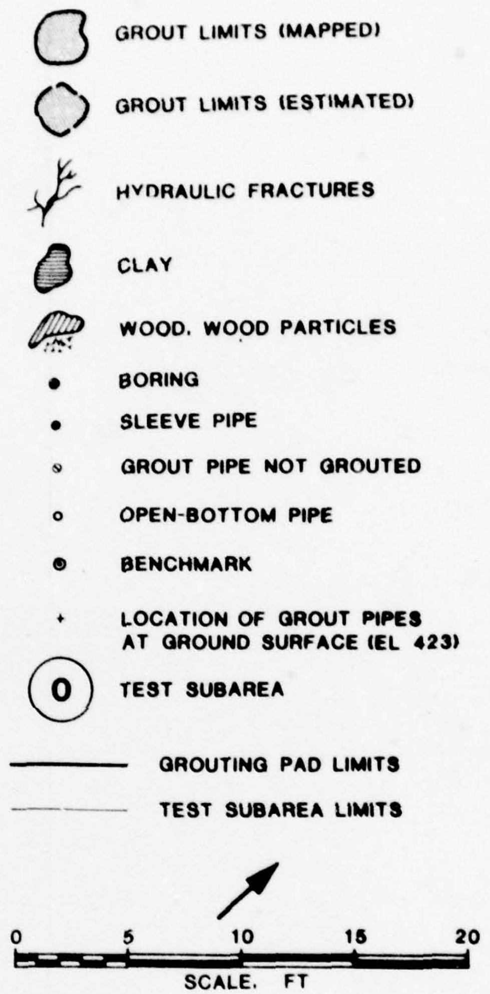

2

CHEMICAL GROUTING TEST PROGRAM

HORIZONTAL SECTION THROUGH TEST AREA AT EL 398

FOUNDATION INVESTIGATION AND TEST PROGRAM
EXISTING LOCKS AND DAM No. 26
ST LOUIS DISTRICT, CORPS OF ENGINEERS
DACW43-78-C-0008

Woodward-Clyde Consultants
Y7C825 Phase IX

Fig. 9.16

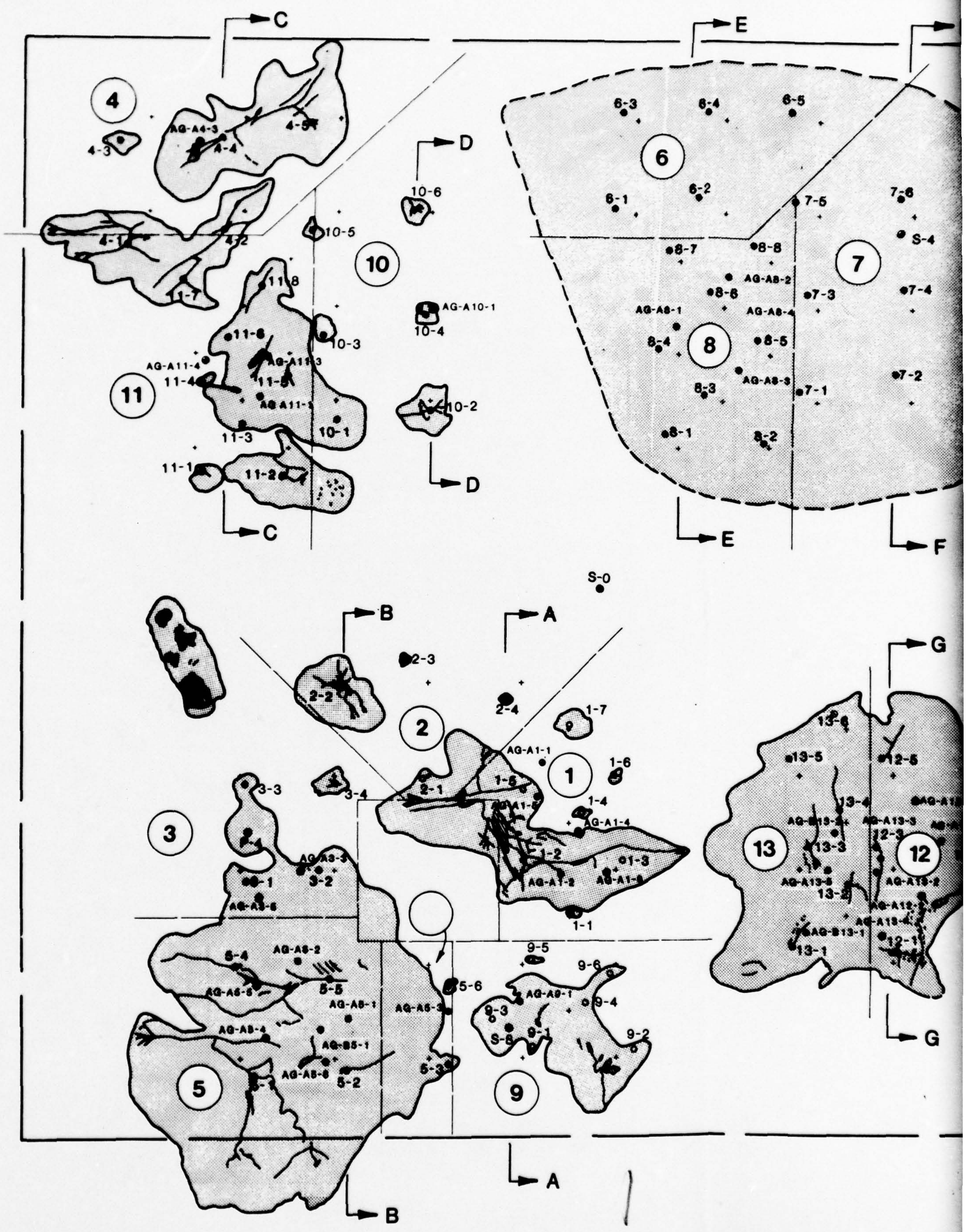

C
E
D
4
4-3
AG-A4-3
4-4
4-5
4-1
4-2
1-7
10-6
10-5
10
11-8
AG-A10-1
10-4
10-3
11-6
AG-A11-4
AG-A11-3
11-4
11-5
11
AG-A11-1
10-2
11-3
10-1
11-1
11-2
6-3
6-4
6-5
6
6-1
6-2
7-5
7-6
S-4
8-7
8-8
7
AG-A8-2
8-6
7-3
AG-A8-1
AG-A8-4
7-4
8-4
8
8-5
AG-A8-3
8-3
7-1
7-2
8-1
8-2
F
S-0
B
A
2-3
G
2-2
2-4
1-7
2
AG-A1-1
1
1-6
3-3
2-1
1-5
3-4
1-4
AG-A1-4
3
AG-A3-3
1-2
1-3
3-2
AG-A1-2
AG-A1-3
3-1
AG-A3-5
1-1
13-6
13-5
12-5
13-4
13
12
AG-A13-3
13-3
12-3
AG-A13-5
AG-A13-2
13-2
AG-B13-1
13-1
12-1
9-5
5-4
AG-A5-2
9-6
5-5
5-6
AG-A5-5
AG-A9-1
AG-A5-1
9-4
AG-A5-3
9-3
AG-A5-4
S-5
9-1
9-2
AG-B5-1
AG-A5-6
5-2
5-3
5
9

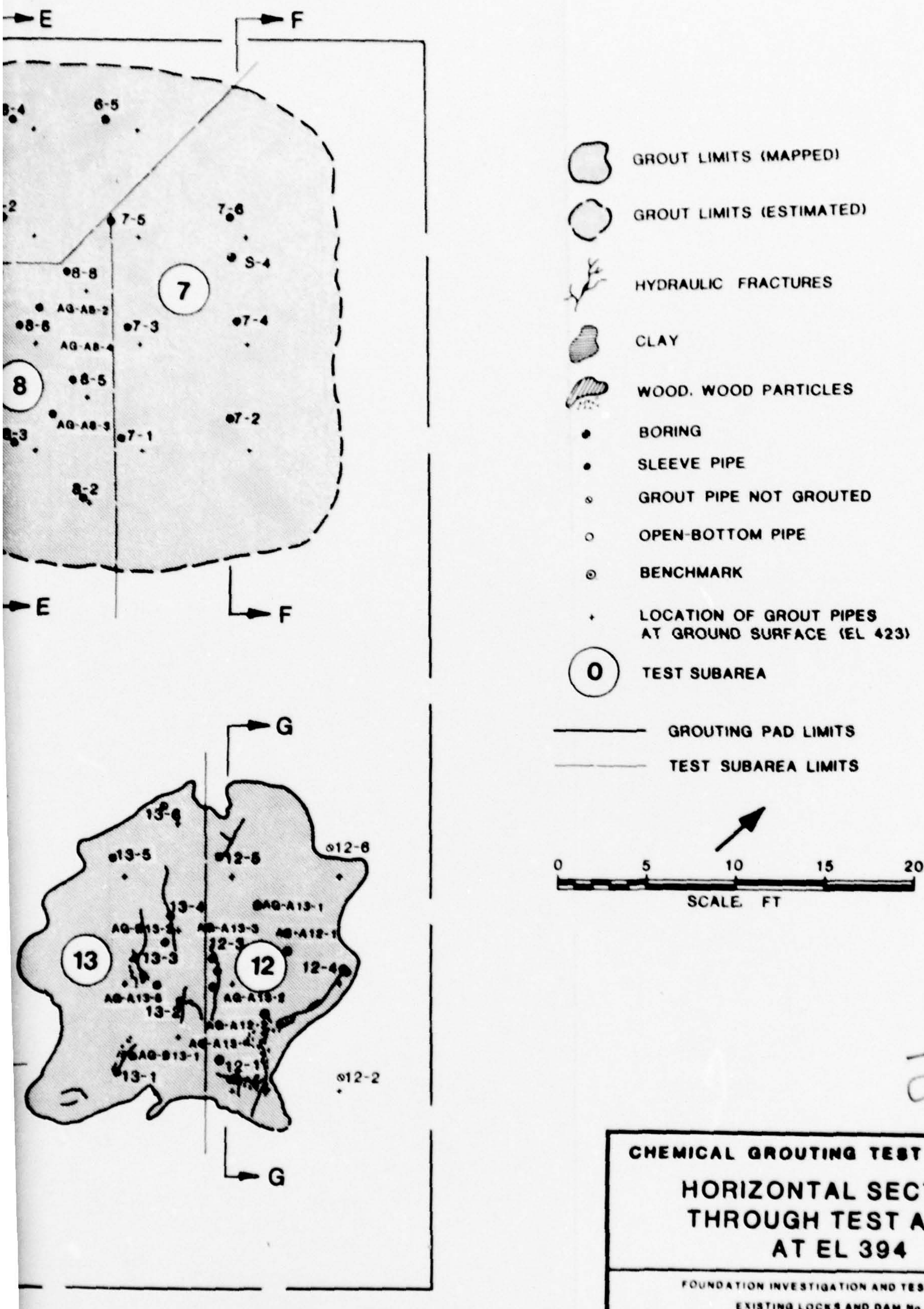

2

CHEMICAL GROUTING TEST PROGRAM

HORIZONTAL SECTION THROUGH TEST AREA AT EL 394

FOUNDATION INVESTIGATION AND TEST PROGRAM
EXISTING LOCKS AND DAM No. 26
ST LOUIS DISTRICT, CORPS OF ENGINEERS.
DACW43-78-C-0005

Woodward-Clyde Consultants
Y7C825 Phase III

Fig. 9.17

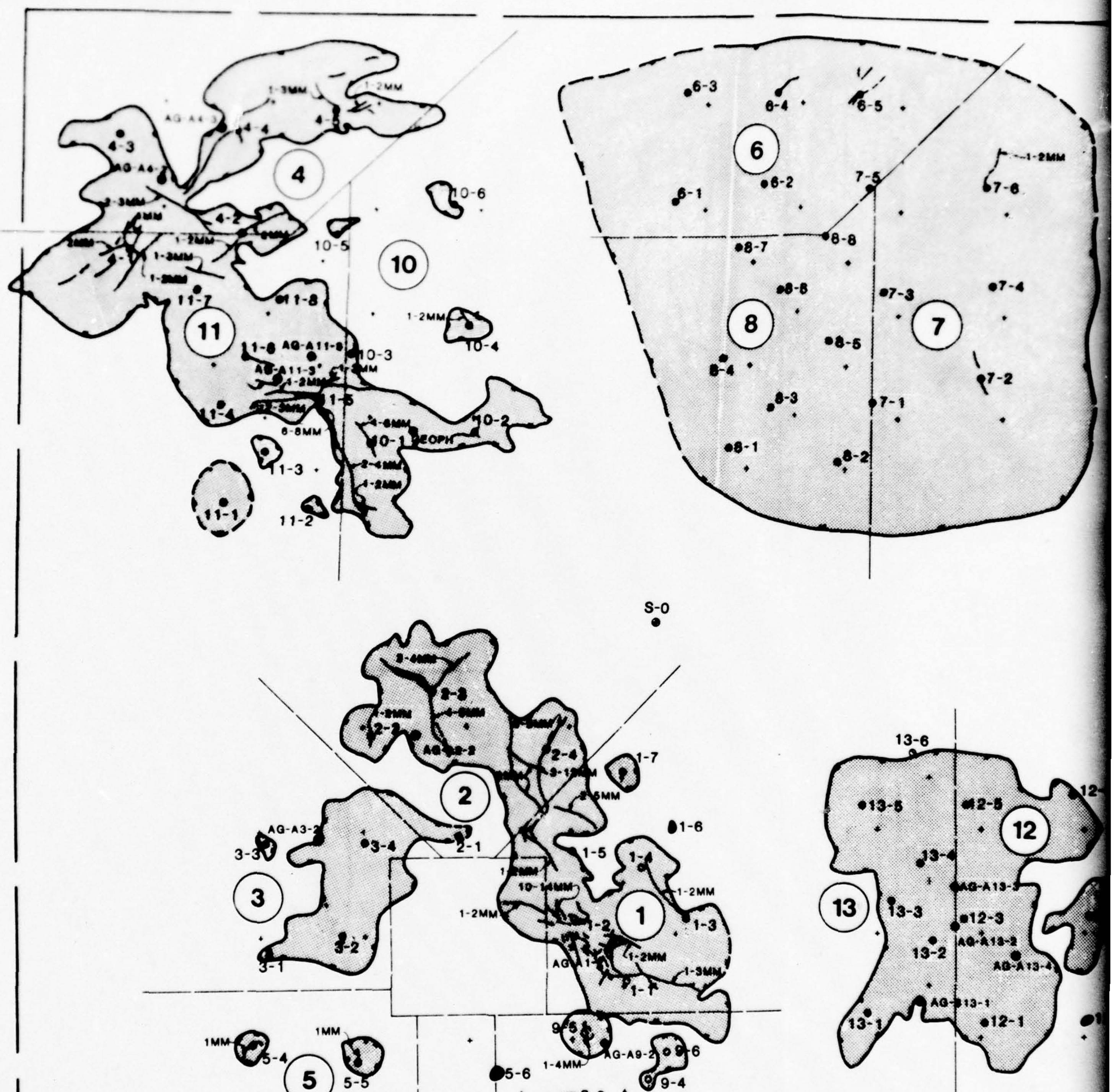

4
AG-A4-3
AG-A4-2
4-3
4-4
4-2
1-3MM
1-2MM
10-6
10-5
10
11
11-7
11-8
AG-A11-8
AG-A11-3
10-3
1-2MM
10-4
11-5
11-4
6-8MM
10-1
10-2
11-3
11-1
11-2
6
6-3
6-4
6-5
6-2
6-1
7-5
7-6
8-8
8-7
7-3
7-4
8
7
8-5
8-4
7-2
8-3
7-1
8-1
8-2
S-0
2
2-3
2-2
AG-A2-2
2-4
1-7
1-6
2-1
3-4
AG-A3-2
3-3
3
3-2
3-1
1-5
1-4
1-2MM
1
1-3
1-1
1-3MM
10-14MM
13-6
13-5
12-5
12
13-4
AG-A13-3
13
13-3
12-3
AG-A13-2
13-2
AG-A13-4
AG-A13-1
13-1
12-1
9-5
9-6
AG-A9-2
1-4MM
1MM
5-4
5
5-5
5-6
9-4
S-8
9-3
9-1
9-2
9
5-1
5-2
5-3

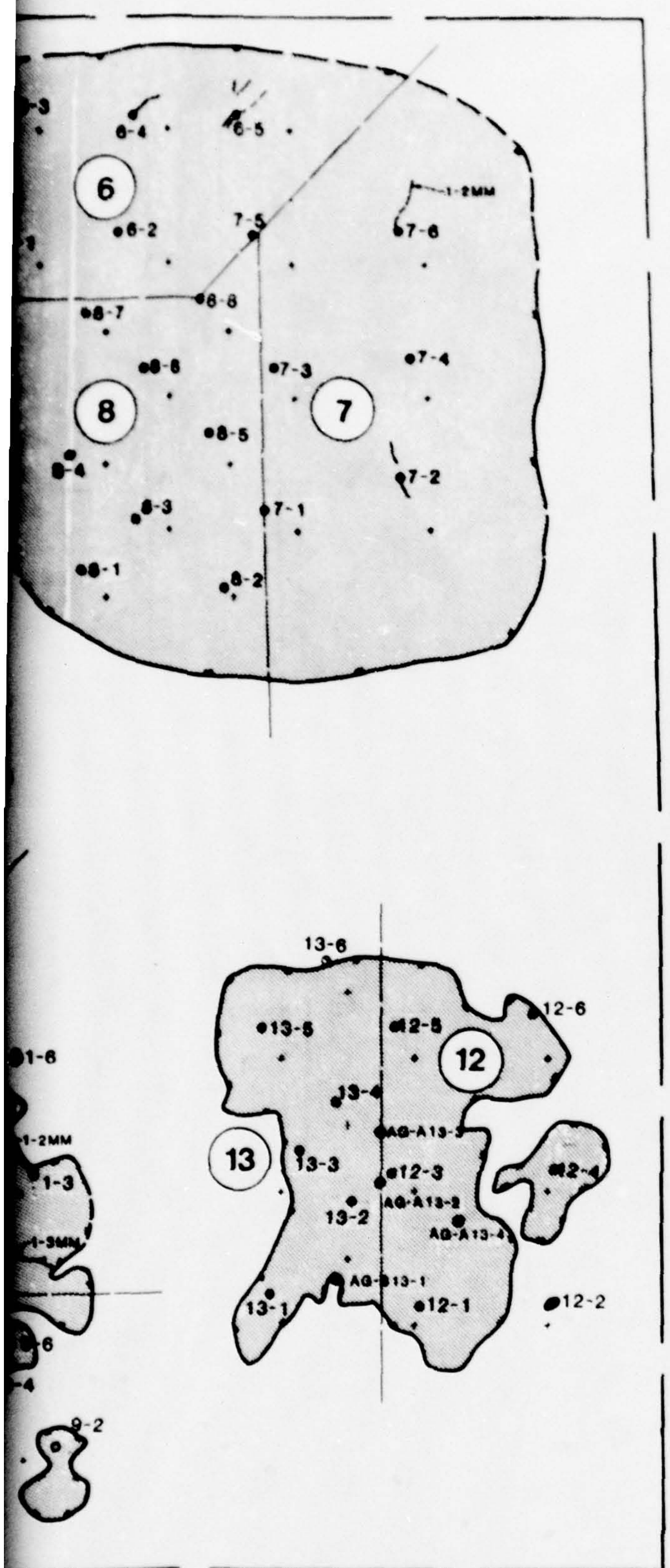

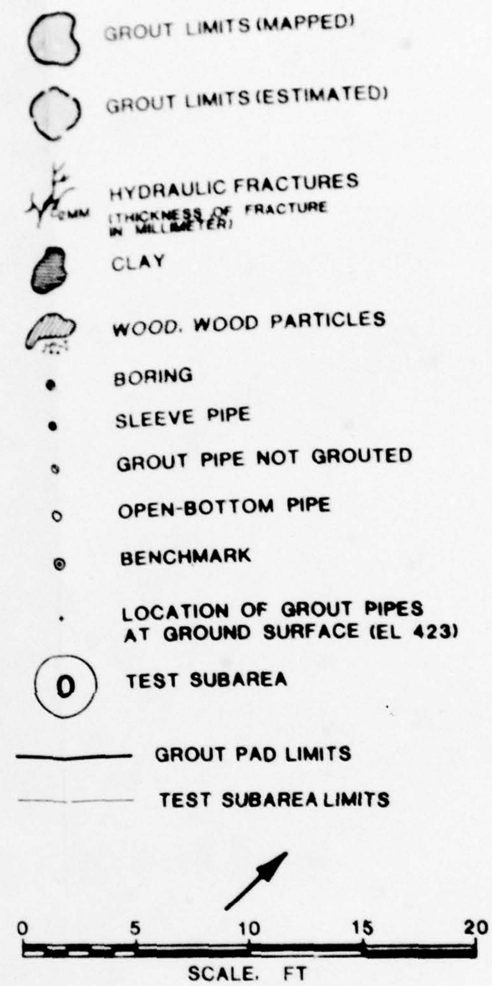

2

CHEMICAL GROUTING TEST PROGRAM

HORIZONTAL SECTION THROUGH TEST AREA AT EL 390

FOUNDATION INVESTIGATION AND TEST PROGRAM
EXISTING LOCKS AND DAM No. 26
ST LOUIS DISTRICT, CORPS OF ENGINEERS.
DACW43-78-C-0005

Woodward-Clyde Consultants
Y7C825 Phase IX

Fig. 9.18

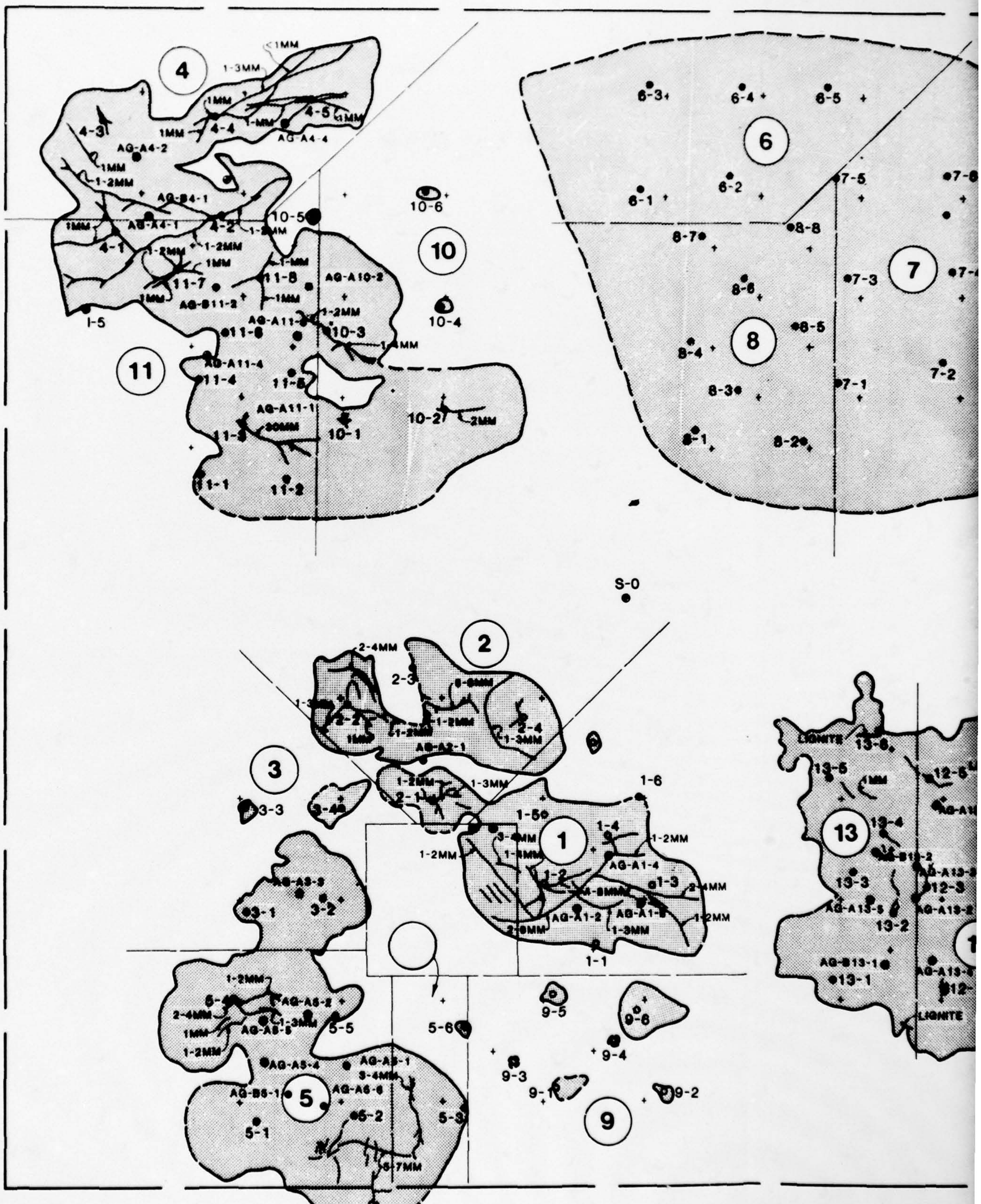

4
1-3MM
1MM
4-3
4-4
4-5
AG-A4-4
AG-A4-2
1-2MM
AG-A4-1
4-2
4-1
10-5
10-6
10
11-7
11-8
AG-A10-2
AG-B11-2
1-5
10-4
10-3
AG-A11-4
11-4
11
11-5
AG-A11-1
10-2
2MM
10-1
11-3
11-1
11-2
6-3
6-4
6-5
6
6-1
6-2
7-5
8-8
8-7
7
7-3
8-6
8-5
8-4
8
7-2
8-3
7-1
8-1
8-2
S-0
2
2-4MM
2-3
2-4
1-3MM
AG-A2-1
3
1-2MM
2-1
3-3
1-6
1-5
1
1-4
1-2MM
AG-A1-4
1-3
1-2
AG-A1-2
1-3MM
1-1
AG-A3-3
3-1
3-2
13
LIGNITE
13-6
13-5
12-5
13-4
13-3
12-3
13-2
AG-B13-1
13-1
5-4
AG-A5-2
2-4MM
1MM
5-5
5-6
9-5
9-6
9-4
9-3
AG-A5-4
AG-A5-1
3-4MM
AG-B5-1
5
5-2
5-1
5-3
9-1
9-2
9
5-7MM

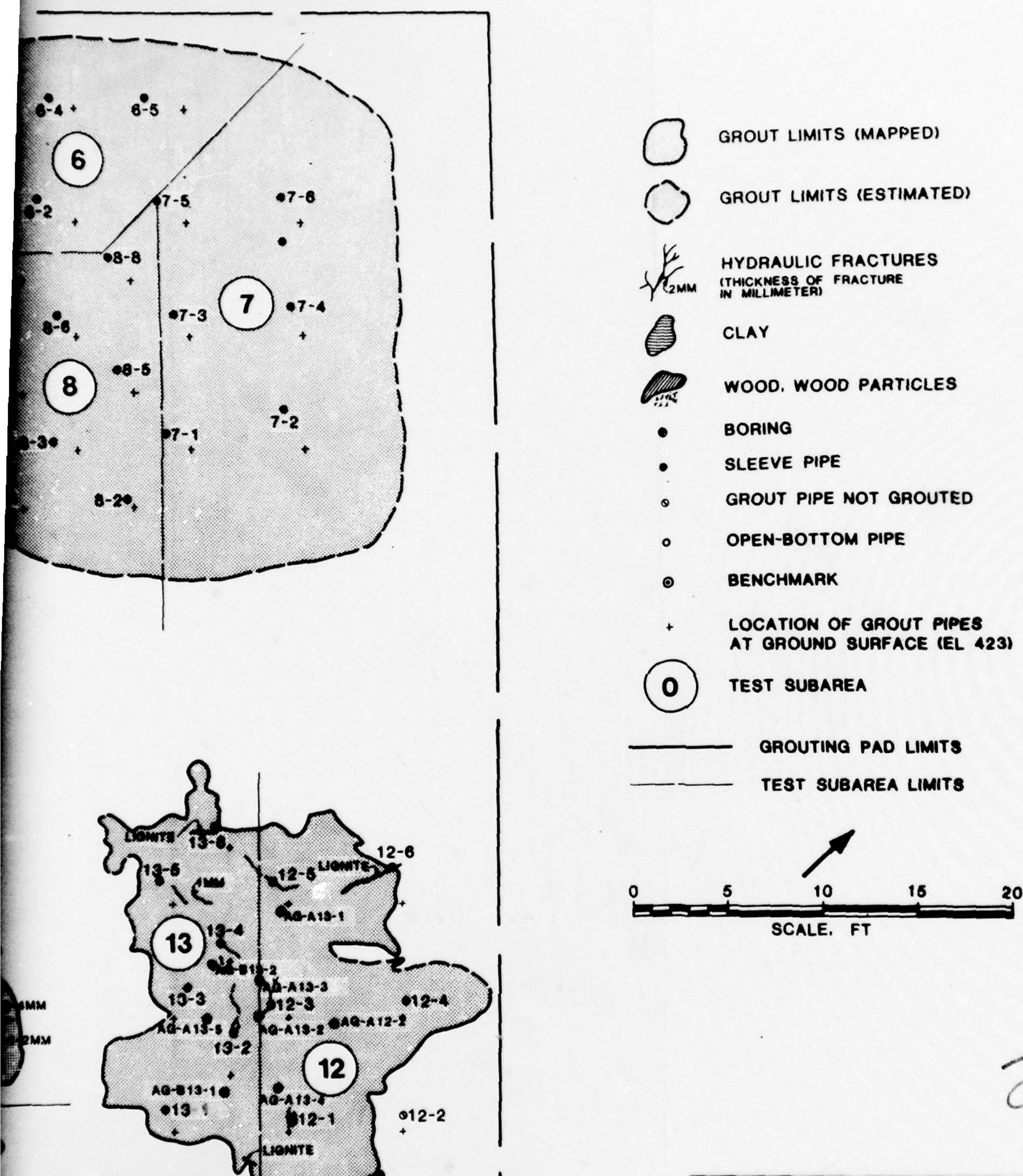

2

CHEMICAL GROUTING TEST PROGRAM

HORIZONTAL SECTION THROUGH TEST AREA AT EL 385

FOUNDATION INVESTIGATION AND TEST PROGRAM
EXISTING LOCKS AND DAM No. 26
ST LOUIS DISTRICT, CORPS OF ENGINEERS.
DACW43-78-C-0005

Woodward-Clyde Consultants

Y7C825 Phase IX

Fig. 9.19

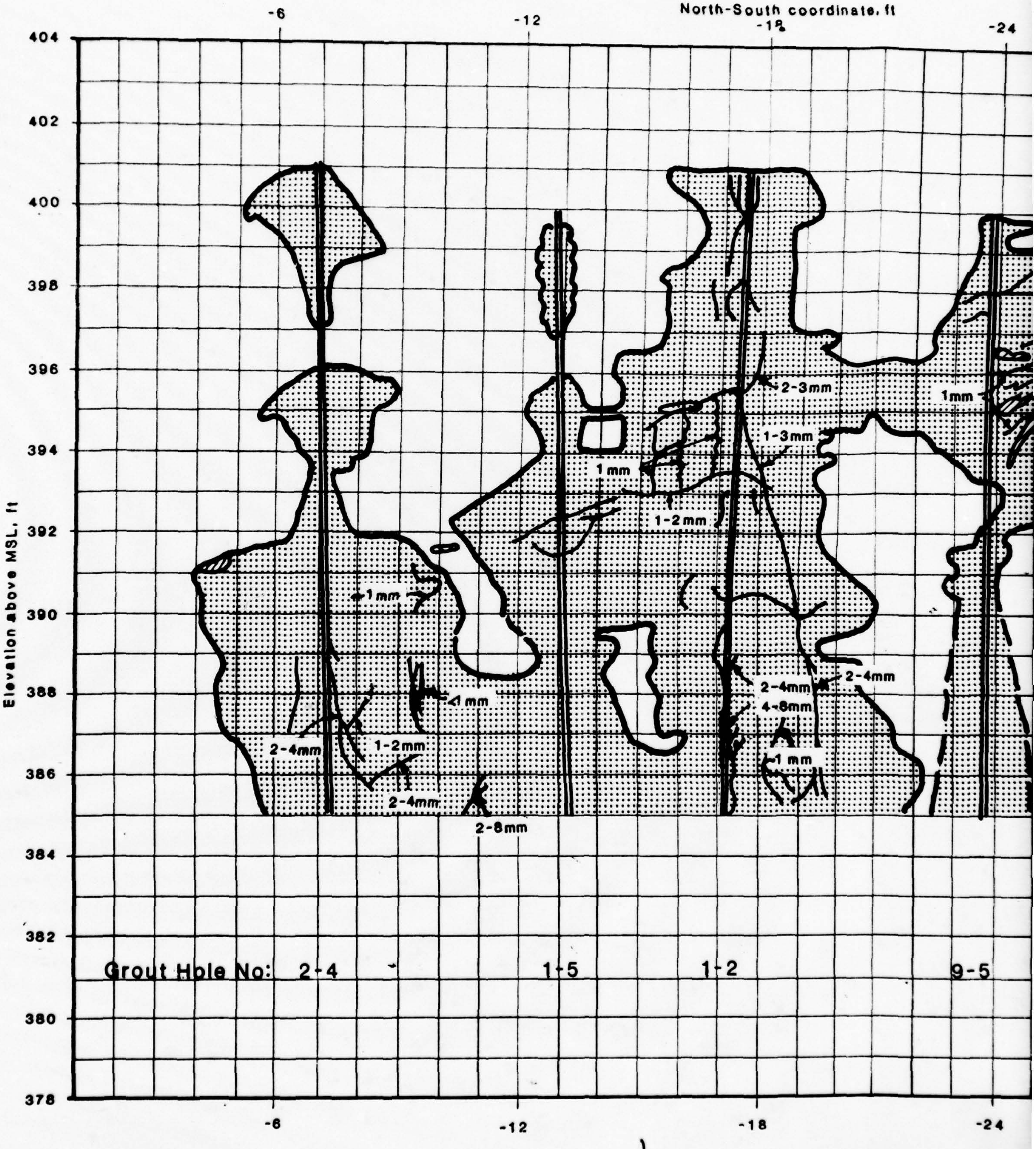
North-South coordinate, ft
-6
-12
-18
-24
Elevation above MSL, ft
404
402
400
398
396
394
392
390
388
386
384
382
380
378
2-3mm
1mm
1-3mm
1 mm
1-2 mm
<1mm
<1 mm
2-4mm
1-2mm
2-4mm
2-8mm
2-4mm
2-4mm
4-8mm
<1 mm
Grout Hole No: 2-4
1-5
1-2
9-5

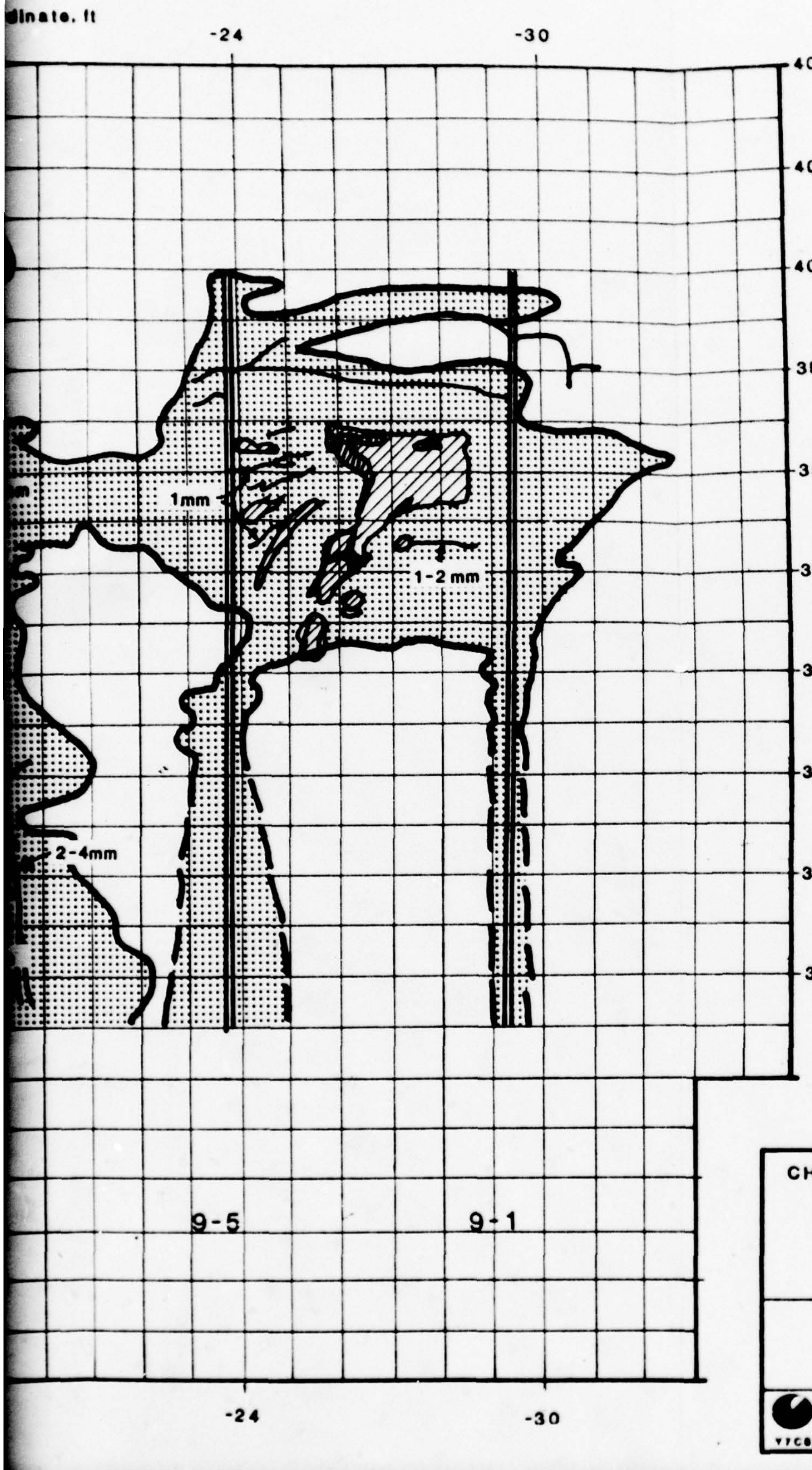

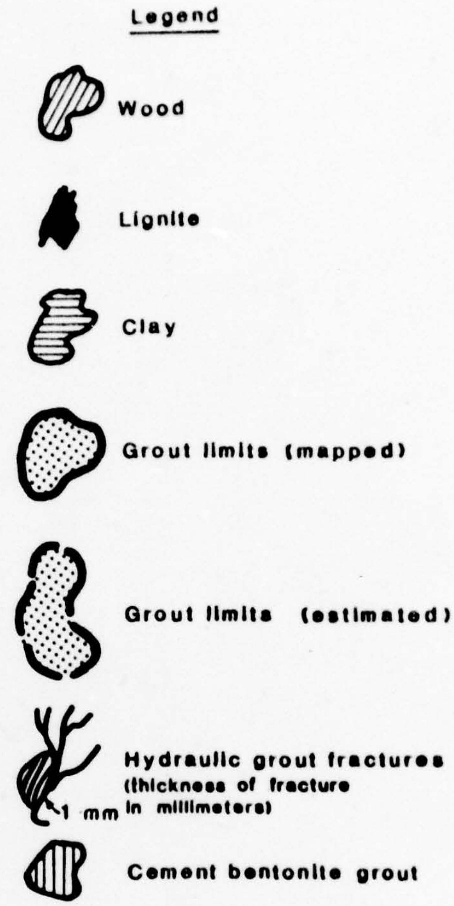

Notes

Grouting was done from el 423

Grout was injected between el 400 and el 380

During grouting groundwater surface varied between el 419.9 and el 407.3

2

CHEMICAL GROUTING TEST PROGRAM

VERTICAL SECTION AA THROUGH TEST AREA

FOUNDATION INVESTIGATION AND TEST PROGRAM
EXISTING LOCKS AND DAM No. 26
ST LOUIS DISTRICT, CORPS OF ENGINEERS
DACW43-78-C-0005

Woodward-Clyde Consultants
Y7C026 Phase II

Fig. 9.20

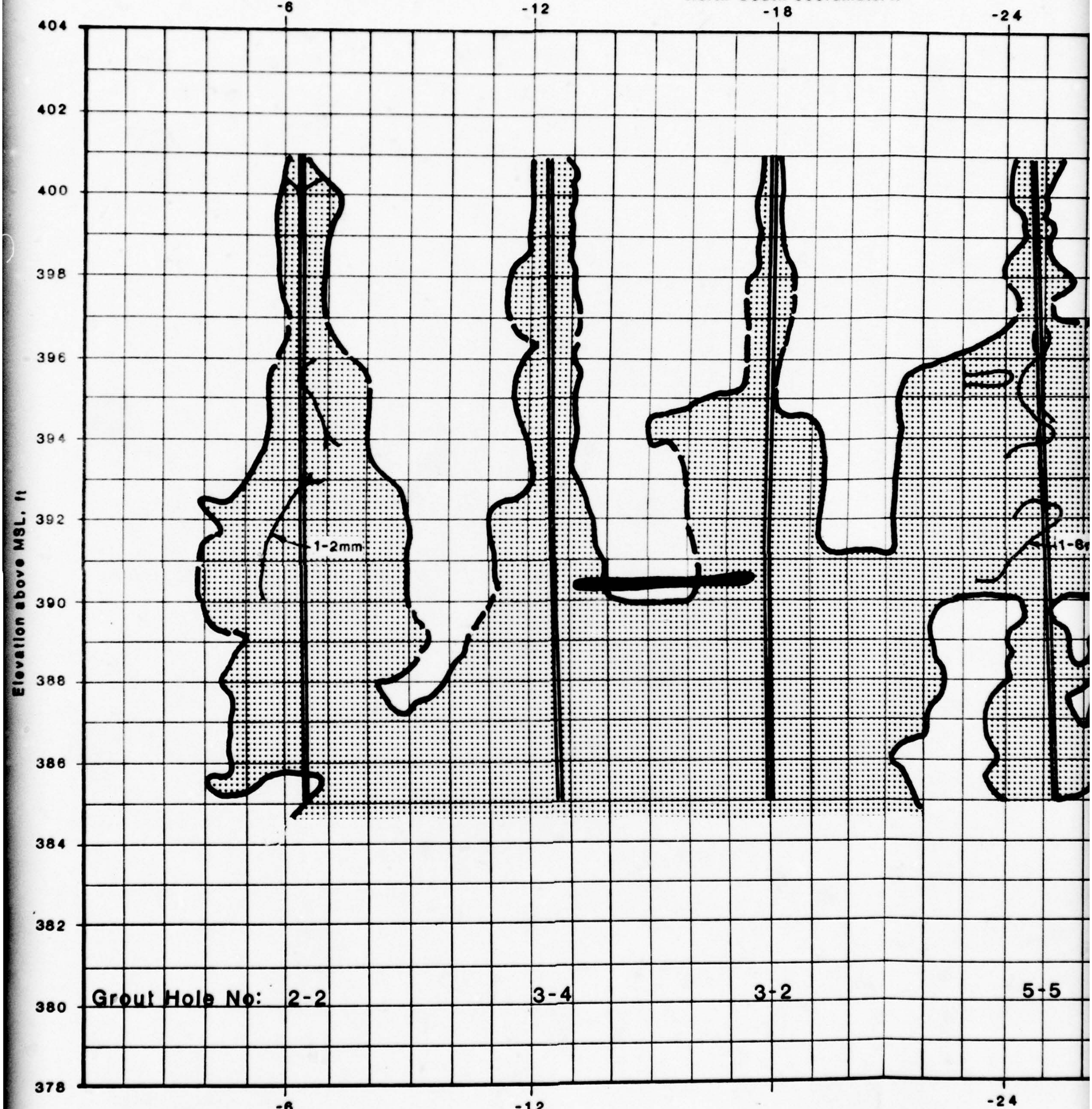

North-South coordinate, ft
-6
-12
-18
-24
Elevation above MSL, ft
404
402
400
398
396
394
392
390
388
386
384
382
380
378
1-2mm
Grout Hole No: 2-2
3-4
3-2
5-5

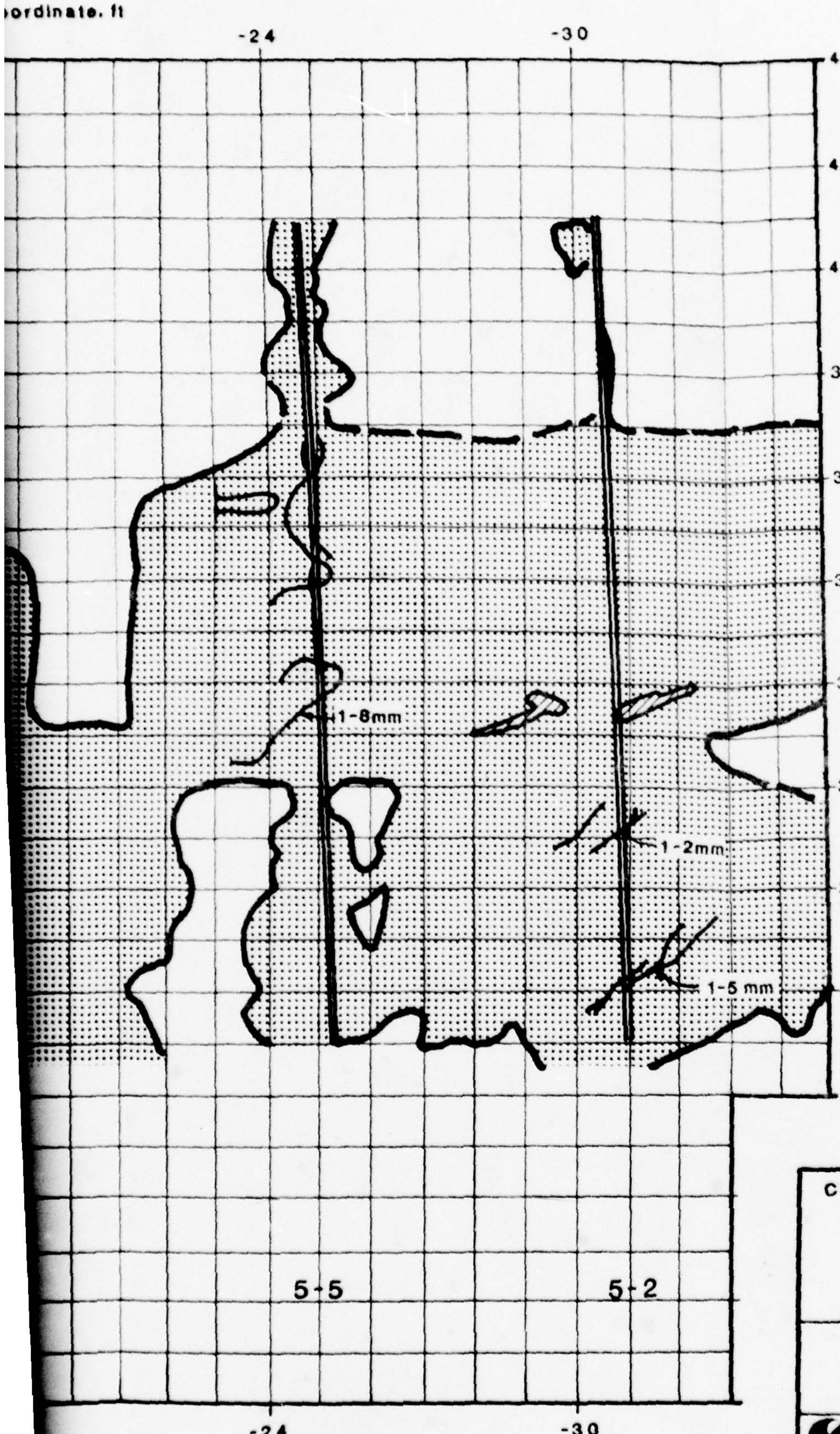

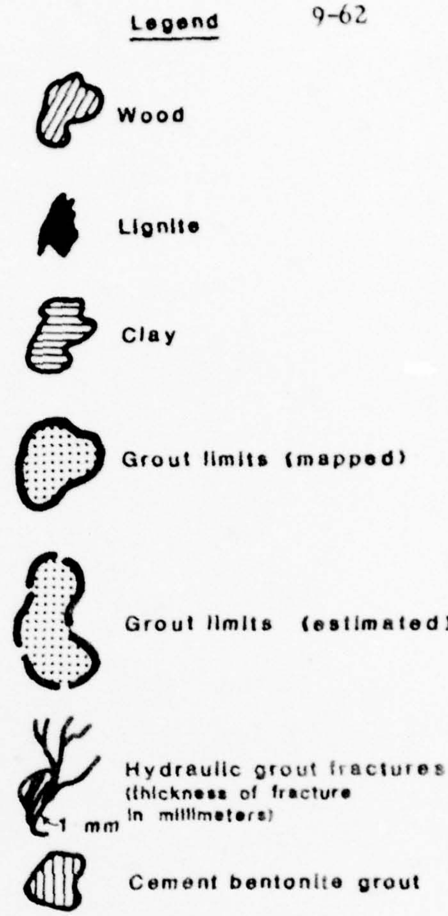

Notes

Grouting was done from el 423

Grout was injected between el 400 and el 380

During grouting groundwater surface varied between el 419.9 and el 407.3

2

CHEMICAL GROUTING TEST PROGRAM

VERTICAL SECTION BB THROUGH TEST AREA

FOUNDATION INVESTIGATION AND TEST PROGRAM
EXISTING LOCKS AND DAM No. 26
ST LOUIS DISTRICT, CORPS OF ENGINEERS.
DACW43-78-C-0005

Woodward-Clyde Consultants

Y7C828 Phase IV

Fig. 9.21

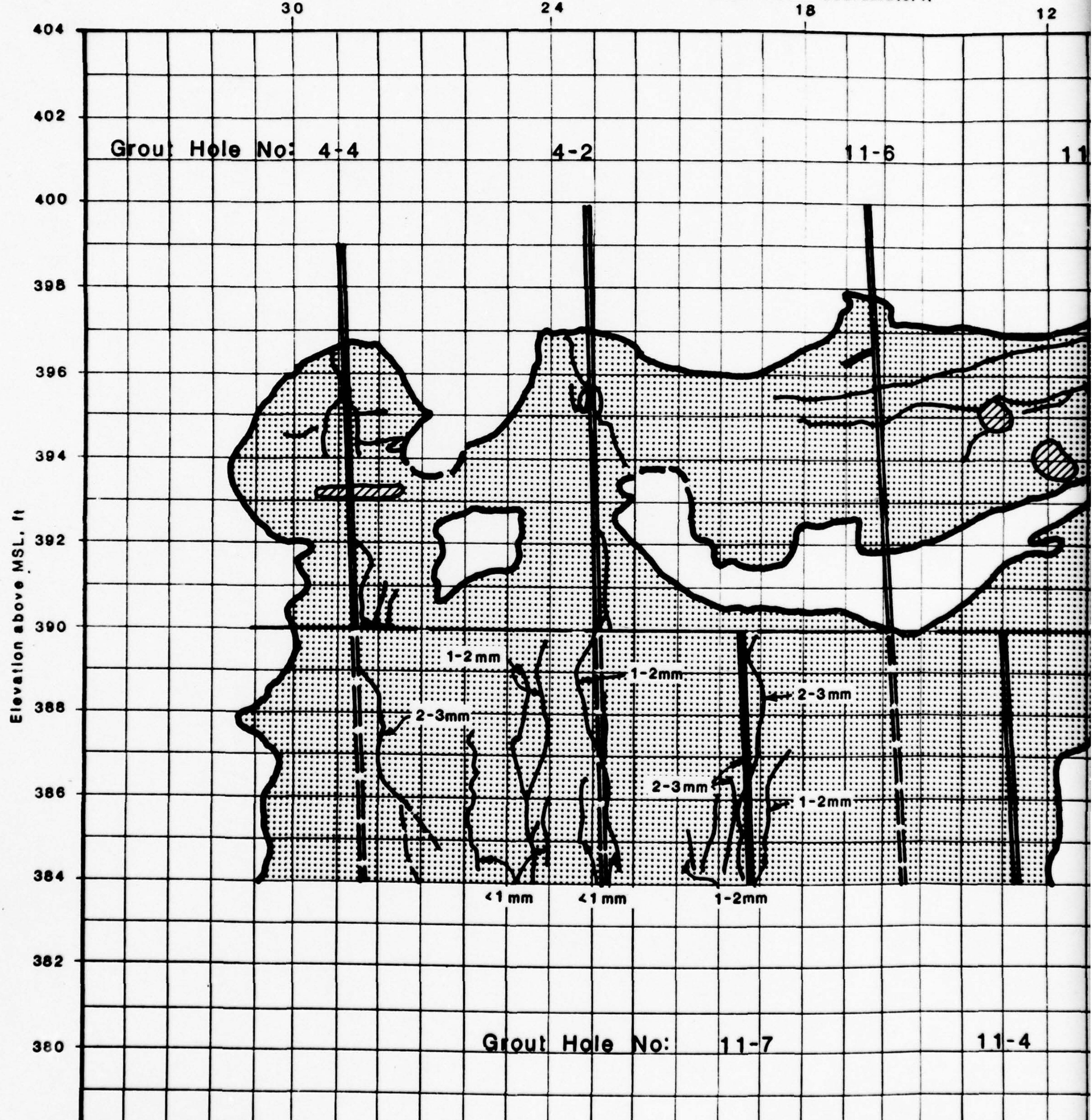

North-South coordinate, ft
30
24
18
12
404
402
400
398
396
394
392
390
388
386
384
382
380
378
Elevation above MSL, ft
Grout Hole No: 4-4
4-2
11-6
1-2mm
1-2mm
2-3mm
2-3mm
2-3mm
1-2mm
<1 mm
<1 mm
1-2mm
Grout Hole No: 11-7
11-4

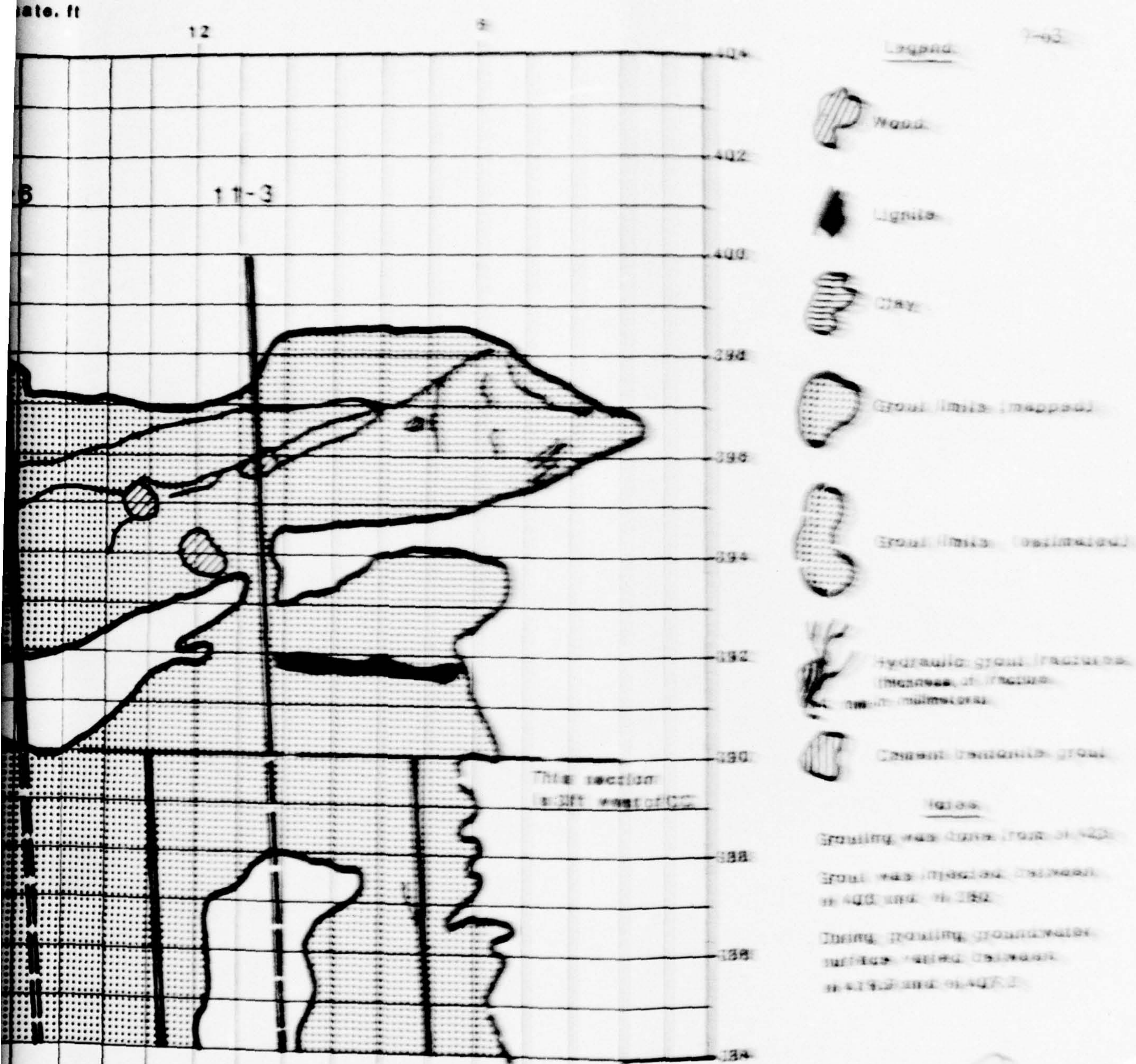

CHEMICAL GROUTING TEST PROGRAM

VERTICAL SECTION C-C'
THROUGH TEST AREA

Fig. 3.22

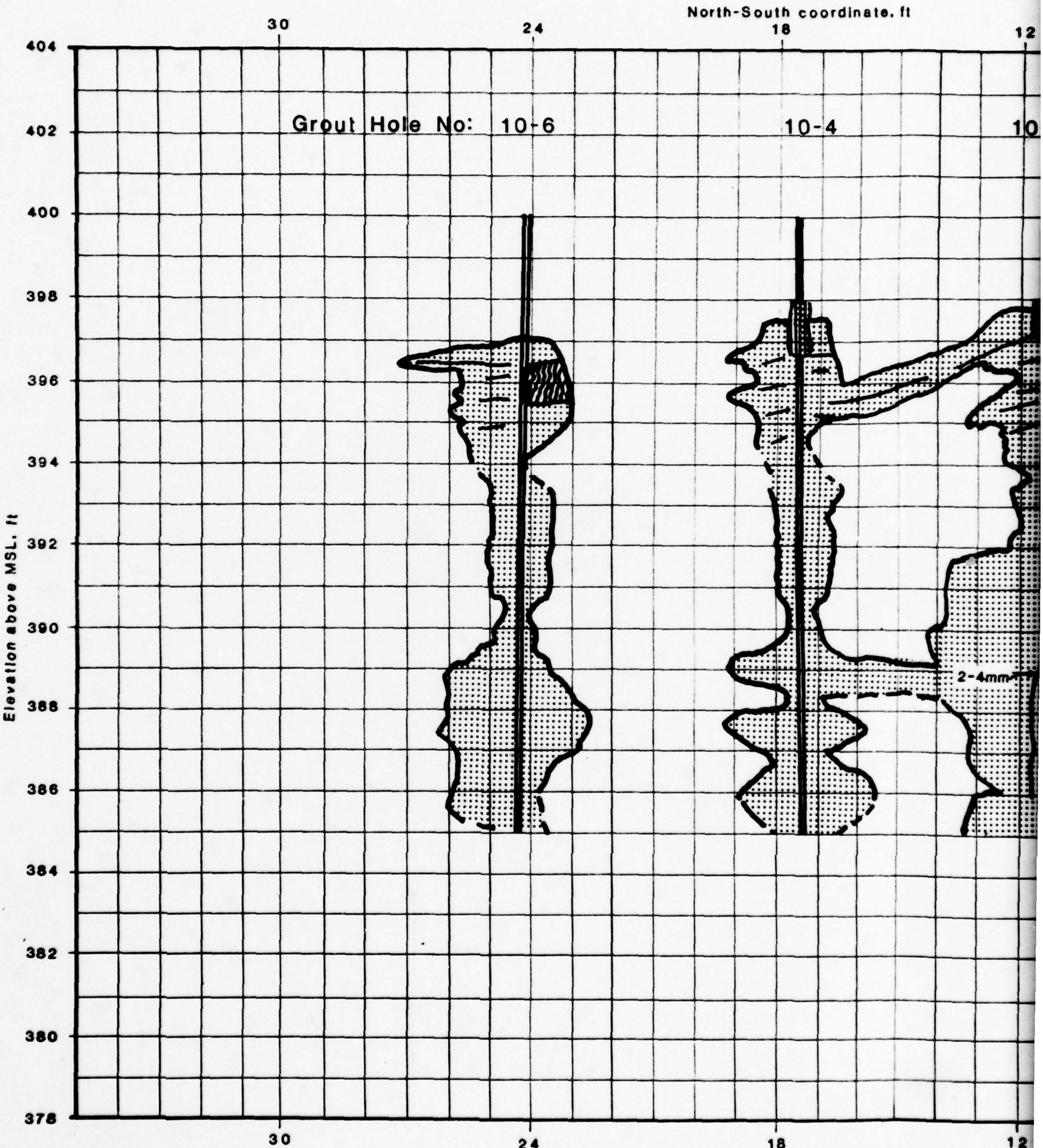
North-South coordinate, ft
30
24
18
12
Grout Hole No: 10-6
10-4
10
2-4mm
Elevation above MSL, ft
404
402
400
398
396
394
392
390
388
386
384
382
380
378

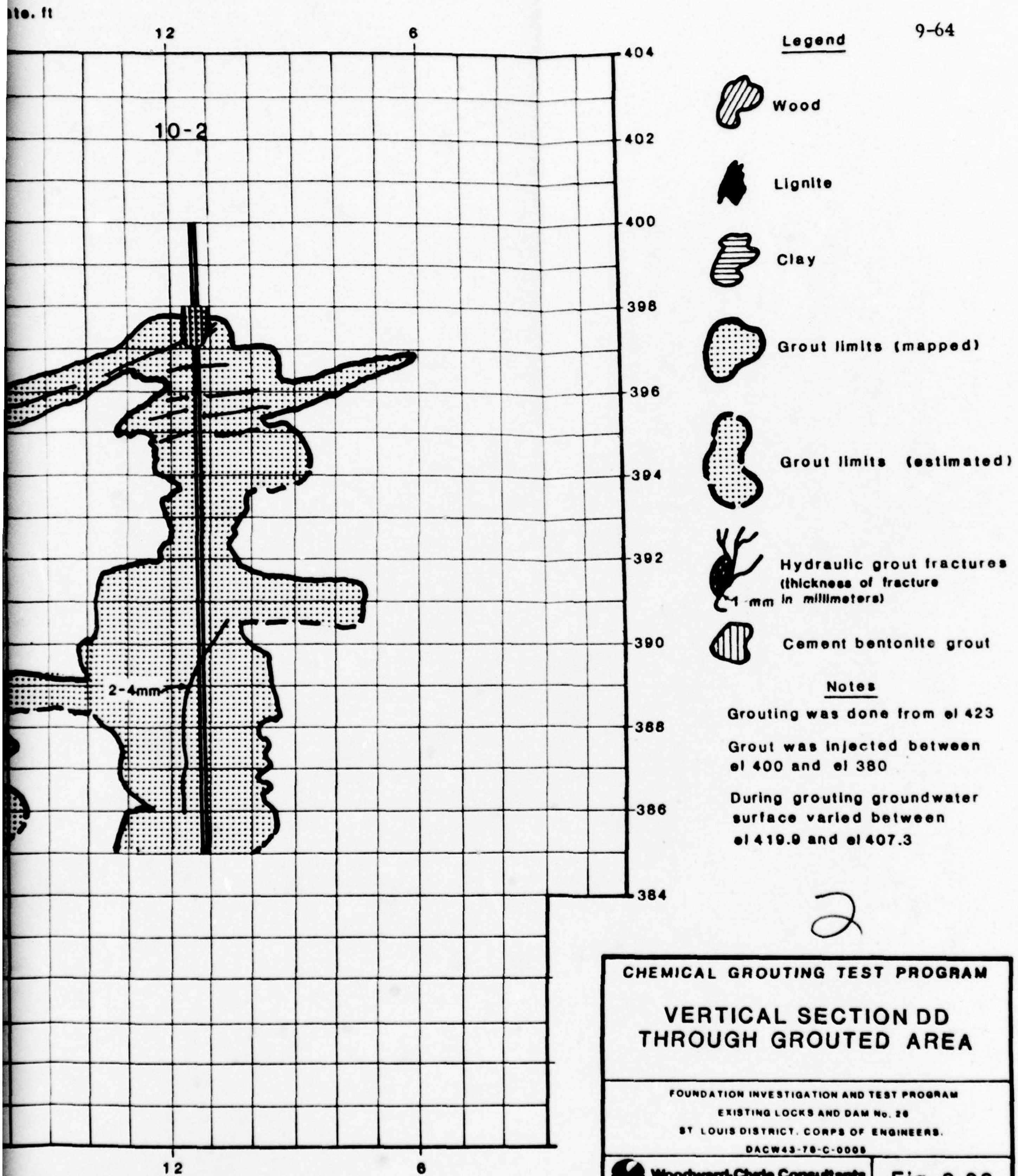

2

CHEMICAL GROUTING TEST PROGRAM

VERTICAL SECTION DD
THROUGH GROUTED AREA

FOUNDATION INVESTIGATION AND TEST PROGRAM
EXISTING LOCKS AND DAM No. 26
ST LOUIS DISTRICT, CORPS OF ENGINEERS.
DACW43-78-C-0005

Woodward-Clyde Consultants

Fig. 9.23

Y7C025 Phase IX

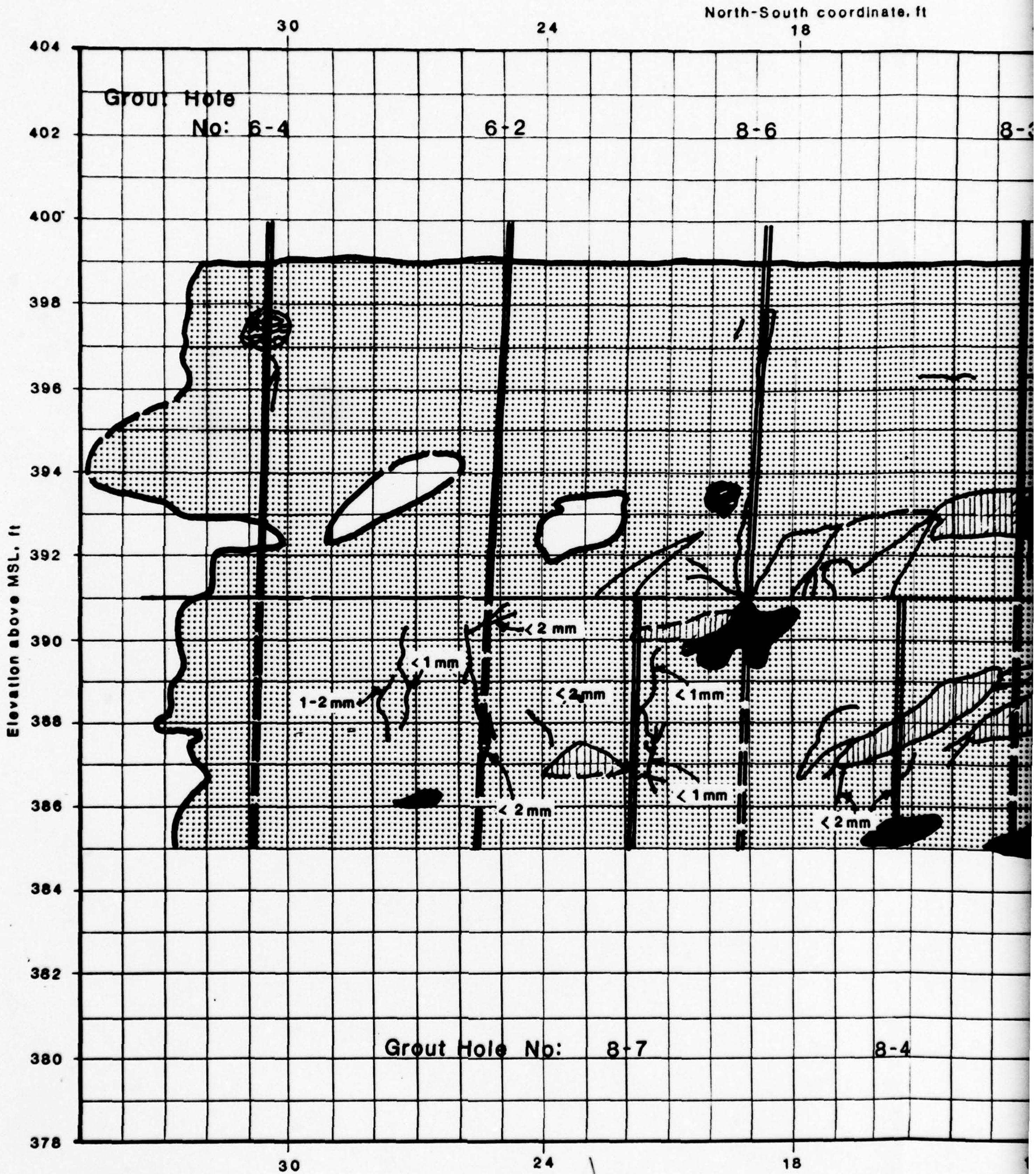
North-South coordinate, ft
30
24
18
404
402
400
398
396
394
392
390
388
386
384
382
380
378
Elevation above MSL, ft
Grout Hole
No: 6-4
6-2
8-6
8-3
< 2 mm
< 1 mm
1-2 mm
< 2 mm
< 1 mm
< 1 mm
< 2 mm
< 2 mm
Grout Hole No: 8-7
8-4
30
24
18

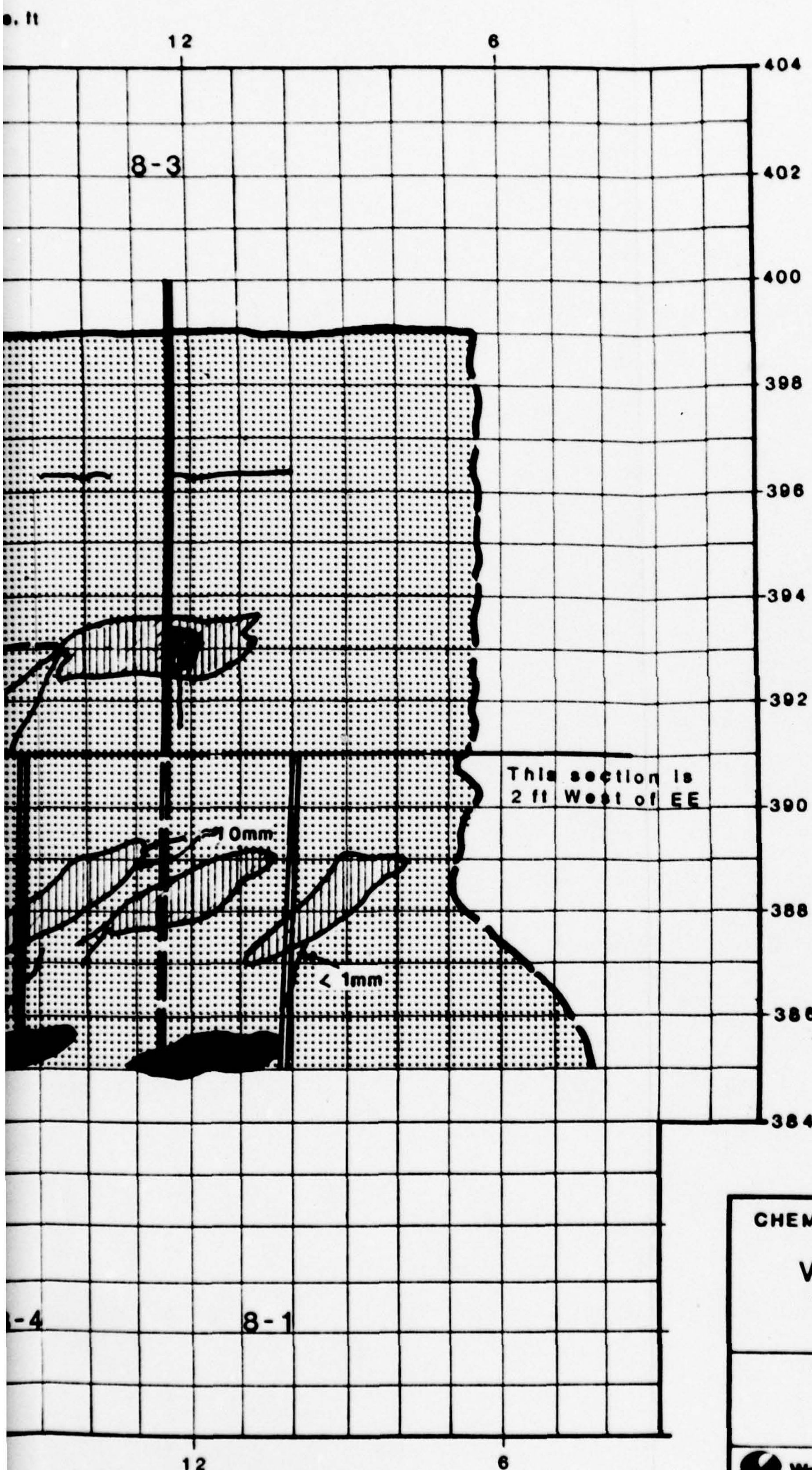

Legend

Wood

Lignite

Clay

Grout limits (mapped)

Grout limits (estimated)

Hydraulic grout fractures (thickness of fracture in millimeters)

Cement bentonite grout

Notes

Grouting was done from el 423

Grout was injected between el 400 and el 380

During grouting groundwater surface varied between el 419.9 and el 407.3

2

CHEMICAL GROUTING TEST PROGRAM

VERTICAL SECTION EE THROUGH TEST AREA

FOUNDATION INVESTIGATION AND TEST PROGRAM
EXISTING LOCKS AND DAM No. 26
ST LOUIS DISTRICT, CORPS OF ENGINEERS.
DACW43-78-C-0006

Woodward-Clyde Consultants

Fig. 9.24

Y7C026 Phase IX

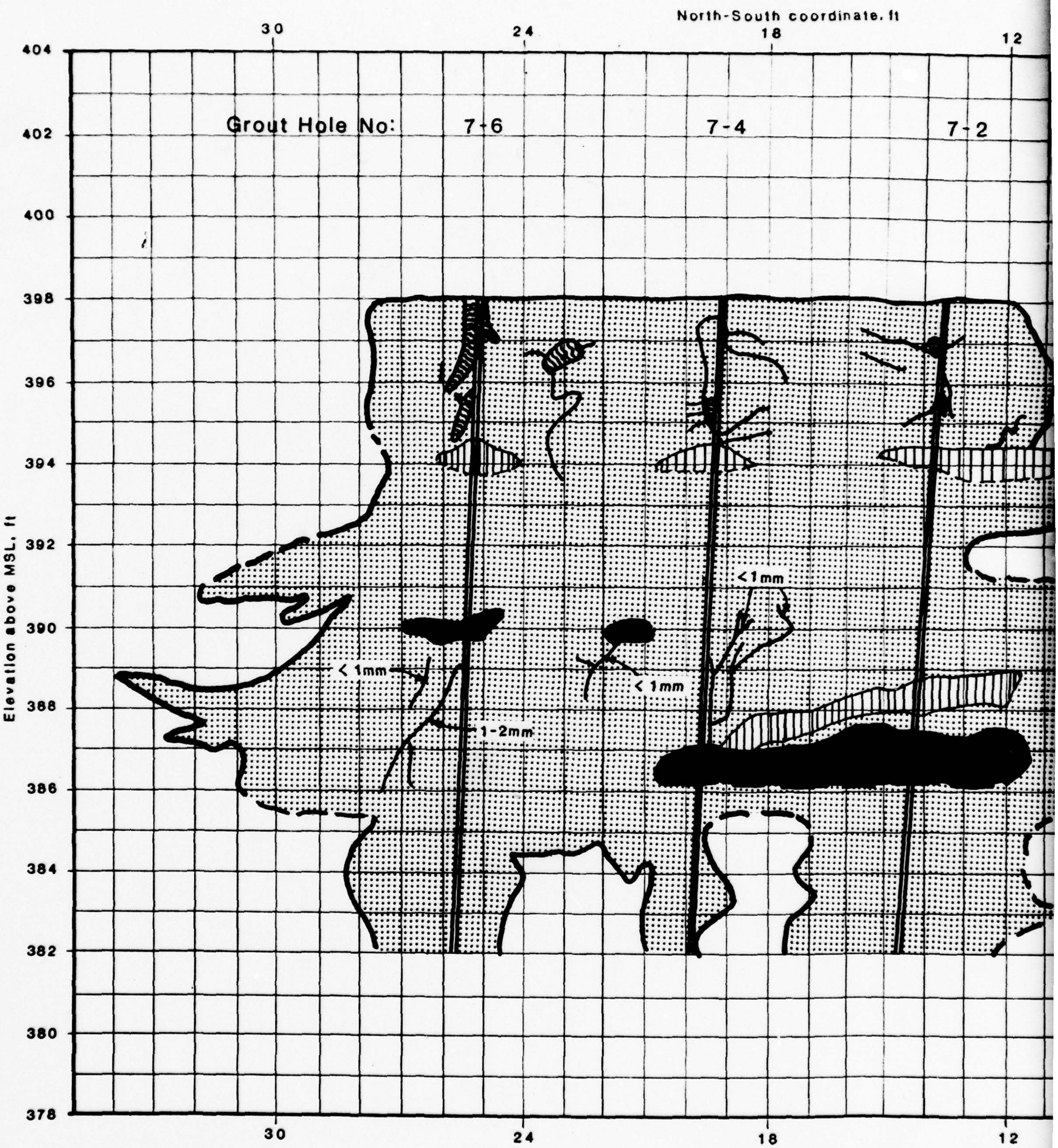
North-South coordinate, ft
30
24
18
12
Grout Hole No:
7-6
7-4
7-2
404
402
400
398
396
394
392
390
388
386
384
382
380
378
Elevation above MSL, ft
< 1mm
1-2mm
< 1mm
<1mm

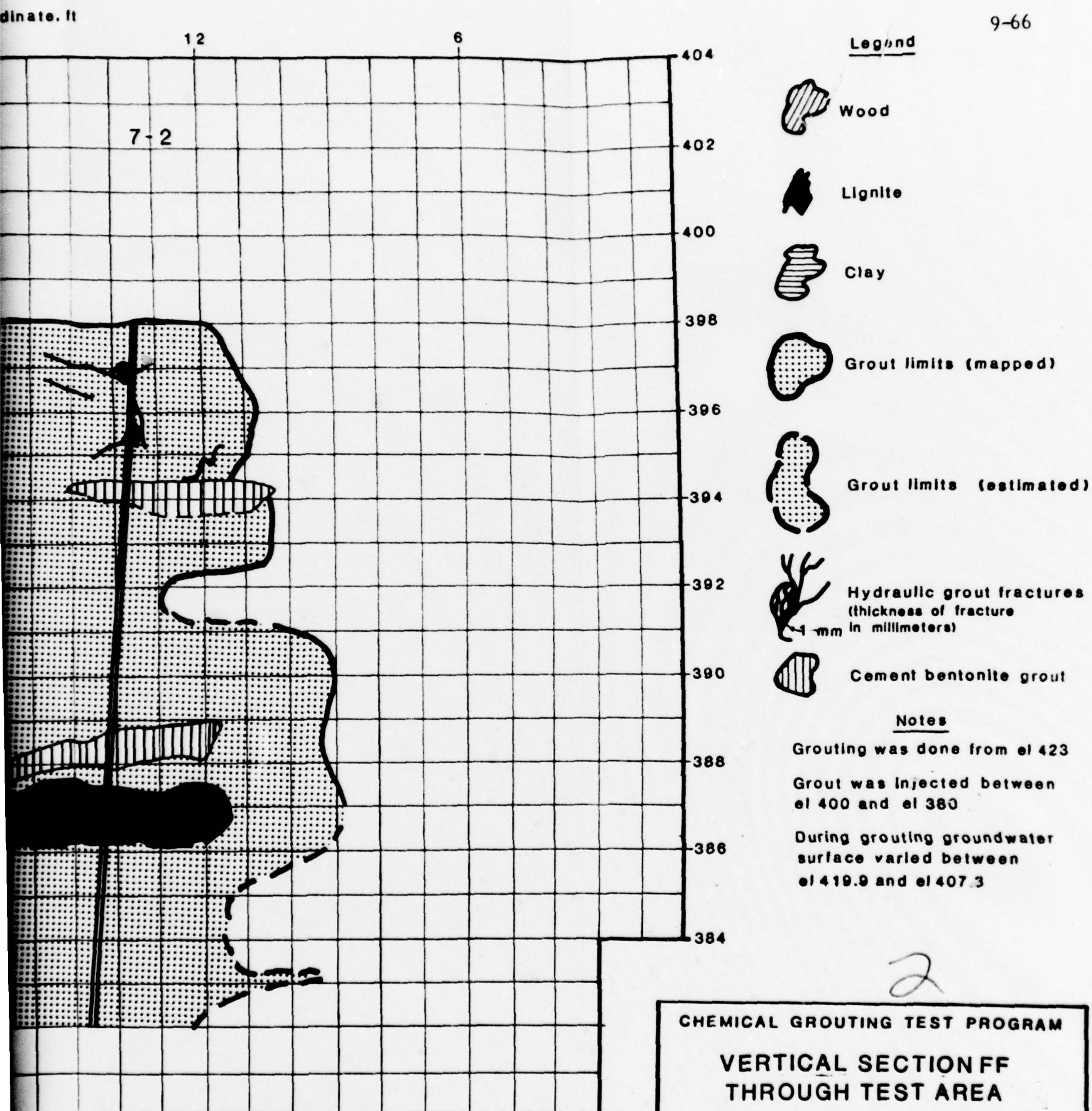

Notes

Grouting was done from el 423

Grout was injected between el 400 and el 380

During grouting groundwater surface varied between el 419.9 and el 407.3

2

CHEMICAL GROUTING TEST PROGRAM

VERTICAL SECTION FF THROUGH TEST AREA

FOUNDATION INVESTIGATION AND TEST PROGRAM
EXISTING LOCKS AND DAM No. 26
ST LOUIS DISTRICT, CORPS OF ENGINEERS.
DACW43-78-C-0005

Woodward-Clyde Consultants

Fig. 9.25

Y7C825 Phase IX

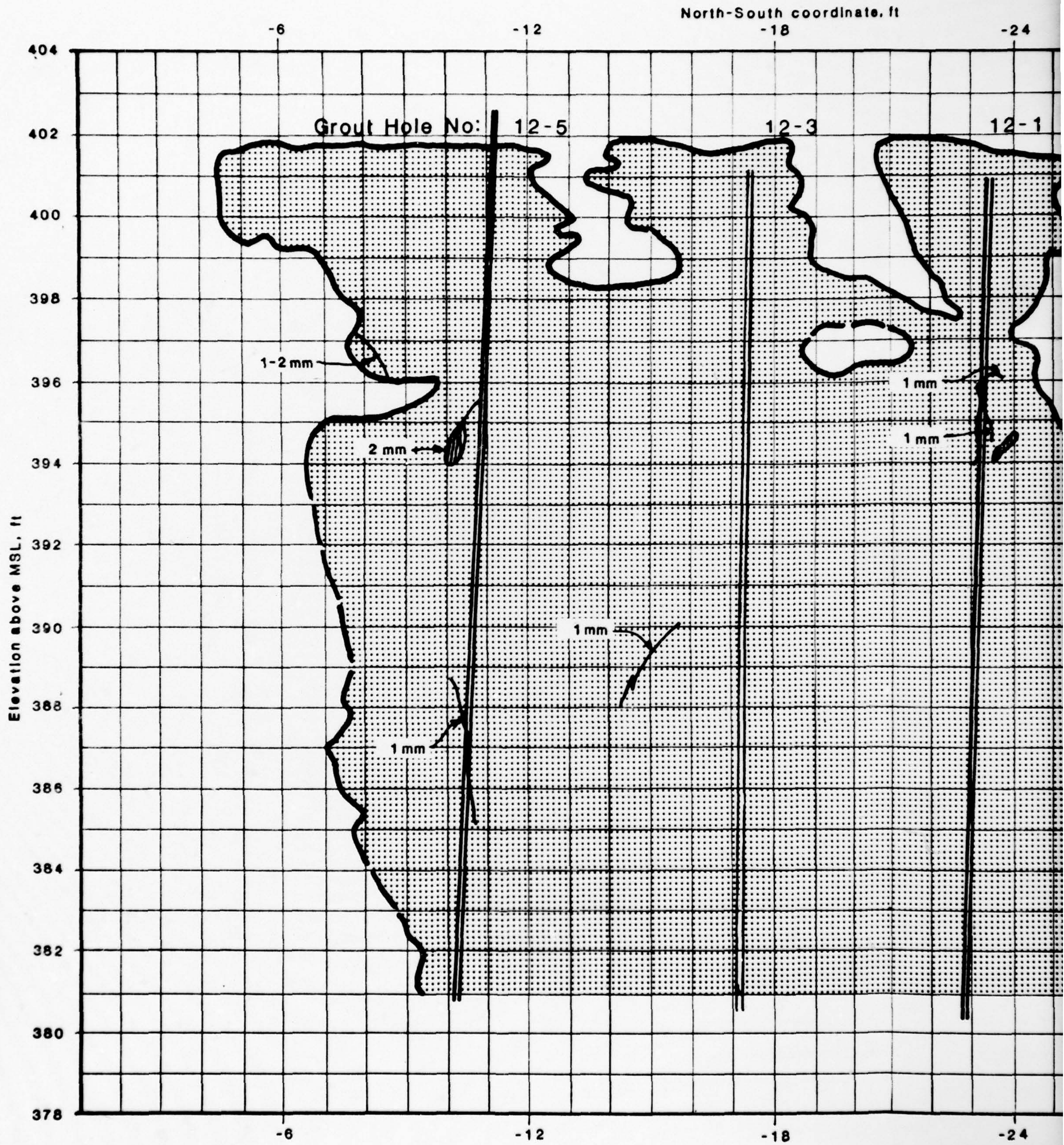

North-South coordinate, ft
-6
-12
-18
-24
Elevation above MSL, ft
404
402
400
398
396
394
392
390
388
386
384
382
380
378
Grout Hole No:
12-5
12-3
12-1
1-2 mm
2 mm
1 mm
1 mm
1 mm
1 mm
1 mm

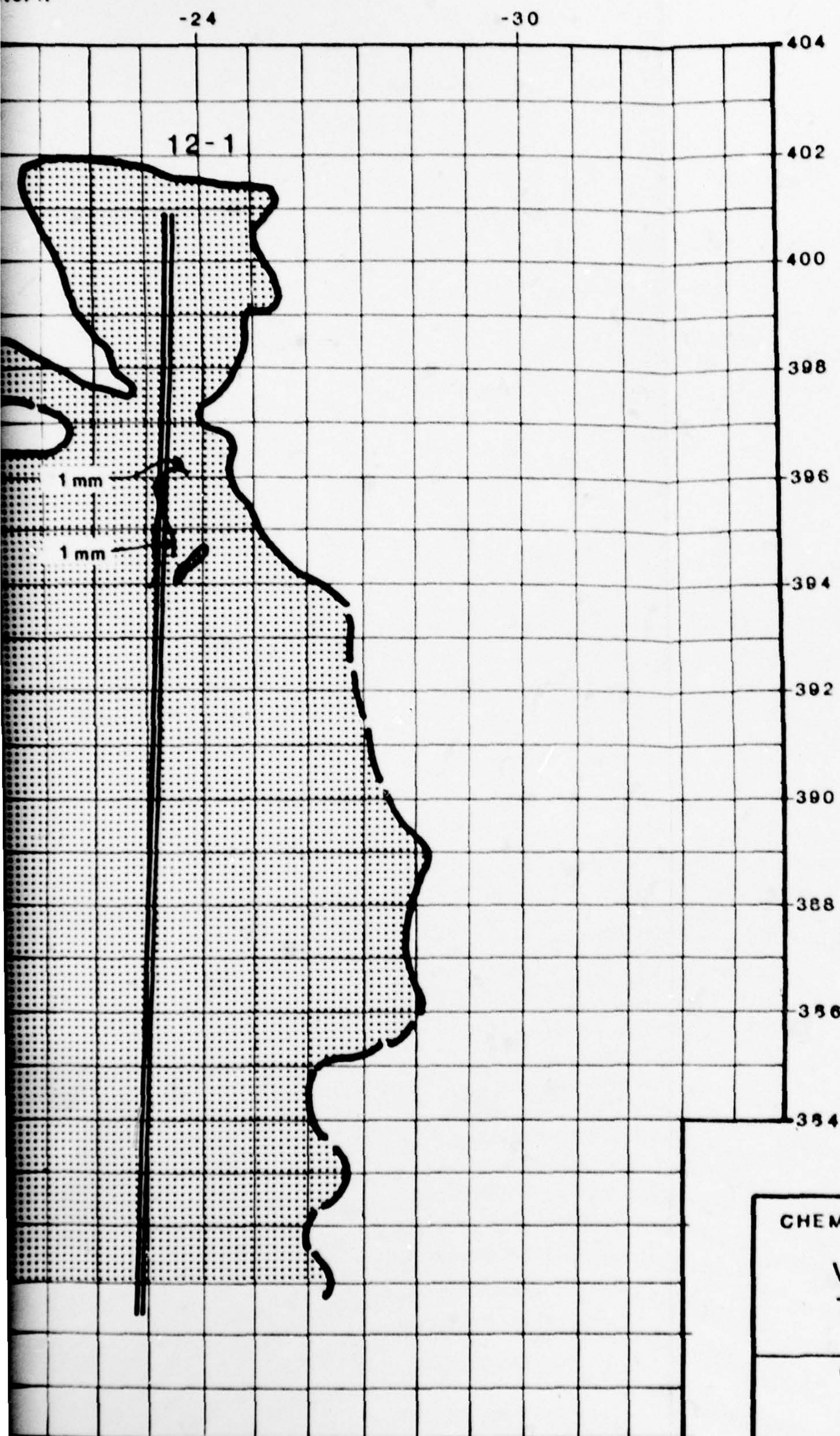

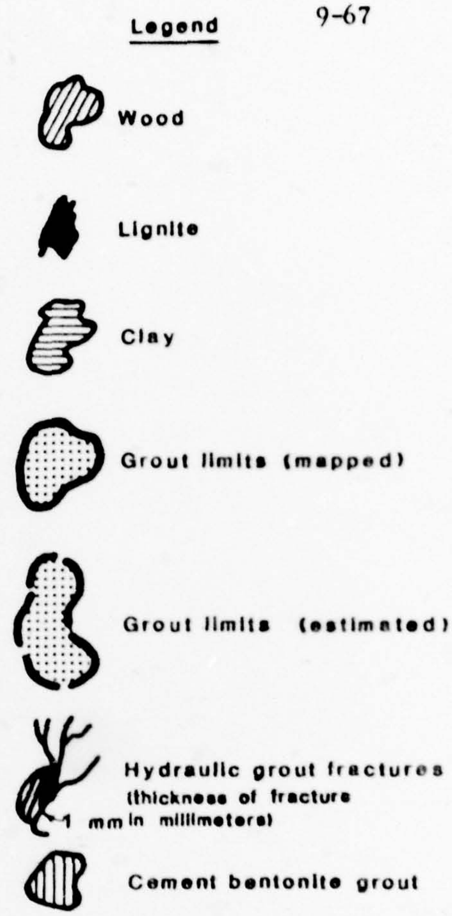

Notes

Grouting was done from el 423

Grout was injected between el 400 and el 380

During grouting groundwater surface varied between el 419.9 and el 407.3

2

CHEMICAL GROUTING TEST PROGRAM

VERTICAL SECTION GG THROUGH TEST AREA

FOUNDATION INVESTIGATION AND TEST PROGRAM
EXISTING LOCKS AND DAM No. 26
ST LOUIS DISTRICT, CORPS OF ENGINEERS
DACW43-78-C-0006

Woodward-Clyde Consultants

Y7C825 Phase IX

Fig. 9.26

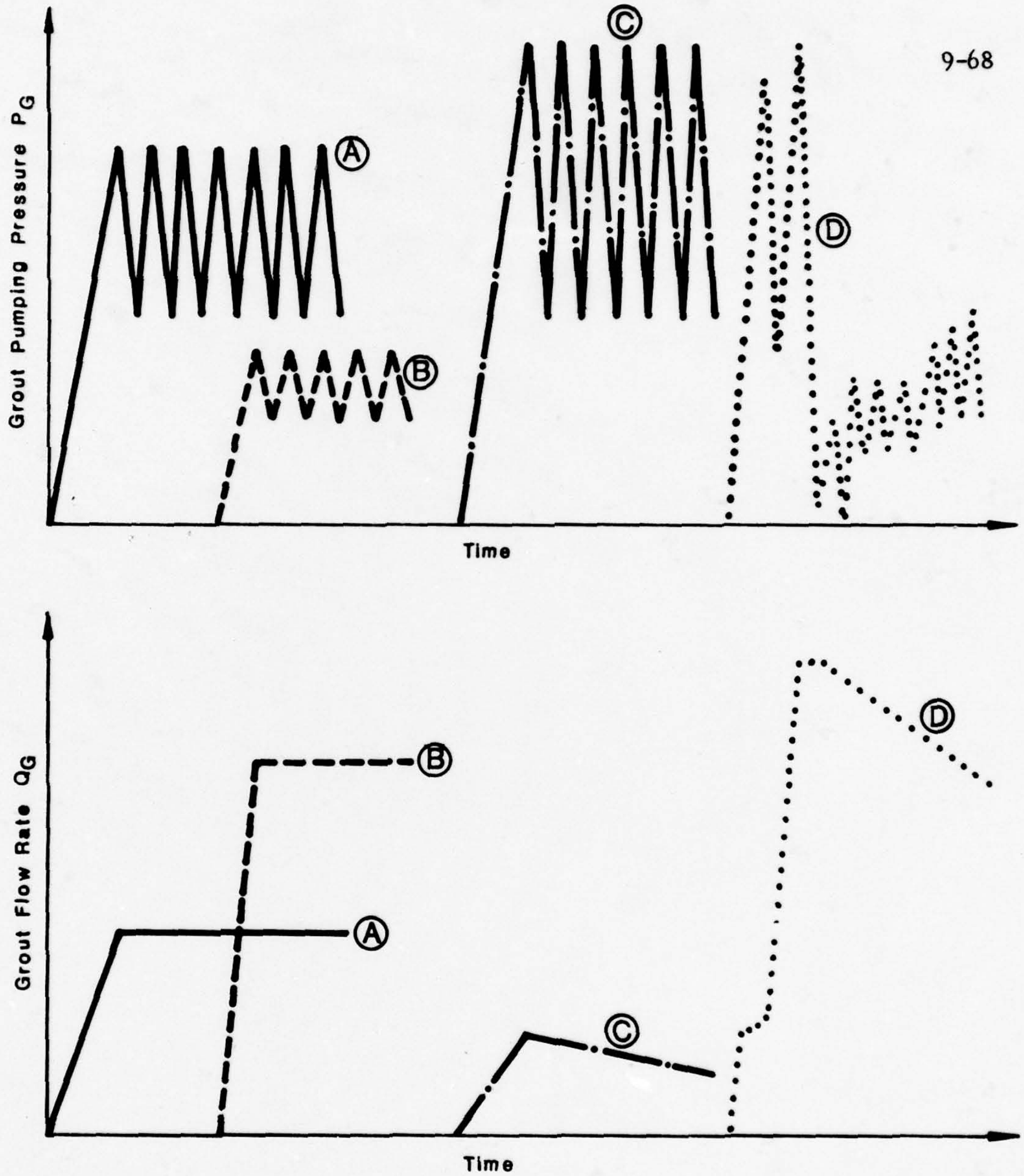

(A) Good grout penetration in fine to medium sand

(B) Good grout penetration in medium to coarse sand

(C) Difficult grout penetration in fine or already grouted sand

(D) Hydraulic fracturing

CHEMICAL GROUTING TEST PROGRAM

IDEALIZED GROUT PUMPING PRESSURE AND RATE RECORDS FOR ALLUVIAL GROUTING

FOUNDATION INVESTIGATION AND TEST PROGRAM
EXISTING LOCKS AND DAM No. 26
ST LOUIS DISTRICT, CORPS OF ENGINEERS.
DACW43-78-C-0005

Woodward-Clyde Consultants

Y7C625 Phase IV

Fig. 9.27

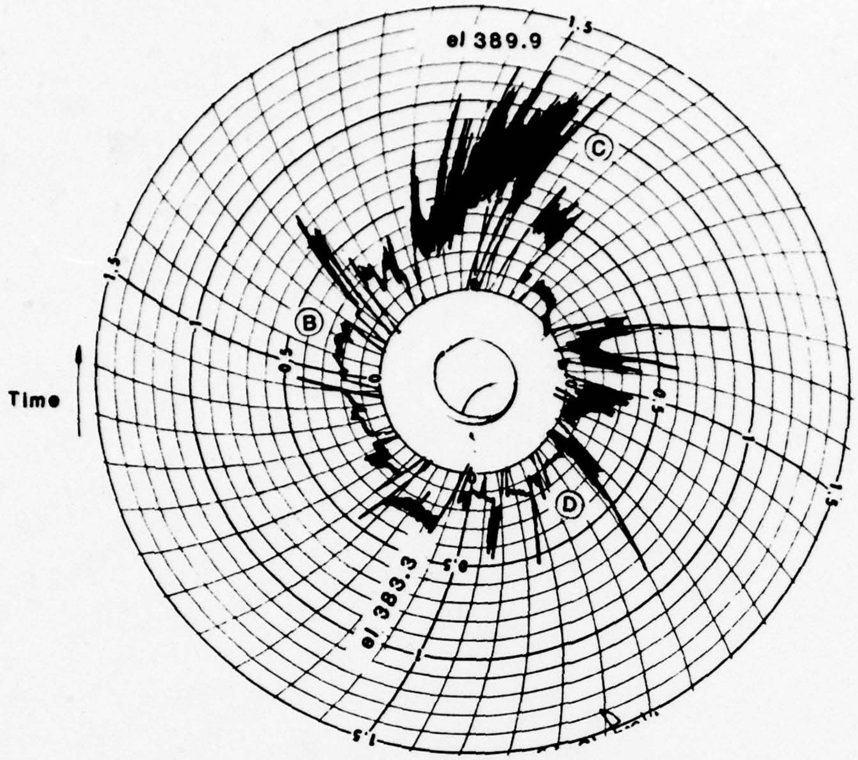

(a) 1 st Stage grouting-Grout Hole 8-4
(el 383.3 to el 398.6)

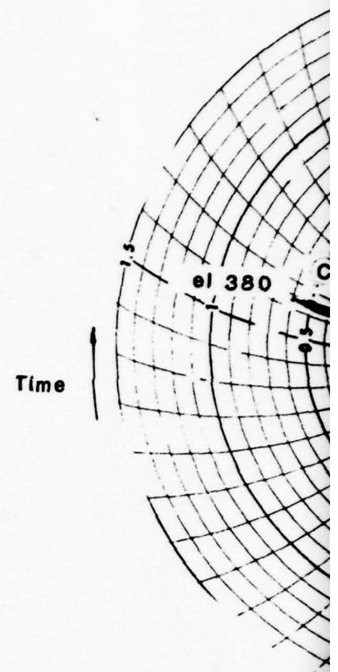

(b) 4 th S

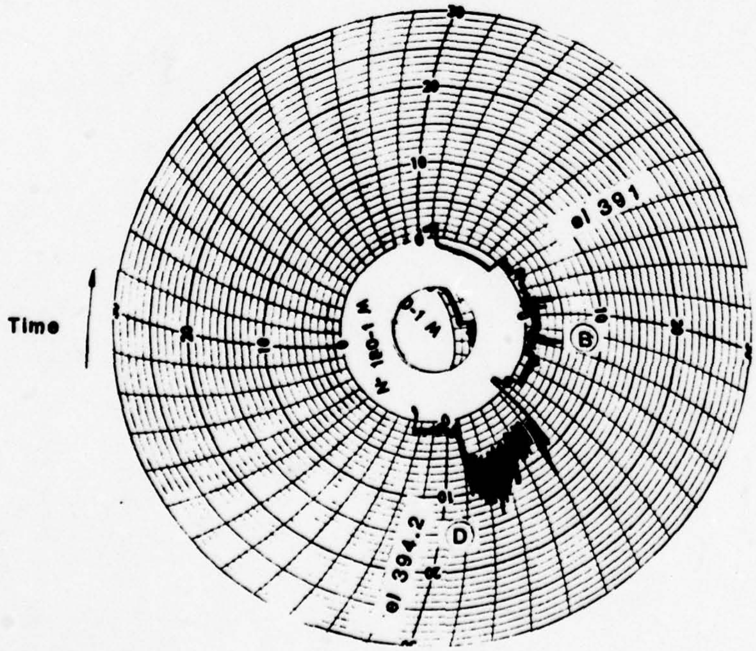

(c) 1 st Stage grouting-Grout Hole 11-8
(el 391 to el 394.2)

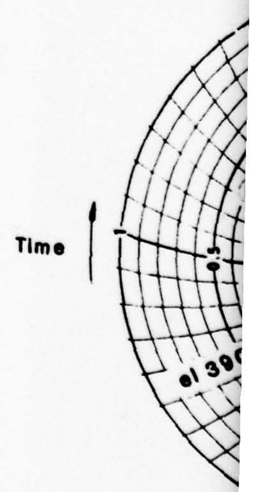

(d) 1 st

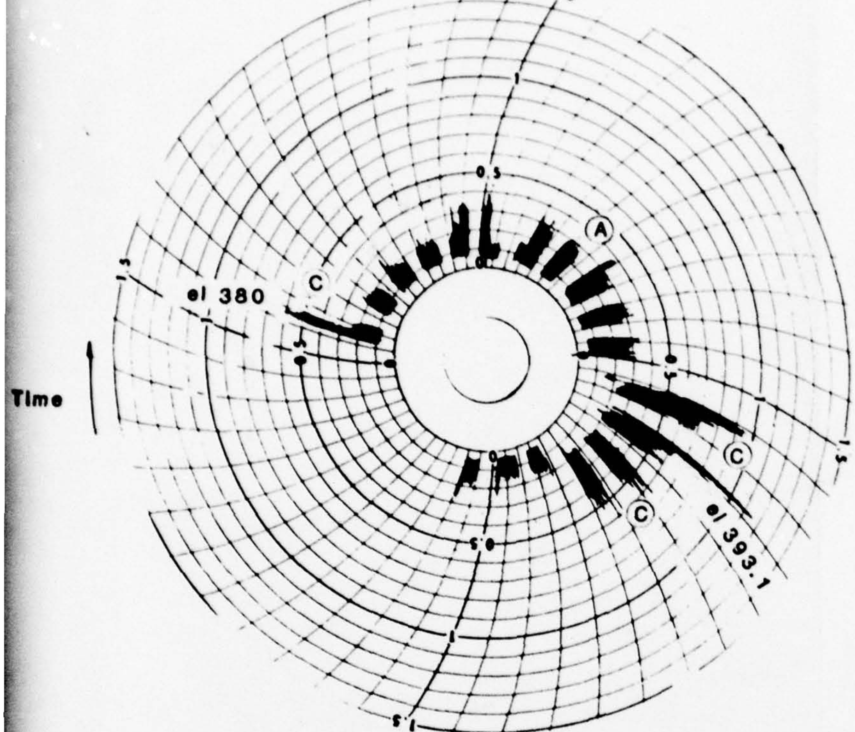

(b) 4 th Stage grouting-Grout Hole 12-1
(el 380 to el 400)

Ⓐ Good grout penetration in fine to medium sand

Ⓑ Good grout penetration in medium to coarse sand

Ⓒ Difficult grout penetration in fine or already grouted sand

Ⓓ Hydraulic fracturing

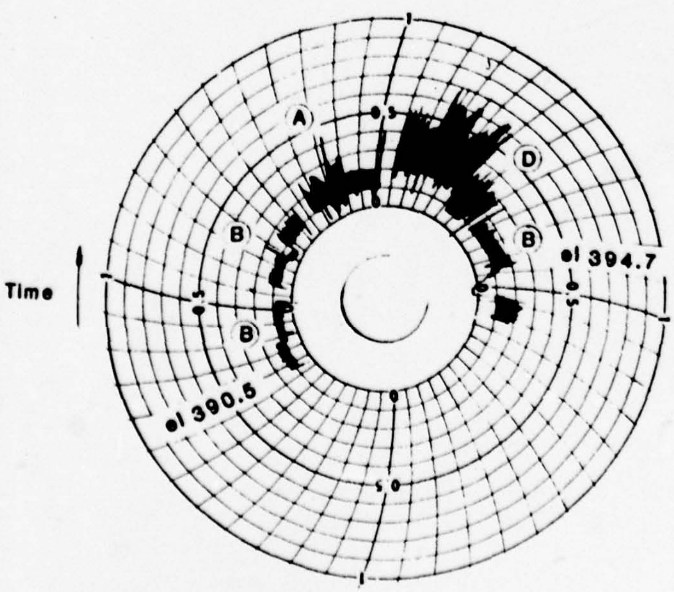

(d) 1 st Stage grouting-Grout Hole 12-1
(el 390.5 to el 394.7)

2

CHEMICAL GROUTING TEST PROGRAM

EXAMPLES AND INTERPRETATION OF ACTUAL GROUT PUMPING PRESSURE RECORDS

FOUNDATION INVESTIGATION AND TEST PROGRAM
EXISTING LOCKS AND DAM No. 26
ST LOUIS DISTRICT, CORPS OF ENGINEERS.
DACW43-78-C-0005

Woodward-Clyde Consultants

Fig. 9.28

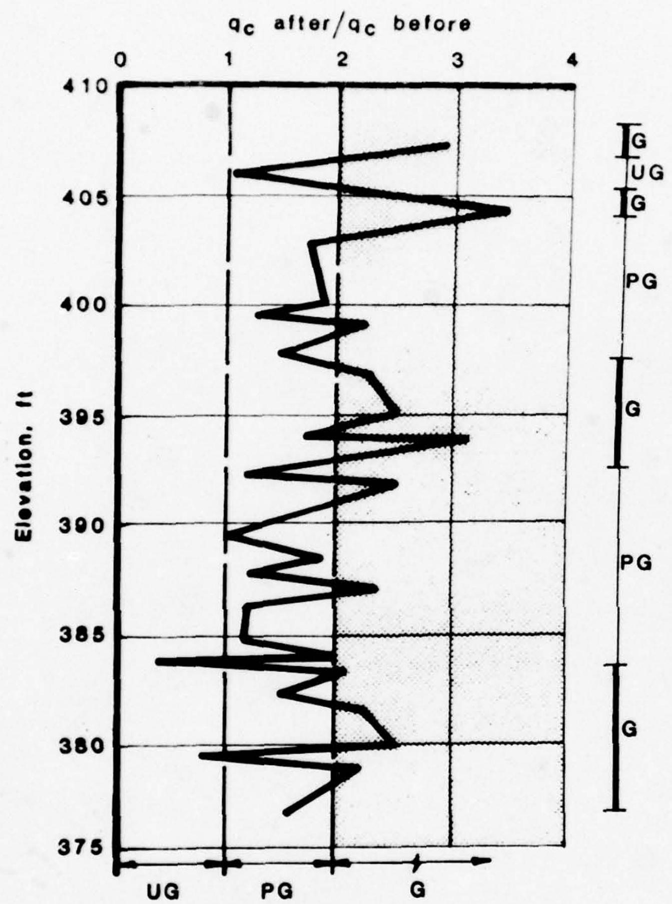

Boring AG-A8-3
Subarea 8
25% Silicate/Aluminate
Grouting method S_3
4-ft spacing

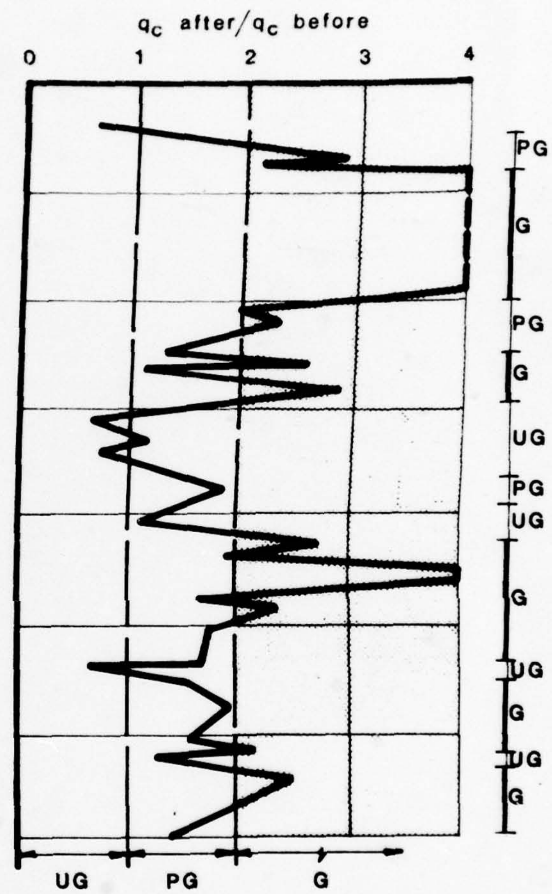

Boring AG-A3-2
Subarea 3
28% Silicate/R600
Grouting method S_2
6-ft spacing

Boring
Subare
45% S
Groutin
6-ft s

Legend

G Grouted soil

PG Poorly grouted soil

UG Ungrouted soil

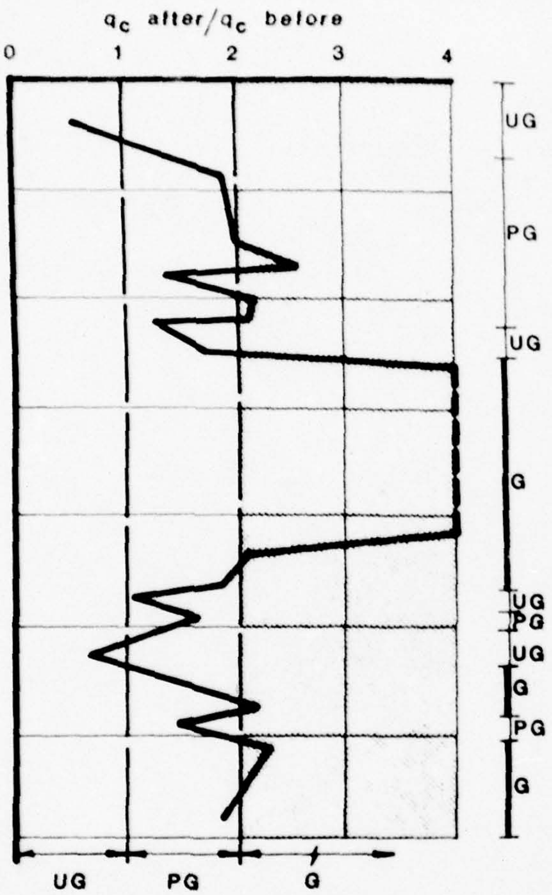

Boring AG-A5-21
Subarea 5
45% Siroc 132
Grouting method S_2
6-ft spacing

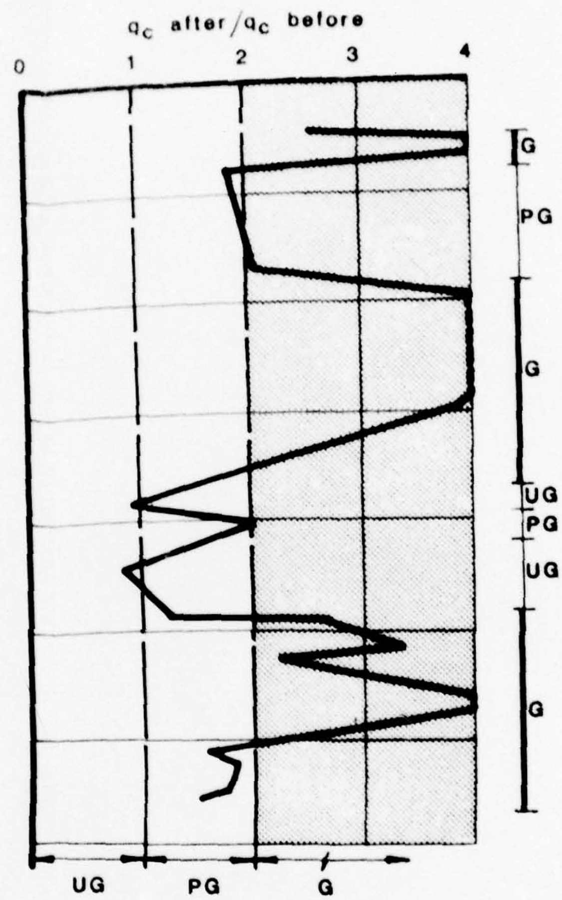

Boring AG-A9-2
Subarea 9
55% Siroc 132/142
Grouting method O_1
4-ft spacing

2

CHEMICAL GROUTING TEST PROGRAM

COMPARISON BETWEEN STATIC CONE PENETRATION RESISTANCE BEFORE AND AFTER GROUTING

FOUNDATION INVESTIGATION AND TEST PROGRAM
EXISTING LOCKS AND DAM No. 26
ST. LOUIS DISTRICT, CORPS OF ENGINEERS.
DACW43-78-C-0006

Woodward-Clyde Consultants

Y7C825 Phase IV

Fig. 9.29

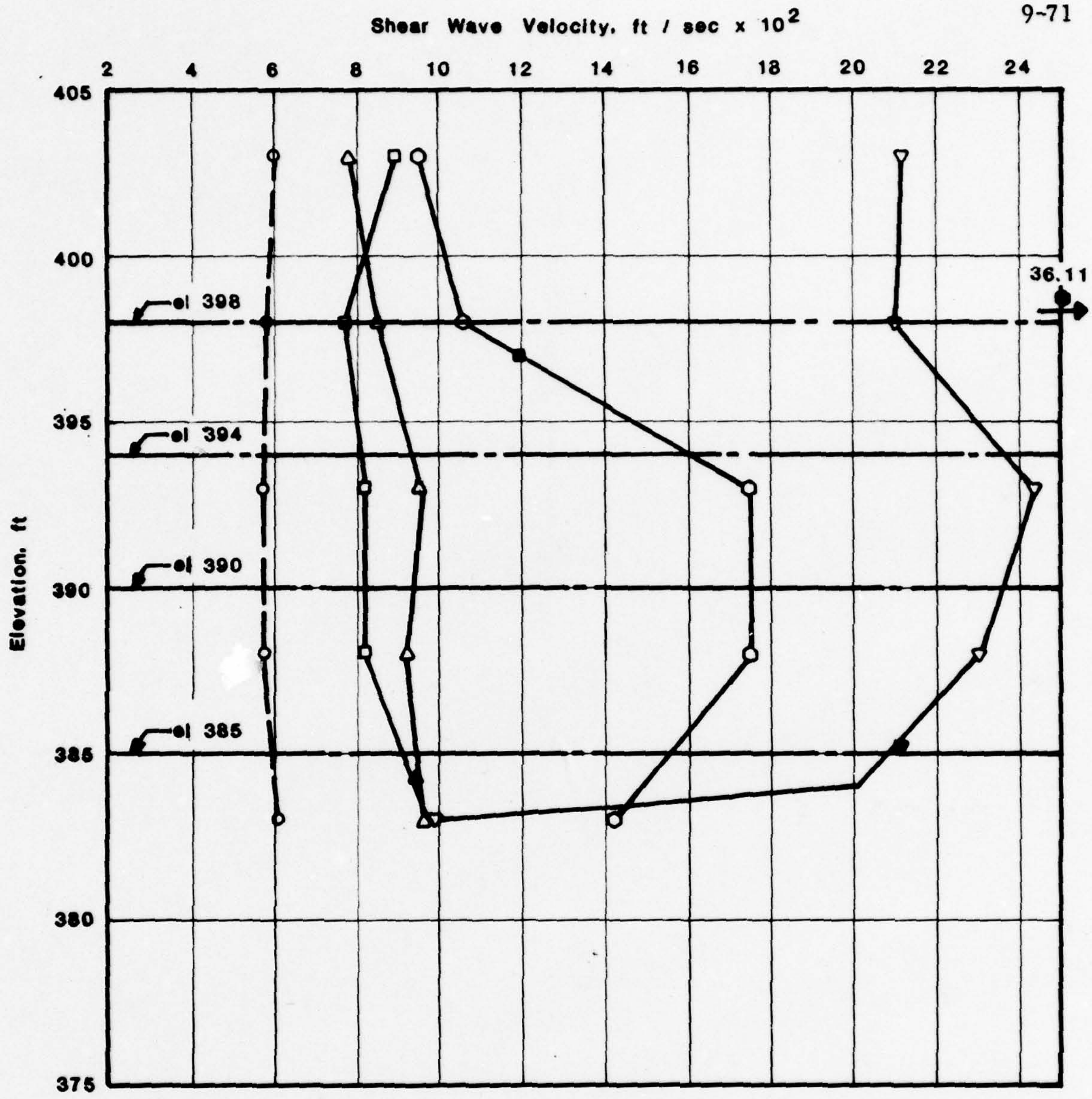

Legend

	Shear Wave Velocity	Lab Sonic Velocity
Average for Ungrouted Soil	○	
Subareas 1 and 9	□	■
Subareas 7 and 8	△	▲
Subareas 10 and 11	○	●
Subareas 12 and 13	▽	▼

CHEMICAL GROUTING TEST PROGRAM

SHEAR WAVE VELOCITY RESULTS FROM INSITU CROSSHOLE MEASUREMENTS AND LABORATORY SONIC VELOCITIES ON EXCAVATION BLOCK SAMPLES

FOUNDATION INVESTIGATION AND TEST PROGRAM
EXISTING LOCKS AND DAM No. 26
ST LOUIS DISTRICT, CORPS OF ENGINEERS.
DACW43-78-C-0005

Woodward-Clyde Consultants

Y7C625 Phase IX

Fig. 9.30

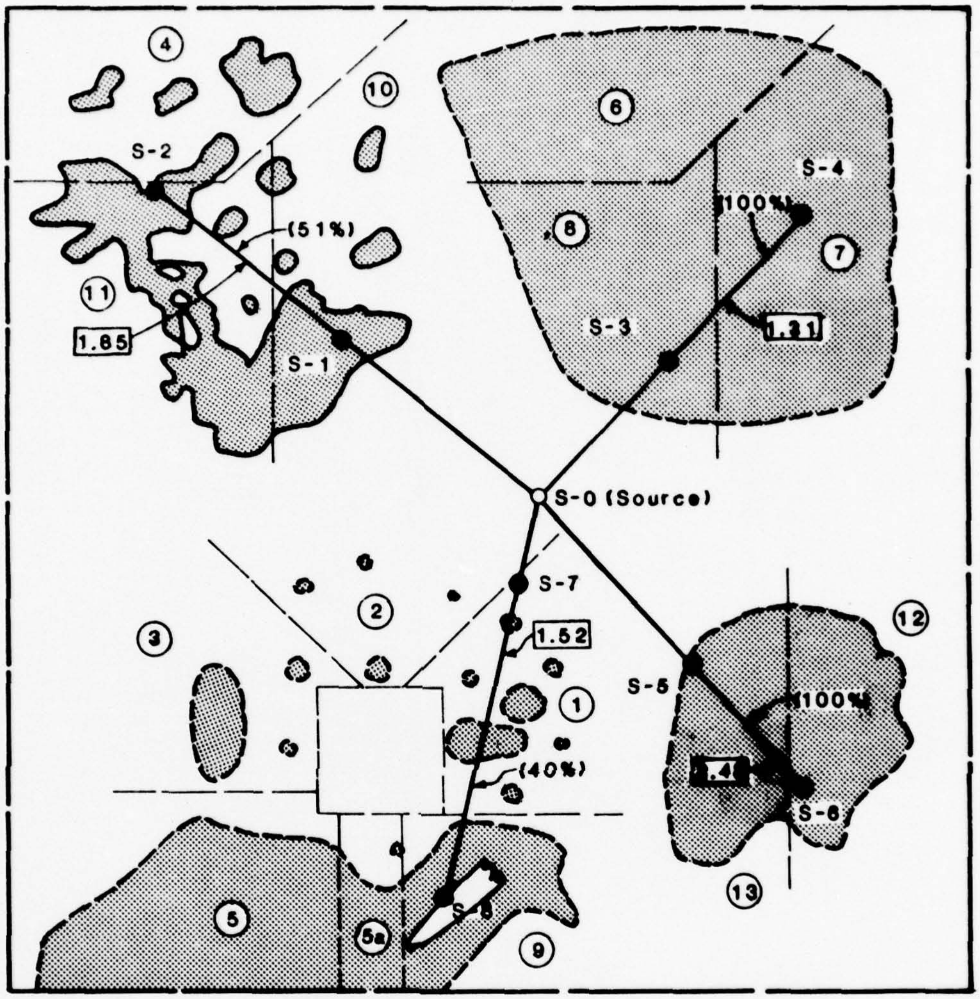

Legend

▬ ▬	Asphalt pad limits	(50%):	Soil mass along wave path is 50% grouted
— —	Test Subarea limits	1.74 :	Shear wave velocity is increased by 1.74 times after grouting
(3)	Test Subarea No.		
• S-1	Geophone location		
○ S-0	Source		

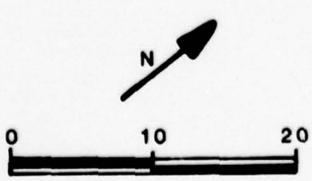

CHEMICAL GROUTING TEST PROGRAM

RELATIVE LOCATION OF GEOPHYSICAL ARRAYS AND GROUTED SOIL AT EL 398

FOUNDATION INVESTIGATION AND TEST PROGRAM
EXISTING LOCKS AND DAM No. 26
ST LOUIS DISTRICT, CORPS OF ENGINEERS.
DACW43-78-C-0005

Woodward-Clyde Consultants

Fig. 9.31

Y7C825 Phase IX

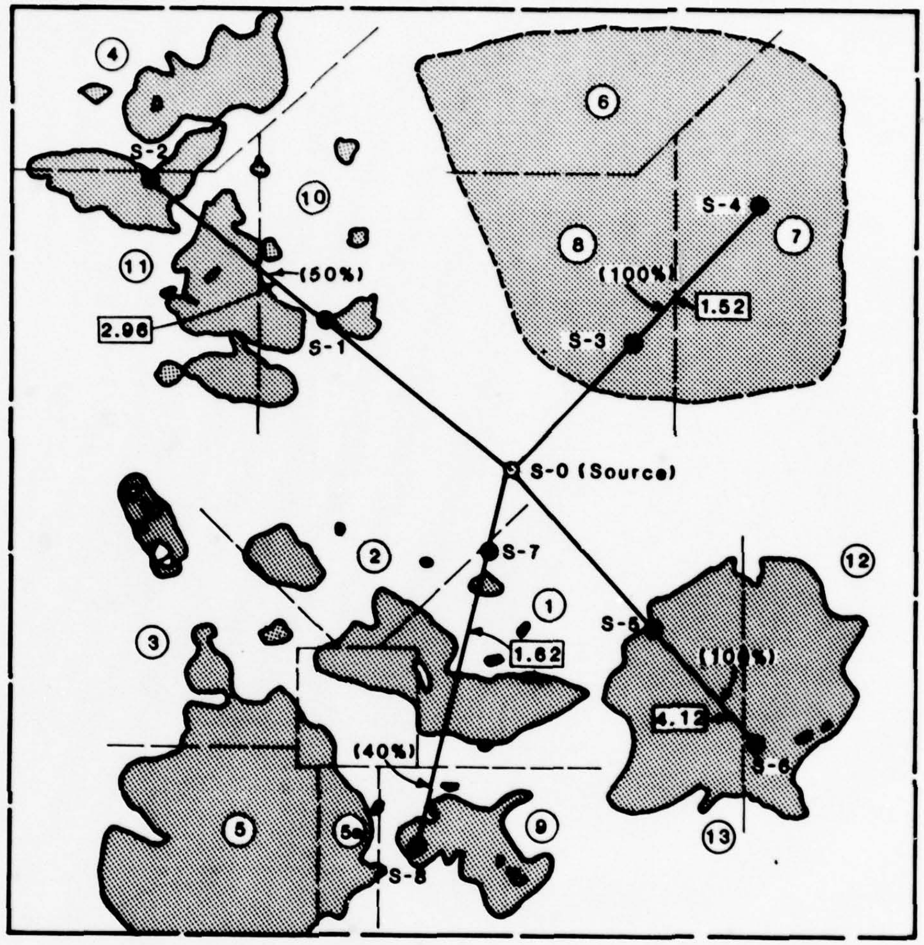

Legend

— —	Asphalt pad limits	(50%):	Soil mass along wave path is 50% grouted
— —	Test Subarea limits	1.74 :	Shear wave velocity is increased by 1.74 times after grouting
③	Test Subarea No.		
● S-1	Geophone location		
○ S-0	Source		

N

0 10 20

Scale, ft

CHEMICAL GROUTING TEST PROGRAM

RELATIVE LOCATION OF GEOPHYSICAL ARRAYS AND GROUTED SOIL AT EL 394

FOUNDATION INVESTIGATION AND TEST PROGRAM
EXISTING LOCKS AND DAM No. 26
ST LOUIS DISTRICT, CORPS OF ENGINEERS.
DACW43-78-C-0005

Woodward-Clyde Consultants

Fig. 9.32

YTC825 Phase IX

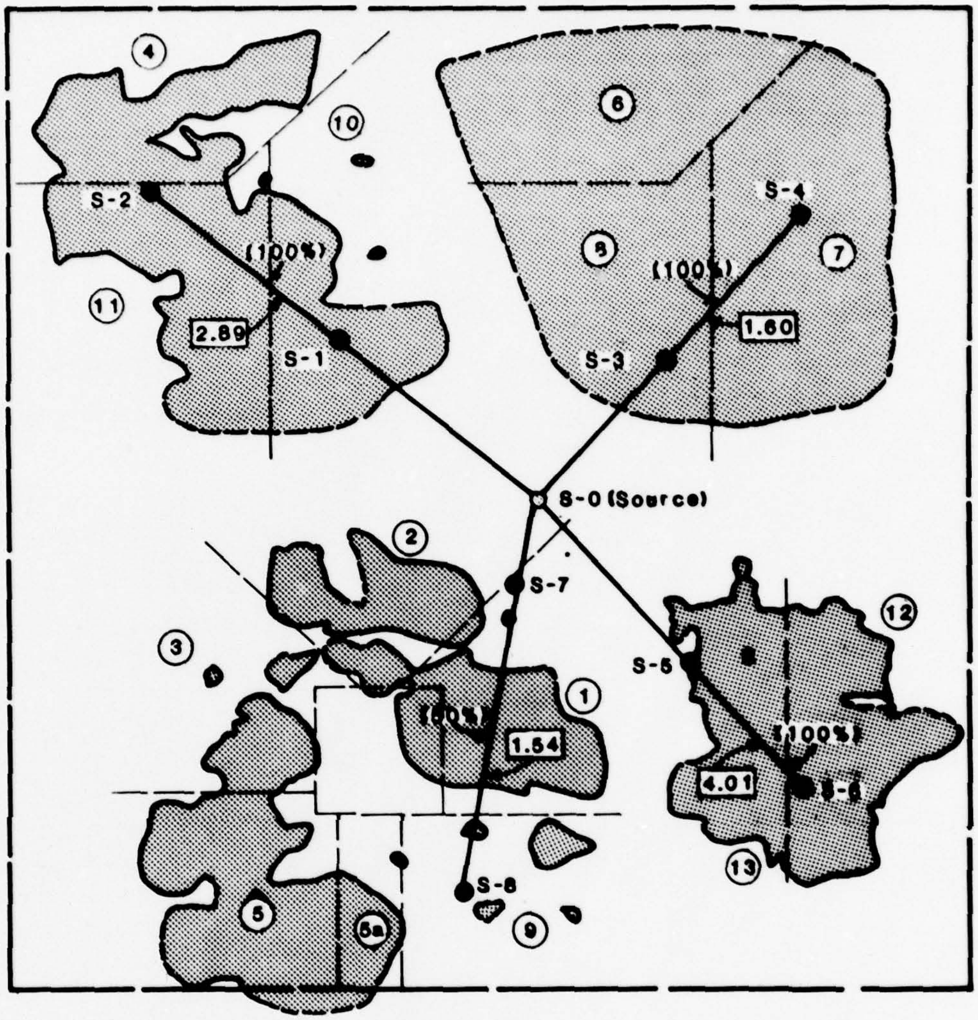

<u>Legend</u>

———	Asphalt pad limits	(50%):	Soil mass along wave path is 50% grouted
— —	Test Subarea limits	1.74 :	Shear wave velocity is increased by 1.74 times after grouting
(3)	Test Subarea No.		
• S-1	Geophone location		
○ S-0	Source		

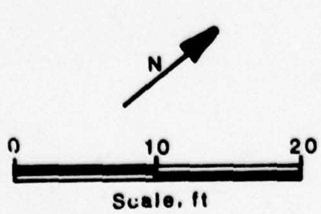

CHEMICAL GROUTING TEST PROGRAM

RELATIVE LOCATION OF GEOPHYSICAL ARRAYS AND GROUTED SOIL AT EL 390

FOUNDATION INVESTIGATION AND TEST PROGRAM
EXISTING LOCKS AND DAM No. 26
ST LOUIS DISTRICT, CORPS OF ENGINEERS.
DACW43-78-C-0008

Woodward-Clyde Consultants

Y7C825 Phase IX

Fig. 9.33

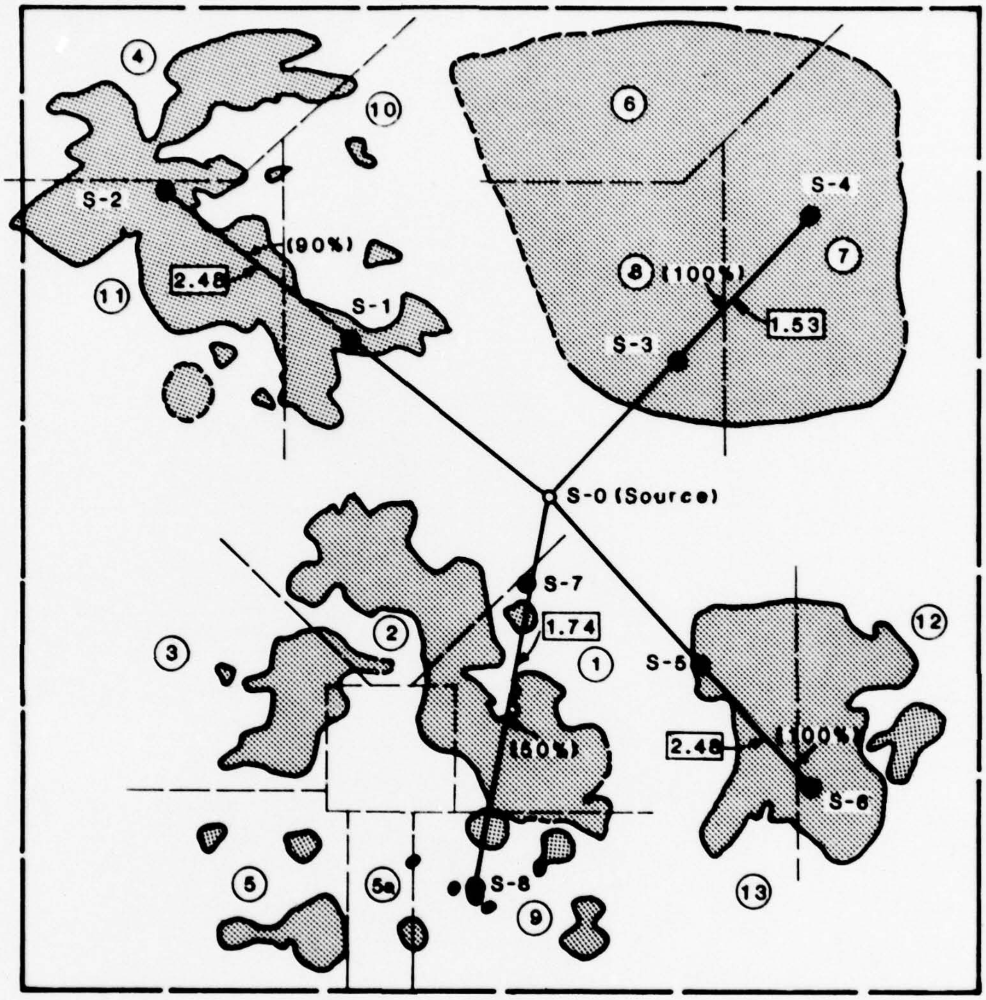

Legend

Asphalt pad limits	
Test Subarea limits	
3	Test Subarea No.
S-1	Geophone location
S-0	Source
(50%):	Soil mass along wave path is 50% grouted
1.74 :	Shear wave velocity is increased by 1.74 times after grouting

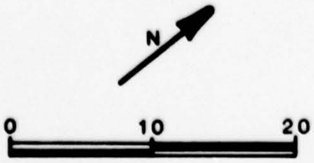

CHEMICAL GROUTING TEST PROGRAM

RELATIVE LOCATION OF GEOPHYSICAL ARRAYS AND GROUTED SOIL AT EL 385

FOUNDATION INVESTIGATION AND TEST PROGRAM
EXISTING LOCKS AND DAM No. 26
ST LOUIS DISTRICT, CORPS OF ENGINEERS.
DACW43-78-C-0005

Woodward-Clyde Consultants

Fig. 9.34

Y7C825 Phase IX

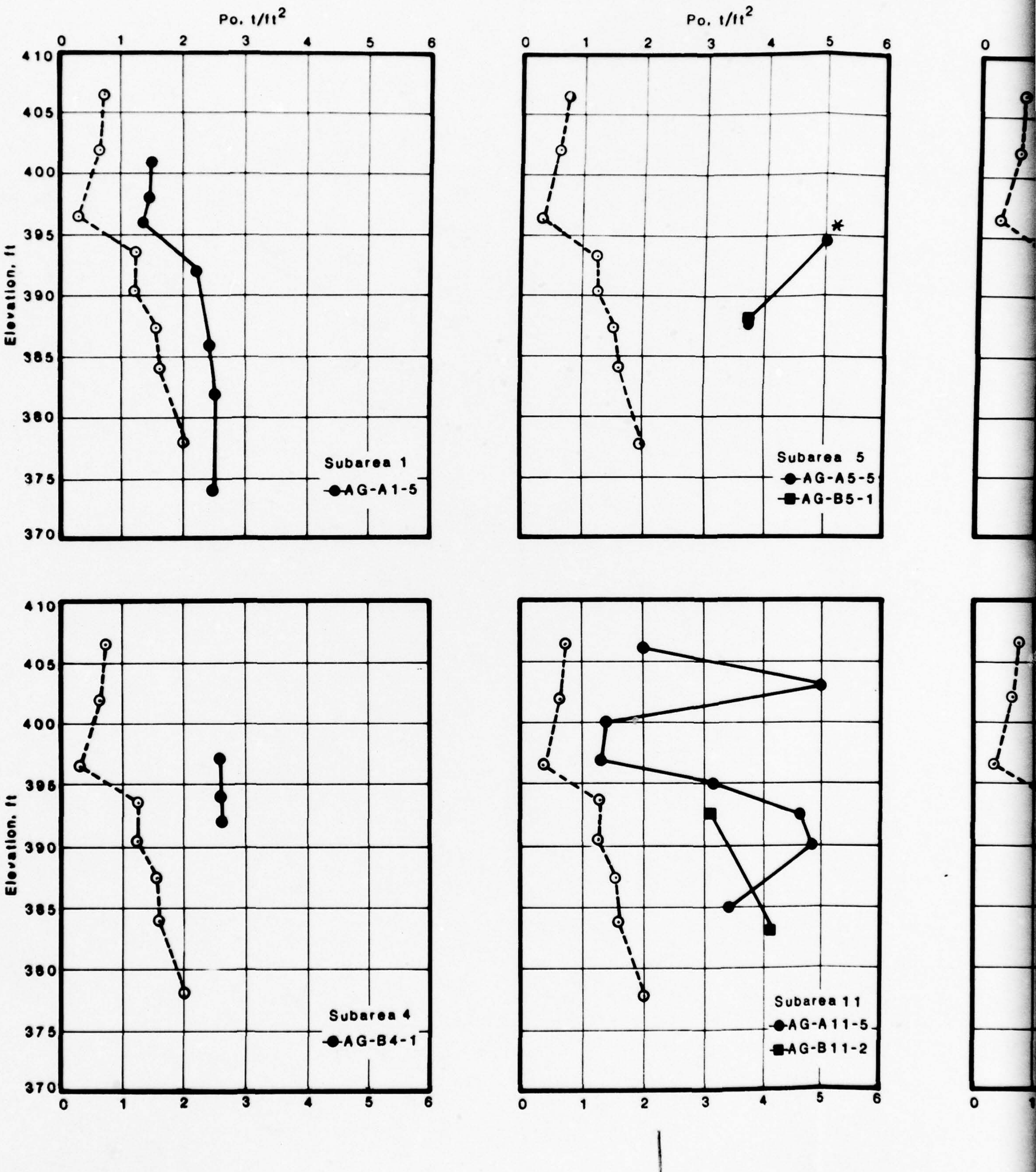

Po, t/ft²
Elevation, ft
Subarea 1
AG-A1-5
Subarea 5
AG-A5-5
AG-B5-1
*
Subarea 4
AG-B4-1
Subarea 11
AG-A11-5
AG-B11-2

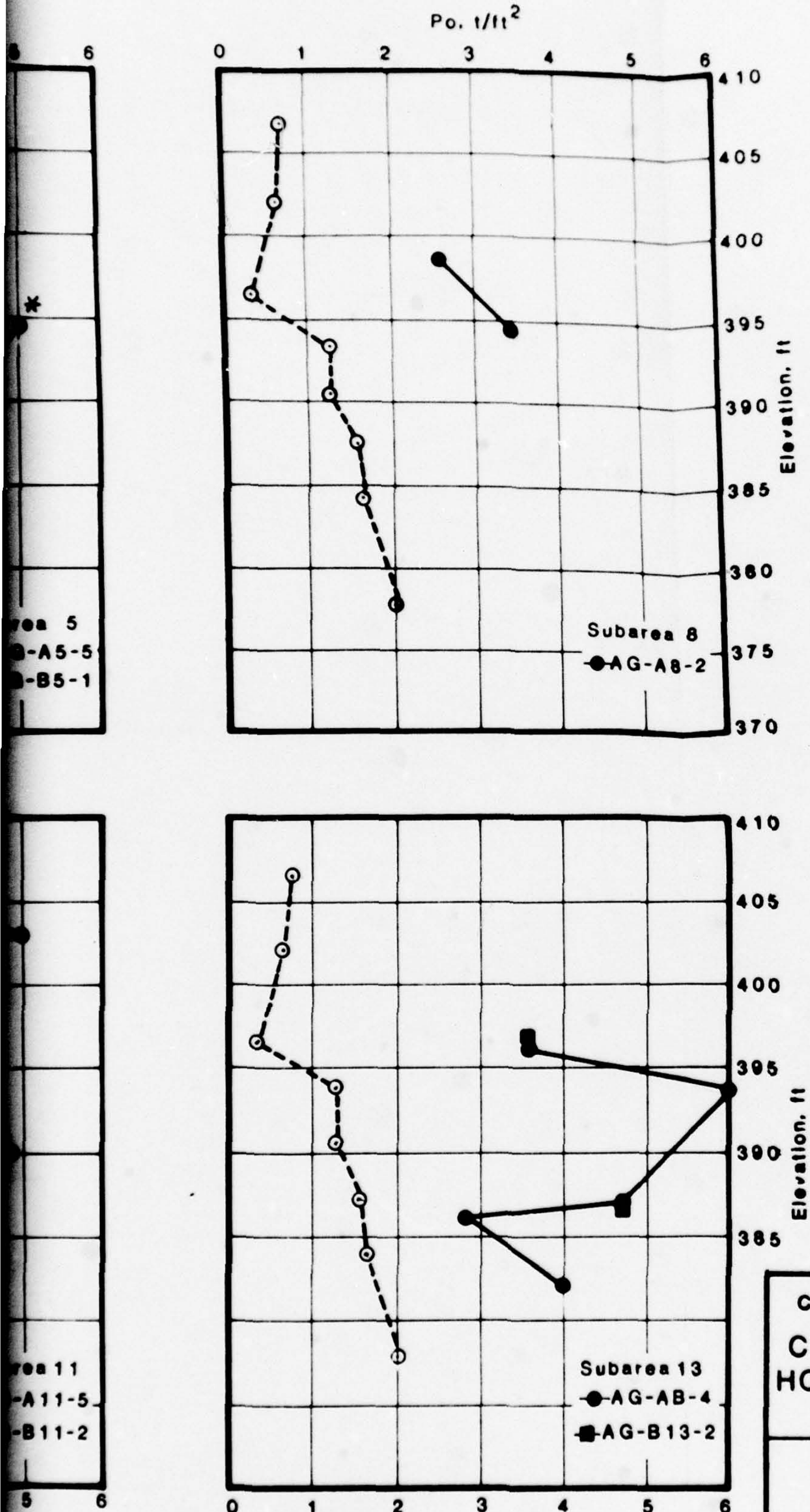

Legend

After grouting

Before grouting Boring (D-27)

* Probe seating difficulty

CHEMICAL GROUTING TEST PROGRAM

COMPARISON BETWEEN IN SITU HORIZONTAL STRESS P_o BEFORE AND AFTER GROUTING

FOUNDATION INVESTIGATION AND TEST PROGRAM
EXISTING LOCKS AND DAM No. 26
ST LOUIS DISTRICT, CORPS OF ENGINEERS.
DACW43-78-C-0005

Woodward-Clyde Consultants
Y7C825 Phase IX

Fig. 9.35

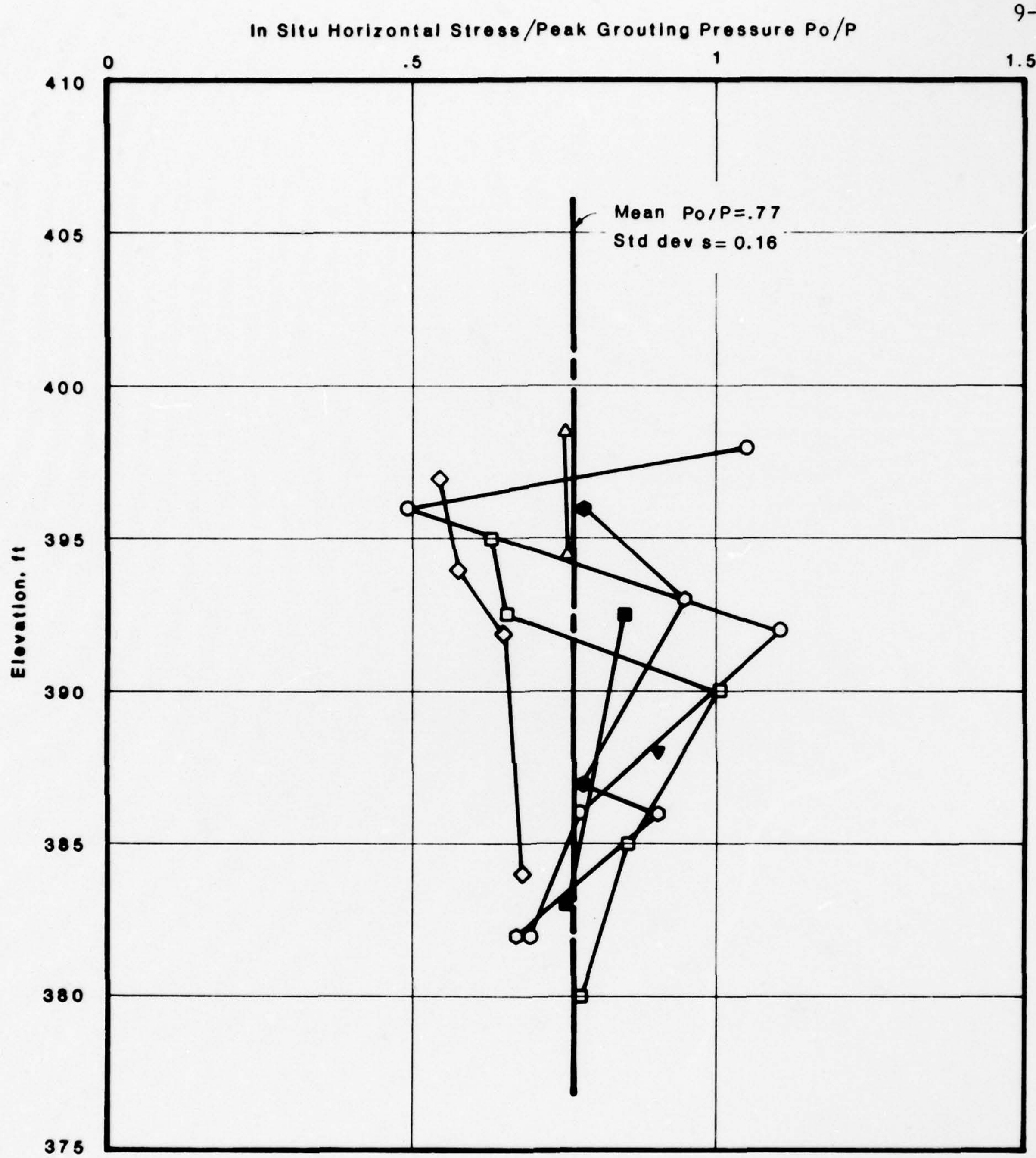

Subarea	el 423	el 402
1	○ AG-A1-5	
4		◇ AG-B4-1
5		▼ AG-B5-1
8	△ AG-A8-2	
11	□ AG-A11-5	■ AG-B11-2
13	⬡ AG-A13-4	⬢ AG-B13-2

CHEMICAL GROUTING TEST PROGRAM

COMPARISON OF GROUTING PRESSURE AND AFTER-GROUTING IN SITU HORIZONTAL STRESS

FOUNDATION INVESTIGATION AND TEST PROGRAM
EXISTING LOCKS AND DAM No. 26
ST LOUIS DISTRICT, CORPS OF ENGINEERS.
DACW43-78-C-0005

Woodward-Clyde Consultants
Y7C825 Phase IX

Fig. 9.36

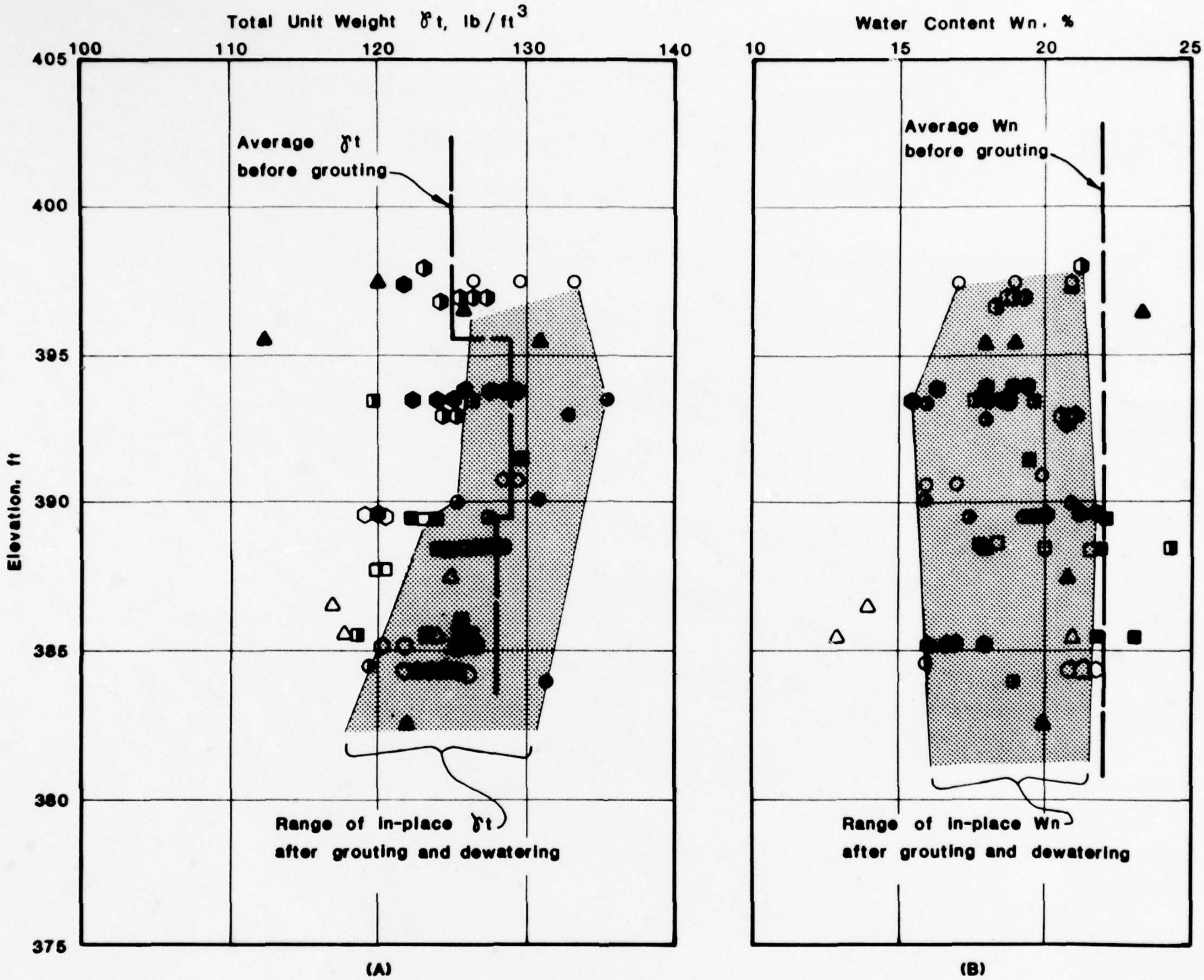

Legend

○ In-place density test

Pitcher undisturbed sample

□ Plymouth Meeting, PA. Lab

△ Kansas City, Mo. Lab

Excavation block and core sample

⬡ Clifton, N.J. Lab

Grout type

○ Low strength

◑ Medium strength

● High strength

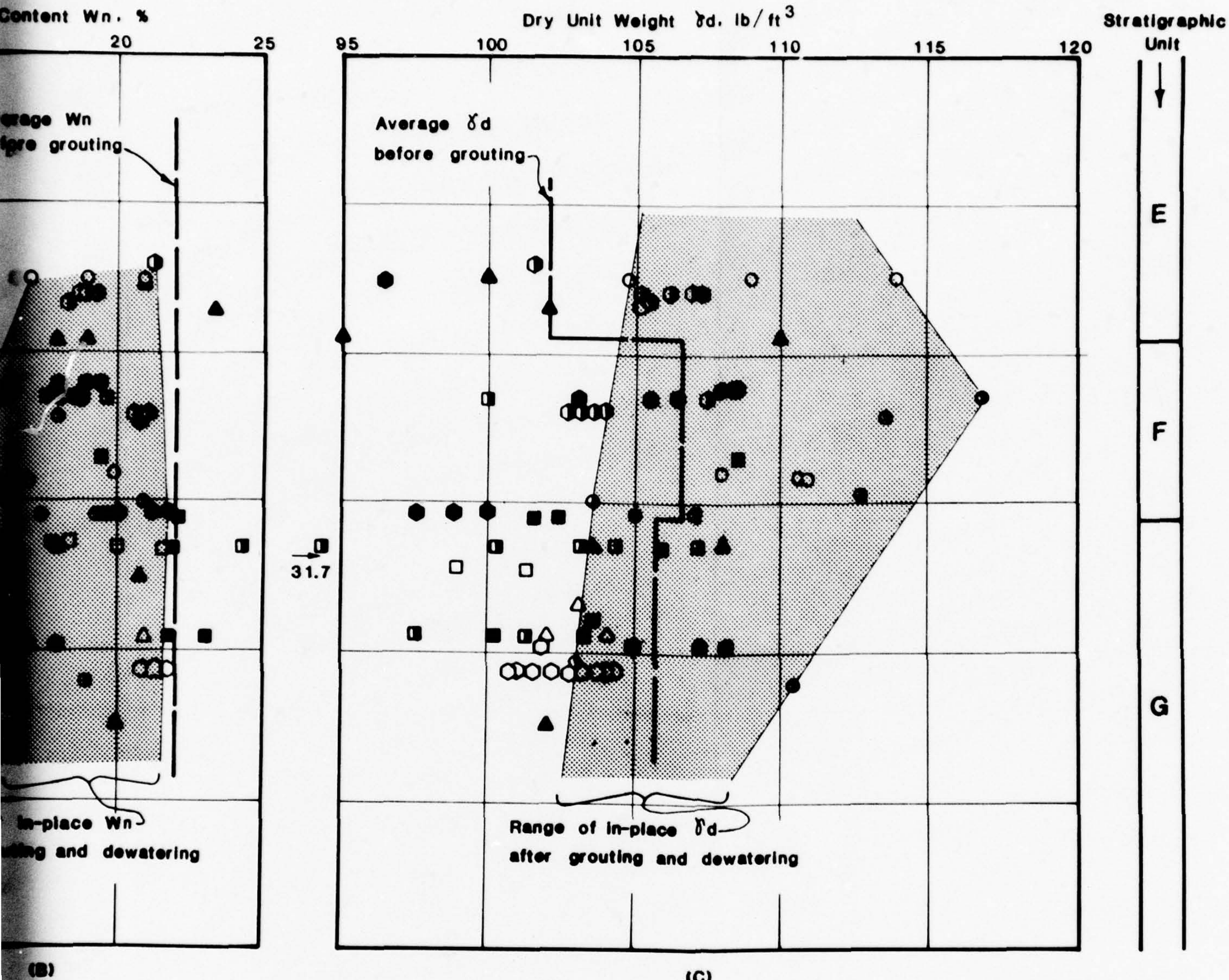

CHEMICAL GROUTING TEST PROGRAM

COMPARISON BETWEEN SOIL UNIT WEIGHT AND WATER CONTENT BEFORE AND AFTER GROUTING

FOUNDATION INVESTIGATION AND TEST PROGRAM
EXISTING LOCKS AND DAM No. 26
ST LOUIS DISTRICT, CORPS OF ENGINEERS.
DACW43-78-C-0005

Woodward-Clyde Consultants
Y7C825 Phase IX

Fig. 9.37

Elastic Deformation Modulus

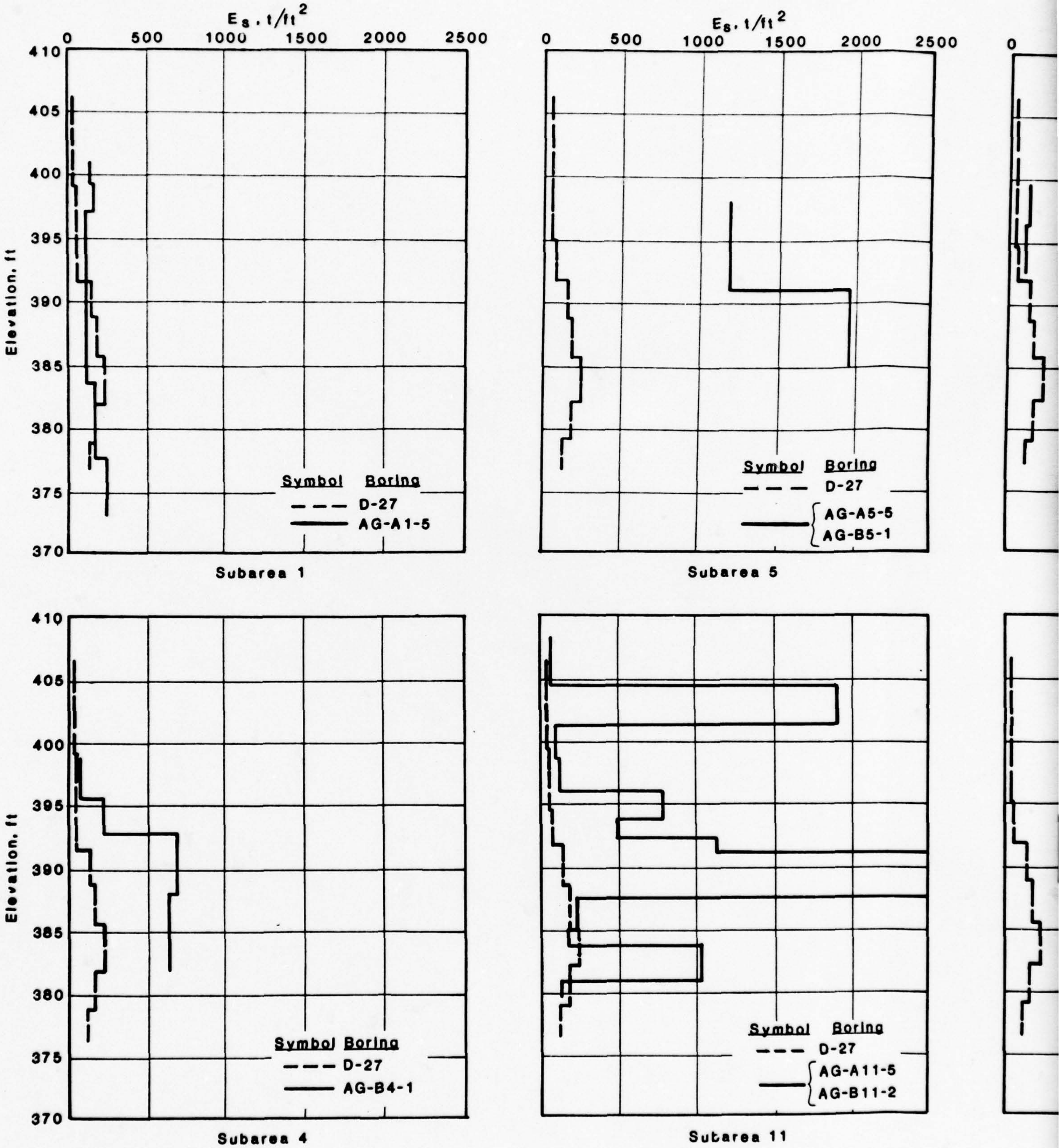

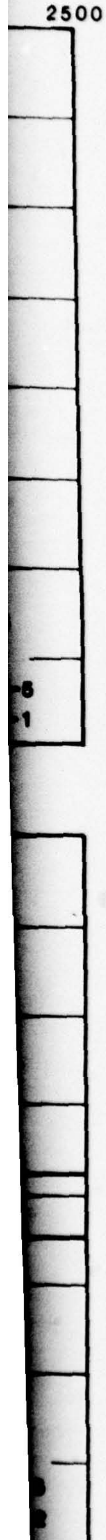

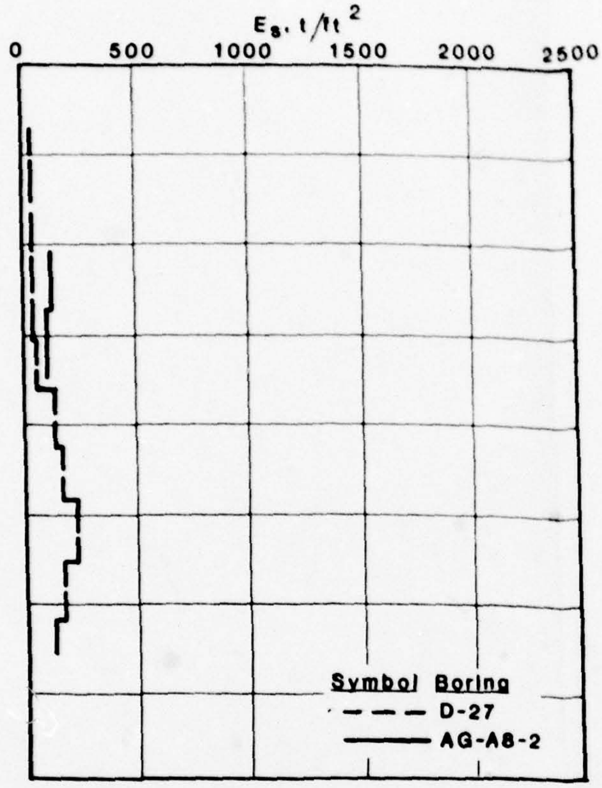

Subarea 8

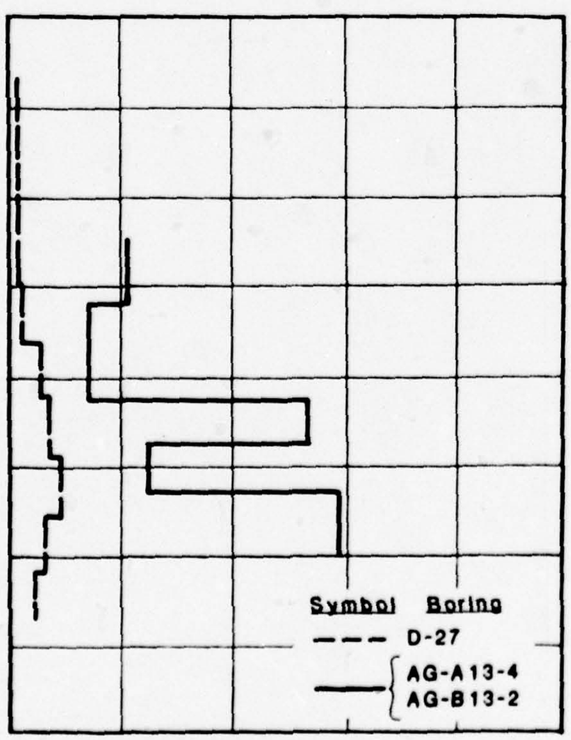

Subarea 13

Legend

——— Modulus after grouting

– – – Modulus before grouting

2

CHEMICAL GROUTING TEST PROGRAM

COMPARISON BETWEEN ELASTIC DEFORMATION MODULUS FROM PRESSUREMETER TESTS BEFORE AND AFTER GROUTING

FOUNDATION INVESTIGATION AND TEST PROGRAM
EXISTING LOCKS AND DAM No. 26
ST. LOUIS DISTRICT, CORPS OF ENGINEERS
DACW43-78-C-0005

Woodward-Clyde Consultants

YTC825 Phase II

Fig. 9.38

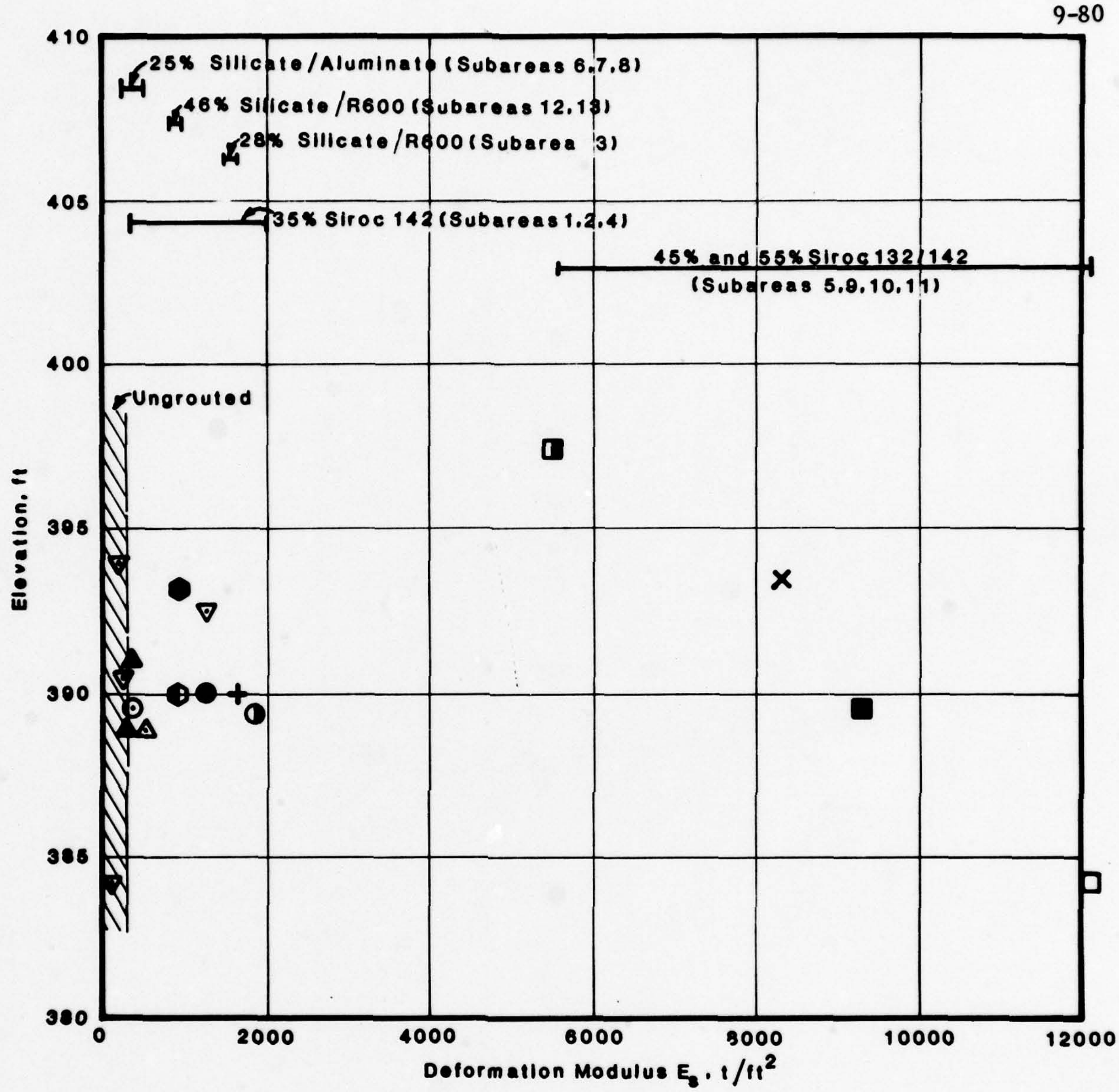

Legend

Symbol	Subarea
○	1
◐	2
+	3
●	4
×	5
△	6
▲	7
▲	8
◧	9
□	10
⬢	12
⬡	13
▽	Ungrouted

CHEMICAL GROUTING TEST PROGRAM

COMPARISON BETWEEN DEFORMATION MODULUS FROM PLATE LOAD TESTS

FOUNDATION INVESTIGATION AND TEST PROGRAM
EXISTING LOCKS AND DAM No. 26
ST LOUIS DISTRICT, CORPS OF ENGINEERS.
DACW43-78-C-0005

Woodward-Clyde Consultants

Y7C825 Phase IX

Fig. 9.39

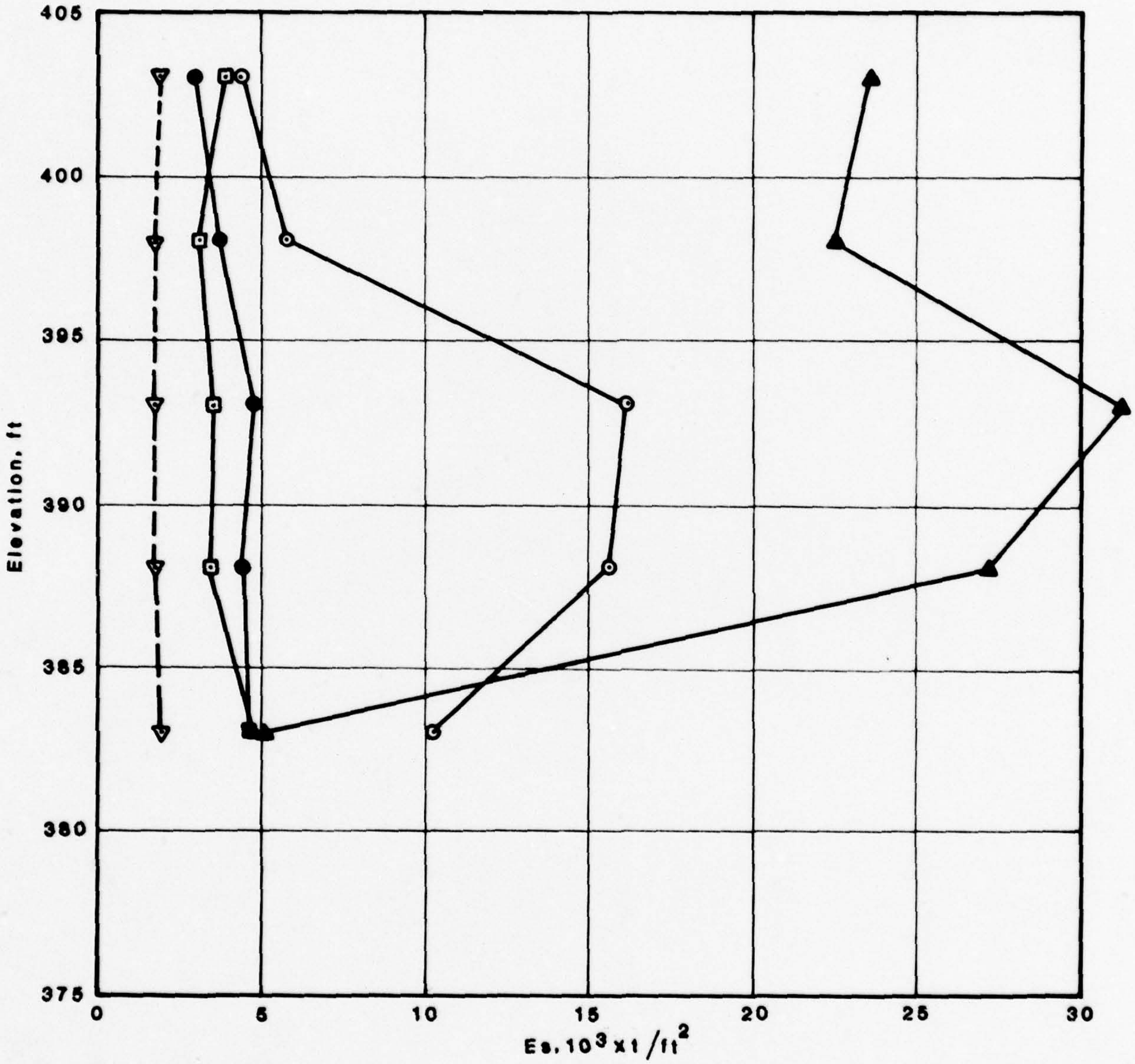

Legend

Array	Test Subareas
⊙ S1-S2	10 and 11
● S3-S4	8 and 7
▲ S5-S6	12 and 13
⊡ S7-S8	1 and 9

▽–▽ Average before grouting

CHEMICAL GROUTING TEST PROGRAM

COMPARISON BETWEEN ELASTIC DEFORMATION MODULUS FROM SHEAR WAVE VELOCITY MEASUREMENTS

FOUNDATION INVESTIGATION AND TEST PROGRAM
EXISTING LOCKS AND DAM No. 26
ST LOUIS DISTRICT, CORPS OF ENGINEERS.
DACW43-78-C-0006

Woodward-Clyde Consultants

Y7C825 Phase IX

Fig. 9.40

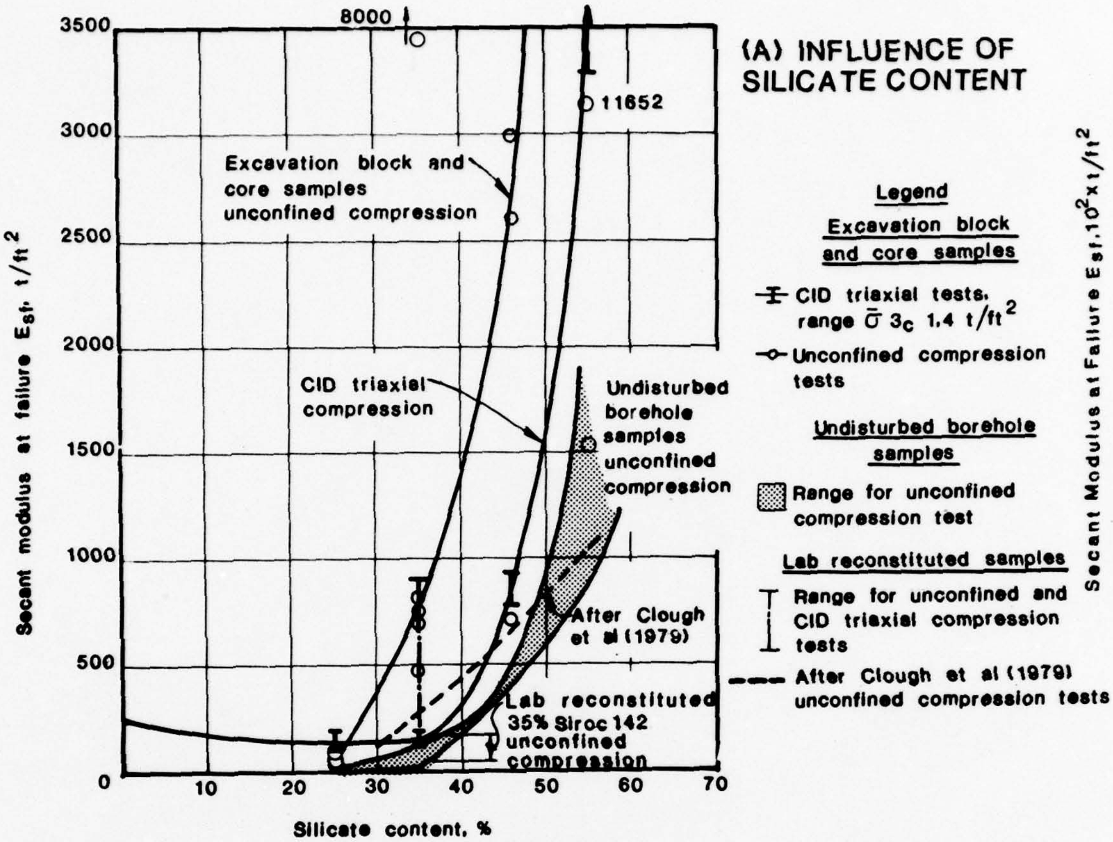

(A) INFLUENCE OF SILICATE CONTENT

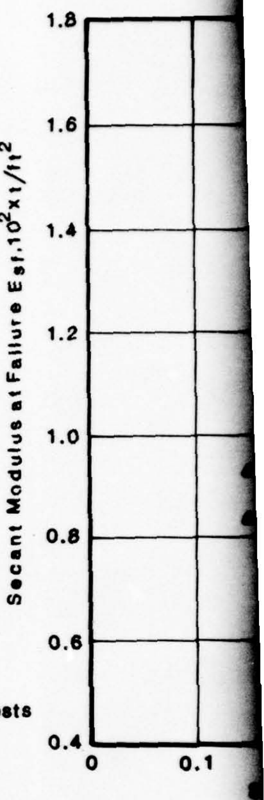

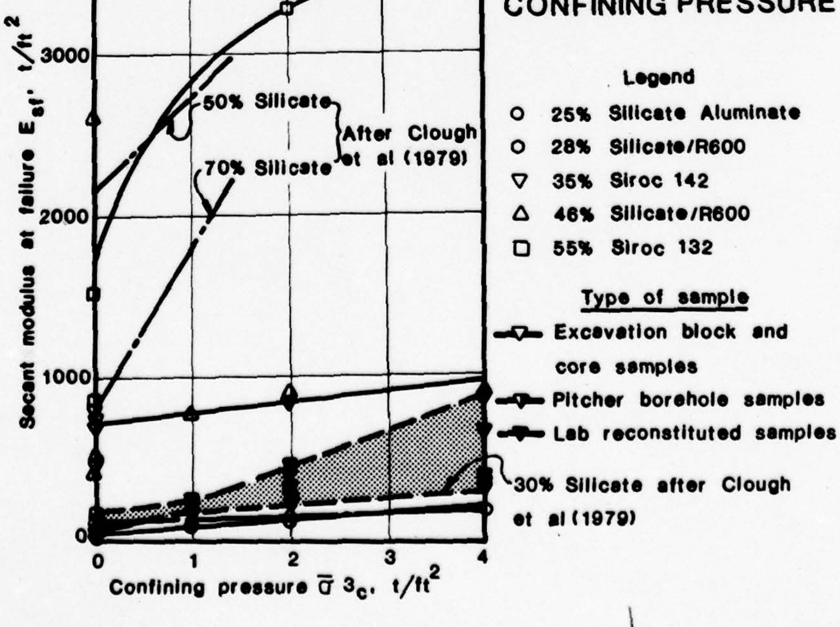

(C) INFLUENCE OF CONFINING PRESSURE

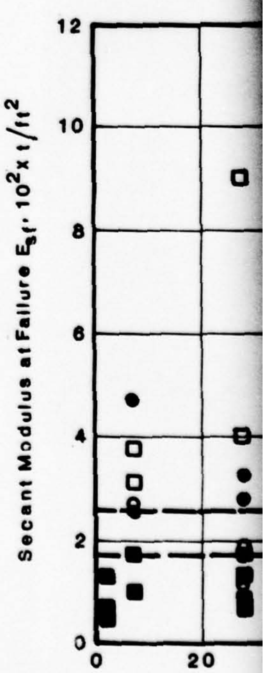

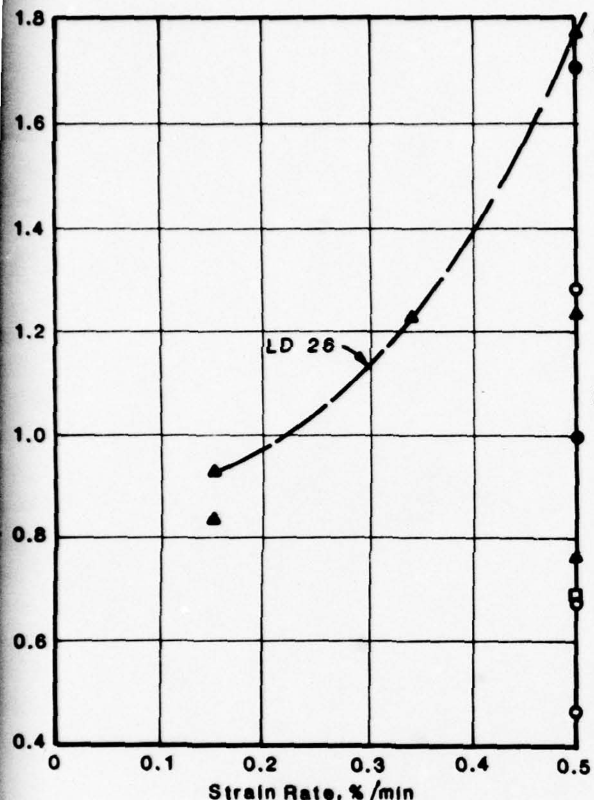

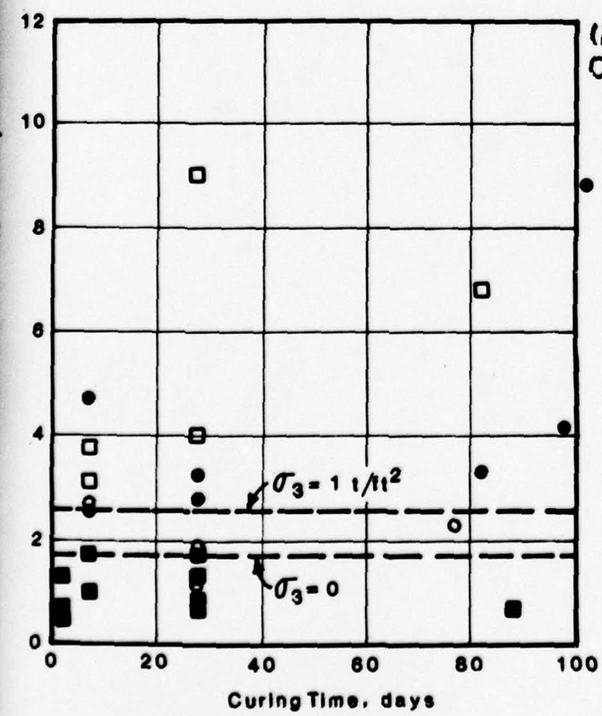

2

CHEMICAL GROUTING TEST PROGRAM

INFLUENCE OF VARIOUS FACTORS ON LABORATORY ELASTIC DEFORMATION MODULUS

FOUNDATION INVESTIGATION AND TEST PROGRAM
EXISTING LOCKS AND DAM No. 26
ST LOUIS DISTRICT, CORPS OF ENGINEERS.
DACW43-78-C-0005

Woodward-Clyde Consultants | Fig. 9.41

Y7C825 Phase IX

Scale, ft

DACW43-78-C-0005

Woodward-Clyde Consultants

Y7C825 Phase IX

Fig. 9.32

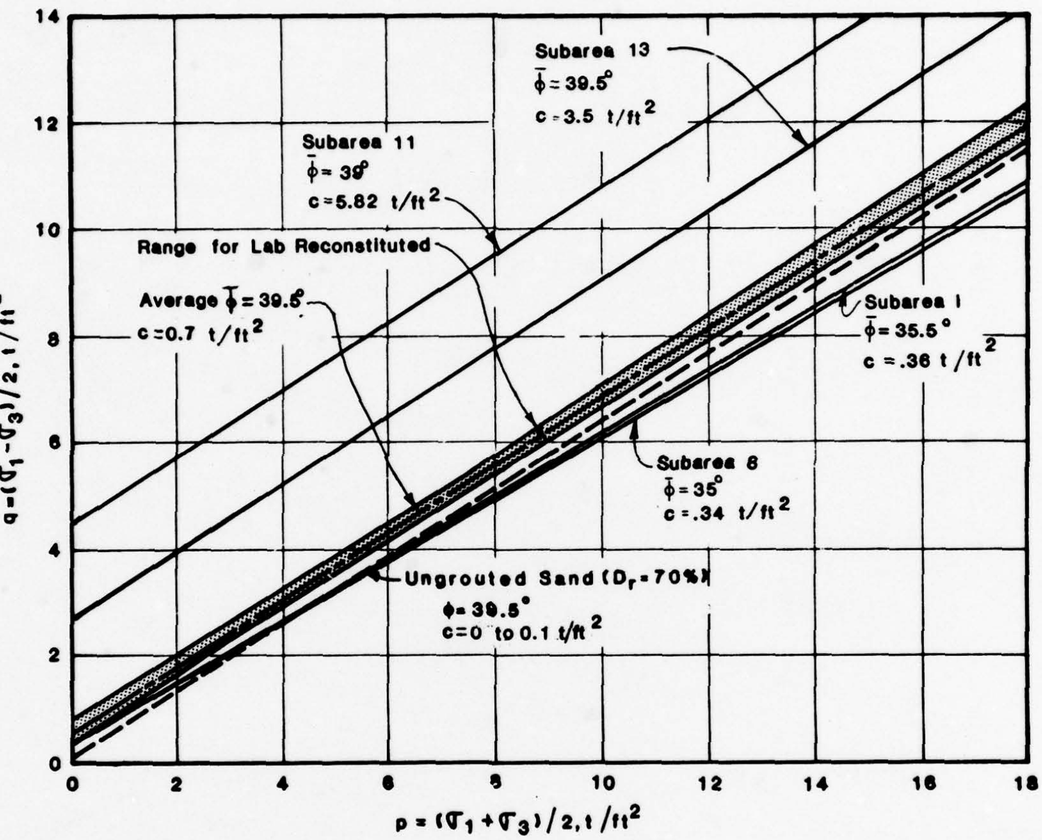

$\sin \phi = \tan \alpha \qquad c = \frac{a}{\cos \phi}$

Notes

Samples tested were:

(1) Undisturbed Osterberg samples taken before grouting

(2) Ungrouted reconstituted sand sample

(3) Reconstituted sand samples grouted in the laboratory with 35% Siroc 142

(4) Grouted excavation block and core samples

CHEMICAL GROUTING TEST PROGRAM

INTERPRETATION OF $\overline{\text{CID}}$ TRIAXIAL TESTS ON UNGROUTED AND GROUTED SAND SAMPLES

FOUNDATION INVESTIGATION AND TEST PROGRAM
EXISTING LOCKS AND DAM No. 26
ST LOUIS DISTRICT, CORPS OF ENGINEERS.
DACW43-78-C-0005

Woodward-Clyde Consultants

Y7C825 Phase IX

Fig. 9.42

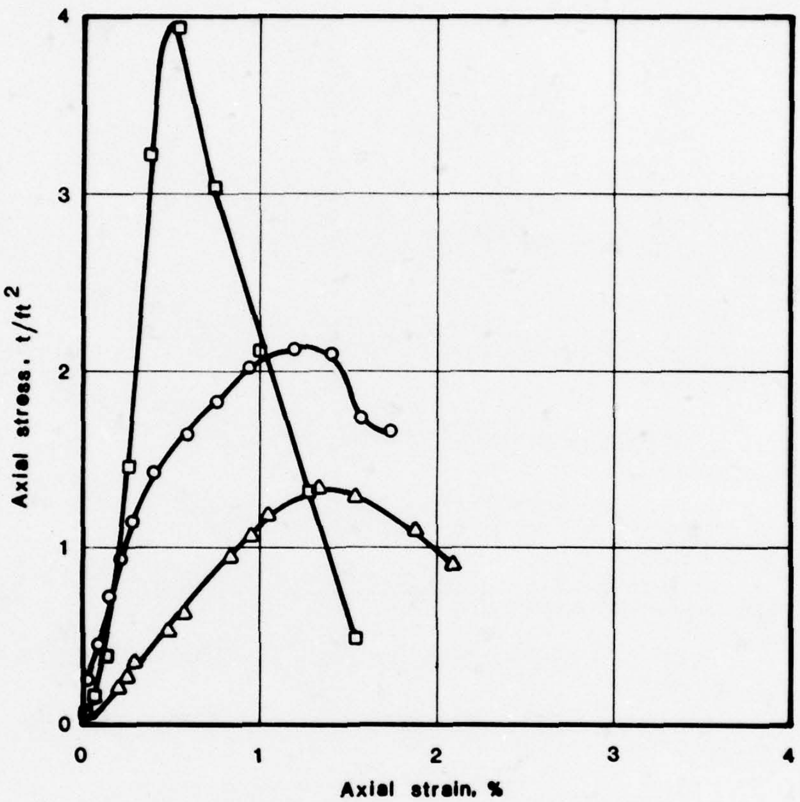

Legend

□ Excavation block samples

○ Lab reconstituted samples

△ Undisturbed borehole samples

CHEMICAL GROUTING TEST PROGRAM

STRESS-STRAIN CURVES FROM UNCONFINED COMPRESSION TESTS FIELD AND LABORATORY SAMPLES GROUTED WITH 35% SIROC 142

FOUNDATION INVESTIGATION AND TEST PROGRAM
EXISTING LOCKS AND DAM No. 26
ST LOUIS DISTRICT, CORPS OF ENGINEERS.
DACW43-78-C-0005

Woodward-Clyde Consultants
Y7C825 Phase IX

Fig. 9.43

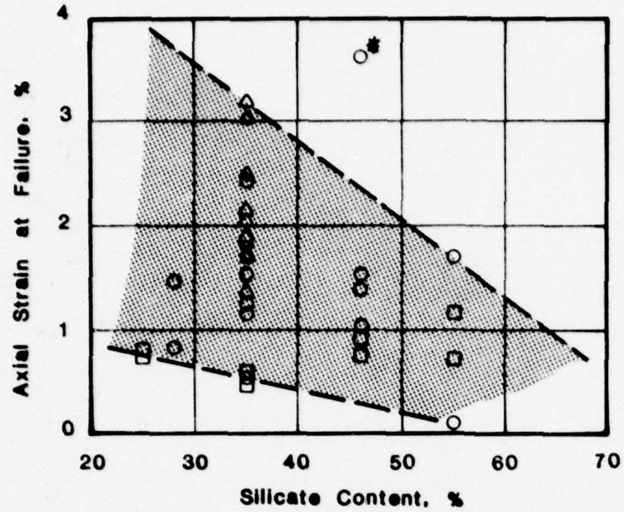

(A) INFLUENCE OF STRAIN AT FAILURE

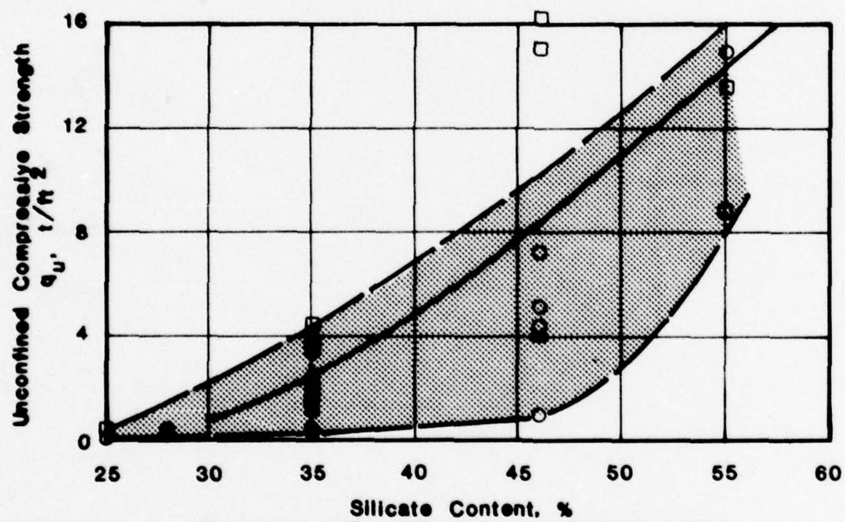

(B) INFLUENCE ON UNCONFINED COMPRESSIVE STRENGTH

Legend

- ○ Undisturbed borehole samples
- △ Lab reconstituted samples
- □ Excavation block and core samples
- * Fracture in samples

CHEMICAL GROUTING TEST PROGRAM

INFLUENCE OF GROUT SILICATE CONTENT ON UNCONFINED STRESS-STRAIN CHARACTERISTICS

FOUNDATION INVESTIGATION AND TEST PROGRAM
EXISTING LOCKS AND DAM No. 26
ST LOUIS DISTRICT, CORPS OF ENGINEERS.
DACW43-78-C-0005

Woodward-Clyde Consultants
Y7C825 Phase IX

Fig. 9.44

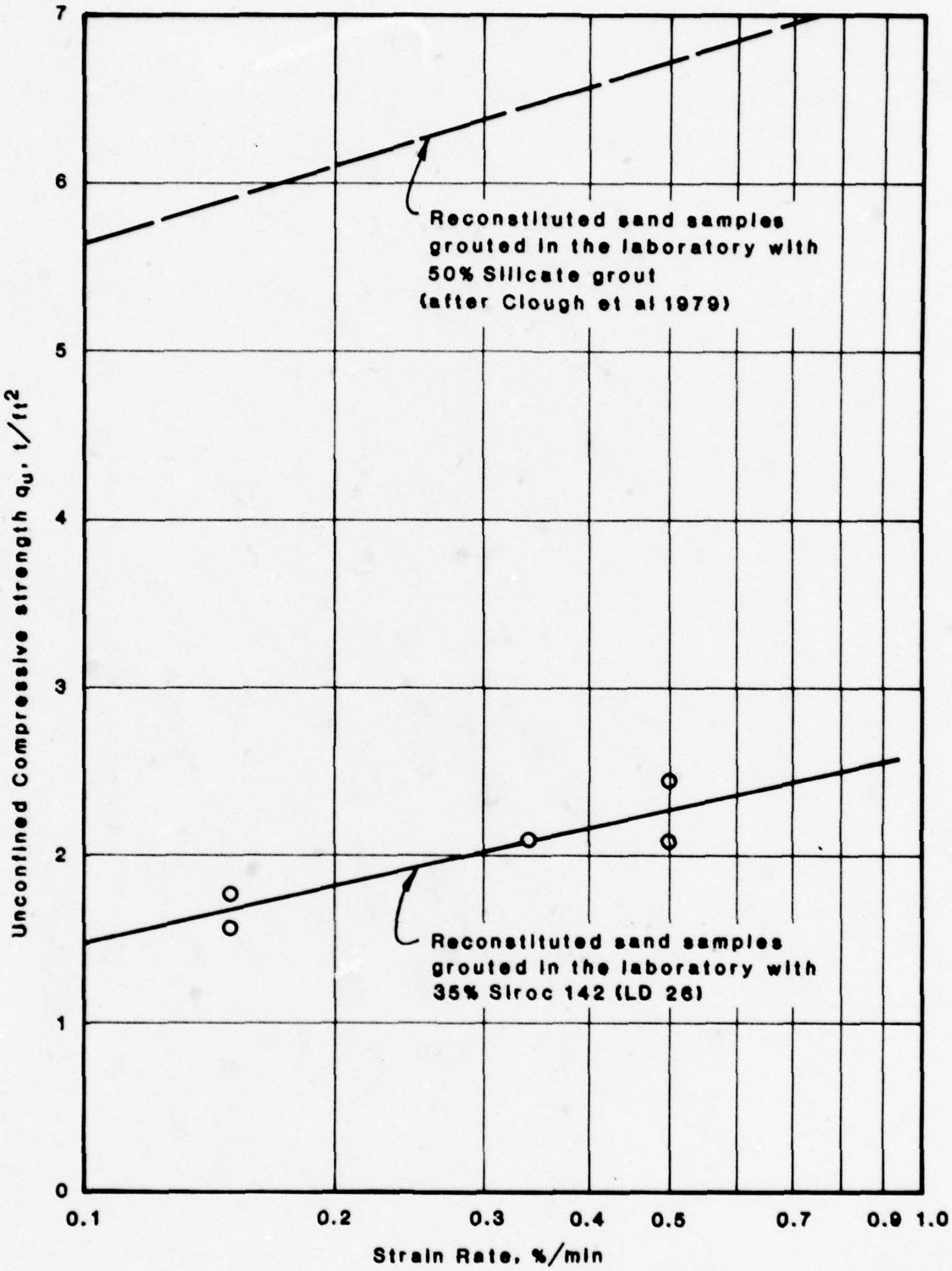

CHEMICAL GROUTING TEST PROGRAM

INFLUENCE OF STRAIN RATE ON UNCONFINED COMPRESSIVE STRENGTH OF GROUTED SAND

FOUNDATION INVESTIGATION AND TEST PROGRAM
EXISTING LOCKS AND DAM No. 26
ST LOUIS DISTRICT, CORPS OF ENGINEERS.
DACW43-78-C-0005

Woodward-Clyde Consultants
Y7C625 Phase IX

Fig. 9.45

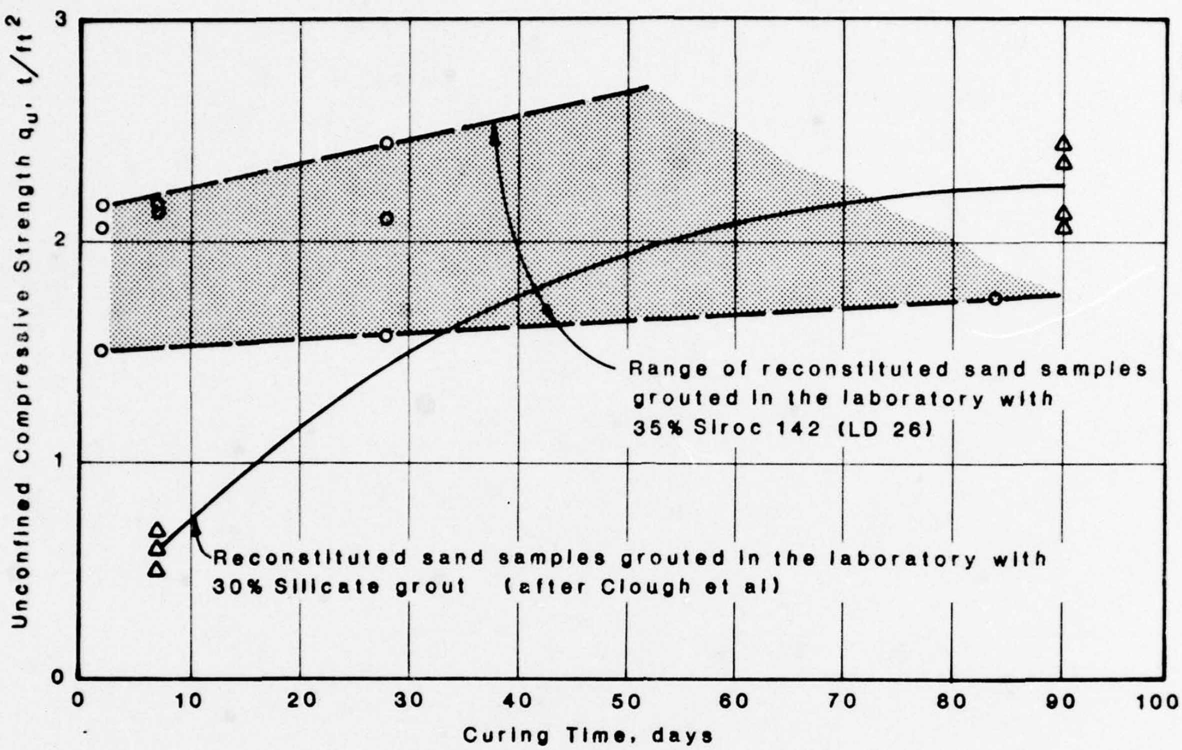

(A) INFLUENCE O
COMPRESSIVE S

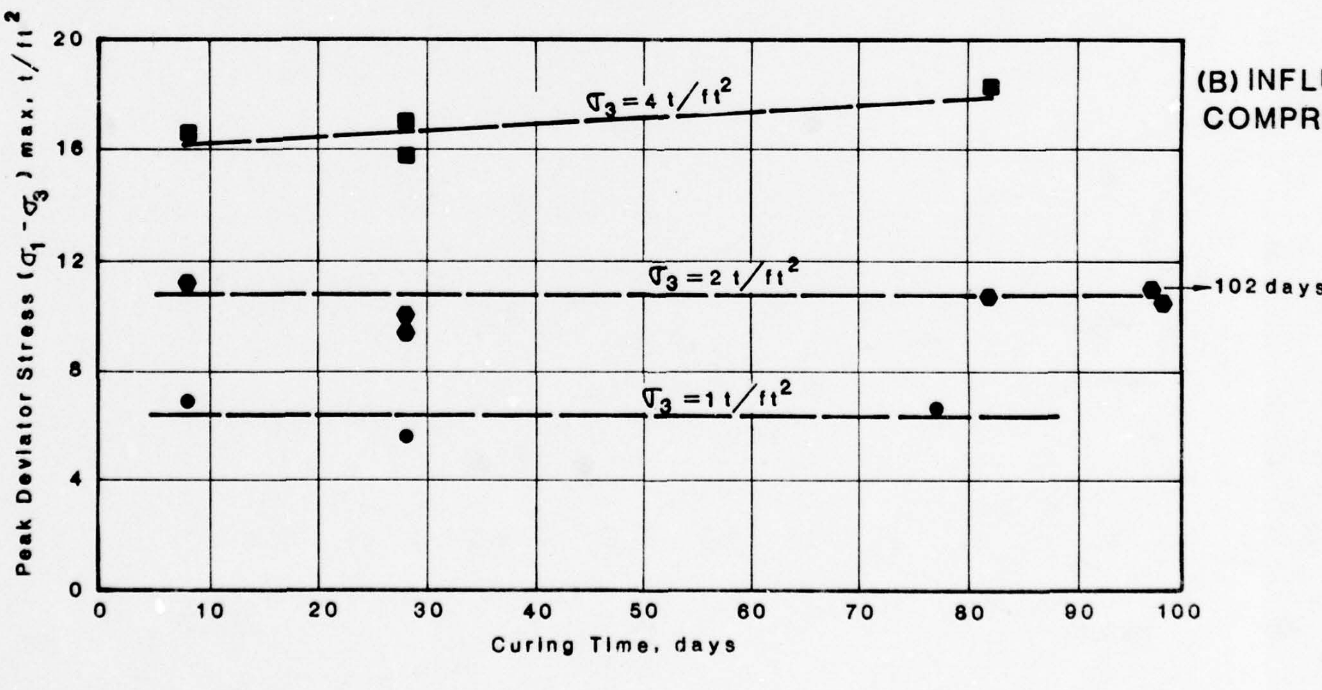

(B) INFLUENCE O
COMPRESSIVE S

(A) INFLUENCE ON UNCONFINED COMPRESSIVE STRENGTH

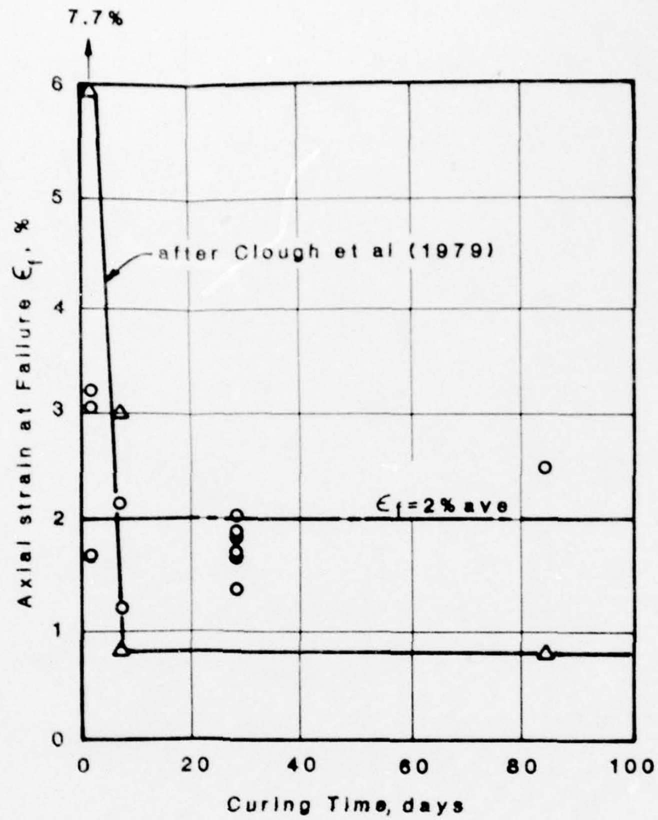

(C) INFLUENCE ON UNCONFINED COMPRESSION AXIAL STRAIN AT FAILURE

(B) INFLUENCE ON TRIAXIAL COMPRESSIVE STRENGTH

Legend

o LD 26 (35% Siroc 142)

Δ Clough et al (1979) (30% Silicate/6% formamide)

—102 days

2

CHEMICAL GROUTING TEST PROGRAM

INFLUENCE OF CURING TIME ON STRESS-STRAIN CHARACTERISTICS OF GROUTED SAND

FOUNDATION INVESTIGATION AND TEST PROGRAM
EXISTING LOCKS AND DAM No. 26
ST LOUIS DISTRICT, CORPS OF ENGINEERS
DACW43-78-C-0005

Woodward-Clyde Consultants

Y7C825 Phase IX

Fig. 9.46

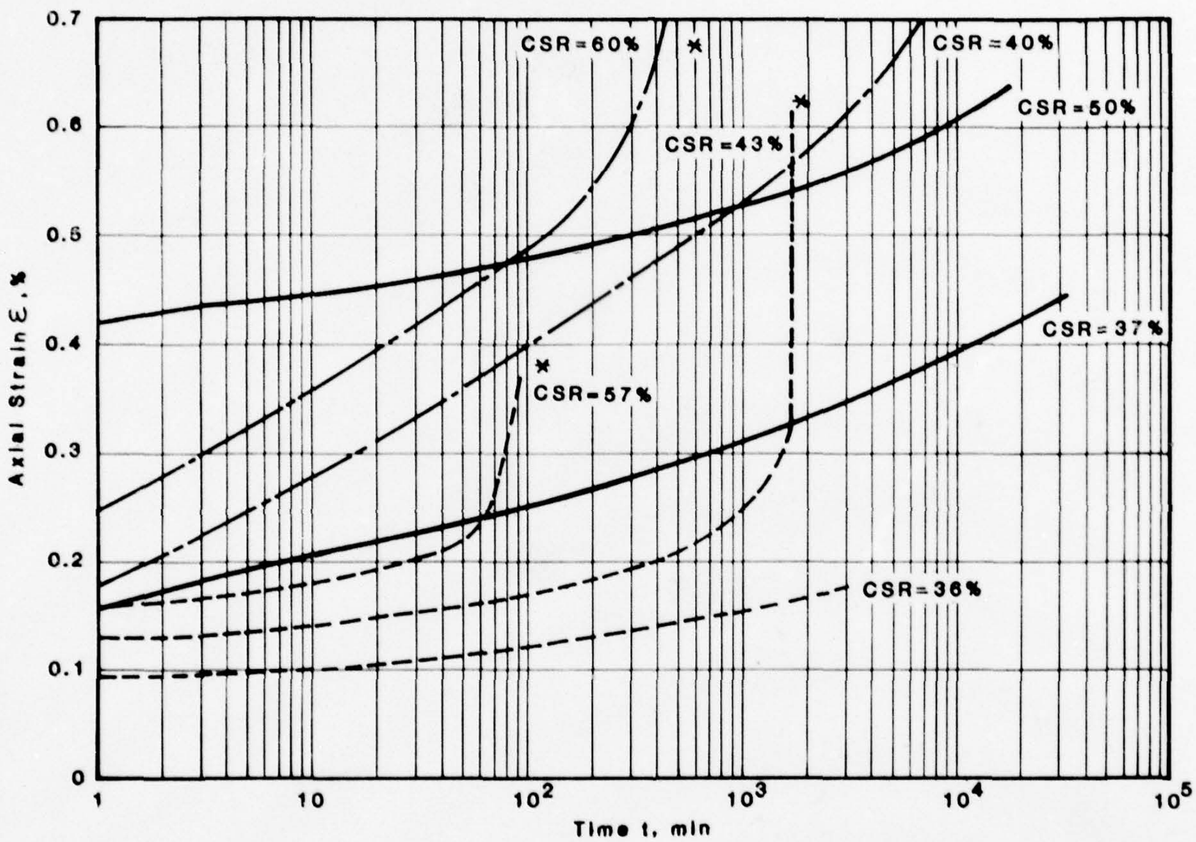

Legend

—— LD 26
35% Siroc 142

– – – Clough et al (1979)
50% Silicate grout

- - - - Koenzen (1978)
70% Silicate grout

* Creep rupture observed

CSR - Constant Stress Ratio = Constant Axial Stress / Unconfined Compressive Strength

CHEMICAL GROUTING TEST PROGRAM

COMPARISON BETWEEN LONG-TERM UNCONFINED BEHAVIOR OF LAB GROUTED SAND USING 35, 50 AND 70% SILICATE GROUTS

FOUNDATION INVESTIGATION AND TEST PROGRAM
EXISTING LOCKS AND DAM No. 26
ST. LOUIS DISTRICT, CORPS OF ENGINEERS.
DACW43-78-C-0005

Woodward-Clyde Consultants

Fig. 9.48

Y7C825 Phase IV

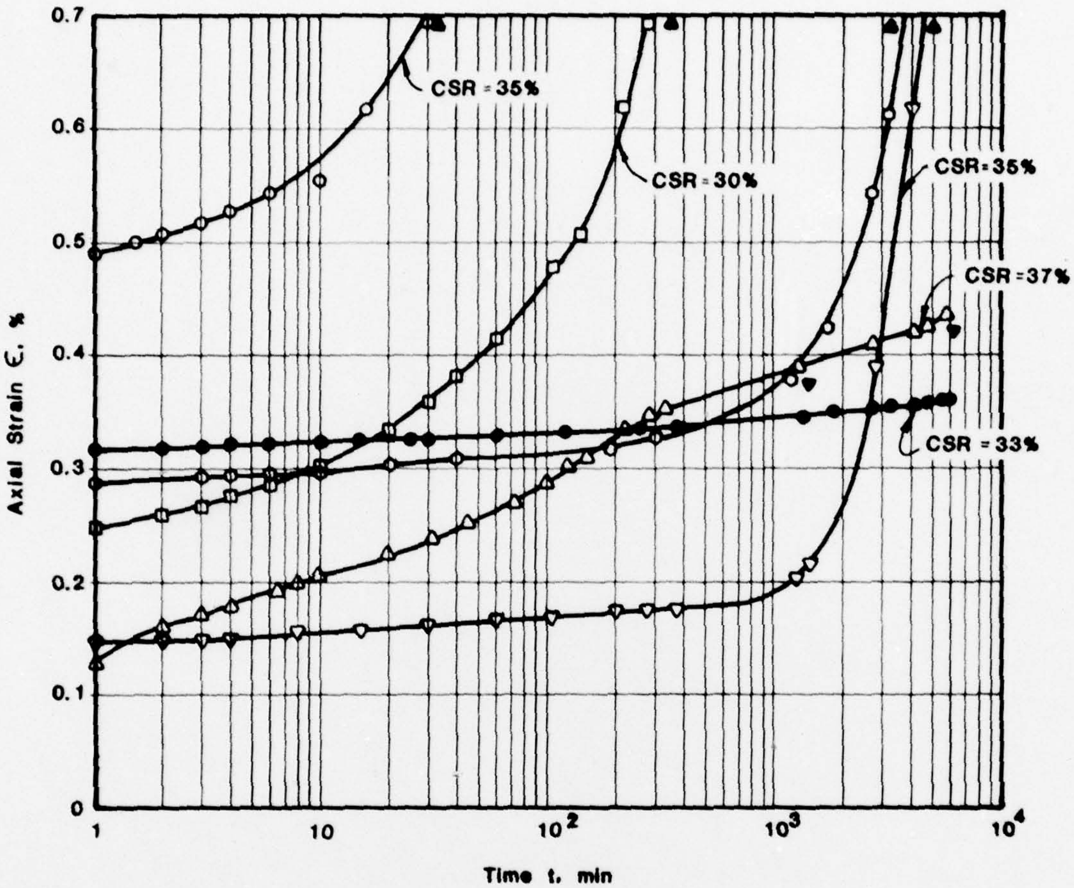

Legend

- ○ Subarea 1
- ● Subarea 11
- □ Subarea 13
- △ Subarea 8
- ▽ Subarea 2
- ▲ Creep rupture
- ▼ Stress dropped off

CHEMICAL GROUTING TEST PROGRAM

RESULTS OF LONG-TERM UNCONFINED COMPRESSION TESTS ON EXCAVATION BLOCK AND CORE SAMPLES

FOUNDATION INVESTIGATION AND TEST PROGRAM
EXISTING LOCKS AND DAM No. 26
ST LOUIS DISTRICT, CORPS OF ENGINEERS.
DACW43-78-C-0005

Woodward-Clyde Consultants
Y7C825 Phase IX

Fig. 9.49

Legend

—— LD 26 35% Siroc 142

— — Koenzen (1978) 70% Silicate Grout

* Creep rupture observed

CSR = Constant Stress Ratio

$$\frac{\sigma_1 - \sigma_3}{(\sigma_1 - \sigma_3)max}$$

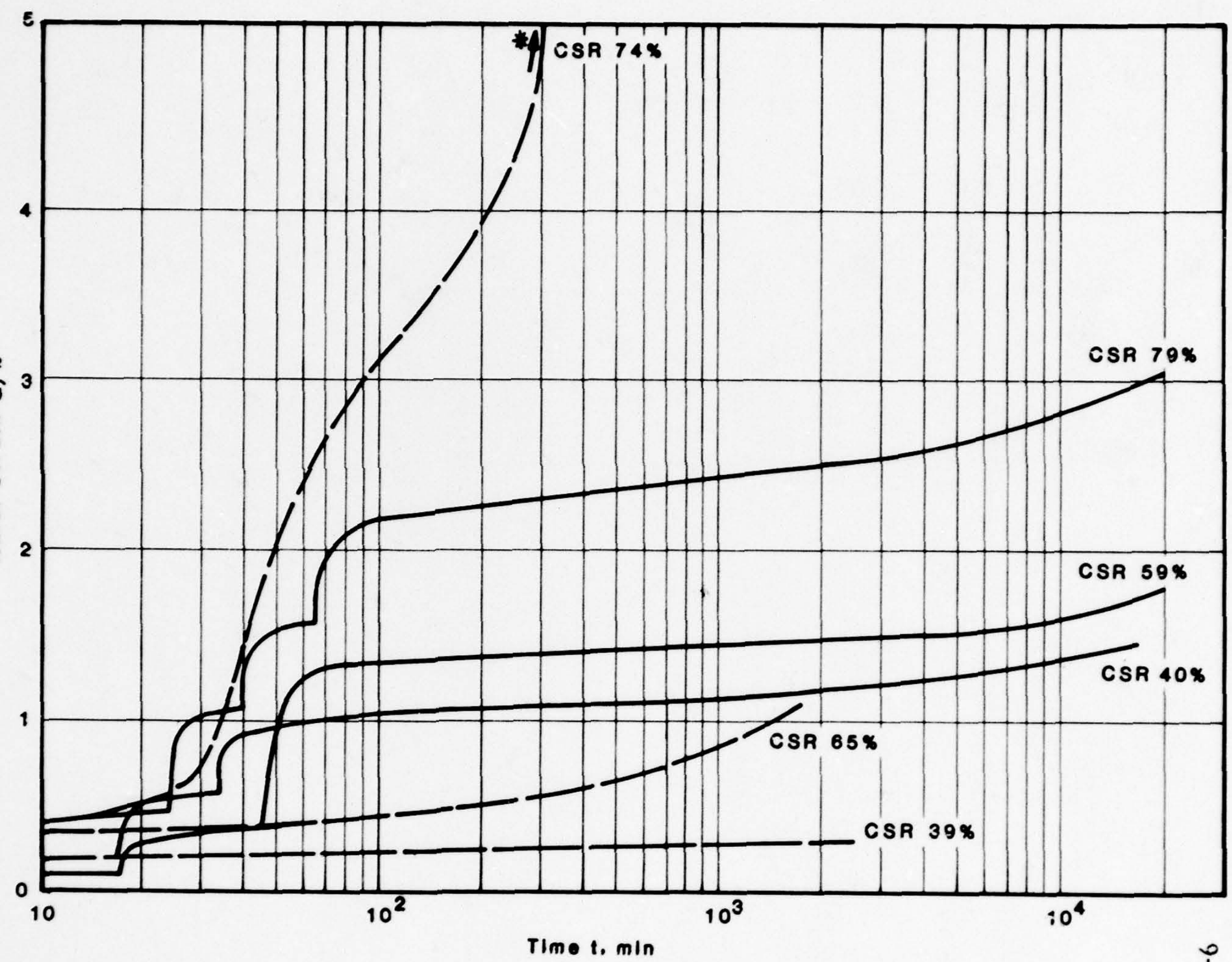

CHEMICAL GROUTING TEST PROGRAM

COMPARISON BETWEEN LONG-TERM TRIAXIAL BEHAVIOR OF LAB GROUTED SAND USING 35% AND 70% SILICATE GROUTS

FOUNDATION INVESTIGATION AND TEST PROGRAM
EXISTING LOCKS AND DAM No. 26
ST LOUIS DISTRICT, CORPS OF ENGINEERS.
DACW43-78-C-0005

Woodward-Clyde Consultants

Y7C825 Phase IX

Fig. 9.50

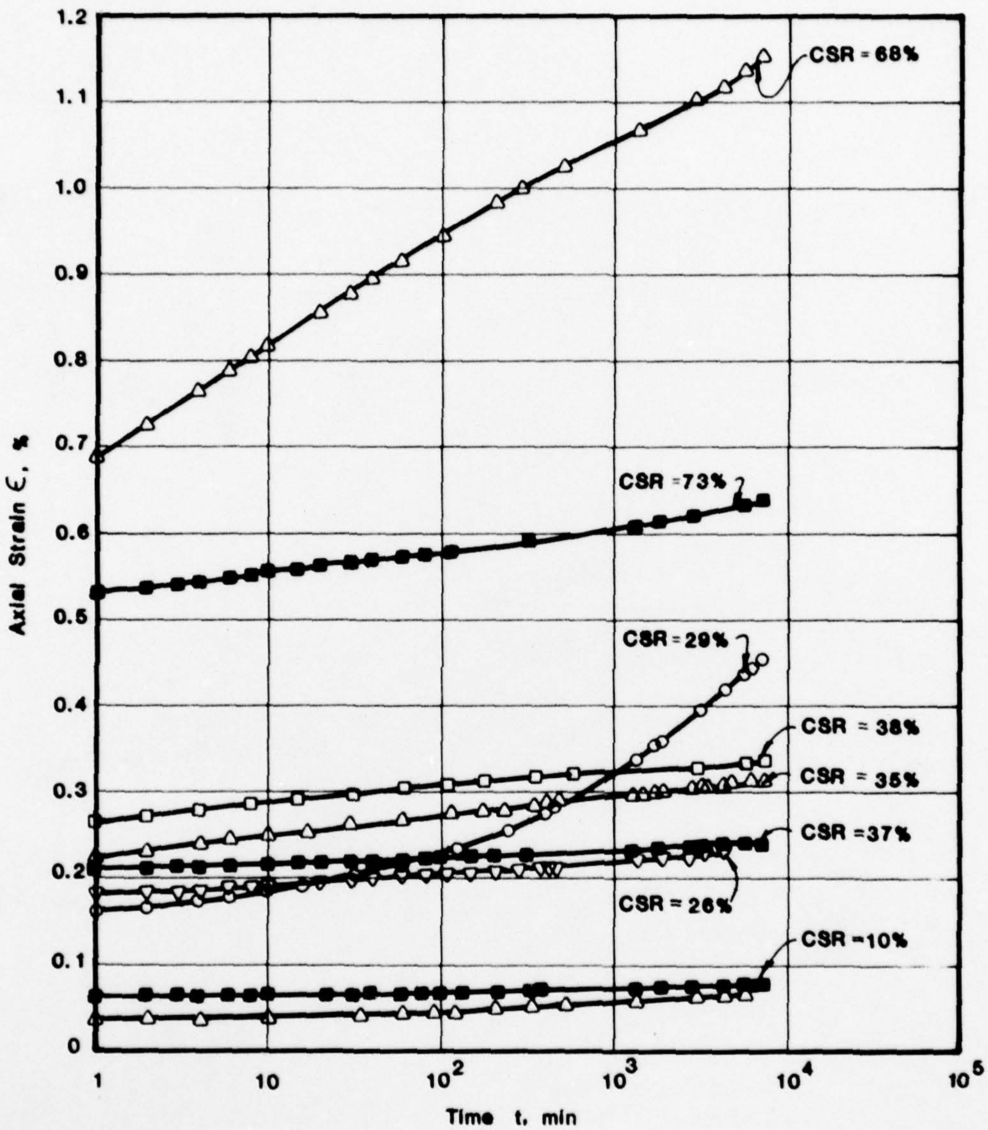

Legend

- □ Subarea 1
- △ Subarea 8
- ○ Subarea 13
- ▽ Subarea 11
- ■ Ungrouted soil

CSR $= \sigma_r / \sigma_r$ max

CHEMICAL GROUTING TEST PROGRAM

RESULTS OF LONG-TERM TRIAXIAL TESTS ON EXCAVATION BLOCK AND CORE SAMPLES

FOUNDATION INVESTIGATION AND TEST PROGRAM
EXISTING LOCKS AND DAM No. 26
ST LOUIS DISTRICT, CORPS OF ENGINEERS.
DACW43-78-C-0005

Woodward-Clyde Consultants

Y7C825 Phase IV

Fig. 9.51

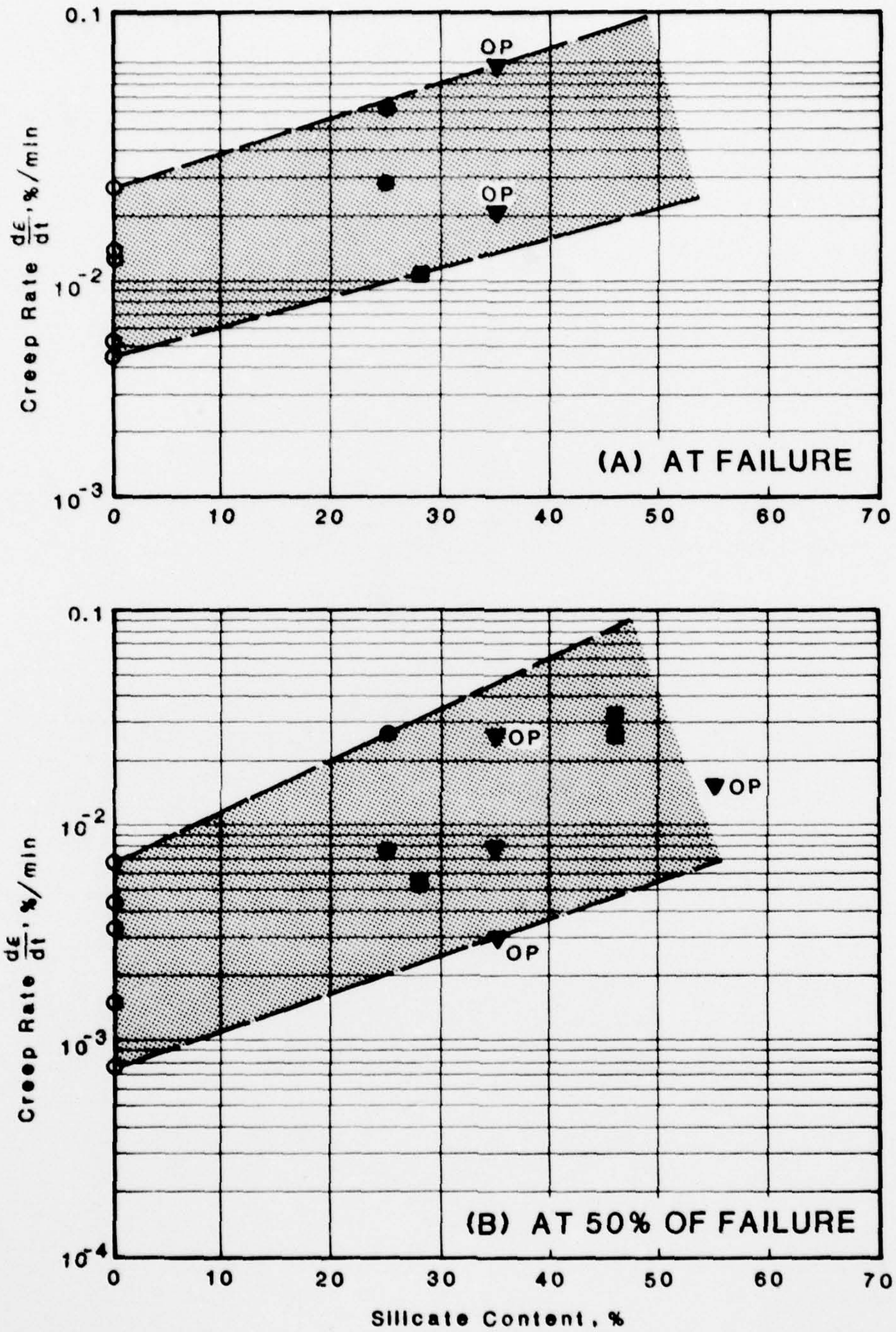

Legend

- O Ungrouted Soil
- ● 25% Silicate/Aluminate
- ■ Silicate/R600 Grouts
- ▼ Siroc Grouts
- OP Open-bottom pipes (all others: sleeve-pipes)

CHEMICAL GROUTING TEST PROGRAM

CREEP RATE VS GROUT SILICATE CONTENT INFERRED FROM PLATE LOAD TEST RESULTS

FOUNDATION INVESTIGATION AND TEST PROGRAM
EXISTING LOCKS AND DAM No. 26
ST. LOUIS DISTRICT, CORPS OF ENGINEERS.
DACW43-78-C-0005

Woodward-Clyde Consultants

Y7C825 Phase IX

Fig. 9.52

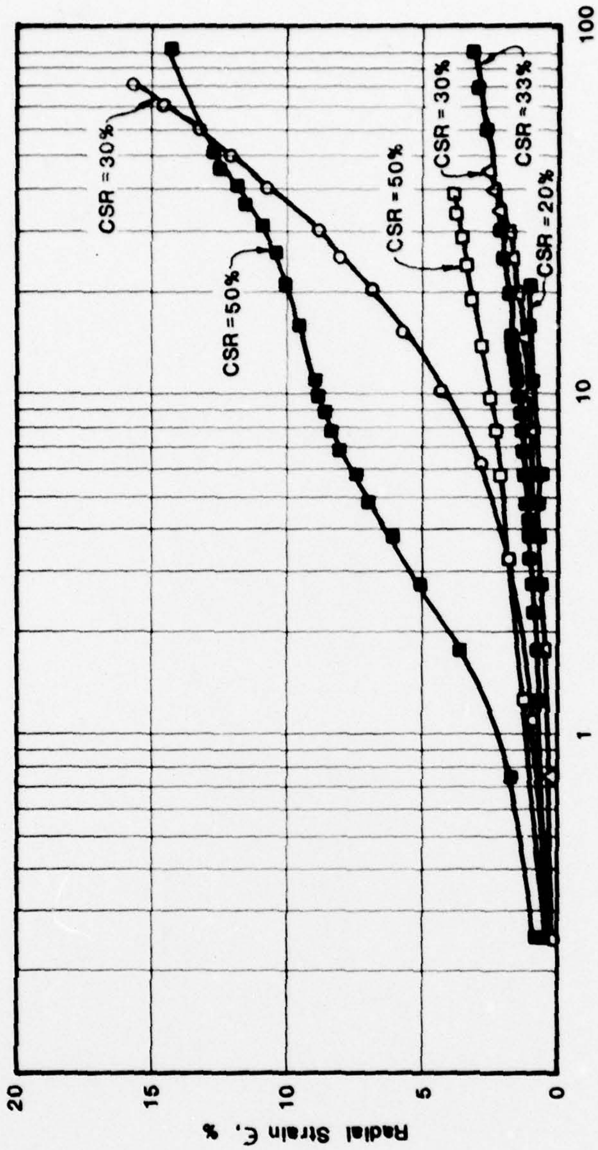

Legend

- ■ 25% Silicate/Aluminate, (Pile driving effects tests)
- △ 45% Siroc 142, Subarea 5
- ○ 46% Silicate/R600, Subarea 13
- □ 55% Siroc 142, Subarea 11

CSR = σ_r / σ_r max

CHEMICAL GROUTING TEST PROGRAM

RESULTS OF LONG TERM PRESSUREMETER TESTS

FOUNDATION INVESTIGATION AND TEST PROGRAM
EXISTING LOCKS AND DAM No. 26
ST LOUIS DISTRICT, CORPS OF ENGINEERS.
DACW43-78-C-0005

Woodward-Clyde Consultants

Y7C825 Phase IV

Fig. 9.53

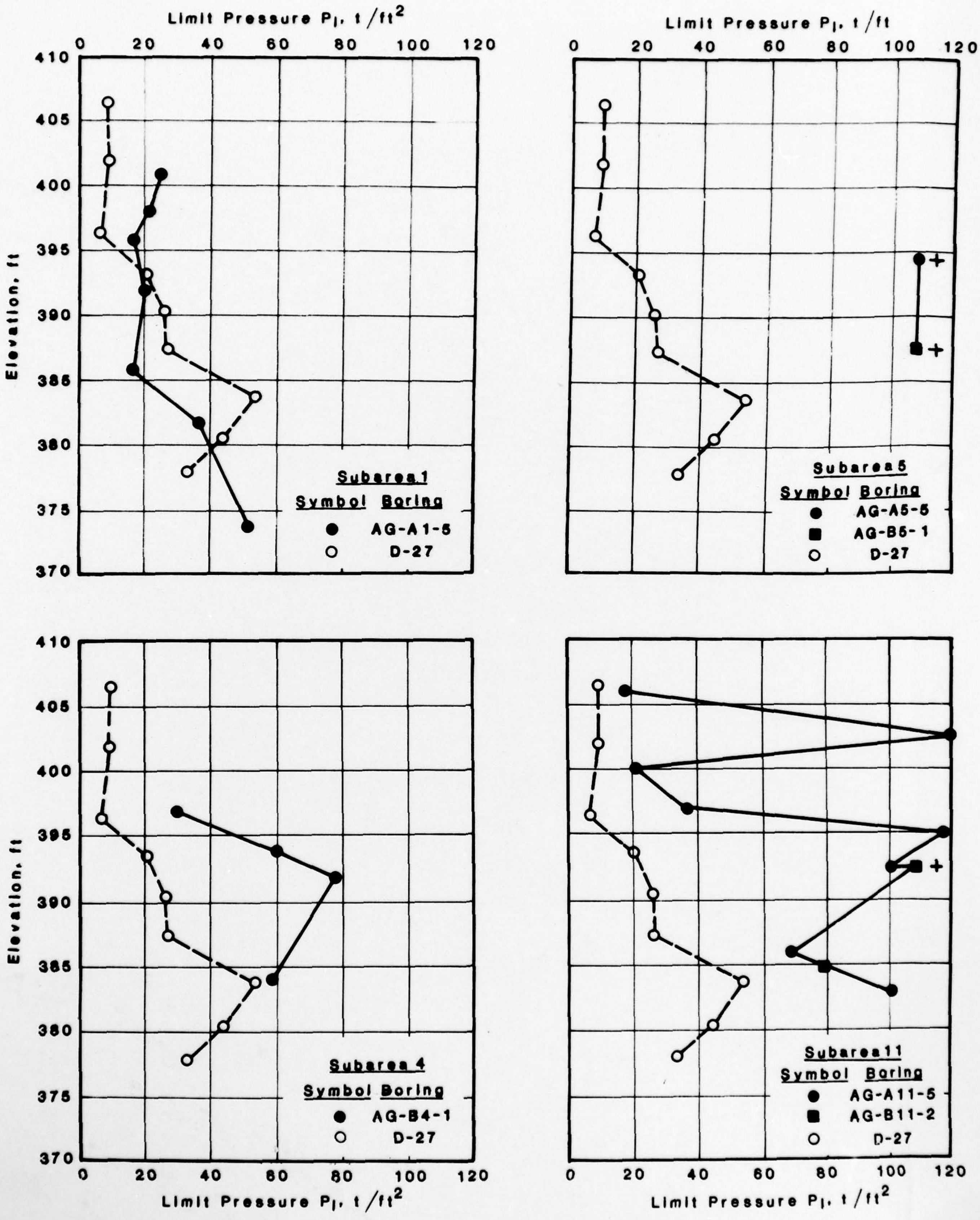

Limit Pressure Pl, t/ft2
0 20 40 60 80 100 120
410 405 400 395 390 385 380 375 370
Elevation, ft
Subarea 1
Symbol Boring
AG-A1-5
D-27
Limit Pressure Pl, t/ft
Subarea 5
Symbol Boring
AG-A5-5
AG-B5-1
D-27
Subarea 4
Symbol Boring
AG-B4-1
D-27
Subarea 11
Symbol Boring
AG-A11-5
AG-B11-2
D-27

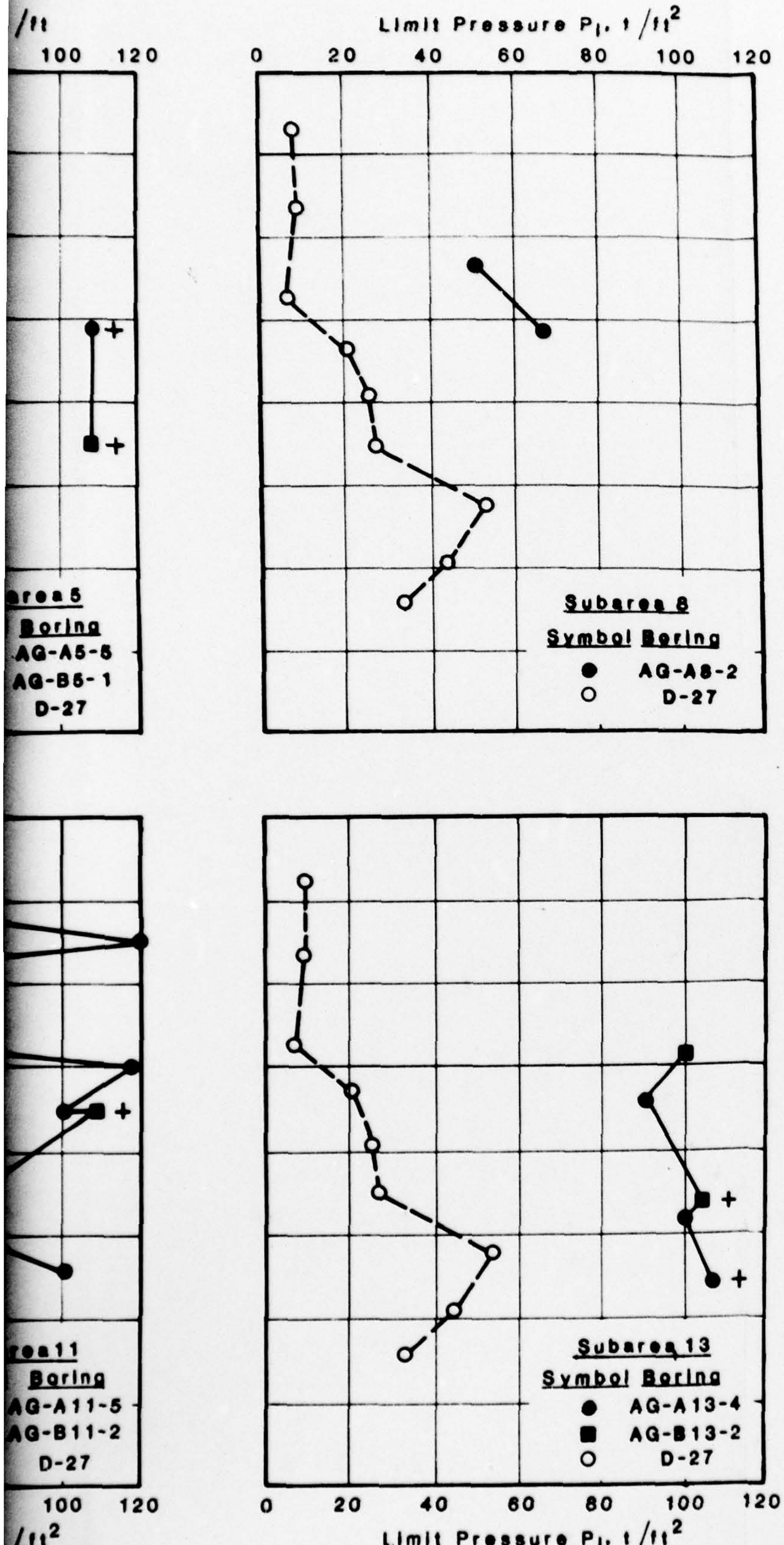

Legend

- Limit pressure after grouting
- Limit pressure before grouting (Boring D-27)
- \+ Failure not approached during test, $P_l > 100$ t /ft^2

CHEMICAL GROUTING TEST PROGRAM

COMPARISON BETWEEN PRESSUREMETER LIMIT PRESSURES MEASURED BEFORE AND AFTER GROUTING

FOUNDATION INVESTIGATION AND TEST PROGRAM
EXISTING LOCKS AND DAM No. 26
ST LOUIS DISTRICT, CORPS OF ENGINEERS.
DACW43-78-C-0008

Woodward-Clyde Consultants

Y7C825 Phase IX

Fig. 9.47

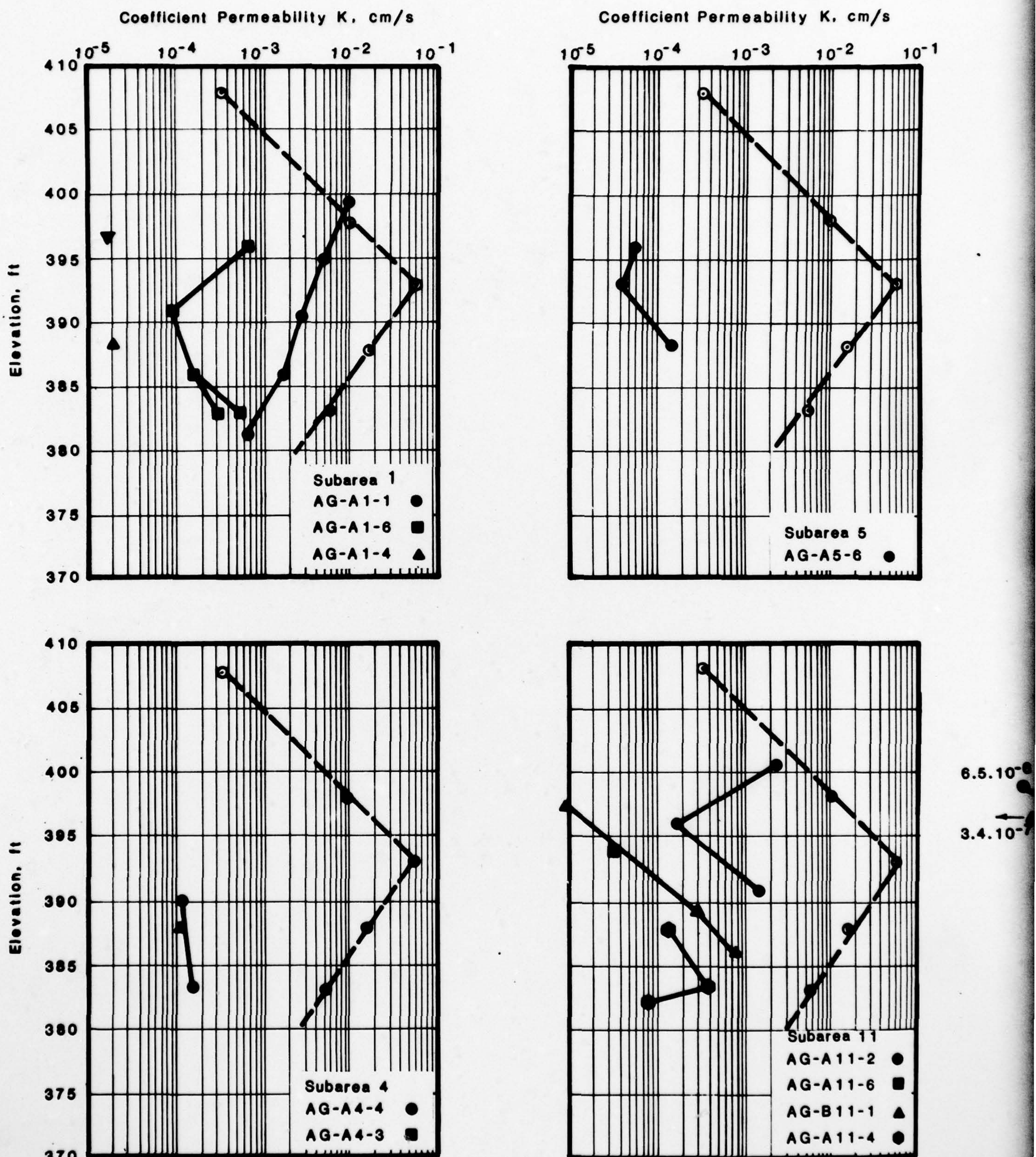

Coefficient Permeability K, cm/s
Coefficient Permeability K, cm/s
10^-5
10^-4
10^-3
10^-2
10^-1
Elevation, ft
410
405
400
395
390
385
380
375
370
Subarea 1
AG-A1-1
AG-A1-6
AG-A1-4
Subarea 5
AG-A5-6
Subarea 4
AG-A4-4
AG-A4-3
Subarea 11
AG-A11-2
AG-A11-6
AG-B11-1
AG-A11-4
6.5.10^-6
3.4.10^-7

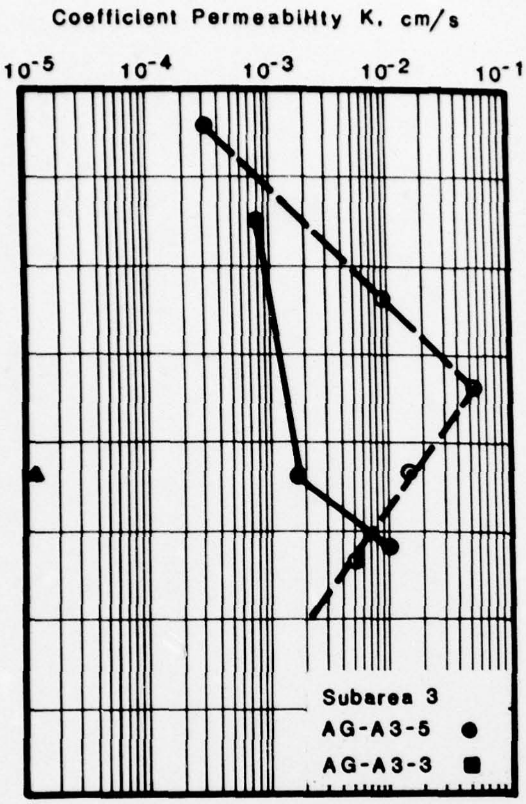

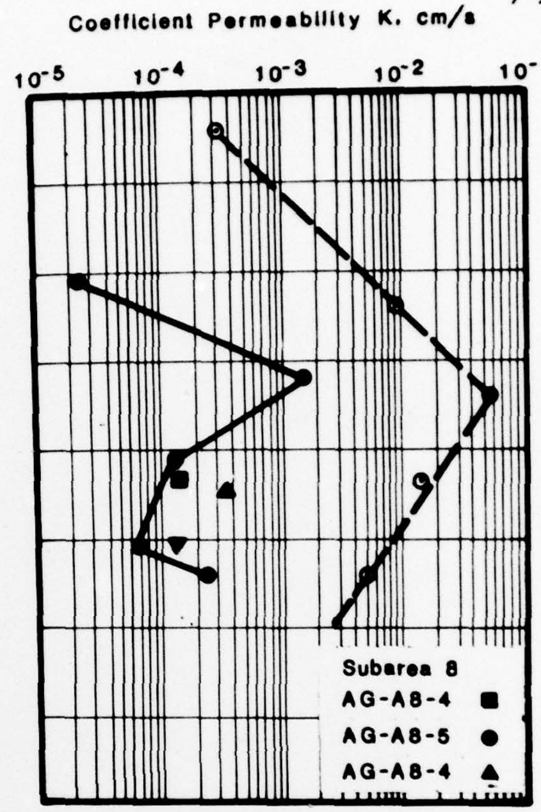

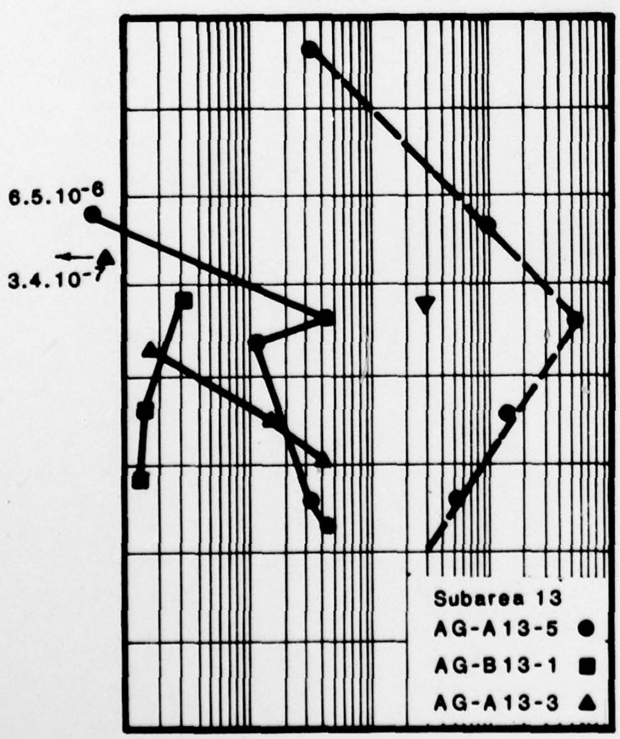

2

Legend

◉ In situ test before grouting

● } In situ test after grouting
■ }
● }

Lab test after grouting

▲ Undisturbed block sample

▼ Excavation block and core sample

CHEMICAL GROUTING TEST PROGRAM

FIELD AND LABORATORY FALLING HEAD PERMEABILITY TEST RESULTS

FOUNDATION INVESTIGATION AND TEST PROGRAM
EXISTING LOCKS AND DAM No. 26
ST LOUIS DISTRICT, CORPS OF ENGINEERS.
DACW43-78-C-0009

Woodward-Clyde Consultants

Y7C825 Phase IX

Fig. 9.54

PHASE IV REPORT

VOLUME II

RESULTS AND INTERPRETATION OF
CHEMICAL GROUTING TEST PROGRAM

SECTION 10

COST ANALYSES

10 COST ANALYSIS

10.1 GENERAL

The total cost of the chemical grouting test program comprised:

(1) engineering costs (design, instrumentation, field supervision, testing,and interpretation);

(2) site-related costs (earthwork, asphalt pad, and dewatering); and

(3) grouting costs (installation of grout pipes, grout components, grout injection, and other costs).

Only the grouting costs are analyzed in this section. All cost elements have been estimated per unit volume (yd^3) of soil to be grouted. The theoretical volume of soil to be grouted in each subarea is indicated in Table 7.1. The grout take, that is the volume of grout actually injected divided by the theoretical volume of soil to be grouted, is also shown for each subarea in this table.

10.2 GROUT PIPE INSTALLATION COST

10.2.1 Drill Rig Cost

GROUT PIPE TYPE	RIGHOURS	RIG HOURLY RATE $	NUMBER OF GROUT PIPES	DRILL RIG COST PER GROUT PIPE $
Open-bottom pipe	23	49.50	17	66.97
Sleeve-pipe	187.5	49.50	57	162.83

10.2.2 Pipe Cost

GROUT PIPE TYPE	PIPE COST $/ft	LENGTH OF PIPE PER GROUT PIPE ft	PIPE COST PER GROUT PIPE $
Open-bottom pipe	0.25	47	11.75
Sleeve-pipe	1.00	45	45.00

10.2.3 Labor Cost

GROUT PIPE TYPE	LABOR COST $	NUMBER OF GROUT PIPES	LABOR COST PER GROUT PIPE $
Open-Bottom pipe	2,361.22	17	138.90
Sleeve-pipe	11,303.26	57	198.30

10.2.4 Sleeve Grouting Cost

This cost applied to sleeve-pipes only. The total cost was $2,954.93 or $51.84 per sleeve-pipe, including labor and materials.

10.2.5 Summary of Grout Pipe Installation Cost

The cost of installing open-bottom pipes was $217.62 per pipe or $4.63 per foot. The cost of installing sleeve-pipes was $457.97 per pipe or $10.18 per foot. This cost is exclusive of mobilization, supervisory personnel, miscellaneous supplies and administration costs, and grouting contractor's profit. Grout pipe installation cost per unit volume of soil to be grouted is presented in Table 10.1 for each test subarea.

10.3 GROUT COST

10.3.1 Grout Components

The grout cost included furnishing and storing grout components. The cost of the grout components delivered at the site were as follows:

Sodium Silicate (Grade 40):	$0.558/gal
Formamide:	$4.11/gal
Sodium Aluminate:	0.302/lb
Calcium Chloride:	$0.015/lb
Cement:	$0.047/lb
Bentonite:	$0.112/lb
R600:	$5.09/gal

10.3.2 **35% Siroc 142** (Grout Type 1)

COMPONENTS	AVERAGE QUANTITY		UNIT COST $	COST $
Sodium Silicate	35	gal	0.558	19.53
Formamide	8	gal	4.11	32.88
Sodium Aluminate	10	lb	0.302	3.02
Water	57	gal	0	0
Total	100	gal		55.43

$55.43/100 gal = $4.15/ft^3 = $111.95/yd^3

10.3.3 **25% Silicate/Aluminate** (Grout Type 2)

COMPONENTS	AVERAGE QUANTITY		UNIT COST $	COST $
Sodium Silicate	25	gal	0.558	13.95
Sodium Aluminate	13	lb	0.302	3.93
Water	75	gal	0	0
Total	100	gal		17.88

$17.88/100 gal = $1.34/ft^3 = $36.10 yd^3

10.3.4 **28% Silicate/R600** (Grout Type 3)

COMPONENTS	AVERAGE QUANTITY		UNIT COST $	COST $
Sodium Silicate	28	gal	0.558	15.62
R600	6	gal	5.09	30.54
Water	66	gal	0	0
Total	100	gal		46.16

$46.16/100 gal = $3.45/ft^3 = $93.22/yd^3

AD-A076 091 WOODWARD-CLYDE CONSULTANTS CHICAGO IL F/G 13/2
RESULTS AND INTERPRETATION OF CHEMICAL GROUTING TEST PROGRAM. V--ETC(U)
JUL 79 J PEREZ , Y LACROIX DACW43-78-C-0005

UNCLASSIFIED NL

4 OF 4

AD
A076091

END
DATE
FILMED
11-79
DDC

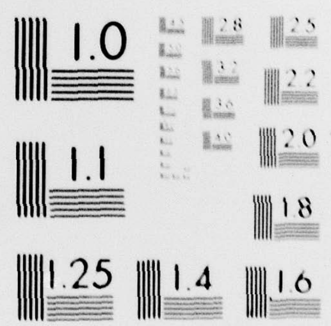

MICROCOPY RESOLUTION TEST CHART
NATIONAL BUREAU OF STANDARDS-1963-A

10.3.5 **55% Siroc 142** (Grout Type 4a)

COMPONENTS	AVERAGE QUANTITY		UNIT COST $	COST $
Sodium Silicate	55	gal	0.558	30.69
Formamide	9	gal	4.11	36.99
Sodium Aluminate	10	lb	0.302	3.02
Water	36	gal	0	0
Total	100	gal		71.00

$71.00/100 gal = $5.31/ft^3 = $143.39/yd^3

10.3.6 **55% Siroc 132** (Grout Type 4b)

COMPONENTS	AVERAGE QUANTITY		UNIT COST $	COST $
Sodium Silicate	55	gal	0.558	30.69
Formamide	9	gal	4.11	36.99
Calcium Chloride	5.6	gal	0.105	0.59
Water	36	gal	0	0
Total	100	gal		68.27

$68.27/100 gal = $5.11/ft^3 = $137.88/yd^3

10.3.7 **46% Silicate/R600** (Grout Type 5)

COMPONENTS	AVERAGE QUANTITY		UNIT COST $	COST $
Sodium Silicate	46.3	gal	0.558	25.84
R600	7.4	gal	5.09	37.67
Water	46.3	gal	0	0
Total	100	gal		63.51

$63.51/100 gal = $4.75/ft^3 = $128.26/yd^3

10.3.8 **45% Siroc 132** (Grout Type 6)

COMPONENTS	AVERAGE QUANTITY	UNIT COST $	COST $
Sodium Silicate	45 gal	0.558	25.11
Formamide	7.5 gal	4.11	30.83
Calcium Chloride	8 lb	0.105	0.84
Water	47.5 gal	0	0
Total	100 gal		56.78

$56.78/100 gal = $4.25/ft^3 = $144.66/yd^3

10.3.9 **Cement-Bentonite (c/w = 0.25)** (Grout Type 7)

COMPONENTS	AVERAGE QUANTITY	UNIT COST $	COST $
Cement	15.6 lb	0.047	0.73
Bentonite (b/w = 0.03)	1.9 lb	0.112	0.21
Water	1 ft^3	0	0
Total	1 ft^3		0.94

$0.94/ft^3 = $25.38/yd^3

10.3.10 **Cement-Bentonite (c/w = 0.4)** (Grout Type 8)

COMPONENTS	AVERAGE QUANTITY	UNIT COST $	COST $
Cement	25 lb	0.047	1.17
Bentonite (b/w = 0.035)	2.5 lb	0.112	0.28
Water	1 ft^3	0	0
Total	1 ft^3		1.45

$1.45/ft^3 = $39.15/yd^3

10.3.11 **Summary of Grout Cost**

Grout cost per test subarea is summarized in Table 10.2.

10.4 GROUT MIXING AND INJECTION COST

The grout mixing and injection cost was calculated for each type of grout on the basis of actual mixing and injection time and non-supervisory labor cost. The actual total mixing and injection time for the entire program was 1,267 hours. The total non-supervisory labor cost for grout mixing and injection was $91,104. Thus, the average grout mixing and injection cost was approximately $71.91 per hour. Grout mixing and injection costs per type of grout are detailed in Table 10.3. Grout mixing and injection costs per subarea are detailed in Table 10.4.

10.5 OTHER COSTS

Other costs included grouting plant mobilization and rental, contractor's supervisory personnel cost, miscellaneous supplies, and contractor's administration and profit. These other costs were distributed among the test subarea proportionally to the sum of grout pipe, grout, and injection costs. The total cost of grouting amounted to $565,560. The sum of grout pipe, grout, and injection costs (Tables 10.1, 10.2, and 10.3) amounted to approximately $183,000. The ratio of other costs to grout pipe, grout, and injection cost was 2.09. Thus other costs amounted to $565,560 minus $183,000 or $382,560. The distribution of other costs among the test subareas is detailed in Table 10.5.

10.6 TOTAL GROUTING COST

The total grouting cost was the sum of all partial costs discussed above. The total grouting cost per subarea is detailed in Table 10.6. It averaged $388.74 per cubic yard of soil to be grouted and varied from a high of $617.66 per cubic yard of soil to be grouted in Subarea 13 to a low of $209.55 per cubic yard of soil to be grouted in Subarea 2, excluding Subarea 5a which was not representative (Section 2.1.2). When related to the grout take (that is to the volume of grout actually injected divided by the volume of soil to be grouted), the grouting cost averaged 9.32 per cubic yard of soil to be grouted and per percent grout take, and ranged from a high of $20.13 per cubic yard of soil to be grouted and per percent grout take in Subarea 9, to a low of $7.14 per cubic yard of soil to be grouted and percent grout take in Subarea 7.

The total grouting cost per grouting method is shown in Table 10.7. Although grouting method S_3 was the most expensive when related to the volume of soil to be grouted ($437/$yd^3$ of soil), it was the least expensive when related to grout take ($8.31/$yd^3$ of soil/percent grout take). Except for grouting Method S_1, the cost for the other three methods was comparable when related to grout take, and averaged approximately $9.32 per cubic yard of soil per percent grout take.

SUBAREA NO.	NO. OF GROUT HOLES	TYPE OF GROUT PIPE (2)	COST PER PIPE $	TOTAL COST FOR GROUT PIPE INSTALLATION $	VOLUME OF SOIL TO BE GROUTED yd^3	COST OF GROUT PIPE INSTALLATION (1) \$/yd^3 of soil
1	7	OP	217.62	1523	91.9	16.57
2	4	OP	217.62	870	105.6	8.24
3	4	SP	457.97	1832	73.8	24.82
4	5	SP	457.97	2290	130.5	17.55
5	4	SP	457.97	1832	109.5	16.73
5a	2	SP	457.97	916	40.5	22.62
6	5	SP	457.97	2290	131.3	17.44
7	6	SP	457.97	2748	151.2	18.17
8	8	SP	457.97	3664	97.9	37.43
9	6	OP	217.62	1306	79.2	16.48
10	6	SP	457.97	2748	158.0	17.39
11	8	SP	457.97	3664	105.1	34.86
12	4	SP	457.97	1832	102.9	17.80
13	5	SP	457.97	2290	64.6	35.45
TOTALS				29962 (SP)	1192.3 (SP)	25.13 (SP)
				3699 (OP)	276.7 (OP)	13.37 (OP)

Notes

(1) *This cost is per cubic yard of soil to be grouted*

(2) *OP: Open-bottom pipe*
SP: Sleeve-pipe

CHEMICAL GROUTING TEST PROGRAM

SUMMARY OF GROUT PIPE INSTALLATION COST PER SUBAREA

FOUNDATION INVESTIGATION AND TEST PROGRAM
EXISTING LOCKS AND DAM No. 26
ST LOUIS DISTRICT, CORPS OF ENGINEERS.
DACW43-78-C-0005

Woodward-Clyde Consultants

Y7C828 Phase III

Table 10.1

SUBAREA NO.	GROUT TYPE	VOLUME OF GROUT INJECTED yd^3	GROUT UNIT COST $/$yd^3$	TOTAL GROUT COST $	VOLUME OF SOIL TO BE GROUTED yd^3	GROUT COST $/$yd^3$ of soil	GROUT[1] TAKE %
1	1	27.65	111.95	3095	91.9	33.68	30.1
2	1	26.48	111.95	2964	105.6	28.07	25.1
3	3	30.85	93.22	2876	73.8	38.97	41.8
4	1	58.61	111.95	6561	130.5	50.28	44.9
5	6	47.28	114.66	5421	109.5	49.50	45.0
5a	2	1.50	36.10	54	40.5	1.34	3.7
6	2	60.64	36.10	2189	131.3	16.67	46.2
7 (2)	2 7	75.61 3.06	36.10 25.38	2827	151.2	18.70	52.5
8 (2)	2 7	49.82 5.14	36.10 25.38	1929	97.9	19.70	56.1
9	4 (3)	16.62	143.39	2383	79.2	30.09	21.0
10	4 (4)	68.08	140.64	9574	158.0	60.60	43.1
11	4 (4)	46.31	140.64	6513	105.1	61.97	44.1
12 (5)	5 7	55.36 0.31	128.26 39.15	7113	102.9	69.12	54.1
13 (5)	5 7	37.19 0.31	128.26 39.15	4782	64.6	74.03	58.1
TOTALS		612 (approx)		58281	1442	40.42 ave	41.7 ave

Notes

(1) *Grout Take = Volume of Grout Injected/Volume of Soil to be Grouted*

(2) *Cement-bentonite (c/w = 0.25) was injected in every grout hole as first stage grouting*

(3) *55% Siroc 142*

(4) *55% Siroc 132/142*

(5) *Cement-bentonite (c/w = 0.25) was injected in one grout hole as first stage grouting*

CHEMICAL GROUTING TEST PROGRAM

SUMMARY OF GROUT COST PER SUBAREA

FOUNDATION INVESTIGATION AND TEST PROGRAM
EXISTING LOCKS AND DAM No. 26
ST LOUIS DISTRICT, CORPS OF ENGINEERS.
DACW43-78-C-[illegible]

Woodward-Clyde Consultants

Y7C828 Phase IX

Table 10.2

	GROUT TYPE	TOTAL VOLUME INJECTED gal	MIXING AND INJECTION TIME hours	TOTAL MIXING AND INJECTION COST $	MIXING AND INJECTION COST $/gal
1	35% Siroc 142 (Subareas 1, 2, 4)	22,768	207.65	14,930	0.66
2	25% Silicate/Aluminate (Subareas 5a, 6, 7, 8)	37,880	416.37	29,940	0.79
3	28% Silicate/R600 (Subarea 3)	6,231	71.87	5,162	0.83
4	55% Siroc 132/142 (Subareas 9, 10, 11)	26,460	251.63	18,090	0.68
5	46% Silicate/R600 (Subareas 12, 13)	18,691	199.77	14,360	0.77
6	45% Siroc 132 (Subarea 5)	9,548	95.37	6,852	0.72
7	Cement-Bentonite (Subareas 7, 8, 12, 13)	1,944	24.67	1,770	0.91
	TOTALS	123,522	1,267 (approx)	91,104	0.74 ave

CHEMICAL GROUTING TEST PROGRAM

GROUT MIXING AND INJECTION COST PER TYPE OF GROUT

FOUNDATION INVESTIGATION AND TEST PROGRAM
EXISTING LOCKS AND DAM No. 26
ST LOUIS DISTRICT, CORPS OF ENGINEERS.
DACW43-78-C-0005

Woodward-Clyde Consultants

Y7C025 Phase IX

Table 10.3

SUBAREA NO.	GROUT TYPE	VOLUME OF GROUT INJECTED gal	MIXING AND INJECTION COST $/gal	MIXING AND INJECTION COST $/subarea	VOLUME OF SOIL TO BE GROUTED yd³	MIXING AND INJECTION COST $/yd³ of soil
1	1	5,584	0.66	3,685	91.9	40.10
2	1	5,348	0.66	3,230	105.6	33.43
3	3	6,231	0.83	5,172	73.8	70.08
4	1	11,836	0.66	7,812	130.5	59.86
5	6	9,548	0.77	7,352	109.5	67.14
5a	2	303	0.79	239	40.5	5.91
6	2	12,246	0.79	9,674	131.3	73.68
7	2 7	15,270 779 (1)	0.79 0.91	12,772	151.2	84.47
8	2 7	10,061 1,039 (1)	0.79 0.91	8,894	97.9	90.84
9	4	3,357	0.68	2,283	79.2	28.82
10	4	13,750	0.68	9,350	158.0	59.18
11	4	9,353	0.68	6,360	105.1	60.51
12	5 7	1,180 63 (1)	0.77 0.91	8,666	102.9	84.22
13	5 7	7,511 63 (1)	0.77 0.91	5,841	64.6	90.41
TOTALS		123,522	0.74 ave	91,102 (approx)	1,442	62.02 ave

Note

(1) Cement-bentonite grout

CHEMICAL GROUTING TEST PROGRAM

SUMMARY OF GROUT MIXING AND INJECTION COST PER SUBAREA

FOUNDATION INVESTIGATION AND TEST PROGRAM
EXISTING LOCKS AND DAM No. 26
ST LOUIS DISTRICT, CORPS OF ENGINEERS.
DACW43-78-C-0085

Woodward-Clyde Consultants

Y7C828 Phase III

Table 10.4

SUBAREA NO.	SUM OF COSTS OF GROUT PIPES, GROUT, AND INJECTION $	OTHER[(1)] COSTS $	VOLUME OF SOIL TO BE GROUTED yd^3	OTHER COSTS $/$yd^3$ of soil
1	8,303	17,353	91.9	183.83
2	7,064	14,764	105.6	139.81
3	9,880	20,649	73.8	279.80
4	16,663	34,826	130.5	266.86
5	14,605	30,524	109.5	278.76
5a	1,209	2,527	40.5	62.39
6	14,153	29,580	131.3	225.28
7	18,347	38,345	151.2	253.61
8	14,487	30,278	97.9	309.27
9	13,163	27,511	79.2	347.36
10	21,672	45,294	158.0	286.67
11	16,537	34,562	105.1	328.85
12	17,611	36,807	102.9	357.70
13	12,913	26,988	64.6	417.77
TOTALS	183,000 (approx)	382,560 (approx)	1,442	265.30 ave

Note

(1) Other costs = (Cost of Grout Pipes, Grout, and Injection) x 2.09

CHEMICAL GROUTING TEST PROGRAM

SUMMARY OF OTHER COSTS PER SUBAREA

FOUNDATION INVESTIGATION AND TEST PROGRAM
EXISTING LOCKS AND DAM No. 26
ST LOUIS DISTRICT, CORPS OF ENGINEERS.
DACW43-75-C-0005

Woodward-Clyde Consultants
Y7C828 Phase II

Table 10.5

SUBAREA NO.	GROUTING[7] METHOD	GROUT[1] PIPE COST $/yd³ of soil	GROUT[2] COST $/yd³ of soil	INJECTION[3] COST $/yd³ of soil	OTHER[4] COSTS $/yd³ of soil	TOTAL[5] COST $/yd³ of soil	GROUT[6] TAKE %	COST $/yd³ of soil/% take
1	O_1	16.57	33.68	40.10	188.83	279.18	30.1	9.28
2	O_1	8.24	28.07	33.43	139.81	209.55	25.1	8.35
3	S_2	24.82	38.97	70.08	279.80	413.67	41.8	9.90
4	S_2	17.55	50.28	59.86	266.86	394.55	44.9	8.79
5	S_2	16.73	49.50	67.14	278.76	412.13	45.0	9.16
5a	S_1	22.62	1.34	5.91	62.76	92.63	3.7	25.04
6	S_3	17.44	16.67	73.68	225.28	333.07	46.2	7.21
7	S_3	18.17	18.70	84.47	253.61	374.95	52.5	7.14
8	S_3	37.43	19.70	90.84	309.27	457.24	56.1	8.15
9	O_1	16.48	30.09	28.82	347.36	422.75	21.0	20.13
10	S_2	17.39	60.60	59.18	286.67	423.84	43.1	9.83
11	S_2	34.86	61.97	60.51	328.85	486.19	44.1	11.02
12	S_3	17.80	69.12	84.22	357.70	528.84	54.1	9.78
13	S_3	35.45	74.03	90.41	417.77	617.66	58.1	10.63
AVERAGES		20.87	39.67	62.02	260.42	388.74 ave	41.7	9.32

Notes

(1) *See Table 10.1*
(2) *See Table 10.2*
(3) *See Table 10.4*
(4) *See Table 10.5*
(5) *= (1) + (2) + (3) + (4)*
(6) *Grout Take = Volume of Grout Injected/Volume of Soil to be Grouted*
(7) *See Section 2.1.2*

CHEMICAL GROUTING TEST PROGRAM

SUMMARY OF TOTAL GROUTING COST PER SUBAREA

FOUNDATION INVESTIGATION AND TEST PROGRAM
EXISTING LOCKS AND DAM No. 26
ST LOUIS DISTRICT, CORPS OF ENGINEERS.
DACW43-78-C-0005

Woodward-Clyde Consultants

Y7C828 Phase II

Table 10.6

GROUTING[(1)] METHOD	VOLUME OF SOIL TO BE GROUTED yd^3	GROUTING COST $/$yd^3$ of soil	AVERAGE[(2)] GROUT TAKE %	COST $/$yd^3$ of soil/% take
O_1	276.7	293.70	25.6	10.13
S_1	40.5	92.63	3.7	25.04
S_2	576.9	425.05	43.9	9.68
S_3	547.9	437.14	52.6	8.31
TOTALS	1442	388.74 ave	41.7	9.32 ave (except S_1)

Notes

(1) *See Section 2 and Table 7.1*

(2) *Average Grout Take =*

$$\frac{\text{Total Volume of Grout Injected by Grouting Method}}{\text{Total Volume of Soil to be Grouted by Grouting Method}}$$

CHEMICAL GROUTING TEST PROGRAM

SUMMARY OF TOTAL GROUTING COST PER GROUTING METHOD

FOUNDATION INVESTIGATION AND TEST PROGRAM
EXISTING LOCKS AND DAM No. 26
ST LOUIS DISTRICT, CORPS OF ENGINEERS.
DACW43-78-C-0006

Woodward-Clyde Consultants
Y7C025 Phase IX

Table 10.7

PHASE IV REPORT

VOLUME II

RESULTS AND INTERPRETATION OF
CHEMICAL GROUTING TEST PROGRAM

REFERENCES

REFERENCES

Auld, B., Fritz, A., and Statton, C. T. (1978) "In Situ Shear Wave Velocity Measurements and Proposed Procedures" Dynamic Geotechnical Testing ASTM, STP 654

Bishop, A. W. and Henkel, D. J. (1962) "The Measurement of Soil Properties in the Triaxial Test" The Triaxial Test, Edward Arnold Publishing Co, London

Caron, D. (1973) "Un Nouveau Style de Perforation: La Boue Auto-Durcissable" (A New Trenching Method: The Self-Hardening Slurry) Proc ITBTP, Paris, November

Clough, G. W., Kuck, W. M., and Kasali, G., (1979) "Behavior of Silicate Stabilized Sands" Journal of Geotechnical Engineering Division, ASCE 105, GT1, Jan

Gibbs, H. J., and Holtz, W. G. (1953) "Research on Determining the Density of Sands by Spoon Penetation Testing" Proc 4th Int Conf of Soil Mechanics and Foundation Engineering, 1, p 35-39

Horn, H. M. (1978) "North American Experience in Soil Sample and Its Influence on the Results of Laboratory Dynamic Testing" ASCE

Hughes, J. M. O., Wroth, C. P., and Windle, D. (1977) "Pressuremeter Tests in Sands" Geotechnique, 27, No. 4, December

Koenzen, J. P. (1978) "Time-Dependent Stress-Strain Analysis of Chemically Stabilized Building Elements" Symposium on Soil Reinforcing and Stabilizing Techniques in Engineering Practice, New Southwater Wales, Australia

Koenzen, J. P. (1978) Personal Communication, Sept

Kolbuszewski, K. J. (1948) "An Experimental Study of the Maximum and Minimum Porosities of Sand" ICSSMFE Roterdam, Vol I

Lambe, T. W. (1951) "Soil Testing for Engineers" John Wiley and Sons, New York

Lucks, A. S. (1970) "Influence of Particle Shape on Strength of Granular Materials" PhD Thesis MIT, June

McClelland Engineers (1975) "Pumping Test and Underseepage Investigations" DM-2, General Design Memorandum, Appendix E, Locks and Dam No. 26 (Replacement)

Meyerhof, G. G. (1974) "Penetration Testing Outside Europe" General Report, Proc European Symposium on Penetration Testing, Stockholm, Sweden, 2.1

Mirafuente, N., Zurflueh, E., and Statton, C. T. (1975) "Improved Shear Wave Measurement Techniques for Better Earthquake Resistant Design" WCC Geotechnical/Enviroinmental Bulletin, VII, No. 2

Schmertmann, J. (1976) "An Updated Correlation Between Relative Density, D_R and Fugro-type Electric Cone Bearing, q_c" Contract Report DACW39-76-M-6646, Waterways Experiment Station, Vicksburg, Mississippi

Soletanche (1978) Personal Communication

Statton, C. T. and Ravneberg, N. M. (1978) "Engineering Geophysics in Present Practice", Annual Meeting SEG

Tallard, R. and Caron, C. (1977) "Chemical Grouts for Soils" Report HWA-RD-77-51, I, II

Terzaghi, K. (1955) "Elevation of Coefficient of Subgrade Reaction" Geotechnique, 5, No. 4, p 297-326

Vesic, A. S. (1970) "Test on Instrumented Piles, Ogeechee River Site" J SMFD, ASCE, 96, SM2, March